

Stony Brook University



OFFICIAL COPY

The official electronic file of this thesis or dissertation is maintained by the University Libraries on behalf of The Graduate School at Stony Brook University.

© All Rights Reserved by Author.

**Development of Antitubercular Agents Targeting FtsZ and Antinociceptive
Agents Targeting Fatty Acid Binding Proteins (FABP)**

A Dissertation Presented

By

Simon Tong

To

The Graduate School

In Partial Fulfillment of the

Requirements

For the Degree of

Doctor of Philosophy

in

Chemistry

Stony Brook University

August 2016

Stony Brook University
The Graduate School

Simon Tong

We, the dissertation committee for the above candidate for the
Doctor of Philosophy degree, hereby recommend
acceptance of this dissertation.

Iwao Ojima – Dissertation Advisor
Distinguished Professor, Department of Chemistry

Dale G. Drueckhammer – Chairperson of Defense
Professor, Department of Chemistry

Joseph W. Lauher – Third Member
Distinguished Teaching Professor, Department of Chemistry

Dale G. Deutsch – Outside member
Professor, Department of Biochemistry and Cell Biology,
Stony Brook University, Stony Brook, NY

This dissertation is accepted by the Graduate School

Nancy Goroff
Interim Dean of the Graduate School

Abstract of the Dissertation

Development of Antitubercular Agents Targeting FtsZ and Antinociceptive Agents

Targeting Fatty Acid Binding Proteins (FABP)

by

Simon Tong

Doctor of Philosophy

in

Chemistry

Stony Brook University

2016

Tuberculosis, responsible for 1.5 million deaths worldwide in 2014, is treated using first and second line drugs. The repertoire of treatments has remained virtually static for decades, but the prevalence of drug resistance has increased. The rise of MDR- and XDR-TB has rendered current treatments ineffective, and new anti-tubercular agents with unique mechanisms of action are needed to overcome this hurdle. Filamenting temperature-sensitive mutant Z (FtsZ) is an essential bacterial cell division protein and a promising target. Inhibition of FtsZ will disrupt cell division, killing bacterial cells. Libraries of 2,5,6- and 2,5,7-trisubstituted benzimidazoles were previously synthesized and tested against *Mtb* H37Rv. Lead compounds enhanced GTPase activity, inhibited polymerization, and promoted depolymerization of FtsZ. For further optimization studies and to diversify our database, a new library of 2,5,6-trisubstituted benzimidazoles, containing a dimethylamino substitution at the 6-position and different substitutions at the 2-position, was synthesized and tested for in vitro activity. The synthesis, biological evaluations, and SAR of these novel benzimidazoles will be presented.

Anandamide (AEA), an endocannabinoid, is linked to the regulation of stress, pain and inflammation. It activates cannabinoid receptors (CB receptors) on the cell surface, leading to pain relief. Through diffusion, anandamide also enters cells, where fatty acid binding protein 5 (FABP5) and fatty acid binding protein 7 (FABP7) transport anandamide for inactivation by fatty acid amide hydrolase (FAAH). Inhibition of FABP5 and FABP7 will arrest inactivation of the

endocannabinoid, lead to higher extracellular anandamide levels, and result in anti-inflammatory and anti-nociceptive effects. Based on these observations, FABP5 and FABP7 make good drug targets. Prior work from our laboratories has determined the crystal structures of FABP5 in complex with AEA, 2-arachidonoylglycerol (2-AG), and SB-FI-26, the current lead compound. The structure of FABP5-SB-FI-26 co-crystal revealed only one enantiomer of SB-FI-26 was present in the binding site of FABP5, prompting the optical resolution of SB-FI-26. In addition, new SB-FI-26 analogues have been designed based on the crystal structure of the FABP5-SB-FI-26 complex, and synthesized to optimize potency. The design and synthesis of novel α -truxillic acid derivatives, as well as optical resolution of SB-FI-26, their biological evaluations, and SAR studies will be presented.

Table of Contents

List of Figures	vii
List of Schemes	ix
List of Tables	xi
List of Abbreviations	xii

Chapter 1

Development of Antitubercular Agents Targeting FtsZ

1.1 Introduction	2
1.1.1 Tuberculosis overview and current treatments	2
1.1.2 FtsZ function and potential as a drug target	5
1.1.3 Discovery Trisubstituted Benzimidazoles	7
1.1.3.1 Benzimidazole as a pharmacophore	7
1.1.3.2 Significance of 2-alkoxycarbonylaminopyridines and 2-carbamoylpteridines	8
1.1.3.3 Synthesis of 2,5,6- and 2,5,7-trisubstituted benzimidazoles	9
1.2 Results and Discussion	15
1.2.1 Synthesis of 2-(dialkylaminomethyl)benzimidazoles	15
1.2.2 Synthesis of 2-alkylthiobenzimidazoles	33
1.2.3 Synthesis of 2-alkoxybenzimidazoles	37
1.2.4 Synthesis of tetrasubstituted benzimidazoles	39
1.2.5. Activity of trisubstituted benzimidazoles on <i>Staphylococcus aureus</i>	45
1.2.6. Resynthesis of hit compounds	47
1.3 Conclusion	50
1.4. Experimental Section	52
1.5. References	103
2.1. Introduction	107

Chapter 2

Development of Antinociceptive Agents Targeting Fatty Acid Binding Proteins (FABP)

2.1.1. Pain and fatty acid binding proteins (FABPs).....	107
2.1.2. Discovery of α -truxillic acid derivatives.....	108
2.1.2.1. In-silico screening.....	108
2.1.2.2. Fluorescence displacement assay	110
2.1.2.3. In-vivo studies of SB-FI-26 and other α -truxillic acid derivatives.....	112
2.1.2.4. Pharmacokinetics of SB-FI-26	115
2.2. Results and discussion	116
2.2.1. Optical resolution of SB-FI-26.....	116
2.2.2. Synthesis of α -truxillic acid derivatives.....	124
2.2.2.1. Synthesis of (-)-incarvillateine analogue.....	124
2.2.2.2. Continuing SAR study.....	127
2.2.2.3. Minimizing hERG activity	130
2.2.2.4. Synthesis of heteroaromatic α -truxillic acids	133
2.2.2.5. Docking study of SB-FI-81 analogues	135
2.2.3. Synthesis of MJN 110	137
2.2.4. Synthesis of KT109 and KT172.....	138
2.3. Conclusion	139
2.4. Experimental Section.....	141
2.5. References.....	163

List of Figures

Chapter 1

Figure 1 Distribution of TB throughout the world in 2014.....	2
Figure 2 First-line anti-tuberculosis drugs	3
Figure 3 Second-line anti-tuberculosis drugs.....	4
Figure 4 Comparison of α -tubulin and β -tubulin with Mtb-FtsZ.....	6
Figure 5 Division of a bacterial cell.....	6
Figure 6 Growth of Mtb cells after treatment with albendazole or thiabendazole	8
Figure 7 FtsZ inhibitors synthesized by the Southern Research Institute.....	9
Figure 8 SAR study from library syntheses	10
Figure 9 Inhibition of FtsZ polymerization.....	12
Figure 10 Malachite Green assay reveals an enhancement of GTPase activity.....	12
Figure 11 Optimization of 2,5,6-trisubstituted benzimidazoles.....	13
Figure 12 Structure of SB-P17G-C2.....	13
Figure 13 FtsZ polymerization in the presence of GTP.....	14
Figure 14 Structure of SB-P17G-A38.....	15
Figure 15 A 2,5,6-trisubstituted benzimidazole with varying functionalities on the 2-position .	15
Figure 16a Hit compounds from library synthesis.....	27
Figure 17 A. Cross-section of hERG channel revealing hERG blocker MK-499 interacting with tyrosine 652 and phenylalanine 656.31 B. top view of hERG tetramer channel.....	40
Figure 18 S. Aureus MIC Assay	47
Figure 19 X-ray diffraction of SB-P17G-A42	50

Chapter 2

Figure 1 Anandamide (AEA).....	108
---------------------------------------	-----

Figure 2 Footprint signature comparison of oleic acid a candidate molecule	110
Figure 3 Fluorescence displacement assay of 48 compounds.....	111
Figure 4 Structures of four most potent compounds from fluorescence displacement assay	111
Figure 5 Structure of (-)-incarvillateine compared to structure of SB-FI-26.....	112
Figure 6 α -Truxillic acid derivatives.....	113
Figure 7 Effects of the four α -truxillic acid derivatives.....	114
Figure 8 Thermal latency in rats with CCI when exposed to SB-FI-26	115
Figure 9 Plasma and brain levels of SB-FI	116
Figure 10 Crystal structure of SB-FI-26 bound to FABP5	117
Figure 11a Racemic SB-FI-26	122
Figure 11b Optical Resolution with L-Phenylalaninol	122
Figure 11c Optical Resolution with D-Phenylalaninol	123
Figure 12 X-ray diffraction of SB-FI-26A.....	124
Figure 13 Structure of natural product (-)-incarvillateine.....	125
Figure 14 SB-FI-26 and SB-FI-101 in the binding site of FAB5	127
Figure 15 Comparison of 2-indanol and 6-epi-incarvilline	128
Figure 16 Overlap of SB-FI-85 regioisomers with SB-FI-26 in the binding site of FABP5 Synthesis of SB-FI-85 was slightly different from the general procedure.	131

List of Schemes

Chapter 1

Scheme 1 Proposed synthesis of 2-(alkylaminomethyl)benzimidazole starting with 4-chloro-5-nitrobenzene-1,2-diamine	16
Scheme 2 Synthesis of 5-chloro-2-chloromethyl-6-nitro-1 <i>H</i> -benzo[d]imidazole	16
Scheme 3 Synthesis of 6-Chloro-2-methoxymethyl-5-nitro-1 <i>H</i> -benzo[d]imidazole.....	17
Scheme 4 Synthesis of 6-Chloro-2-dimethylaminomethyl-5-nitro-1 <i>H</i> -benzo[d]imidazole.....	17
Scheme 5 Attempted synthesis of 6- <i>N,N</i> -Dimethylamino-2-dimethylaminomethyl-5-nitro-1 <i>H</i> -benzo[d]imidazole in different heating conditions.	18
Scheme 6 Synthesis of alternative starting material.....	19
Scheme 7 Synthesis of 5-Dimethylamino-2-dimethylaminomethyl-6-nitro-1 <i>H</i> -benzo[d]imidazole	20
Scheme 8 Synthesis of 1-amino-5-chloro-4-nitro-2-(<i>p</i> -toluenesulfonylamino) benzene.....	21
Scheme 9 Synthesis of 1-amino-5- <i>N,N</i> -dimethylamino-4-nitro-2-(<i>p</i> -toluenesulfonylamino) benzene	22
Scheme 10 Synthesis of 1,2-diamino-4- <i>N,N</i> -dimethylamino-5-nitro benzene	22
Scheme 11 Alternative synthesis of 5-Dimethylamino-2-dimethylaminomethyl-6-nitro-1 <i>H</i> -benzo[d]imidazole.....	23
Scheme 12 Synthesis of 5-Amino-6- <i>N,N</i> -dimethylamino-2- <i>N,N</i> -dialkylaminomethyl-1 <i>H</i> -benzo[d]imidazoles	25
Scheme 13 Library Synthesis	25
Scheme 14 Resynthesis of dialkylaminomethyl benzimidazoles.....	30
Scheme 15 Synthesis of 6-(4-fluorophenoxy)-dialkylaminomethyl benzimidazoles	33
Scheme 16 Synthesis of 2-alkylthio benzimidazoles	35
Scheme 17 Conversion of 1-alkoxybenzimidazoles to 2-alkoxybenzimidazoles	37
Scheme 18 Synthesis of benzimidazole <i>N</i> -oxide hydrochloride salt	38

Scheme 19 Synthesis of 2-alkoxybenzimidazoles.....	39
Scheme 20 Synthesis of Tetrasubstituted 1-Carbamate Benzimidazoles.....	42
Scheme 21 Attempts at Alkylating Trisubstituted Benzimidazoles.....	42
Scheme 22 Synthesis of Tetrasubstituted 1-Alkyl Benzimidazoles.....	44
Resynthesis Scheme 1 Resynthesis of 2-cyclohexyl-5-(4-bromobenzamido)-6-piperidin-1-yl-1 <i>H</i> -benzo[d]imidazole.....	48
Resynthesis Scheme 2 Resynthesis of 2-cyclohexyl-5-(4-ethylbenzamido)-6-piperidin-1-yl-1 <i>H</i> -benzo[d]imidazole.....	48
Resynthesis Scheme 3 Resynthesis of 2-cyclohexyl-5-(2,4-difluorobenzamido)-6-pyrrolidin-1-yl-1 <i>H</i> -benzo[d]imidazole.....	49
Resynthesis Scheme 4 Resynthesis of 2-cyclohexyl-5-(2-fluoro-4-trifluoromethylbenzamido)-6- <i>N,N</i> -dimethylamino-1 <i>H</i> -benzo[d]imidazole.....	49

Chapter 2

Scheme 1 Optical resolution with (1 <i>R</i> ,2 <i>S</i>)-2-amino-1,2-diphenylethanol.....	118
Scheme 2 Optical resolution with (S)-1-(1-naphthyl)ethylamine.....	119
Scheme 3 Optical resolution with L-phenylalaninol and D-phenylalaninol.....	120
Scheme 4 Synthesis of (-)-incarvillateine analog.....	126
Scheme 5 Synthesis of SB-FI-85.....	132
Scheme 6 Synthesis of heteroaromatic cyclobutane diacids.....	134
Scheme 7 Synthesis of MJN 110.....	138
Scheme 8 Synthesis of KT109 and KT172.....	139

List of Tables

Chapter 1

Table 1 MIC values and cytotoxicity of 2,5,6 and 2,5,7-trisubstituted benzimidazoles	11
Table 2: Conditions used to optimize the synthesis of 5-Dimethylamino-2-dimethylaminomethyl-6-nitro-1 <i>H</i> -benzo[d]imidazole	21
Table 3 MIC of 2-(dialkylaminomethyl)benzimidazoles compared to 2-cyclohexylbenzimidazoles	31
Table 4 MIC of 2-thiobenzimidazoles	36
Table 5 Activities of tetrasubstituted benzimidazoles.....	45

Chapter 2

Table 1 Binding affinities of α -truxillic acid derivatives	113
Table 2 Conditions tested in optical resolution using (1 <i>R</i> ,2 <i>S</i>)-2-amino-1,2-diphenylethanol...	118
Table 3 Conditions tested in optical resolution using (<i>S</i>)-1-(1-naphthyl)ethylamine	119
Table 4 Conditions tested in optical resolution using L-phenylalaninol.....	121
Table 5 Synthesis of α -truxillic acid derivatives.....	129
Table 6 Docking results of α -truxillic acid analogues using various alcohols.....	136

List of Abbreviations

2-AG	2-Arachidonoylglycerol
AcCN	Acetonitrile
AIDS	Acquired immune deficiency syndrome
AEA	Anandamide
CB receptor	Cannabinoid receptor
CDC	Center for disease control and prevention
CDI	Carbonyldiimidazole
¹³ C NMR	Carbon-13 nuclear magnetic resonance
DCM	Dichloromethane
DIPEA	Diisopropylethylamine
DMAP	Dimethylaminopyridine
DMF	Dimethylformamide
DMSO	Dimethylsulfoxide
DNA	Deoxynucleic acid

<i>E. coli</i>	<i>Escherichia coli</i>
EDC·HCl	1-Ethyl-3-(3-dimethylaminopropyl)carbodiimide hydrochloride
EtOAc	Ethyl acetate
EtOH	ethanol
FAAH	Fatty acid amide hydrolase
FABP	Fatty acid binding protein
FDA	Food and drug administration
FIA	Flow injection analysis
GDP	Guanosine diphosphate
GTP	Guanosine triphosphate
GTPase	Guanosine triphosphatase
HCl	Hydrochloric acid
hERG	Human ether-a-go-go-related gene
HIV	Human immunodeficiency virus
¹ H NMR	Proton nuclear magnetic resonance
HPLC	High pressure liquid chromatography
HRMA	High resolution mass spectrometry
IP	Intraperitoneal
IPA	Isopropyl alcohol
mp	Melting point
MABA	Microplate Alamar blue assay
MDR-TB	Multidrug resistant tuberculosis
MeCN	Acetonitrile
MeOH	Methanol
MIC	Minimum inhibitory concentration

MRSA	Methicillin-resistant <i>Staphylococcus aureus</i>
Ms-Cl	Methanesulfonyl chloride (mesyl chloride)
<i>Mtb</i>	<i>Mycobacterium tuberculosis</i>
NBD-stearate	12-N-methyl-(7-nitrobenz-2-oxa-1,3-diazo)aminostearic acid
PDB	Protein data bank
PEG	Polyethyleneglycol
<i>S. aureus</i>	<i>Staphylococcus aureus</i>
SAR	Structure-activity relationship
SRI	Southern Research Institute
TB	Tuberculosis
TBAF	Tetrabutylammonium fluoride
TEM	Transmission electron microscopy
TEA	Triethylamine
TES-Cl	Triethylsilyl chloride
TFA	Trifluoroacetic acid
THF	Tetrahydrofuran
TLC	Thin layer chromatography
Ts-Cl	4-Toluenesulfonyl chloride (tosyl chloride)
UV	Ultraviolet
WHO	World Health Organization
XDR-TB	Extensively drug-resistant tuberculosis

Chapter 1

Development of Antitubercular Agents Targeting FtsZ

1.1 Introduction.....	2
1.1.1 Tuberculosis overview and current treatments.....	2
1.1.2 FtsZ function and potential as a drug target.....	5
1.1.3 Discovery Trisubstituted Benzimidazoles.....	7
1.1.3.1 Benzimidazole as a pharmacophore	7
1.1.3.2 Significance of 2-alkoxycarbonylaminopyridines and 2-carbamoylpteridines	8
1.1.3.3 Synthesis of 2,5,6- and 2,5,7-trisubstituted benzimidazoles	9
1.2 Results and Discussion	15
1.2.1 Synthesis of 2-(dialkylaminomethyl)benzimidazoles	15
1.2.2 Synthesis of 2-alkylthiobenzimidazoles.....	33
1.2.3 Synthesis of 2-alkoxybenzimidazoles	37
1.2.4 Synthesis of tetrasubstituted benzimidazoles.....	39
1.2.5. Activity of trisubstituted benzimidazoles on <i>Staphylococcus aureus</i>	45
1.2.6. Resynthesis of hit compounds.....	47
1.3 Conclusion	50
1.4. Experimental Section.....	52
1.5. References.....	103

1.1 Introduction

1.1.1 Tuberculosis overview and current treatments

Tuberculosis (TB) is a disease caused by *Mycobacterium tuberculosis* (*Mtb*).¹ This disease has claimed the lives of 1.5 million people in 2014 alone, and 500,000 of them had HIV coinfection.² Most of the fatalities are prevalent in developing countries (**Figure 1**).³ TB is usually localized to the lungs. It is known to spread through the air, and some of the ways an infected person can spread the bacteria are by coughing, sneezing and spitting.^{1,3} According to the World Health Organization, one-third of the world's population is infected with *Mtb* bacteria, but only about 5-10% of people infected with *Mtb* develop the active form of TB in their life time.³ People may or may not show symptoms based on the condition of their immune system.

Estimated TB incidence rates, 2014

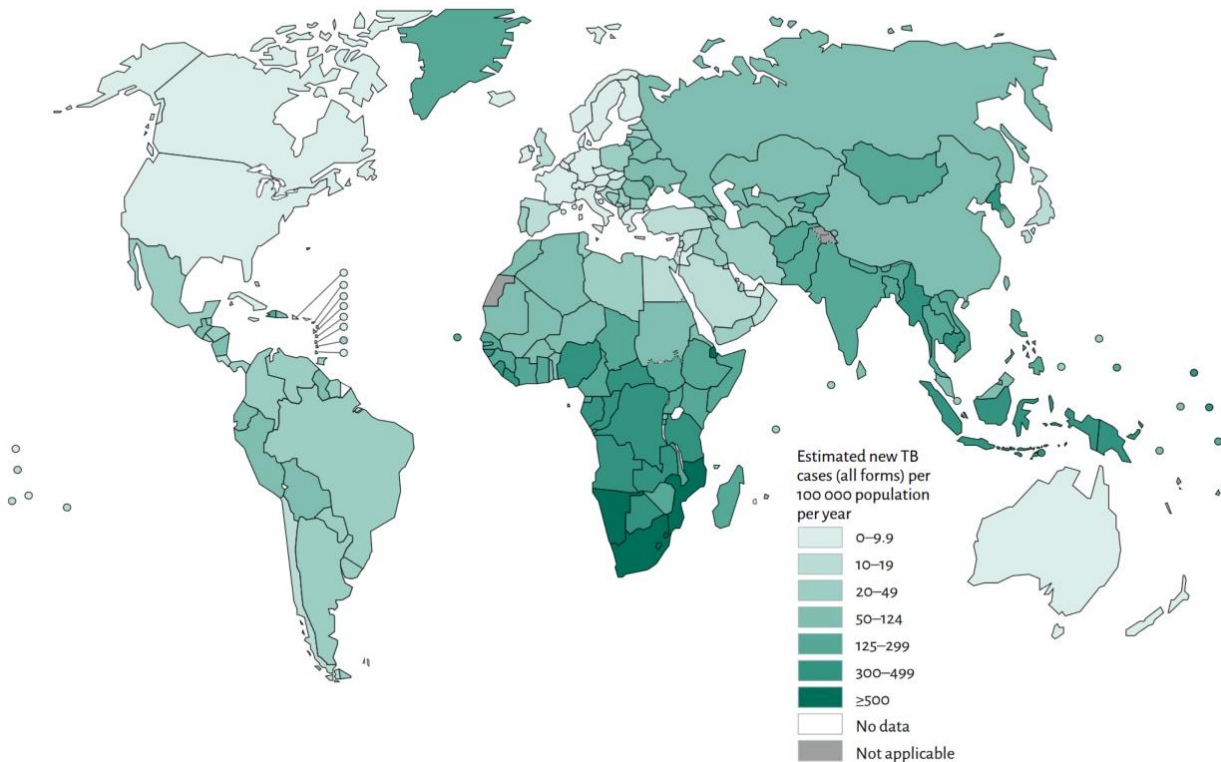


Figure 1 Distribution of TB throughout the world in 2014.³

Most of the people infected with *Mtb*, with healthy immune systems, have latent TB infection. When people have this form of TB, no symptoms are shown. The immune system sends macrophages and help T-cells to "wall off" the bacteria and keep their growth at bay, but the infection is never fully cured.⁴ The immune system cannot kill all the bacteria; it can only keep

the growth of the bacteria in check. However, when a person's immune system is weakened, the bacteria get a chance to progress into active form of TB infection. Symptoms of active form of TB infection primarily include, coughing (sometimes containing sputum or blood), chest pains, weakness, weight loss, fever and night sweats.⁵ In addition to the aforementioned symptoms, the macrophages release neutral proteases and reactive oxygen species, which results in the necrosis of lung tissue.⁶ Interestingly, people may be infected with latent TB for a long period, sometimes even years, before showing symptoms of active TB.⁴ People infected with HIV are more susceptible to TB because they are immunocompromised. TB is one of the most prevalent causes of death in patients with HIV.³

There are four first line drugs available for treating TB, isoniazid, pyrazinamide, rifampin, and ethambutol (**Figure 2**). These drugs, used in combination, can eradicate TB infection, but it may take up to six months to get rid of the infection completely. This is due to the slow growing nature of *Mtb* bacteria.⁷ Consequently, the antibiotics take longer to be effective. Since the treatment takes a long time, most patients do not finish all of the prescribed medications. Poor patient compliance could give bacteria time to mutate and possibly build up resistance to the first line drugs.⁷

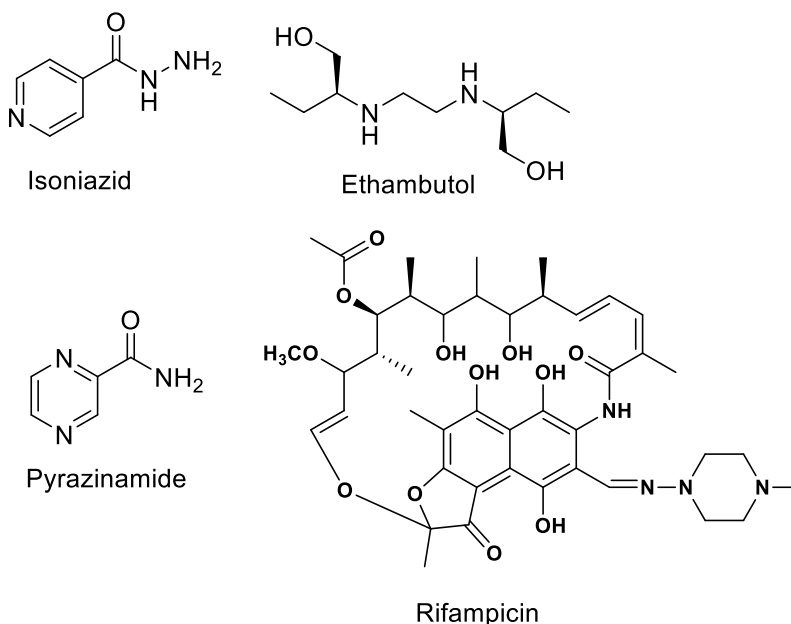


Figure 2 First-line anti-tuberculosis drugs.

This new form of TB is known as multi drug resistant tuberculosis (MDR-TB), which cannot be cured with first-line drugs. Second-line antibiotics are employed to cure MDR-TB

infection, but the treatment duration is very long, taking up to two years, and cause to more harmful side effects (**Figure 3**). When bacteria develop resistance to even second-line antibiotics, it gives rise to extensively drug resistant tuberculosis (XDR-TB).² There are very few treatment options available for this form of tuberculosis. Two drugs recently approved for treatment of MDR-TB are Delamanid, approved in Europe in 2014, and Bedaquiline, approved by the FDA in 2012.^{8,9} These two compounds are the newest in the arsenal against drug-resistant tuberculosis, as they are the first approved anti-TB drugs in 40 years.¹⁰ They inhibit mycolic acid synthesis and ATP synthase, respectively, but they also carry serious cardiotoxicity side effects. Recently, Delamanid and Bedaquiline have been used in successful treatment of XDR-TB.¹¹

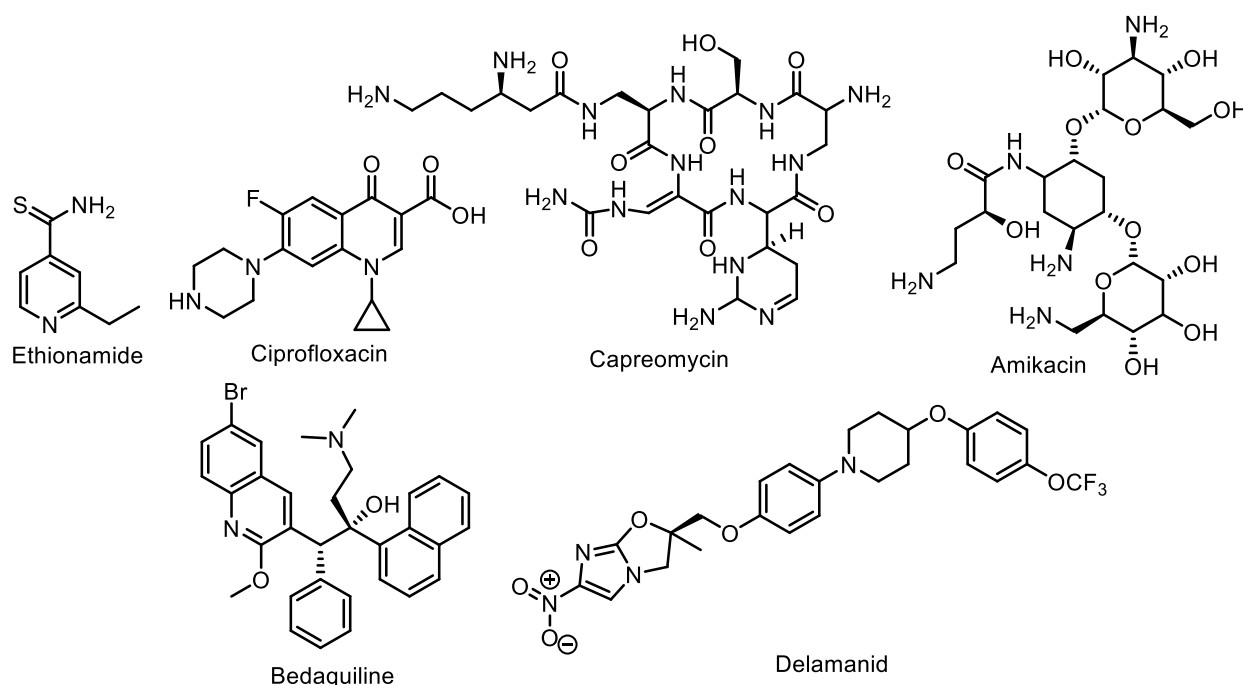


Figure 3 Second-line anti-tuberculosis drugs.

With the increasing prevalence of MDR-TB and XDR-TB and the toxic side effects of newer drug compounds, there is a motivation to find novel drug targets so that new and safer forms of treatment can be developed. The target needs to be essential for bacterial cells, so that disruption of the target will prove fatal for the cell. Additionally, it should be extremely difficult for bacteria to acquire resistances through mutations of this target. One protein found to fit both of these criteria is filamentous temperature sensitive protein Z (FtsZ).⁸

1.1.2 FtsZ function and potential as a drug target

Filamentous temperature sensitive protein Z (FtsZ) is an important prokaryotic protein involved in cell division of bacteria.¹² In addition to being present in *Mtb*, this protein is highly essential and crucial for the growth of a number of infectious bacteria and is the most abundant of all the cell division proteins.¹² If a novel compound disrupts the functioning of FtsZ, it can potentially be used as a broad spectrum antibiotic.

Before going further with drug discovery, it is important that the function of the target is well understood. Tubulin and FtsZ share 7% sequence identity but have high structural homology.¹¹ Both proteins contain two domains, N-terminal and C-terminal, bisected by the H7 helix (H7).^{13,14} The N-terminal domain consists of helices H1-H6 and strands S1-S6 and also contains the nucleotide binding site. The C-terminal domain consists of helices H8-H10 and strands S7-S10 and houses the vital T7 loop (**Figure 4**). The GTPase active site is located at the interface of two FtsZ monomers. The nucleotide-binding site of a FtsZ monomer combined with the T7 loop of another FtsZ monomer forms the active site (Figure 1). During cell division, GTP binds to FtsZ, which activates the polymerization of FtsZ into protofilaments.¹⁵ The units of FtsZ monomers in protofilaments vary. These protofilaments associate together laterally at the center of bacterial cells, forming a Z-ring.¹⁵ The Z-ring is a highly dynamic structure, which continuously exchange the FtsZ monomers from the cytoplasm.¹⁵ Other proteins are recruited to the Z-ring to form a septum which forms the platform for cytokinesis.¹⁵ When GTP is hydrolyzed to GDP, it causes the protofilaments to bend leading to the constriction of the Z-ring.¹⁵ The septum is attached to the cell membrane, so contracting the septum will cause the bacterial cells to start pinching and divide (**Figure 3**).¹⁵ Inhibiting the proper functioning of FtsZ may lead to the arrest of bacterial growth, giving the drugs time to kill the bacteria. Hence, FtsZ is an ideal target due to its crucial role in bacterial cell division. Since FtsZ and tubulin share functional and structural similarities, known tubulin inhibitors can be used as the starting point for the development of novel anti-FtsZ agents.¹⁵ These known tubulin inhibitors can be chemically modified to reverse their affinity, making it specific to FtsZ and diminishing its binding capacity to tubulin, as any tubulin activity in drug compounds will lead to cytotoxicity in humans.¹⁵

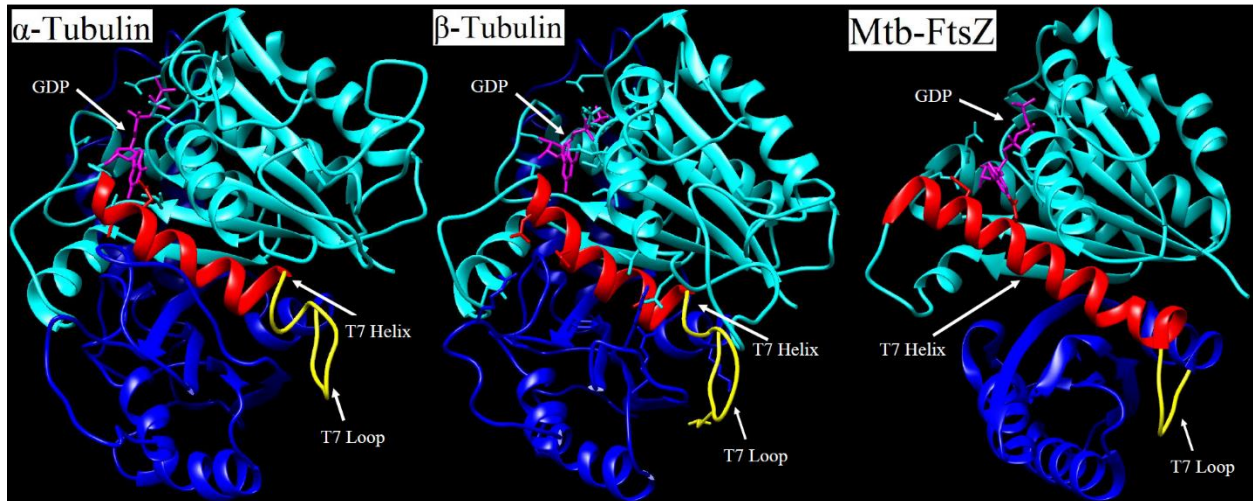


Figure 4 Comparison of α -tubulin and β -tubulin with Mtb-FtsZ. Cyan is the N-terminal domain. Red is the H7 helix. Yellow is the T7 loop. Blue is the C-terminal domain. The magenta molecule is GDP, which sits in the nucleotide binding site. (PDB entries 1TUB for tubulins and 1RLU for FtsZ).

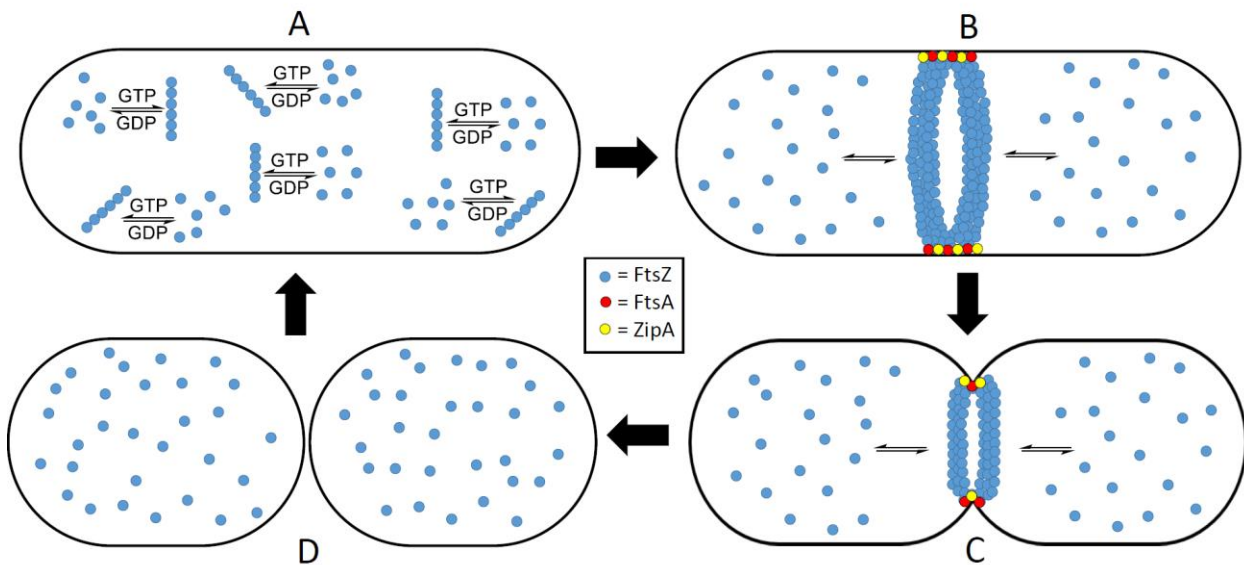


Figure 5 Division of a bacterial cell. A) FtsZ monomers and protofilaments are in equilibrium. GTP binding initiates polymerization bidirectionally. B) FtsA and ZipA are recruited to form the Z-ring. C) Hydrolysis of GTP to GDP causes a contraction of the septum, and cytokinesis begins. D) Cytokinesis finishes and the initial parent cell is split into two daughter cells.¹⁶

1.1.3 Discovery Trisubstituted Benzimidazoles

1.1.3.1 Benzimidazole as a pharmacophore

Two compounds, albendazole and thiabendazole, are known inhibitors of tubulin, which is involved in eukaryotic cell division.^{17,18} These compounds were tested to determine their activity against FtsZ. Albendazole and thiabendazole were found to be moderately active with MIC₉₉ values of 61 μ M and 80 μ M, respectively against H37Rv *Mtb* cells.¹⁹ Treatment of *Mtb* with these two compounds for 3 days reduced the growth of the bacteria substantially (**Figure 6**). Individual bacterial cells were elongated after the treatment, and there was little to no septum formation.¹⁷ This showed that treatment of *Mtb* with albendazole and thiabendazole does inhibit FtsZ. Even though these two compounds inhibit FtsZ, they cannot be used for treatment of TB because they inhibit tubulin polymerization and are therefore cytotoxic. Albendazole and thiabendazole need to be modified to make them more active towards FtsZ with no cytotoxicity. Both albendazole and thiabendazole have a benzimidazole core structure. Benzimidazoles is a privileged pharmacophore which has been studied extensively in past. However, there are very few trisubstituted benzimidazoles, which are known in literature, and these compounds have not been tested for their anti-TB activity.

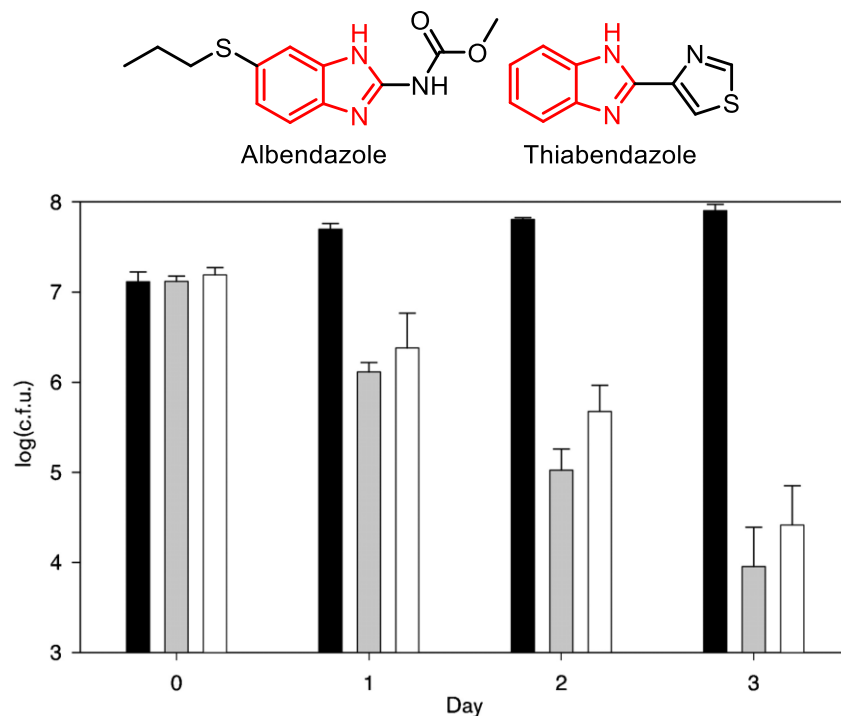


Figure 6 Growth of *Mtb* cells after treatment with albendazole or thiabendazole. Black bars are the control; Gray bars are *Mtb* treated with albendazole, and white bars are *Mtb* treated with thiabendazole. After three days of treatment, growth of the *Mtb* that were exposed to albendazole or thiabendazole was significantly decreased.¹⁷

1.1.3.2 Significance of 2-alkoxycarbonylaminopyridines and 2-carbamoylpteridines

The Southern Research Institute (SRI) tested a series of 200 compounds, initially designed as tubulin inhibitors, for anti-TB activity.²⁰ The homology of tubulin and FtsZ lead researchers to hypothesize that the compounds would be FtsZ inhibitors. Of the 200 compounds, SRI-3072 and SRI-7614 were found to have MIC values of 0.28 μM and 19 μM , respectively, against H37Rv.²⁰ FtsZ polymerization was inhibited in a dose-dependent manner and also inhibited GTPase activity.²⁰ Tubulin activity was nonexistent even at 100 μM . SRI-3072 and SRI-7614 were found to be FtsZ specific.²⁰ Later, a 2-carbamoyl pteridine analogue of SRI-3072 was synthesized and was found to be eight times as active as SRI-3072.²¹

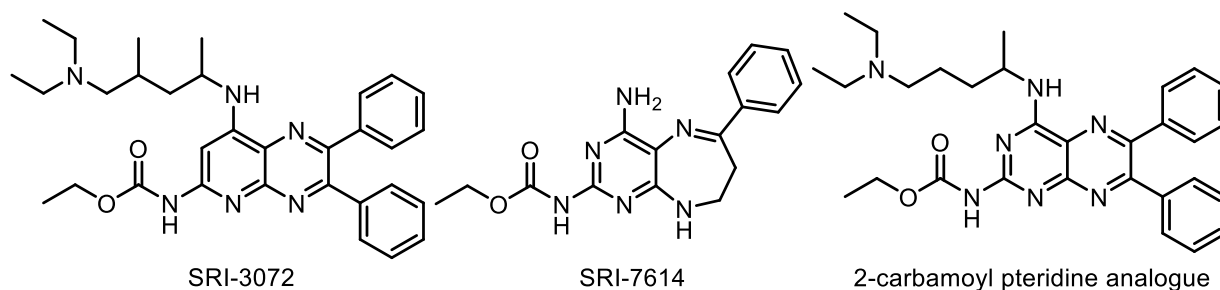


Figure 7 FtsZ inhibitors synthesized by the Southern Research Institute.

1.1.3.3 Synthesis of 2,5,6- and 2,5,7-trisubstituted benzimidazoles

By combining the benzimidazole pharmacophore, from thiabendazole and albendazole, with the substitution patterns of the SRI compounds, the trisubstituted benzimidazoles were developed as novel anti-TB agents. An initial library of 349 compounds, consisting of 2,5,6- and 2,5,7-trisubstituted benzimidazoles, were synthesized and evaluated on H37Rv strain *Mtb*.¹⁹ The compounds were screened for activity using the microplate Alamar Blue Assay (MABA) which showed that several compounds were effective inhibitors of *Mtb* growth. Of the 349 compounds in the library, there were 26 with MIC values $\leq 5 \mu\text{g/mL}$.¹⁹ 9 of the 26 compounds were resynthesized. Based on the results from the library, a cyclohexyl group at the 2-position and a diethylamino group at the 6-position were crucial for activity (**Figure 8**).¹⁹ The SAR study from the first library gave much insight into the future synthesis of trisubstituted benzimidazole, and a second library of 238 compounds, with various dialkylamine groups at the 6-position and cyclohexyl at the 2-position, was synthesized.¹⁹ The second library had 54 hit compounds, which were active at $\leq 5 \mu\text{g/mL}$. The number of hit compounds was significantly higher than the previous library. Of the 54 compounds, two compounds were resynthesized. All 11 of the resynthesized compounds were retested on MABA as well as tested for cytotoxicity on Vero cells (**Table 1**).¹⁹ None of the compounds were found to be cytotoxic.

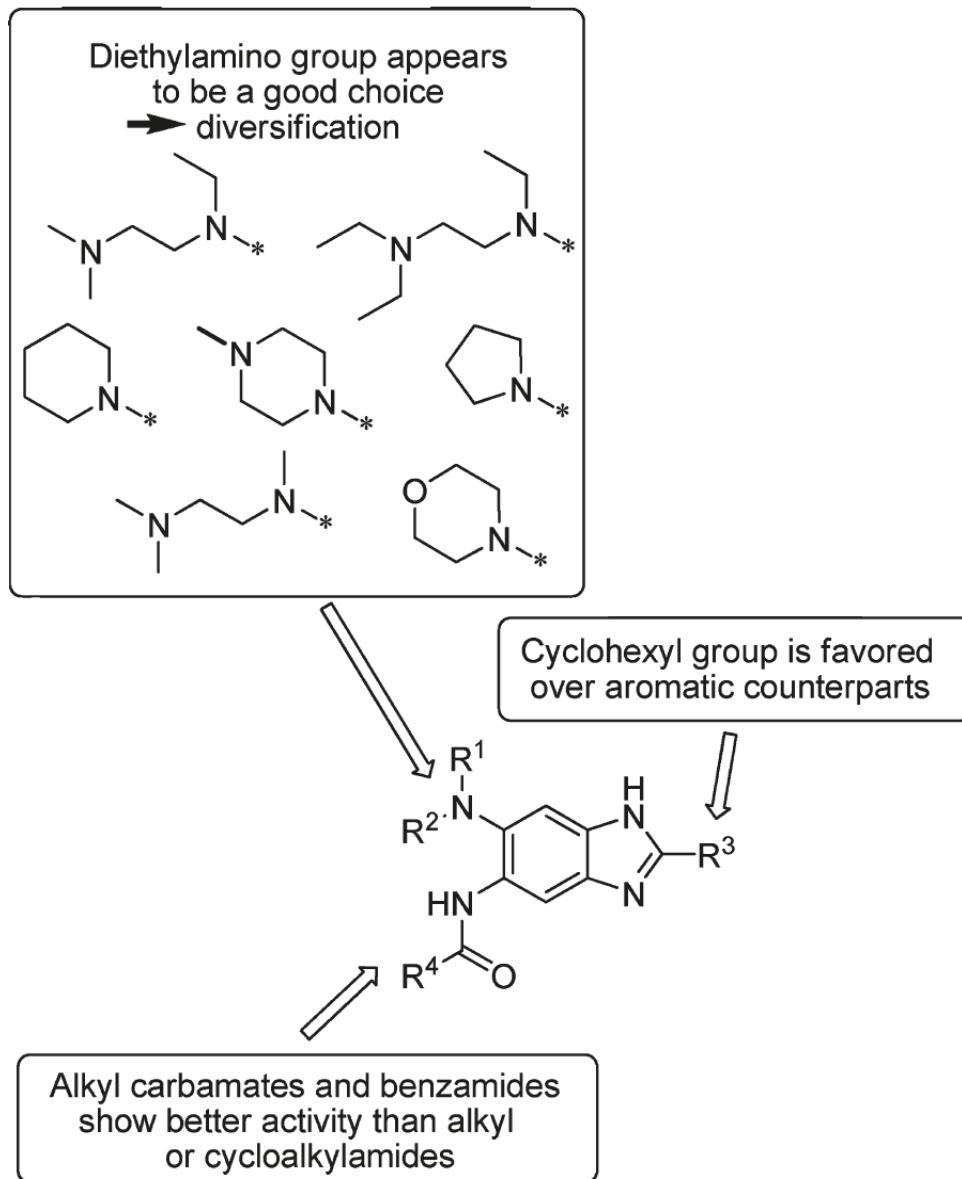
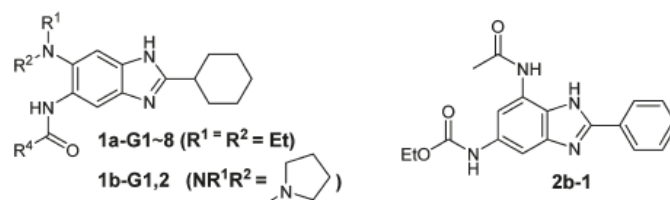


Figure 8 SAR study from library syntheses.

Table 1 MIC values and cytotoxicity of 2,5,6 and 2,5,7-trisubstituted benzimidazoles.

Entry	Benzimidazole	R_4	MIC ₉₉ (μM) <i>Mtb</i> strains						Cytotoxicity (IC ₅₀ μM) Vero cells
			H37Rv	W210	NHN20	NHN335	NHN382	TN587	
1	1a-G1		7.9						>400
2	1a-G2		4.3						>400
3	1a-G3		7.4						>400
4	1a-G4		4.2	4.2	4.2	4.2	4.2	4.2	>400
5	1a-G5		14.1						>400
6	1a-G6		15.1						>400
7	1a-G7		2.0	4.0	4.0	4.0	2.0	4.0	>400
8	1a-G8		3.8						>400
9	1b-G1		1.0	1.0	1.0	1.0	1.0	1.0	>200
10	1b-G2		3.7	3.7	3.7	3.7	3.7	3.7	>200
11	2b-1	Me	2.3	4.6	2.3	2.3	2.3	2.3	>200

Even though the compounds killed *Mtb* cells, the target of the trisubstituted benzimidazoles were still not known. A polymerization assay with *Mtb* FtsZ was performed using a fluorimeter to measure light scattering, and the compounds were shown to inhibit polymerization in a dose-dependent manner (**Figure 9**).¹⁹ In addition to a polymerization assay, the a Malachite Green assay was performed to determine the GTPase activity of the FtsZ when exposed to the trisubstituted benzimidazoles.¹⁹ The compounds were found to accelerate the GTPase activity of the protein (**Figure 10**).¹⁹ The hypothesis was the accelerated GTPase activity would rapidly hydrolyze any bound GTP to GDP and push the FtsZ protofilament equilibrium towards the monomers, thus inhibiting polymerization.

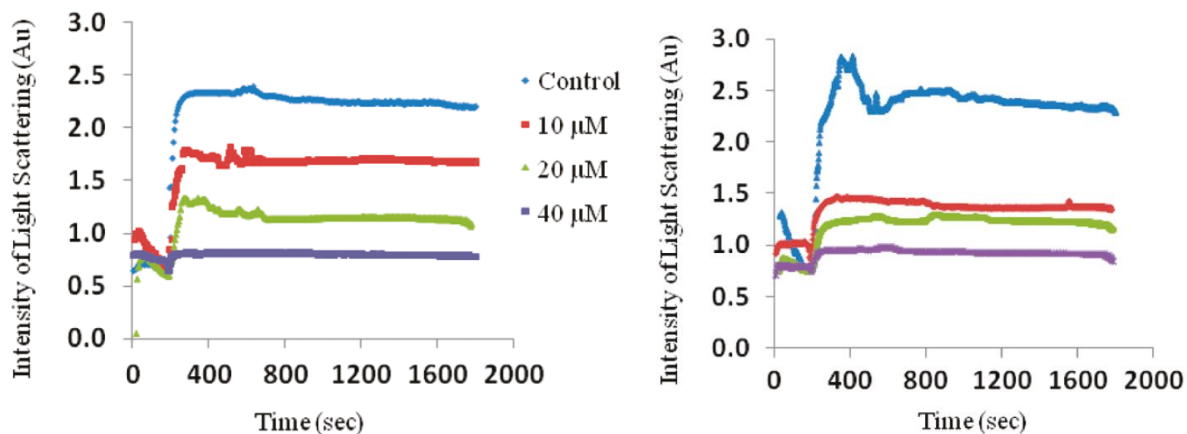


Figure 9 Inhibition of FtsZ polymerization by 1a-G4 (left) and 1a-G7 (right).

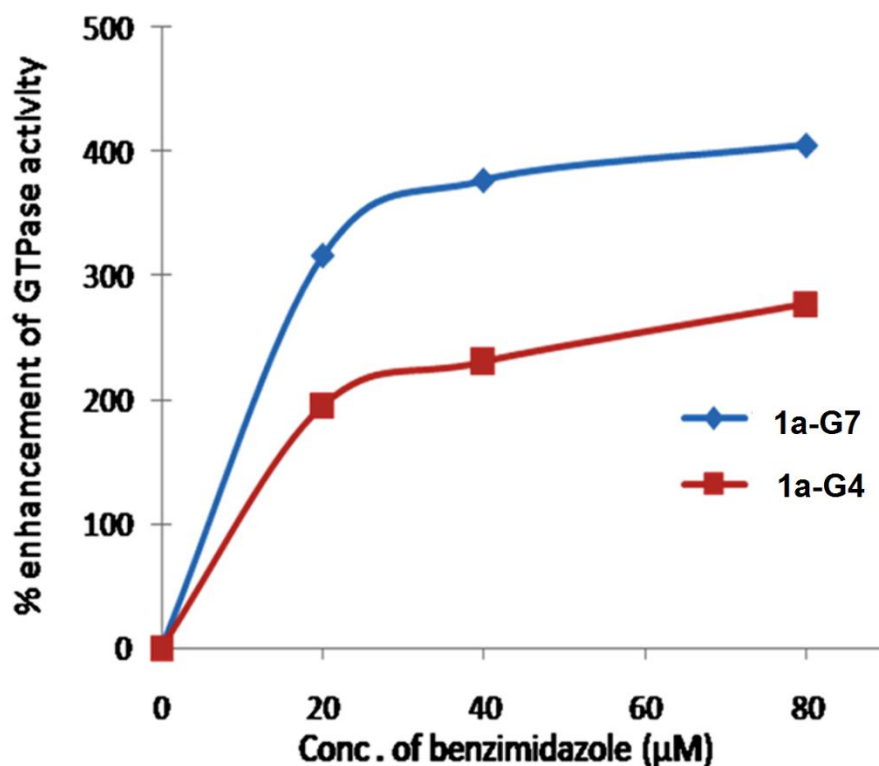


Figure 10 Malachite Green assay reveals an enhancement of GTPase activity.

With the numerous hit compounds from the previous libraries, 2,5,6-trisubstituted benzimidazoles were chosen to be optimized for anti-TB activity. A library of 63 compounds were synthesized.²² Several dialkylamines were used to vary the 6-position and different acyl chlorides, chloroformates, and isocyanates were used to obtain amide, carbamate, and urea functionalities, respectively, at the 5-position (**Figure 11**).²² Certain benzamides and carbamates, at the 5-position, improved activities of compounds, but addition the urea moiety at the 5-position was deleterious to activity. Of the dialkylamines on the 6-position, the dimethylamino group resulted

in good to excellent activities, making the addition of the dimethylamino group a major breakthrough in improving potency.²² A highly active compound, SB-P17G-C2, was found to be the most potent 2,5,6-trisubstituted benzimidazole synthesized, with an MIC of 0.06 µg/ mL for H37Rv strain *Mtb* (**Figure 12**).²² This compound was active against four different strains of *Mtb*, H37Rv (drug sensitive), W210 (drug sensitive), NHN382 (isoniazid-resistant, Kat G S315T mutation), and TN587 (isoniazid-resistant Kat G S315T mutation).²² Transmission electron microscopy (TEM) was used to visualize FtsZ inhibition by the benzimidazoles. Addition of GTP to FtsZ resulted in a dense protofilament buildup on the TEM grid. FtsZ pretreated with SB-P17G-C2 resulted in less populated grids, and addition of the benzimidazole after polymerization resulted in the disassembly of FtsZ filaments (**Figure 13**).²² The compound was able to inhibit FtsZ polymerization and enhance FtsZ depolymerization on preformed protofilaments.

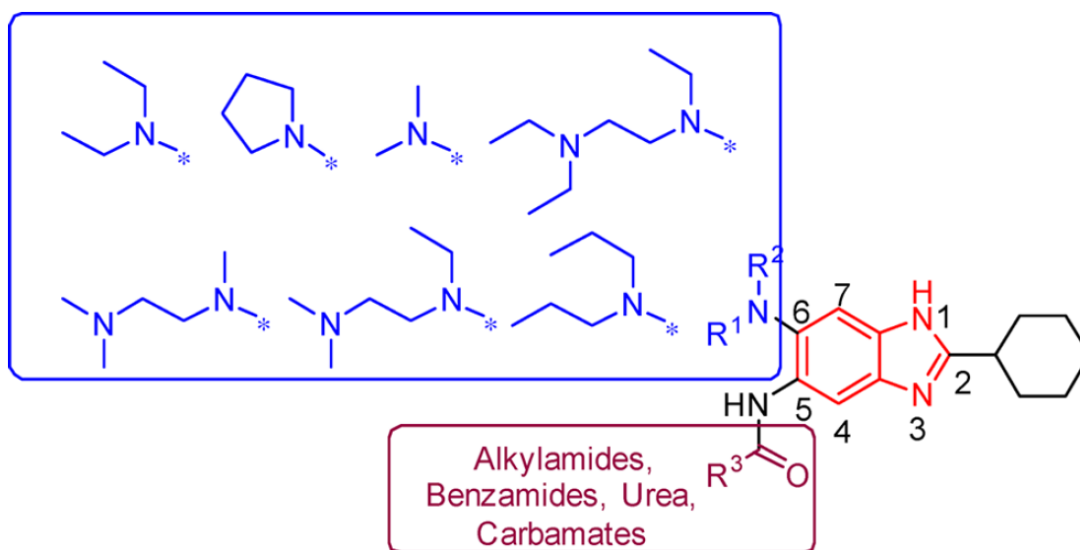


Figure 11 Optimization of 2,5,6-trisubstituted benzimidazoles.

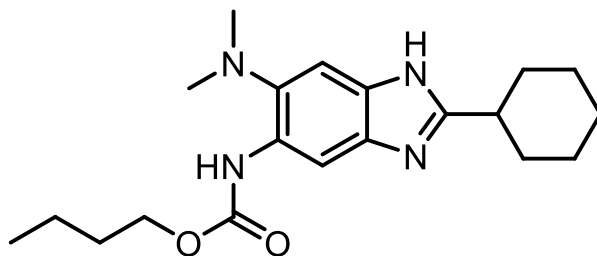


Figure 12 Structure of SB-P17G-C2.

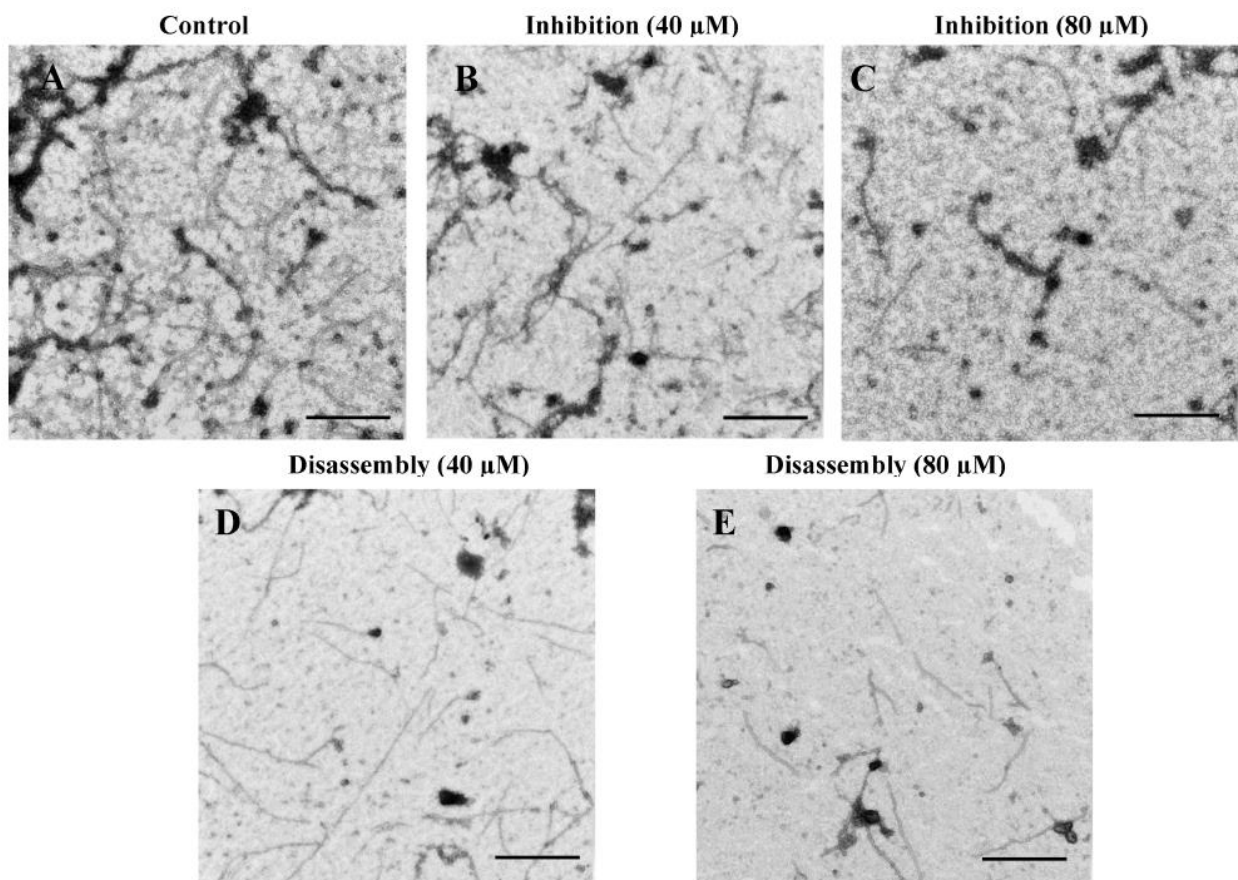


Figure 13 A. The control sample of FtsZ polymerized in the presence of GTP. B, C. Pretreatment of FtsZ with SB-P17G-C2 at 40 μ M and 80 μ M resulted in less densely populated grids. D, E. Treatment of preformed protofilaments with SB-P17G-C2 at 40 μ M and 80 μ M resulted in depolymerization.

Even though SB-P17G-C2 was highly potent, all compounds with carbamates at the 5-position were metabolically unstable. In plasma, the carbamate was quickly hydrolyzed, and compounds were rendered inactive. To improve the metabolic stability, a series of compounds, with benzamides at the 5-position, were synthesized. An amide functionality was much more robust than carbamates, and there was little to no loss in activity. Unfortunately, even the amide compounds exhibited hydrolysis, so a series of fluorinated benzamides were synthesized to help improve the stability. One compound, SB-P17G-A38, was found to be metabolically stable as well as active, with an MIC value of 0.16 μ g/ mL (**Figure 14**). This compound was chosen to be the lead compound.

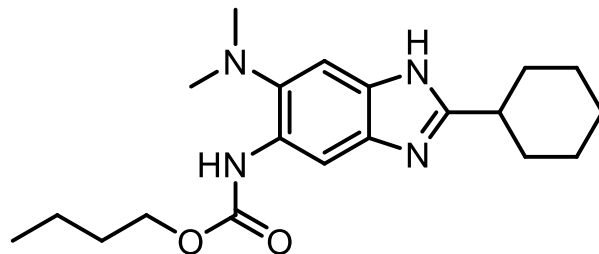


Figure 14 Structure of SB-P17G-A38

1.2 Results and Discussion

In the Ojima lab, functionalities on the 5, 6, and 7 positions of benzimidazole have been explored extensively, but variation at the 2-position of benzimidazole is not as well studied. The purpose of this project is to synthesize various benzimidazoles with different functionalities at the 2-position to develop a new series of benzimidazole libraries (**Figure 15**).

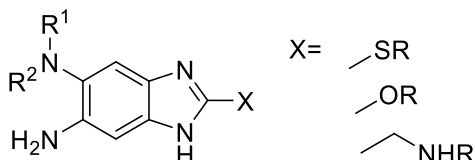
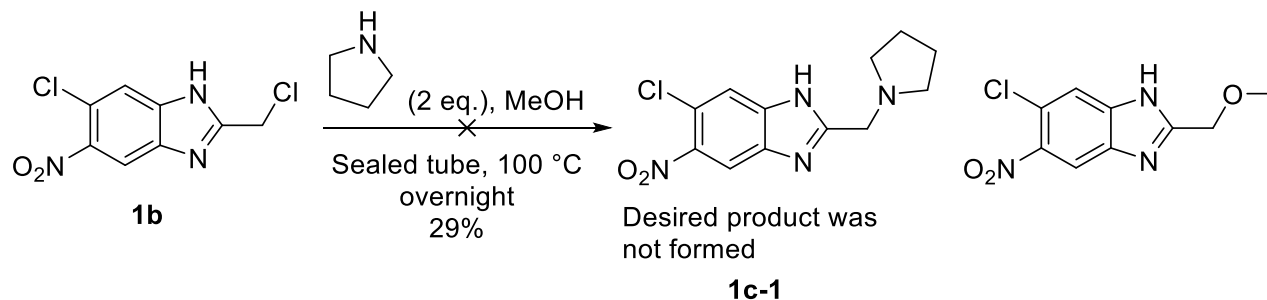


Figure 15 A 2,5,6-trisubstituted benzimidazole with varying functionalities on the 2-position

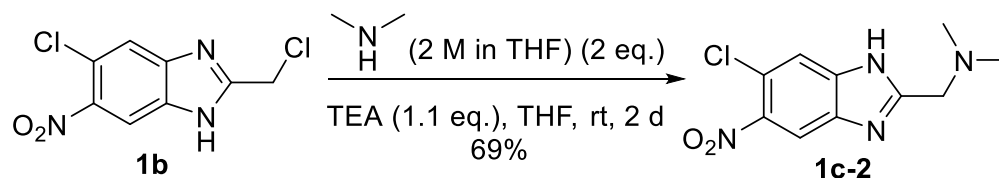
1.2.1 Synthesis of 2-(dialkylaminomethyl)benzimidazoles

The initial plan for synthesis of 2-(dialkylaminomethyl)benzimidazoles was starting with commercially available 4-chloro-1,2-diamino-5-nitrobenzene, and cyclizing it with chloroacetic acid. The cyclized product would then be nucleophilically attacked by a dialkylamine. The resulting benzimidazole would be subjected to a nucleophilic aromatic substitution, with dimethyl amine, and a subsequent reduction of the nitro group, with tin chloride, to obtain a “final intermediate,” which would be used in library synthesis to obtain hundreds of trisubstituted benzimidazoles for preliminary MIC determination (**Scheme 1**).



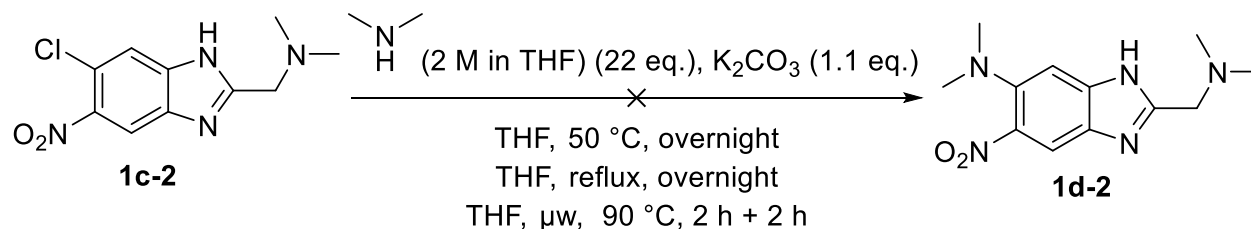
Scheme 3: Synthesis of 6-Chloro-2-methoxymethyl-5-nitro-1H-benzo[d]imidazole

The procedure was changed to avoid any unwanted side reactions, which were observed in the previous condition. The next procedure used tetrahydrofuran (THF) as the solvent, dimethyl amine as a nucleophile, and TEA as a base (**Scheme 4**). This reaction took place in two days at room temperature. The yield for this reaction was 69% yield. In order to improve the yield, potassium iodide was added and the reaction mixture was heated in subsequent nucleophilic substitutions in a later scheme.



Scheme 4: Synthesis of 6-Chloro-2-dimethylaminomethyl-5-nitro-1H-benzo[d]imidazole

The product of the previous step was used in a nucleophilic aromatic substitution. Various conditions were used to push the reaction to form desired product. First, the reaction mixture, consisting of dimethylamine and potassium carbonate in THF, was heated to 50 °C overnight. TLC, as well as MS analysis, of the reaction mixture revealed no consumption of starting material. The reaction mixture was then heated to reflux overnight, and analysis also revealed no formation of desired product. The reaction was then performed in the microwave (**Scheme 4**). After four hours of being heated at 90 °C, there was no product formation. The lack for formation of product may be attributed to chlorine being a poor leaving group compared to fluorine in nucleophilic aromatic substitutions due to the difference in electronegativity. Fluorine is more inductively electron withdrawing and can stabilize the resulting anionic intermediate, resulting from a nucleophilic attack onto the benzene ring, better than chlorine, so a better leaving group was needed to make the reaction work.

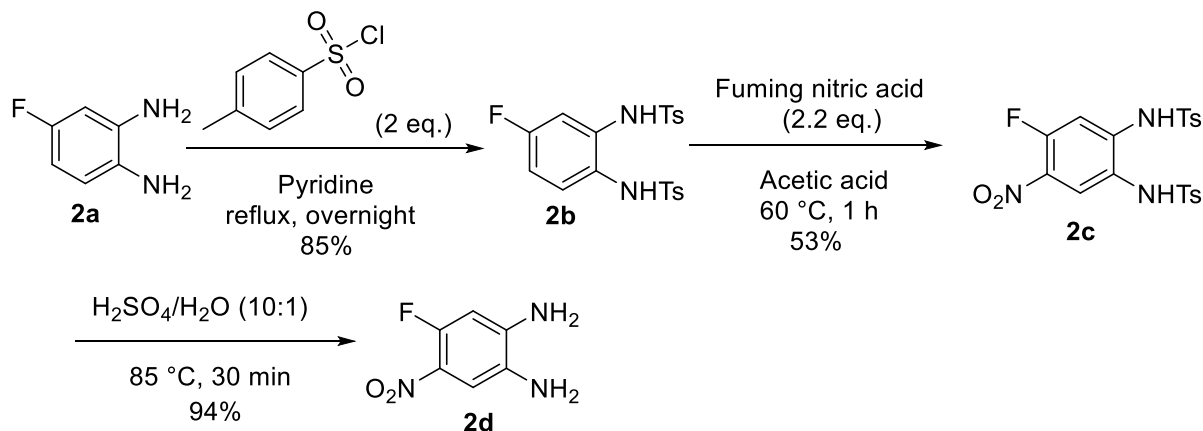


Scheme 5: Attempted synthesis of 6-N,N-Dimethylamino-2-dimethylaminomethyl-5-nitro-1H-benzo[d]imidazole in different heating conditions.

As aromatic nucleophilic substitution of chloride did not work, it was decided that fluorine would be a better alternative. Fluorine, being more electronegative, was thought to stabilize the anionic intermediate better than chlorine and as a result, the nucleophilic attack by dimethylamine would occur more readily. Unfortunately, 1,2-diamino-4-fluoro-5-nitrobenzene, **2d**, was expensive to purchase. However, 1,2-diamino-4-fluoro-5-nitrobenzene, **2d**, could be synthesized from commercially available and relatively inexpensive 5-fluorobenzene-1,2-diamine, **2a**, following the procedure by Nasielski-Hinkens *et. al.*²³ The first reaction in the scheme below was the protection of the phenylenediamine with tosyl groups (**Scheme 6**). This was performed in pyridine with *p*-toluenesulfonyl chloride. The reaction was heated to reflux and left to react overnight. The reaction went to completion and the desired product was isolated in 85% yield.

Subsequently, 4-fluoro-1,2-di (*p*-toluenesulfonylamino) benzene, **2b**, was nitrated with fuming nitric acid in acetic acid at 60 °C for 2 hours. The reaction mixture was initially a slurry, which became a solution as the reaction progressed. After completion of the reaction, the desired product precipitated out of solution and made the whole reaction mixture a solid. The crude solid was broken apart and washed with cold ethanol and filtered to give 4-fluoro-5-nitro-1,2-di (*p*-toluenesulfonylamino) benzene, **2c**, in 53 % yield.

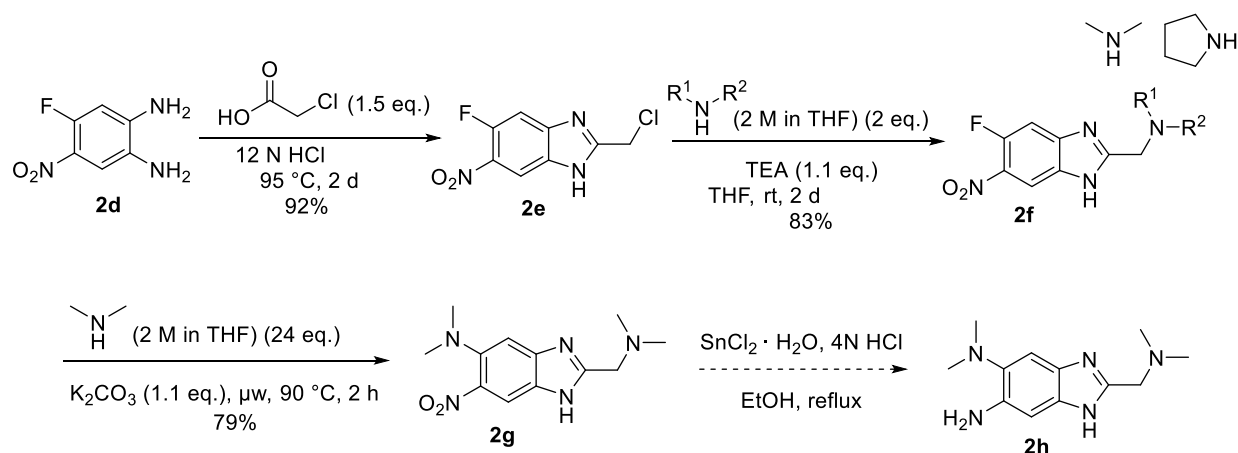
Deprotection was performed in a 10:1 ratio of concentrated sulfuric acid to water. Initially, the reaction mixture was a slurry, which became a solution as the reaction progressed. The reaction was monitored through small-scale basification using saturated aqueous sodium bicarbonate and extraction with ethyl acetate. After small-scale work-up, the crude mixture was monitored on TLC. After consumption of starting material, the reaction mixture was diluted, basified and extracted with DCM. After purification, 1,2-diamino-4-fluoro-5-nitrobenzene, **2d**, was isolated as the product in 94% yield.



Scheme 6: Synthesis of alternative starting material

The next step of the synthesis was to make 2-chloromethyl-5-fluoro-6-nitro-1*H*-benzo[d]imidazole, **2e**. 1,2-Diamino-4-fluoro-5-nitrobenzene, **2d**, was dissolved into 12 N aqueous hydrochloric acid, and chloroacetic acid was added to the solution (**Scheme 7**). Reaction was nearly identical to synthesis of 5-chloro-2-chloromethyl-6-nitro-1*H*-benzo[d]imidazole, **1b** above (**Scheme 2**). The desired product was obtained in 92% yield.

The next step of the synthesis was to perform a nucleophilic substitution to replace the chlorine on the 2-chloromethyl-5-fluoro-6-nitro-1*H*-benzo[d]imidazole, **2e**. The procedure used was similar to that of the synthesis of 6-chloro-2-dimethylaminomethyl-5-nitro-1*H*-benzo[d]imidazole, **1c-2** (**Scheme 6**). After completion of the reaction, the solvent was evaporated, and the reaction mixture was purified by flash column chromatography without a workup. Pyrrolidine was also used a nucleophile following the same procedure.



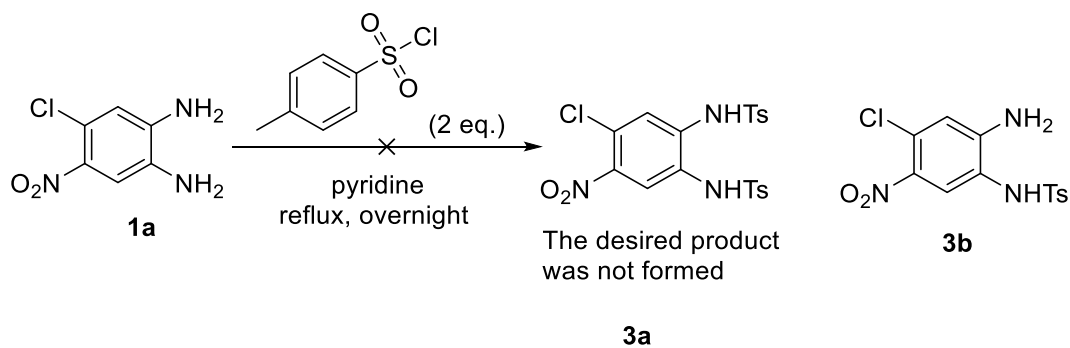
Scheme 7: Synthesis of 5-Dimethylamino-2-dimethylaminomethyl-6-nitro-1H-benzo[d]imidazole

The next reaction was to replace the aromatic fluorine with a dimethyl amino group in a nucleophilic aromatic substitution. The starting material, 5-fluoro-2-dimethylaminomethyl-6-nitro-1H-benzo[d]imidazole, **2f**, was dissolved in a 2 M solution of dimethyl amine in THF, and potassium carbonate was added to the solution (**Scheme 6**). This mixture was heated in a microwave reactor for 2 hours at 300 Watts using a microwave vial. After heating, a new spot appeared on TLC. The reaction mixture was worked up and purified by alumina column. Purification was difficult because the reaction never went to completion and the starting material and desired product had R_f difference of < 0.1 . During column purification, the starting material co-eluted with the product regardless of elution conditions, and yields were only 30-40%. Only once, a good yield of 79% was observed, which could not be reproduced. Different conditions were tested to improve the yield (**Table 2**). Concentrated reaction mixture with more equivalents of dimethylamine was used to push the reaction, but the reaction still did not go to completion with 43% yield. In another trial, addition of more base did not make any difference with a moderate yield of 40%. A different base, like lithium hydroxide, did not have any effect on yield. The low yields and the difficulty in purifying the material made this step the bottleneck of the synthetic route. The synthetic route was reimagined to improve the yield and ease of purification, as described below.

Table 2: Conditions used to optimize the synthesis of 5-Dimethylamino-2-dimethylaminomethyl-6-nitro-1*H*-benzo[d]imidazole

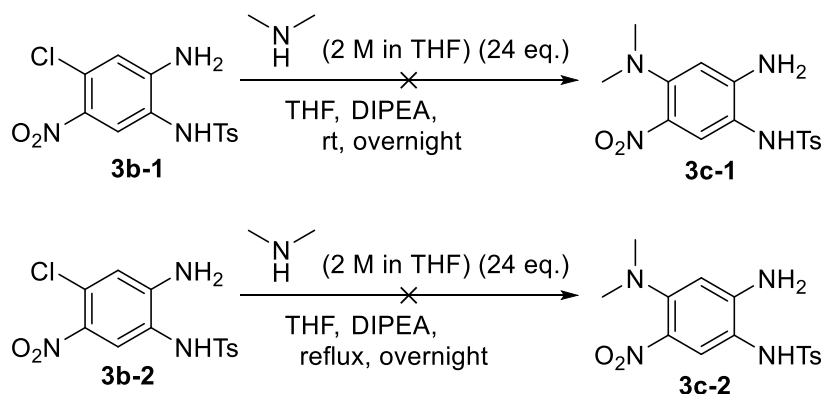
Dimethyl Amine (2 M in THF)	Base equivalents	Base	Time
48 eq.	1.1 eq.	Potassium carbonate	2 hours
24 eq.	2 eq.	Potassium carbonate	2 hours
24 eq.	1.1 + 0.5 eq.	Lithium hydroxide	2 + 2 hours

Since the nucleophilic aromatic substitution could not be optimized and the column purification was difficult, a new scheme was developed to try and circumvent the low yield. Another possible starting material to use for the synthesis was 4-chloro-1,2-diamino-5-nitro benzene, **1a**. The compound would be ditosylated followed by a nucleophilic aromatic substitution to replace the chlorine with the desired secondary amine (**Scheme 8**). The tosylation of 4-chloro-1,2-diamino-5-nitro benzene, **1a**, following previous conditions gave only monotosylated compound, **3b**, with 85 % yield instead of the desired product. The amino group *para* to the nitro group is thought to be more deactivated than the meta substituent, making it less reactive as a nucleophile. The tosyl group was thought to be on the 1-amino group.



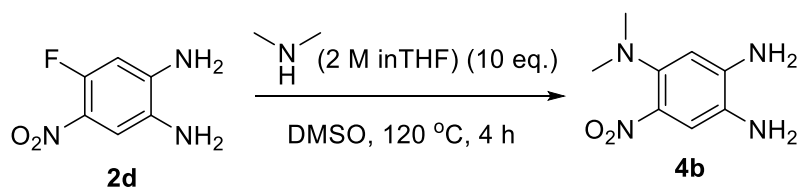
Scheme 8: Synthesis of 1-amino-5-chloro-4-nitro-2-(*p*-toluenesulfonylamino) benzene

Even though only one tosyl group was added, this compound was still used for the nucleophilic aromatic substitution of chlorine by dimethylamine (**Scheme 9**). This reaction was performed at room temperature overnight in THF. Even after refluxing the reaction mixture overnight, no product formation was observed. The nucleophilic attack may not have worked because the starting material was not electron deficient enough. Since no product could be formed, the usage of 4-chloro-1,2-diamino-5-nitro benzene, **1a**, as the starting material was abandoned.



Scheme 9: Synthesis of 1-amino-5-*N,N*-dimethylamino-4-nitro-2-(*p*-toluenesulfonylamino) benzene

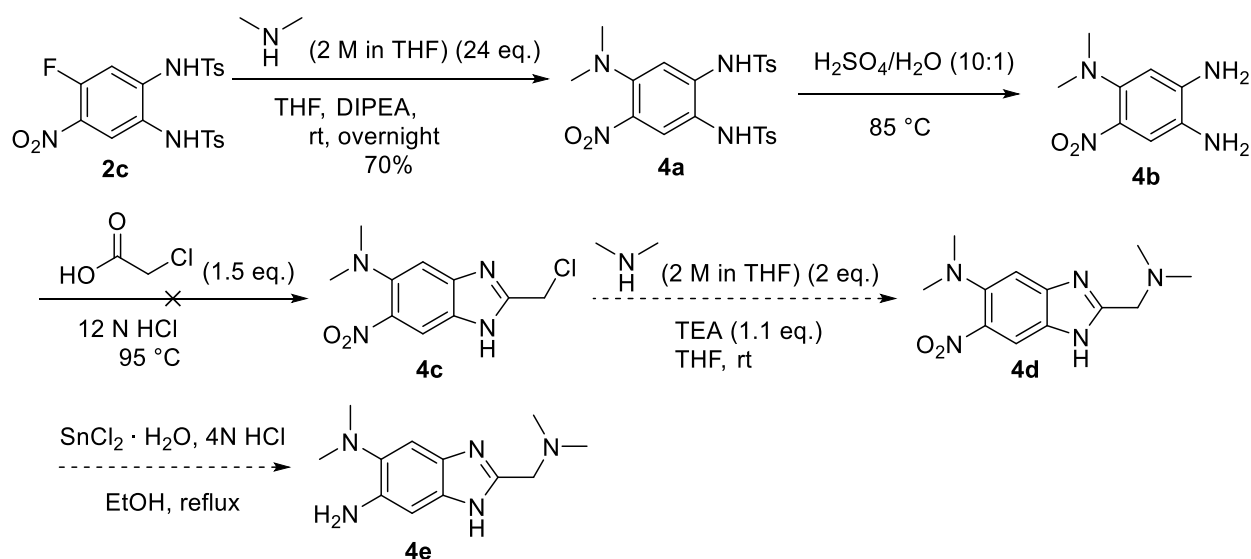
In another attempt, nucleophilic aromatic substitution of the fluorine on 1,2-diamino-4-fluoro-5-nitrobenzene, **2d**, was explored (**Scheme 10**). Starting material was treated with dimethylamine (2 M solution in THF) in dimethylsulfoxide (DMSO) and heated for 4 hours.²⁴ After completion of reaction, the purification of the reaction mixture was unsuccessful due to the close *R_f* of starting material and product. ¹H NMR of the crude sample confirmed that the product, **4b**, was made, but the sample was not pure enough for a melting point or for full characterization. This route of synthesis was also abandoned.



Scheme 10: Synthesis of 1,2-diamino-4-*N,N*-dimethylamino-5-nitro benzene

A new scheme involved performing a nucleophilic aromatic substitution on 4-fluoro-5-nitro-1,2-di (*p*-toluenesulfonylamino) benzene, **2c**, followed by deprotection and cyclization (**Scheme 11**). The first step of the nucleophilic aromatic substitution with dimethylamine gave the desired product, **4a**, in 70% yield, and the reaction was performed at room temperature. The tosyl groups deactivated the amine groups enough to make nucleophilic aromatic substitutions occur readily. The reaction was left overnight to ensure all of the starting material was consumed. A large excess of dimethylamine was used to push the reaction to completion. This large excess was not needed, and was reduced in later attempts.

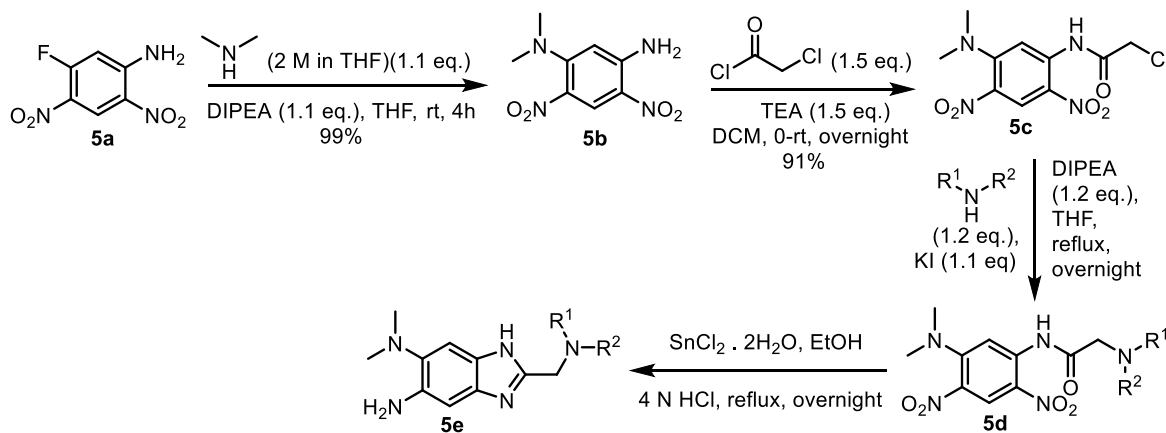
The next reaction in the series was to deprotect the amines (**Scheme 11**), which was performed in an aqueous solution of sulfuric acid and heated to 80 °C for an hour. After the consumption of the starting material, a small aliquot of the crude reaction mixture was removed and a small-scale basification and work-up was performed, and the mixture was analyzed by FIA, which confirmed the formation of product, **4b**. The reaction mixture was worked-up and purified by flash column on alumina. The product was cyclized using chloroacetic acid. The reaction was run for a day in 12 N HCl and heated to 95 °C. Small-scale extraction followed by FIA showed no peaks corresponding to either the starting material or the desired product, **4c**. TLC of the crude reaction mixture showed a complex mixture with no obvious major product. The reaction was repeated twice more to ensure nothing was performed incorrectly in prior steps, but each reaction lead to the same result, a complex mixture on TLC and no peaks on FIA corresponding to the desired product. The starting material, 1,2-diamino-4-*N,N*-dimethylamino-5-nitrobenzene, **4b**, is unstable at room temperature. TLC of the compound the day after purification revealed several new spots. After discovery of the degradation, the material was used immediately after purification and drying to reduce loss of the material.



Scheme 11: Alternative synthesis of 5-Dimethylamino-2-dimethylaminomethyl-6-nitro-1H-benzo[d]imidazole

A working method for developing the 2-(dialkylaminomethyl)benzimidazoles was finally developed using a scheme similar to synthesis of previous benzimidazoles (**Scheme 12**). Dimethylamine, dissolved in tetrahydrofuran, was used in a nucleophilic aromatic substitution

with commercially available 2,4-dinitro-5-fluoroaniline, **5a**, in the presence of diisopropylethylamine at room temperature. This afforded 5-*N,N*-dimethylamino-2,4-dinitro aniline, **5b**, as a yellow solid in 90% yield. In the following step, 5-*N,N*-dimethylamino-2,4-dinitro aniline, **5b**, was reacted with chloroacetyl chloride in dichloromethane in the presence of triethylamine. Initial addition of chloroacetyl chloride was performed at 0 °C, and the reaction mixture was allowed to warm to room temperature. The reaction mixture was left to stir at room temperature overnight. This reaction afforded 1-dchloromethylcarboxamido-5-*N,N*-dimethylamino-2,4-dinitro benzene, **5c**, as a yellow solid in 91% yield. 1-Chloromethylcarboxamido-5-*N,N*-dimethylamino-2,4-dinitro benzene, **5c**, was used in the following step in S_N2 reactions with various different dialkylamines. The starting materials, 1-dchloromethylcarboxamido-5-*N,N*-dimethylamino-2,4-dinitro benzene (**5c**), dialkylamine nucleophile, potassium iodide, and TEA were dissolved in THF and heated to reflux overnight. The amines used were dimethylamine (**5d-1**), dipropylamine (**5d-2**), morpholine (**5d-3**), *N*-methyl piperazine (**5d-4**), piperidine (**5d-5**), pyrrolidine (**5d-6**), and *N*-methyl aniline (**5d-7**). The reactions afforded the desired compounds and yields ranging from 71% to 93%. In the following step, each of compounds was reduced and cyclized using tin chloride dihydrate dissolved in ethanol and 4 N hydrochloric acid. These reactions afforded final intermediates, **5e-1 – 5e-7**, with yields ranging from 62% to 91%.



Amine	Yield
1. Dimethylamine	62%
2. Dipropylamine	78%
3. Morpholine	69%
4. <i>N</i> -methyl piperazine	45%
5. Piperidine	91%
6. Pyrrolidine	77%
7. <i>N</i> -methyl aniline	72%

Amine	Yield
1. Dimethylamine	83%
2. Dipropylamine	71%
3. Morpholine	78%
4. <i>N</i> -methyl piperazine	74%
5. Piperidine	93%
6. Pyrrolidine	79%
7. <i>N</i> -methyl aniline	88%

of active compounds. The 2-piperidin-1-ylmethyl compounds had 10 hits. The 2-pyrrolidin-1-ylmethyl compounds had 5 hits, and the 2-morpholin-1-ylmethyl compounds had 4 hits.

From the preliminary results, large aliphatic groups with at least four carbons attached to the nitrogen were required for activity, since none of the dimethylamino compounds were active. Five and six membered rings were well tolerated since there were numerous hit compounds with pyrrolidine, piperidine and morpholine, though heteroatoms at the 4-position of the ring may be detrimental to activity, since there were fewer hits with morpholine, and no hits with *N*-methyl piperazine. The activity of the aromatic *N*-methyl aniline compounds were surprising, since it deviated so much from the established cyclohexyl group in the lead compounds.

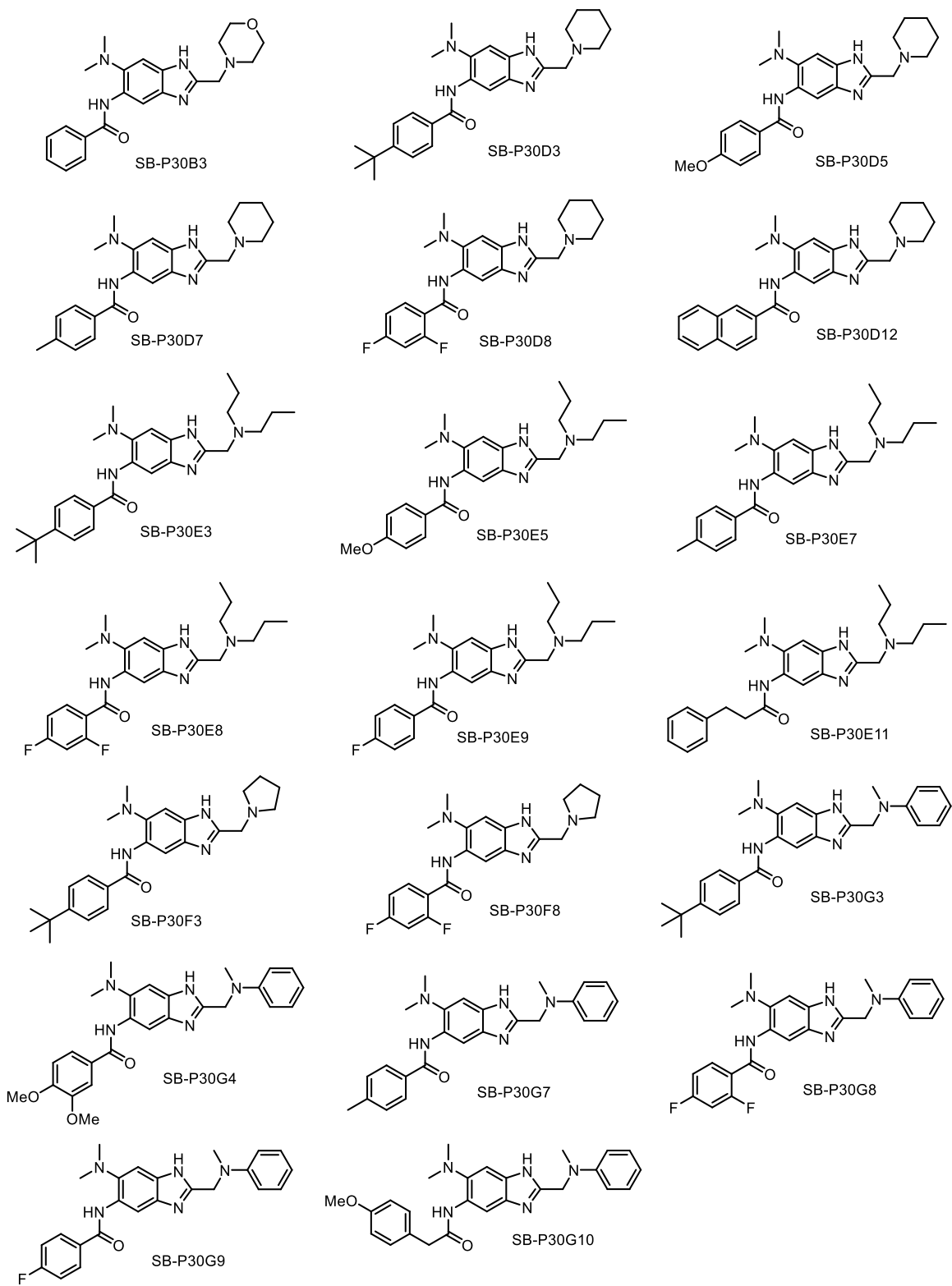


Figure 16a Hit compounds from library synthesis (Plate 30)

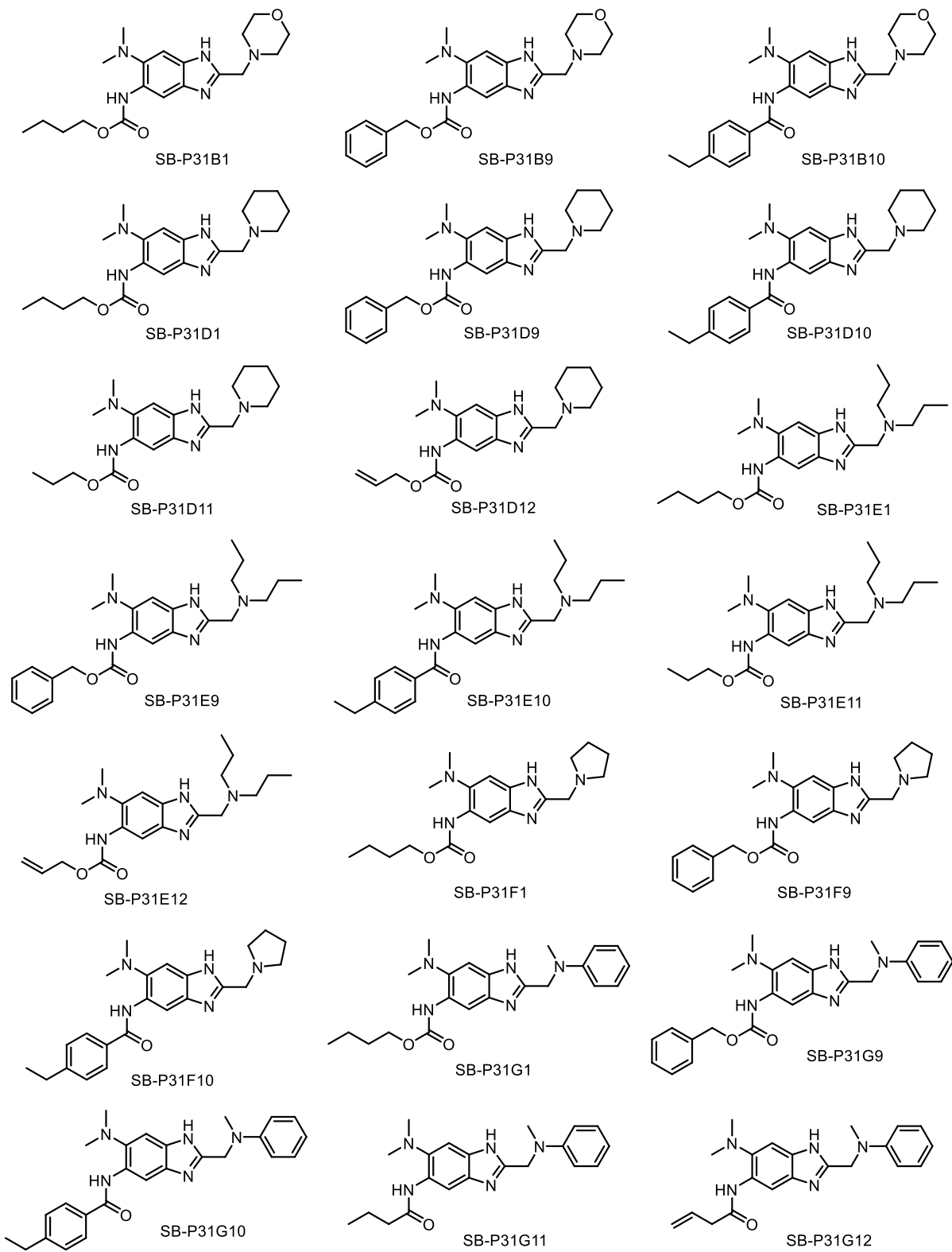


Figure 16b Hit compounds from library synthesis (Plate 31)

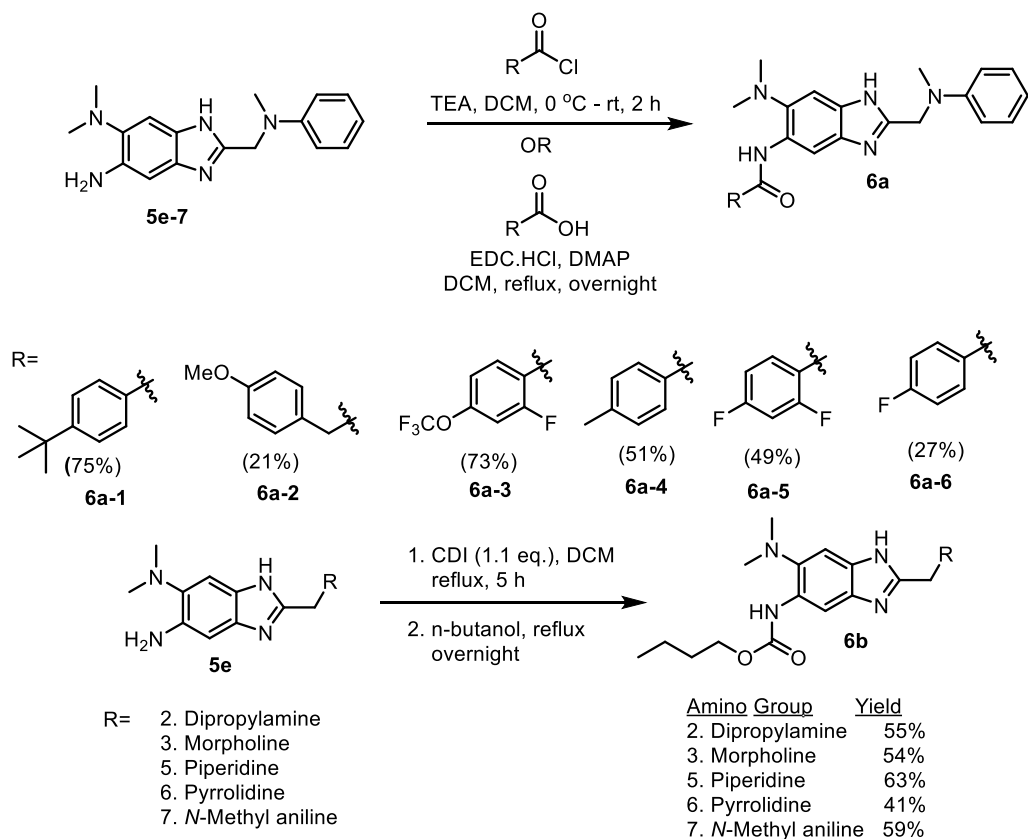
Since the active compounds obtained from the library synthesis were preliminary hits, they needed to be resynthesized for accurate MIC determination. The same procedures were followed in the scheme above to resynthesize the final intermediates. Only the 2-piperidin-1-ylmethyl, 2-dipropylaminomethyl, 2-pyrrolidin-1-ylmethyl, 2-morpholin-1-ylmethyl, and 2-*N*-methylanilinylmethyl compounds were synthesized, since there were not hits with the other two functional groups. The first series of compounds to be resynthesized was the 2-(*N*-methylanilinylmethyl)benzimidazoles. The final intermediate, 5-amino-6-*N,N*-dimethylamino-2-(*N*-methyl-*N*-phenylamino)methyl-1*H*-benzo[d]imidazole, was acylated using various acyl chlorides, in the presence of triethyl amine (TEA), to afford six different 5-amido-6-*N,N*-dimethylamino-2-(*N*-methyl-*N*-phenylamino)methyl-1*H*-benzo[d]imidazoles, **6a-1** – **6a-6**, in yields ranging from 21% – 75% (**Scheme 14**).

After synthesis of the six compounds, there was a realization that synthesis of all 41 hit compounds would be extremely time consuming, and the information gained from it may not have been fruitful. Since the purpose of this project was to optimize the 2-position of the trisubstituted benzimidazoles, synthesis of the butyl carbamates of each 2-(dialkylaminomethyl)benzimidazole would be sufficient for comparing activities. The butyl carbamate was the optimized 5-position functional group for *in-vitro* studies, and SB-P17G-C2, the most active compound *in-vitro*, was used as the gold standard for comparing variations in the 2-position. This method would save time as fewer compounds would need to be resynthesized for comparisons.

Butyl carbamate hit compounds containing 2-piperidin-1-ylmethyl (**5e-5**), 2-dipropylaminomethyl (**5e-2**), 2-pyrrolidin-1-ylmethyl (**5e-6**), 2-morpholin-1-ylmethyl (**5e-3**), and 2-*N*-methylanilinylmethyl (**5e-7**) groups at the 2-position were resynthesized using the exact same procedure (**Scheme 14**). Carbonyldiimidazole and the benzimidazole final intermediate, in the presence of dichloromethane, were heated under reflux for 5 hours. This afforded an isocyanate, which was further reacted, with the addition of *n*-butanol, under reflux overnight. This one-pot, two-step reaction afforded a carbamate functional group at the 5-position, **6b-2** – **6b-7**, in yields ranging from 41-63%.

After resynthesis of hit compounds, they were sent to Colorado State University for accurate MIC determination. Preliminary and accurate MIC determinations both used the alamarBlue assay on H37Rv *M. tuberculosis* strain. The library of compounds was synthesized in high throughput manner and the purity of each compound was unknown. The purpose of

resynthesis of the compounds was to ensure a higher level of purity, at least 95%, so the MIC can be accurately determined without possible impurities skewing the results.

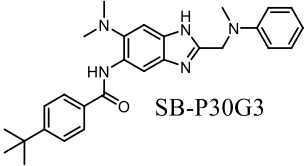
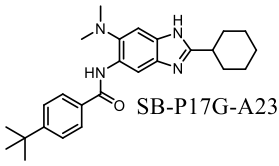
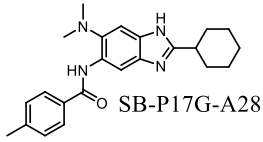
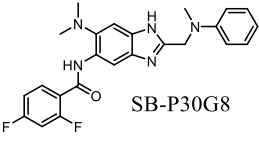
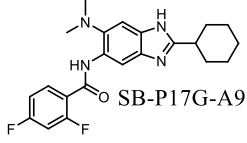
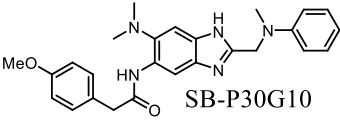
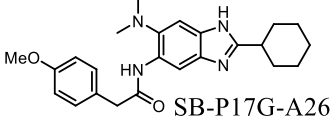
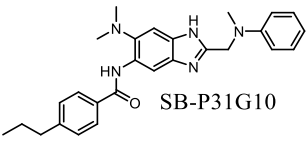
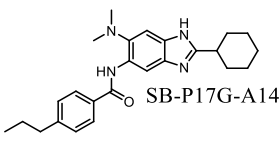
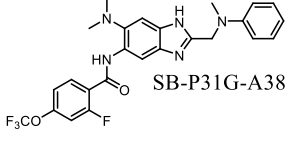
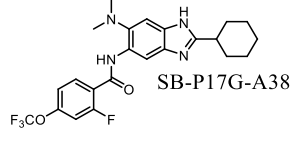
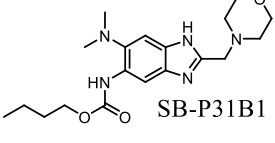
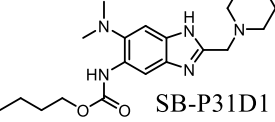


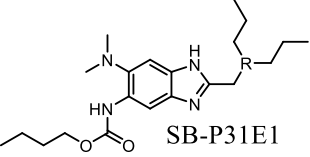
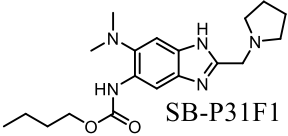
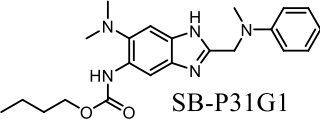
Scheme 14 Resynthesis of dialkylaminomethyl benzimidazoles

The addition of *N*-methylanilinylmethyl group to the 2-position was detrimental to activity compared to a cyclohexyl group, as none of the aniline compounds had MICs close to the compounds containing cyclohexyl groups at the 2-position (**Table 3**). The most active amide compounds were SB-P30G7 and SB-P30G8, which both had MIC values of 1.25 $\mu\text{g}/\text{mL}$, but the cyclohexyl analogues, SB-P17G-A28 and SB-P17G-A9, both had MIC value of 0.31 $\mu\text{g}/\text{mL}$. The cyclohexyl group is far more conducive to compound activity than the *N*-methylanilinylmethyl functionality. When comparing the carbamates, the only functional group with MIC close to the cyclohexyl compound, SB-P17G-C2, was the piperidin-1-ylmethyl compound, SB-P31D1. Even slight deviations from the piperidine made drastic changes in activity. The addition of an oxygen to the ring in the morpholin-1-ylmethyl compound, SB-P31B1, changed the MIC from 0.09 $\mu\text{g}/\text{mL}$ to 1.6 $\mu\text{g}/\text{mL}$. Removal of one carbon from piperidin-1-ylmethyl to pyrrolidin-1-ylmethyl

also caused an increase in MIC from 0.09 $\mu\text{g}/\text{mL}$ to 1.6 $\mu\text{g}/\text{mL}$. Overall, none of the 2-(dialkylaminomethyl)benzimidazoles were as active as the 2-cyclohexylbenzimidazoles.

Table 3 MIC of 2-(dialkylaminomethyl)benzimidazoles compared to 2-cyclohexylbenzimidazoles

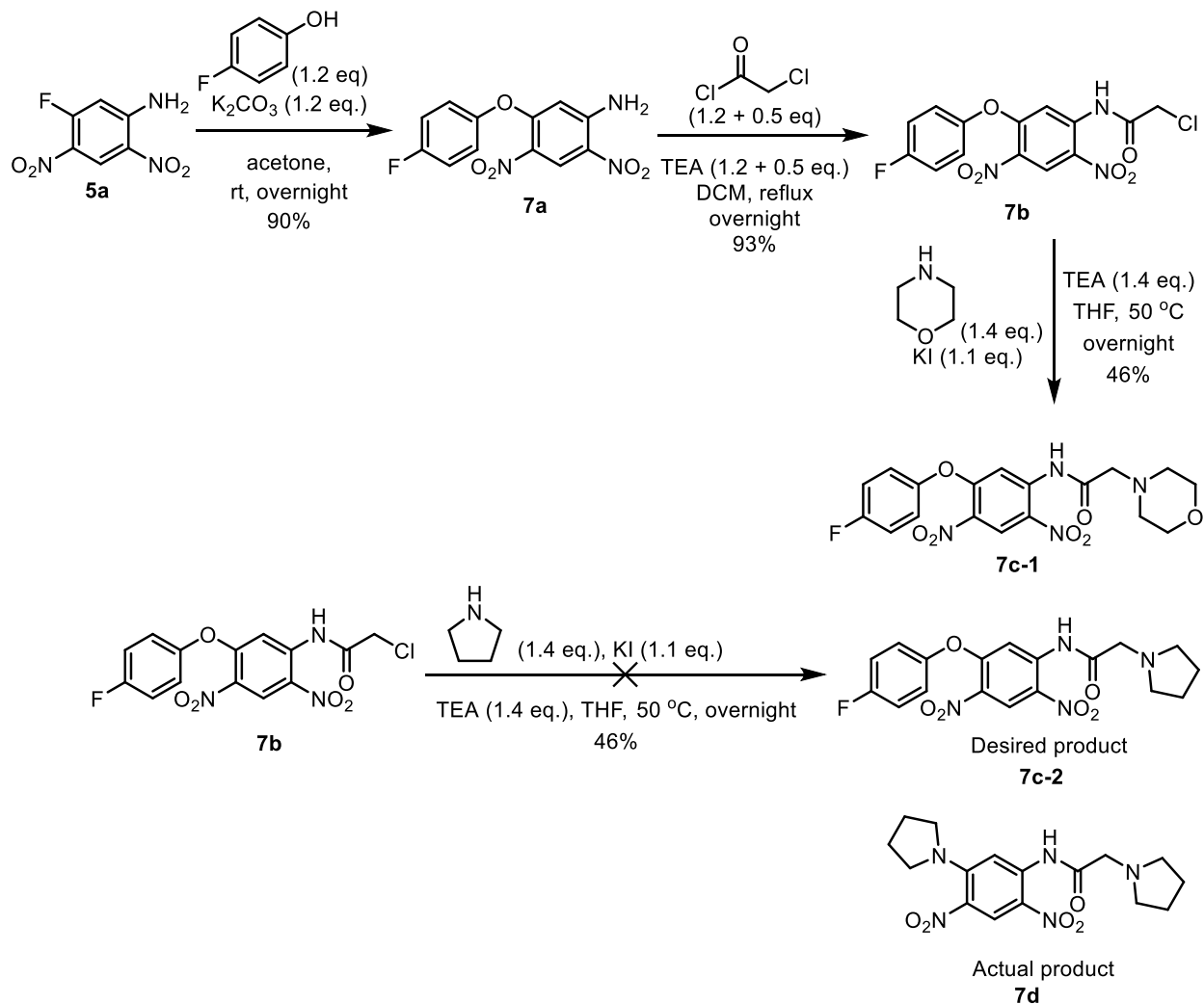
Compound	MIC <i>Mtb</i> H37Rv ($\mu\text{g}/\text{mL}$)	MIC <i>Mtb</i> H37Rv ($\mu\text{g}/\text{mL}$)	Compound
 SB-P30G3	2.5	0.63	 SB-P17G-A23
 SB-P30G7	1.25	0.31	 SB-P17G-A28
 SB-P30G8	1.25	0.31	 SB-P17G-A9
 SB-P30G10	>10	>10	 SB-P17G-A26
 SB-P31G10	5	0.63	 SB-P17G-A14
 SB-P31G-A38	0.19	0.019	 SB-P17G-A38
 SB-P31B1	1.6	0.06	 SB-P17G-C2
 SB-P31D1	0.09		

 SB-P31E1	0.16
 SB-P31F1	1.6
 SB-P31G1	0.16

A new series of 2-dialkylanimomethylbenzimidazoles was attempted with the 4-fluorophenoxy group at the 6-position (**Scheme 15**). Previously synthesized 2-cyclohexyl benzimidazoles with the 4-fluorophenoxy group at the 6-position showed good antitubercular activity, and the exploration of the 2-position was extended to this class of benzimidazoles. 4-Fluorophenol was used in a nucleophilic aromatic substitution with commercially available 2,4-dinitro-5-fluoroaniline, **5a**, in the presence of potassium carbonate at room temperature. This afforded 5-(4-fluorophenoxy)-2,4-dinitro aniline, **7a**, as a yellow solid in 90% yield. In the following step, 5-(4-fluorophenoxy)-2,4-dinitro aniline, **7a**, was reacted with chloroacetyl chloride in dichloromethane in the presence of triethylamine. Initial addition of chloroacetyl chloride was performed at 0 °C, and the reaction mixture was refluxed after addition of chloroacetyl chloride. This reaction afforded 1-chloromethylcarboxamido-5-(4-fluorophenoxy)-2,4-dinitro benzene, **7b**, as a light yellow solid in 93% yield.

1-Chloromethylcarboxamido-5-(4-fluorophenoxy)-2,4-dinitro benzene, **7b**, was used in the following step in an S_N2 reaction with morpholine in the presence of triethylamine at 50 °C. The reaction afforded 1-morpholinomethylcarboxamido-5-(4-fluorophenoxy)-2,4-dinitro benzene, **7c-1**, as a yellow solid in 55% yield. The S_N2 reaction was also performed with pyrrolidine and dimethylamine as the nucleophiles, following the morpholine procedure, but disubstitution occurred in both cases. Both the chloride and 4-fluorophenoxy groups were disubstituted with pyrrolidinyl, **7d**, and *N,N*-dimethylamino groups. Performing the substitution reactions at room temperature still resulted in the formation of disubstituted products. It is surprising to see the 4-fluorophenoxy group be such a good leaving group. The added electron

withdrawing capacity of the fluorine may stabilize the resulting phenoxy anion, making it a good leaving group. In order to move forward in this synthetic scheme, the disubstitution issue needs to be addressed in the future.



Scheme 15 Synthesis of 6-(4-fluorophenoxy)-dialkylaminomethyl benzimidazoles

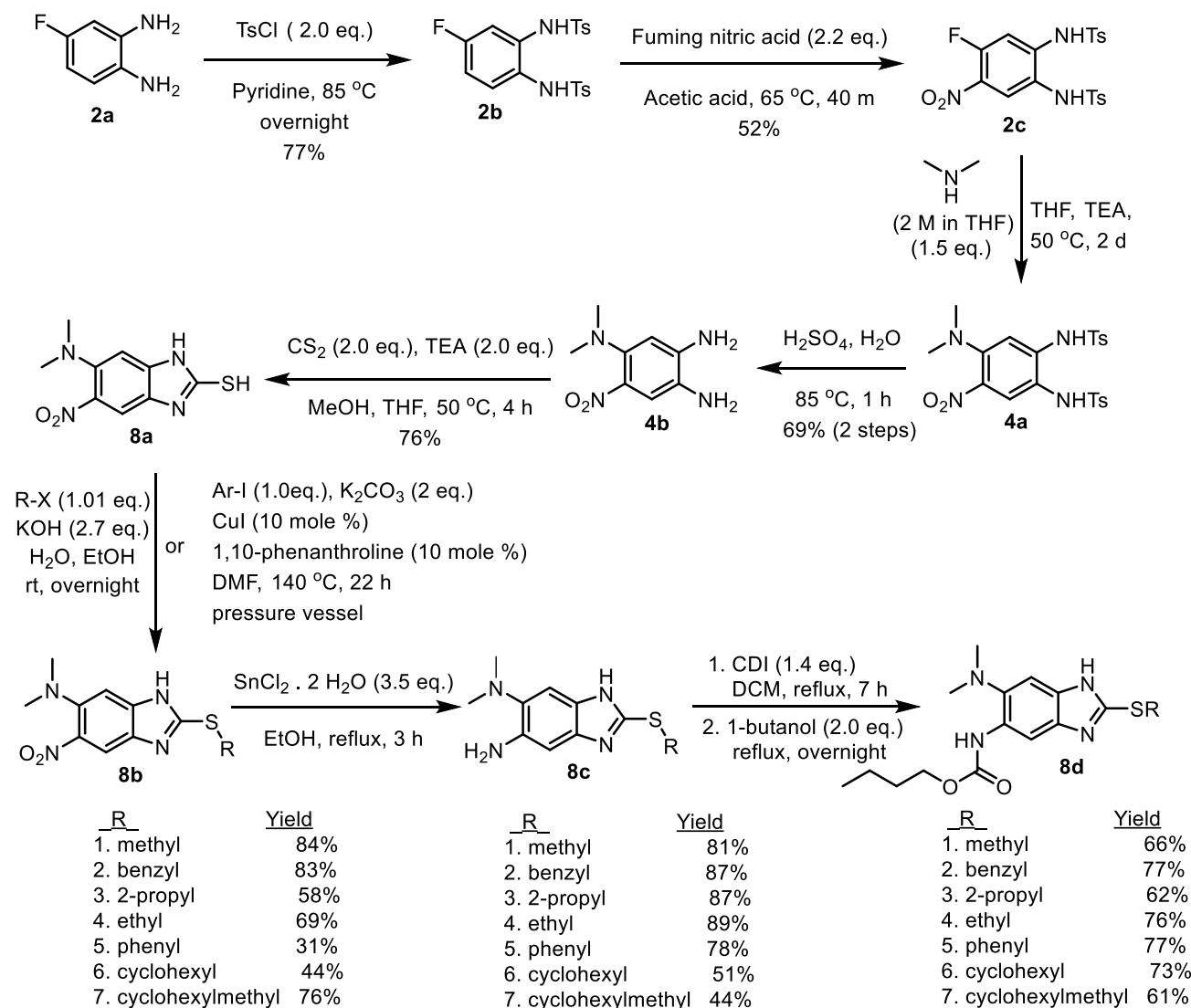
1.2.2 Synthesis of 2-alkylthiobenzimidazoles

After successful synthesis of the 2-(dialkylaminomethyl)benzimidazoles, the next goal was to synthesize the 2-alkylthiobenzimidazoles. The scheme was developed using a previously synthesized material, 1,2-diamino-4-*N,N*-dimethylamino-5-nitro benzene, **4b**. This compound was unstable at room temperature and gave a complex mixture when cyclized under acidic conditions, but when this compound was first synthesized for the 2-

(dialkylaminomethyl)benzimidazoles, a small batch of 1,2-diamino-4-*N,N*-dimethylamino-5-nitro benzene, **4b**, was reacted with carbon disulfide in the presence of TEA in THF. Surprisingly, the desired 2-thiobenzimidazole, **8a**, was obtained. With the success of the cyclization, additional steps were added to complete the scheme to obtain a series of 2-alkylthiobenzimidazoles butyl carbamates for MIC determination (**Scheme 16**).

p-Toluenesulfonyl chloride was used in the protection of commercially available 1,2-diamino-4-fluoro benzene, **2a**, in the presence of pyridine, at 85 °C overnight. This afforded 4-fluoro-1,2-di (*p*-toluenesulfonylamino) benzene, **2b**, as a light brown solid in 85% yield.²³ In the following step, 4-fluoro-1,2-di (*p*-toluenesulfonylamino) benzene, **2b**, was nitrated, in the presence of fuming nitric acid, at 65 °C in 40 minutes to afford 4-fluoro-5-nitro-1,2-di (*p*-toluenesulfonylamino) benzene, **2c**, as a white solid in 65% yield.²³ 4-fluoro-5-nitro-1,2-di (*p*-toluenesulfonylamino) benzene, **2c**, was reacted with dimethylamine, dissolved in THF, in a nucleophilic aromatic substitution to afford 4-*N,N*-dimethylamino-5-nitro-1,2-di (*p*-toluenesulfonylamino) benzene, **4a**, which was used in the following step crude. Deprotection of dimethylamino-5-nitro-1,2-di (*p*-toluenesulfonylamino) benzene, **4a**, was performed in the presence of sulfuric acid and water at 85 °C in 1.5 hours.²³ This afforded 1,2-diamino-4-*N,N*-dimethylamino-5-nitro benzene, **4b**, as a dark red solid in 69% yield over two steps. Since 1,2-diamino-4-*N,N*-dimethylamino-5-nitro benzene, **4b**, was unstable at room temperature, it was purified and immediately used in the following step to avoid degradation. 1,2-Diamino-4-*N,N*-dimethylamino-5-nitro benzene, **4b**, was reacted with carbon disulfide in the presence of TEA at 50 °C in 4 hours to afford 6-*N,N*-dimethylamino-5-nitro -2-thio-1*H*-benzo[d]imidazole, **8a**, as a red solid in 76% yield.²⁵⁻²⁷ In the following step, 6-*N,N*-dimethylamino-5-nitro -2-thio-1*H*-benzo[d]imidazole, **8a**, was alkylated using methyl iodide (**8b-1**), benzyl bromide (**8b-2**), isopropyl iodide (**8b-3**), ethyl iodide (**8b-4**), cyclohexyl bromide (**8b-6**), or cyclohexylmethyl bromide (**8b-7**) in the presence of potassium hydroxide, to give the desired compounds in yields ranging from 44% to 84%.^{25,26} 6-*N,N*-dimethylamino-5-nitro -2-thio-1*H*-benzo[d]imidazole, **8a**, was reacted with iodobenzene in the presence of cuprous iodide and 1,10-phenanthroline at 140 °C in a pressure vessel for 22 h. This reaction afforded 6-*N,N*-dimethylamino-5-nitro-2-(phenylthio)-1*H*-benzo[d]imidazole, **8b-5**, as a red solid in 31% yield.²⁸ The six alkylated/ arylated 2-thiobenzimidazoles were reduced, in the presence of tin (II) chloride hydrate, to afford the desired products, **8c-1 – 8c-7**, in yields ranging from 44% to 89%. The final intermediates, were reacted with carbonyldiimidazole, forming isocyanates. *n*-Butanol was then added to the same reaction mixture to make the final compounds, **8d-1 – 8d-7**, with

carbamate functionalities at the 5-position, in yields ranging from 61% to 77% in a one-pot, two-step reaction.

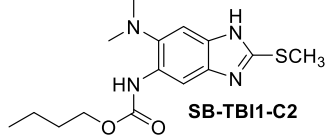
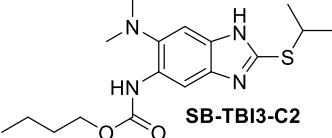
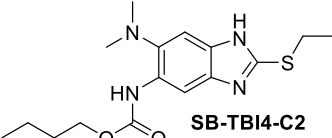
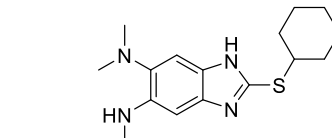
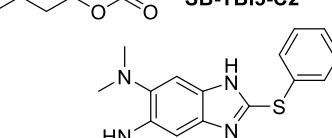


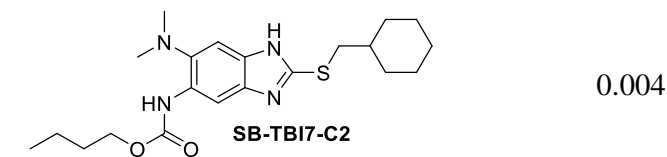
Scheme 16 Synthesis of 2-alkylthio benzimidazoles

Final compounds were purified and sent to collaborators at Colorado State University and Rutgers University for accurate MIC determination (**Table 4**). MIC values were determined by serial dilution of compound solutions in 96-well plates. AlamarBlue agent was added after 6 days of incubation to determine cell viability. The compound with the lowest activity of the 2-alkylthiobenzimidazoles was SB-TBI2-C2, with an MIC value of 6.25 $\mu\text{g}/\text{mL}$. Similar to the *N,N*-dimethylamino-2-*N,N*-dimethylaminomethyl-1*H*-benzo[d]imidazoles, which had no hits from the library screen, small alkyl groups at the 2-position is detrimental to activity. Even with the addition of an extra carbon on SB-TBI4-C2 changes the activity by nearly an order of magnitude, 0.78 $\mu\text{g}/\text{mL}$,

and changing the alkyl group from an ethyl group to an isopropyl group further improves activity, 0.31 $\mu\text{g}/\text{mL}$. The two compounds with aromatic rings on the thiol, SB-TBI2-C2 and SB-TBI6-C2, showed moderate activity, with both compounds having MIC values of 0.31 $\mu\text{g}/\text{mL}$. The two most active compounds were SB-TBI5-C2, with an MIC of <0.02 $\mu\text{g}/\text{mL}$, and SB-TBI7-C2, with an MIC of 0.004 $\mu\text{g}/\text{mL}$. The most active cyclohexyl compound, SB-P17G-C2, has an MIC of 0.008 $\mu\text{g}/\text{mL}$. SB-TBI7-C2 is more active by a factor of 2. Overall, some form of a cyclohexyl ring is needed for favorable activity in the trisubstituted benzimidazoles, since the most active compounds from both the 2-(dialkylaminomethyl)benzimidazoles and 2-alkylthiobenzimidazoles contain saturated six-membered rings.

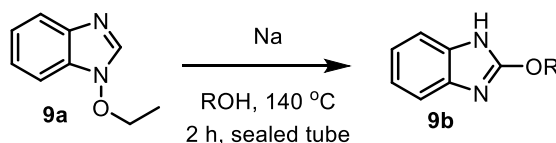
Table 4 MIC of 2-thiobenzimidazoles

Compound	MIC <i>Mtb</i> H37Rv ($\mu\text{g}/\text{mL}$)
 SB-P17G-C2	0.008
 SB-TBI1-C2	6.25
 SB-TBI2-C2	0.31
 SB-TBI3-C2	0.31
 SB-TBI4-C2	0.78
 SB-TBI5-C2	<0.02
 SB-TBI6-C2	0.31



1.2.3 Synthesis of 2-alkoxybenzimidazoles

After successful synthesis of 2-alkylthiobenzimidazoles, the next series of benzimidazoles to be synthesized was the 2-alkoxybenzimidazoles, **9b**. The scheme was designed based on the conversion of a 1-alkoxybenzimidazole, **9a**, to a 2-alkoxybenzimidazole, **9b**, in the presence of alcohol and sodium metal (**Scheme 17**).²⁹ Combining sodium metal with the alcohol would create alkoxide, which would perform a nucleophilic attack at the 2-position and release the alcohol at the 1-position as the leaving group. This reaction takes place most likely through the use of a sealed tube and heating to 140 °C, pushing the reaction was to take place.²⁹ In order to synthesize the desired 1-alkoxybenzimidazole, the benzimidazole N-oxide needed to be made (**Scheme 18**).³⁰

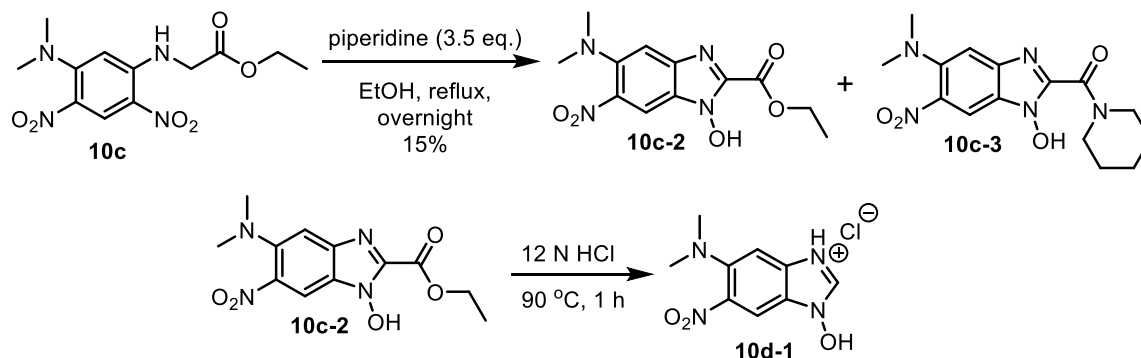


Scheme 17 Conversion of 1-alkoxybenzimidazoles to 2-alkoxybenzimidazoles

Commercially available 1,5-difluoro-2,4-dinitrobenzene, **10a**, was reacted with dimethylamine, dropwise, in the presence of diisopropylethylamine to afford 5-fluoro-*N,N*-dimethylamino-2,4-dinitrobenzene, **10b**, in 90% yield. In the following step, 5-fluoro-*N,N*-dimethylamino-2,4-dinitrobenzene, **10b**, was reacted with glycine ethyl ester hydrochloride in the presence of sodium bicarbonate, in a nucleophilic aromatic substitution, affording *N*-(5-*N,N*-dimethylamino-2,4-dinitro)-glycine ethyl ester, **10c**, in 97% yield as a yellow solid (**Scheme 19**).

N-(5-*N,N*-dimethylamino-2,4-dinitro)-glycine ethyl ester, **10c**, was initially cyclized in the presence of piperidine to afford 3-hydroxy-6-*N,N*-dimethylamino-5-nitro-1*H*-benzimidazole-2-carboxylic acid ethyl ester, **10c-2**, in 15% yield.³⁰ Another product formed in this step was 3-hydroxy-6-*N,N*-dimethylamino-5-nitro-1*H*-benzimidazole-2-carboxylic acid piperidinyl ester, **10c-3**, which was not surprising since piperidine can also act as a nucleophile. The benzimidazole-2-carboxylic acid ethyl ester was hydrolyzed and decarboxylated in the presence of concentrated hydrochloric acid affording 3-hydroxy-6-*N,N*-dimethylamino-5-nitro-1*H*-benzimidazole

hydrochloride salt, **10d-1**, in quantitative yield as a white solid.³⁰ This route of synthesis worked, but was far from optimized because the cyclization step was low yielding and also produced side product (**Scheme 18**).

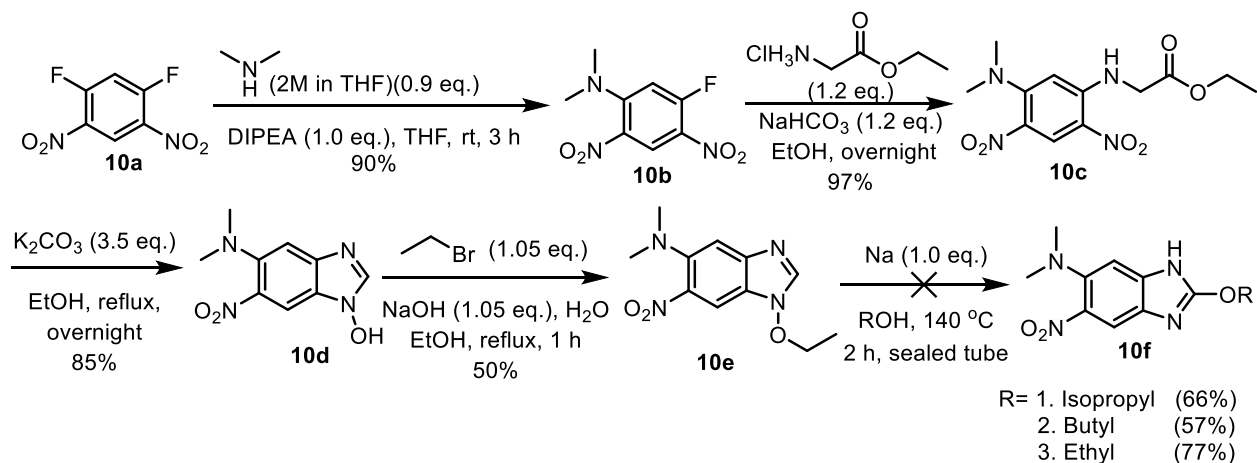


Scheme 18 Synthesis of benzimidazole N-oxide hydrochloride salt

In an alternate route, 3-hydroxy-6-*N,N*-dimethylamino-5-nitro-1*H*-benzimidazole, **10d**, was obtained from cyclization of *N*-(5-*N,N*-dimethylamino-2,4-dinitro)-glycine ethyl ester, **10c**, in the presence of potassium carbonate in 85% yield over two steps. This procedure was discovered serendipitously when a series of bases were tested for optimizing the cyclization step. The bases used were TEA, sodium hydroxide, and potassium carbonate. Usage of TEA resulted in no reaction, and sodium hydroxide gave a complex mixture on TLC. Potassium carbonate was found to perform the cyclization, ester hydrolysis, and decarboxylation all in one pot. The product formed was also the desired N-oxide and not the N-oxide hydrochloride salt, which would have needed to be neutralized before the next synthetic step (**Scheme 19**).

The optimized procedure was *N*-(5-*N,N*-dimethylamino-2,4-dinitro)-glycine ethyl ester, **10c**, dissolved in 190 proof ethanol, refluxed with potassium carbonate (**Scheme 19**). The water content was important. If 200 proof ethanol was used, the ester hydrolysis and decarboxylation did not go to completion, and the reaction mixture contained an amalgam of 3-hydroxy-6-*N,N*-dimethylamino-5-nitro-1*H*-benzimidazole-2-carboxylic acid ethyl ester, **10c-2**, and 3-hydroxy-6-*N,N*-dimethylamino-5-nitro-1*H*-benzimidazole, **10d**. The presence of water was believed to generate hydroxide *in-situ* to push the ester hydrolysis to completion. In the next step, 3-hydroxy-6-*N,N*-dimethylamino-5-nitro-1*H*-benzimidazole, **10d**, was ethylated using ethyl bromide in the presence of sodium hydroxide affording 3-ethoxy-6-*N,N*-dimethylamino-5-nitro-1*H*-benzimidazole, **10e**, in 50% yield (**Scheme 19**). 3-ethoxy-6-*N,N*-dimethylamino-5-nitro-1*H*-benzimidazole, **10e**, was then reacted with ethanol, isopropanol or n-butanol in the presence of

sodium metal. The desired product was 2-alkoxy-6-*N,N*-dimethylamino-5-nitro-1*H*-benzimidazole, **10f**, but the product obtained from the reactions were 1-ethoxy-6-*N,N*-dimethylamino-5-nitro-1*H*-benzimidazole in 77% yield, 1-isopropoxy-6-*N,N*-dimethylamino-5-nitro-1*H*-benzimidazole in 66% yield, and 1-butoxy-6-*N,N*-dimethylamino-5-nitro-1*H*-benzimidazole in 57% yield (**Scheme 19**). This method of synthesis was abandoned.



Scheme 19 Synthesis of 2-alkoxybenzimidazoles

1.2.4 Synthesis of tetrasubstituted benzimidazoles

The human ether-a-go-go related gene (hERG) codes for the α -subunit of the potassium ion channel, which is a channel responsible for controlling the electrical activity of the heart.^{31,32} Inhibition of the potassium channel leads to long QT syndrome, which is potentially lethal.³² The hERG channel is promiscuous to many drug compounds, and many have been taken off the market because of this lethal side effect.^{31,32} Some strategies for reducing hERG activity are increasing the polarity (LogP) of compounds and reducing aromaticity of compounds.³¹ The protein is a homo-tetramer, and within the binding site of the hERG channel, there are four tyrosine-652 and four phenylalanine-656, which are thought to pi-pi stack with aromatic rings in drug compounds (**Figure 17**).^{31,32} The protein also contains lipophilic binding sites, which will interact with hydrophobic molecules, and basic nitrogen functional groups on compounds may also pose a problem with hERG blockage.³¹ The trisubstituted benzimidazoles contain many aromatic rings, are lipophilic molecules, and contain a basic nitrogen in the imidazole ring. These factors pose as another hurdle for the project, as hERG inhibition is a serious concern for newly developed drug compounds. Acylation of the basic nitrogen on the imidazole ring would block the nitrogen from

interacting with the hERG channel, which was the initial strategy for addressing this problem. A series of tetrasubstituted benzimidazoles were synthesized and analyzed *in-vitro* for activities.

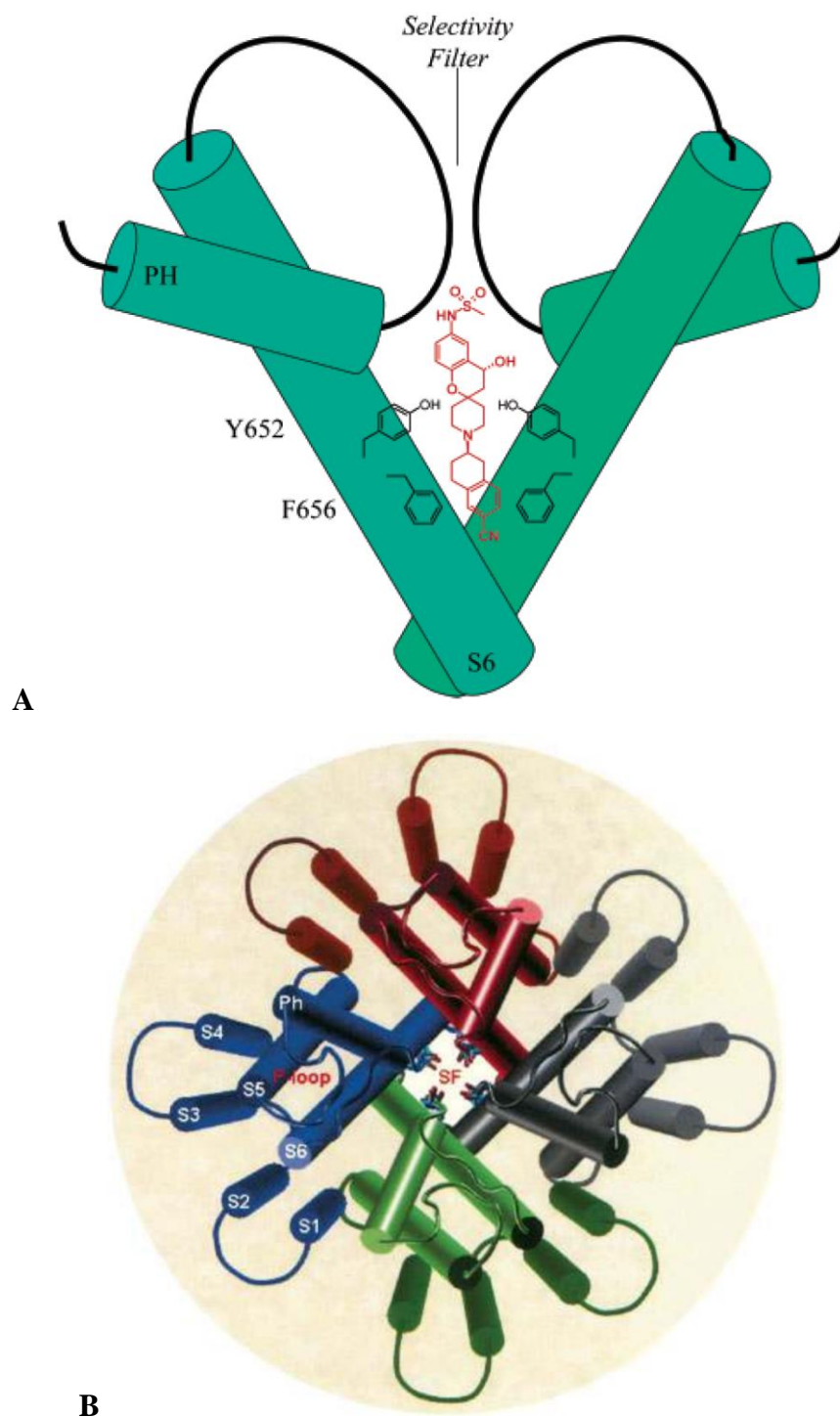
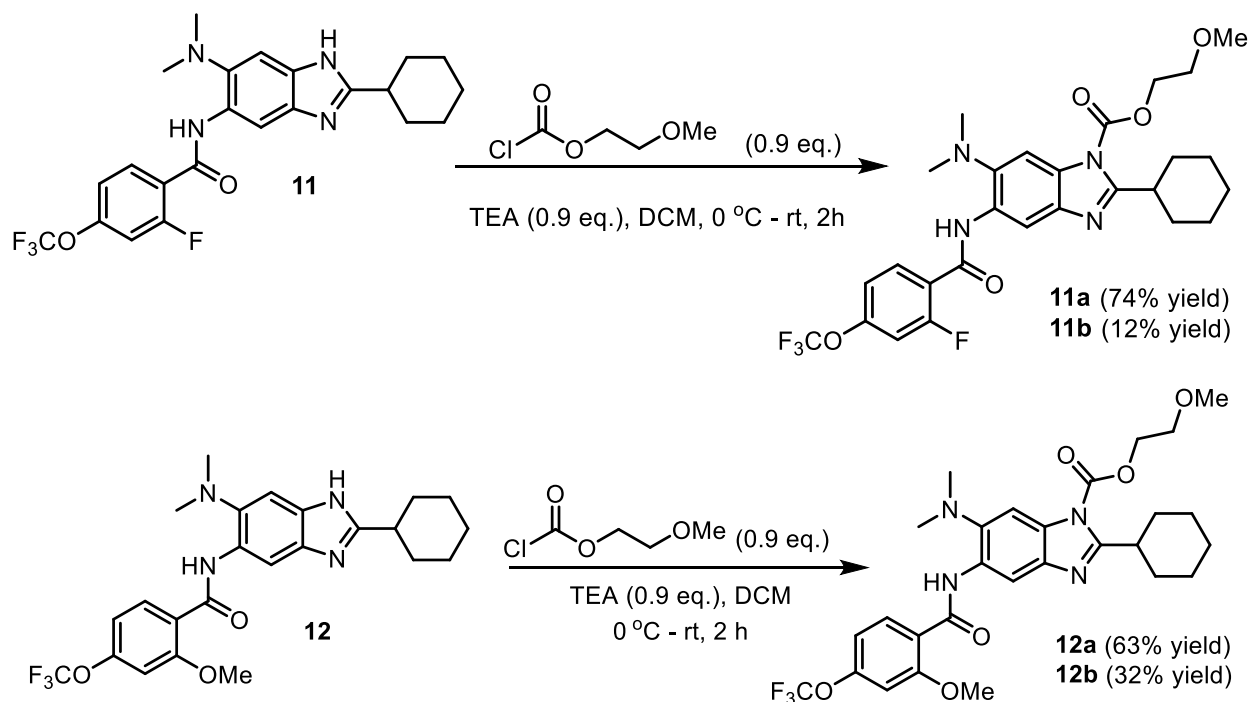


Figure 17 A. Cross-section of hERG channel revealing hERG blocker MK-499 interacting with tyrosine 652 and phenylalanine 656.³¹ B. top view of hERG tetramer channel.³³

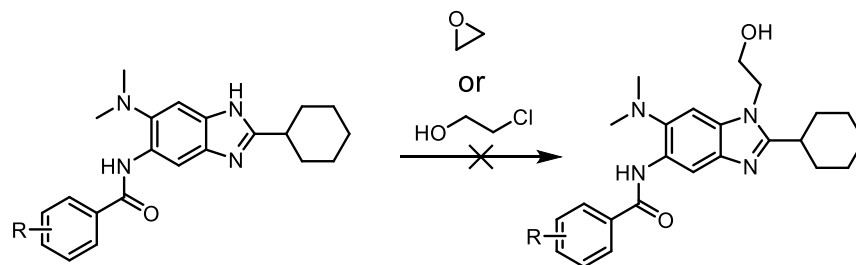
Acylation of the nitrogen on the benzimidazole was thought to improve hERG activity through blocking the basic nitrogen. Tetrasubstituted benzimidazoles were synthesized using two hit compounds, SB-P17G-A38 (**11**), and SB-P17G-A55 (**12**), as starting materials to functionalize the nitrogen on the benzimidazole ring. 2-Cyclohexyl-5-(2-fluoro-4-trifluoromethoxy)benzamido-6-*N,N*-dimethylamino-1*H*-benzo[d]imidazole, **11**, was acylated, in the presence of 2-methoxyethyl chloroformate and triethylamine, to give 2-cyclohexyl-5-(2-fluoro-4-trifluoromethoxy)benzamido-1-(2-methoxyethoxy)carbonyl-6-*N,N*-dimethylamino-1*H*-benzo[d]imidazole, **11a**, and 2-cyclohexyl-5-(2-fluoro-4-trifluoromethoxy)benzamido-3-(2-methoxyethoxy)carbonyl-6-*N,N*-dimethylamino-1*H*-benzo[d]imidazole, **11b**, as regioisomers in 74% yield and 12% yield respectively (**Scheme 20**).

2-Cyclohexyl-5-(2-methoxy-4-trifluoromethoxy)benzamido-6-*N,N*-dimethylamino-1*H*-benzo[d]imidazole, **12**, was acylated, in the presence of 2-methoxyethyl chloroformate and triethylamine, to give 2-cyclohexyl-5-(2-methoxy-4-trifluoromethoxy)benzamido-1-(2-methoxyethoxy)carbonyl-6-*N,N*-dimethylamino-1*H*-benzo[d]imidazole, **12a**, and 2-cyclohexyl-5-(2-methoxy-4-trifluoromethoxy)benzamido-3-(2-methoxyethoxy)carbonyl-6-*N,N*-dimethylamino-1*H*-benzo[d]imidazole, **12b**, as regioisomers in 63% yield and 34% yield respectively (**Scheme 20**).



Scheme 20 Synthesis of Tetrasubstituted 1-Carbamate Benzimidazoles

In addition to acylating the nitrogen, alkylation was also a possibility, since a hydrophilic group, such as a hydroxy or carboxylate group, could be added to make the compounds more polar, as well as block the basic nitrogen. Both changes to the compounds would dampen the hERG activity. Various methods were used to alkylate the nitrogen of the trisubstituted benzimidazoles. Two different nucleophiles, 2-chloroethanol and ethylene oxide, were used. Used in conjunction with different combinations with numerous bases, solvents, and heating conditions, the reactions were still unsuccessful. The resulting reaction mixtures often showed complex mixtures on TLC with no definite major product. Simple alkylation of trisubstituted benzimidazoles turned out to be not so simple at all. Another method was needed to obtain the desired tetrasubstituted benzimidazoles.



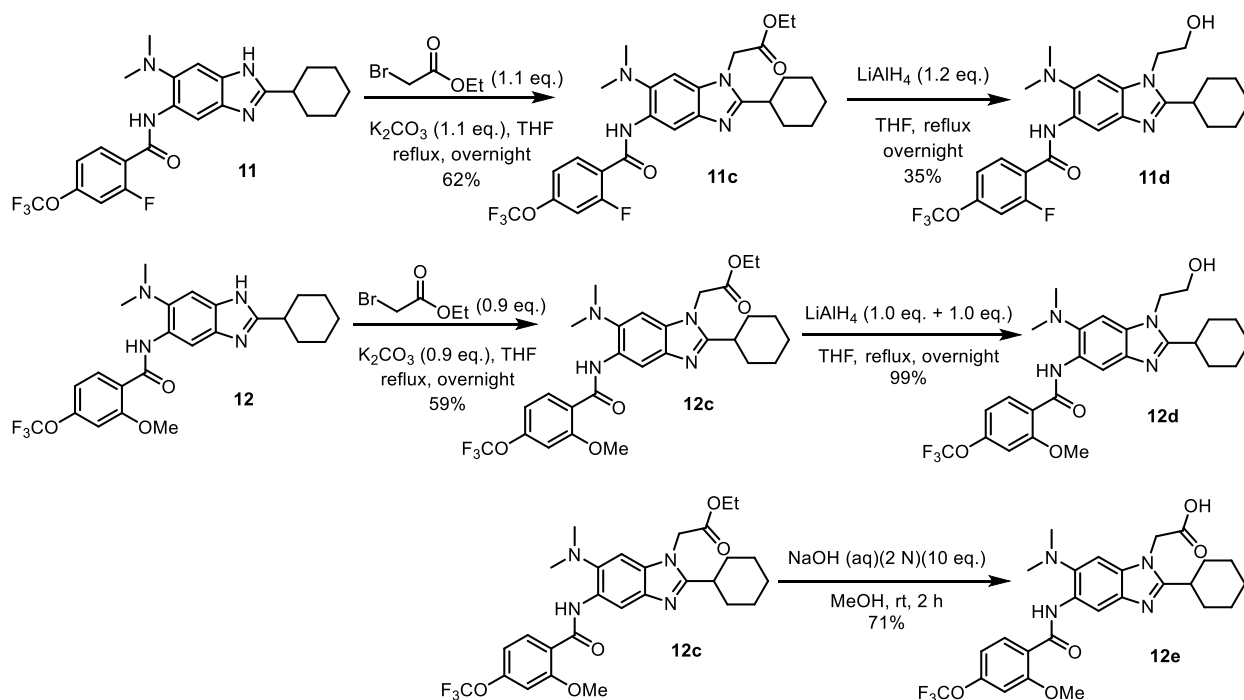
	Solvent	Base	Electrophile	Temperature
1	DMF	Cs ₂ CO ₃	2-Chloroethanol	130 °C
2	DMF	NaH	2-Chloroethanol	100 °C
3	EtOH	<i>t</i> -BuOK	2-Chloroethanol	Reflux
4	THF	TEA	2-Chloroethanol	Reflux
5	THF	LDA	2-Chloroethanol	Reflux
6	THF	K ₂ CO ₃	2-Chloroethanol	Reflux
7	THF	K ₂ CO ₃	Ethylene oxide	Reflux

Scheme 21 Attempts at Alkylating Trisubstituted Benzimidazoles

In order to synthesize tetrasubstituted benzimidazoles with a hydroxy ethyl group at the 1-position, 2-Cyclohexyl-5-(2-fluoro-4-trifluoromethoxy)benzamido-6-*N,N*-dimethylamino-1*H*-benzo[d]imidazole, **11**, was alkylated with ethyl bromoacetate, in the presence of potassium carbonate, to give 2-cyclohexyl-1-ethoxycarbonylmethyl-5-(2-fluoro-4-trifluoromethoxy)benzamido-6-*N,N*-dimethylamino-1*H*-benzo[d]imidazole, **11c**, in 62% yield.

Cyclohexyl-5-(2-methoxy-4-trifluoromethoxy)benzamido-6-*N,N*-dimethylamino-1*H*-benzo[d]imidazole, **12**, was also alkylated with ethyl bromoacetate, in the presence of potassium carbonate, to give 2-cyclohexyl-1-ethoxycarbonylmethyl-5-(2-methoxy-4-trifluoromethoxy)benzamido-6-*N,N*-dimethylamino-1*H*-benzo[d]imidazole, **12c**, in 59% yield.

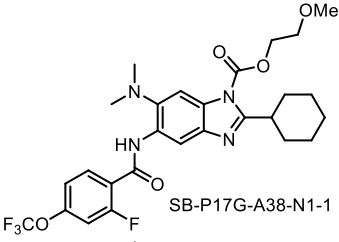
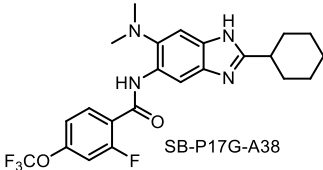
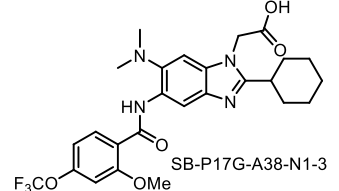
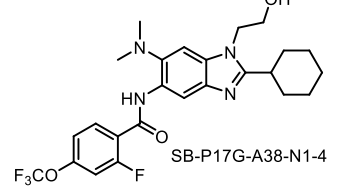
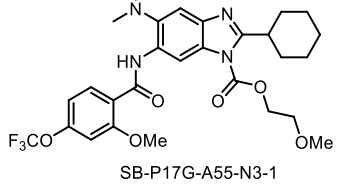
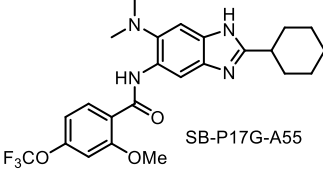
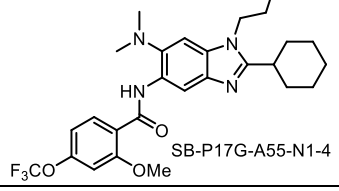
2-Cyclohexyl-1-ethoxycarbonylmethyl-5-(2-fluoro-4-trifluoromethoxy)benzamido-6-*N,N*-dimethylamino-1*H*-benzo[d]imidazole, **11c**, was reduced using lithium aluminum hydride in THF giving 2-cyclohexyl-5-(2-fluoro-4-trifluoromethoxy)benzamido-1-hydroxyethyl-6-*N,N*-dimethylamino-1*H*-benzo[d]imidazole, **11d**, in 35% yield. 2-Cyclohexyl-1-ethoxycarbonylmethyl-5-(2-methoxy-4-trifluoromethoxy)benzamido-6-*N,N*-dimethylamino-1*H*-benzo[d]imidazole, **12c**, was also reduced using lithium aluminum hydride in THF to give 2-cyclohexyl-1-hydroxyethyl-5-(2-methoxy-4-trifluoromethoxy)benzamido-6-*N,N*-dimethylamino-1*H*-benzo[d]imidazole, **12d**, in 99% yield. 2-Cyclohexyl-1-ethoxycarbonylmethyl-5-(2-methoxy-4-trifluoromethoxy)benzamido-6-*N,N*-dimethylamino-1*H*-benzo[d]imidazole, **12c**, was hydrolyzed using 2 N aqueous sodium hydroxide in methanol to give 1-carboxymethyl-2-cyclohexyl-5-(2-methoxy-4-trifluoromethoxy)benzamido-6-*N,N*-dimethylamino-1*H*-benzo[d]imidazole, **12e**, in 71% yield.



Scheme 22 Synthesis of Tetrasubstituted 1-Alkyl Benzimidazoles

Five of the tetrasubstituted benzimidazoles were submitted for biological testing on H37rv strain *M. tuberculosis*. Analogues of SB-P17G-A38, the current lead compound, were inactive. The acylated compound, SB-P17G-A38-N1-1 showed the best activity of the tetrasubstituted compounds, but still had an MIC, 0.19 $\mu\text{g}/\text{mL}$, an order of magnitude greater than the MIC of SB-P17G-A38, 0.019 $\mu\text{g}/\text{mL}$ (**Table 5**). The SB-P17-A55 analogues were also inactive (**Table 5**). Overall, none of the compounds synthesized had desirable activities, so they were not brought forward for hERG activity assays. The typical trend seen in optimizing hERG activity was the loss of *M. tuberculosis* activity whenever hERG blockage was decreased, and in the case of the tetrasubstituted benzimidazoles, the trend was also seen. The activity of the compounds needed to stay relatively similar, so there would be no tradeoff in activity for *M. tuberculosis* and hERG. Even though the tetrasubstituted benzimidazoles were inactive, the scope of functional groups was small, and additional studies need to be performed to obtain a more complete picture on the activity of tetrasubstituted benzimidazoles.

Table 5 Activities of tetrasubstituted benzimidazoles

Compound	MIC <i>Mtb</i> H37Rv ($\mu\text{g/ mL}$)	MIC <i>Mtb</i> H37Rv ($\mu\text{g/ mL}$)	Compound
 SB-P17G-A38-N1-1	0.19	0.019	 SB-P17G-A38
 SB-P17G-A38-N3-1	>14		
 SB-P17G-A38-N1-3	17		
 SB-P17G-A38-N1-4	1.56		
 SB-P17G-A55-N3-1	12	5	 SB-P17G-A55
 SB-P17G-A55-N1-4	6.25		

1.2.5. Activity of trisubstituted benzimidazoles on *Staphylococcus aureus*

In addition to *M. tuberculosis*, many different bacterial species utilize FtsZ for cell division. Another bacteria that plagues hospitals due to antibiotic resistance is MRSA. In testing for activity in *S. aureus*, six compounds were tested in an assay for the determination of MICs of each

compound. *S. Aureus* cells were suspended in media and incubated at 37 °C. Compound concentrations started at 62.5 µg/ mL and were serially diluted until the final concentration was 0.06 µg/ mL. When the optical density of the cell culture was 0.1 at 600 nm, the suspension was diluted and added to each of the rows in a 96-well plate. Seven rows of a 96-well plate were used in the experiment. The top row was the control, which only contained media and *S. aureus* cells. Rows A-F contained compounds in varying concentrations (**Figure 18**). After adding the cells, the plates were covered and incubated at 37 °C overnight, and the next day, there was no inhibition of growth observed in any of the wells. Even at concentrations of 62.5 µg/ mL, there was still growth of *S. aureus*. From these results, the six benzimidazoles used were not active against *S. aureus*, but additional studies need to be performed to find hit compounds. In the future, another method, agar diffusion assay, will be used to determine if the benzimidazoles have antibacterial activity against *S. aureus*. In an agar diffusion assay, a set concentration of compounds are added to small plates. These plates are placed onto an agar plate that contains a bacterial lawn of *S. aureus*. If the compounds are active against *S. aureus*, the area around the small compound containing plates will show no bacterial growth. Using this method, many compounds can be screened more quickly compared to the MIC method. This work was performed under the supervision of Professor Stephen Walker at the School of Dental Medicine at Stony Brook University.

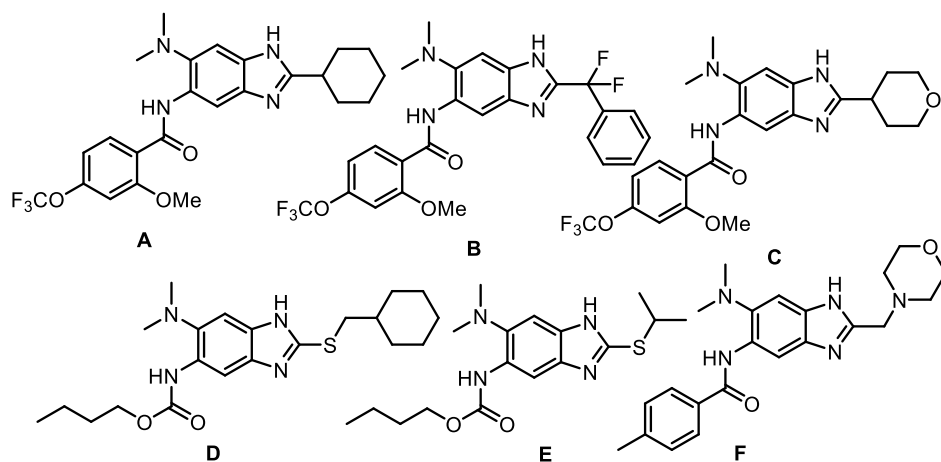
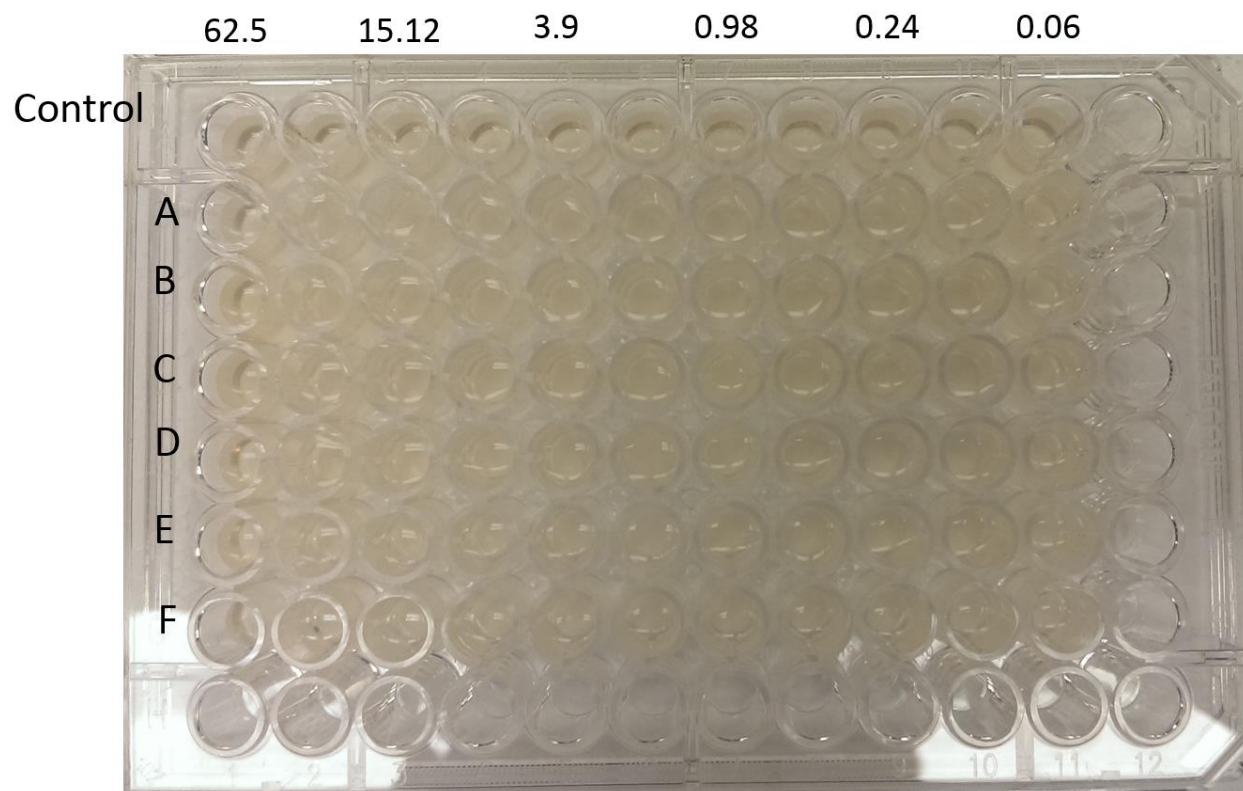
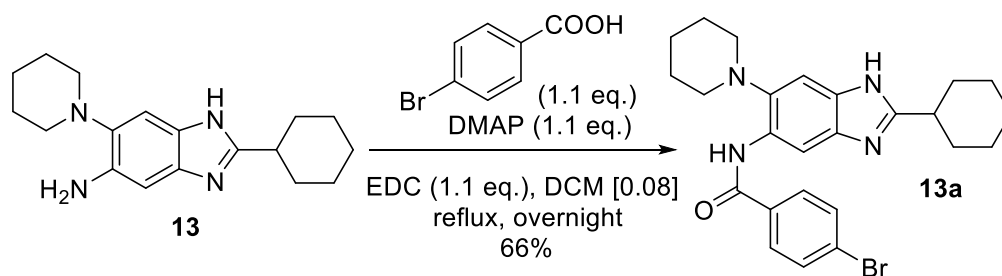


Figure 18 *S. Aureus* MIC Assay

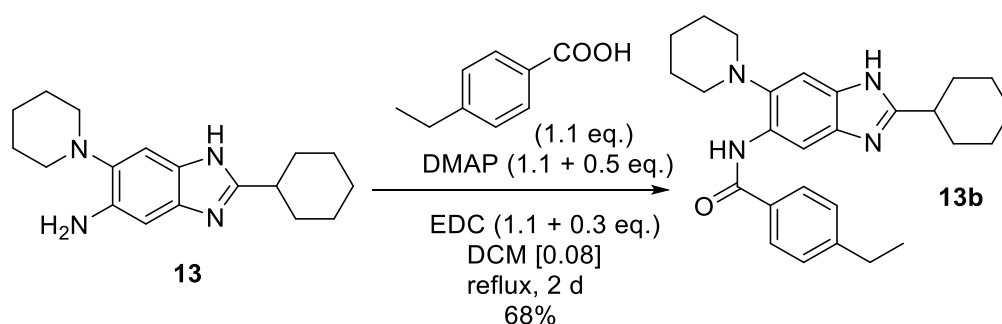
1.2.6. Resynthesis of hit compounds

Preliminary screening of previously synthesized trisubstituted benzimidazole library showed several compounds with good activity against *Mtb*. A few of these compounds needed to be resynthesized to obtain their accurate MIC values. Accordingly, three hit compounds were synthesized. Both 2-cyclohexyl-5-(4-bromobenzamido)-6-piperidin-1-yl-1*H*-benzo[d]imidazole, **13a**, and 2-cyclohexyl-5-(4-ethylbenzamido)-6-piperidin-1-yl-1*H*-benzo[d]imidazole, **13b**, were

synthesized from final intermediate, **13**. The final intermediate was coupled with corresponding carboxylic acid using 1-ethyl-3-(3-dimethylaminopropyl) carbodiimide (EDC) and 4-dimethylaminopyridine (DMAP). In both reactions, the starting material could not be consumed even after further addition of EDC and DMAP and longer reaction duration. The reaction was stopped even though it had not gone to completion, and the product was isolated. 2-cyclohexyl-5-(4-bromobenzamido)-6-piperidin-1-yl-1*H*-benzo[d]imidazole, **13a**, had solubility issues. It did not dissolve in many organic solvents, not even in DMSO. However, 2-cyclohexyl-5-(4-ethylbenzamido)-6-piperidin-1-yl-1*H*-benzo[d]imidazole, **13b**, did not have solubility issues.

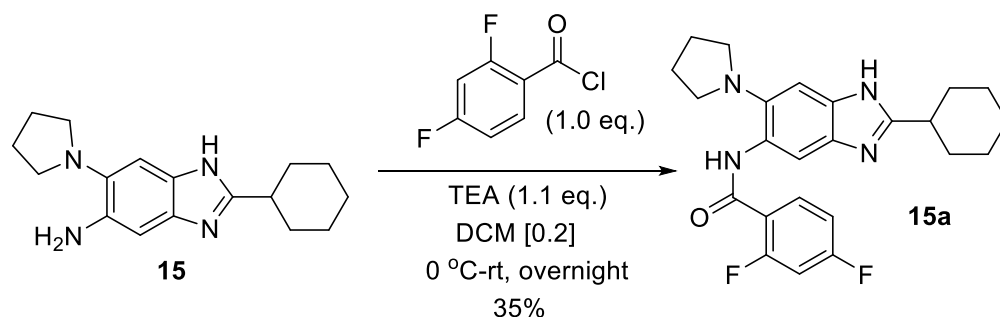


Resynthesis Scheme 1: Resynthesis of 2-cyclohexyl-5-(4-bromobenzamido)-6-piperidin-1-yl-1*H*-benzo[d]imidazole



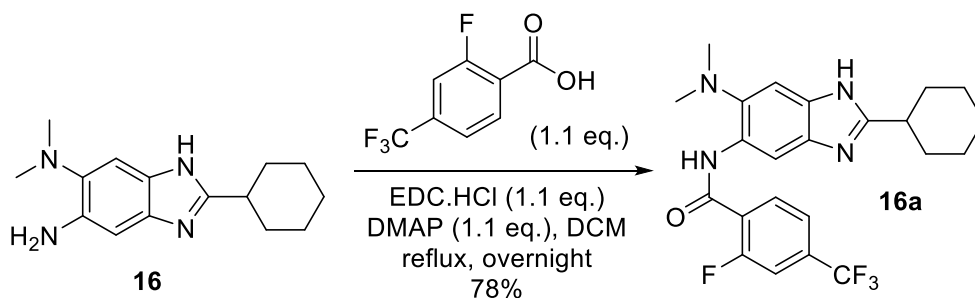
Resynthesis Scheme 2: Resynthesis of 2-cyclohexyl-5-(4-ethylbenzamido)-6-piperidin-1-yl-1*H*-benzo[d]imidazole

2-Cyclohexyl-5-(2,4-difluorobenzamido)-6-pyrrolidin-1-yl-1*H*-benzo[d]imidazole, **15a**, was synthesized by using an acyl chloride. The intermediate, **15**, was treated with 2,4-difluorobenzoyl chloride in DCM and triethylamine as a base. The reaction was stirred overnight to get the desired product in 35 % yield. The low yield could be attributed to the formation of the undesirable disubstituted product.



Resynthesis Scheme 3: Resynthesis of 2-cyclohexyl-5-(2,4-difluorobenzamido)-6-pyrrolidin-1-yl-1*H*-benzo[d]imidazole

2-Cyclohexyl-5-(2-fluoro-4-trifluoromethylbenzamido)-6-*N,N*-dimethylamino-1*H*-benzo[d]imidazole (SB-P17G-A42), **16a**, was resynthesized for X-ray diffraction. Final intermediate, 5-amino-6-*N,N*-dimethylamino-2-cyclohexyl-1*H*-benzo[d]imidazole, **16**, was dissolved in DCM and to the was solution was added 2-fluoro-4-trifluoromethyl benzoic acid, EDC·HCl, and DMAP. The reaction mixture was heated under reflux overnight. The mixture was extracted with water and DCM and purified by column to obtain the desired product in 78% yield (**Scheme 4**). The compound was recrystallized in acetonitrile and the X-ray diffraction was carried out by Matthew Freitag (**Figure 19**).



Resynthesis Scheme 4: Resynthesis of 2-cyclohexyl-5-(2-fluoro-4-trifluoromethylbenzamido)-6-*N,N*-dimethylamino-1*H*-benzo[d]imidazole

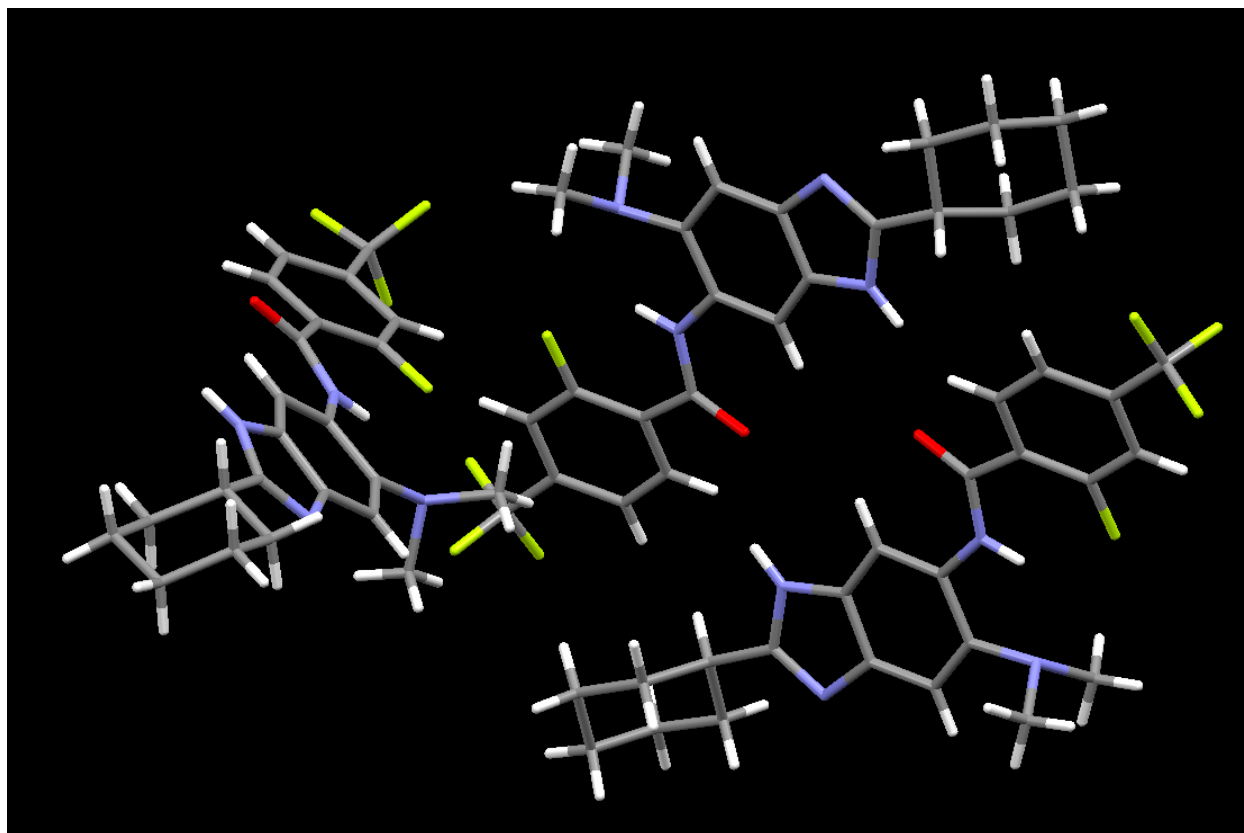


Figure 19 X-ray diffraction of SB-P17G-A42

1.3 Conclusion

Exploration of the 2-position of the 2,5,6-trisubstituted benzimidazoles was performed. The 2-dialkylaminomethylbenzimidazoles were less active than the 2-cyclohexylbenzimidazoles. Comparison of the 2-(*N*-methyl-*N*-phenylamino)benzimidazoles revealed at least a four-fold difference in activity, in favor of the cyclohexyl group at the 2-position. Of all the carbamate compounds synthesized, the 2-piperidinyl group showed the best activity, but it still could not match the MIC of SB-P17G-C2 (**Table 3**). Synthesis of 2-alkylthiobenzimidazoles yielded better results. The 2-cyclohexylmethylthio group of SB-TBI7-C2 showed promise. It was highly active, with an MIC of 0.004 $\mu\text{g}/\text{mL}$, and it is similar in activity to the 2-cyclohexyl group of SB-P17G-C2, with an MIC of 0.008 $\mu\text{g}/\text{mL}$ (**Table 4**). The 2-cyclohexylthio group may also be a highly active functional group, but it is unknown until the endpoint MIC is determined by collaborators at Rutgers University. Looking at the 2-dialkylaminomethylbenzimidazoles and 2-alkylthiobenzimidazoles, there is a preference for cyclohexyl at the 2-position. Changing a

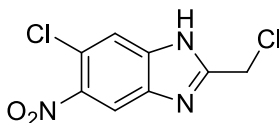
piperidine group to a pyrrolidine group alters the MIC by over an order of magnitude, and addition of aromatic groups to the 2-position is detrimental to activity. (**Table 3** and **Table 4**). The goal of finding a more active functional group at the 2-position has been achieved.

Investigation into the 2-alkoxybenzimidazoles lead to the synthesis of 3-alkoxybenzimidazole. Ultimately, the series of compounds could not be synthesized. Even though it was a failure, an interesting reaction was found. In literature, there is only one example of using an aldol type reaction for ring closure and formation of benzimidazole N-oxides.²⁹ The reaction required three steps to obtain the N-oxide from an ester. In the attempted synthesis of the 2-alkoxybenzimidazoles, the N-oxide formation was optimized to a three-step-one-pot process.

Synthesis of tetrasubstituted benzimidazoles was thought to dampen the hERG activity of the compounds. The trisubstituted benzimidazoles were acylated and alkylated using different procedures. The addition of carboxymethyl and hydroxyethyl would increase the polarity while blocking the basic nitrogen of the benzimidazole, but addition of acyl and alkyl groups to the nitrogens of the benzimidazoles disrupted activity. The best tetrasubstituted benzimidazole, SB-P17G-A38-N1-1, had an MIC 10-fold, 0.19 $\mu\text{g}/\text{mL}$, more than the MIC, 0.019 $\mu\text{g}/\text{mL}$, of the lead compound, SB-P17G-A38 (**Table 5**). The extra substitution may have decreased cardiotoxicity, but the loss of activity is too steep a price.

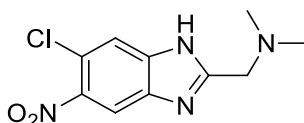
1.4. Experimental Section

5-Chloro-2-chloromethyl-6-nitro-1*H*-benzo[d]imidazole



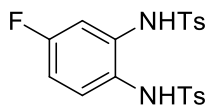
To a solution of 1,2-diamino-4-chloro-5-nitro benzene (500 mg, 2.70 mmol.) in 12 N hydrochloric acid (5 mL) was added chloroacetic acid (332 mg, 3.51 mmol.). The reaction mixture was heated to 90 °C, while stirring, overnight. The reaction mixture, while being cooled in an ice bath, was basified with sodium carbonate, extracted with ethyl acetate, dried over magnesium sulfate, filtered, and rotary evaporated. A flash column on silica gel, using ethyl acetate and hexanes (1:1), was used to purify the crude compound to afford the pure compound as a red-orange solid. 566 mg, 92% yield; mp 165-168 °C; ¹H NMR (400 MHz, Acetone-D₆) δ 4.99 (s, 2 H), 6.29 (s, 0.5 H), 6.92 (s, 0.5 H), 7.85 (s, 1 H), 8.28 (s, 1 H); ¹³C NMR (100 MHz, Acetone-D₆) δ 37.53, 101.9, 105.3, 114.2, 116.8, 119.8, 143.9, 155.0; MS (FIA) *m/z* 245.9 (M+1)⁺.

5-Chloro-2-dimethylaminomethyl-6-nitro-1*H*-benzo[d]imidazole



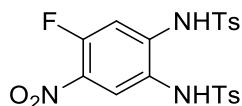
To a solution of 5-chloro-2-chloromethyl-6-nitro-1*H*-benzo[d]imidazole (50 mg, 0.20 mmol.) in DMF (2 mL), was added dimethylamine (2 M solution in THF, 0.11 mL) and TEA (31 μL). The reaction mixture was left stirring at room temperature overnight. Upon completion, the reaction mixture was diluted with ethyl acetate, washed with brine and water, dried over magnesium sulfate, and rotary evaporated. A flash column on alumina, using ethyl acetate and hexanes (1:1), was used to purify the crude mixture to afford the pure compound as a light yellow solid. 35 mg, 69% yield; mp 172-175 °C; ¹H NMR (400 MHz, Acetone-D₆) δ 2.31 (s, 6 H), 3.78 (s, 2 H), 7.77 (s, 1 H), 8.21 (s, 1 H); ¹³C NMR (100 MHz, Acetone-D₆) δ 45.91, 58.05, 112.8, 114.4, 115.6, 117.6, 120.0, 144.1, 159.7; MS (FIA) *m/z* 255.1 (M+1)⁺

4-Fluoro-1,2-di (*p*-toluenesulfonylamino) benzene



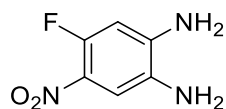
To a solution of 1,2-diamino-4-fluoro benzene (10 g, 79 mmol.) in pyridine (20 mL), was added a solution of *p*-toluenesulfonyl chloride (30 g, 158 mmol.) in pyridine (50 mL), dropwise. After addition, the reaction mixture was heated to 90 °C and stirred overnight. Upon completion of the reaction, the mixture was allowed to cool to room temperature and was added to a solution of water (264 mL) and 12 N hydrochloric acid (66 mL). The precipitate was filtered, and the filtrate was washed with water. The compound was allowed to air dry giving a white solid.¹³ 29 g, 85% yield; mp, ¹H NMR (400 MHz, CDCl₃) δ 2.38 (s, 6 H), 6.75 (m, 1 H), 6.84 (m, 1 H), 7.05 (dd 1 H, *J* = 2.84 Hz, 10.0 Hz), 7.35 (qd, 4 H, *J* = 0.64 Hz, 6.68 Hz), 7.55 (dt, 2 H, *J* = 1.86 Hz, 8.32 Hz), 7.72 (dt, 2 H, *J* = 1.86 Hz, 8.32 Hz); ¹³C NMR (100 MHz, CDCl₃) δ 21.39, 110.3, 110.6, 112.8, 113.0, 125.7, 125.8, 128.2, 128.3, 129.6, 129.7, 130.4, 130.5, 135.7, 135.8, 136.2, 136.8, 145.1, 145.2, 160.5, 163.0. The analytical data was consistent with literature values.²³

4-fluoro-5-nitro-1,2-di (*p*-toluenesulfonylamino) benzene



To 4-fluoro-1,2-di (*p*-toluenesulfonylamino) benzene (8 g, 18 mmol.) was added glacial acetic acid (30 mL) forming a slurry. A fuming nitric acid (1.9 mL) and acetic acid (2.5 mL) solution was added slowly to the slurry. The slurry was heated to 60 °C and stirred for 2 hours until the reaction mixture formed a solid that could no longer be stirred. The solid was filtered and washed with ethyl acetate, and the solid air dried. The product was an off white solid.¹³ 4.7 g, 53% yield; mp 212-215 °C; ¹H NMR (400 MHz, CDCl₃) δ 2.43 (s, 6 H), 6.35 (s, 1 H), 7.12 (d, 1 H, *J* = 7.4 Hz), 7.28 (d, 2 H, *J* = 8 Hz), 7.33 (d, 2 H, *J* = 8.04 Hz), 7.41 (d, 1H, *J* = 12.6 Hz), 7.49 (d, 2H, = 8.32 Hz), 7.84 (d, 2 H, *J* = 8.4 Hz), 8.26 (s, 1 H); ¹³C NMR (100 MHz, CDCl₃) δ 21.93, 31.19, 107.8, 108.1, 126.8, 127.9, 128.0, 130.3, 130.4, 133.6, 135.4, 145.6, 146.0; MS (FIA) *m/z* 452.0 (M+1)⁺. The analytical data was consistent with literature values.²³

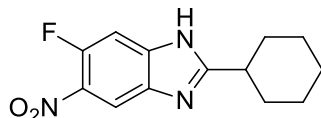
1,2-Diamino-4-fluoro-5-nitro benzene



To 4-fluoro-5-nitro-1,2-di (*p*-toluenesulfonylamino) benzene (4.7 g, 9.8 mmol.) was added a solution of sulfuric acid (22 mL) and water (2.2 mL) forming a slurry. The reaction mixture was

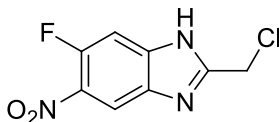
heated to 85 °C and stirred for 30 minutes. As the reaction mixture was heated, the slurry became a homogeneous solution. The completion of the reaction was confirmed by TLC, the reaction mixture turned into a dark brown homogeneous solution. The reaction mixture was cooled to room temperature and added to ice cold water (400 mL). The diluted solution was basified to pH 10, using ammonium hydroxide solution, while being cooled in an ice bath. After basification, a red solid crashed out of solution. The mixture was extracted with ethyl acetate, dried over magnesium sulfate, filtered, rotary evaporated, and vacuum dried to get the desired product as a red solid.¹³ 1.6 g, 94% yield; 186-189 °C; ¹H NMR (400 MHz, Acetone-D₆) δ 6.40 (d, 1 H, *J* = 13.6 Hz), 7.41 (d, 1 H, *J* = 7.48 Hz); ¹³C NMR (100 MHz, Acetone-D₆) δ 100.5, 100.6, 100.8, 100.9, 111.4, 111.5, 116.7, 132.9, 148.7, 148.8, 154.7, 157.1, 174.9; MS (FIA) *m/z* 172.0 (M+1)⁺. The analytical data was consistent with literature values.²³

2-Cyclohexyl-5-fluoro-6-nitro-1*H*-benzo[d]imidazole



To a solution of 1,2-diamino-4-fluoro-5-nitrobenzene (100 mg, 0.58 mmol) in ethanol (6 mL) and DMSO (1 mL), was added the sodium bisulfite adduct of cyclohexanal (138 mg) and stirred at room temperature overnight. The reaction mixture was diluted with ethyl acetate, washed with water, dried over magnesium sulfate, and rotary evaporated. The crude compound was purified by flash chromatography on silica gel using ethyl acetate/ethanol (1:1) as eluent to afford the product as a light yellow solid.¹¹ 69 mg, 83% yield; mp 131-134 °C; ¹H NMR (400 MHz, Acetone D₆) δ 1.31 (t, 1 H, *J* = 12.2 Hz), 1.43 (q, 2 H, *J* = 12.4 Hz), 1.63-1.73 (m, 3 H), 1.81-1.84 (m, 2 H), 2.10 (d, 2 H, *J* = 11.5 Hz), 2.98 (m, 1 H), 7.44 (d, 1 H, *J* = 11.7 Hz), 8.24 (d, 1 H, *J* = 6.68 Hz); ¹³C NMR (100 MHz, Acetone D₆) δ 26.53, 32.08, 39.24, 67.54, 103.4, 113.7, 133.6, 133.7, 151.7, 154.2, 165.8; MS (FIA) *m/z* 264.1 (M+1)⁺

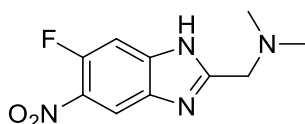
2-Chloromethyl-5-fluoro-6-nitro-1*H*-benzo[d]imidazole



To a solution of 1,2-diamino-4-fluoro-5-nitrobenzene (500 mg, 2.90 mmol.) in 12 N hydrochloric acid (5 mL) was added 2-chloroacetic acid (411 mg, 4.35 mmol.). The reaction

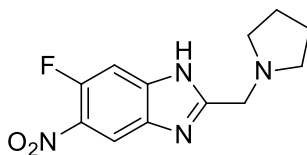
mixture was heated to 90 °C, while stirring, overnight. The reaction mixture was basified with sodium bicarbonate in ice bath, extracted with ethyl acetate, dried over magnesium sulfate, filtered, and rotary evaporated. A flash column on silica gel, using ethyl acetate and hexanes (1:1), was used to purify the crude compound to afford the pure compound as a light orange solid. 566 mg, 92% yield; ¹H NMR (400 MHz, Acetone-D₆) δ 4.991 (s, 2 H), 7.57 (d, 1 H, *J* = 11.44 Hz), 8.37 (d, 1 H, *J* = 6.76 Hz); ¹³C NMR (100 MHz, Acetone-D₆) δ 38.50, 103.6, 115.5, 134.7, 134.8, 152.0, 154.6, 156.2; MS (FIA) *m/z* 230.1 (M+1)⁺

5-Fluoro-2-dimethylaminomethyl-6-nitro-1*H*-benzo[d]imidazole



To a solution of 2-chloromethyl-5-fluoro-6-nitro-1*H*-benzo[d]imidazole (105 mg, 0.46 mmol.), dissolved in THF, was added 2 M dimethylamine solution dissolved in THF (1.84 mL) and TEA (70 μL). The reaction mixture was left stirring at room temperature for 2 days. Upon completion, the reaction mixture was rotary evaporated. A flash column on alumina, using ethyl acetate and hexanes (1:1), was used to purify the crude mixture to afford the pure compound as a red-orange solid. 90 mg, 83% yield; mp 150-152 °C; ¹H NMR (400 MHz, Acetone-D₆) δ 2.31 (s, 6 H), 3.78 (s, 2 H), 7.50 (d, 1 H, *J* = 11.64 Hz), 8.31 (d, 1 H, *J* = 6.8 Hz); ¹³C NMR (100 MHz, Acetone-D₆) δ 45.9, 58.0, 103.3, 114.3, 133.9, 134.0, 151.7, 154.2, 159.9; MS (FIA) *m/z* 239.1 (M+1)⁺

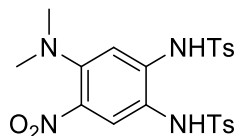
5-Fluoro-2-pyrrolidinylmethyl-6-nitro-1*H*-benzo[d]imidazole



To a solution of 2-chloromethyl-5-fluoro-6-nitro-1*H*-benzo[d]imidazole (100 mg, 0.44 mmol.) in DMF, was added pyrrolidine (0.48 mmol.) and TEA (68 μL). The reaction mixture was left stirring at room temperature overnight. Upon completion, the reaction mixture was diluted with ethyl acetate, washed with brine and water, dried over magnesium sulfate, and rotary evaporated. A flash column on alumina, using ethyl acetate and hexanes (1:1), was used to purify the crude mixture to afford the pure compound as a yellow solid (50 mg, 43% yield). ¹H NMR

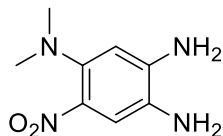
(400 MHz, Acetone-D₆) δ 1.77 (m, 4 H), 2.62 (m, 4 H), 3.96 (s, 2 H), 7.50 (d, 1 H, $J = 11.68$), 8.30 (d, 1 H, $J = 6.8$ Hz); ¹³C NMR (100 MHz, Acetone-D₆) δ 14.36, 23.30, 24.82, 32.31, 35.27, 54.17, 54.91, 133.9, 151.7, 154.2, 160.3; MS (FIA) m/z 265.0 (M+1)⁺

4-*N,N*-Dimethylamino-5-nitro-1,2-di (*p*-toluenesulfonylamino) benzene



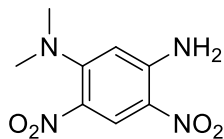
To a solution of 4-fluoro-5-nitro-1,2-di (*p*-toluenesulfonylamino) benzene (100 mg, 0.21 mmol.) and DIPEA (0.23 mmol) in tetrahydrofuran (1.0 mL) was added a solution of 2 M dimethylamine in tetrahydrofuran (115 μ L). The mixture was stirred at room temperature overnight. The reaction mixture was diluted with ethyl acetate, washed with water and dried over anhydrous magnesium sulfate. The compound was purified on column chromatography on silica gel with 1:1 ethyl acetate: hexanes. The pure compound was obtained as an amber solid.¹¹ 75 mg, 70% crude yield; ¹H NMR (500 MHz, CDCl₃) δ 2.42 (s, 6 H), 2.82 (s, 6 H), 6.87 (s, 1 H), 7.02 (s, 1 H), 7.26 (d, $J = 7.93$ Hz, 3 H), 7.31 (d, $J = 8.24$ Hz, 2 H), 7.52 (d, $J = 8.24$ Hz, 2 H), 7.84 (d, $J = 8.24$ Hz, 2 H); ¹³C NMR (126 MHz, CDCl₃) δ 21.6, 42.4, 106.9, 113.8, 127.7, 127.7, 128.1, 129.8, 129.9, 132.4, 133.9, 135.6, 140.2, 144.7, 145.0, 146.9; MS (FIA) m/z 505.1 (M+1)⁺.

1,2-Diamino-4-*N,N*-dimethylamino-5-nitro benzene



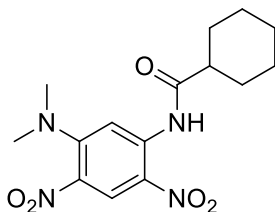
To a solution of 1,2-Diamino-4-fluoro-5-nitrobenzene (50 mg, 0.29 mmol.), dissolved in anhydrous DMF (10 mL), was added dimethylamine solution (2 M in THF) (1.5 mL, 3.0 mmol.). The mixture was heated to 120 °C for 1 hour in a sealed tube. Upon completion, the reaction mixture was diluted with ethyl acetate and the washed with 5 % aqueous lithium chloride solution three times. The organic layer was collected, dried over magnesium sulfate, and evaporated on a rotary evaporator. The crude mixture was purified by column chromatography on alumina, using ethyl acetate as the eluent. This reaction was also performed in the microwave, and the reaction went to completion in 30 minutes. The compound was a red solid.¹⁴ 72.3 mg, 98% yield; ¹H NMR (500 MHz, CDCl₃) δ 2.79 (s, 6 H), 3.16 (br. s., 2 H), 4.26 (br. s., 2 H), 6.26 (s, 1 H), 7.52 (s, 1 H); ¹³C NMR (126 MHz, CDCl₃) δ 43.6, 103.1, 116.8, 125.5, 130.7, 144.3, 145.5;

5-*N,N*-Dimethylamino-2,4-dinitro aniline



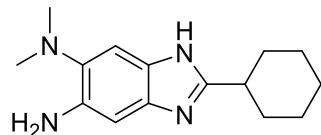
To a solution of 2,4-dinitro-5-fluoroaniline (9.00 g, 44.6 mmol) and DIPEA (8.53 mL, 49.0 mmol) in THF (200 mL) was added a solution of 2 M dimethylamine (24.5 mL, 49 mmol.), dissolved in THF, dropwise. The mixture was stirred at room temperature for 4 h. The reaction mixture was diluted with DCM, washed with water three times and dried over anhydrous magnesium sulfate. The solvent was evaporated to afford 5-*N,N*-dimethylamino-2,4-dinitro aniline as an orange solid.¹¹ 9.30 g, 92% yield; mp 157-160 °C; ¹H NMR (400 MHz, CDCl₃) δ 2.94 (s, 6 H), 6.00 (s, 1 H), 6.37 (s, 2 H), 8.81 (s, 1 H); ¹³C NMR (100 MHz, CDCl₃) δ 42.57, 100.7, 123.8, 128.9, 130.6, 147.9, 150.8. The analytical data was consistent with literature values.²²

1-Cyclohexanecarboxamido-5-*N,N*-dimethylamino-2,4-dinitro benzene



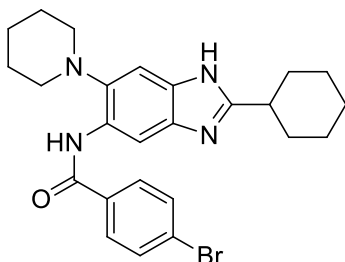
A solution of 5-*N,N*-dimethylamino-2,4-dinitro aniline (7.00 g, 31.0 mmol.) and cyclohexanecarbonyl chloride (4.97 mL, 37.1 mmol.) in pyridine (150 mL) was refluxed overnight. The reaction mixture was evaporated to get yellow residue. The reaction mixture was washed with methanol to obtain the product 1-cyclohexanecarboxamido-5-(*N,N*-dimethylamino)-2,4-dinitro benzene as yellow solid.¹¹ 10 g, 97% yield; mp ; ¹H NMR (300 MHz, CDCl₃) δ 1.23 – 1.39 (m, 4 H), 1.51-1.61 (m, 3 H), 1.75 (m, 1 H), 1.84-1.89 (m, 2 H), 2.00-2.05 (m, 2 H), 2.38 (m, 1 H), 3.06 (s, 6 H), 8.60 (s, 1 H), 8.85 (s, 1 H), 11.0 (s, 1H); ¹³C NMR (75 MHz, CDCl₃) δ 25.2, 25.3, 25.4, 29.2, 42.3, 42.4, 47.0, 76.7, 77.0, 77.3, 105.8, 124.7, 127.1, 131.1, 138.5, 149.9, 175.7. The analytical data was consistent with literature values.²²

5-Amino-2-cyclohexyl-6-*N,N*-dimethylamino-1*H*-benzo[d]imidazole



To a solution of 1-cyclohexanecarboxamido-5-*N,N*-dimethylamino-2,4-dinitro benzene (10.1 g, 30.0 mmol.) in ethanol (200 mL) was added solid stannous chloride dihydrate (47.4 g, 210 mmol). Concentrated hydrochloric acid (75 mL) was added to the reaction mixture such that the final concentration of HCl was 4 N in the reaction flask. The reaction mixture was refluxed for 4 h. Upon completion, the reaction mixture was basified with 30% sodium hydroxide solution. Excess stannous chloride formed a soluble salt in excess base. The desired product was extracted with DCM and purified by flash chromatography on alumina using ethyl acetate as eluent to afford the product as a light brown solid.¹¹ 5.5 g, 71% yield; mp ; ¹H NMR (300 MHz, CDCl₃) δ 1.23-1.37 (m, 4 H), 1.59-1.68 (m, 3 H), 1.79-1.84 (m, 2 H), 2.04-2.11 (m, 2 H), 2.64 (s, 6 H), 2.82 (m, 1 H), 6.81 (s, 1 H), 7.26 (s, 1 H); ¹³C NMR (75 MHz, CDCl₃) δ 25.7, 26.0, 38.6, 44.5, 76.7, 77.0, 77.3, 98.7, 106.5, 132.9, 134.3, 137.8, 138.1, 158.0. The analytical data was consistent with literature values.²²

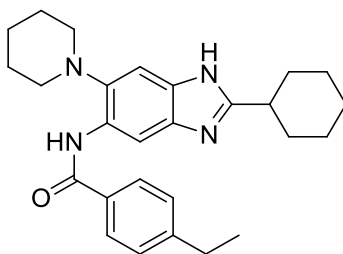
2-Cyclohexyl-5-(4-bromobenzamido)-6-piperidin-1-yl-1*H*-benzo[d]imidazole



To a solution of 5-piperidyl-2-cyclohexyl-6-dimethylamino-1*H*-benzo[d]imidazole (100 mg, 0.34 mmol.) in DCM (4.2 mL) was added DMAP (45 mg, 0.37 mmol.), EDC (57.2 mg, 0.37 mmol.), and 4-bromo benzoic acid (74.1 mg, 0.37 mmol.). The reaction mixture was refluxed overnight. The reaction mixture was diluted with ethyl acetate and washed with a sodium bicarbonate solution and dried over magnesium sulfate. The crude mixture was purified by column chromatography on silica gel with 1:1 ethyl acetate: hexanes. The pure compound was obtained as a light yellow solid; 107 mg, 66% yield; mp >260 °C; ¹H NMR (400 MHz, DMSO-*D*₆) (mixture of tautomers) δ 1.27-1.34 (m, 1 H), 1.36-1.43 (m, 2 H), 1.57 (m, 4 H), 1.68 (d, 5 H, *J* = 4.5 Hz), 1.77-1.84 (m, 2 H), 1.98-2.01 (m, 2 H), 2.79 (m, 5 H), 3.42 (s, 6 H), 7.24 (s, 0.4 H), 7.44 (s, 0.6

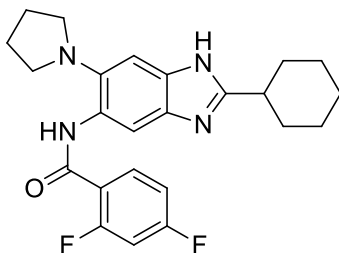
H), 7.79-7.90 (m, 4 H), 8.33 (s, 0.4 H), 8.39 (s, 0.7 H), 9.73 (s, 0.4 H), 9.89 (s, 0.7 H), 11.99 (s, 0.4 H), 12.02 (s, 0.6 H); ^{13}C NMR (100 MHz, DMSO- D_6) (mixture of tautomers) δ 24.1, 25.9, 26.0, 27.1, 27.2, 31.7, 38.1, 38.2, 54.4, 54.5, 102.0, 111.3, 125.9, 128.5, 129.3, 131.4, 132.5, 134.5, 139.4, 140.0, 159.6, 159.8, 163.2; HRMS (ESI) m/z calculated for $\text{C}_{25}\text{H}_{29}\text{BrN}_4\text{O}_5$ ($\text{M}+\text{H}$) $^+$: 481.1589, found 481.1601 (Δ -0.67 ppm)

2-Cyclohexyl-5-(4-ethylbenzamido)-6-piperidin-1-yl-1H-benzo[d]imidazole



The same procedure used to make 2-cyclohexyl-5-(4-bromobenzamido)-6-piperidin-1-yl-1H-benzo[d]imidazole was used to make this compound. White solid; 97 mg, 68% yield; mp 213-216 $^{\circ}\text{C}$; ^1H NMR (400 MHz, CDCl_3) δ 1.04-1.17 (m, 3 H), 1.31 (t, 3 H, $J = 7.6$ Hz), 1.51-1.68 (m, 6 H), 1.79 (s, 5 H), 1.95 (d, 2 H, $J = 12.5$ Hz), 2.66-3.14 (m, 5 H), 7.39 (d, 2 H, $J = 8.04$), 7.58 (s, 1 H), 7.94 (d, 2 H, $J = 8.12$), 8.97 (s, 1 H), 10.14 (s, 1H), 10.95 (s, 1 H); ^{13}C NMR (100 MHz, CDCl_3) 15.5, 24.2, 25.8, 26.1, 27.6, 29.1, 32.0, 38.7, 55.0, 101.5, 111.6, 127.2, 128.7, 129.2, 131.5, 133.2, 129.0, 139.7, 148.7, 160.0, 165.6; HRMS (ESI) m/z calculated for $\text{C}_{27}\text{H}_{34}\text{N}_4\text{O}$ ($\text{M}+\text{H}$) $^+$: 431.2805, found 431.2809 (Δ -0.9 ppm).

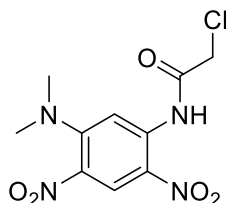
2-Cyclohexyl-5-(2,4-difluorobenzamido)-6-pyrrolidin-1-yl-1H-benzo[d]imidazole



To a solution of 5-pyrrolidyl-2-cyclohexyl-6-dimethylamino-1H-benzo[d]imidazole (100 mg, 0.35 mmol.) in DCM (1.8 mL) was added TEA (39 mg, 0.39 mmol.) and 2,4-difluorobenzoyl chloride (61.8 mg, 0.35 mmol), while cooling the reaction mixture in an ice bath. After the addition, the reaction mixture was left to warm up to room temperature and stirred overnight. After completion, the reaction mixture was diluted with ethyl acetate and washed with a sodium

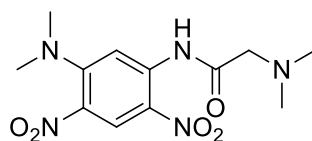
bicarbonate solution and dried over magnesium sulfate. The crude mixture was purified by column chromatography on silica gel with 1:1 ethyl acetate: hexanes. The pure compound was obtained as a white solid. 52 mg, 35% yield; mp 218-221 °C; ¹H NMR (400 MHz, DMSO-D₆) (mixture of two tautomers) δ 1.34-1.43 (m, 3 H), 1.57 (m, 2 H), 1.60 (m, 1H), 1.98 (m, 1 H), 2.81 (m, 1 H), 3.01 (s, 4 H), 3.32 (s, 3 H), 7.27 (m, 1.4 H), 7.49 (s, 1.5 H), 8.09 (s, 1 H), 8.33 (s, 0.4 H), 8.44 (s, 0.6 H), 9.92 (s, 0.4 H), 10.13 (d, 0.6 H, *J* = 10.9 Hz), 11.93 (s, 0.4 H), 11.99 (s, 0.6 H); ¹³C NMR (100 MHz, DMSO-D₆) (mixture of two tautomers) δ 14.0, 22.3, 24.0, 26.0, 31.3, 37.9, 53.4, 102.3, 104.6, 104.9, 105.1, 110.1, 112.5, 112.7, 115.6, 119.0, 132.3, 133.2, 133.3, 135.4, 139.7, 159.3; HRMS (ESI) *m/z* calculated for C₂₄H₂₆F₂N₄O₅ (M+H)⁺: 425.2147, found 425.2149 (Δ -0.42 ppm).

1-Chloroacetylcarboxamido-5-*N,N*-dimethylamino-2,4-dinitro benzene



To a solution of 5-*N,N*-dimethylamino-2,4-dinitro aniline (1.00 g, 3.31 mmol.) in DCM (20 mL) was added chloroacetyl chloride (315 μL, 3.96 mmol.) and TEA (553 μL, 3.96 mmol.). The reaction mixture was refluxed overnight. Upon consumption of starting material, the reaction mixture was diluted with DCM (30 mL), washed thrice with water (50 mL), and dried over anhydrous magnesium sulfate. The crude product was purified on by flash column chromatography on silica gel with 1:3 ethyl acetate: hexanes as the eluent to obtain 1-chloroacetylcarboxamido-5-*N,N*-dimethylamino-2,4-dinitro benzene as a yellow solid. 93% yield; mp 152 °C – 153 °C; ¹H NMR (500 MHz, CDCl₃) δ 3.07 (s, 6 H), 4.26 (s, 2 H), 8.48 (s, 1 H), 8.81 (s, 1 H), 11.83 (br. s., 1 H); ¹³C NMR (126 MHz, CDCl₃) δ 42.5, 43.2, 106.2, 125.1, 127.3, 131.7, 137.2, 149.8, 166.0; HRMS (ESI) *m/z* calculated for C₁₀H₁₁ClN₄O₅ (M+H)⁺: 303.0491, found 303.049 (Δ 0.26 ppm).

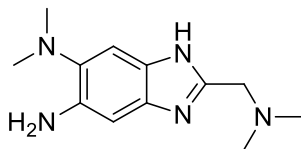
1-*N,N*-dimethylaminomethylcarboxamido-5-*N,N*-dimethylamino-2,4-dinitro benzene



To a solution of 1-Chloromethylcarboxamido-5-*N,N*-dimethylamino-2,4-dinitro benzene in THF (10 mL) was added DIPEA (0.35 mL, 2.0 mmol.) and 2 M dimethylamine in THF (0.35 mL, 2.0

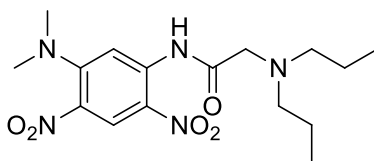
mmol.). The reaction mixture was stirred under reflux conditions overnight. The reaction mixture was evaporated to get yellow residue. The residue was dissolved in DCM, washed three times with water, and dried over anhydrous magnesium sulfate. The crude mixture was purified using flash column chromatography on silica gel and 1:1 ethyl acetate: hexanes. The compound was obtained as a yellow solid. 428 mg, 83% yield; mp 134-137 °C; ¹H NMR (300 MHz, CDCl₃) δ 2.42 (s, 6 H), 3.05 (s, 6 H), 3.16 (s, 2 H), 8.58 (s, 1 H), 8.86 (s, 1 H), 12.29 (s, 1 H); ¹³C NMR (126 MHz, CDCl₃) δ 44.4, 45.3, 57.5, 98.2, 107.0, 133.2, 134.1, 138.3, 138.3, 150.1; HRMS (ESI) *m/z* calculated for C₁₂H₁₇N₅O₅ (M+H)⁺: 312.1302, found 312.1305 (Δ -0.9 ppm).

5-Amino-6-*N,N*-dimethylamino-2-*N,N*-dimethylaminomethyl-1*H*-benzo[d]imidazole



To a solution of 1-*N,N*-dimethylaminomethylcarboxamido-5-*N,N*-dimethylamino-2,4-dinitro benzene (428 mg, 1.37 mmol.) in ethanol (10 mL) was added solid stannous chloride dihydrate (2.17 g, 9.62 mmol). Concentrated hydrochloric acid (2 mL) was added to the reaction mixture such that the final concentration of HCl was 4 N in the reaction flask. The reaction mixture was refluxed overnight. Upon completion, the reaction mixture was basified with 30% sodium hydroxide solution. Excess stannous chloride formed a soluble salt in excess base. The desired product was extracted with DCM and purified by flash chromatography on alumina using a solution of 3% methanol in DCM as eluent to afford the product as a dark brown solid. 1198 mg, 62 % yield; ¹H NMR (300 MHz, CDCl₃) δ 2.31 (s, 6 H), 2.64 (s, 6 H), 3.70 (s, 2 H), 6.73 (s, 1 H), 7.23 (s, 1 H); ¹³C NMR (126 MHz, CDCl₃) δ 44.4, 45.3, 57.5, 98.2, 107.0, 133.3, 134.1, 138.3, 138.3, 150.1; MS (FIA) *m/z* 234.1 (M+1)⁺.

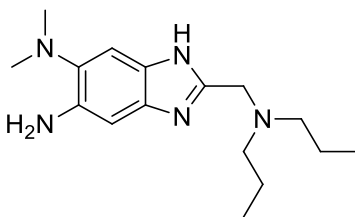
5-*N,N*-Dimethylamino-1-*N,N*-dipropylaminomethylcarboxamido-2,4-dinitro benzene



This compound was synthesized using the same procedure used to synthesize 5-Amino-6-*N,N*-dimethylamino-2-*N,N*-dimethylaminomethyl-1*H*-benzo[d]imidazole. 344 mg, 71% yield; mp 94-

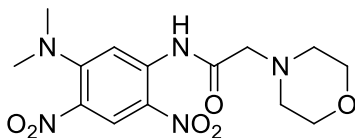
97 °C; ¹H NMR (300 MHz, CDCl₃) δ 0.88 (t, 6 H), 1.52 (m, 4 H), 2.54 (t, 4 H), 3.05 (s, 6 H), 3.25 (s, 2 H), 8.64 (s, 1 H), 8.87 (s, 1 H), 12.36 (s, 1 H); ¹³C NMR (126 MHz, CDCl₃) δ 11.6, 20.3, 42.4, 57.7, 59.9, 106.1, 125.2, 127.3, 131.2, 137.9, 149.9, 173.1; HRMS (ESI) *m/z* calculated for C₁₆H₂₅N₅O₅ (M+H)⁺: 368.1928, found 368.1934 (Δ -1.41 ppm).

5-Amino-6-*N,N*-dimethylamino-2-*N,N*-dipropylaminomethyl-1*H*-benzo[d]imidazole



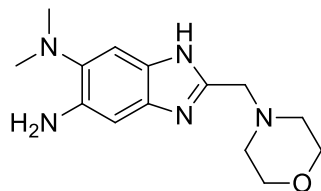
This compound was synthesized using the same procedure used to synthesize 1-*N,N*-dimethylaminomethylcarboxamido-5-*N,N*-dimethylamino-2,4-dinitro benzene. 235 mg, 78% yield; ¹H NMR (300 MHz, CDCl₃) δ 0.83 (t, 6 H), 1.45 (m, 4 H), 2.42 (t, 4 H), 2.64 (s, 6 H), 3.78 (s, 2 H), 6.79 (s, 1 H), 7.23 (s, 1 H);.

5-*N,N*-Dimethylamino-1-morpholin-1-ylmethylcarboxamido-2,4-dinitro benzene



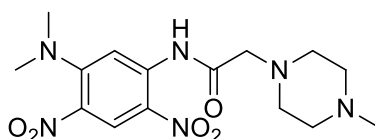
This compound was synthesized using the same procedure used to synthesize 1-*N,N*-dimethylaminomethylcarboxamido-5-*N,N*-dimethylamino-2,4-dinitro benzene. 362 mg, 78% yield; ¹H NMR (500 MHz, CDCl₃) δ 2.52 (br. s., 4H), 2.90 (s, 6H), 3.09 (s, 2H), 3.67 (br. s., 4H), 8.36 (s, 1H), 8.51 (s, 1H), 12.11 (s, 1H); ¹³C NMR (126 MHz, CDCl₃) δ 42.0, 53.3, 62.2, 66.2, 105.3, 124.4, 126.7, 130.7, 137.3, 149.3, 170.4; HRMS (ESI) *m/z* calculated for C₁₄H₁₉N₅O₆ (M+H)⁺: 354.1408, found 354.1412 (Δ -1.11 ppm).

5-Amino-6-*N,N*-dimethylamino-2-morpholin-1-ylmethyl-1*H*-benzo[d]imidazole



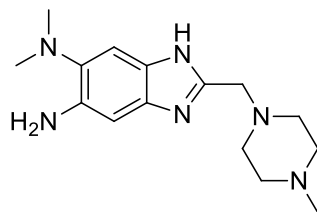
This compound was synthesized using the same procedure used to synthesize 1-*N,N*-dimethylaminomethylcarboxamido-5-*N,N*-dimethylamino-2,4-dinitro benzene. 76 mg, 28% yield; ^1H NMR (300 MHz, CDCl_3) δ 2.48 (s, 4 H), 2.64 (s, 6 H), 3.65 (s, 4 H), 3.71 (s, 2 H), 6.79 (s, 1 H), 7.24 (s, 1 H); ^{13}C NMR (126 MHz, CHLOROFORM-d) δ 44.5, 53.7, 56.8, 66.8, 77.2, 98.3, 107.1, 132.9, 133.9, 138.5, 149.6;

5-*N,N*-Dimethylamino-1-*N*-methylpiperazin-1-ylaminomethylcarboxamido-2,4-dinitro benzene



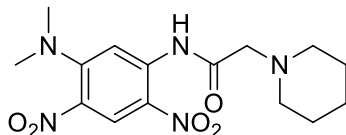
This compound was synthesized using the same procedure used to synthesize 1-*N,N*-dimethylaminomethylcarboxamido-5-*N,N*-dimethylamino-2,4-dinitro benzene. 359 mg, 74% yield; ^1H NMR (500 MHz, CDCl_3) δ 2.28 (s, 3H), 2.53 (br. s., 4H), 2.62 (br. s., 4H), 2.99 (s, 6H), 3.17 (s, 2H), 8.53 (s, 1H), 8.75 (s, 1H), 12.21 (s, 1H); ^{13}C NMR (126 MHz, CDCl_3) δ 42.4, 45.8, 53.4, 54.6, 62.2, 105.9, 125.0, 127.2, 131.2, 137.8, 149.8, 171.1; HRMS (ESI) m/z calculated for $\text{C}_{15}\text{H}_{22}\text{N}_6\text{O}_5$ ($\text{M}+\text{H}^+$): 367.1724, found 367.1728 (Δ -0.97 ppm).

5-Amino-6-*N,N*-dimethylamino-2-*N*-methylpiperazin-1-ylmethyl-1*H*-benzo[d]imidazole



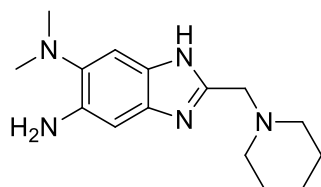
This compound was synthesized using the same procedure used to synthesize 1-*N,N*-dimethylaminomethylcarboxamido-5-*N,N*-dimethylamino-2,4-dinitro benzene. 170 mg, 45% yield; ^1H NMR (300 MHz, CDCl_3) δ 2.23 (s, 3 H), 2.39 (s, 4 H), 2.52 (s, 4 H), 2.63 (s, 6 H), 3.70 (s, 2 H), 6.78 (s, 1 H), 7.23 (s, 1 H); ^{13}C NMR (126 MHz, CDCl_3) δ 44.5, 45.9, 53.3, 53.4, 55.0, 56.4, 77.2, 95.2, 109.8, 131.0, 136.3, 138.4, 149.9;

5-*N,N*-Dimethylamino-1-piperadin-1-ylmethylcarboxamido-2,4-dinitro benzene



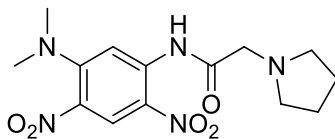
This compound was synthesized using the same procedure used to synthesize 1-*N,N*-dimethylaminomethylcarboxamido-5-*N,N*-dimethylamino-2,4-dinitro benzene. 432 mg, 93% yield; mp 152-154 °C; ¹H NMR (300 MHz, CDCl₃) δ 1.45 (br. s., 2H), 1.68 (td, *J* = 5.38, 10.91 Hz, 4H), 2.52 (br. s., 4H), 3.01 (s, 6H), 3.12 (s, 2H), 8.57 (s, 1H), 8.77 (s, 1H), 12.34 (br. s., 1H); ¹³C NMR (126 MHz, CDCl₃) δ 23.4, 25.7, 42.4, 54.9, 63.2, 105.9, 125.1, 127.2, 131.1, 137.9, 149.8, 171.9; HRMS (ESI) *m/z* calculated for C₁₅H₂₂N₆O₅ (M+H)⁺: 352.1615, found 352.1622 (Δ -1.77 ppm).

5-Amino-6-*N,N*-dimethylamino-2-piperidin-1-ylmethyl-1*H*-benzo[d]imidazole



This compound was synthesized using the same procedure used to synthesize 1-*N,N*-dimethylaminomethylcarboxamido-5-*N,N*-dimethylamino-2,4-dinitro benzene. 224 mg, 91% yield; ¹H NMR (300 MHz, CDCl₃) δ 1.46 (d, 2 H), 1.58 (m, 4 H), 2.45 (s, 4 H), 2.68 (s, 6 H), 3.68 (s, 2 H), 6.75 (s, 1 H), 7.35 (s, 1 H), 9.36 (s, 1 H); ¹³C NMR (126 MHz, CDCl₃) δ 23.6, 25.5, 44.3, 54.3, 56.9, 60.1, 98.3, 106.7, 133.0, 134.2, 137.9, 138.0, 150.2; MS (FIA) *m/z* 274.1 (M+1)⁺.

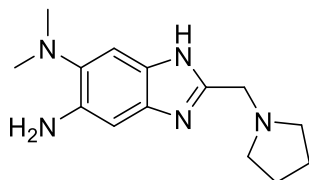
5-*N,N*-Dimethylamino-1-pyrrolidin-1-ylmethylcarboxamido-2,4-dinitro benzene



This compound was synthesized using the same procedure used to synthesize 1-*N,N*-dimethylaminomethylcarboxamido-5-*N,N*-dimethylamino-2,4-dinitro benzene. 352 mg, 79% yield; mp 94-95 °C; ¹H NMR (500 MHz, CDCl₃) δ 1.83 (br. s., 4H), 2.66 (br. s., 4H), 2.97 (s, 6H), 3.30 (s, 2H), 8.45 (s, 1H), 8.64 (s, 1H), 12.18 (s, 1H); ¹³C NMR (126 MHz, CDCl₃) δ 23.8, 42.1,

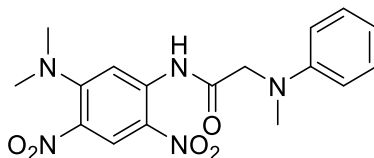
54.0, 59.1, 105.5, 124.7, 126.9, 130.8, 137.6, 149.5, 171.5; HRMS (ESI) m/z calculated for $C_{14}H_{19}N_5O_5$ ($M+H$)⁺: 338.1459, found 338.1466 (Δ -2.07 ppm).

5-Amino-6-*N,N*-dimethylamino-2-piperidin-1-ylmethyl-1*H*-benzo[d]imidazole



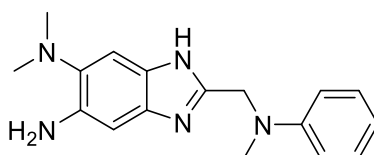
This compound was synthesized using the same procedure used to synthesize 1-*N,N*-dimethylaminomethylcarboxamido-5-*N,N*-dimethylamino-2,4-dinitro benzene. ¹H NMR (500 MHz, CDCl₃) δ ppm 1.78 (dt, $J=6.48, 3.32$ Hz, 4 H) 2.59 - 2.70 (m, 10 H) 3.88 (s, 2 H) 6.74 (s, 1 H) 7.23 (s, 1 H); ¹³C NMR (126 MHz, CDCl₃) δ 23.5, 44.5, 53.8, 54.2, 77.2, 98.2, 107.1, 133.4, 134.0, 138.3, 150.6; MS (FIA) m/z 260.1 ($M+1$)⁺.

5-*N,N*-Dimethylamino-1-(*N*-methyl-*N*-phenylamino)methylcarboxamido-2,4-dinitro benzene



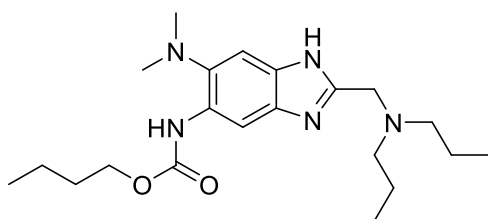
This compound was synthesized using the same procedure used to synthesize 1-*N,N*-dimethylaminomethylcarboxamido-5-*N,N*-dimethylamino-2,4-dinitro benzene. mp 142-144 °C; ¹H NMR (500 MHz, CDCl₃) δ 3.06 (s, 6 H), 3.18 (s, 3 H), 4.05 (s, 2 H), 6.78 - 6.83 (m, 2 H), 6.86 (s, 1 H), 7.23 - 7.30 (m, 2 H), 8.61 (s, 1 H), 8.78 (s, 1 H), 11.94 (s, 1 H); ¹³C NMR (126 MHz, CDCl₃) δ 40.4, 42.5, 59.9, 106.1, 113.5, 119.2, 125.1, 127.3, 129.4, 131.5, 137.7, 148.7, 150.0, 171.4; HRMS (ESI) m/z calculated for $C_{17}H_{19}N_5O_5$ ($M+H$)⁺: 374.1459, found 374.1463 (Δ -1.12 ppm).

5-Amino-6-*N,N*-dimethylamino-2-(*N*-methyl-*N*-phenylamino)methyl-1*H*-benzo[d]imidazole



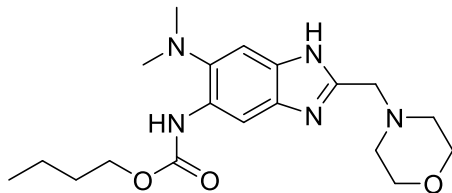
This compound was synthesized using the same procedure used to synthesize 1-*N,N*-dimethylaminomethylcarboxamido-5-*N,N*-dimethylamino-2,4-dinitro benzene. mp 120-122 °C; ¹H NMR (500 MHz, CDCl₃) δ ppm 2.66 (s, 6 H) 3.00 (s, 3 H) 4.60 (s, 2 H) 6.68 - 6.86 (m, 4 H) 7.13 - 7.26 (m, 3 H); ¹³C NMR (126 MHz, CDCl₃) δ 39.4, 44.6, 52.2, 76.9, 77.2, 77.4, 77.4, 98.6, 107.1, 113.1, 117.9, 129.4, 133.8, 138.3, 138.6, 149.5, 151.1; HRMS (ESI) *m/z* calculated for C₁₇H₂₁N₅ (M+H)⁺: 296.187, found 296.1868 (Δ 0.54 ppm).

5-Butyloxycarbonylamino-6-*N,N*-dimethylamino-2-*N,N*-dipropylaminomethyl-1*H*-benzo[d]imidazole



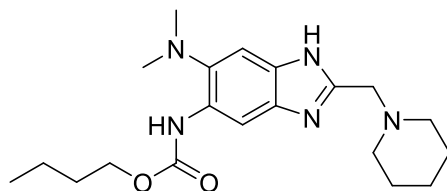
To a solution of 5-Amino-6-*N,N*-dimethylamino-2-*N,N*-dipropylaminomethyl-1*H*-benzo[d]imidazole (100 mg, 0.26 mmoles), dissolved in DCM (2 mL), was added carbonyldiimidazole (CDI) (46 mg, 0.28 mmoles). The reaction mixture was heated to reflux for 7 hours. After consumption of starting material, which was monitored by TLC, 1-butanol (26 μL, 0.28 mmoles) was added to the solution. The reaction mixture was reacted overnight under reflux. Upon completion of the reaction, the reaction mixture was diluted with DCM (30 mL) and washed thrice with water (20 mL X 3). The organic layer was collected, dried over anhydrous magnesium sulfate. The crude mixture was purified through flash column on alumina with 2% methanol in DCM as the eluent. The desired product was obtained as a light brown solid. 55 mg, 54% yield; mp 176-178 °C; ¹H NMR (500 MHz, CDCl₃) δ 0.80 (t, *J* = 7.32 Hz, 6 H), 0.89 (t, *J* = 7.48 Hz, 3 H), 1.31 - 1.48 (m, 6 H), 1.62 (quin, *J* = 7.10 Hz, 2 H), 2.30 - 2.46 (m, 4 H), 2.58 (s, 6 H), 3.75 (s, 2 H), 4.12 (t, *J* = 6.71 Hz, 2 H), 7.43 (br. s., 1 H), 8.15 (s, 1 H), 8.12 (s, 1 H), 9.52 (br. s., 1 H); ¹³C NMR (126 MHz, CDCl₃) δ 11.8, 13.8, 19.1, 20.3, 31.1, 45.6, 53.1, 56.8, 64.9, 99.4, 110.8, 129.9, 130.5, 138.6, 138.9, 154.0, 154.2; HRMS (ESI) *m/z* calculated for C₂₁H₃₅N₅O₂ (M+H)⁺: 390.2864, found 390.2864 (Δ -0.09 ppm).

5-Butyloxycarbonylamino-6-*N,N*-dimethylamino-2-*N,N*-morpholinylmethyl-1*H*-benzo[d]imidazole



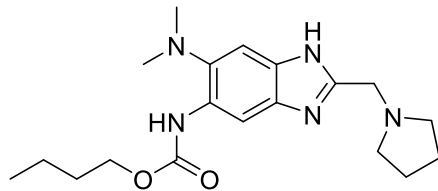
This compound was synthesized using the same procedure used to synthesize 5-Butyloxycarbonylamino-6-*N,N*-dimethylamino-2-*N,N*-dipropylaminomethyl-1*H*-benzo[d]imidazole. 74 mg, 54% yield; mp 146-147 °C; ¹H NMR (500 MHz, CDCl₃) δ 0.97 (t, *J* = 7.32 Hz, 3 H), 1.45 (dq, *J* = 14.95, 7.53 Hz, 2 H), 1.64 - 1.76 (m, 2 H), 2.45 - 2.60 (m, 4 H), 2.66 (s, 6 H), 3.54 - 3.76 (m, 4 H), 3.78 (s, 2 H), 4.20 (t, *J* = 6.71 Hz, 2 H), 7.52 (br. s., 1 H), 8.21 (br. s., 2 H), 9.72 (br. s., 1 H); ¹³C NMR (126 MHz, CDCl₃) δ 14.0, 19.3, 31.3, 45.8, 54.0, 57.1, 65.1, 67.1, 99.6, 111.2, 130.4, 131.1, 138.7, 139.1, 151.5, 154.3; HRMS (ESI) *m/z* calculated for C₁₉H₂₉N₅O₃ (M+H)⁺: 376.2343, found 376.2347 (Δ -0.89 ppm).

5-Butyloxycarbonylamino-6-*N,N*-dimethylamino-2-*N,N*-piperidinylmethyl-1*H*-benzo[d]imidazole



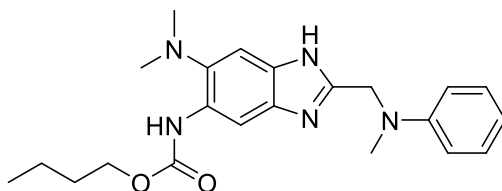
This compound was synthesized using the same procedure used to synthesize 5-Butyloxycarbonylamino-6-*N,N*-dimethylamino-2-*N,N*-dipropylaminomethyl-1*H*-benzo[d]imidazole. 86 mg, 63% yield; mp 160-161 °C; ¹H NMR (500 MHz, CDCl₃) δ 0.97 (t, *J* = 7.32 Hz, 3 H), 1.39 - 1.52 (m, 4 H), 1.59 (quin, *J* = 5.57 Hz, 4 H), 1.66 - 1.74 (m, 2 H), 2.47 (br. s., 4 H), 2.66 (s, 6 H), 3.73 (s, 2 H), 4.20 (t, *J* = 6.71 Hz, 2 H), 7.51 (br. s., 1 H), 8.20 (br. s., 1 H), 9.73 (br. s., 1 H); ¹³C NMR (126 MHz, CDCl₃) δ 13.8, 19.1, 23.9, 26.0, 31.1, 45.6, 54.9, 57.2, 64.9, 99.4, 110.9, 128.2, 129.0, 130.0, 130.8, 138.7, 152.5, 154.0; HRMS (ESI) *m/z* calculated for C₂₀H₃₁N₅O₂ (M+H)⁺: 374.2551, found 374.2551 (Δ -0.23 ppm).

5-Butyloxycarbonylamino-6-*N,N*-dimethylamino-2-*N,N*-pyrrolidinylmethyl-1*H*-benzo[d]imidazole



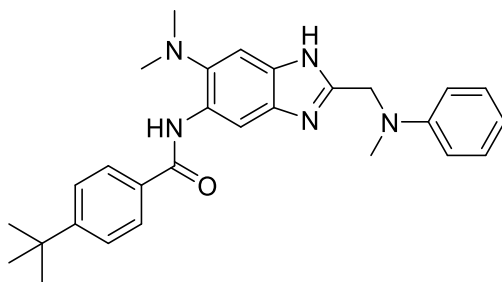
This compound was synthesized using the same procedure used to synthesize 5-Butyloxycarbonylamino-6-*N,N*-dimethylamino-2-*N,N*-dipropylaminomethyl-1*H*-benzo[d]imidazole. 58 mg, 41% yield; mp 135-137 °C; ¹H NMR (500 MHz, CDCl₃) δ 0.96 (t, *J* = 7.48 Hz, 3 H), 1.38 - 1.50 (m, 2 H), 1.63 - 1.73 (m, 2 H), 1.82 (dt, *J* = 6.56, 3.13 Hz, 4 H), 2.55 - 2.72 (m, 10 H), 3.91 (s, 2 H), 4.19 (t, *J* = 6.71 Hz, 2 H), 7.50 (br. s., 1 H), 8.18 (br. s., 2 H), 10.19 (br. s., 1 H); ¹³C NMR (126 MHz, CDCl₃) δ 14.0, 19.3, 23.9, 31.3, 45.8, 54.1, 54.6, 65.1, 99.7, 111.1, 130.1, 131.2, 139.0, 152.8, 154.2; HRMS (ESI) *m/z* calculated for C₁₉H₂₉N₅O₂ (M+H)⁺: 360.2394, found 360.2396 (Δ -0.58 ppm).

5-Butyloxycarbonylamino-6-*N,N*-dimethylamino-2-(*N*-methyl-*N*-phenylamino)methyl-1*H*-benzo[d]imidazole



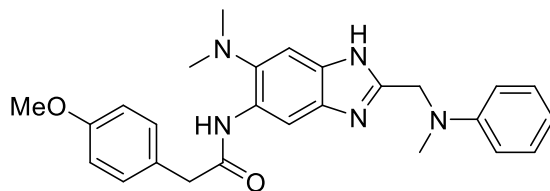
This compound was synthesized using the same procedure used to synthesize 5-Butyloxycarbonylamino-6-*N,N*-dimethylamino-2-*N,N*-dipropylaminomethyl-1*H*-benzo[d]imidazole. 79 mg, 59% yield; ¹H NMR (500 MHz, CDCl₃) δ 0.96 (t, *J* = 7.48 Hz, 3 H), 1.36 - 1.54 (m, 2 H), 1.57 - 1.77 (m, 2 H), 2.65 (s, 6 H), 3.00 (s, 3 H), 4.16 (t, *J* = 6.71 Hz, 2 H), 4.63 (s, 2 H), 6.70 - 6.87 (m, 3 H), 7.18 - 7.26 (m, 2 H), 7.45 (br. s., 1 H), 8.13 (br. s., 1 H), 8.19 (br. s., 1 H); ¹³C NMR (500 MHz, CDCl₃) δ 13.9, 19.3, 31.2, 39.7, 45.7, 52.6, 65.1, 99.9, 110.7, 113.4, 118.4, 129.6, 130.1, 131.1, 139.1, 139.3, 149.6, 152.7, 154.2; HRMS (ESI) *m/z* calculated for C₂₂H₂₉N₅O₂ (M+H)⁺: 396.2394, found 396.2395 (Δ -0.16 ppm).

5-(4-Tert-butyl)benzamido-6-*N,N*-dimethylamino-2-(*N*-methyl-*N*-phenylamino)methyl-1*H*-benzo[d]imidazole



A solution of 5-amino-6-*N,N*-dimethylamino-2-(*N*-methyl-*N*-phenylamino)methyl-1*H*-benzo[d]imidazole (100 mg, 0.34 mmoles.) and in DCM (3.0 ml) was chilled to 0 °C and 4-tert-butylbenzoyl chloride (0.30 mmoles.) was added dropwise. After addition, the reaction mixture was stirred and left to warm to room temperature. The reaction was monitored by TLC. Upon completion of the reaction, the reaction mixture was diluted with DCM (25 mL), washed with water (20 mL) thrice, and dried over anhydrous magnesium sulfate. The crude mixture was purified using flash column chromatography on silica gel with 1:2 ethyl acetate: hexanes. The pure compound was obtained as a yellow solid. 112 mg, 75% yield; mp 111-112 °C ¹H NMR (500 MHz, CDCl₃) δ ppm 1.37 (s, 9 H) 2.75 (br. s., 6 H) 3.02 (s, 3 H) 4.68 (s, 2 H) 6.76 - 6.84 (m, 3 H) 7.23 (dd, *J*=8.85, 7.32 Hz, 2 H) 7.52 (m, *J*=8.55 Hz, 2 H) 7.60 (br. s., 1 H) 7.87 (m, *J*=8.54 Hz, 2 H) 8.70 (br. s., 1 H) 9.76 (br. s., 1 H) 9.89 (br. s., 1 H); ¹³C NMR (500 MHz, CDCl₃) δ 31.2, 35.0, 39.6, 45.8, 52.6, 101.5, 110.8, 113.5, 118.4, 125.8, 126.9, 129.5, 130.0, 132.6, 139.8, 149.5, 152.9, 155.1, 165.0; HRMS (ESI) *m/z*. calculated for C₂₈H₃₃N₅O (M+H)⁺: 456.2758, found 456.2757 (Δ 0.13 ppm).

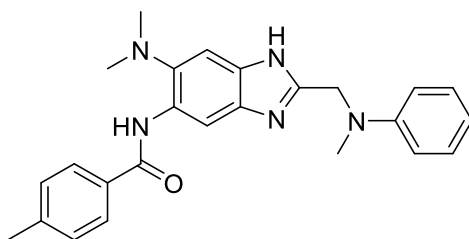
5-(4-Methoxyphenyl)ethanamido-6-*N,N*-dimethylamino-2-(*N*-methyl-*N*-phenylamino)methyl-1*H*-benzo[d]imidazole



This compound was synthesized using the same procedure used to synthesize 5-(4-Tert-butyl)benzamido-6-*N,N*-dimethylamino-2-(*N*-methyl-*N*-phenylamino)methyl-1*H*-benzo[d]imidazole. 43 mg, 29% yield; ¹H NMR (500 MHz, CDCl₃) δ ppm 2.36 (s, 6 H) 3.00 (s, 3 H) 3.66 (s, 2 H) 3.83 (s, 3 H) 4.65 (s, 2 H) 6.73 - 6.84 (m, 3 H) 6.93 (d, *J*=8.54 Hz, 2 H) 7.14 -

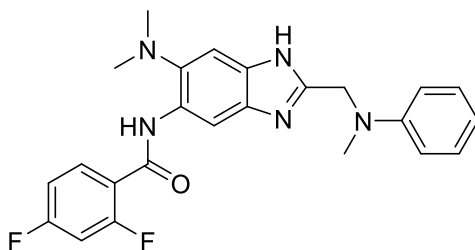
7.26 (m, 4 H) 7.38 (br. s., 1 H) 8.58 (br. s., 1 H) 8.85 (br. s., 1 H); ^{13}C NMR (500 MHz, CDCl_3) δ 39.6, 44.6, 45.4, 52.7, 55.6, 101.9, 110.0, 113.7, 114.6, 118.5, 126.9, 129.6, 129.7, 131.0, 139.6, 149.7, 153.0, 159.2, 169.8; HRMS (ESI) m/z calculated for $\text{C}_{26}\text{H}_{29}\text{N}_5\text{O}_2$ ($\text{M}+\text{H}$) $^+$: 444.2394, found 444.2374 (Δ 4.6 ppm)

5-(4-Methyl)benzamido-6-*N,N*-dimethylamino-2-(*N*-methyl-*N*-phenylamino)methyl-1*H*-benzo[d]imidazole



This compound was synthesized using the same procedure used to synthesize 5-(4-Tert-butyl)benzamido-6-*N,N*-dimethylamino-2-(*N*-methyl-*N*-phenylamino)methyl-1*H*-benzo[d]imidazole. 71 mg, 50% yield; mp 178-181 °C; ^1H NMR (500 MHz, CDCl_3) δ ppm 2.43 (s, 3 H) 2.72 (s, 6 H) 2.99 (s, 3 H) 4.64 (s, 2 H) 6.66 - 6.86 (m, 3 H) 7.12 - 7.24 (m, 2 H) 7.29 (m, $J=7.93$ Hz, 2 H) 7.51 (br. s., 1 H) 7.82 (m, $J=8.24$ Hz, 2 H) 8.72 (s, 1 H) 9.71 (br. s., 1 H); ^{13}C NMR (500 MHz, CDCl_3) δ 21.5, 39.5, 45.8, 52.4, 102.6, 109.9, 113.4, 118.2, 127.0, 129.4, 129.5, 129.7, 132.6, 139.8, 142.1, 149.5, 153.0, 165.1; HRMS (ESI) m/z calculated for $\text{C}_{25}\text{H}_{27}\text{N}_5\text{O}$ ($\text{M}+\text{H}$) $^+$: 414.2288, found 414.229 (Δ -0.29 ppm).

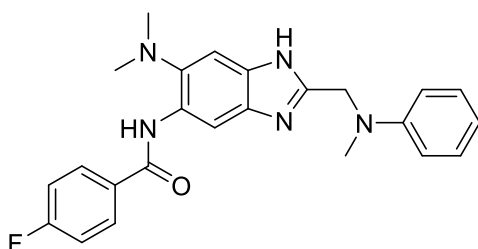
5-(2,4-Difluoro)benzamido-6-*N,N*-dimethylamino-2-(*N*-methyl-*N*-phenylamino)methyl-1*H*-benzo[d]imidazole



This compound was synthesized using the same procedure used to synthesize 5-(4-Tert-butyl)benzamido-6-*N,N*-dimethylamino-2-(*N*-methyl-*N*-phenylamino)methyl-1*H*-benzo[d]imidazole. 73 mg, 49% yield; mp 130-134 °C; ^1H NMR (500 MHz, CDCl_3) δ ppm 2.71

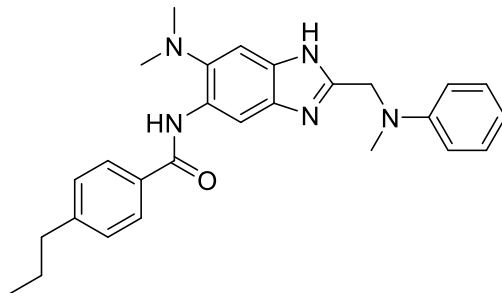
(s, 6 H) 2.98 (s, 3 H) 4.63 (s, 2 H) 6.63 - 6.82 (m, 3 H) 6.85 - 7.05 (m, 2 H) 7.18 (t, $J=7.82$ Hz, 2 H) 7.51 (br. s., 1 H) 8.07 - 8.26 (m, 1 H) 8.76 (br. s., 1 H) 10.20 (d, $J=12.48$ Hz, 1 H); ^{13}C NMR (126 MHz, CDCl_3) δ 39.3, 45.5, 52.2, 104.0, 104.2, 104.3, 104.5, 112.2, 112.2, 112.3, 112.4, 113.1, 117.9, 118.4, 118.4, 118.5, 118.5, 129.1, 129.6, 133.5, 133.6, 133.6, 133.7, 139.9, 149.3, 153.3, 159.5, 159.6, 159.9, 159.9, 161.5, 161.6, 163.6, 163.7, 165.6, 165.7; HRMS (ESI) m/z calculated for $\text{C}_{24}\text{H}_{23}\text{F}_2\text{N}_5\text{O}$ ($\text{M}+\text{H}$) $^+$: 436.1943, found 436.1946 (Δ -0.55 ppm).

6-*N,N*-Dimethylamino-5-(4-fluoro)benzamido-2-(*N*-methyl-*N*-phenylamino)methyl-1*H*-benzo[d]imidazole



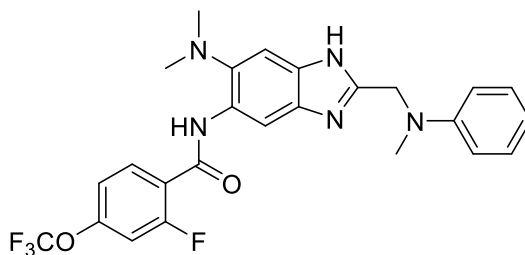
This compound was synthesized using the same procedure used to synthesize 5-(4-Tert-butyl)benzamido-6-*N,N*-dimethylamino-2-(*N*-methyl-*N*-phenylamino)methyl-1*H*-benzo[d]imidazole. 37 mg, 26% yield; ^1H NMR (500 MHz, CDCl_3) δ ppm 2.73 (s, 6 H) 3.01 (s, 3 H) 4.67 (s, 2 H) 6.74 - 6.84 (m, 3 H) 7.12 - 7.25 (m, 4 H) 7.53 (s, 1 H) 7.91 (dd, $J=8.70, 5.34$ Hz, 2 H) 8.67 (s, 1 H) 9.68 (s, 1 H); ^{13}C NMR (126 MHz, CDCl_3) δ 39.5, 45.8, 52.4, 113.4, 113.4, 115.7, 115.9, 118.3, 118.4, 129.2, 129.3, 129.3, 129.4, 129.5, 129.8, 131.5, 131.5, 139.8, 149.3, 149.4, 153.1, 163.7, 163.8, 165.7; HRMS (ESI) m/z calculated for $\text{C}_{24}\text{H}_{24}\text{FN}_5\text{O}$ ($\text{M}+\text{H}$) $^+$: 418.2038, found 418.2041 (Δ -0.88 ppm).

6-*N,N*-Dimethylamino-2-(*N*-methyl-*N*-phenylamino)methyl-5-(4-propyl)benzamido-1*H*-benzo[d]imidazole



This compound was synthesized using the same procedure used to synthesize 5-(4-Tert-butyl)benzamido-6-*N,N*-dimethylamino-2-(*N*-methyl-*N*-phenylamino)methyl-1*H*-benzo[d]imidazole. 99 mg, 66% yield; ^1H NMR (500 MHz, CDCl_3) δ 0.95 (t, $J = 7.32$ Hz, 3 H), 1.67 (sxt, $J = 7.45$ Hz, 2 H), 2.64 (t, $J = 7.63$ Hz, 2 H), 2.71 (br. s., 6 H), 2.94 (s, 3 H), 4.59 (s, 2 H), 6.65 - 6.78 (m, 3 H), 7.15 (dd, $J = 8.70, 7.17$ Hz, 2 H), 7.24 - 7.31 (m, 2 H), 7.55 (br. s., 1 H), 7.82 (d, $J = 8.24$ Hz, 2 H), 8.72 (br. s., 1 H), 9.72 (br. s., 1 H), 10.80 (br. s., 1 H); ^{13}C NMR (126 MHz, CDCl_3) δ 13.9, 24.4, 38.0, 39.6, 45.8, 52.4, 102.1, 110.7, 113.5, 118.1, 127.1, 129.0, 129.4, 129.7, 131.3, 132.9, 139.9, 146.9, 149.6, 153.2, 165.2; HRMS (ESI) m/z calculated for $\text{C}_{27}\text{H}_{31}\text{N}_5\text{O}$ ($\text{M}+\text{H}$) $^+$: 442.2601, found 442.2602 (Δ -0.12 ppm).

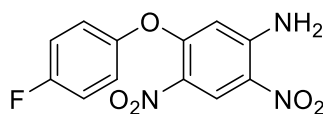
6-*N,N*-Dimethylamino-2-5-(2-fluoro-4-trifluoromethoxy)benzamido-*N*-methyl-*N*-phenylamino)methyl-1*H*-benzo[d]imidazole



A solution of 5-amino-6-*N,N*-dimethylamino-2-(*N*-methyl-*N*-phenylamino)methyl-1*H*-benzo[d]imidazole (100 mg, 0.34 mmoles.) and in DCM (4.0 ml) was added 1-ethyl-3-(3-dimethylaminopropyl)carbodiimide hydrochloride ($\text{EDC}\cdot\text{HCl}$)(78 mg, 0.41 mmoles) and *N,N*-4-dimethylaminopyridine (DMAP)(50 mg, 0.41 mmoles). After addition, the reaction mixture was stirred under reflux overnight. The reaction was monitored by TLC, and upon completion of the reaction, the reaction mixture was diluted with DCM (30 mL), washed thrice with water (20 mL X 3), and dried over anhydrous magnesium sulfate. The crude mixture was purified using flash column chromatography on silica gel with 1:2 ethyl acetate: hexanes. The pure compound was

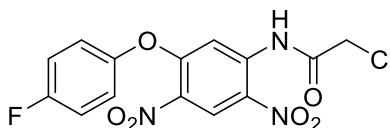
obtained as a beige solid. 124 mg, 73% yield; mp 73-75 °C; ¹H NMR (500 MHz, CDCl₃) δ 2.72 (s, 6 H), 2.99 (s, 3 H), 4.66 (s, 2 H), 6.73 - 6.80 (m, 3 H), 7.07 (d, *J* = 11.90 Hz, 1 H), 7.14 (d, *J* = 8.85 Hz, 1 H), 7.17 - 7.23 (m, 2 H), 7.52 (s, 1 H), 8.20 (t, *J* = 8.85 Hz, 1 H), 8.75 (s, 1 H), 10.23 (d, *J* = 12.51 Hz, 1 H); ¹³C NMR (126 MHz, CDCl₃) δ 39.4, 45.6, 52.3, 103.7, 108.7, 108.9, 109.2, 113.3, 116.7, 117.1, 118.3, 119.1, 120.5, 120.6, 121.2, 123.2, 129.4, 129.8, 132.5, 133.5, 133.5, 137.7, 140.1, 149.3, 151.8, 151.9, 153.2, 159.2, 159.6, 159.7, 161.2; HRMS (ESI) *m/z* calculated for C₂₅H₂₃F₄N₅O₂ (M+H)⁺: 502.1861, found 502.1859 (Δ 0.23 ppm).

5-(4-Fluorophenoxy)-2,4-dinitro aniline



To a solution of 2,4-dinitro-5-fluoroaniline in acetone was added 4-fluorophenol and potassium carbonate. The reaction mixture was stirred at room temperature overnight. The reaction was monitored by TLC. Upon completion of the reaction, the solvent was evaporated using a rotary evaporator. The resulting solid was washed with water, filtered, and washed thrice more with water, and the compound was lyophilized to afford a yellow solid. 7.0 g, 90% yield; ¹H NMR (300 MHz, CDCl₃) δ 6.00 (s, 1 H), 6.44 (s, 2 H), 7.09-7.20 (m, 4 H), 9.05 (s, 1 H). The analytical data was consistent with literature values.³⁴

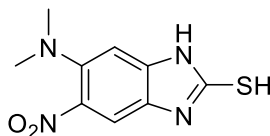
1-Chloromethylcarboxamido-5-(4-fluorophenoxy)-2,4-dinitro benzene



A solution of 5-(4-fluorophenoxy)-2,4-dinitro aniline (2.00 g, 6.40 mmol.) and TEA (777 mg, 7.68 mmol.) in DCM (7 ml) was chilled to 0 °C and chloro acetylchloride (867 mg, 7.68 mmol.) was added dropwise. After addition, the reaction mixture was heated to reflux and stirred overnight. The reaction mixture diluted with DCM (50 mL), washed with water (50 mL) thrice, and dried over anhydrous magnesium sulfate. The crude mixture was purified using flash column chromatography on silica gel with 1:1 ethyl acetate: hexanes. The pure compound was obtained as a yellow solid. 2.32 g, 93% yield; ¹H NMR (500 MHz, CDCl₃) δ ppm 4.18 (s, 2 H) 7.06 - 7.24 (m, 4 H) 8.47 (s, 1 H) 9.07 (s, 1 H) 11.73 (br. s, 1 H); ¹³C NMR (126 MHz, CDCl₃) δ 43.09, 108.8,

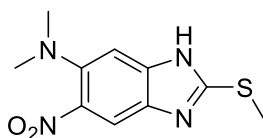
117.5, 117.7, 122.5, 122.6, 125.7, 129.5, 133.9, 138.9, 149.0, 149.0, 157.7, 159.8, 161.8, 166.1;
MS (FIA) m/z (M+1)⁺.

6-*N,N*-Dimethylamino-5-nitro -2-thio-1*H*-benzo[d]imidazole



To a solution of 1,2-Diamino-4-*N,N*-dimethylamino-5-nitro benzene (1.0 g, 5.09 mmol.) in THF (10 mL) and methanol (10mL) was added carbon disulfide (776 mg, 10.19 mmol.) and TEA (1.03 g, 10.19 mmol.). The reaction mixture was heated to 50 °C for 4 hours. The reaction is complete when a red solid crashes out of solution and the reaction mixture is clear and colorless. The reaction mixture is monitored by FIA to ensure all starting material is consumed. The solvent was evaporated off in a rotary evaporator, giving a red solid. The solid was washed with water (20 mL), filtered, and washed with more water (20 mL X3). After the water washes, the solid was rinsed with methanol (10 mL). The solid was allowed to dry in air overnight, and under vacuum the next day. 980 mg, 76% yield; ¹H NMR (500 MHz, DMSO) δ 6.55 (s, 1H), 7.31 (s, 1H), 12.40 (br. s., 1H), 12.48 (br. s., 1H); ¹³C NMR (126 MHz, DMSO) δ 39.8, 39.9, 43.3, 98.7, 106.7, 125.4, 136.1, 136.1, 136.8, 144.2, 171.2 MS (FIA) m/z 239.1 (M+1)⁺.

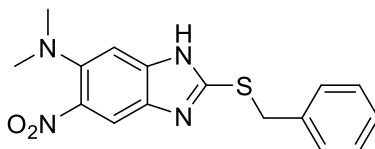
6-*N,N*-Dimethylamino-2-(methylthio)-5-nitro-1*H*-benzo[d]imidazole



To 6-*N,N*-dimethylamino-5-nitro -2-thio-1*H*-benzo[d]imidazole (500 mg, 2.1 mmol.) was added water (5 mL), ethanol (5 mL), and potassium hydroxide (318 mg, 5.67 mmol.) resulting in a red-black solution. Methyl iodide (301 mg, 2.12 mmol.) was added to the reaction mixture, and the reaction mixture was allowed to stir at room temperature overnight. The reaction was monitored by FIA for the consumption of starting material. The reaction mixture was diluted with water (30 mL) and extracted with DCM (30 mL X3) and dried over anhydrous magnesium sulfate. The crude mixture was purified using flash column chromatography on silica gel with 1:1 ethyl acetate: hexanes. The pure compound was obtained as a red solid. 444 mg, 84% yield; ¹H NMR (500

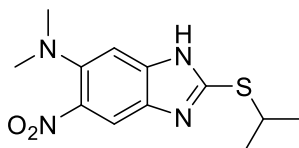
MHz, CDCl₃) δ 2.60 (s, 6 H), 2.66 (s, 3 H), 6.79 (s, 1 H), 7.22 (s, 1 H); ¹³C NMR (126 MHz, CDCl₃) δ 15.17, 44.42, 98.40, 105.8, 134.0, 135.6, 137.7, 138.1, 149.2; HRMS (ESI) m/z calculated for C₁₀H₁₂N₄O₂S (M+H)⁺: 253.0754, found 253.0756 (Δ -1.01 ppm).

2-(Benzylthio)-6-*N,N*-dimethylamino-5-nitro-1*H*-benzo[d]imidazole



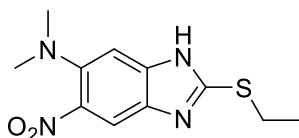
This compound was synthesized using the same procedure used to synthesize 6-*N,N*-Dimethylamino-2-(methylthio)-5-nitro-1*H*-benzo[d]imidazole. 334 mg, 83% yield; ¹H NMR (500 MHz, CDCl₃) δ 2.81 (s, 6 H), 4.54 (s, 2 H), 7.12 (s, 1 H), 7.23-7.37 (m, 5 H), 8.05 (s, 1 H); ¹³C NMR (126 MHz, CDCl₃) δ 37.11, 44.01, 102.6, 113.4, 127.9, 128.8, 128.9, 136.1, 138.4, 144.2, 154.3, 155.9; HRMS (ESI) m/z calculated for C₁₆H₁₆N₄O₂S (M+H)⁺: 329.1067, found 367.1072 (Δ -1.46 ppm); MS (FIA) m/z 209.1 (M+1)⁺.

6-*N,N*-Dimethylamino-2-(isopropylthio)-5-nitro-1*H*-benzo[d]imidazole



This compound was synthesized using the same procedure used to synthesize 6-*N,N*-Dimethylamino-2-(methylthio)-5-nitro-1*H*-benzo[d]imidazole. 68 mg, 58% yield; ¹H NMR (500 MHz, CDCl₃) δ 1.41 (d, 6 H, J 6.8 Hz), 2.81 (s, 6 H), 4.01 (p, 1 H, J 6.75 Hz), 7.17 (s, 1 H), 8.11 (s, 1 H); ¹³C NMR (126 MHz, CDCl₃) δ 23.65, 39.12, 44.25, 103.2, 113.4, 134.0, 138.6, 143.0, 144.3, 154.4; MS (FIA) m/z 281.1 (M+1)⁺.

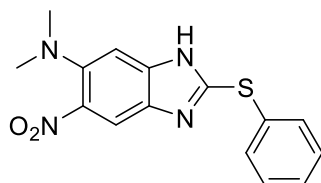
6-*N,N*-Dimethylamino-2-(ethylthio)-5-nitro-1*H*-benzo[d]imidazole



This compound was synthesized using the same procedure used to synthesize 6-*N,N*-dimethylamino-2-(methylthio)-5-nitro-1*H*-benzo[d]imidazole. 230 mg, 69% yield; ¹H NMR (500

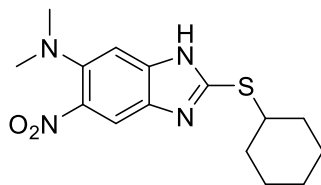
MHz, CDCl₃) δ 1.42 (t, 3 H, J 7.38 Hz), 2.80 (s, 6 H), 3.31 (q, 2 H, J 7.37 Hz), 7.12 (s, 1 H), 8.04 (s, 1 H); ¹³C NMR (126 MHz, CDCl₃) δ 14.92, 26.96, 44.10, 102.9, 112.9, 133.5, 138.2, 142.8, 144.2, 155.2; HRMS (ESI) *m/z* calculated for C₁₁H₁₄N₄O₂S (M+H)⁺: 267.091, found 267.0916 (Δ -1.99 ppm).

6-*N,N*-Dimethylamino-5-nitro-2-(phenylthio)-1*H*-benzo[d]imidazole



To a solution of 6-*N,N*-dimethylamino-5-nitro-2-thio-1*H*-benzo[d]imidazole (100 mg, 0.4 mmole.) in dimethylformamide (2 mL) was added iodobenzene (81.6 mg, 0.4 mmol.), cuprous iodide (7.6 mg, 0.04 mmol.), 1,10-phenanthroline (7.2 mg, 0.04 mmol.), and potassium carbonate (110 mg, 0.8 mmol.). The reaction mixture was heated in a pressure vessel for 22 hours at 140 °C. The reaction was monitored by FIA. Upon completion of the reaction, the reaction mixture was diluted with ethyl acetate (40 mL) and washed thrice with brine (80 mL) and thrice with water (80 mL), and dried over anhydrous magnesium sulfate. The crude mixture was purified using flash column chromatography on silica gel and 1:3 ethyl acetate: hexanes. The pure compound was obtained as a red solid. 41 mg, 31% yield; ¹H NMR (500 MHz, CDCl₃) δ 2.79 (s, 6 H), 7.05 (s, 1 H), 7.27-7.29 (m, 3 H), 7.45-7.54 (m, 2 H), 7.89 (s, 1 H); ¹³C NMR (126 MHz, CDCl₃) δ 44.12, 100.4, 116.8, 128.7, 129.7, 129.8, 130.1, 133.8, 134.9, 139.0, 144.3; MS (FIA) *m/z* 315.1 (M+1)⁺.

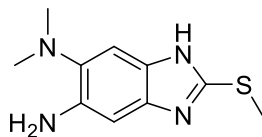
6-*N,N*-Dimethylamino-5-nitro-2-(cyclohexylthio)-1*H*-benzo[d]imidazole



This compound was synthesized using the same procedure used to synthesize 6-*N,N*-dimethylamino-2-(methylthio)-5-nitro-1*H*-benzo[d]imidazole. 310 mg, 58% yield; ¹H NMR (500 MHz, CDCl₃) δ 1.21 - 1.44 (m, 3 H), 1.46 - 1.65 (m, 3 H), 1.74 (dt, *J* = 13.28, 3.89 Hz, 2 H), 2.04 - 2.18 (m, 2 H), 2.83 (s, 6 H), 3.73 - 3.96 (m, 1 H), 7.16 (br. s., 1 H), 8.07 (br. s., 1 H); ¹³C NMR

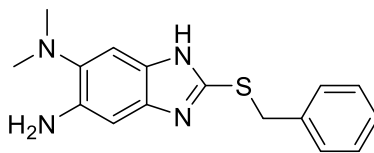
(126 MHz, CDCl₃) δ 154.3, 144.1, 142.4, 138.3, 133.7, 113.2, 102.6, 46.6, 44.0, 33.4, 25.6, 25.3; HRMS (ESI) m/z calculated for C₁₅H₂₀N₄O₂S (M+H)⁺: 321.138, found 321.1385 (Δ -1.57 ppm).

5-Amino-6-*N,N*-dimethylamino-2-(methylthio)-1*H*-benzo[d]imidazole



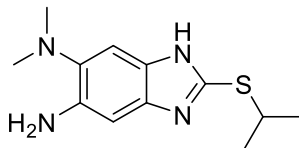
To a solution of 6-*N,N*-dimethylamino-2-(methylthio)-5-nitro-1*H*-benzo[d]imidazole (444 mg 1.8 mmol.), dissolved in ethanol (10 mL), was added solid stannous chloride dehydrate (1.42 g, 6.3 mmol.). The reaction mixture was refluxed for 3 hours. The reaction was monitored by TLC for the consumption of starting material. After completion of the reaction, the reaction mixture was diluted with water (100 mL), and solid sodium carbonate was added until the solution was basic. The reaction mixture was extracted thrice with DCM (50 mL) and dried over anhydrous magnesium sulfate. The crude mixture was purified using flash column chromatography on alumina using a 1.5% methanol/ DMC solution. The pure compound was obtained as a beige solid. 315 mg, 81% yield; ¹H NMR (500 MHz, CDCl₃) δ 2.60 (s, 6 H), 2.66 (s, 3 H), 6.79 (s, 1 H), 7.22 (s, 1 H); ¹³C NMR (126 MHz, CDCl₃) δ 15.17, 44.42, 98.40, 105.8, 134.0, 135.6, 137.7, 138.1, 149.2; MS (FIA) m/z 223.1 (M+1)⁺.

5-Amino-2-(benzylthio)-6-*N,N*-dimethylamino-1*H*-benzo[d]imidazole



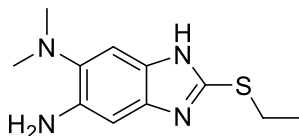
This compound was synthesized using the same procedure used to synthesize 5-amino-6-*N,N*-dimethylamino-2-(methylthio)-1*H*-benzo[d]imidazole. 265 mg, 87% yield; ¹H NMR (500 MHz, CDCl₃) δ 2.59 (s, 6 H), 4.41 (s, 2 H), 1.17 (s, 1 H), 7.15-7.23 (m, 5 H), 7.28 (s, 1 H); ¹³C NMR (126 MHz, CDCl₃) δ 37.93, 44.30, 98.30, 106.1, 127.2, 128.4, 128.7, 133.8, 135.2, 136.7, 138.0, 138.4, 146.7.

5-Amino-6-*N,N*-dimethylamino-2-(isopropylthio)-1*H*-benzo[d]imidazole



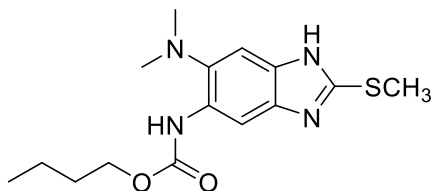
This compound was synthesized using the same procedure used to synthesize 5-amino-6-*N,N*-dimethylamino-2-(methylthio)-1*H*-benzo[d]imidazole. 272 mg, 87% yield; ¹H NMR (500 MHz, CDCl₃) δ 1.32 (d, 6 H, J 5.15 Hz), 2.63 (s, 6 H), 3.87 (s, 1 H), 6.86 (s, 1 H), 7.33 (s, 1 H); ¹³C NMR (126 MHz, CDCl₃) δ 23.43, 38.93, 44.45, 98.42, 106.3, 134.1, 135.5, 138.0, 138.4, 146.4; MS (FIA) *m/z* 251.1 (M+1)⁺.

5-Amino-6-*N,N*-dimethylamino-2-(ethylthio)-1*H*-benzo[d]imidazole



This compound was synthesized using the same procedure used to synthesize 5-amino-6-*N,N*-dimethylamino-2-(methylthio)-1*H*-benzo[d]imidazole. 241 mg, 89% yield; ¹H NMR (500 MHz, CDCl₃) δ 1.35 (t, 3 H, J 7.38), 2.63 (s, 6 H), 3.22 (q, 2 H, J 7.37), 6.84 (s, 1 H), 7.29 (s, 1H); ¹³C NMR (126 MHz, CDCl₃) δ 14.91, 27.38, 44.34, 98.29, 106.0, 134.0, 135.5, 137.7, 138.1, 147.4; MS (FIA) *m/z* 237.1 (M+1)⁺.

5-Butyloxycarbonylamino-6-*N,N*-dimethylamino-2-(methylthio)-1*H*-benzo[d]imidazole



To a solution of 5-Amino-6-*N,N*-dimethylamino-2-(methylthio)-1*H*-benzo[d]imidazole (100 mg, 0.45 mmoles), dissolved in DCM (2 mL), was added carbonyldiimidazole (CDI) (87 mg, 0.54 mmoles). The reaction mixture was heated to reflux for 7 hours. After consumption of starting material, which was monitored by TLC, 1-butanol (50 μL, 0.54 mmoles) was added to the solution. The reaction mixture was reacted overnight under reflux. Upon completion of the reaction, the reaction mixture was diluted with DCM (50 mL) and washed thrice with water (50 mL X 3). The organic layer was collected, dried over anhydrous magnesium sulfate. The crude mixture was

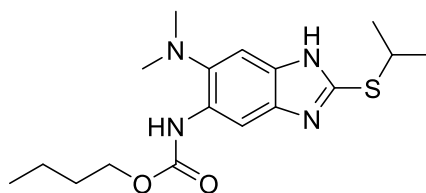
purified through flash column on silica gel with 2:1 hexanes: ethyl acetate. The desired product was obtained as a white solid. 96 mg, 66% yield; mp 159-160 °C; ¹H NMR (500 MHz, CDCl₃) δ 0.97 (t, *J* = 7.32 Hz, 3 H), 1.34 - 1.55 (m, 2 H), 1.58 - 1.82 (m, 2 H), 2.64 (br. s., 6 H), 2.72 (s, 3 H), 4.28 (br. s., 2 H), 7.52 (br. s., 1 H), 8.30 (s, 1 H), 8.28 (s, 1 H), 11.30 (br. s., 1 H); ¹³C NMR (126 MHz, CDCl₃) δ 13.7, 14.8, 19.1, 30.9, 45.6, 65.3, 99.2, 109.7, 129.1, 132.7, 138.4, 139.3, 150.8, 154.4; HRMS (ESI) *m/z* calculated for C₁₅H₂₂N₄O₂S (M+H)⁺: 323.1536, found 323.1533 (Δ 0.86 ppm).

5-Butyloxycarbonylamino-6-*N,N*-dimethylamino-2-(benzylthio)-1*H*-benzo[d]imidazole



This compound was synthesized using the same procedure used to synthesize 5-Butyloxycarbonylamino-6-*N,N*-dimethylamino-2-(methylthio)-1*H*-benzo[d]imidazole. 104 mg, 77% yield; mp 126-127 °C; ¹H NMR (500 MHz, CDCl₃) δ 0.95 (t, *J* = 7.32 Hz, 3 H), 1.43 (dq, *J* = 15.03, 7.40 Hz, 2 H), 1.57 - 1.78 (m, 2 H), 2.66 (s, 6 H), 4.26 (t, *J* = 6.71 Hz, 2 H), 4.52 (s, 2 H), 7.20 - 7.31 (m, 3 H), 7.32 - 7.40 (m, 2 H), 7.56 (br. s., 1 H), 8.30 (br. s., 2 H), 10.84 (br. s., 1 H); ¹³C NMR (126 MHz, CDCl₃) δ 13.7, 19.1, 30.9, 37.4, 45.6, 65.3, 99.2, 110.0, 127.5, 128.6, 128.9, 129.4, 132.4, 136.8, 138.7, 139.4, 149.0, 154.3; HRMS (ESI) *m/z* calculated for C₂₁H₂₆N₄O₂S (M+H)⁺: 399.1849, found 399.1848 (Δ 0.25 ppm).

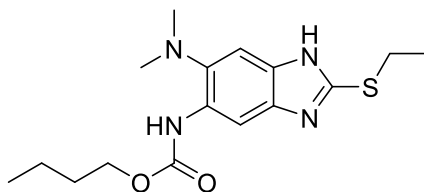
5-Butyloxycarbonylamino-6-*N,N*-dimethylamino-2-(isopropylthio)-1*H*-benzo[d]imidazole



This compound was synthesized using the same procedure used to synthesize 5-Butyloxycarbonylamino-6-*N,N*-dimethylamino-2-(methylthio)-1*H*-benzo[d]imidazole. 88 mg, 62% yield; mp 165-166 °C; ¹H NMR (500 MHz, CDCl₃) δ 0.98 (t, *J* = 7.32 Hz, 3 H), 1.39 (d, *J* = 7.02 Hz, 6 H), 1.43 - 1.54 (m, 2 H), 1.72 (quin, *J* = 7.10 Hz, 2 H), 2.65 (s, 6 H), 3.94 (dt, *J* = 13.43,

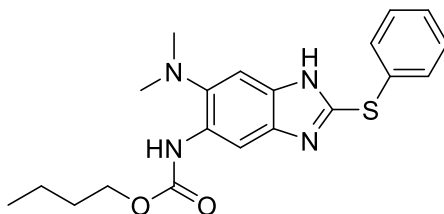
6.71 Hz, 1 H), 4.30 (t, $J = 6.41$ Hz, 2 H), 7.53 (br. s., 1 H), 8.32 (br. s., 2 H), 11.05 (br. s., 1 H); ^{13}C NMR (126 MHz, CDCl_3) δ 13.8, 19.2, 23.6, 31.0, 38.9, 45.7, 65.4, 76.8, 77.1, 77.3, 99.3, 110.1, 129.5, 132.2, 138.8, 139.9, 148.7, 154.4; HRMS (ESI) m/z calculated for $\text{C}_{17}\text{H}_{26}\text{N}_4\text{O}_2\text{S}$ ($\text{M}+\text{H}$) $^+$: 351.1849, found 351.1846 (Δ 0.79 ppm).

5-Butyloxycarbonylamino-6-*N,N*-dimethylamino-2-(ethylthio)-1*H*-benzo[d]imidazole



This compound was synthesized using the same procedure used to synthesize 5-Butyloxycarbonylamino-6-*N,N*-dimethylamino-2-(methylthio)-1*H*-benzo[d]imidazole. 108 mg, 76% yield; mp 136-138 °C; ^1H NMR (500 MHz, CDCl_3) δ 0.98 (t, $J = 7.17$ Hz, 3 H), 1.40 (t, $J = 7.48$ Hz, 3 H), 1.47 (dq, $J = 14.61, 7.24$ Hz, 2 H), 1.62 - 1.81 (m, 2 H), 2.65 (s, 6 H), 3.28 (q, $J = 7.43$ Hz, 2 H), 4.29 (br. s., 2 H), 7.53 (br. s., 1 H), 8.30 (br. s., 2 H), 10.96 (br. s., 1 H); ^{13}C NMR (126 MHz, CDCl_3) δ 13.8, 15.0, 19.1, 27.1, 31.0, 45.6, 65.4, 99.2, 109.9, 129.2, 132.4, 138.5, 139.5, 149.5, 154.4; HRMS (ESI) m/z calculated for $\text{C}_{16}\text{H}_{24}\text{N}_4\text{O}_2\text{S}$ ($\text{M}+\text{H}$) $^+$: 337.1693, found 337.1692 (Δ 0.35 ppm).

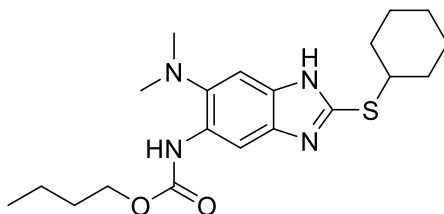
5-Butyloxycarbonylamino-6-*N,N*-dimethylamino-2-(phenylthio)-1*H*-benzo[d]imidazole



This compound was synthesized using the same procedure used to synthesize 5-Butyloxycarbonylamino-6-*N,N*-dimethylamino-2-(methylthio)-1*H*-benzo[d]imidazole. 103 mg, 77% yield; mp 172-173 °C; ^1H NMR (500 MHz, CDCl_3) δ 0.95 (t, $J = 7.32$ Hz, 3 H), 1.33 - 1.51 (m, 2 H), 1.57 - 1.77 (m, 2 H), 2.63 (s, 6 H), 4.21 (t, $J = 6.71$ Hz, 2 H), 7.14 - 7.25 (m, 3 H), 7.39 (dd, $J = 8.09, 1.37$ Hz, 2 H), 7.45 (br. s., 1 H), 8.20 (br. s., 1 H), 8.28 (br. s., 1 H); ^{13}C NMR (126 MHz, CDCl_3) δ 13.7, 19.1, 30.9, 45.4, 65.1, 77.2, 127.9, 129.3, 130.0, 131.2, 131.8, 139.2, 146.4,

154.2; HRMS (ESI) m/z calculated for $C_{20}H_{24}N_4O_2S$ ($M+H$)⁺: 385.1693, found 385.1691 (Δ 0.52 ppm).

5-Butyloxycarbonylamino-2-(cyclohexylthio)-6-*N,N*-dimethylamino-1*H*-benzo[d]imidazole



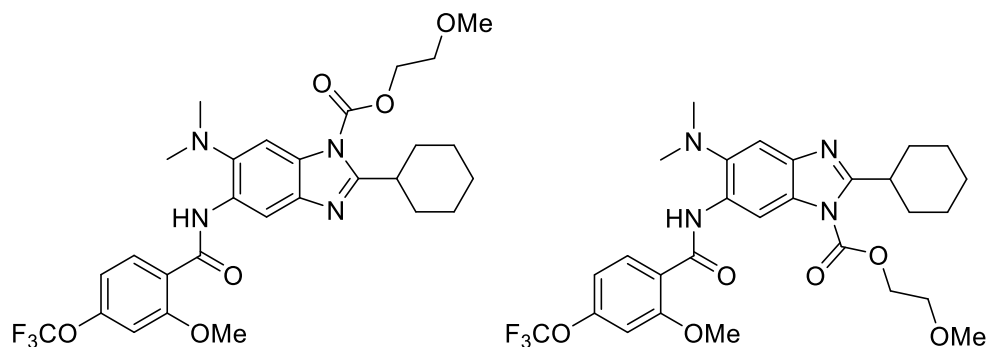
This compound was synthesized using the same procedure used to synthesize 5-Butyloxycarbonylamino-6-*N,N*-dimethylamino-2-(methylthio)-1*H*-benzo[d]imidazole. 97 mg, 73% yield; mp 129-132 °C; ¹H NMR (500 MHz, CDCl₃) δ 0.98 (t, J = 7.32 Hz, 3 H), 1.19 - 1.31 (m, 1 H), 1.31 - 1.42 (m, 2 H), 1.42 - 1.53 (m, 4 H), 1.58 (dt, J = 8.39, 4.04 Hz, 1 H), 1.66 - 1.80 (m, 4 H), 2.01 - 2.15 (m, 2 H), 2.66 (s, 6 H), 3.65 - 3.81 (m, 1 H), 4.30 (br. s., 2 H), 7.54 (br. s., 1 H), 8.29 (br. s., 2 H), 10.55 (br. s., 1 H); ¹³C NMR (126 MHz, CDCl₃) δ 13.8, 19.1, 25.5, 25.8, 31.0, 33.6, 45.6, 46.7, 65.3, 99.1, 110.2, 129.5, 132.1, 138.6, 139.6, 148.3, 154.4; HRMS (ESI) m/z calculated for $C_{20}H_{30}N_4O_2S$ ($M+H$)⁺: 391.2162, found 391.2161 (Δ 0.23 ppm).

5-Butyloxycarbonylamino-2-(cyclohexylmethylthio)-6-*N,N*-dimethylamino-1*H*-benzo[d]imidazole



This compound was synthesized using the same procedure used to synthesize 5-Butyloxycarbonylamino-6-*N,N*-dimethylamino-2-(methylthio)-1*H*-benzo[d]imidazole. 81 mg, 61% yield; 109-110 °C; ¹H NMR (500 MHz, CDCl₃) δ 0.91 - 1.06 (m, 5 H), 1.07 - 1.29 (m, 3 H), 1.37 - 1.55 (m, 2 H), 1.56 - 1.79 (m, 6 H), 1.85 (d, J = 13.12 Hz, 2 H), 2.59 (br. s., 1 H), 2.65 (s, 5 H), 3.22 (d, J = 7.02 Hz, 2 H), 4.31 (t, J = 6.56 Hz, 2 H), 7.52 (s, 1 H), 8.27 (br. s., 1 H), 8.31 (br. s., 1 H), 10.81 (br. s., 1 H); ¹³C NMR (126 MHz, CDCl₃) δ 13.8, 19.1, 25.9, 26.2, 31.0, 32.5, 37.7, 39.7, 45.6, 65.4, 99.1, 109.8, 129.1, 132.4, 138.4, 139.4, 150.3, 154.4; HRMS (ESI) m/z calculated for $C_{21}H_{32}N_4O_2S$ ($M+H$)⁺: 405.2319, found 405.2317 (Δ 0.43 ppm).

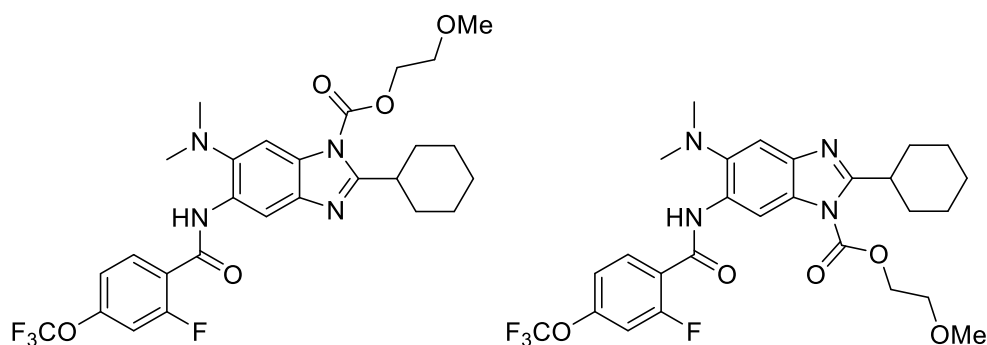
2-Cyclohexyl-6-*N,N*-dimethylamino-5-(2-methoxy-4-trifluoromethoxy)benzamido-1-(2-methoxyethoxy)carbonyl-1*H*-benzo[d]imidazole and **2-Cyclohexyl-6-*N,N*-dimethylamino-5-(2-methoxy-4-trifluoromethoxy)benzamido-3-(2-methoxyethoxy)carbonyl-1*H*-benzo[d]imidazole**



To a solution of 2-Cyclohexyl-5-(2-methoxy-4-trifluoromethoxy)benzamido-6-*N,N*-dimethylamino-1*H*-benzo[d]imidazole (120 mg, 0.25 mmoles), in DCM (10 mL) and chilled in an ice bath, was slowly added 2-methoxyethyl chloroformate (28 μ L, 0.24 mmoles) and triethylamine (33 μ L, 0.24 mmoles). The reaction mixture was allowed to warm up to room temperature and was stirred overnight. The reaction was monitored by TLC. Upon completion, the reaction mixture was diluted with DCM, washed thrice with water, and dried over magnesium sulfate. The crude mixture was purified by flash column on silica gel with 1.5% methanol in DCM as the eluent. Two regioisomers were obtained as a white solids. 87 mg, 63% yield; mp 159-161 $^{\circ}$ C; ^1H NMR (500 MHz, CDCl_3) δ 1.33 (qt, $J = 12.72, 3.51$ Hz, 1 H), 1.39 - 1.51 (m, 2 H), 1.69 (qd, $J = 12.41, 3.05$ Hz, 2 H), 1.78 (d, $J = 12.51$ Hz, 1 H), 1.83 - 1.93 (m, 2 H), 2.12 (d, $J = 12.21$ Hz, 2 H), 2.75 (s, 6 H), 3.41 - 3.65 (m, 4 H), 3.86 - 4.01 (m, 2 H), 4.08 (s, 3 H), 4.58 - 4.73 (m, 2 H), 6.88 (s, 1 H), 6.93 - 7.08 (m, 1 H), 7.58 (s, 1 H), 8.39 (d, $J = 8.55$ Hz, 1 H), 9.31 (s, 1 H), 11.02 (s, 1 H); ^{13}C NMR (126 MHz, CDCl_3) δ 26.1, 26.3, 31.9, 38.6, 45.4, 56.1, 59.1, 66.7, 69.8, 99.9, 104.3, 106.9, 110.8, 112.8, 117.2, 119.3, 121.1, 121.3, 123.4, 129.8, 131.6, 134.0, 138.2, 141.3, 150.5, 152.3, 158.1, 160.9, 161.5; 45 mg, 32% yield; ^1H NMR (500 MHz, CDCl_3) δ 1.25 - 1.49 (m, 3 H), 1.60 - 1.83 (m, 3 H), 1.83 - 2.00 (m, 2 H), 2.10 (d, $J = 11.90$ Hz, 2 H), 2.77 (s, 6 H), 3.40 - 3.61 (m, 4 H), 3.73 - 3.93 (m, 2 H), 4.06 (s, 3 H), 4.50 - 4.74 (m, 2 H), 6.70 - 6.93 (m, 1 H), 6.93 - 7.08 (m, 1 H), 7.89 (s, 1 H), 8.39 (d, $J = 8.55$ Hz, 1 H), 9.01 (s, 1 H), 10.93 (s, 1 H); ^{13}C NMR (126 MHz, CDCl_3) δ 26.0, 26.4, 31.9, 38.8, 45.5, 56.1, 59.0, 66.2, 70.1, 76.8, 77.0, 77.3, 104.2, 107.3, 111.0,

112.8, 117.3, 119.3, 121.2, 123.4, 128.8, 129.8, 131.6, 134.3, 138.3, 139.4, 141.2, 150.4, 152.2, 152.3, 152.3, 158.1, 160.6, 161.6; HRMS (ESI) m/z calculated for $C_{28}H_{33}N_4O_6$ ($M+H$)⁺: 579.2425, found 579.2427 (Δ -0.43 ppm).

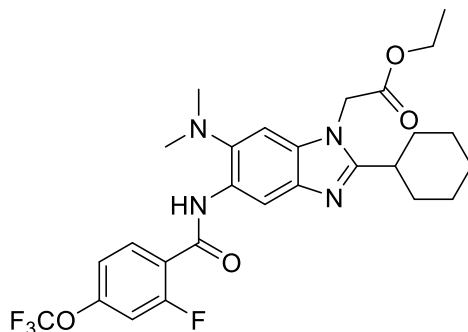
2-Cyclohexyl-6-*N,N*-dimethylamino-5-(2-fluoro-4-trifluoromethoxy)benzamido-1-(2-methoxyethoxy)carbonyl-1*H*-benzo[d]imidazole and 2-Cyclohexyl-6-*N,N*-dimethylamino-5-(2-fluoro-4-trifluoromethoxy)benzamido-3-(2-methoxyethoxy)carbonyl-1*H*-benzo[d]imidazole



This compound was synthesized using the same procedure used to synthesize 2-Cyclohexyl-6-*N,N*-dimethylamino-5-(2-methoxy-4-trifluoromethoxy)benzamido-1-(2-methoxyethoxy)carbonyl-1*H*-benzo[d]imidazole. 84 mg, 74% yield; ¹H NMR (500 MHz, CDCl₃) δ 2.72 (s, 6 H), 3.52 (s, 3 H), 3.57 (tt, J = 11.60, 3.20 Hz, 1 H), 3.86 - 4.01 (m, 2 H), 4.53 - 4.76 (m, 2 H), 6.99 - 7.16 (m, 1 H), 7.19 (d, J = 8.55 Hz, 1 H), 7.60 (s, 1 H), 8.27 (t, J = 8.70 Hz, 1 H), 9.25 (s, 1 H), 10.11 (d, J = 12.51 Hz, 1 H); ¹³C NMR (126 MHz, CDCl₃) δ 26.0, 26.3, 31.8, 38.6, 45.4, 59.0, 66.8, 69.8, 77.2, 99.9, 106.6, 108.7, 108.9, 111.2, 116.8, 119.1, 120.7, 120.8, 121.2, 123.3, 129.8, 130.9, 133.6, 133.6, 138.5, 141.2, 150.4, 151.8, 151.9, 159.3, 159.5, 159.5, 161.1, 161.3; HRMS (ESI) m/z calculated for $C_{27}H_{30}F_4N_4O_5$ ($M+H$)⁺: 567.2225, found 567.2228 (Δ -0.48 ppm). 14 mg, 12% yield; ¹H NMR (500 MHz, CDCl₃) δ 1.31 - 1.54 (m, 4 H), 1.65 (br. s., 2 H), 1.68 - 1.83 (m, 3 H), 1.83 - 1.95 (m, 2 H), 2.11 (d, J = 11.90 Hz, 2 H), 2.66 - 2.81 (m, 6 H), 3.43 - 3.63 (m, 4 H), 3.76 - 3.87 (m, 2 H), 4.57 - 4.69 (m, 2 H), 7.01 - 7.13 (m, 1 H), 7.18 (d, J = 8.55 Hz, 1 H), 7.93 (s, 1 H), 8.30 (t, J = 8.70 Hz, 1 H), 8.97 (s, 1 H), 10.05 (d, J = 12.21 Hz, 1 H); ¹³C NMR (126 MHz, CDCl₃) δ 26.0, 26.4, 31.8, 38.8, 45.4, 59.0, 66.3, 70.0, 77.2, 107.7, 108.6, 108.8, 110.7, 116.7, 119.2, 120.7, 120.8, 121.2, 129.1, 131.0, 133.9, 133.9, 139.4, 141.1, 150.4, 151.8,

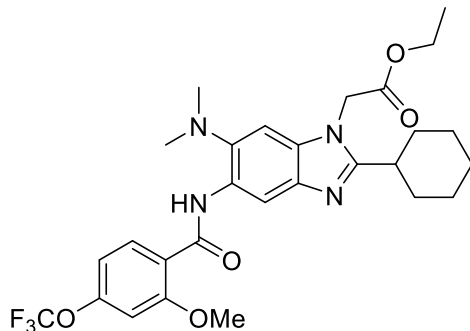
151.9, 159.2, 159.5, 160.8, 161.2; HRMS (ESI) m/z calculated for $C_{27}H_{30}F_4N_4O_5$ (M+H)⁺: 567.2225, found 567.2228 (Δ -0.55 ppm).

2-Cyclohexyl-6-*N,N*-dimethylamino-5-(2-fluoro-4-trifluoromethyl)benzamido-1-ethoxycarbonylmethyl-1*H*-benzo[d]imidazole



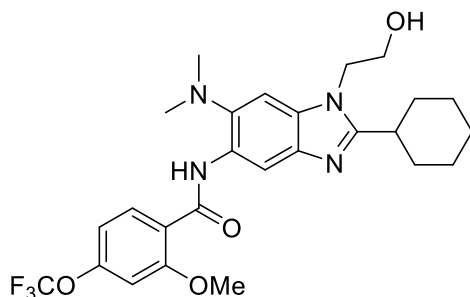
2-Cyclohexyl-5-(2-methoxy-4-trifluoromethoxy)benzamido-6-*N,N*-dimethylamino-1*H*-benzo[d]imidazole (100 mg, 0.21 mmoles), in THF (10 mL), was added ethyl bromoacetate (22 μ L, 0.20 mmoles) and potassium carbonate (28 mg, 0.20 mmoles). The reaction mixture was stirred under reflux overnight. The reaction was monitored by TLC. Upon completion, the reaction mixture was diluted with DCM (25 mL), washed thrice with water (25 mL X 3), and dried over magnesium sulfate. The crude mixture was purified by flash column on silica gel with 3% methanol in DCM as the eluent. The desired compound was obtained as a white solid. 75 mg, 62% yield; ¹H NMR (500 MHz, CDCl₃) δ 1.25 (t, J = 7.17 Hz, 3 H), 1.30 - 1.46 (m, 3 H), 1.69 - 1.78 (m, 1 H), 1.78 - 1.86 (m, 2 H), 1.86 - 2.00 (m, 3 H), 2.43 (br. s., 1 H), 2.55 - 2.78 (m, 6 H), 4.23 (q, J = 7.22 Hz, 2 H), 4.82 (s, 2 H), 6.98 - 7.10 (m, 2 H), 7.15 (d, J = 8.54 Hz, 1 H), 8.27 (t, J = 8.85 Hz, 1 H), 8.98 (s, 1 H), 10.00 (d, J = 12.21 Hz, 1 H); ¹³C NMR (126 MHz, CDCl₃) δ 14.0, 25.6, 26.2, 29.6, 31.7, 36.4, 37.0, 44.8, 45.5, 45.7, 62.0, 100.6, 108.5, 108.8, 110.7, 116.6, 117.0, 119.1, 120.8, 120.9, 121.2, 123.2, 129.4, 131.3, 133.8, 133.8, 139.4, 140.2, 151.6, 151.6, 151.7, 151.7, 159.1, 159.2, 159.3, 159.3, 161.1, 167.5; HRMS (ESI) m/z calculated for $C_{27}H_{30}F_4N_4O_4$ (M+H)⁺: 551.2276, found 551.2277 (Δ -0.17 ppm).

2-Cyclohexyl-6-*N,N*-dimethylamino-5-(2-methoxy-4-trifluoromethyl)benzamido-1-ethoxycarbonylmethyl-1*H*-benzo[d]imidazole



This compound was synthesized using the same procedure used to synthesize 2-Cyclohexyl-6-*N,N*-dimethylamino-5-(2-fluoro-4-trifluoromethyl)benzamido-3-ethoxycarbonylmethyl-1*H*-benzo[d]imidazole. 66 mg, 59% yield; ^1H NMR (500 MHz, CDCl_3) δ 1.25 (t, $J = 7.02$ Hz, 3 H), 1.32 - 1.52 (m, 3 H), 1.62 - 1.78 (m, 1 H), 1.78 - 2.02 (m, 6 H), 2.58 - 2.81 (m, 7 H), 3.92 - 4.14 (m, 3 H), 4.23 (q, $J = 7.02$ Hz, 2 H), 4.80 (s, 2 H), 6.82 (s, 1 H), 6.87 - 6.98 (m, 1 H), 7.01 (s, 1 H), 8.37 (d, $J = 8.85$ Hz, 1 H), 9.04 (s, 1 H), 10.87 (s, 1 H); ^{13}C NMR (126 MHz, CDCl_3) δ 14.0, 25.7, 26.2, 31.7, 31.7, 36.3, 44.8, 45.5, 45.7, 56.0, 61.9, 100.0, 104.1, 111.1, 112.6, 117.2, 119.2, 121.3, 121.3, 123.3, 130.0, 131.0, 134.1, 139.5, 140.3, 152.0, 157.9, 158.9, 161.2, 167.5; HRMS (ESI) m/z calculated for $\text{C}_{28}\text{H}_{33}\text{F}_3\text{N}_4\text{O}_5$ ($\text{M}+\text{H}$) $^+$: 563.2476, found 563.248 (Δ -0.77 ppm).

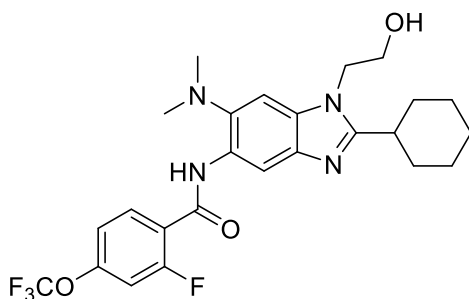
2-Cyclohexyl-6-*N,N*-dimethylamino-5-(2-methoxy-4-trifluoromethyl)benzamido-1-hydroxyethyl-1*H*-benzo[d]imidazole



To a solution of 2-Cyclohexyl-6-*N,N*-dimethylamino-5-(2-methoxy-4-trifluoromethyl)benzamido-1-ethoxycarbonylmethyl-1*H*-benzo[d]imidazole (52 mg, 0.09 mmoles), dissolved in THF (2 mL), was added lithium aluminum hydride (14 mg, 0.36 mmoles). The reaction mixture was heated to reflux after evolution of gas was absent. The reaction was monitored by TLC. Upon completion, the reaction was quenched with water (15 mL). DCM (25 mL) was added to the reaction mixture and the organic layer was washed thrice with water (20 mL X 3). The organic layer was collected and dried over anhydrous magnesium sulfate. The crude

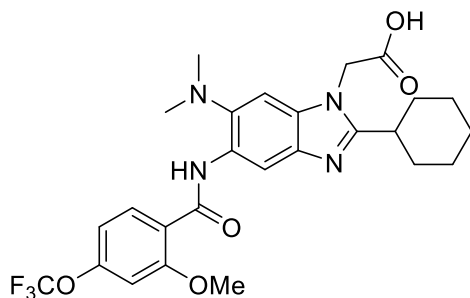
mixture was purified by flash column on silica gel with 2% methanol in DCM as the eluent. The desired product was obtained as a white solid. 47 mg, 99% yield; ^1H NMR (500 MHz, MeOD) δ 1.35 - 1.53 (m, 3 H), 1.69 - 1.83 (m, 3 H), 1.88 (d, $J = 12.82$ Hz, 2 H), 1.97 (d, $J = 12.21$ Hz, 2 H), 2.62 - 2.86 (m, 6 H), 3.05 (t, $J = 3.20$ Hz, 1 H), 3.88 (t, $J = 5.34$ Hz, 2 H), 4.13 (s, 3 H), 4.33 (t, $J = 5.34$ Hz, 2 H), 7.05 (d, $J = 8.85$ Hz, 1 H), 7.11 (s, 1 H), 7.45 (s, 1 H), 8.27 (d, $J = 8.85$ Hz, 1 H), 8.82 (s, 1 H); ^{13}C NMR (126 MHz, MeOD) δ 27.1, 27.5, 33.2, 37.4, 46.1, 47.1, 57.4, 61.6, 103.5, 106.3, 110.6, 113.9, 118.9, 120.9, 122.0, 123.0, 125.0, 131.1, 132.5, 134.8, 139.6, 142.4, 154.0, 160.2, 161.6, 163.6; HRMS (ESI) m/z calculated for $\text{C}_{26}\text{H}_{31}\text{F}_3\text{N}_4\text{O}_4$ ($\text{M}+\text{H}$) $^+$: 521.237, found 521.2375 (Δ -0.91 ppm).

2-Cyclohexyl-6-*N,N*-dimethylamino-5-(2-fluoro-4-trifluoromethyl)benzamido-1-hydroxyethyl-1*H*-benzo[d]imidazole



This compound was synthesized using the same procedure used to synthesize 2-Cyclohexyl-6-*N,N*-dimethylamino-5-(2-methoxy-4-trifluoromethyl)benzamido-1-hydroxyethyl-1*H*-benzo[d]imidazole. 25 mg, 35% yield; ^1H NMR (500 MHz, MeOD) δ 1.35 - 1.55 (m, 3 H), 1.69 - 1.84 (m, 3 H), 1.90 (d, $J = 13.12$ Hz, 2 H), 1.99 (d, $J = 12.21$ Hz, 2 H), 2.64 - 2.86 (m, 6 H), 2.96 - 3.17 (m, 1 H), 3.88 (t, $J = 5.34$ Hz, 2 H), 4.35 (t, $J = 5.34$ Hz, 2 H), 7.33 (s, 1 H), 7.34 - 7.38 (m, 1 H), 7.48 (s, 1 H), 8.12 - 8.30 (m, 1 H), 8.74 (s, 1 H); ^{13}C NMR (500 MHz, MeOD) δ 27.1, 27.5, 33.1, 37.5, 46.1, 47.1, 61.7, 103.8, 110.5, 110.7, 110.8, 118.4, 120.8, 122.5, 122.6, 122.9, 130.4, 132.9, 134.5, 134.5, 139.9, 142.3, 153.4, 160.9, 161.7, 162.0, 162.9; HRMS (ESI) m/z calculated for $\text{C}_{25}\text{H}_{28}\text{F}_4\text{N}_4\text{O}_3$ ($\text{M}+\text{H}$) $^+$: 509.217, found 509.2173 (Δ -0.54 ppm).

2-Cyclohexyl-6-*N,N*-dimethylamino-5-(2-methoxy-4-trifluoromethyl)benzamido-1-carboxymethyl-1*H*-benzo[d]imidazole



To a solution of 2-cyclohexyl-6-*N,N*-dimethylamino-5-(2-methoxy-4-trifluoromethyl)benzamido-1-ethoxycarbonylmethyl-1*H*-benzo[d]imidazole, in methanol (2 mL), was added 2 N NaOH (aq) (1 mL). The slurry was stirred at room temperature for 3 hours. The reaction was monitored by TLC. Upon completion of the reaction, the slurry became a homogeneous solution. The reaction mixture was acidified using 1 N HCl (5 mL) and the solid was filtered. The solid was washed thrice with water and allowed to air dry. The desired compound was obtained as a white solid. 67 mg, 71% yield; mp >230 °C; ¹H NMR (500 MHz, MeOD) δ 1.35 - 1.47 (m, 1 H), 1.53 (q, *J* = 12.92 Hz, 2 H), 1.63 - 1.76 (m, 2 H), 1.85 (d, *J* = 12.51 Hz, 1 H), 1.94 (d, *J* = 13.12 Hz, 2 H), 2.15 (d, *J* = 11.90 Hz, 2 H), 2.82 (s, 6 H), 3.18 (t, *J* = 12.05 Hz, 1 H), 4.16 (s, 3 H), 5.02 (s, 2 H), 7.09 (d, *J* = 8.55 Hz, 1 H), 7.16 (s, 1 H), 7.66 (s, 1 H), 8.31 (d, *J* = 8.55 Hz, 1 H), 8.97 (s, 1 H); ¹³C NMR (500 MHz, MeOD) δ 25.1, 25.4, 30.4, 35.4, 44.2, 56.0, 104.0, 104.6, 104.9, 112.4, 119.4, 119.9, 121.4, 129.0, 132.7, 133.4, 143.5, 152.8, 157.2, 158.9, 162.5, 170.1; HRMS (ESI) *m/z* calculated for C₂₆H₂₉F₃N₄O₅ (M+H)⁺: 535.2163, found 535.2166 (Δ -0.5 ppm).

Single Crystal X-ray diffraction (XRD)

Crystals were selected and mounted on glass fibers using epoxy adhesive. Each crystal was centered, and the X-ray intensity data were measured on an Oxford Gemini A Enhance diffractometer by using graphite-monochromated Cu radiation. The data was collected using the CrysAlis Pro 38.41 software,³⁵ Wingx 2014.1,³⁶ Olex2 1.2,³⁷ and SHELX 2013.³⁸ The X-ray diffraction was carried out by Matthew Freitag

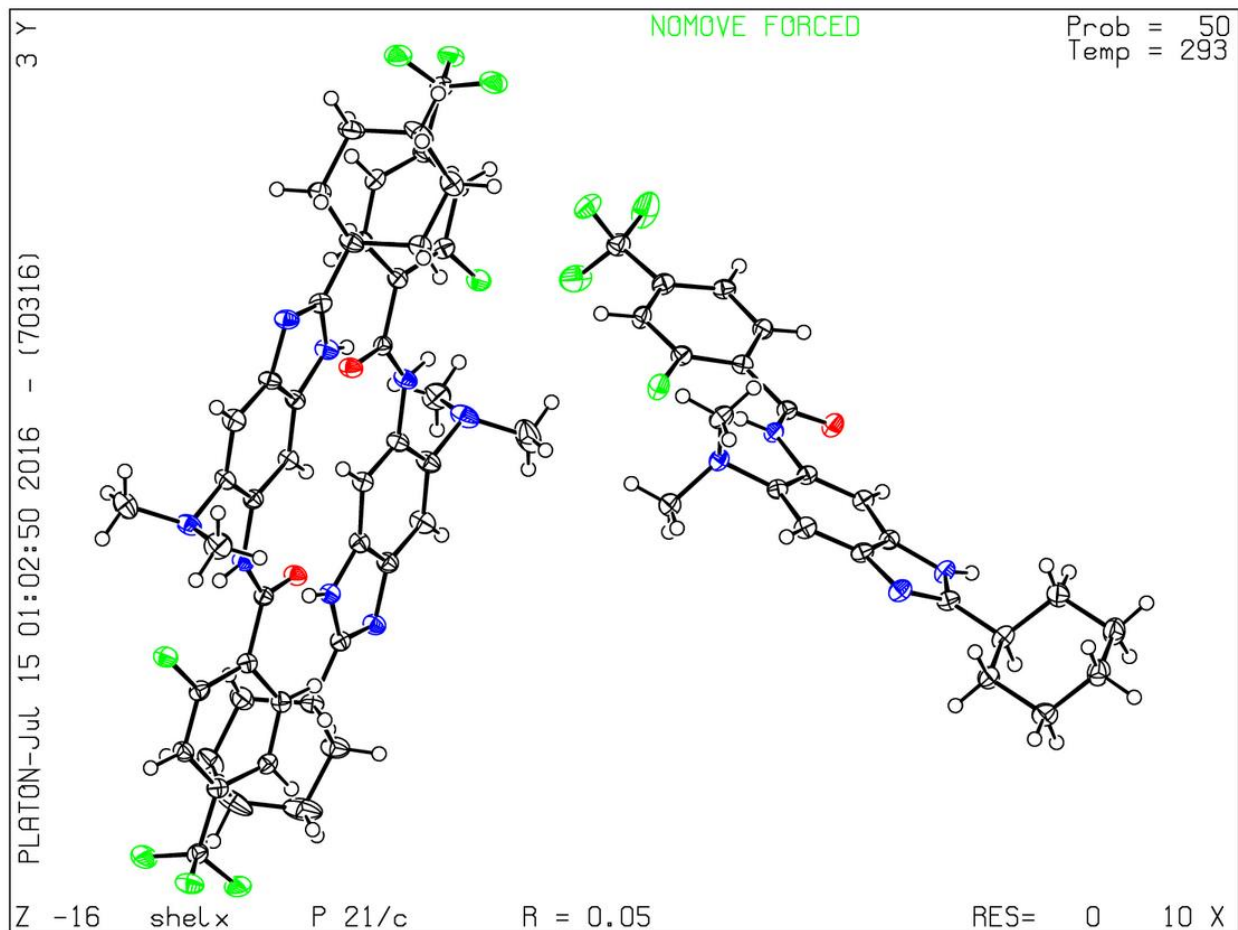


Table 1 Crystal data and structure refinement for sb-p17g-a42

Identification code	sb-p17g-a42
Empirical formula	C ₆₉ H ₇₂ F ₁₂ N ₁₂ O ₃
Formula weight	1345.38
Temperature/K	293(2)
Crystal system	monoclinic
Space group	P2 ₁ /c
a/Å	34.6958(6)
b/Å	6.63840(10)
c/Å	27.6706(5)
α/°	90
β/°	94.352(2)
γ/°	90

Volume/Å ³	6354.84(19)
Z	4
ρ _{calc} /cm ³	1.406
μ/mm ⁻¹	0.958
F(000)	2808.0
Crystal size/mm ³	? × ? × ?
Radiation	CuKα (λ = 1.54184)
2Θ range for data collection/°	7.666 to 146.366
Index ranges	-35 ≤ h ≤ 42, -8 ≤ k ≤ 4, -33 ≤ l ≤ 25
Reflections collected	21062
Independent reflections	11882 [R _{int} = 0.0305, R _{sigma} = 0.0449]
Data/restraints/parameters	11882/0/871
Goodness-of-fit on F ²	1.037
Final R indexes [I ≥ 2σ (I)]	R ₁ = 0.0468, wR ₂ = 0.1192
Final R indexes [all data]	R ₁ = 0.0647, wR ₂ = 0.1396
Largest diff. peak/hole / e Å ⁻³	0.27/-0.31

Table 2 Fractional Atomic Coordinates ($\times 10^4$) and Equivalent Isotropic Displacement Parameters ($\text{\AA}^2 \times 10^3$) for sb-p17g-a42. U_{eq} is defined as 1/3 of of the trace of the orthogonalised U_{II} tensor.

Atom	x	y	z	U(eq)
F32	2786.3(4)	5807(2)	496.2(5)	27.5(3)
F64	480.5(4)	-4948(2)	2567.3(5)	26.1(3)
F61	182.0(4)	-11938(2)	1937.1(5)	30.9(3)
F62	396.0(4)	-11938(2)	1230.8(6)	34.0(3)
F29	3060.5(4)	12712(2)	1167.3(5)	29.5(3)
F30	2816.1(4)	12702(2)	1856.8(6)	34.1(3)
F63	-111.0(4)	-10233(2)	1363.7(6)	35.9(4)
O18	1959.3(5)	3510(2)	1376.8(6)	22.7(3)
O50	1307.6(4)	-2845(2)	1665.5(6)	21.9(3)
N9	1376.7(5)	-2957(3)	624.5(6)	18.2(4)
N16	2192.9(5)	3214(3)	634.0(6)	20.2(4)

F31	3337.5(4)	11043(2)	1760.7(6)	36.6(4)
N2	1514.8(5)	-3779(3)	-129.2(7)	21.6(4)
C49	1116.0(6)	-3466(3)	1995.6(7)	17.3(4)
N48	1091.6(5)	-2492(3)	2417.5(6)	18.6(4)
C59	590.1(6)	-6053(3)	2190.6(8)	19.1(4)
C26	2868.2(6)	8595(3)	1002.6(8)	21.3(4)
C23	2257.6(6)	7328(3)	1515.5(8)	18.3(4)
N34	1844.5(6)	4250(3)	3210.6(7)	22.1(4)
C57	484.6(6)	-8963(3)	1695.2(8)	19.2(4)
C58	379.4(6)	-7768(3)	2076.6(8)	20.0(4)
C7	1771.6(6)	250(3)	716.3(8)	18.2(4)
C22	2366.3(6)	6128(3)	1137.1(8)	18.5(4)
C1	1320.9(6)	-4280(3)	242.9(8)	18.3(4)
C54	896.2(6)	-5411(3)	1927.3(8)	18.0(4)
N51	918.3(6)	-1484(3)	3288.2(7)	24.1(4)
C56	800.9(6)	-8448(3)	1442.7(8)	19.6(4)
C27	2667.4(6)	6856(3)	878.8(8)	20.3(4)
C55	1000.0(6)	-6683(3)	1557.9(7)	18.3(4)
C28	2991.5(7)	11541(3)	1545.5(8)	23.1(5)
C39	1528.4(6)	429(3)	2332.4(8)	18.4(4)
N19	2399.0(6)	2126(3)	-226.8(7)	29.3(5)
C38	1276.8(6)	-719(3)	2588.9(8)	18.5(4)
N41	1956.2(5)	3511(3)	2443.0(7)	21.4(4)
C60	239.6(6)	-10771(3)	1555.0(8)	21.7(5)
C40	1694.6(6)	2090(3)	2576.6(8)	18.1(4)
C17	2155.8(6)	4167(3)	1057.5(8)	17.5(4)
C35	1625.3(6)	2578(3)	3055.5(8)	19.5(4)
C5	2126.0(7)	837(4)	-8.7(8)	23.6(5)
C25	2758.5(6)	9710(3)	1393.9(8)	20.5(4)
C3	1713.7(6)	-2029(3)	13.6(8)	20.8(4)
C37	1190.2(6)	-198(3)	3067.9(8)	20.3(4)

C8	1626.1(6)	-1483(3)	482.6(8)	19.5(4)
C36	1367.2(7)	1440(4)	3303.4(8)	23.0(5)
C33	2036.0(6)	4744(3)	2836.1(8)	20.0(4)
C42	2326.1(6)	6412(4)	2834.5(8)	22.0(5)
C4	1967.0(7)	-862(4)	-234.1(8)	25.5(5)
C24	2448.8(6)	9102(3)	1646.4(8)	19.4(4)
C6	2023.3(6)	1405(3)	461.1(8)	19.5(4)
C10	1046.2(6)	-6020(3)	246.7(8)	19.7(4)
C53	1100.9(8)	-2714(4)	3679.6(10)	34.0(6)
C11	636.1(7)	-5256(4)	306.9(9)	28.0(5)
C52	581.6(7)	-389(4)	3441.3(10)	33.4(6)
C43	2254.6(7)	8031(3)	3209.7(9)	25.2(5)
C15	1064.6(8)	-7292(4)	-213.7(9)	29.6(5)
C44	2547.8(7)	9753(4)	3175.9(10)	29.6(5)
F96	3730.0(4)	526(2)	787.3(5)	27.2(3)
F93	3526.6(4)	7487(2)	82.3(6)	34.0(3)
F94	3271.4(5)	5728(2)	-499.1(6)	44.2(4)
F95	3799.2(5)	7342(3)	-583.1(7)	51.1(5)
O82	4645.1(5)	-1746(2)	57.5(6)	24.1(3)
N80	4350.0(5)	-1970(3)	763.3(7)	18.4(4)
N83	4058.3(5)	-2975(3)	1580.6(7)	19.7(4)
N73	5173.8(5)	-8134(3)	950.0(7)	20.7(4)
C71	4778.8(6)	-4966(3)	763.1(8)	18.5(4)
C86	4216.8(6)	896(3)	231.1(8)	17.9(4)
C72	4899.3(6)	-6667(3)	1028.7(8)	18.4(4)
N66	4948.1(6)	-8877(3)	1668.3(7)	22.3(4)
C90	3688.7(6)	3299(3)	272.8(8)	21.1(4)
C68	4477.8(6)	-5995(3)	1665.5(8)	21.1(4)
C81	4423.4(6)	-1060(3)	346.1(8)	17.6(4)
C89	3837.0(7)	4439(3)	-92.5(8)	21.9(5)
C91	3883.4(6)	1590(3)	430.0(8)	19.4(4)

C70	4500.6(6)	-3792(3)	964.4(7)	17.3(4)
C92	3611.1(7)	6248(4)	-276.6(9)	24.9(5)
C65	5189.8(6)	-9395(3)	1346.1(8)	19.9(4)
C74	5467.5(7)	-11116(3)	1408.7(8)	21.5(5)
C88	4177.2(6)	3865(3)	-285.3(8)	20.5(4)
C87	4362.0(6)	2111(3)	-123.2(8)	19.7(4)
C75	5353.2(6)	-12571(3)	1799.8(8)	23.4(5)
C67	4761.8(6)	-7168(3)	1476.4(8)	19.9(4)
C69	4345.3(6)	-4308(3)	1408.7(8)	18.4(4)
C85	4191.0(7)	-1966(4)	2031.7(9)	27.3(5)
C78	6170.6(7)	-12093(4)	1603.4(10)	32.2(6)
C79	5883.3(7)	-10352(4)	1524.6(10)	29.8(5)
C84	3690.2(7)	-3987(4)	1626.5(10)	31.3(6)
C77	6048.3(7)	-13561(4)	1987.6(9)	29.5(5)
C76	5638.8(7)	-14317(4)	1861.4(10)	28.5(5)
C12	335.9(7)	-6948(4)	259.4(9)	31.4(6)
C45	2959.0(8)	8975(4)	3257.1(10)	36.2(6)
C46	3036.1(8)	7331(4)	2888.3(13)	43.8(7)
C47	2741.0(7)	5613(4)	2912.0(12)	37.6(6)
C13	358.7(9)	-8080(5)	-210.3(10)	45.2(8)
C21	2218.8(8)	3329(4)	-625.7(10)	37.3(6)
C14	761(1)	-8953(5)	-239.3(11)	47.4(8)
C20	2732.3(8)	1035(5)	-382.6(12)	46.2(7)

Table 3 Anisotropic Displacement Parameters ($\text{\AA}^2 \times 10^3$) for sb-p17g-a42. The Anisotropic displacement factor exponent takes the form: $-2\pi^2[h^2a^{*2}U_{11}+2hka^*b^*U_{12}+\dots]$.

Atom	U_{11}	U_{22}	U_{33}	U_{23}	U_{13}	U_{12}
F32	30.6(7)	26.5(7)	27.2(7)	-8.5(6)	14.0(6)	-6.8(6)
F64	30.2(7)	24.7(7)	25.0(7)	-8.6(6)	12.3(5)	-7.0(6)
F61	37.3(8)	23.2(7)	32.5(8)	1.8(6)	5.0(6)	-9.9(6)
F62	37.5(8)	26.4(7)	39.5(8)	-16.3(6)	12.2(6)	-6.3(6)

F29	32.2(7)	20.9(7)	35.8(8)	1.6(6)	5.4(6)	-6.8(6)
F30	37.7(8)	27.4(7)	38.7(8)	-13.8(6)	11.7(6)	-7.8(6)
F63	26.7(7)	29.6(7)	49.1(9)	-6.1(7)	-12.4(6)	-3.6(6)
O18	27.4(8)	20.9(8)	20.9(8)	-1.8(6)	8.4(6)	-5.7(7)
O50	24.9(8)	21.7(8)	19.9(8)	-1.9(6)	6.9(6)	-5.3(7)
N9	20.3(8)	19.7(9)	14.7(8)	-2.2(7)	2.5(6)	-2.0(7)
N16	23.2(9)	22.1(9)	15.6(9)	-0.5(7)	3.2(7)	-7.3(8)
F31	29.1(7)	25.6(7)	52.2(10)	-0.5(7)	-15.4(7)	-4.2(6)
N2	23.4(9)	22.8(9)	18.4(9)	-2.6(8)	1.2(7)	-4.1(8)
C49	17.7(10)	17.8(10)	16.2(10)	-1.3(8)	0.1(8)	-0.3(8)
N48	20.5(8)	18.8(9)	16.9(9)	-0.9(7)	4.3(7)	-5.3(7)
C59	22.9(10)	18.9(10)	15.9(10)	-2.0(8)	4.3(8)	1.2(9)
C26	22(1)	20.0(11)	22.3(11)	0.2(9)	4.5(8)	-2.7(9)
C23	18.4(10)	19.3(10)	17.3(10)	1.9(8)	2.7(8)	-0.2(9)
N34	28.1(10)	20.2(9)	18.1(9)	-3.5(7)	2.2(7)	-5.1(8)
C57	21.3(10)	17.9(10)	18(1)	0.5(8)	-1.7(8)	-0.3(9)
C58	19.9(10)	21.0(11)	19.4(10)	-0.9(9)	3.6(8)	-3.2(9)
C7	20(1)	19.3(10)	15(1)	0.2(8)	-0.3(8)	-1.4(9)
C22	18.3(10)	20.3(10)	16.6(10)	0.1(8)	-0.8(8)	-0.8(9)
C1	19.4(10)	18.6(10)	16.5(10)	-0.5(8)	-1.1(8)	0.5(9)
C54	19.2(10)	18.3(10)	16.1(10)	0.1(8)	-0.6(8)	0.0(9)
N51	27.8(10)	25.8(10)	19.3(9)	-1.8(8)	6.4(7)	-9.1(8)
C56	21.4(10)	18.7(10)	18.6(10)	-1.7(8)	1.0(8)	2.5(9)
C27	24.5(11)	19.6(11)	17.2(10)	0.0(8)	2.7(8)	0.7(9)
C55	19.3(10)	20.1(10)	15.6(10)	3.1(8)	2.8(8)	-0.2(9)
C28	25.5(11)	19.4(11)	24.3(11)	1.0(9)	1.2(9)	0.0(9)
C39	20(1)	20.3(10)	14.8(10)	-0.2(8)	1.6(8)	-0.9(9)
N19	35.0(11)	33.4(11)	20.6(10)	-4.1(9)	9.2(8)	-14.1(9)
C38	18.9(10)	18.3(10)	17.9(10)	-1.8(8)	-1.4(8)	0.5(9)
N41	26.7(9)	22.2(9)	15.4(9)	-2.5(7)	3.0(7)	-4.4(8)
C60	22.6(11)	20.0(11)	22.5(11)	-3.6(9)	1.6(8)	1.2(9)

C40	17.9(10)	18.3(10)	18.3(10)	2.1(8)	1.8(8)	-2.9(9)
C17	16.6(9)	17.2(10)	18.5(10)	-0.4(8)	-0.2(8)	1.2(8)
C35	23.7(10)	18.3(10)	16.5(10)	-2.1(8)	1.0(8)	-5.1(9)
C5	25.5(11)	26.1(12)	19.3(11)	-0.9(9)	3.0(9)	-7.4(10)
C25	19.8(10)	18.1(10)	23.1(11)	0.5(9)	-2.7(8)	-1.1(9)
C3	21.6(10)	21.7(11)	19.1(11)	-1.8(9)	0.3(8)	-1.7(9)
C37	19.3(10)	22.0(11)	19.8(11)	-0.9(9)	2.3(8)	-4.3(9)
C8	19.7(10)	21.9(11)	16.7(10)	-1.0(8)	0.6(8)	-1.3(9)
C36	26.5(11)	26.4(12)	16.6(10)	-2.6(9)	4.7(8)	-3.5(10)
C33	24.5(11)	19.5(10)	15.8(10)	-1.1(8)	-0.7(8)	-0.9(9)
C42	25.5(11)	24.0(11)	16.6(10)	-0.7(9)	2.4(8)	-8.3(9)
C4	30.6(12)	30.7(12)	15.6(10)	-4.8(9)	5.3(9)	-7.5(10)
C24	22(1)	18.6(10)	17.6(10)	-0.3(8)	1.5(8)	3.2(9)
C6	21.2(10)	21.2(10)	15.6(10)	-1.6(8)	-1.8(8)	-3.3(9)
C10	24.8(11)	18.3(10)	15.8(10)	0.1(8)	-0.7(8)	-3.2(9)
C53	40.1(14)	32.1(13)	31.2(13)	7.3(11)	11.0(11)	-1.3(12)
C11	23.7(11)	26.7(12)	33.3(13)	4.3(10)	-0.2(9)	-3.9(10)
C52	26.4(12)	38.7(14)	36.0(14)	2.6(12)	8.1(10)	-6.4(11)
C43	25.1(11)	20.4(11)	30.5(12)	-4.1(9)	5.8(9)	-4.8(9)
C15	39.9(14)	27.0(12)	23.0(12)	-6.7(10)	9.3(10)	-9.5(11)
C44	32.9(13)	21.9(12)	34.9(13)	-8.2(10)	8.6(10)	-9.7(10)
F96	28.7(7)	24.8(7)	29.9(7)	12.1(6)	14.2(6)	6.2(6)
F93	39.7(8)	22.2(7)	39.9(8)	-1.4(6)	1.6(6)	9.7(6)
F94	44.6(9)	31.6(8)	52.2(10)	2.8(7)	-24.3(8)	4.5(7)
F95	54(1)	40.9(9)	62.5(11)	35.5(9)	30.5(9)	20.6(8)
O82	27.4(8)	22.2(8)	23.8(8)	4.8(7)	9.1(6)	5.2(7)
N80	20.5(9)	16.5(9)	18.6(9)	0.7(7)	4.2(7)	1.8(7)
N83	21.7(9)	19.8(9)	18.0(9)	-0.3(7)	3.5(7)	3.2(8)
N73	24.5(9)	19.3(9)	18.8(9)	2.0(7)	4.7(7)	5.8(8)
C71	21.8(10)	18.9(10)	15(1)	1.9(8)	1.5(8)	0.7(9)
C86	20.6(10)	17.4(10)	15.5(10)	1.8(8)	0.1(8)	-1.3(9)

C72	20.2(10)	18.2(10)	16.6(10)	-1.2(8)	0.1(8)	1.0(9)
N66	28.7(10)	19.6(9)	18.7(9)	4.0(7)	3.3(7)	3.9(8)
C90	20.8(10)	22.0(11)	21.1(11)	0.7(9)	5.5(8)	4.2(9)
C68	26.1(11)	21.6(11)	16.2(10)	1.4(9)	5.3(8)	0.3(9)
C81	20.1(10)	16.7(10)	16.1(10)	1.9(8)	2.7(8)	-0.6(8)
C89	25.1(11)	19.6(11)	20.7(11)	2.2(9)	-0.1(8)	1.7(9)
C91	23(1)	17.2(10)	18.7(10)	3.0(8)	5.9(8)	-0.1(9)
C70	19.9(10)	16(1)	15.8(10)	0.5(8)	-0.2(8)	1.0(8)
C92	28.1(12)	21.6(11)	25.1(12)	4.6(9)	2.8(9)	1.3(10)
C65	26.3(11)	17.5(10)	16(1)	2.1(8)	1.8(8)	0.3(9)
C74	28.1(11)	21.1(11)	15.2(10)	1.3(9)	1.2(8)	6.9(9)
C88	26.0(11)	18(1)	17.7(10)	1.6(8)	3.2(8)	-1.7(9)
C87	20.6(10)	20.3(10)	18.5(10)	-2.1(8)	3.6(8)	-0.5(9)
C75	22.7(11)	22.1(11)	25.1(11)	4.7(9)	-0.6(8)	2.6(9)
C67	25.4(11)	16.5(10)	17.8(10)	2.8(8)	1.6(8)	1.0(9)
C69	20.1(10)	17.8(10)	17(1)	-0.3(8)	0.7(8)	-0.2(9)
C85	32.0(12)	24.6(12)	25.7(12)	-7(1)	5.3(9)	3.6(10)
C78	26.0(12)	29.6(13)	41.7(15)	8.8(11)	7.4(10)	5.5(11)
C79	25.6(12)	23.7(12)	41.0(14)	12.9(11)	8.9(10)	0.6(10)
C84	24.4(12)	27.4(12)	42.7(15)	-9.6(11)	6.1(10)	-1.1(10)
C77	27.4(12)	29.7(13)	31.1(13)	5.9(11)	0.9(10)	6.3(10)
C76	30.8(12)	21.7(11)	32.3(13)	10.7(10)	-1.6(10)	0.6(10)
C12	24.0(11)	38.2(14)	30.9(13)	6.2(11)	-4.5(9)	-9.4(11)
C45	29.9(13)	37.7(15)	40.5(15)	-6.2(12)	-1.1(11)	-18.7(12)
C46	26.6(13)	33.9(15)	72(2)	-10.6(15)	14.7(13)	-6.6(12)
C47	26.7(13)	25.4(13)	62.1(19)	-12.3(13)	12.8(12)	-5.0(11)
C13	50.1(16)	62(2)	22.0(13)	1.2(13)	-4.5(11)	-39.3(16)
C21	43.8(15)	31.4(14)	38.9(15)	7.6(12)	18.1(12)	-1.9(12)
C14	72(2)	40.2(16)	31.6(14)	-18.9(13)	17.2(14)	-27.6(16)
C20	31.1(14)	53.8(18)	55.4(19)	15.2(16)	14.5(13)	-6.3(14)

Table 4 Bond Lengths for sb-p17g-a42.

Atom	Atom	Length/Å	Atom	Atom	Length/Å
F32	C27	1.357(3)	C25	C24	1.386(3)
F64	C59	1.353(2)	C3	C4	1.390(3)
F61	C60	1.338(3)	C3	C8	1.403(3)
F62	C60	1.332(3)	C37	C36	1.387(3)
F29	C28	1.340(3)	C33	C42	1.497(3)
F30	C28	1.336(3)	C42	C43	1.528(3)
F63	C60	1.338(3)	C42	C47	1.534(3)
O18	C17	1.236(3)	C10	C11	1.532(3)
O50	C49	1.240(3)	C10	C15	1.533(3)
N9	C1	1.376(3)	C11	C12	1.530(3)
N9	C8	1.383(3)	C43	C44	1.538(3)
N16	C17	1.347(3)	C15	C14	1.523(4)
N16	C6	1.405(3)	C44	C45	1.518(4)
F31	C28	1.341(3)	F96	C91	1.356(2)
N2	C1	1.315(3)	F93	C92	1.339(3)
N2	C3	1.393(3)	F94	C92	1.333(3)
C49	N48	1.343(3)	F95	C92	1.326(3)
C49	C54	1.504(3)	O82	C81	1.237(3)
N48	C38	1.406(3)	N80	C81	1.344(3)
C59	C58	1.376(3)	N80	C70	1.415(3)
C59	C54	1.399(3)	N83	C69	1.440(3)
C26	C27	1.378(3)	N83	C84	1.457(3)
C26	C25	1.388(3)	N83	C85	1.460(3)
C23	C24	1.386(3)	N73	C65	1.377(3)
C23	C22	1.390(3)	N73	C72	1.391(3)
N34	C33	1.314(3)	C71	C70	1.390(3)
N34	C35	1.395(3)	C71	C72	1.394(3)
C57	C56	1.388(3)	C86	C87	1.393(3)
C57	C58	1.391(3)	C86	C91	1.396(3)

C57	C60	1.505(3)	C86	C81	1.505(3)
C7	C6	1.394(3)	C72	C67	1.401(3)
C7	C8	1.395(3)	N66	C65	1.315(3)
C22	C27	1.396(3)	N66	C67	1.391(3)
C22	C17	1.501(3)	C90	C91	1.374(3)
C1	C10	1.498(3)	C90	C89	1.392(3)
C54	C55	1.394(3)	C68	C69	1.386(3)
N51	C37	1.441(3)	C68	C67	1.389(3)
N51	C53	1.461(3)	C89	C88	1.385(3)
N51	C52	1.466(3)	C89	C92	1.502(3)
C56	C55	1.385(3)	C70	C69	1.421(3)
C28	C25	1.502(3)	C65	C74	1.496(3)
C39	C38	1.393(3)	C74	C75	1.526(3)
C39	C40	1.395(3)	C74	C79	1.540(3)
N19	C5	1.442(3)	C88	C87	1.387(3)
N19	C20	1.457(4)	C75	C76	1.525(3)
N19	C21	1.464(4)	C78	C77	1.526(3)
C38	C37	1.424(3)	C78	C79	1.531(3)
N41	C33	1.373(3)	C77	C76	1.522(3)
N41	C40	1.379(3)	C12	C13	1.509(4)
C40	C35	1.403(3)	C45	C46	1.531(4)
C35	C36	1.391(3)	C46	C47	1.537(4)
C5	C4	1.383(3)	C13	C14	1.519(5)
C5	C6	1.424(3)			

Table 5 Bond Angles for sb-p17g-a42.

Atom	Atom	Atom	Angle/°	Atom	Atom	Atom	Angle/°
C1	N9	C8	106.76(17)	C7	C8	C3	123.1(2)
C17	N16	C6	129.27(19)	C37	C36	C35	118.2(2)
C1	N2	C3	105.10(18)	N34	C33	N41	113.11(19)
O50	C49	N48	123.6(2)	N34	C33	C42	124.5(2)

O50	C49	C54	119.18(19)	N41	C33	C42	122.29(19)
N48	C49	C54	117.25(18)	C33	C42	C43	112.01(18)
C49	N48	C38	129.72(18)	C33	C42	C47	111.6(2)
F64	C59	C58	116.73(18)	C43	C42	C47	110.3(2)
F64	C59	C54	120.32(19)	C5	C4	C3	118.5(2)
C58	C59	C54	122.9(2)	C23	C24	C25	119.3(2)
C27	C26	C25	118.5(2)	C7	C6	N16	124.04(19)
C24	C23	C22	122.1(2)	C7	C6	C5	121.8(2)
C33	N34	C35	104.61(18)	N16	C6	C5	114.19(19)
C56	C57	C58	120.3(2)	C1	C10	C11	110.01(19)
C56	C57	C60	121.30(19)	C1	C10	C15	110.61(18)
C58	C57	C60	118.37(19)	C11	C10	C15	111.7(2)
C59	C58	C57	118.7(2)	C12	C11	C10	112.3(2)
C6	C7	C8	115.94(19)	C42	C43	C44	109.84(19)
C23	C22	C27	116.3(2)	C14	C15	C10	111.4(2)
C23	C22	C17	116.80(19)	C45	C44	C43	110.9(2)
C27	C22	C17	126.9(2)	C81	N80	C70	129.32(18)
N2	C1	N9	112.91(19)	C69	N83	C84	112.23(18)
N2	C1	C10	124.33(19)	C69	N83	C85	112.55(17)
N9	C1	C10	122.64(19)	C84	N83	C85	111.02(19)
C55	C54	C59	116.5(2)	C65	N73	C72	106.74(18)
C55	C54	C49	117.10(18)	C70	C71	C72	115.65(19)
C59	C54	C49	126.41(19)	C87	C86	C91	116.2(2)
C37	N51	C53	112.54(19)	C87	C86	C81	117.15(19)
C37	N51	C52	112.95(19)	C91	C86	C81	126.64(19)
C53	N51	C52	111.92(19)	N73	C72	C71	131.8(2)
C55	C56	C57	119.5(2)	N73	C72	C67	104.80(18)
F32	C27	C26	116.48(19)	C71	C72	C67	123.4(2)
F32	C27	C22	120.34(19)	C65	N66	C67	104.86(18)
C26	C27	C22	123.1(2)	C91	C90	C89	118.6(2)
C56	C55	C54	121.9(2)	C69	C68	C67	118.5(2)

F30	C28	F29	106.60(18)	O82	C81	N80	123.8(2)
F30	C28	F31	107.00(19)	O82	C81	C86	119.38(19)
F29	C28	F31	106.43(18)	N80	C81	C86	116.80(18)
F30	C28	C25	112.66(19)	C88	C89	C90	120.2(2)
F29	C28	C25	112.08(19)	C88	C89	C92	121.8(2)
F31	C28	C25	111.68(19)	C90	C89	C92	118.0(2)
C38	C39	C40	115.95(19)	F96	C91	C90	116.75(18)
C5	N19	C20	113.0(2)	F96	C91	C86	119.86(19)
C5	N19	C21	112.5(2)	C90	C91	C86	123.4(2)
C20	N19	C21	110.6(2)	C71	C70	N80	124.68(19)
C39	C38	N48	125.03(19)	C71	C70	C69	122.1(2)
C39	C38	C37	121.8(2)	N80	C70	C69	113.18(18)
N48	C38	C37	113.19(19)	F95	C92	F94	107.9(2)
C33	N41	C40	107.03(18)	F95	C92	F93	106.5(2)
F62	C60	F63	107.07(19)	F94	C92	F93	105.43(19)
F62	C60	F61	106.77(18)	F95	C92	C89	112.7(2)
F63	C60	F61	106.35(18)	F94	C92	C89	111.7(2)
F62	C60	C57	112.75(18)	F93	C92	C89	112.18(19)
F63	C60	C57	111.59(18)	N66	C65	N73	113.02(19)
F61	C60	C57	111.94(18)	N66	C65	C74	124.02(19)
N41	C40	C39	131.9(2)	N73	C65	C74	122.91(19)
N41	C40	C35	104.98(18)	C65	C74	C75	111.47(18)
C39	C40	C35	123.11(19)	C65	C74	C79	110.97(19)
O18	C17	N16	123.4(2)	C75	C74	C79	110.52(19)
O18	C17	C22	119.35(19)	C89	C88	C87	119.5(2)
N16	C17	C22	117.26(18)	C88	C87	C86	122.1(2)
C36	C35	N34	129.5(2)	C76	C75	C74	111.03(19)
C36	C35	C40	120.2(2)	C68	C67	N66	129.5(2)
N34	C35	C40	110.26(19)	C68	C67	C72	119.9(2)
C4	C5	C6	120.6(2)	N66	C67	C72	110.58(19)
C4	C5	N19	123.2(2)	C68	C69	C70	120.4(2)

C6	C5	N19	116.3(2)	C68	C69	N83	122.56(19)
C24	C25	C26	120.5(2)	C70	C69	N83	117.03(19)
C24	C25	C28	121.1(2)	C77	C78	C79	111.7(2)
C26	C25	C28	118.4(2)	C78	C79	C74	111.8(2)
C4	C3	N2	130.0(2)	C76	C77	C78	110.8(2)
C4	C3	C8	120.1(2)	C77	C76	C75	111.2(2)
N2	C3	C8	109.89(19)	C13	C12	C11	111.1(2)
C36	C37	C38	120.7(2)	C44	C45	C46	110.7(2)
C36	C37	N51	123.1(2)	C45	C46	C47	110.5(2)
C38	C37	N51	116.18(19)	C42	C47	C46	111.0(2)
N9	C8	C7	131.6(2)	C12	C13	C14	110.1(2)
N9	C8	C3	105.33(19)	C13	C14	C15	110.9(3)

Table 6 Hydrogen Atom Coordinates ($\text{\AA}\times 10^4$) and Isotropic Displacement Parameters ($\text{\AA}^2\times 10^3$) for sb-p17g-a42.

Atom	x	y	z	U(eq)
H9	1276	-3032	898	22
H16	2342	3795	442	24
H48	940	-3033	2612	22
H26	3073	9012	828	26
H23	2050	6928	1686	22
H58	171	-8121	2251	24
H7	1705	612	1024	22
H56	879	-9282	1198	23
H55	1209	-6337	1384	22
H39	1582	107	2017	22
H41	2051	3607	2166	26
H36	1315	1770	3618	28
H42	2298	7048	2514	26
H4	2028	-1215	-544	31
H24	2370	9876	1901	23

H10	1125	-6872	526	24
H53A	1321	-3396	3567	51
H53B	919	-3688	3780	51
H53C	1183	-1865	3949	51
H11A	629	-4629	623	34
H11B	570	-4238	63	34
H52A	662	510	3702	50
H52B	397	-1331	3549	50
H52C	466	372	3173	50
H43A	2280	7450	3532	30
H43B	1994	8554	3152	30
H15A	1024	-6429	-496	36
H15B	1319	-7889	-218	36
H44A	2512	10378	2859	36
H44B	2503	10769	3417	36
H80	4188	-1356	932	22
H73	5308	-8234	702	25
H71	4878	-4639	470	22
H90	3463	3686	408	25
H68	4379	-6334	1958	25
H74	5460	-11854	1101	26
H88	4281	4649	-522	25
H87	4590	1734	-255	24
H75A	5346	-11857	2105	28
H75B	5096	-13094	1712	28
H85A	4227	-2944	2287	41
H85B	4001	-996	2114	41
H85C	4431	-1294	1991	41
H78A	6189	-12807	1300	39
H78B	6424	-11556	1703	39
H79A	5958	-9519	1259	36

H79B	5892	-9524	1814	36
H84A	3607	-4617	1324	47
H84B	3501	-3018	1709	47
H84C	3721	-4991	1876	47
H77A	6225	-14695	2011	35
H77B	6061	-12894	2300	35
H76A	5563	-15201	2117	34
H76B	5632	-15088	1563	34
H12A	380	-7873	529	38
H12B	79	-6380	272	38
H45A	3000	8433	3583	43
H45B	3139	10078	3227	43
H46A	3295	6804	2956	53
H46B	3019	7902	2565	53
H47A	2785	4621	2665	45
H47B	2776	4957	3225	45
H13A	300	-7176	-481	54
H13B	169	-9158	-230	54
H21A	2139	2461	-892	56
H21B	2401	4297	-728	56
H21C	1997	4018	-519	56
H14A	772	-9690	-541	57
H14B	816	-9890	26	57
H20A	2843	227	-120	69
H20B	2922	1979	-479	69
H20C	2652	181	-652	69

1.5. References

- (1) WHO. Tuberculosis (TB) <http://www.who.int/topics/tuberculosis/en/> (accessed Jul 11, 2016).
- (2) WHO. Tuberculosis <http://www.who.int/mediacentre/factsheets/fs104/en/> (accessed Jul 11, 2016).
- (3) WHO. *Global Tuberculosis Report 2015*, 20th ed.; WHO Press: Geneva, 2015.
- (4) CDC. Latent TB Infection and TB Disease <http://www.cdc.gov/tb/topic/basics/tbinfectiondisease.htm> (accessed Jul 11, 2016).
- (5) CDC. Signs & Symptoms <http://www.cdc.gov/tb/topic/basics/signsandSYMPTOMS.htm> (accessed Jul 11, 2016).
- (6) Dobos, K. M.; Spotts, E. a.; Quinn, F. D.; King, C. H. Necrosis of Lung Epithelial Cells during Infection with Mycobacterium Tuberculosis Is Preceded by Cell Permeation. *Infect. Immun.* **2000**, *68* (11), 6300–6310.
- (7) Golan, D. E.; Tashjian Jr., A. H.; Armstrong, E. J.; Armstrong, A. W. *Principles of Pharmacology: The Pathophysiologic Basis of Drug Therapy*, 2nd Editio.; Williams & Wilkins: Philadelphia, PA, 2008.
- (8) European Medicines Agency. Delytba http://www.ema.europa.eu/ema/index.jsp?curl=pages/medicines/human/medicines/002552/human_med_001699.jsp&mid=WC0b01ac058001d124 (accessed Jul 11, 2016).
- (9) FDA. News & Events <http://www.fda.gov/NewsEvents/Newsroom/PressAnnouncements/ucm333695.htm> (accessed Jul 11, 2016).
- (10) Gupta, R.; Gao, M.; Cirule, A.; Xiao, H.; Geiter, L. J.; Wells, C. D. Delamanid for Extensively Drug-Resistant Tuberculosis. *N. Engl. J. Med.* **2015**, *373* (3), 291–292.
- (11) Tadolini, M.; Lingsang, R. D.; Tiberi, S.; Enwerem, M.; D'Ambrosio, L.; Sadutshang, T. D.; Centis, R.; Migliori, G. B. First Case of Extensively Drug-Resistant Tuberculosis Treated with Both Delamanid and Bedaquiline. *Eur. Respir. J.* **2016**, ERJ – 00637–02016.
- (12) Awasthi, D.; Kumar, K.; Ojima, I. Therapeutic Potential of FtsZ Inhibition: A Patent Perspective. *Expert Opin. Ther. Pat.* **2011**, *21* (5), 657–679.
- (13) Li, X.; Ma, S. Advances in the Discovery of Novel Antimicrobials Targeting the Assembly of Bacterial Cell Division Protein FtsZ. *Eur. J. Med. Chem.* **2015**, *95*, 1–15.
- (14) Nogales, E.; Wolf, S. G.; Downing, K. H. Structure of the Alpha Beta Tubulin Dimer by Electron Crystallography. *Nature* **1998**, *391* (6663), 199–203.
- (15) Kumar, K.; Awasthi, D.; Berger, W. T.; Tonge, P. J.; Slayden, R. A.; Ojima, I. Discovery of Anti-TB Agents That Target the Cell-Division Protein FtsZ. *Future Med. Chem.* **2010**, *2* (8), 1305–1323.
- (16) Haranahalli, K.; Tong, S.; Ojima, I. Recent Advances in the Discovery and Development of Antibacterial Agents Targeting the Cell-Division Protein FtsZ. *Bioorg. Med. Chem.* **2016**.

- (17) Slayden, R. A. Identification of Cell Cycle Regulators in Mycobacterium Tuberculosis by Inhibition of Septum Formation and Global Transcriptional Analysis. *Microbiology* **2006**, *152* (6), 1789–1797.
- (18) Sarcina, M. Effects of Tubulin Assembly Inhibitors on Cell Division in Prokaryotes in Vivo. *FEMS Microbiol. Lett.* **2000**, *191* (1), 25–29.
- (19) Kumar, K.; Awasthi, D.; Lee, S.-Y.; Zanardi, I.; Ruzsicska, B.; Knudson, S.; Tonge, P. J.; Slayden, R. A.; Ojima, I. Novel Trisubstituted Benzimidazoles, Targeting Mtb FtsZ, as a New Class of Antitubercular Agents. *J. Med. Chem.* **2011**, *54* (1), 374–381.
- (20) White, E. L. 2-Alkoxy-carbonylaminopyridines: Inhibitors of Mycobacterium Tuberculosis FtsZ. *J. Antimicrob. Chemother.* **2002**, *50* (1), 111–114.
- (21) Reynolds, R. C.; Srivastava, S.; Ross, L. J.; Suling, W. J.; White, E. L. A New 2-Carbamoyl Pteridine That Inhibits Mycobacterial FtsZ. *Bioorg. Med. Chem. Lett.* **2004**, *14* (12), 3161–3164.
- (22) Awasthi, D.; Kumar, K.; Knudson, S. E.; Slayden, R. A.; Ojima, I. SAR Studies on Trisubstituted Benzimidazoles as Inhibitors of Mtb FtsZ for the Development of Novel Antitubercular Agents. *J. Med. Chem.* **2013**, *56* (23), 9756–9770.
- (23) Nasielski-Hinkens, R.; Levêque, P.; Castelet, D.; Nasielski, J. The Four 6-Halo-7-Nitroquinoxalines. *Heterocycles* **1987**, *26* (9), 2433.
- (24) Turesky, R. J.; Goodenough, A. K.; Ni, W.; McNaughton, L.; LeMaster, D. M.; Holland, R. D.; Wu, R. W.; Felton, J. S. Identification of 2-Amino-1,7-dimethylimidazo[4,5- G]Quinoxaline: An Abundant Mutagenic Heterocyclic Aromatic Amine Formed in Cooked Beef. *Chem. Res. Toxicol.* **2007**, *20* (3), 520–530.
- (25) Valdez, J.; Cedillo, R.; Hernández-Campos, A.; Yépez, L.; Hernández-Luis, F.; Navarrete-Vázquez, G.; Tapia, A.; Cortés, R.; Hernández, M.; Castillo, R. Synthesis and Antiparasitic Activity of 1H-Benzimidazole Derivatives. *Bioorg. Med. Chem. Lett.* **2002**, *12* (16), 2221–2224.
- (26) Iddon, B.; Kutschy, P.; Robinson, A. G.; Suschitzky, H.; Kramer, W.; Neugebauer, F. A. 2H-Benzimidazoles (Isobenzimidazoles). Part 7. A New Route to Triclabendazole [5-Chloro-6-(2,3-Dichlorophenoxy)-2-Methylthio-1H-Benzimidazole] and Congeneric Benzimidazoles. *J. Chem. Soc. Perkin Trans. 1* **1992**, No. 22, 3129.
- (27) VanAllan, J. A.; Deacon, B. D. 2-MERCAPTOBENZIMIDAZOLE. *Org. Synth.* **1950**, *30* (September), 56.
- (28) Sekar, R.; Srinivasan, M.; Marcelis, A. T. M.; Sambandam, A. S-Arylation of Mercaptobenzimidazoles Using Cu(I) Catalysts—experimental and Theoretical Observations. *Tetrahedron Lett.* **2011**, *52* (26), 3347–3352.
- (29) Takahashi, S.; Kano, H. Benzimidazole N-Oxides. II. The Reactivity of 1-Alkoxybenzimidazoles. *Chem. Pharm. Bull. (Tokyo)*. **1964**, *12* (3), 282–291.
- (30) Harvey, I. W.; McFarlane, M. D.; Moody, D. J.; Smith, D. M. O-Nitroaniline Derivatives. Part 9. Benzimidazole N-Oxides Unsubstituted at N-1 and C-2. *J. Chem. Soc. Perkin Trans. 1* **1988**, No. 3, 681.

- (31) Jamieson, C.; Moir, E. M.; Rankovic, Z.; Wishart, G. Medicinal Chemistry of hERG Optimizations: Highlights and Hang-Ups. *J. Med. Chem.* **2006**, *49* (17), 5029–5046.
- (32) Wang, S.; Li, Y.; Xu, L.; Li, D.; Hou, T. Recent Developments in Computational Prediction of hERG Blockage. *Curr. Top. Med. Chem.* **2013**, *13* (11), 1317–1326.
- (33) Recanatini, M.; Poluzzi, E.; Masetti, M.; Cavalli, A.; De Ponti, F. QT Prolongation through hERG K⁺ Channel Blockade: Current Knowledge and Strategies for the Early Prediction during Drug Development. *Med. Res. Rev.* **2005**, *25* (2), 133–166.
- (34) Park, B.; Awasthi, D.; Chowdhury, S. R.; Melief, E. H.; Kumar, K.; Knudson, S. E.; Slayden, R. A.; Ojima, I. Design, Synthesis and Evaluation of Novel 2,5,6-Trisubstituted Benzimidazoles Targeting FtsZ as Antitubercular Agents. *Bioorg. Med. Chem.* **2014**, *22* (9), 2602–2612.
- (35) Oxford Diffraction. CrysAlis Pro. Oxford Diffraction Ltd: Abingdon, England 2016.
- (36) Farrugia, L. J. WinGX and ORTEP for Windows: An Update. *J. Appl. Crystallogr.* **2012**, *45* (4), 849–854.
- (37) Dolomanov, O. V.; Bourhis, L. J.; Gildea, R. J.; Howard, J. A. K.; Puschmann, H. OLEX2 : A Complete Structure Solution, Refinement and Analysis Program. *J. Appl. Crystallogr.* **2009**, *42* (2), 339–341.
- (38) Gruene, T.; Hahn, H. W.; Luebben, A. V.; Meilleur, F.; Sheldrick, G. M. Refinement of Macromolecular Structures against Neutron Data with SHELXL2013. *J. Appl. Crystallogr.* **2014**, *47* (1), 462–466.

Chapter 2

Development of Antinociceptive Agents Targeting Fatty Acid Binding Proteins (FABP)

2.1.1. Pain and fatty acid binding proteins (FABPs).....	107
2.1.2. Discovery of α -truxillic acid derivatives.....	108
2.1.2.1. In-silico screening.....	108
2.1.2.2. Fluorescence displacement assay	110
2.1.2.3. In-vivo studies of SB-FI-26 and other α -truxillic acid derivatives.....	112
2.1.2.4. Pharmacokinetics of SB-FI-26	115
2.2. Results and discussion	116
2.2.1. Optical resolution of SB-FI-26.....	116
2.2.2. Synthesis of α -truxillic acid derivatives	124
2.2.2.1. Synthesis of (-)-incarvillateine analogue.....	124
2.2.2.2. Continuing SAR study.....	127
2.2.2.3. Minimizing hERG activity	130
2.2.2.4. Synthesis of heteroaromatic α -truxillic acids	133
2.2.2.5. Docking study of SB-FI-81 analogues	135
2.2.3. Synthesis of MJN 110	137
2.2.4. Synthesis of KT109 and KT172.....	138
2.3. Conclusion	139
2.4. Experimental Section.....	141
2.5. References.....	163

2.1. Introduction

2.1.1. Pain and fatty acid binding proteins (FABPs)

Pain management is a major issue in healthcare. Chronic pain, a persistent disorder that can last weeks, months, or years, afflicts 100 million Americans.¹ Chronic pain carries an annual economic cost of \$560-\$635 billion, which consists of healthcare cost, \$261-\$300 billion, and loss of productivity, \$297-\$336 billion.¹ Current drugs used in pain treatment, such as opioids, activate opioid receptors, located throughout the central and peripheral nervous system, to cause analgesia.² These compounds have unwanted side effects, such as constipation, drowsiness, nausea, and vomiting.² They are contraindicated with antidepressants, antihistamines, sleeping pills, and alcohol, and prolonged use can lead to tolerance and dependence.² Another pain medication is the cannabinoid Δ^9 -tetrahydrocannabinol, the active compound in marijuana. It elicits analgesia through activation of the G-protein-coupled cannabinoid receptor (CB₁), leading to anti-nociceptive and anti-hyperalgesic effects. Unfortunately, well-known side effects of THC administration are hallucinations, paranoia, altered senses, changes in mood, impaired body movement, impaired memory, and difficulty thinking and problem-solving.³ These adverse side effects make the therapeutic window of exogenous cannabinoids narrow, and it is difficult to achieve desired pain relief without the psychoactive effects of the drug.⁴ Endocannabinoids, innate CB₁ receptor agonists, are essential in the regulation of stress, pain and inflammation in the body, and they are biosynthesized in small quantities and rapidly degraded.⁴⁻⁶ Inhibition of the degradation pathway of endocannabinoids is a viable method to regulate pain without the psychedelic effects of exogenous cannabinoids.

Fatty acids play numerous important roles in the body, but the hydrophobic nature of the compounds requires the utilization of protein chaperones and transporters to shuttle these lipids throughout the cells. These transporter proteins are fatty acid binding proteins (FABPs), which are tissue specific, and include FABP1 (liver FABP), FABP3 (heart FABP), FABP4 (adipocyte FABP), FABP5 (epidermal FABP), FABP7 (brain FABP), and FABP8 (myelin FABP).⁶ Anandamide, an endocannabinoid that is linked to the regulation of stress, pain, and inflammation, uses these fatty acid binding proteins, specifically FABP5 and FABP7, as transporters. Through diffusion, anandamide also enters the cell where FABP5 and FABP7 transport the anandamide for inactivation in FAAH (fatty acid amide hydrolase), which is abundant in pancreas, brain, kidney,

and skeletal muscle.⁷ FABPs play a critical role in the endocannabinoid degradation pathway, and inhibition of FABP5 and FABP7 would arrest inactivation, leading to higher extracellular anandamide levels, which will result in anti-inflammatory and anti-nociceptive effects (**Figure 1**). The tissue specific nature of FABPs make it attractive as drug targets, since drug compounds can be designed to inhibit one type of fatty acid binding protein, reducing off target side effects. Inhibitors of FABP5 and FABP7 can be anti-inflammatory and anti-nociceptive drugs.

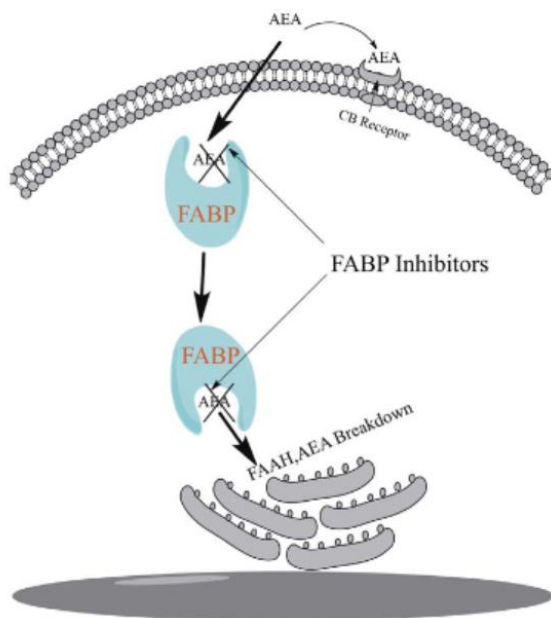


Figure 1 Anandamide (AEA) can either bind to the CB receptor or enter the cell through diffusion. Binding to the CB receptor causes anti-inflammatory and anti-nociceptive effects. Diffusion into the cell leads transportation of AEA by fatty acid binding proteins (FABPs) and inactivation of AEA by fatty acid amide hydrolase (FAAH). Inhibition of FABPs will hamper AEA breakdown, resulting in pain relief.⁸

2.1.2. Discovery of α -truxillic acid derivatives

2.1.2.1. In-silico screening

Typical computational screening programs, such as DOCK, give a score that is a sum of the intermolecular interactions, electrostatic and steric. Conversely, footprint similarity (FPS) scoring is a type of DOCK scoring function that takes an energy score and breaks it down into residue interactions and scores it based on the electrostatic, steric, and hydrogen bonding

contributions of each amino acid residue.⁹ This results in a distinct signature between the target and ligand. The identification of amino acid interactions is useful in determining how high affinity ligands bind to target molecules. These signatures can be used to compare compounds and predict interactions are within a binding site. One way this can be done is by analyzing a known, high affinity, reference and comparing it to an unknown potential binder. If the FPS scores are similar, the unknown compound may be a tight binder.

In order propagate anandamide activation of CB₁ receptors in the central and peripheral nervous systems, specific FABPs needed to be targeted. FABP5 (epidermal FABP) is present throughout the body in the tongue, adipose tissue, dendritic cells, mammary glands, brain neurons, kidneys, liver, lungs, and testis, but it is most concentrated in the epidermal skin cells.⁸ FABP7 (brain FABP) is found only during embryonic development.⁸ Both proteins bind fatty acids with high affinity, with FABP7 showing higher binding affinities *in-vitro*.⁸ Both FABP5 and FABP7 were selected as targets for the localization of each protein in the body, and only FABP7 was used in the *in-silico* screening.

Oleic acid, a high affinity natural ligand of FABP7, was used as the reference in the docking studies.¹⁰ The project started with *in-silico* screening of one million commercially available compounds, from ChemDiv, utilizing FPS scoring was conducted on FABP7 (PDB: 1FE3, 2.8 Å resolution) with oleic acid as the reference compound. Each compound screened had its own footprint signature, which was compared to the footprint signature of oleic acid (**Figure 2**). In **Figure 2**, there is favorable overlap between oleic acid, the reference compound, and a potential ligand from the ChemDiv database. The overlap in FPS score means the compound from the ChemDiv database will bind to FABP7 in a similar fashion to oleic acid, even though the structures of the compounds are vastly different. The goal of the virtual screening was to find compounds that interacted with the same amino acids, in the binding site of FABP7, as oleic acid. After several stages of virtual screenings, 48 compounds were purchased and assayed *in-vitro* against FABP5.

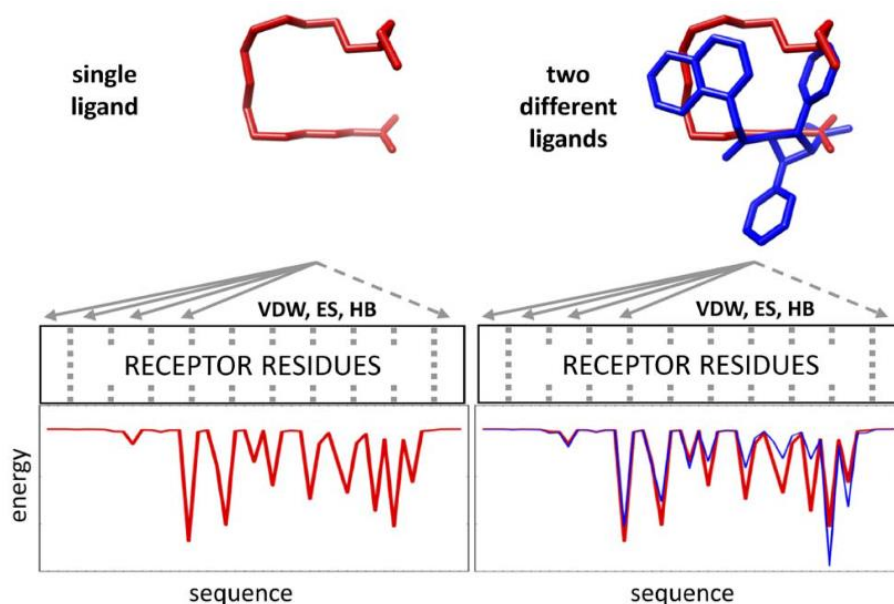


Figure 2 Footprint signature of oleic acid (red) is compared to the footprint signature of a candidate molecule (blue).⁸

2.1.2.2. Fluorescence displacement assay

The 48 purchased compounds were tested in a fluorescence displacement assay to determine the degree to which the compounds displaced NBD-stearate from FABP5. Fatty acid binding protein-NDB-stearate complex is fluorescent. As the NBD-stearate is displaced by FABP inhibitors, the fluorescence decreases. The larger the decrease in fluorescence, the higher the binding affinity of the compound being tested. FABP5 was chosen for the *in-vitro* assays for its ease of expression compared to FABP7. The experiment was performed using 10 μM of the 48 purchased compounds to displace 1 μM of NBD-stearate from FABP5. Arachidonic acid, a strong inhibitor of FABP5, was used as the positive control, and NBD-stearate with FABP5 was used as the negative control (**Figure 3**). Buffer and NBD-stearate was used to show NDB-stearate does not fluoresce when not bound to a FABP. About one-third of the compounds displaced NBD-stearate, causing a decrease in fluorescence (**Figure 3**). The four most potent compounds showed at least 50% inhibition of FABP5 were selected for further evaluation (**Figure 4**). Of the four compounds, SB-FI-26 was the most potent. All four compounds showed a carboxylate moiety, which is similar to the reference compound, oleic acid. The carboxylate group is thought to be critical for FABP activity.

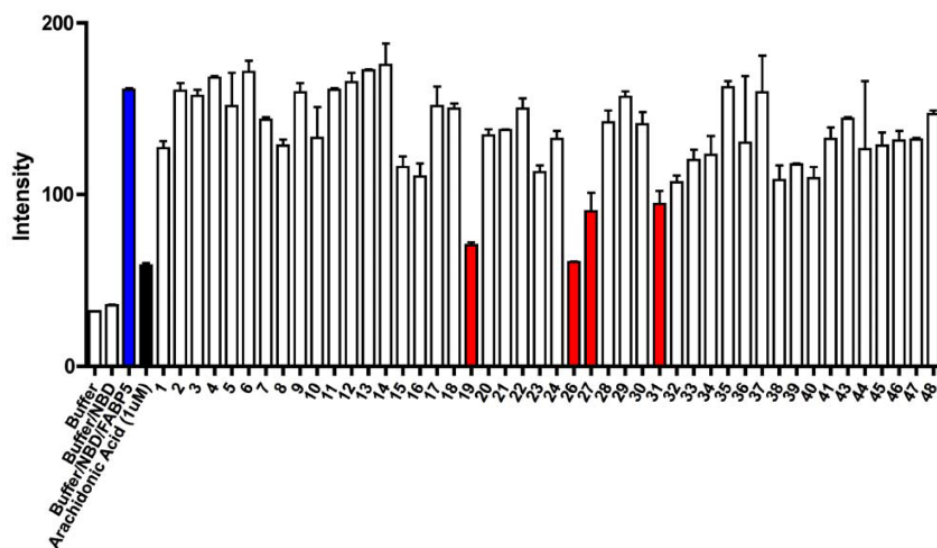


Figure 3 Fluorescence displacement assay of 48 compounds. Arachidonic acid (black), a compound that binds strongly with FABP5, was used as a control. The four most potent compounds red showed greater than 50% inhibition.⁸

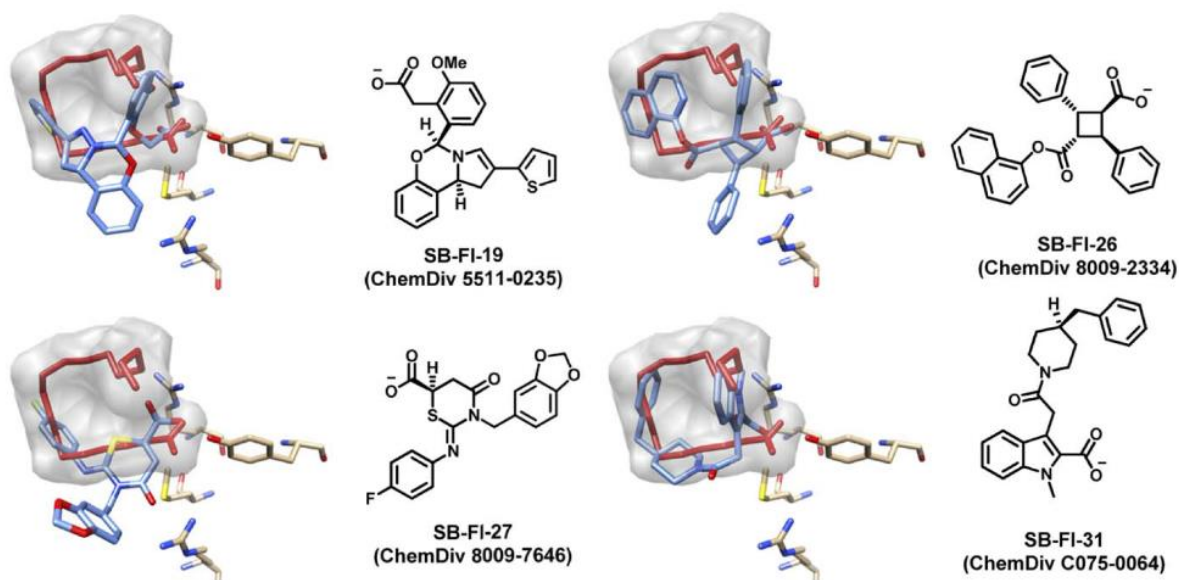


Figure 4 Left - Predicted binding pose of test compounds compared to oleic acid (red). Right - Structural formulae of four most potent compounds from the fluorescence displacement assay.⁸

The structure of SB-FI-26 was incorrectly provided by the vendor. In the database, the compound was supposed to be an α -truxillic acid, but the γ -truxillic acid derivative, SB-FI-49, was purchased and tested on the preliminary fluorescence displacement assay. The α -truxillic acid mono naphthyl ester, SB-FI-26, and γ -truxillic acid mono naphthyl ester, SB-FI-49, were later synthesized and retested *in-vitro*. SB-FI-26 showed a K_i value of $0.93 \pm 0.08 \mu\text{M}$, and SB-FI-49

showed a K_i value of $0.75 \pm 0.07 \mu\text{M}$. Even though SB-FI-49 was the most potent compound, it had poor solubility in DMSO ($200 \mu\text{M}$) compared to SB-FI-26 in DMSO (1 mM). SB-FI-26 also shares the α -truxillic acid core with (-)-incarvillateine, a natural product that has pain relieving properties (**Figure 5**). Based on the activity, the unique α -truxillic acid scaffold, and the structural similarity to (-)-incarvillateine, SB-FI-26 was chosen for further development as an anti-nociceptive agent.

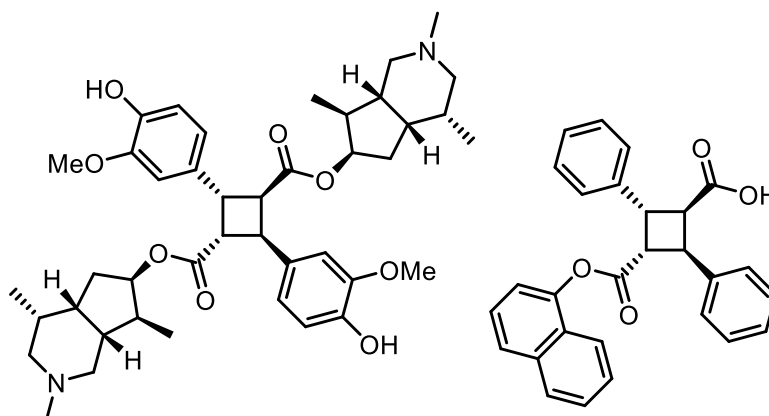


Figure 5 Left – structure of (-)-incarvillateine. Right – structure of SB-FI-26. Both compounds share an α -truxillic acid core.

2.1.2.3. In-vivo studies of SB-FI-26 and other α -truxillic acid derivatives

Analogues of SB-FI-26 were synthesized as part of an SAR study to determine which functional groups are needed to optimize the activity of the molecule. Three α -truxillic acid derivatives, SB-FI-50, SB-FI-56, SB-FI-60, SB-FI-71, SB-FI-72, and SB-FI-73, were synthesized (**Figure 6**). Various functional groups were used to diversify the ester group in hopes of developing a compound with much higher binding affinity. The 2-naphthol monoester was synthesized to explore the different positions on the naphthalene ring. The 1-naphthylamine monoamide and diamide were synthesized to find more stable functional groups, since the ester was thought to be too labile in living systems. Aliphatic groups were also explored, but SB-FI-26 was still the most active compound of the series. SB-FI-60 showed similar activity, but was not as active. The diamide, SB-FI-62, was a weak binder.

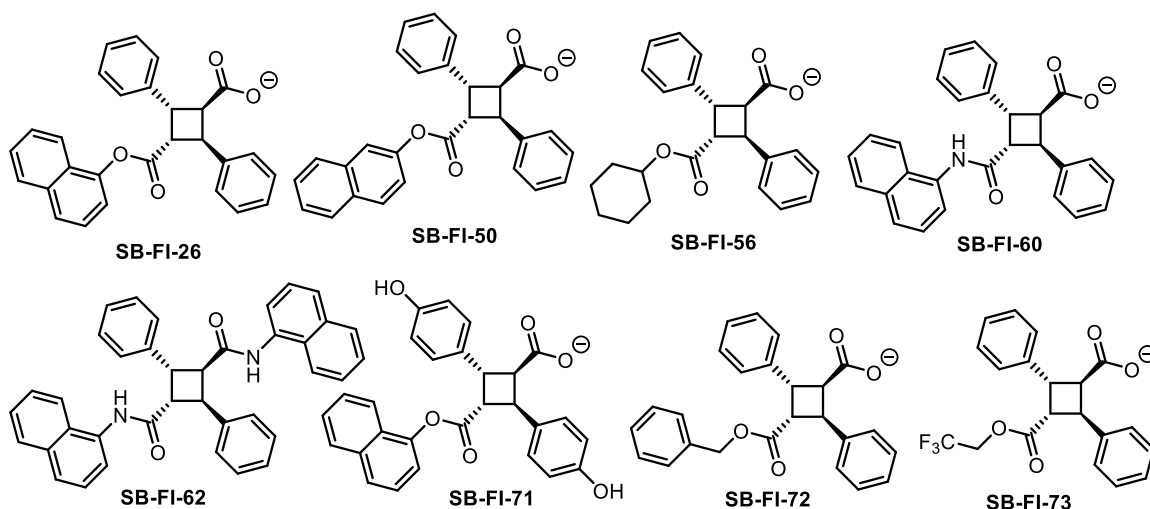


Figure 6 α -Truxillic acid derivatives.

Table 1 Binding affinities of α -truxillic acid derivatives.

Compound	K _i (μ M)	
	FABP5	FABP7
SB-FI-26	0.93 \pm 0.05	0.38 \pm 0.04
SB-FI-50	1.34 \pm 0.20	0.61 \pm 0.12
SB-FI-60	1.55 \pm 0.03	0.32 \pm 0.01
SB-FI-62	3.27 \pm 0.69	6.08 \pm 0.48
SB-FI-71	>10	1.90 \pm 0.34
SB-FI-72	4.11 \pm 0.57	1.06 \pm 0.13
SB-FI-73	>10	---

Fluorescence displacement assays showed the α -truxillic acid derivatives inhibited FABP5 and FABP7, but there was no evidence that the compounds actually reduced pain. SB-FI-26, SB-FI-50, SB-FI-60, and SB-FI-62 were tested in various pain models in mice. Four different experiments were performed on mice to model inflammatory, visceral, and neuropathic pain (**Figure 7**). In the carrageenan inflammatory pain model, α -truxillic acid derivatives were administered via intraperitoneal (ip) injection followed by injection of 1% λ - the paws of mice. Paw edema and thermal hyperalgesia were measured. SB-FI-26 and SB-FI-50 showed reduction in paw edema and thermal hyperalgesia, while SB-FI-60 and SB-FI-62 were ineffective. The formalin inflammatory pain model involved administration of α -truxillic acid derivatives followed by injection of formalin into a paw. The formalin pain model is expressed in two phases.⁸ In the first phase, involves direct activation of pain receptors and the second phase involves inflammation.⁸ SB-FI-26 was found to reduce pain in both phases, while SB-FI-50 and SB-FI-60 only reduced pain in the first phase of the experiment.¹¹ SB-FI-62 was ineffective in the formalin

test. For the visceral pain model, α -truxillic acid derivatives were first administered subcutaneously, and a 0.6% acetic acid solution was then injected i.p.¹¹ The number of writhes were recorded, and SB-FI-26 reduced writhing caused by the acetic acid injection, while SB-FI-50, SB-FI-60, and SB-FI-62 did not change the number of writhes.¹¹ In the neuropathic pain model, chronic constriction injury (CCI) of the sciatic nerve was emulated through surgical tying of the nerve using chromic gut.¹¹ SB-FI-26 was administered and reactions to mechanical and thermal stimuli were measured, and the compound improved pain thresholds for thermal stimuli, but it did not have any effect on mechanical thresholds (**Figure 8**).¹¹ Overall, SB-FI-26 was shown to be the best compound of the four tested. Even though *in-vitro* experiments showed similar Ki values, SB-FI-26 was effect at reducing pain in inflammatory, visceral, and neuropathic models, while the other three compounds did not perform as well.

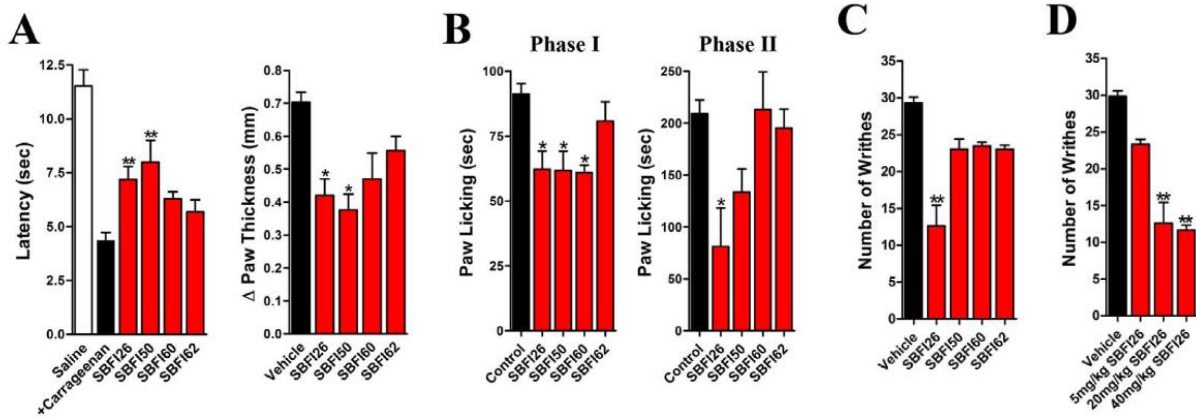


Figure 7 a) Effects of the four α -truxillic acid derivatives on carrageenan induced hyperalgesia (left) and paw edema (right) in mice. b) Effects of α -truxillic acid derivatives on the first phase (left) and second phase (right) of formalin induced inflammatory pain model in mice. c) Effects of α -truxillic acid derivatives on the acetic acid induced visceral pain model in mice. d) Dose dependent effect of SB-FI-26 on acetic acid induced visceral pain model in mice.¹¹

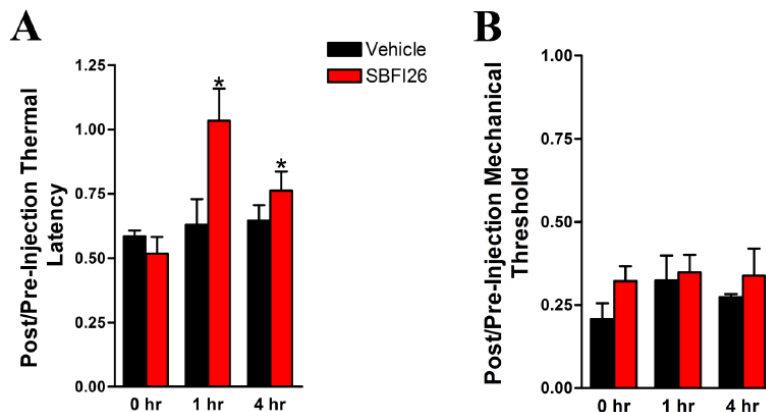
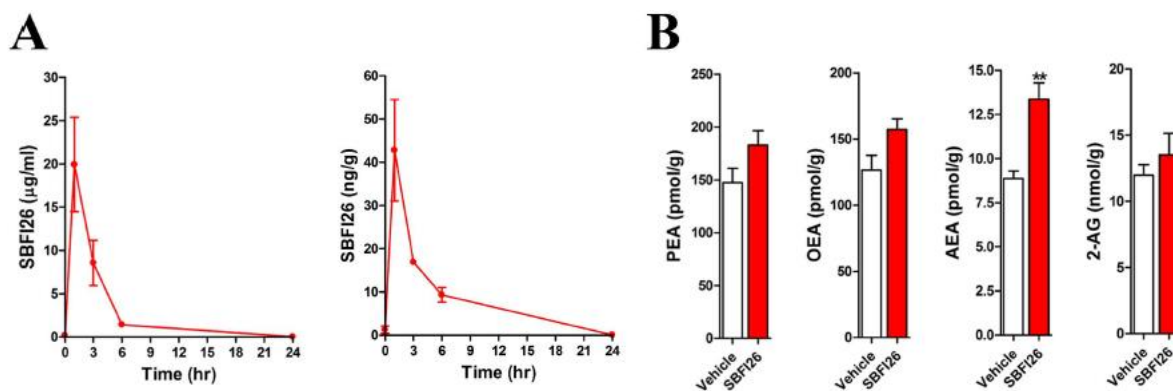


Figure 8 Left – thermal latency in rats with CCI when exposed to SB-FI-26. Effects persisted up to 4 hours. Right – mechanical threshold in rats with CCI when exposed to SB-FI-26.

2.1.2.4. Pharmacokinetics of SB-FI-26

Intraperitoneal injection of SB-FI-26 into mice showed a peak in plasma and brain levels within an hour of injection (**Figure 9A**).¹¹ The half-life of the compound was about 3 hours, and the compound was completely eliminated from the body within 24 hours.¹¹ Brain levels of SB-FI-26 were lower than in the plasma. The hydrophilic carboxylate moiety may disrupt the compound's ability to cross the blood-brain barrier. Administration of SB-FI-26 into mice lead to increased anandamide levels, while other endocannabinoids, such as 2-arachidonylglycerol, remained steady (**Figure 9B**).¹¹ Furthermore, liver extracts, from mice administered with SB-FI-26, used in [¹⁴C] anandamide hydrolysis experiments showed normal levels of anandamide hydrolysis, signifying that SB-FI-26 did not inhibit FAAH (**Figure 9C**).¹¹ These data support the hypothesis that SB-FI-26 inhibits FABP5 and FABP7, increasing the levels of anandamide and leading to analgesia.



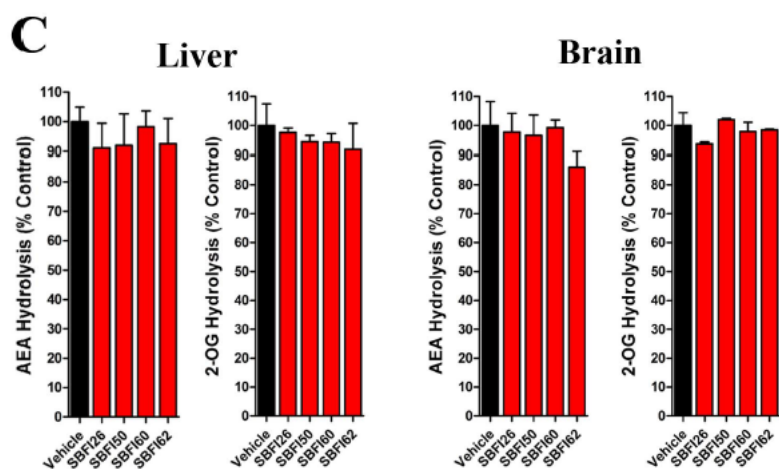


Figure 9 A – Plasma and brain levels of SB-FI-26 after i.p. injection. B – Endocannabinoid levels after administration of SB-FI-26. Anandamide levels increase, while other endocannabinoids stay relatively static. C – Anandamide hydrolysis in the liver and brain after administration of SB-FI-26. Anandamide hydrolysis remains normal.

2.2. Results and discussion

2.2.1. Optical resolution of SB-FI-26

After the resolution of a co-crystal structure of SB-FI-26 bound to FABP5 from the Li group, the crystal structure shows SB-FI-26 sitting in the fatty acid binding pocket, with the free carboxylate of SB-FI-26 interacting with two amino acids, tyrosine 129 and arginine 131. The carboxylate forms one hydrogen bond with the hydroxy group of tyrosine and two hydrogen bonds with the guaninium of arginine. This is identical to the interactions 2-arachidonoyl glycerol has with FABP5. It was also found that only the *S,S* enantiomer of SB-FI-26 appeared in the binding site (**Figure 10**). This led to the hypothesis that one enantiomer of SB-FI-26 bound more tightly to the protein than the other, and usage of a racemic mixture would hamper the activity of the compound, so the optical resolution of SB-FI-26 was initiated. This was performed to obtain optically pure SB-FI-26 to determine if one enantiomer had a higher affinity for FABP5 than the other. Various chiral resolving agents, (1*R*,2*S*)-2-amino-1,2-diphenylethanol, (*S*)-1-(1-naphthyl)ethylamine, and L-phenylalaninol, were purchased.

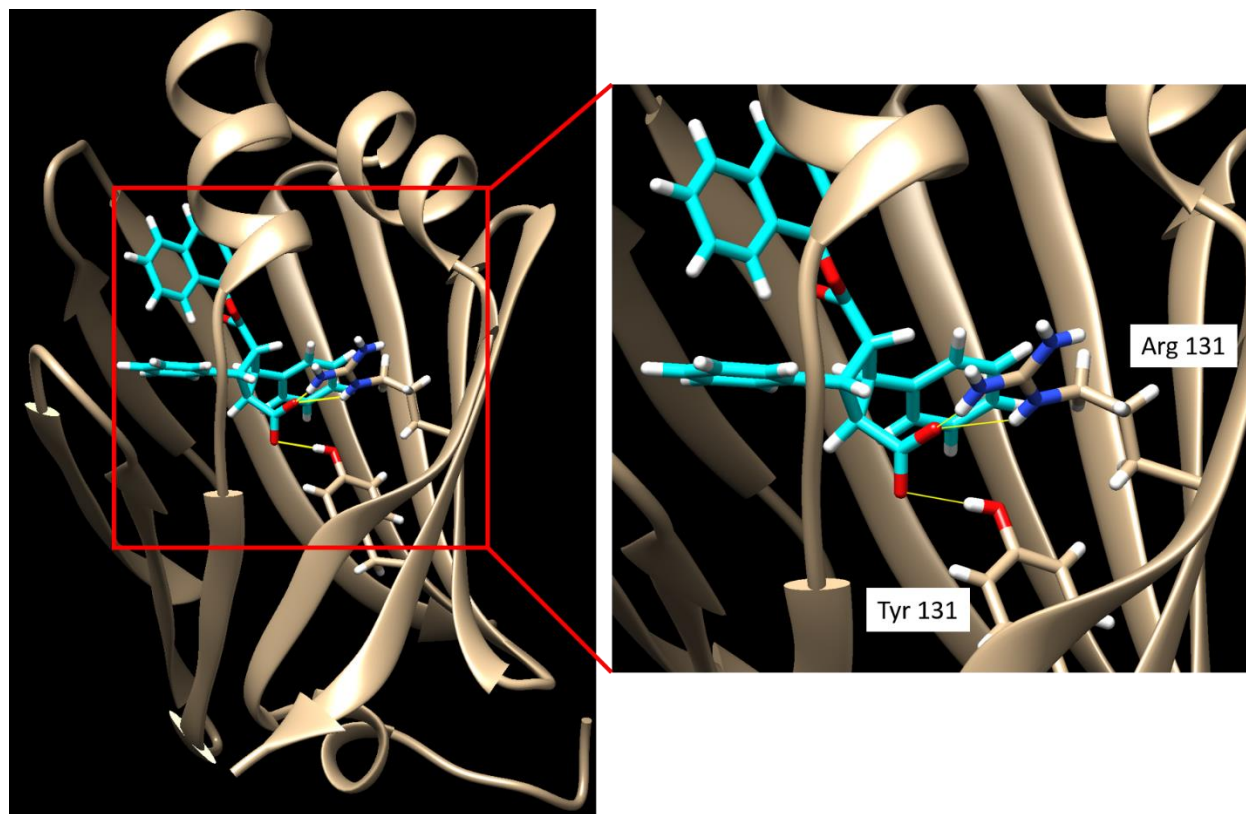
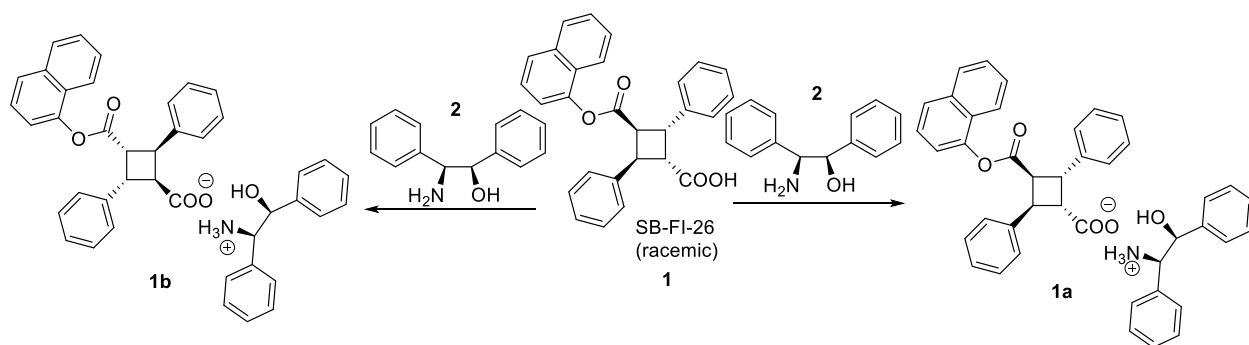


Figure 10 Crystal structure of SB-FI-26 bound to FABP5

Small amounts of SB-FI-26, **1**, and resolving agent were dissolved in various solvents and allowed to recrystallize as diastereomeric salts. (1R,2S)-2-Amino-1,2-diphenylethanol, **2**, was the first resolving agent tested. Solvents used for recrystallization were ethanol, isopropanol, and acetonitrile. Each trial was tested on a 30 mg scale with concentrations of 30 mg/ mL, 60 mg/ mL, and 86 mg/ mL. After seeing no crystal formation at these concentrations with all solvents, 50 μ L of water was added to help promote nucleation. Only isopropanol showed small amounts of crystal formation. An additional 50 μ L of water was added to the remaining three samples, and crystal formation was observed in the ethanol and acetonitrile samples. No crystal formation occurred in the methanol sample and further addition of water resulted in compound precipitating out of solution (**Table 2**). Resolution of SB-FI-26 with (1R,2S)-2-amino-1,2-diphenylethanol, **2**, resulted in few crystals and any successful crystal formation resulted in racemic SB-FI-26 after acidic workup and subsequent chiral HPLC analysis. (1R,2S)-2-Amino-1,2-diphenylethanol, **2**, was a poor resolving agent for SB-FI-26, **1**, since crystal formation was difficult, and crystals that were formed remained as racemic mixtures.



Scheme 1 Optical resolution with (1R,2S)-2-amino-1,2-diphenylethanol

Table 2 Conditions tested in optical resolution using (1R,2S)-2-amino-1,2-diphenylethanol

Solvent	Solvent quantity	Crystals formation
MeOH	1000 μ L MeOH	No crystal formation
	500 μ L MeOH	No crystal formation
	350 μ L MeOH	No crystal formation
	350 μ L MeOH, 50 μ L water	No crystal formation
	350 μ L MeOH, 100 μ L water	No crystal formation
EtOH	1000 μ L EtOH	No crystal formation
	350 μ L EtOH	No crystal formation
	350 μ L EtOH, 50 μ L water	No crystal formation
	350 μ L EtOH, 100 μ L water	Small crystals after overnight
IPA	1000 μ L IPA	No crystal formation
	350 μ L IPA	No crystal formation
	350 μ L IPA, 50 μ L water	Small crystals after overnight
MeCN	1000 μ L MeCN	No crystal formation
	350 μ L MeCN	No crystal formation
	350 μ L MeCN, 50 μ L water	No crystal formation
	350 μ L MeCN, 100 μ L water	Small crystals after overnight

Resolution with (S)-1-(1-naphthyl)ethylamine, **3**, was performed on a 30 mg scale of SB-FI-26, **1**, with one equivalent of resolving agent dissolved in methanol, isopropanol, or acetonitrile, with a final concentration of 25 mg/ mL. (S)-1-(1-Naphthyl)ethylamine, **3**, gave better results, with small crystals forming after dissolving samples in methanol and acetonitrile, but the crystals

remained small even after leaving the solutions to sit for 48 hours. Larger crystals formed with isopropanol. Two other methanol samples were made with DCM and water added to them to promote nucleation. The resulting crystals were larger with the methanol water sample. Both the isopropanol and methanol/water samples were acidified, extracted, and analyzed on HPLC, and both samples were nearly racemic with a 10% enantiomeric excess. (S)-1-(1-Naphthyl)ethylamine, **3**, was unsuitable for optical resolution as numerous iterations would need to be performed to obtain even a mediocre amount of enantiomeric excess.

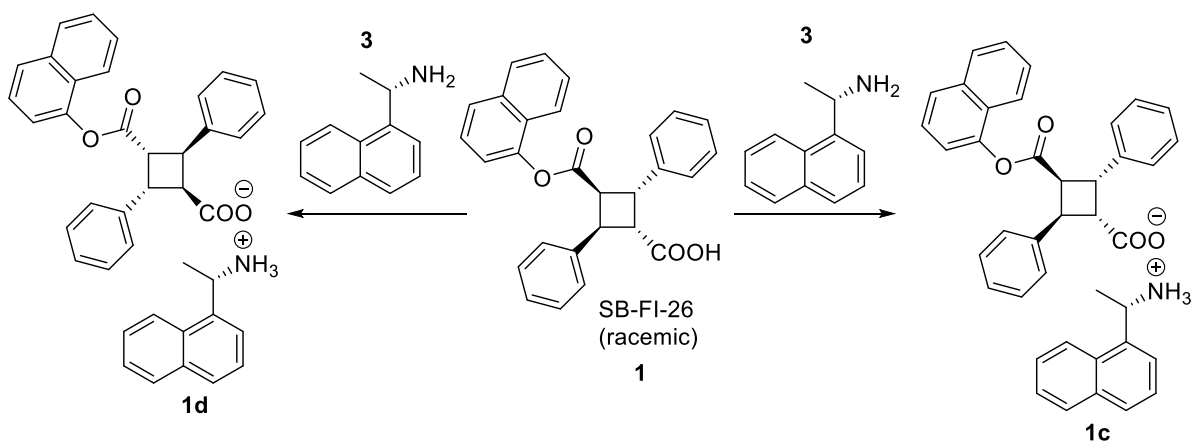


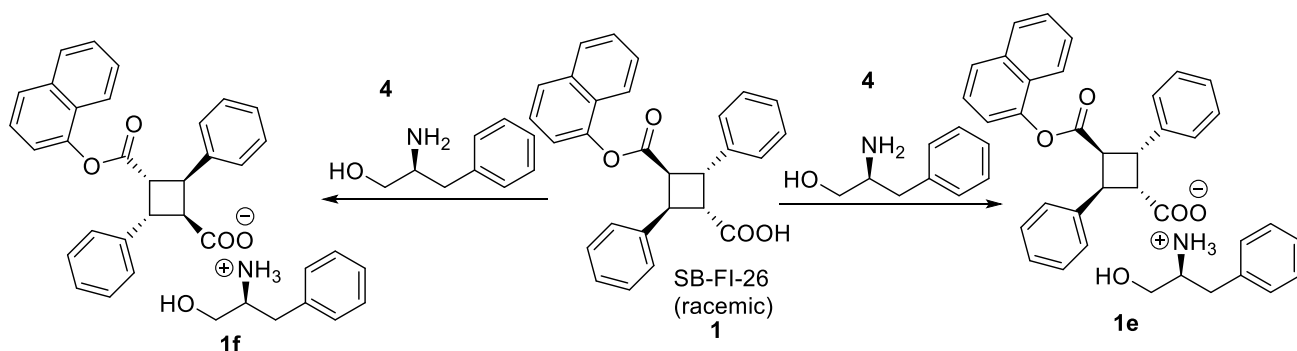
Table 3 Conditions tested in optical resolution using (S)-1-(1-naphthyl)ethylamine

Solvent	Solvent quantity	Time & crystal formation
MeOH	1200 μ L MeOH	Small crystals after 48 hrs.
MeOH / DCM	1200 μ L MeOH, 500 μ L DCM	Small crystals after 48 hrs.
MeOH / water	1200 μ L MeOH, 300 μ L water	Small crystals after 3 hrs.
IPA	1200 μ L IPA	Crystal formation after 48 hrs.
MeCN	1200 μ L MeCN	Small crystals after 3 hrs.

The next trial was with L-phenylalaninol, **4**, at a 30 mg scale with SB-FI-26, **1**, and one equivalent of resolving agent (**Scheme 3**). Methanol, ethanol, isopropanol, or acetonitrile were used to dissolve SB-FI-26, **1**, and L-phenylalaninol, **4**. Resolution with L-phenylalaninol, **4**, gave larger crystals in methanol and water than resolution with (S)-1-(1-naphthyl)ethylamine, **3**, in isopropanol. There was no crystal formation with isopropanol, ethanol, and acetonitrile. Various other solvents, such as acetone, hexanes, or water, were added to the solution to facilitate crystal

formation, but only small crystals were formed. The solid from the methanol/water sample were collected, extracted with 1 N HCl and ethyl acetate, and analyzed on chiral HPLC. The sample showing an enantiomeric excess of 80%. L-phenylalaninol, **4**, was chosen as the resolving agent, and the solvent was methanol. The resolution was scaled up to 100 mg of SB-FI-26, **1**. After the first resolution in methanol, the resulting SB-FI-26, **1**, showed an optical purity of 89% enantiomeric excess. The sample was resolved a second time to 99% enantiomeric excess in 36% yield. The sample was labelled SB-FI-26A, **1e**, since its absolute stereochemistry was unknown (**Figure 11b**). D-phenylalaninol, **4a**, was purchased for resolution of the other enantiomer, and the second enantiomer was resolved at 95% enantiomeric excess with 65% yield, following the same procedure for the optical resolution of SB-FI-26A, **1e**. The second enantiomer was labelled SB-FI-26B, **1g**, (**Figure 11c**). In a recent optical resolution with D-phenylalaninol, **4a**, acetone was used as the solvent, and after one resolution, SB-FI-26, **1**, was found to be 93% ee. Acetone was found to be a better solvent than methanol for optical resolution of SB-FI-26, **1**.

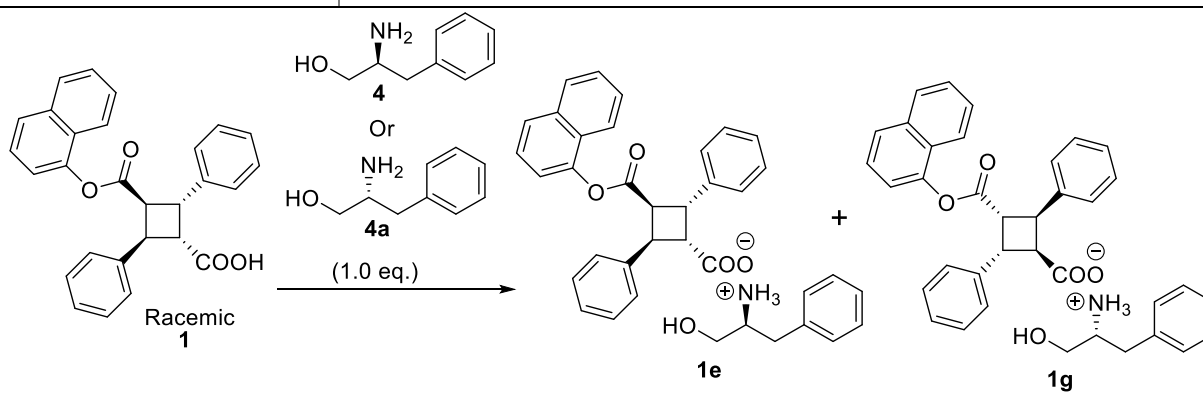
Resolution of the two enantiomers required two cycles of diastereomeric salt formation. After the first iteration, the enantiomeric excess was approximately 90%, and second resolution was needed to ensure at least 95% enantiomeric excess. Racemic SB-FI-26, **1**, was run on a Chiralcel ODH column with 65% isopropanol and 35% hexanes as the eluent. The mixture had retention times as 4.3 and 6.7 minutes (**Figure 11a**). SB-FI-26A, **1e**, corresponded to the enantiomer at 6.7 minutes and SB-FI-26B, **1g**, corresponded to the enantiomer at 4.3 minutes (**Figure 11b, 11c**).



Scheme 3 Optical resolution with L-phenylalaninol and D-phenylalaninol

Table 4 Conditions tested in optical resolution using L-phenylalaninol

Solvent	Solvent quantity	Time & crystal
MeOH/water	1200 mL MeOH, 200 mL water	Crystal formation after overnight.
MeOH/acetone/DCM	1200 mL MeOH, 200 mL acetone, 300 mL DCM	Small crystals after 3 hrs.
MeOH/acetone/hexanes	1200 mL MeOH, 100 mL Acetone, 300 mL Hexanes	Small crystals after 3hrs.
EtOH	1200 mL EtOH	No crystal formation
IPA	1800 mL IPA	No crystal formation
IPA/acetone/hexanes	1800 mL IPA, 200 mL acetone, 300 mL Hexanes	Small crystals after 8 hrs.
MeCN	1000 mL MeCN	No crystal formation
MeCN/acetone/hexanes	1000 mL MeCN, 200 mL acetone, 300 mL Hexanes	Small crystals after 8 hrs.



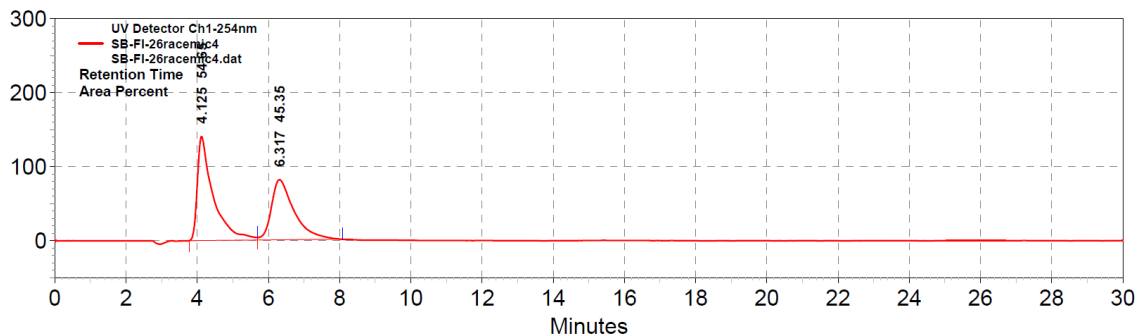
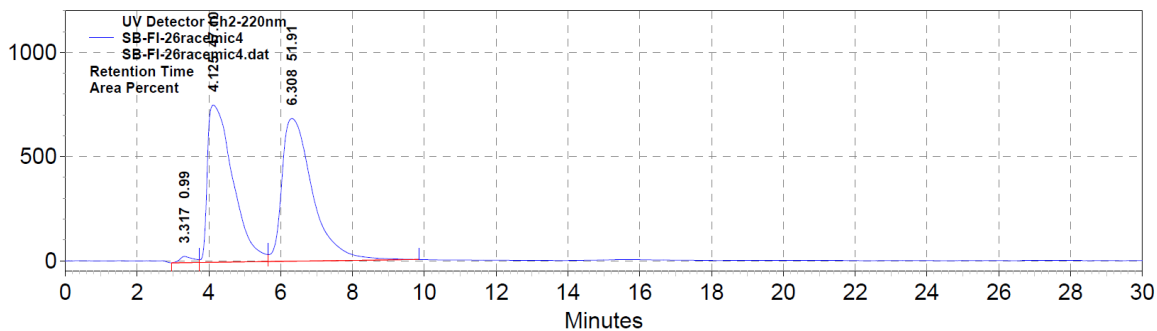


Figure 11a Racemic SB-FI-26 (65%: 35% IPA: hexanes Chiralcel ODH).

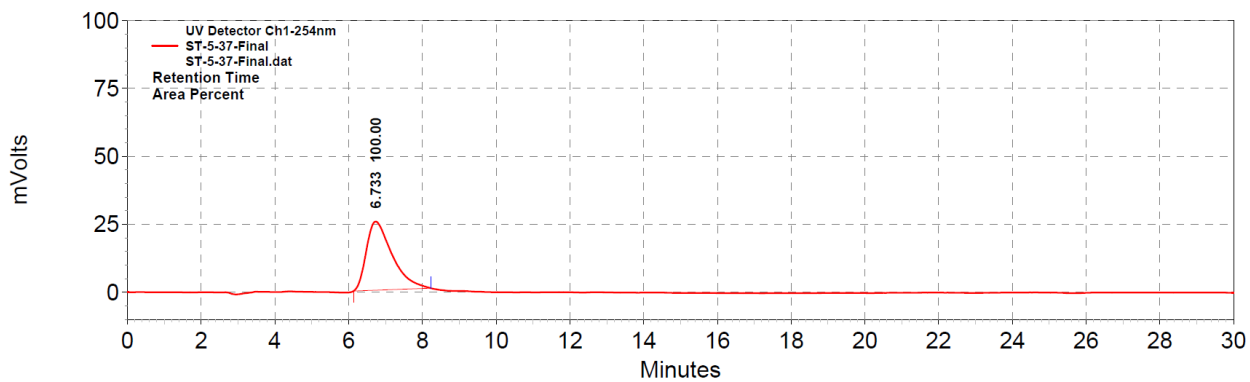
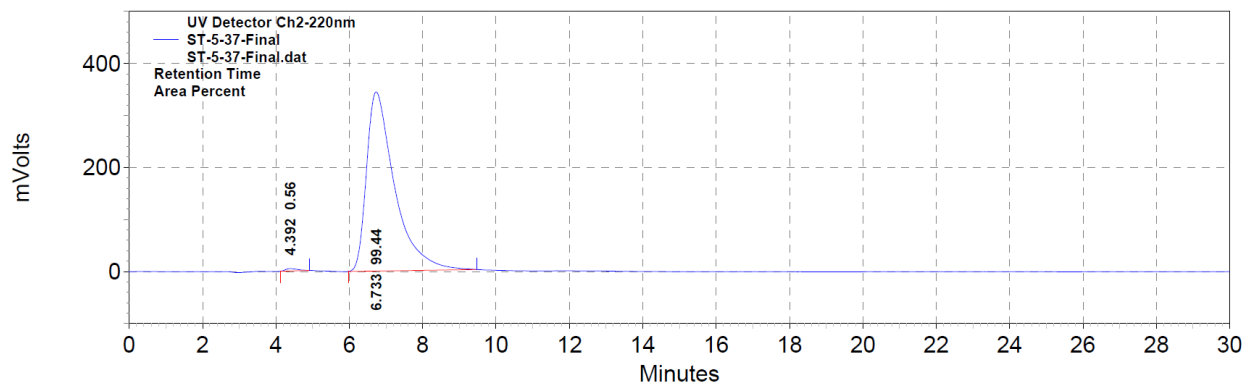


Figure 11b Optical Resolution with L-Phenylalaninol.

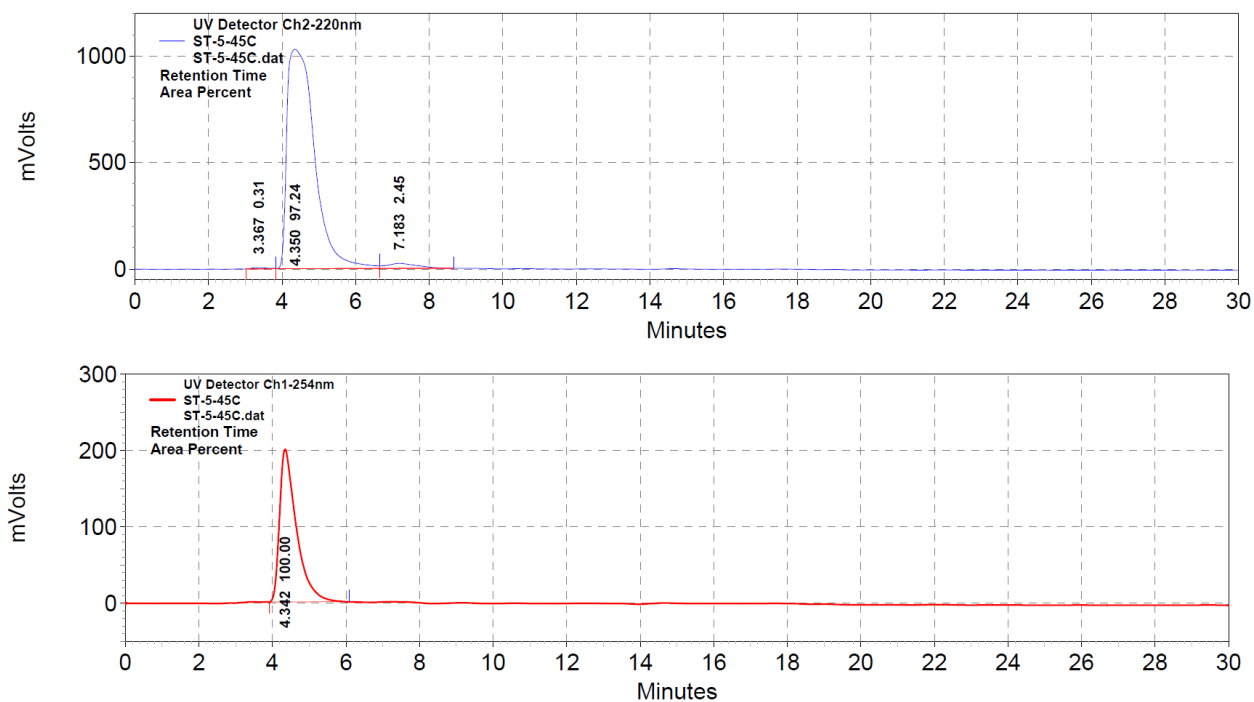


Figure 11c Optical Resolution with D-Phenylalaninol

Both optically pure samples were submitted for X-ray diffraction, and SB-FI-26A was found to be the (R,R) enantiomer (**Figure 12**). SB-FI-26B was found to be the (S,S) enantiomer. Fluorescence displacement assay of the two enantiomers showed little difference in activity SB-FI-26A K_i values of $0.71 \pm 0.08 \mu\text{M}$ and $0.92 \pm 0.22 \mu\text{M}$ for FABP5 and FABP7, respectively. SB-FI-26B had K_i values of $0.79 \pm 0.15 \mu\text{M}$ and $0.45 \pm 0.01 \mu\text{M}$ for FABP5 and FABP7, respectively. Comparing K_i values for FABP5, the two compounds are within error of each other. The only significant difference in K_i is for FABP7, but activity for FABP7 does not translate to analgesic effects *in-vivo*.^{5,6} The crystal structure for SB-FI-26A was determined by Matthew Freitag.

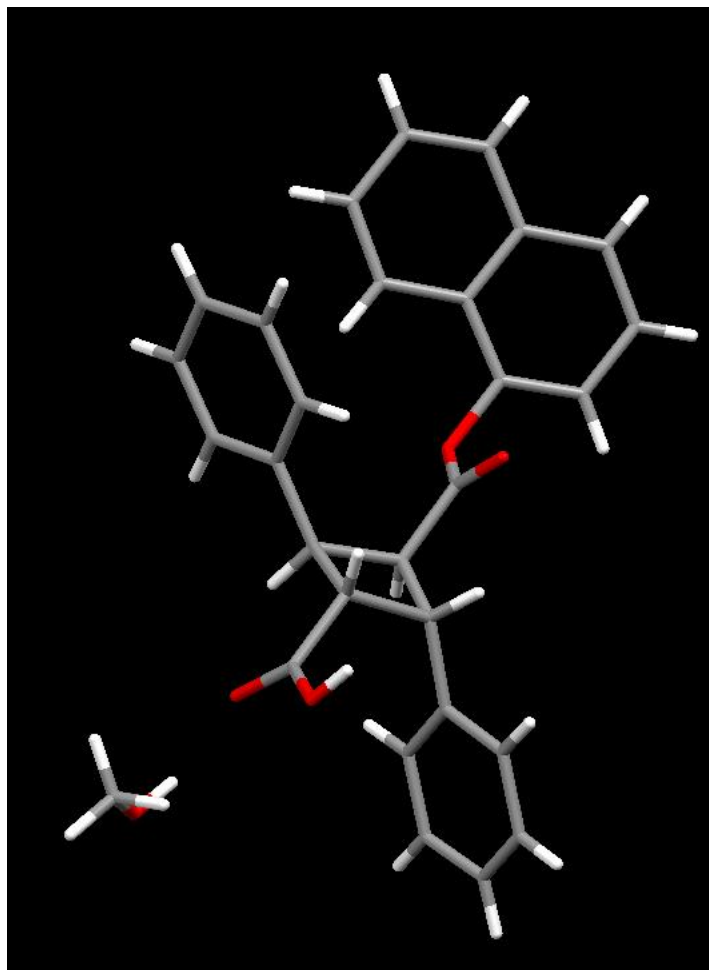


Figure 12 X-ray diffraction of SB-FI-26A.

2.2.2. Synthesis of α -truxillic acid derivatives

2.2.2.1. Synthesis of (-)-incarvillateine analogue

(-)-Incarvillateine is a monoterpene alkaloid natural product from *Incarvillea sinensis*, a plant from northern China.^{8,12} It is used as traditional medicine for pain relief and treating rheumatism.¹² In formalin pain models in mice, this compound showed analgesic activity.¹² It contains an α -truxillic acid core and bears striking similarity to the α -truxillic acid monoesters that have been tested as FABP inhibitors. A compound, SB-FI-101, was synthesized to mimic the 4-hydroxy-3-methoxy substitution patterns on the phenyl rings. (-)-Incarvillateine relieves pain through an opioid receptor agonist mechanism. (-)-Incarvillateine was ineffective in a formalin pain model, where mice were pretreated with κ -opioid receptor antagonist, nor-binaltorphimine, and μ -opioid receptor antagonist, β -funtaltramine, while (-)-incarvillateine still produced

analgesia when administered to mice pretreated with a δ -opioid receptor antagonist, naltrindole.¹³ The natural product elicits analgesia through activation of specific opioid receptors. Even though it potentially acts through a different mechanism, synthesis of this compound was interesting and provided important information as to what substitution patterns are tolerated on the phenyl rings.

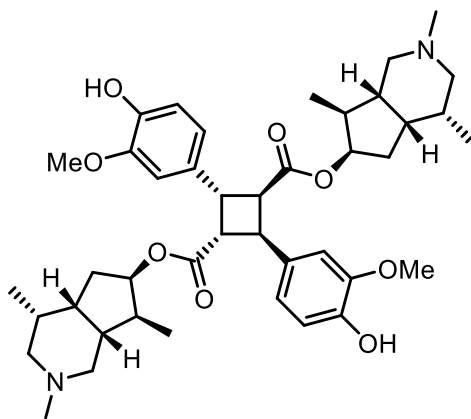
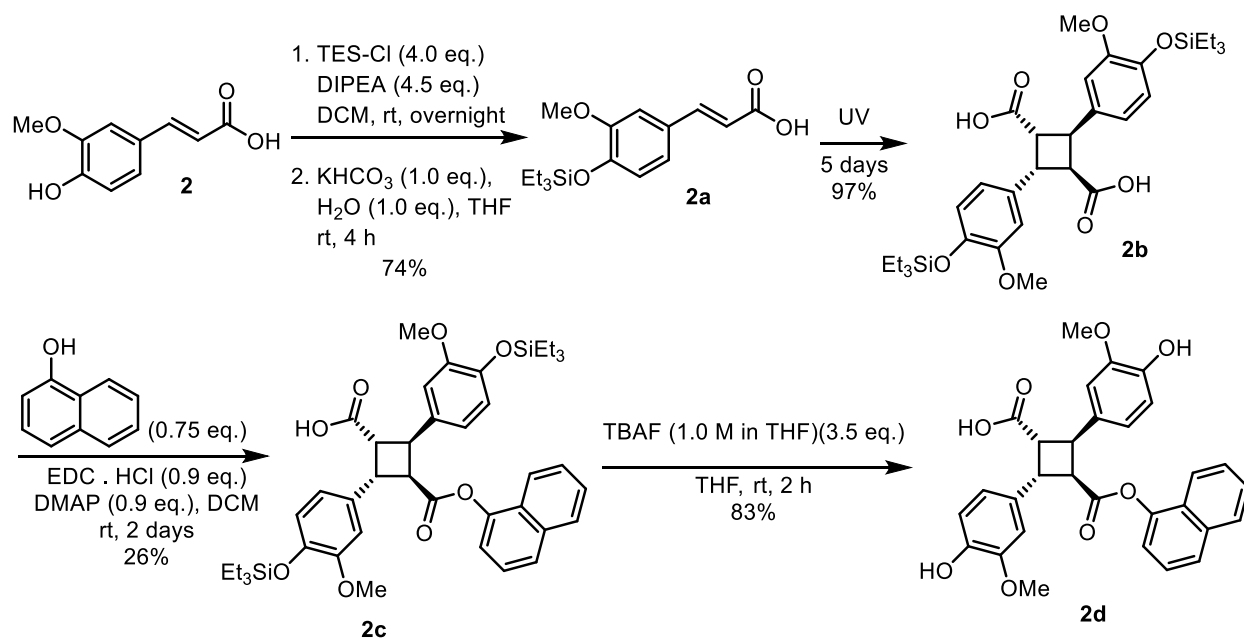


Figure 13 Structure of natural product (-)-incarvillateine

The synthesis started with commercially available (E)-3-(4-hydroxy-3-methoxyphenyl)-2-propenoic acid, **2**, which was silylated using triethylsilylchloride, in the presence of diisopropylethylamine (**Scheme 4**). The resulting product was the disilylated product which was subsequently reacted with potassium bicarbonate to afford (2E)-3-(3-methoxy-4-triethylsiloxyphenyl)-2-propenoic acid, **2a**, in 74% yield (**Scheme 4**). (2E)-3-(3-Methoxy-4-triethylsiloxyphenyl)-2-propenoic acid, **2a**, was then photodimerized using a UV reactor affording 2,4-bis(3-methoxy-4-triethylsiloxy)phenylcyclobutane-1,3-dicarboxylic acid, **2b**, as the product in 97% yield. In the following reaction, 2,4-bis(3-methoxy-4-triethylsiloxy)phenylcyclobutane-1,3-dicarboxylic acid, **2b**, was coupled with 1-naphthol, in the presence of dimethylaminopyridine and 1-(3-dimethylaminopropyl)-3-ethylcarbodiimide hydrochloride, to afford 2,4-bis(3-methoxy-4-triethylsiloxy)phenylcyclobutane-1,3-dicarboxylic acid mono-1-naphthyl ester, **2c**, as the product in 26% yield (**Scheme 4**). 2,4-bis(3-methoxy-4-triethylsiloxy)phenylcyclobutane-1,3-dicarboxylic acid mono-1-naphthyl ester, **2c**, was then reacted with tetrabutylammonium fluoride to obtain 2,4-bis(3-methoxy-4-hydroxy)phenylcyclobutane-1,3-dicarboxylic acid mono-1-naphthyl ester, **2d**, as the product in 83% yield (**Scheme 4**). The compound was sent out for testing in the Deutsch group in the Department of Biochemistry and Cell Biology.



Scheme 4 Synthesis of (-)-incarvillateine analog

Results from the fluorescence displacement assay showed poor activity for FABP5, with a $K_i > 10 \mu\text{M}$. The compound showed activity for FABP3 and FABP7 with K_i values of $1.31 \pm 0.19 \mu\text{M}$ and $2.97 \pm 0.11 \mu\text{M}$, respectively. Compared to SB-FI-26, SB-FI-101 is far less active and potentially more detrimental to health, since it binds better to FABP3, a fatty acid binding protein in the heart. Inhibition of FABP3 disrupts cardiac lipid transport, leading to altered heart homeostasis as well as old-age cardiac hypertrophy.^{11,14} Even though this compound was inactive, it shows that substitutions on the phenyl rings may be detrimental to activity. When looking at the FABP5-SB-FI-26 co-crystal structure, there is little space around the phenyl rings, and any additions to the rings may require changes in binding pose of the compound, within the binding site, to accommodate the substituents (**Figure 14**). This change in binding pose may lead to less effective contacts within the binding site, resulting in lower activity.

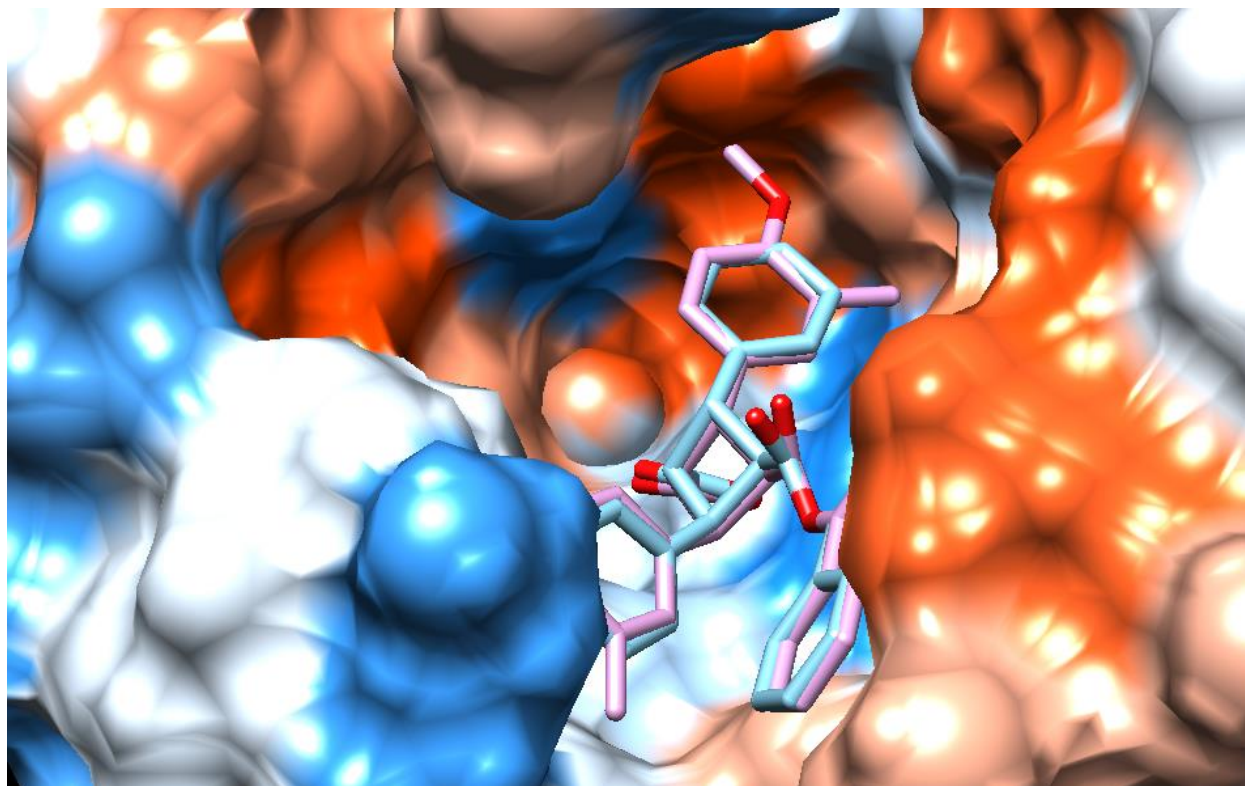


Figure 14 SB-FI-26 (blue) and SB-FI-101 (pink) in the binding site of FAB5.

2.2.2.2. Continuing SAR study

A series of α -truxillic acid derivatives were synthesized as a continuation of the SAR study. Since a byproduct of monoester synthesis is formation of the diester, both monoesters and diesters were isolated and sent for K_i determination. The general procedure started with commercially available *trans*-cinnamic acid, **3**, which was exposed to UV light at 360 nm to induce the [2+2] photocycloaddition. The resulting product was α -truxillic acid, **3a**. The acid was then chlorinated with thionyl chloride, in the presence of catalytic DMF, under reflux to obtain the diacid chloride, **3b**. In order to determine what substitutions were needed for activity at the ester moiety, the diacid chloride was substituted with numerous alcohols. Several benzyl alcohols were used to synthesize analogues. The monoesters, **3c**, showed good activity, but were about 50% less active than SB-FI-26 at inhibiting FABP5 and were nearly an order of magnitude less active than SB-FI-26 at inhibiting FABP7. Diester compounds, **3d**, were complete inactive, which is consistent with the hypothesis that a free carboxylate group is needed for activity, as both natural substrates, AEA and 2-AG, are carboxylic acids.

Aside from benzyl alcohols, 2-indanol was used as a nucleophile. This compound was chosen as a potential analogue to 6-*epi*-incarvilline, the alcohol moiety on (-)-incarvillateine.¹²

Both compounds contain a 5/6 ring system on the alcohol, but 2-indanol contains an aromatic ring, compared to the aliphatic ring of 6-*epi*-incarvilline. It was to be a hybrid between 6-*epi*-incarvilline and 1-naphthol. Maintaining the aromaticity meant not having to deal with extra chiral centers and mixtures of four stereoisomers. Only two enantiomers would be obtained when keeping the alcohol achiral, and imitation of the 5/6 ring system may improve activity. SB-FI-77, **3c-5**, showed good binding activity, but was not as active as SB-FI-26, with SB-FI-77, **3c-5**, having a K_i of $1.57 \pm 0.15 \mu\text{M}$ compared to SB-FI-26, **3c-1**, having a K_i of $0.93 \pm 0.08 \mu\text{M}$ for FABP5. These values are not far from each other, but the K_i difference for FABP7 binding is much farther apart, with $0.38 \pm 0.04 \mu\text{M}$ for SB-FI-26 and $2.78 \pm 0.24 \mu\text{M}$ for SB-FI-77. Overall, this compound is nowhere near as active as the lead.

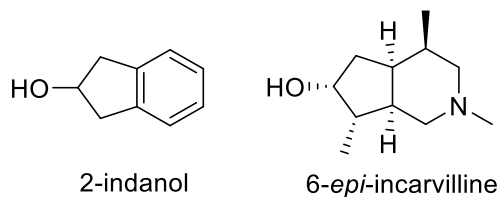
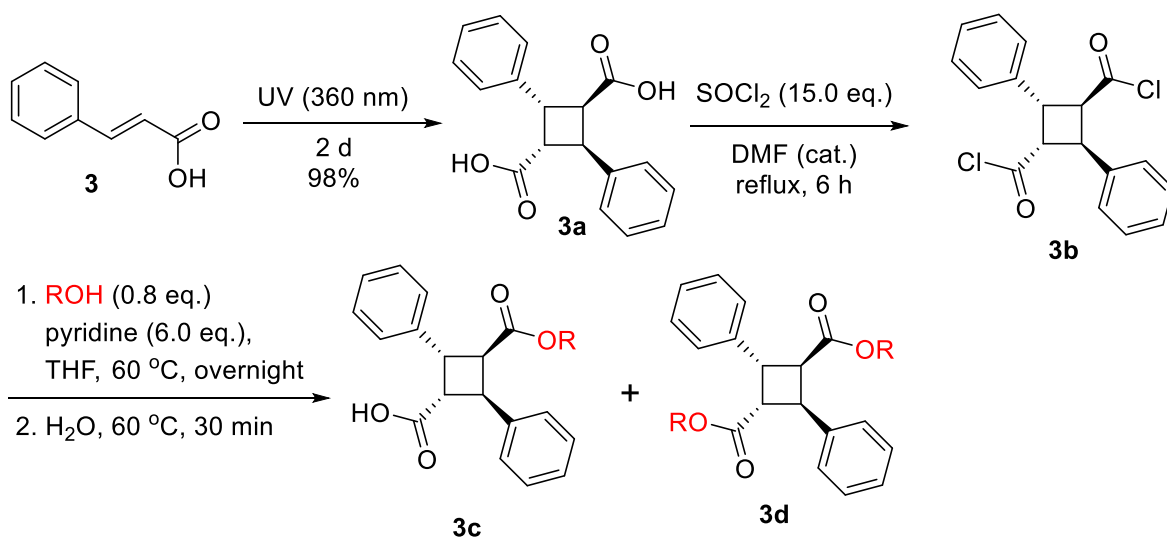


Figure 15 Comparison of 2-indanol and 6-*epi*-incarvilline.

Another compound was synthesized from 3-hydroxyphenyl acetylene (SB-FI-84), **3c-9**. This compound was an intermediate for synthesis of SB-FI-85, **3c-10**, but it was sent for biological testing and showed slightly better activity than SB-FI-26 for binding to FABP5. Its FABP7 binding affinity has not been determined. Even though it has slightly better activity, the difference is not great enough to justify replacing SB-FI-26 as the new lead. Further testing would need to be performed, but it may not be worth it for a compound with marginally better binding.

Table 5 Synthesis of α -truxillic acid derivatives

ROH	SB Code	Yield	Ki	
			FABP5	FABP7
Naphthol	1 SB-FI-26	-	0.93±0.08 μ M	0.38±0.04 μ M
benzyl alcohol (diester)	2 SB-FI-74	43%	>10 μ M	>10 μ M
4-methoxy benzyl alcohol	3 SB-FI-75	40%	-	-
4-methoxy benzyl alcohol (diester)	4 SB-FI-76	12%	>10 μ M	>10 μ M
2-indanol	5 SB-FI-77	34%	1.57±0.15 μ M	2.78±0.24 μ M
4-fluorobenzyl alcohol	6 SB-FI-78	34%	2.68±0.08 μ M	2.39±0.28 μ M
4-fluorobenzyl alcohol (diester)	7 SB-FI-79	15%	>10 μ M	>10 μ M
4-bromobenzyl alcohol	8 SB-FI-80	44%	1.61±0.26 μ M	2.68±0.07 μ M
3-hydroxyphenylacetylene	9 SB-FI-84	31%	0.83±0.0027 μ M	-
3-(1-(2-(2-(2-ethoxyethoxy)ethoxy)ethyl)-1H-1,2,3-triazol-4-yl)phenol	10 SB-FI-85	94%	>10 μ M	>10 μ M
tetrahydropyran-4-methanol (diester)	11 SB-FI-86	43%	-	-
2-iodophenol	12 SB-FI-90	21%	-	-
2-phenylphenol	13 SB-FI-91	30%	-	-

2.2.2.3. Minimizing hERG activity

The human ether-a-go-go related gene (hERG) codes for the α -subunit of the potassium ion channel, which is a channel responsible for controlling the electrical activity of the heart.^{15,16} Inhibition of the potassium channel leads to long QT syndrome, which is potentially lethal.¹⁶ The hERG channel is promiscuous to many drug compounds, and many have been taken off the market because of this lethal side effect.^{15,16} Some strategies for reducing hERG activity are increasing the polarity (LogP) of compounds and reducing aromaticity of compounds.¹⁵ The protein is a homo-tetramer, and within the binding site of the hERG channel, there are four tyrosine-652 and four phenylalanine-656, which are thought to pi-pi stack with aromatic rings in drug compounds.^{15,16} The protein also contains lipophilic binding sites, which will interact with hydrophobic molecules.¹⁵ Most α -truxillic acid monoester derivatives are highly lipophilic, but this lipophilicity increases the hERG binding potential and makes formulation of the compounds difficult for later use as drugs. Another caveat is the compounds need some degree of lipophilicity to bind to the fatty acid binding proteins, so a balance needs to be reached for having decreased hERG binding, improved formulation, and tight binding to the target.

Tetrahydropyran-4-methanol was used as a nucleophile for synthesis of SB-FI-85 and SB-FI-86. The extra oxygen on the ring changes the cLogP from 5.96 for SB-FI-26 to 3.83 for SB-FI-85. This increase in polarity will make the compound more easily soluble for biological experiments, but the activity has yet to be determined. By improving solubility and reducing aromaticity, the hERG activity was also thought to be minimized. The disubstituted compound with tetrahydropyran-4-methanol was synthesized starting with α -truxillic acid, which was chlorinated with thionyl chloride and subsequently substituted in the presence of pyridine. The compound was purified and sent out for *in vitro* analysis.

Structural analysis of FABP5, by Longfei Wei, revealed that 5 and 6 positions of the 1-naphthyl group in SB-FI-26 are quite exposed, and a series of SB-FI-26 analogues, with a multitude of substituents on the 5 and 6 positions, were designed based on this structural analysis and the compounds were evaluated using a pharmacophore-guided docking strategy using the program MOE. Of the various compounds, many showed favorable binding energies with the lead compound, and SB-FI-85 showed binding energies of -10.9 Kcal/ mole and -11.0 Kcal/ mole, for the two possible regioisomers, compared to the binding of SB-FI-26, which was -9.00 Kcal/ mole.

The regioisomers of the compound also showed good overlap with SB-FI-26 in the binding site of FABP5 (**Figure 16**).

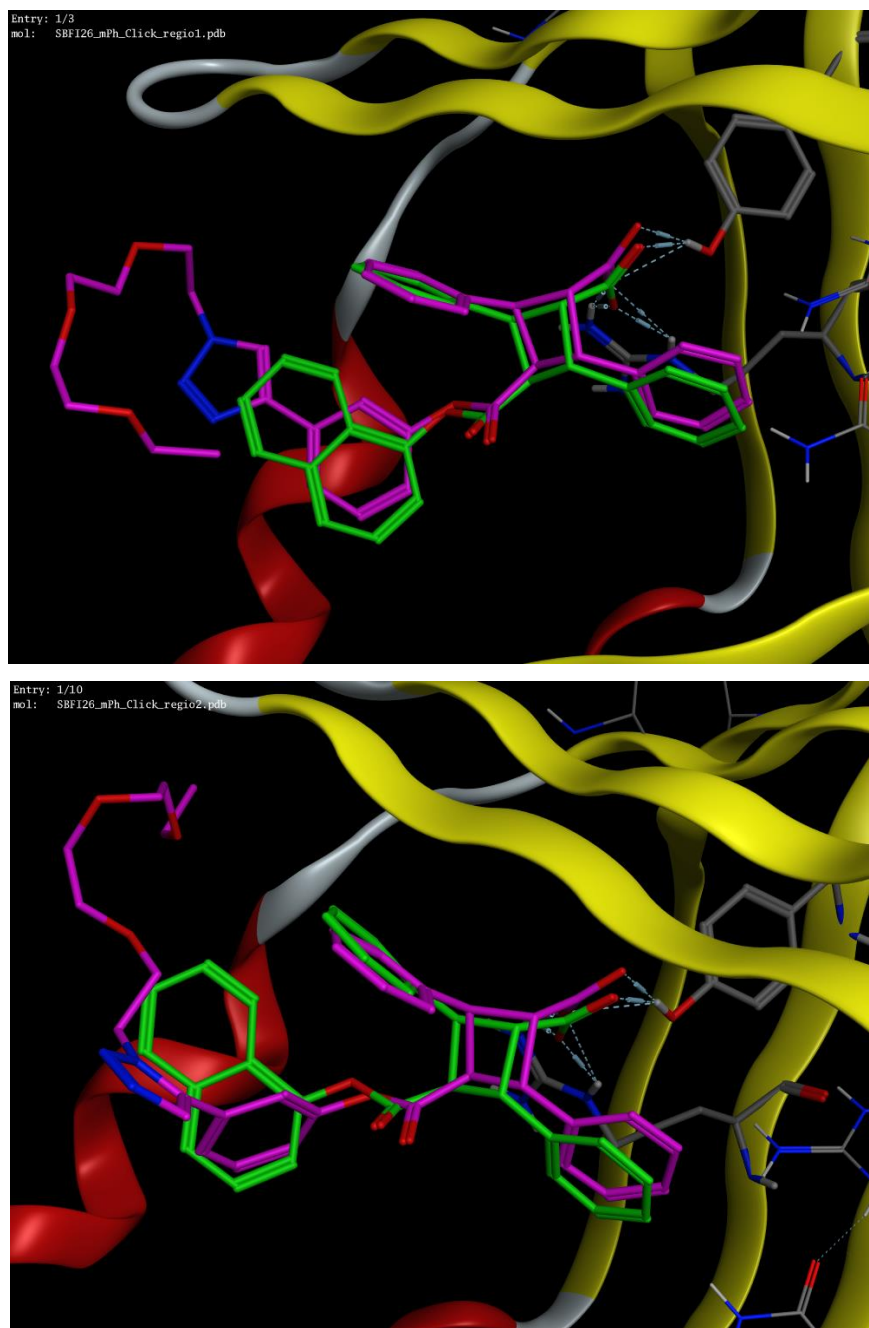
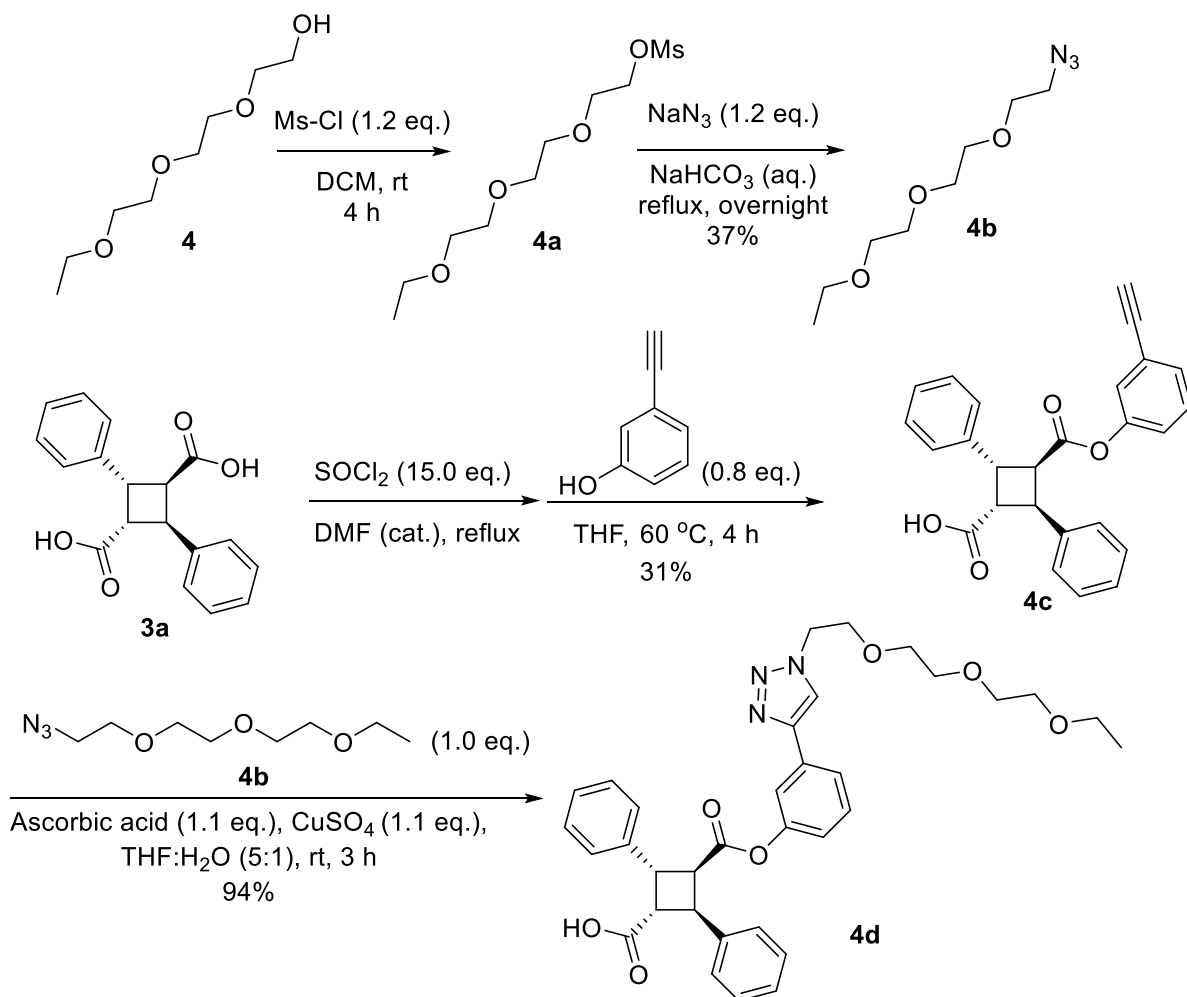


Figure 16 Overlap of SB-FI-85 regioisomers with SB-FI-26 in the binding site of FABP5

Synthesis of SB-FI-85 was slightly different from the general procedure.

First, triethylene glycol monoethyl ether, **4**, was mesylated in DCM at room temperature. The mesylated product, **4a**, was used crude in the next step, which was nucleophilic substitution

with sodium azide in aqueous sodium bicarbonate under reflux overnight. The yield was 37% over two steps. After formation of the azide product, **4b**, it was coupled with α -truxillic acid hydroxy phenyl acetylene monoester, **4c**, in a copper click reaction to make a 1,2,3-triazole. The monoester, SB-FI-84, was synthesized starting from α -truxillic acid, which was chlorinated with thionyl chloride, in the presence of catalytic DMF, and subsequently substituted with 3-hydroxyphenyl acetylene, in the presence of pyridine. The resulting compound, SB-FI-85, **4d**, was tested in fluorescence displacement assay and was found to be inactive in inhibiting FABP5 and FABP7. Addition of the polyethylene glycol (PEG) chain improved solubility, but completely abolished activity. Addition of a PEG chain may not be a good approach to balancing activity and solubility, but more compounds may need to be synthesized to obtain a better picture.

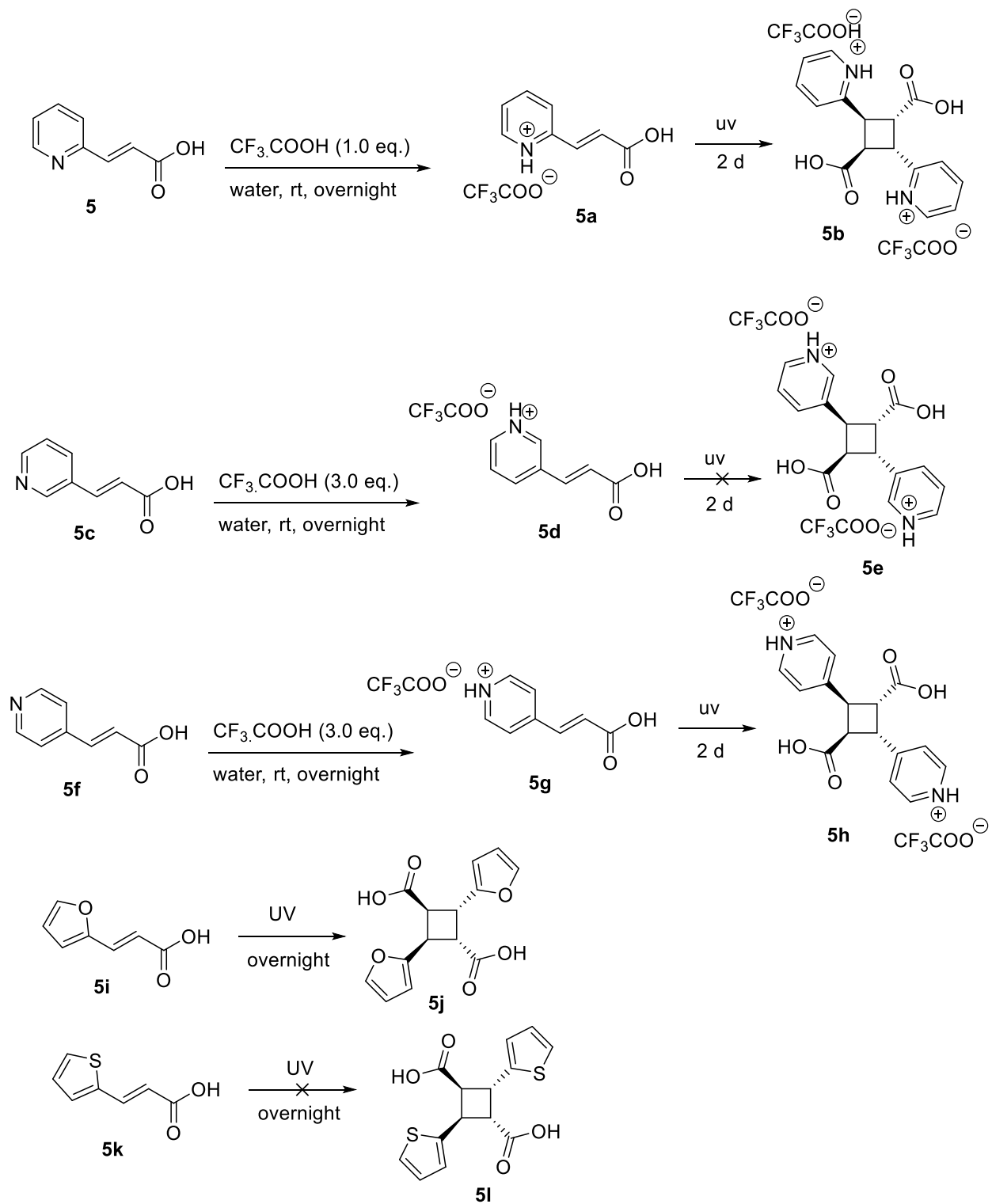


Scheme 5 Synthesis of SB-FI-85.

2.2.2.4. Synthesis of heteroaromatic α -truxillic acids

As part of synthesizing compounds that do not inhibit the hERG channel, the phenyl rings on α -truxillic acid were altered to heteroaromatic rings in hopes of improving solubility. Pyridyl acrylic acids (**5**, **5c**, **5f**) were used in cyclization, but it was found they do not cyclize. Acid activation to the pyridinium salt (**5a**, **5d**, **5g**) improves cyclization. 2-Pyridyl acrylic acid (**5**), 3-pyridyl acrylic acid (**5c**), and 4-pyridyl acrylic acid (**5f**) were individually suspended in water and trifluoroacetic acid was slowly added to the slurry until the solution became clear and no compound persisted. The solutions were allowed to air dry to form the pyridinium salts, **5a**, **5d**, **5g**. The salts were exposed to UV at 360 nm to initiate the [2+2] cycloaddition. It was found 3-pyridinium acrylic acid, **5d**, did not cyclize, but 2-pyridinium acrylic acid, **5a**, and 4-pyridinium acrylic acid cyclized, **5g**, and were confirmed by ^1H NMR. The two successful cyclizations will be carried forward to make SB-FI-26 analogues. When making the salt solution with trifluoroacetic acid, the addition of acid needs to be slow and heating should not be used to improve solubility. Heating the solution improves solubility, but the crystals formed, after drying, do not completely photocyclize into the α -truxillic acid. The solution needs to be dried slowly and completely, since wet crystals also do not photocyclize completely.

Following the approach used for heteroaromatic modification, 3-(2-thiophene) acrylic acid, **5i**, and 3-(2-furyl) acrylic acid, **5k**, were exposed to UV at 360 nm. After overnight, they were analyzed on ^1H NMR, and new proton signals indicated cyclization had occurred for 3-(2-furyl) acrylic acid, **5i**. This was also confirmed by FIA. 3-(2-thiophene) acrylic acid, **5k**, did not cyclize under UV, but 3-(2-furyl) acrylic acid, **5i**, readily cyclizes under UV. Unfortunately, the stereochemistry of the resulting compound is unknown. Further analysis will be required to determine the stereochemistry, but SB-FI-26 analogues will be synthesized from the compound in the future.

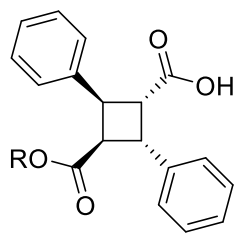


Scheme 6 Synthesis of heteroaromatic cyclobutane diacids.

2.2.2.5. Docking study of SB-FI-81 analogues

A new lead, SB-FI-81, was synthesized, by Kongzhen Hu, and shown to have a binding affinity that is better than SB-FI-26 by a factor of approximately 5-fold. Unfortunately, four possible stereoisomers exist for SB-FI-26, since it was synthesized using a chiral alcohol, *trans*-2-phenyl cyclohexanol. The 2-position of alcohols had not been previously explored, the extra stereoisomers brought about from using a chiral alcohol, and the lipophilicity of SB-FI-81 motivated the continued search for an even more potent compound. A series of compounds were virtually constructed and screened on AutoDock. Emphasis was placed on phenols with substituents at the 2-position. Usage of phenol instead of cyclohexanol limits the number of stereoisomers.

Fifteen compounds were docked to determine binding scores, and the cLogP was also determined for all of the compounds to find a balance between favorable binding and increased polarity. The two compounds, **B** and **C**, showed better binding energy scores than SB-FI-81. Using 2-(3-pyridyl)phenol for the monoester gave an energy score of -8.72 Kcal/ mole, which is more favorable compared to the -8.52 Kcal/ mole of SB-FI-81 (**Table 6**). The 2-(3-pyridyl)phenol monoester, **B**, also had a cLogP of 4.72, which is far more polar than the cLogP of SB-FI-81 at 7.17 (**Table 6**). The second compound with more favorable binding energy was the 2-phenylphenol monoester, which had an energy score of -8.67 and a cLogP of 6.11. The 2-phenylphenol monoester, **C**, is still lipophilic, but it is more polar than SB-FI-81. It is also the aromatic analogue of SB-FI-81, since the cyclohexane ring was replaced by a benzene ring. A third compound that looked interesting was the 2-iodophenol monoester, which showed slightly lower binding energy, -8.46 Kcal/ mole, compared to SB-FI-81, but I can be used as a precursor for Suzuki coupling for the formation of the 2-(3-pyridyl)phenol monoester. Compounds **C** and **D** were synthesized and sent out for biological testing, and compound **B** looks like a promising compound, which should be synthesized in the future. For the rest of the compounds that were screened, the binding score decreased as the polarity increased. There is a delicate balance in finding a compound with good activity as well as high polarity.

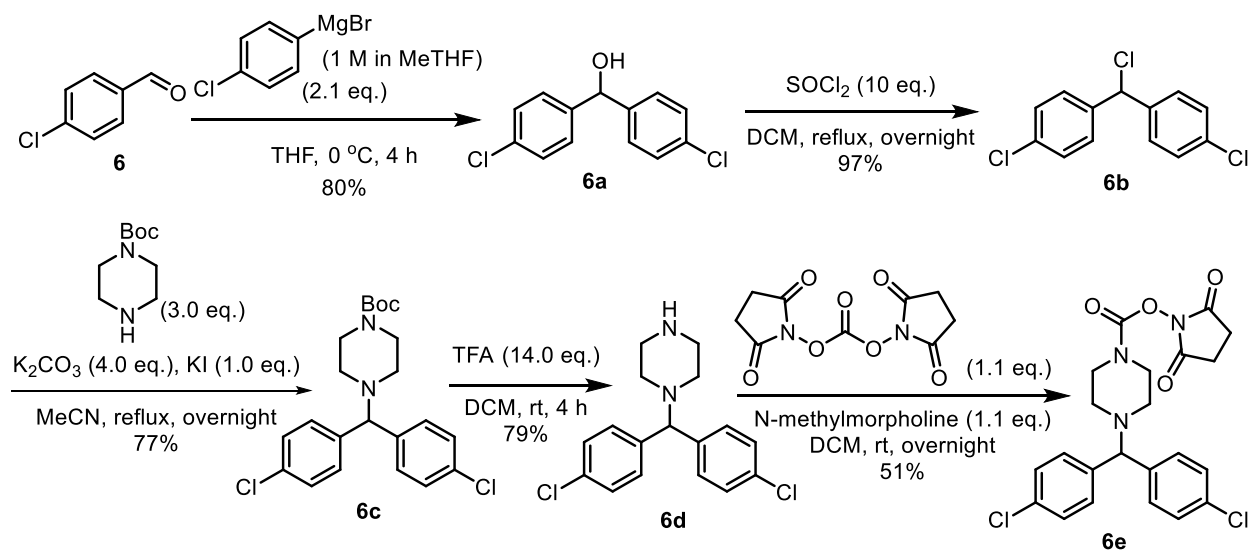
Table 6 Docking results of α -truxillic acid analogues using various alcohols

	Alcohol (-OR)	cLogP	Binding Score (Kcal/ mole)
A		7.17	-8.52
B		4.72	-8.71
C		6.11	-8.67
D		5.77	-8.46
E		4.72	-8.42
F		4.35	-7.82
G		5.19	-7.78
H		4.93	-7.57
I		6.84	-7.53
J		4.00	-7.47

K		6.07	-7.35
L		5.79	-7.16
M		6.07	-7.13
N		4.61	-7.08
O		4.26	-7.07
P		3.38	-6.86

2.2.3. Synthesis of MJN 110

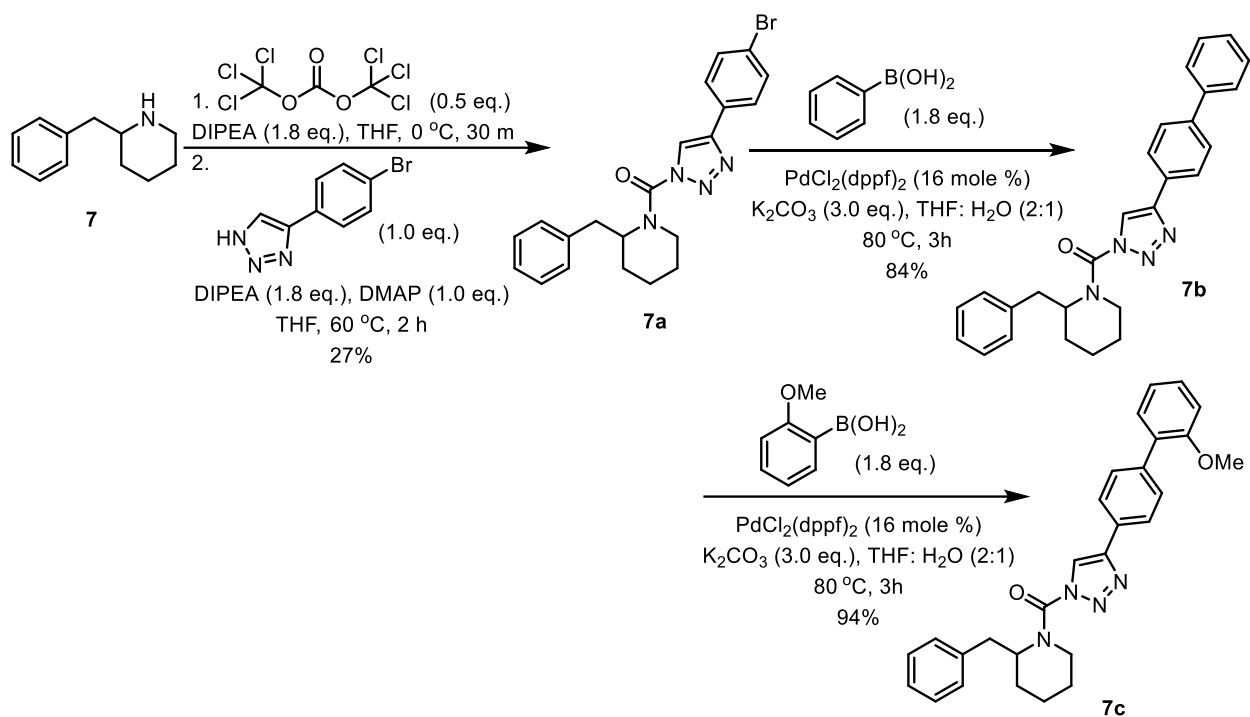
MJN 110, **6e**, was synthesized for a collaborator. The synthesis started with 4-chlorobenzaldehyde, **6**, which was reacted with 4-chlorophenylmagnesium bromide in THF at 0 °C for 4 hours.²¹ This resulted in formation of 4,4'-dichlorodiphenylmethanol, **6a**, in 80% yield. In the following step, 4,4'-dichlorodiphenylmethanol, **6a**, was chlorinated with thionyl chloride in DCM under reflux overnight to give 4,4'-dichlorodiphenylchloromethane, **6b**, in 97% yield.²¹ 4,4'-dichlorodiphenylchloromethane, **6b**, was then reacted with 1-Boc-piperazine with potassium carbonate and potassium chloride in acetonitrile under reflux overnight to give tert-butyl 4-(4,4'-dichlorodiphenyl)methylpiperazine-1-carboxylate, **6c**, as the product in 77% yield.²¹ After nucleophilic substitution, the compound was deprotected with trifluoroacetic acid in DCM at room temperature for 4 hours to obtain 1-(4,4'-dichlorodiphenyl)methylpiperazine, **6d**, as the product in 79% yield.²¹ After deprotection, the compound was acylated using *N,N*'-disuccinimidyl carbonate with *N*-methylmorpholine in DCM at room temperature overnight to obtain MJN110, **6e**, as the final product in 51% yield.²¹ MJN110, **6e**, was characterized and sent out to Dr. Kaczocha for testing.



Scheme 7 Synthesis of MJN 110

2.2.4. Synthesis of KT109 and KT172

2-Benzylpiperidine, **7**, was initially reacted with triphosgene, while being chilled in an ice bath.²² Upon completion of the reaction, the reaction mixture was worked up in ethyl acetate and water. After workup, 4-(4-bromophenyl)-1H-1,2,3-triazole was added to the reaction mixture and stirred while heated. The reaction afforded [4-(4-bromophenyl)-1H-1,2,3-triazol-1-yl][2-(phenylmethyl)-1-piperidinyl]-methanone, **7a**, in 27% yield as a yellow solid.²² In the subsequent step, [4-(4-bromophenyl)-1H-1,2,3-triazol-1-yl][2-(phenylmethyl)-1-piperidinyl]-methanone, **7a**, was reacted with phenylboronic acid in a Suzuki Coupling to afford (4-[1,1'-biphenyl]-4-yl)-1H-1,2,3-triazol-1-yl[2-(phenylmethyl)-1-piperidinyl]-methanone, **7b**, in 84% yield as an off white solid.²² In a parallel synthesis, [4-(4-bromophenyl)-1H-1,2,3-triazol-1-yl][2-(phenylmethyl)-1-piperidinyl]-methanone, **7a**, was reacted with 2-methoxyphenylboronic acid in a Suzuki Coupling to afford [4-(2'-methoxy[1,1'-biphenyl]-4-yl)-1H-1,2,3-triazol-1-yl][2-(phenylmethyl)-1-piperidinyl]-methanone, **7c**, in 94% yield as an off white solid.²² The compounds were synthesized in a gram scale and given to Dr. Martin Kaczocho from the anesthesiology department at the hospital.



Scheme 8 Synthesis of KT109 and KT172

2.3. Conclusion

Since the co-crystal structure of FABP5 and SB-FI-26 only contained one enantiomer of SB-FI-26, optical resolution was performed to obtain enantiomerically pure compound for Ki determination. Unfortunately, there was no difference in binding between the two enantiomers. This is peculiar since the protein contained only one enantiomer, but it is also an indication that the protein does not bind one enantiomer over another and the use of a racemic mixture can be used without the fear of decreased efficacy. The reason behind why the protein is bound exclusively to one enantiomer, even though there is no difference in activity, is unknown, and further testing is needed to fully elucidate the binding mechanism.

Synthesis of a series of α -truxillic acid derivatives has broadened the understanding of the ester functionality and the acid as a whole. Monoester compound showed activity and diester compounds were completely inactive, supporting the hypothesis that the carboxylate group is necessary for activity. The (-)-incarvillateine analogue, SB-FI-101, was less active than SB-FI-26. When looking into the binding site of FABP5, the area around the phenyl rings are tight and may not provide enough room for substituents on the para or meta positions (**Figure 14**). This may have resulted in unfavorable binding in the active site, leading to lowered activity. The ortho

positions on the phenyl rings have more space within the protein binding site and may be able to accommodate larger substituents. The mechanism of (-)-incarvillateine may also be different from the mechanism seen in the α -truxillic acid derivatives. The differences can explain the poor activity of SB-FI-101, since it was now partially modified to act on a different target. Virtual screening of SB-FI-85 showed great overlap with SB-FI-26, and the PEG chain would have improved the solubility of the compound, making it a great candidate, but the actual activity of the compound was poor. Addition of the PEG chain severely reduced activity. Further studies need to be done using the virtual screening approach to perfect the method.

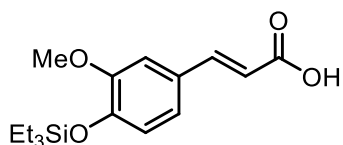
With the advent of SB-FI-81, a new series of compounds, which have not been previously explored, need to be studied (**Table 6, A**). The ortho position of the ester moiety has not been well studied, and two compounds, SB-FI-90 and SB-FI-91, with ortho substitutions on the aromatic group of the ester have been synthesized based on a docking study. The activities have yet to be determined, but they look promising. Overall, the investigation of the SAR of the α -truxillic acid derivatives are still in its nascent stages. Much more needs to be done to get a complete picture into what functional groups and what positions on the molecule can be altered to improve activity.

2.4. Experimental Section

Optical resolution of SB-FI-26

To a solution of α -diphenylcyclobutane-1,3-dicarboxylic acid mono-1-naphthyl ester (SB-FI-26) (100 mg, 0.24 mmoles) in acetone (3 mL) was added L-phenylalaninol (36 mg, 0.24 mmoles) and heated until the reaction mixture was clear and homogeneous. The solution was allowed to cool to room temperature and left on a benchtop overnight. After crystal formation, the mother liquor was removed, and the crystals were washed with cold methanol (3 mL). Hydrochloric acid (12 N) (1.0 mL) was added to the crystals and extracted thrice with ethyl acetate (5 mL X 3). The organic layer was collected, dried over magnesium sulfate, and analyzed on chiral HPLC with 65% isopropanol and 35% hexanes as the eluent. The exact same procedure, using D-phenylalaninol instead of L-phenylalaninol, was used to optically resolve the other enantiomer.

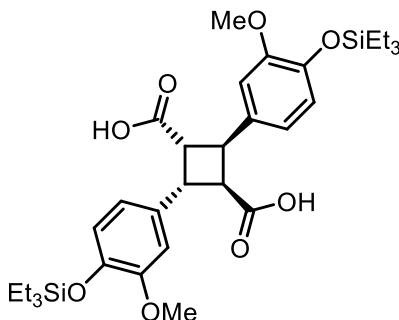
(2E)-3-(3-Methoxy-4-triethylsiloxyphenyl)-2-Propenoic acid



To a chilled solution of (E)-3-(4-hydroxy-3-methoxyphenyl)-2-propenoic acid (400 mg, 2.1 mmoles) in dichloromethane (4 mL) was added diisopropylethylamine (10.3 mmoles) and chlorotriethylsilane (8.2 mmoles). The reaction mixture was left to stir at room temperature overnight. The reaction was monitored by TLC. Upon consumption of the starting material, the reaction mixture was diluted with dichloromethane (30 mL), washed twice with 0.5 M HCl (15 mL), and dried over anhydrous magnesium sulfate. The crude mixture was dissolved in tetrahydrofuran (4 mL) and to the solution was added potassium bicarbonate (2.1 mmoles) and water (2.1 mmoles). The reaction mixture was stirred at room temperature for 5 hours. Upon completion of the reaction, the reaction mixture was diluted with dichloromethane (30 mL), washed twice with 0.5 M HCl (15 mL), and dried over anhydrous magnesium sulfate. The crude mixture was purified using flash column chromatography on silica gel with 1:2 ethyl acetate: hexanes as the eluent affording the product as a white solid. 479 mg, 74% yield; ^1H NMR (500 MHz, CDCl_3) δ 0.69 - 0.83 (m, 6 H), 0.91 - 1.07 (m, 9 H), 3.86 (s, 3 H), 6.32 (d, $J = 15.87$ Hz, 1 H), 6.79 - 6.93 (m, 1 H), 7.00 - 7.13 (m, 2 H), 7.74 (d, $J = 15.87$ Hz, 1 H); ^{13}C NMR (126 MHz,

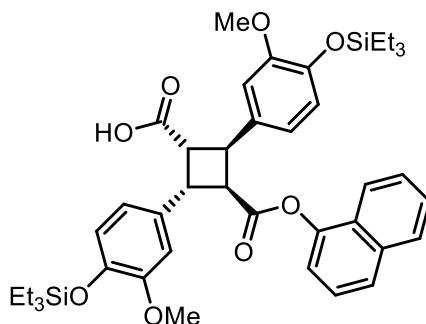
CDCl₃) δ 5.1, 5.4, 6.6, 55.5, 110.9, 114.9, 120.9, 122.7, 127.8, 147.2, 148.0, 151.2, 172.7; HRMS (ESI) *m/z* calculated for C₁₆H₂₄O₄Si (M+H)⁺: 309.1517, found 309.1525 (Δ -2.64 ppm).

2,4-Bis(3-methoxy-4-triethylsiloxy)phenylcyclobutane-1,3-dicarboxylic acid



(2E)-3-(3-Methoxy-4-triethylsiloxyphenyl)-2-Propenoic acid (1.0 g, 3.2 mmoles) was charged to jacketed flask. The reaction vessel was radiated with 365 nm mercury lamp for 5 days under cooling. The reaction was monitored by ¹H NMR, and desired functionalized alpha-truxillic acid was obtained as off-white powder. 959 mg, 97% yield; m.p. 215-218 °C. ¹H NMR (300 MHz, CDCl₃) δ ppm 0.57 - 0.77 (m, 13 H) 0.86 - 1.04 (m, 20 H) 3.77 (s, 6 H) 3.87 (dd, *J*=10.80, 7.26 Hz, 2 H) 4.30 (dd, *J*=10.15, 7.54 Hz, 2 H) 6.67 - 6.84 (m, 6 H). HRMS (ESI) *m/z* calculated for C₃₂H₄₈O₈Si₂ (M+H)⁺: 617.296, found 617.2955 (Δ 0.88 ppm).

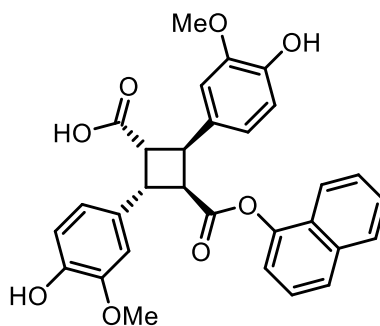
2,4-Bis(3-methoxy-4-triethylsiloxy)phenylcyclobutane-1,3-dicarboxylic acid mono-1-naphthyl ester



To a solution of 2,4-bis(3-methoxy-4-triethylsiloxy)phenylcyclobutane-1,3-dicarboxylic acid (300 mg, 0.49 mmoles), in DCM (10 mL), was added dimethylaminopyridine (0.04 mmoles) and 1-(3-dimethylaminopropyl)-3-ethylcarbodiimide hydrochloride (0.44 mmoles). The mixture was allowed to stir for 4 hours at room temperature. After 4 hours, 1-naphthol (0.36 mmoles), in dichloromethane (20 mL) was added to the reaction mixture dropwise. The reaction was allowed

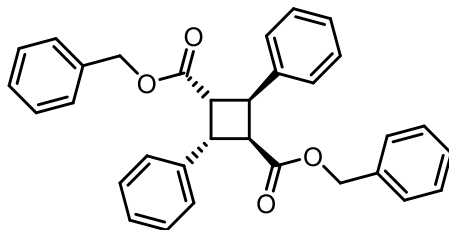
to stir at room temperature for 24 hours. The reaction was monitored by TLC. Upon completion of the reaction, the reaction mixture was diluted with dichloromethane (30 mL), washed thrice with water (20 mL), and dried over anhydrous magnesium sulfate. The resulting crude mixture was purified using flash column chromatography on silica gel with 1:6 ethyl acetate: hexanes as the eluent to afford the desired compound as an off white solid. 71 mg, 26% yield; $^1\text{H NMR}$ (300 MHz, CDCl_3) δ ppm 0.55 - 0.77 (m, 13 H) 0.82 - 1.05 (m, 18 H) 3.75 (s, 3 H) 3.70 (s, 3 H) 3.96 (dd, $J=10.34, 7.36$ Hz, 1 H) 4.26 (dd, $J=10.24, 7.26$ Hz, 1 H) 4.37 - 4.61 (m, 2 H) 6.40 (d, $J=7.45$ Hz, 1 H) 6.63 - 6.76 (m, 1 H) 6.76 - 6.95 (m, 5 H) 7.14 - 7.46 (m, 4 H) 7.59 (d, $J=8.01$ Hz, 1 H) 7.73 (d, $J=8.01$ Hz, 1 H).

2,4-Bis(3-methoxy-4-hydroxy)phenylcyclobutane-1,3-dicarboxylic acid mono-1-naphthyl ester



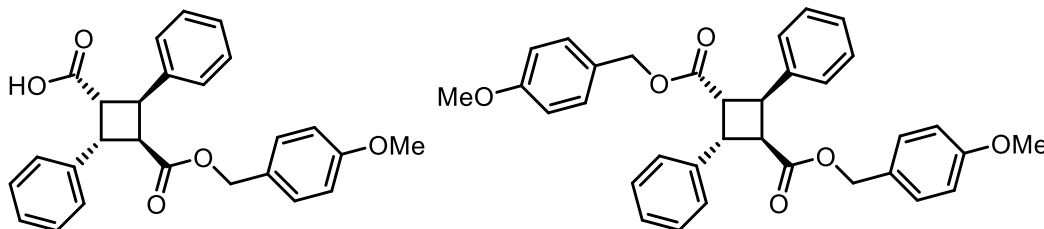
To a solution of 2,4-bis(3-methoxy-4-triethylsiloxy)phenylcyclobutane-1,3-dicarboxylic acid mono-1-naphthyl ester (56 mg, 0.08 mmoles), in 20:1 tetrahydrofuran: acetic acid (2.0 mL total), was added 1.0 M tetrabutylammonium fluoride in THF (0.27 mmoles). The reaction was allowed to stir at room temperature for two hours. The reaction was monitored by TLC. Upon consumption of the starting material, the reaction mixture was diluted with ethyl acetate (30 mL), washed thrice with water (15 mL), and dried over anhydrous magnesium sulfate. The crude mixture was purified using flash column chromatography on silica gel with 3% methanol in dichloromethane as the eluent. 34 mg, 83% yield; $^1\text{H NMR}$ (400 MHz, Acetone- d_6) δ ppm 3.79 (s, 3 H) 3.89 (s, 3 H) 4.02 (dd, $J=10.29, 7.53$ Hz, 1 H) 4.43 (dd, $J=10.29, 7.53$ Hz, 1 H) 4.51 - 4.67 (m, 2 H) 6.66 (d, $J=7.53$ Hz, 1 H) 6.82 (d, $J=8.03$ Hz, 1 H) 6.88 - 6.99 (m, 2 H) 7.04 (br. s., 1 H) 7.07 - 7.15 (m, 2 H) 7.20 (s, 1 H) 7.34 (d, $J=7.78$ Hz, 2 H) 7.46 (s, 1 H) 7.72 (d, $J=8.03$ Hz, 1 H) 7.85 (s, 1 H); HRMS (ESI) m/z calculated for $\text{C}_{30}\text{H}_{26}\text{O}_8$ ($\text{M}+\text{H}$) $^+$: 515.17, found 515.1743 (Δ -8.34 ppm).

α -2,4-Diphenylcyclobutane-1,3-dicarboxylic acid di-benzyl ester (SB-FI-74)



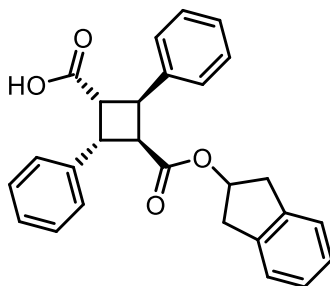
α -Truxillic acid (200 mg, 0.66 mmol) suspended in thionyl chloride (2 mL), was added three drops of DMF and heated to reflux for 3 h. The excess thionyl chloride and DMF was removed *in vacuo* and truxillic acyl chloride was obtained, which was used directly in the subsequent reaction. To the solution of α -truxillic acyl chloride in THF (10 mL) was added benzyl alcohol (1.3 mmol) and pyridine (4.0 mmoles), and the reaction mixture was heated to reflux overnight. The reaction was quenched with addition of distilled water (10 mL) and stirring at 60 °C for 30 minutes. The resulted solution was diluted with ethyl acetate (15 mL) and washed thrice with aqueous copper sulfate (5 mL X 3) and thrice with water (5 mL X 3). The organic layer was collected, dried over MgSO₄, and concentrated *in vacuo*. The crude mixture was purified through flash column on silica gel with 1% acetic acid, 20% ethyl acetate, and 79% hexanes as the eluent. The desired product was isolated as a white solid. 110 mg, 43% yield; mp ; ¹H NMR (500 MHz, ACETONE-d₆) δ 3.99 - 4.17 (m, 2 H), 4.52 (dd, *J* = 10.38, 7.32 Hz, 2 H), 4.64 (d, *J* = 12.21 Hz, 2 H), 4.81 (d, *J* = 12.51 Hz, 2 H), 6.98 - 7.08 (m, 4 H), 7.23 - 7.30 (m, 7 H), 7.30 - 7.36 (m, 4 H), 7.36 - 7.45 (m, 4 H); ¹³C NMR (126 MHz, ACETONE-d₆) δ 42.6, 47.5, 66.9, 128.0, 128.7, 128.8, 129.1, 129.2, 129.3, 136.9, 140.1, 172.3; HRMS (ESI) *m/z* calculated for C₃₂H₂₈O₄ (M+H)⁺: 477.206, found 477.2059 (Δ 0.34 ppm).

α -2,4-Diphenylcyclobutane-1,3-dicarboxylic acid mono-(4-methoxy)benzyl ester (SB-FI-75) and α -2,4-diphenylcyclobutane-1,3-dicarboxylic acid di-(4-methoxy)benzyl ester (SB-FI-76)



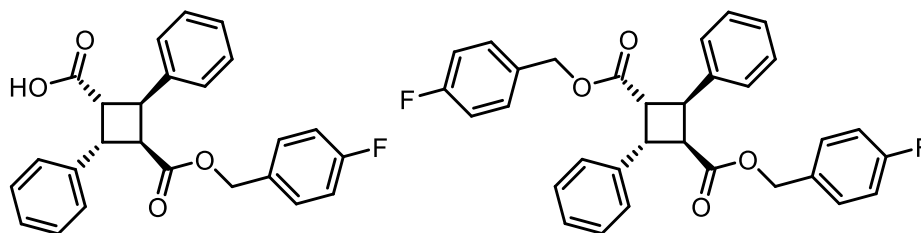
α -Truxillic acid (200 mg, 0.66 mmol) suspended in thionyl chloride (2 mL), was added three drops of DMF and heated to reflux for 3 h. The excess thionyl chloride and DMF was removed *in vacuo* and truxillic acyl chloride was obtained, which was used directly in the subsequent reaction. To the solution of α -truxillic acyl chloride in THF (10 mL) was added 4-methoxybenzyl alcohol (0.53 mmol) and pyridine (4.0 mmoles), and the reaction mixture was heated to reflux overnight. The reaction was quenched with addition of distilled water (10 mL) and stirring at 60 °C for 30 minutes. The resulted solution was diluted with ethyl acetate (15 mL) and washed thrice with aqueous copper sulfate (5 mL X 3) and thrice with water (5 mL X 3). The organic layer was collected, dried over MgSO₄, and concentrated *in vacuo*. The crude mixture was purified through flash column on silica gel with 1% acetic acid, 20% ethyl acetate, and 79% hexanes as the eluent. Disubstituted product and monosubstituted were collected as white solids. Monosubstituted: 110 mg, 40% yield; m.p. 99-102 °C; ¹H NMR (500 MHz, ACETONE-d₆) δ 3.78 (s, 3 H), 3.93 - 4.07 (m, 2 H), 4.40 - 4.50 (m, 2 H), 4.58 (d, *J* = 11.90 Hz, 1 H), 4.74 (d, *J* = 11.90 Hz, 1 H), 6.79 - 6.87 (m, 2 H), 6.93 - 7.03 (m, 2 H), 7.21 - 7.39 (m, 8 H), 7.41 (d, *J* = 7.32 Hz, 2 H); ¹³C NMR (126 MHz, ACETONE-d₆) δ 42.4, 42.7, 47.1, 47.6, 55.6, 66.7, 114.6, 127.7, 127.8, 128.6, 128.7, 129.1, 129.2, 130.9, 140.3, 160.6, 172.5, 173.1; HRMS (ESI) *m/z* calculated for C₂₆H₂₄O₅ (M+H)⁺: 434.1962, found 434.1964 (Δ -0.42 ppm). Disubstituted: 53 mg, 12% yield; m.p. 145-148 °C; ¹H NMR (500 MHz, ACETONE-d₆) δ 3.78 (s, 6 H), 3.97 - 4.08 (m, 2 H), 4.47 (dd, *J* = 10.38, 7.32 Hz, 2 H), 4.56 (d, *J* = 12.21 Hz, 2 H), 4.73 (d, *J* = 12.21 Hz, 2 H), 6.78 - 6.86 (m, 4 H), 6.93 - 7.01 (m, 4 H), 7.23 - 7.30 (m, 2 H), 7.30 - 7.40 (m, 8 H); ¹³C NMR (126 MHz, ACETONE-d₆) δ 42.5, 47.5, 55.6, 66.7, 114.6, 127.9, 128.6, 129.3, 130.9, 140.1, 160.6, 172.3; HRMS (ESI) *m/z* calculated for C₂₆H₂₄O₅ (M+H)⁺: 554.2536, found 554.2537 (Δ 0.2 ppm)

α -2,4-Diphenylcyclobutane-1,3-dicarboxylic acid mono-2-indanyl ester (SB-FI-77)



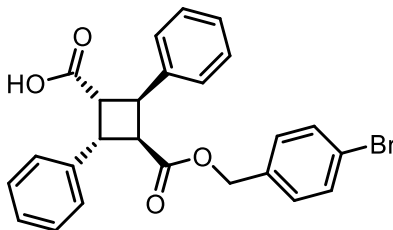
This compound was synthesized using the procedure for α -2,4-diphenylcyclobutane-1,3-dicarboxylic acid mono-(4-methoxy)benzyl ester. 142 mg, 34% yield; ^1H NMR (500 MHz, Acetone- d_6) δ 2.05 (dt, $J = 4.35, 2.25$ Hz, 1 H), 2.10 (dd, $J = 17.09, 2.44$ Hz, 1 H), 2.74 (dd, $J = 16.94, 2.59$ Hz, 1 H), 2.87 (dd, $J = 16.94, 6.26$ Hz, 1 H), 3.11 (dd, $J = 17.09, 6.41$ Hz, 1 H), 3.90 (dd, $J = 10.68, 6.71$ Hz, 1 H), 3.97 - 4.07 (m, 1 H), 4.36 - 4.48 (m, 2 H), 5.14 - 5.21 (m, 1 H), 7.05 - 7.18 (m, 4 H), 7.19 - 7.25 (m, 1 H), 7.27 - 7.37 (m, 7 H), 7.40 (d, $J = 7.32$ Hz, 2 H); ^{13}C NMR (126 MHz, ACETONE- d_6) δ 39.8, 40.0, 42.3, 42.6, 46.9, 47.5, 76.0, 125.3, 125.5, 127.3, 127.4, 127.7, 127.9, 128.7, 128.7, 129.1, 129.2, 140.1, 140.4, 141.4, 173.1; HRMS (ESI) m/z calculated for $\text{C}_{27}\text{H}_{24}\text{O}_4$ (M+H) $^+$: 413.1747, found 413.1749 (Δ -0.43 ppm).

α -2,4-Diphenylcyclobutane-1,3-dicarboxylic acid mono-(4-fluoro)benzyl ester (SB-FI-78)
and **α -2,4-diphenylcyclobutane-1,3-dicarboxylic acid di-(4-fluoro)benzyl ester (SB-FI-79)**



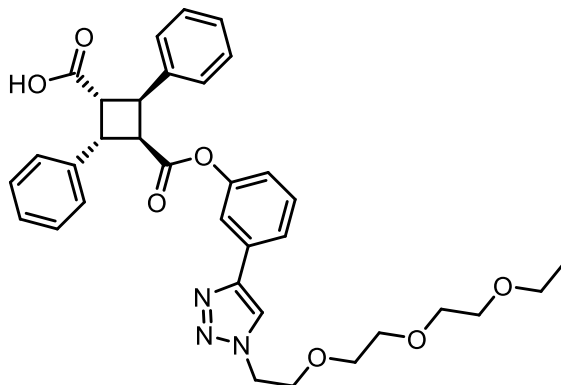
This compound was synthesized using the procedure for α -2,4-diphenylcyclobutane-1,3-dicarboxylic acid mono-(4-methoxy)benzyl ester. Monosubstituted: 73 mg, 34% yield; m.p. 145-148 $^{\circ}\text{C}$; ^1H NMR (500 MHz, ACETONE- d_6) δ 4.03 (dd, $J = 10.38, 7.32$ Hz, 2 H), 4.35 - 4.58 (m, 2 H), 4.68 (d, $J = 12.21$ Hz, 1 H), 4.80 (d, $J = 12.21$ Hz, 1 H), 6.93 - 7.14 (m, 4 H), 7.21 - 7.45 (m, 10 H), 10.63 (br. s., 1 H); ^{13}C NMR (126 MHz, ACETONE- d_6) δ 42.4, 42.7, 47.2, 47.6, 66.1, 115.8, 116.0, 127.8, 127.9, 128.6, 128.7, 129.2, 129.3, 131.2, 131.3, 133.1, 140.2, 140.3, 162.4, 164.3, 172.4, 173.0; HRMS (ESI) m/z calculated for $\text{C}_{25}\text{H}_{21}\text{FO}_4$ (M+H) $^+$: 405.1497, found 405.1502 (Δ -1.3 ppm). Disubstituted: 40 mg, 15% yield; m.p. 103-105 $^{\circ}\text{C}$; ^1H NMR (500 MHz, ACETONE- d_6) δ 4.06 (dd, $J = 10.53, 7.48$ Hz, 2 H), 4.51 (dd, $J = 10.38, 7.32$ Hz, 2 H), 4.66 (d, $J = 12.21$ Hz, 2 H), 4.78 (d, $J = 12.51$ Hz, 2 H), 6.93 - 7.17 (m, 8 H), 7.20 - 7.44 (m, 10 H); ^{13}C NMR (126 MHz, ACETONE- d_6) δ 42.5, 47.4, 66.1, 115.8, 116.0, 128.0, 128.6, 129.3, 131.3, 131.3, 133.1, 133.1, 140.0, 162.4, 164.3, 172.2; HRMS (ESI) m/z calculated for $\text{C}_{32}\text{H}_{26}\text{F}_2\text{O}_4$ (M+H) $^+$: 513.1872, found 513.1882 (Δ -2 ppm).

α -2,4-Diphenylcyclobutane-1,3-dicarboxylic acid mono-(4-bromo)benzyl ester (SB-FI-80)



This compound was synthesized using the procedure for α -2,4-diphenylcyclobutane-1,3-dicarboxylic acid mono-(4-methoxy)benzyl ester. 109 mg, 44% yield; m.p. 175-177 °C; ^1H NMR (500 MHz, ACETONE- d_6) δ 3.92 - 4.11 (m, 2 H), 4.40 - 4.57 (m, 2 H), 4.69 (d, J = 12.82 Hz, 1 H), 4.78 (d, J = 12.51 Hz, 1 H), 6.96 (d, J = 8.54 Hz, 2 H), 7.20 - 7.29 (m, 2 H), 7.32 (t, J = 7.48 Hz, 4 H), 7.35 - 7.40 (m, 2 H), 7.40 - 7.49 (m, 4 H); ^{13}C NMR (126 MHz, ACETONE- d_6) δ 42.4, 42.7, 47.2, 47.5, 66.0, 122.3, 127.8, 127.9, 128.6, 128.7, 129.2, 129.3, 131.0, 132.3, 136.4, 140.2, 140.3, 172.4, 173.1; HRMS (ESI) m/z calculated for $\text{C}_{25}\text{H}_{21}\text{BrO}_4$ ($\text{M}+\text{H}$) $^+$: 465.0696, found 465.0697 (Δ -0.27 ppm).

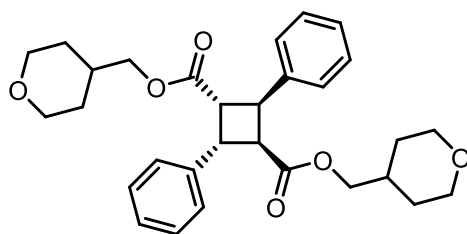
α -2,4-Diphenylcyclobutane-1,3-dicarboxylic acid mono-(3-(1-(2-(2-(2-ethoxyethoxy)ethoxy)ethyl)-1H-1,2,3-triazol-4-yl)phenyl ester (SB-FI-85)



To a solution of α -2,4-diphenylcyclobutane-1,3-dicarboxylic acid mono-(3-ethynyl)phenyl ester, dissolved in degassed THF (8 mL) and water (1.5 mL), was added cupric sulfate pentahydrate (81 mg, 0.32 mmoles), ascorbic acid (57 mg, 0.32 mmoles), and 1-azido-2-(2-(2-ethoxyethoxy)ethoxy)ethane (60 mg, 0.30 mmoles). The reaction was kept under nitrogen while stirring at room temperature overnight. Upon completion of the reaction, the reaction mixture was diluted with water (20 mL) and extracted thrice with DCM (25 mL X 3). The crude mixture was

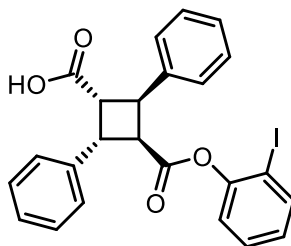
purified with flash column on silica gel with 3.5% methanol and DCM as the eluent. 180 mg, 94% yield; ^1H NMR (500 MHz, ACETONE- d_6) δ 1.07 (t, $J = 7.02$ Hz, 6 H), 3.39 (q, $J = 7.02$ Hz, 4 H), 3.43 - 3.49 (m, 4 H), 3.49 - 3.55 (m, 4 H), 3.55 - 3.61 (m, 4 H), 3.61 - 3.71 (m, 4 H), 3.93 (t, $J = 5.19$ Hz, 4 H), 4.06 - 4.19 (m, 2 H), 4.27 - 4.36 (m, 2 H), 4.54 - 4.72 (m, 8 H), 6.28 - 6.43 (m, 2 H), 6.96 (t, $J = 1.83$ Hz, 2 H), 7.21 - 7.32 (m, 4 H), 7.33 - 7.44 (m, 6 H), 7.44 - 7.54 (m, 8 H), 7.57 (d, $J = 7.32$ Hz, 4 H), 7.69 (d, $J = 7.93$ Hz, 2 H), 8.22 (s, 2 H); ^{13}C NMR (126 MHz, ACETONE- d_6) δ 15.6, 42.3, 42.9, 47.0, 47.6, 51.0, 66.8, 70.1, 70.6, 71.2, 71.3, 119.5, 121.7, 122.4, 123.4, 127.8, 128.3, 128.7, 129.0, 129.2, 129.5, 130.4, 133.7, 140.1, 140.2, 146.8, 152.1, 171.3, 173.1; HRMS (ESI) m/z calculated for $\text{C}_{34}\text{H}_{37}\text{N}_3\text{O}_7$ ($\text{M}+\text{H}$) $^+$: 600.2704, found 600.2705 (Δ -0.13 ppm).

α -2,4-Diphenylcyclobutane-1,3-dicarboxylic acid di-tetrahydropyran-4-methyl ester (SB-FI-86)



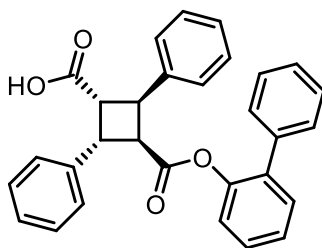
This compound was synthesized using the procedure for α -2,4-diphenylcyclobutane-1,3-dicarboxylic acid mono-(4-methoxy)benzyl ester. 177 mg, 21% yield; ^1H NMR (500 MHz, ACETONE- d_6) δ 0.91 - 1.10 (m, 4 H), 1.16 - 1.31 (m, 4 H), 1.38 - 1.55 (m, 2 H), 3.17 (tt, $J = 11.71, 2.33$ Hz, 4 H), 3.58 (d, $J = 6.41$ Hz, 4 H), 3.67 - 3.81 (m, 4 H), 3.90 - 4.08 (m, 2 H), 4.48 (dd, $J = 10.38, 7.32$ Hz, 2 H), 7.19 - 7.31 (m, 2 H), 7.31 - 7.46 (m, 8 H); ^{13}C NMR (126 MHz, ACETONE- d_6) δ 35.2, 42.5, 47.7, 67.8, 67.8, 69.4, 127.9, 128.7, 129.3, 140.3, 172.3; HRMS (ESI) m/z calculated for $\text{C}_{30}\text{H}_{36}\text{O}_6$ ($\text{M}+\text{H}$) $^+$: 493.2585, found 493.2591 (Δ -1.24 ppm).

α -2,4-Diphenylcyclobutane-1,3-dicarboxylic acid mono-1-(2-iodo)phenyl ester (SB-FI-90)



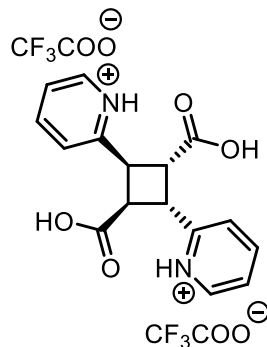
This compound was synthesized using the procedure for α -2,4-diphenylcyclobutane-1,3-dicarboxylic acid mono-(4-methoxy)benzyl ester. 177 mg, 21% yield; ^1H NMR (500 MHz, ACETONE- d_6) δ 3.97 (t, $J = 10.53$ Hz, 2 H), 4.19 (t, $J = 10.38$ Hz, 2 H), 4.52 (t, $J = 10.22$ Hz, 2 H), 4.83 (t, $J = 10.68$ Hz, 2 H), 5.86 (dd, $J = 7.93, 1.22$ Hz, 2 H), 6.87 - 7.00 (m, 2 H), 7.09 - 7.22 (m, 2 H), 7.24 - 7.31 (m, 2 H), 7.31 - 7.45 (m, 10 H), 7.51 (dd, $J = 7.02, 3.97$ Hz, 8 H), 7.79 (dd, $J = 7.93, 1.22$ Hz, 2 H); ^{13}C NMR (126 MHz, ACETONE- d_6) δ 42.8, 45.4, 47.0, 47.3, 91.1, 123.5, 127.4, 127.6, 128.2, 128.5, 129.3, 129.4, 129.8, 130.2, 139.2, 140.0, 143.0, 152.1, 170.0, 172.8; HRMS (ESI) m/z calculated for $\text{C}_{24}\text{H}_{19}\text{IO}_4$ ($\text{M}+\text{H}$) $^+$: 499.0401, found 499.0407 (Δ -1.19 ppm).

α -2,4-Diphenylcyclobutane-1,3-dicarboxylic acid mono-1-(2-phenyl)phenyl ester (SB-FI-91)



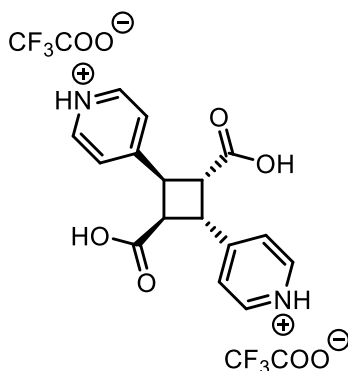
This compound was synthesized using the procedure for α -2,4-diphenylcyclobutane-1,3-dicarboxylic acid mono-(4-methoxy)benzyl ester. 177 mg, 21% yield; mp 195-196 $^{\circ}\text{C}$; ^1H NMR (500 MHz, ACETONE- d_6) δ 3.81 (dt, $J = 11.67, 10.49$ Hz, 2 H), 4.39 (t, $J = 10.07$ Hz, 1 H), 4.68 (t, $J = 10.68$ Hz, 1 H), 5.99 (dd, $J = 8.09, 1.07$ Hz, 1 H), 7.11 - 7.19 (m, 3 H), 7.20 - 7.28 (m, 2 H), 7.28 - 7.40 (m, 11 H), 7.40 - 7.46 (m, 2 H); ^{13}C NMR (126 MHz, ACETONE- d_6) δ 42.3, 45.4, 46.8, 47.0, 123.4, 127.1, 127.4, 128.1, 128.4, 129.2, 129.3, 129.6, 129.8, 131.3, 135.8, 138.5, 139.2, 143.2, 148.7, 170.6, 172.9; HRMS (ESI) m/z calculated for $\text{C}_{30}\text{H}_{24}\text{O}_4$ ($\text{M}+\text{H}$) $^+$: 449.1747, found 449.1754 (Δ -1.55 ppm).

α -2,4-Di(pyridin-2-ium)cyclobutane-1,3-dicarboxylic acid trifluoroacetate



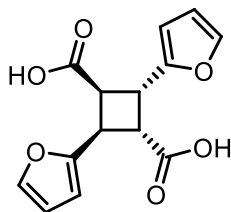
To a suspension of 3-(2-pyridyl)acrylic acid (100 mg, 0.67 mmoles), in water (5 mL), was added trifluoroacetic acid (3.35 mmoles), resulting in a clear and light yellow solution. The solution was allowed to air dry over several days. The resulting salt was broken up into a powder using a spatula. The powder was evenly spread on a glass petri dish and irradiated in a UV reaction at 365 nm for 3 days. The reaction was monitored by ^1H NMR for disappearance of starting material. The desired product was obtained as a light brown solid. 134 mg, 76% yield; ^1H NMR (300 MHz, D_2O) δ 4.26 - 4.42 (m, 2 H), 7.92 (d, $J = 6.71$ Hz, 2 H), 8.08 (d, $J = 8.20$ Hz, 2 H), 8.54 (s, 2 H), 8.68 (d, $J = 5.59$ Hz, 2 H); MS (FIA) m/z 299.1 ($\text{M}+1$) $^+$.

α -2,4-Di(pyridin-4-ium)cyclobutane-1,3-dicarboxylic acid trifluoroacetate



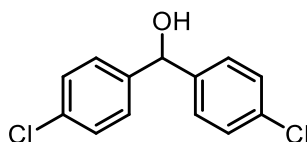
This compound was synthesized following the procedure for α -2,4-di(pyridin-2-ium)cyclobutane-1,3-dicarboxylic acid trifluoroacetate. 155 mg, 88% yield; ^1H NMR (300 MHz, D_2O) δ 4.26 (dd, $J = 10.43, 7.26$ Hz, 2 H), 4.67 (dd, $J = 10.34, 7.54$ Hz, 2 H), 8.03 (d, $J = 6.15$ Hz, 4 H), 8.73 (d, $J = 6.33$ Hz, 4 H). The analytical data was consistent with literature values.¹⁷

2,4-Di(furan-2-yl)cyclobutane-1,3-dicarboxylic acid



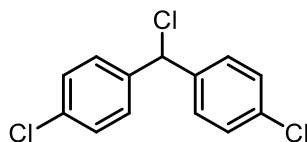
This compound was synthesized following the procedure for 2,4-Bis(3-methoxy-4-triethylsilyloxy)phenylcyclobutane-1,3-dicarboxylic acid. 100 mg, quant.; $^1\text{H NMR}$ (300 MHz, ACETONE- d_6) δ 3.80 - 3.90 (m, 2 H), 4.04 - 4.38 (m, 2 H), 6.10 (d, $J = 3.17$ Hz, 2 H), 6.18 - 6.40 (m, 2 H), 7.17 - 7.52 (m, 2 H).

Bis(4-chlorophenyl)methanol²¹



To a stirring solution of 4-chlorobenzaldehyde (2.0 g, 14.2 mmol) in dry THF (60 mL) at 0 °C under N_2 was added 4-chlorophenyl)magnesium bromide (30 mL, 29.9 mmol, 1.0 M in MeTHF). After 4 h, the reaction was quenched with water (50 mL) and the aqueous layer extracted with DCM (40 mL X 3). The combined organic layers were dried over anhydrous magnesium sulfate and concentrated under reduced pressure. The mixture was purified by flash chromatography (5–15% EtOAc/hexanes) to give bis(4-chlorophenyl)methanol as a white solid. 2.7 g, 75% yield; $^1\text{H NMR}$ (300 MHz, CDCl_3) δ 2.18 (br. s., 1 H), 5.76 (s, 1 H), 7.07 - 7.44 (m, 7 H). The analytical data was consistent with literature values.²¹

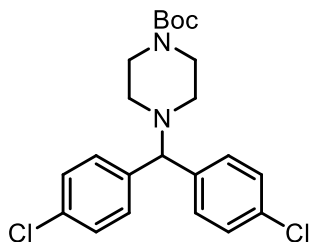
4,4'-(Chloromethylene)bis(chlorobenzene)²¹



To a stirring solution of bis(4-chlorophenyl)methanol (200 mg, 0.79 mmol) in dry DCM (5 mL) at room temperature under N_2 was added thionylchloride (574 μL , 7.9 mmol). After stirred at 65 °C for overnight, the reaction was quenched with saturated aqueous NaHCO_3 (20 mL) and the aqueous layer was extracted thrice with DCM (3 \times 10 mL). The combined organic layers were dried over anhydrous magnesium sulfate and concentrated under reduced pressure. The crude product

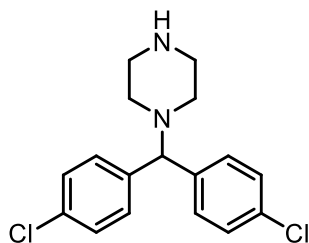
was used without further purification. 209 mg, 97% yield; $^1\text{H NMR}$ (300 MHz, CDCl_3) δ 6.07 (s, 1 H), 7.29 - 7.40 (m, 8 H). The analytical data was consistent with literature values.²¹

***tert*-Butyl 4-(bis(4-chlorophenyl)methyl)piperazine-1-carboxylate**²¹



To a solution of 4,4'-(chloromethylene)bis(chlorobenzene) (125 mg, 0.5 mmol) in MeCN (5 mL) was added *tert*-butyl piperazine-1-carboxylate (261 mg, 1.4 mmol), KI (83 mg, 0.5 mmol), and K_2CO_3 (318 mg, 2.3 mmol) at room temperature. After stirring under reflux 4 hours, the reaction, which was monitored by TLC, was complete. The reaction was quenched with water (20 mL) and the aqueous layer was extracted thrice with DCM (10 mL X 3). The combined organic layers were dried over anhydrous magnesium sulfate and concentrated under reduced pressure. The mixture was purified by flash chromatography (10% EtOAc/hexanes) to give *tert*-butyl 4-(bis(4-chlorophenyl)methyl)piperazine-1-carboxylate as a white solid. 163 mg, 77% yield; $^1\text{H NMR}$ (300 MHz, CDCl_3) δ 1.44 (s, 9 H), 2.31 (br. s., 4 H), 3.25 - 3.56 (m, 4 H), 4.19 (s, 1 H), 7.21 - 7.36 (m, 8 H). The analytical data was consistent with literature values.²¹

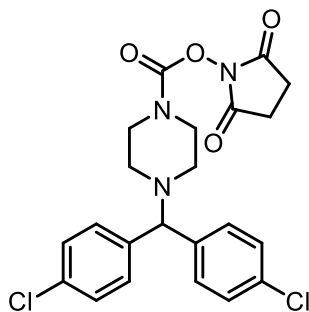
1-(Bis(4-chlorophenyl)methyl)piperazine²¹



To a solution of *tert*-butyl 4-(bis(4-chlorophenyl)methyl)piperazine-1-carboxylate (130 mg, 0.31 mmol), dissolved in DCM (5 mL), was added TFA (331 μL , 4.32 mmol). The reaction mixture was allowed to stir at room temperature overnight. The reaction was monitored by TLC, and upon consumption of the starting material, the reaction was quenched with saturated NaHCO_3 (20 mL) and extracted thrice with DCM (15 mL X 3). The crude mixture was purified with flash

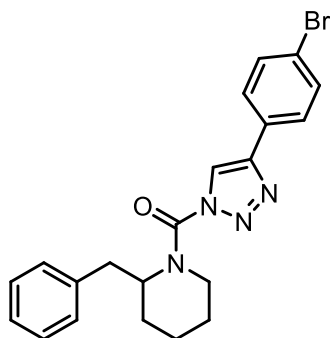
column on silica gel with 4% methanol and DCM as the eluent. 79 mg, 79% yield; $^1\text{H NMR}$ (300 MHz, CDCl_3) δ 2.38 (br. s., 4 H), 2.93 (br. s., 4 H), 3.52 (br. s., 1 H), 4.21 (s, 1 H), 7.24 (br. s., 3 H), 7.28 - 7.47 (m, 5 H). The analytical data was consistent with literature values.²¹

2,4-Dioxopyrrolidin-1-yl 4-(bis(4-chlorophenyl)methyl)piperazine-1-carboxylate²¹



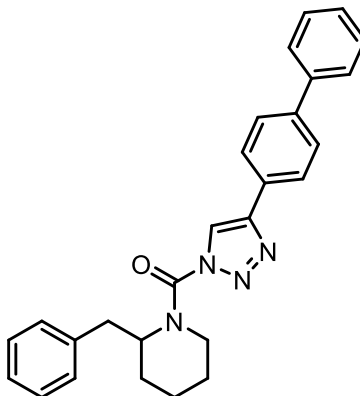
To a solution of 1-(bis(4-chlorophenyl)methyl)piperazine, dissolved in DCM (5 mL), was added N,N' -disuccinimidyl carbonate (77 mg, 0.3 mmoles) and N -methylmorpholine (81 μL , 0.74 mmoles). The reaction mixture was stirred at room temperature overnight. A stream of nitrogen was passed over the reaction mixture to remove the solvent and to the remaining residue was added EtOAc (20 mL). The resulting precipitate was filtered off and the filtrate was concentrated and purified by SiO_2 flash chromatography (50% EtOAc/hexanes) provided the title compound (180 mg, 78%) as a white solid. 71 mg, 51% yield; $^1\text{H NMR}$ (300 MHz, CDCl_3) δ 2.44 (br. s., 4 H), 2.82 (s, 4 H), 3.53 (br. s., 2 H), 3.64 (br. s., 2 H), 4.25 (s, 1 H), 7.23 - 7.37 (m, 9 H). The analytical data was consistent with literature values.²¹

(2-Benzylpiperidin-1-yl)(4-(4-bromophenyl)-1H-1,2,3-triazol-1-yl)methanone²²



To a solution of 2-benzylpiperidine (500 mg, 2.85 mmol) in THF (25 mL) was treated with DIPEA (1.5 mL, 8.55 mmol) and triphosgene (423 mg, 1.43 mmol), and the reaction mixture was stirred for 30 min at 4 °C. The mixture was poured into water and extracted with ethyl acetate. The organic layer was washed with water and brine, dried over anhydrous magnesium sulfate and concentrated under reduced pressure. The intermediate was dissolved in THF (30 mL), and DIPEA (1.5 mL, 8.55 mmol), DMAP (348 mg, 2.85 mmol) and 4-(4-bromophenyl)-1H-1,2,3-triazole (639 mg, 2.85 mmol) were added to the solution. The mixture was stirred for 2 h at 60 °C and poured into saturated aqueous NH₄Cl solution. The mixture was extracted with ethyl acetate, washed with water, dried over anhydrous magnesium sulfate. The crude mixture was purified by flash column on silica gel with ethyl acetate: hexane 1:5 as the eluent. 320 mg, 27% yield; ¹H NMR (500 MHz, CDCl₃) δ 1.69 - 1.88 (m, 5 H), 1.91 (br. s., 1 H), 2.67 (br. s., 1 H), 3.06 - 3.30 (m, 1 H), 3.35 (br. s., 1 H), 4.34 (d, *J* = 13.12 Hz, 1 H), 4.82 (br. s., 1 H), 6.83 - 7.07 (m, 1 H), 7.08 - 7.31 (m, 5 H), 7.31 - 7.47 (m, 1 H), 7.57 (d, *J* = 8.24 Hz, 2 H), 7.65 (br. s., 2 H). The analytical data was consistent with literature values.²²

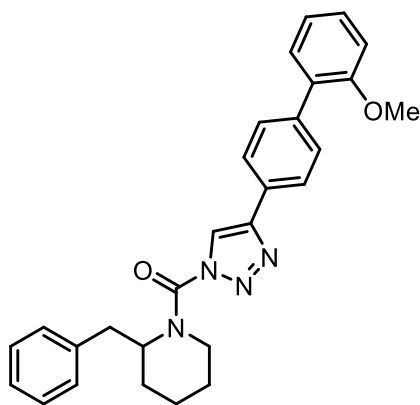
(4-([1,1'-Biphenyl]-4-yl)-1H-1,2,3-triazol-1-yl)(2-benzylpiperidin-1-yl)methanone²²



A solution of (2-benzylpiperidin-1-yl)(4-(4-bromophenyl)-1H-1,2,3-triazol-1-yl)methanone

(850 mg, 2.0 mmol) in THF (73 mL) and water (36 mL) was treated with phenylboronic acid (488 mg, 4.0 mmol), K_2CO_3 (829 mg, 6.0 mmol) and $PdCl_2(dppf)$ (55 mg, 0.075 mmol), and the reaction mixture was stirred for 2 h at 80 °C under N_2 . The mixture was poured into water and extracted with ethyl acetate. The organic layer was washed with water, dried over anhydrous magnesium sulfate. The crude mixture was purified by flash column on silica gel with 1:4 ethyl acetate: hexanes as the eluent. (709 mg, 84 %). 1H NMR (500 MHz, $CDCl_3$) δ 1.63 - 1.85 (m, 4 H), 1.85 - 2.09 (m, 3 H), 2.74 (br. s., 1 H), 3.27 (br. s., 1 H), 3.40 (br. s., 1 H), 4.40 (d, $J = 13.43$ Hz, 1 H), 4.90 (br. s., 1 H), 7.15 - 7.37 (m, 4 H), 7.37 - 7.44 (m, 1 H), 7.44 - 7.58 (m, 2 H), 7.62 - 7.79 (m, 4 H), 7.91 (br. s., 2 H). The analytical data was consistent with literature values.²²

(2-Benzylpiperidin-1-yl)(4-(2'-methoxy-[1,1'-biphenyl]-4-yl)-1H-1,2,3-triazol-1-yl)methanone²²



A solution of (2-benzylpiperidin-1-yl)(4-(4-bromophenyl)-1H-1,2,3-triazol-1-yl)methanone (300 mg, 0.71 mmol) in THF (24 mL) and water (12 mL) was treated with 2-methylphenylboronic acid (173 mg, 1.42 mmol), K_2CO_3 (294 mg, 2.13 mmol) and $PdCl_2(dppf)$ (77.4 mg, 0.11 mmol), and the reaction mixture was stirred for 2 h at 80 °C under N_2 . The mixture was poured into water and extracted with ethyl acetate. The organic layer was washed with water, dried over anhydrous magnesium sulfate. The crude mixture was purified by flash column on silica gel with 1:4 ethyl acetate: hexanes as the eluent. (281 mg, 87%). 1H NMR (400 MHz, $CDCl_3$) δ 1.70 - 1.99 (m, 6 H), 3.24 (br. s., 1 H), 3.37 (t, $J = 11.54$ Hz, 1 H), 3.77 - 3.97 (m, 3 H), 4.38 (d, $J = 13.80$ Hz, 1 H), 4.89 (br. s., 1 H), 6.87 - 7.14 (m, 4 H), 7.17 (br. s., 1 H), 7.20 - 7.30 (m, 4 H), 7.30 - 7.43 (m, 2 H), 7.59 - 7.66 (m, 2 H), 7.85 (d, $J = 6.78$ Hz, 2 H). The analytical data was consistent with literature values.²²

Single Crystal X-ray diffraction (XRD)

Crystals were selected and mounted on glass fibers using epoxy adhesive. Each crystal was centered, and the X-ray intensity data were measured on an Oxford Gemini A Enhance diffractometer by using graphite-monochromated Cu radiation. The data was collected using the CrysAlis Pro 38.41 software,¹⁷ Wingx 2014.1,¹⁸ Olex2 1.2,¹⁹ and SHELX 2013.²⁰ The crystal structure for SB-FI-26A was determined by Matthew Freitag.

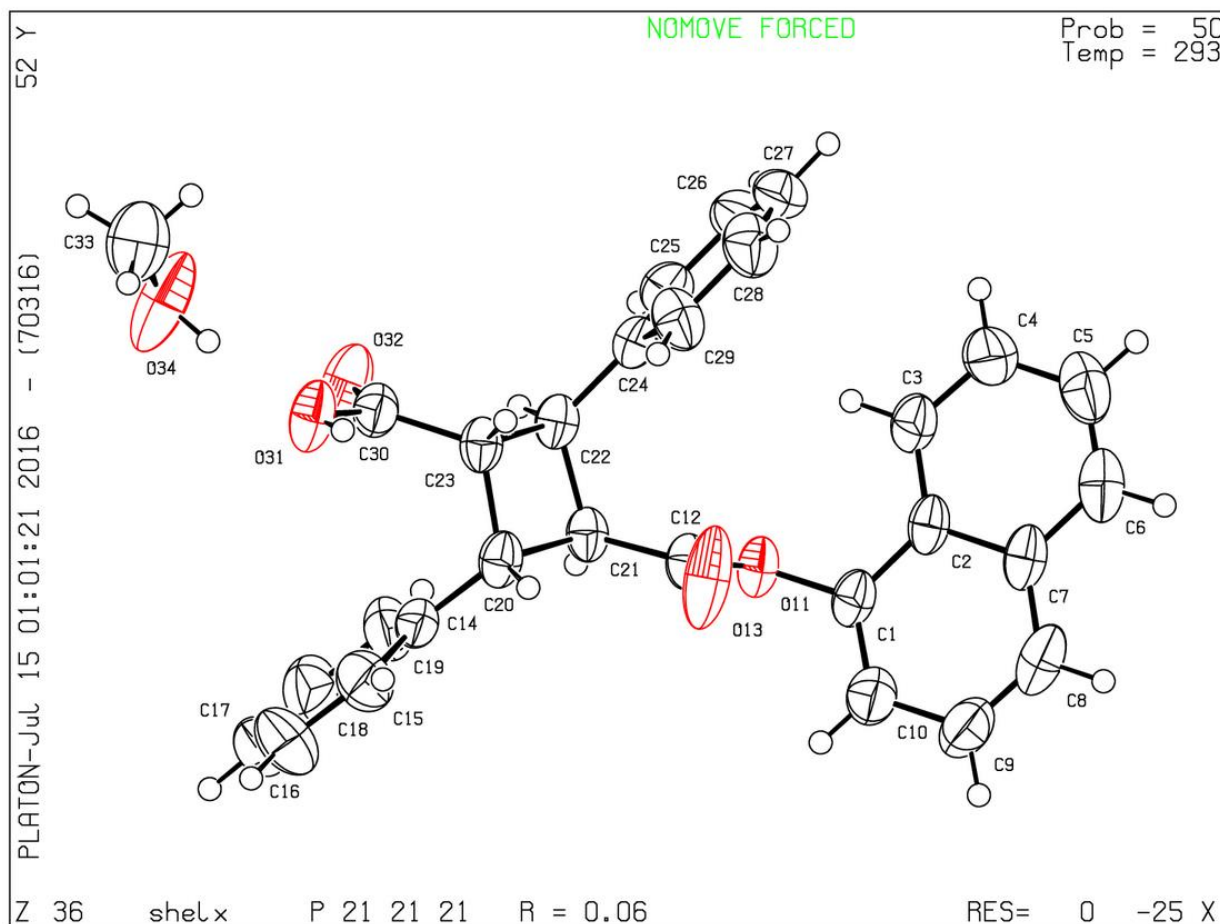


Table 1 Crystal data and structure refinement for SB-FI-26A.

Identification code	SB-FI-26 A
Empirical formula	C ₃₀ H ₂₈ O ₄
Formula weight	452.52
Temperature/K	293(2)
Crystal system	orthorhombic

Space group	P2 ₁ 2 ₁ 2 ₁
a/Å	5.9061(2)
b/Å	8.3860(5)
c/Å	47.6746(19)
α /°	90
β /°	90
γ /°	90
Volume/Å ³	2361.25(19)
Z	4
$\rho_{\text{calc}}/\text{cm}^3$	1.273
μ/mm^{-1}	0.666
F(000)	960.0
Crystal size/mm ³	? × ? × ?
Radiation	CuK α (λ = 1.54184)
2 Θ range for data collection/°	7.418 to 146.328
Index ranges	-5 ≤ h ≤ 7, -10 ≤ k ≤ 9, -56 ≤ l ≤ 58
Reflections collected	6076
Independent reflections	3943 [R _{int} = 0.0396, R _{sigma} = 0.0392]
Data/restraints/parameters	3943/0/313
Goodness-of-fit on F ²	1.187
Final R indexes [I ≥ 2 σ (I)]	R ₁ = 0.0607, wR ₂ = 0.1537
Final R indexes [all data]	R ₁ = 0.0696, wR ₂ = 0.1602
Largest diff. peak/hole / e Å ⁻³	0.24/-0.31
Flack parameter	0.0(3)

Table 2 Fractional Atomic Coordinates ($\times 10^4$) and Equivalent Isotropic Displacement Parameters ($\text{\AA}^2 \times 10^3$) for SB-FI-26A. U_{eq} is defined as 1/3 of of the trace of the orthogonalised U_{ij} tensor.

Atom	x	y	z	U(eq)
O11	12254(5)	12069(4)	10822.0(6)	48(3)
O32	6516(6)	13212(6)	11852.7(7)	68(3)
O31	9195(6)	13183(7)	12166.5(6)	65(3)

C1	14134(8)	12124(7)	10639.8(9)	47(3)
C2	14554(9)	13568(7)	10496.0(9)	46(3)
C21	10659(8)	11975(6)	11277.0(8)	40(3)
C12	12743(8)	12153(6)	11101.5(9)	45(3)
O13	14593(6)	12340(8)	11181.5(7)	93(3)
C23	10335(8)	13231(6)	11680.6(9)	43(3)
C20	11226(8)	11549(6)	11588.6(9)	45(3)
C22	9477(8)	13545(6)	11378.6(9)	41(3)
C30	8497(10)	13225(6)	11902.5(10)	49(3)
C6	16953(12)	15040(9)	10169.0(11)	69(3)
C7	16485(10)	13611(7)	10314.2(9)	53(3)
C14	10133(9)	10100(6)	11711.8(10)	48(3)
C25	8385(9)	15690(7)	11043.3(11)	51(3)
O34	3414(8)	13546(9)	12264.3(9)	108(4)
C24	9950(8)	15101(6)	11234.2(9)	43(3)
C3	13206(10)	14936(7)	10522(1)	54(3)
C29	11881(11)	15991(7)	11280.9(11)	59(3)
C8	17823(10)	12231(9)	10284.0(11)	69(3)
C4	13709(13)	16290(8)	10374.9(11)	69(3)
C27	10647(11)	17972(7)	10952.4(11)	64(3)
C10	15433(11)	10812(8)	10603.4(11)	61(3)
C9	17296(12)	10858(9)	10421.4(12)	72(3)
C5	15601(13)	16338(9)	10197.4(12)	76(4)
C15	11248(14)	9305(8)	11927.1(13)	78(3)
C26	8746(11)	17099(7)	10902.3(11)	63(3)
C19	8089(12)	9502(7)	11624.8(12)	66(3)
C28	12242(12)	17425(7)	11141.7(11)	66(3)
C18	7165(14)	8156(8)	11746.2(14)	84(4)
C16	10300(20)	7960(11)	12049.1(17)	112(4)
C17	8320(20)	7383(9)	11957.4(17)	105(4)
C33	4125(14)	14668(11)	12463.7(14)	95(4)

Table 3 Anisotropic Displacement Parameters ($\text{\AA}^2 \times 10^3$) for SB-FI-26A. The Anisotropic displacement factor exponent takes the form: $-2\pi^2[h^2a^2U_{11}+2hka*b*U_{12}+\dots]$.

Atom	U ₁₁	U ₂₂	U ₃₃	U ₂₃	U ₁₃	U ₁₂
O11	41(3)	72(4)	32(3)	2.3(15)	3.7(13)	-3.0(19)
O32	40(3)	109(4)	54(4)	-13(2)	7.3(17)	-12(2)
O31	53(4)	103(4)	37(3)	-1(2)	6.6(16)	-3(3)
C1	42(4)	67(4)	32(4)	-1(2)	1.8(19)	2(3)
C2	42(4)	68(4)	27(3)	-1(2)	0.4(19)	-5(3)
C21	36(4)	50(4)	35(4)	-1(2)	0.2(19)	-13(2)
C12	45(4)	55(4)	35(4)	-3(2)	3(2)	-10(3)
O13	43(4)	196(7)	41(3)	-10(3)	2.0(17)	-41(3)
C23	40(4)	54(4)	34(4)	-2(2)	0.8(19)	-10(2)
C20	36(4)	64(4)	35(4)	2(2)	-0.1(19)	-1(3)
C22	31(4)	55(4)	37(4)	-2(2)	-0.8(18)	-7(2)
C30	55(4)	50(4)	42(4)	-5(2)	9(2)	-9(3)
C6	68(5)	94(6)	44(4)	4(3)	10(3)	-19(4)
C7	45(4)	81(5)	33(4)	-2(2)	3(2)	-8(3)
C14	56(4)	52(4)	38(4)	4(2)	11(2)	10(3)
C25	36(4)	60(4)	58(4)	-1(2)	0(2)	3(3)
O34	47(4)	214(8)	63(4)	-41(4)	9(2)	-2(4)
C24	36(4)	53(4)	40(4)	-3(2)	4(2)	-1(2)
C3	54(4)	69(4)	37(4)	1(2)	4(2)	2(3)
C29	70(5)	60(4)	47(4)	4(2)	-5(3)	-18(3)
C8	51(4)	110(6)	45(4)	-7(3)	11(2)	9(4)
C4	90(5)	66(5)	51(4)	7(3)	4(3)	9(4)
C27	93(5)	40(4)	58(4)	2(2)	12(3)	2(3)
C10	64(5)	69(5)	51(4)	4(3)	10(3)	7(3)
C9	69(5)	88(5)	58(4)	-1(3)	15(3)	25(4)
C5	97(6)	82(5)	50(4)	11(3)	6(3)	-20(4)
C15	90(6)	81(5)	61(4)	24(3)	4(4)	23(4)

C26	72(5)	57(4)	60(4)	7(3)	-2(3)	12(3)
C19	75(5)	66(5)	57(4)	7(3)	12(3)	-15(4)
C28	78(5)	61(4)	60(4)	-6(3)	5(3)	-26(3)
C18	99(6)	72(5)	82(5)	-6(4)	31(4)	-24(4)
C16	164(10)	91(7)	81(6)	46(5)	17(6)	31(7)
C17	171(10)	55(5)	89(6)	13(4)	55(6)	2(6)
C33	98(7)	122(7)	65(5)	-4(4)	2(4)	-7(6)

Table 4 Bond Lengths for SB-FI-26A.

Atom	Atom	Length/Å	Atom	Atom	Length/Å
O11	C12	1.365(5)	C7	C8	1.409(8)
O11	C1	1.410(5)	C14	C19	1.371(9)
O32	C30	1.194(7)	C14	C15	1.390(8)
O31	C30	1.325(6)	C25	C26	1.376(8)
C1	C10	1.352(8)	C25	C24	1.388(7)
C1	C2	1.413(7)	O34	C33	1.402(9)
C2	C3	1.402(7)	C24	C29	1.381(8)
C2	C7	1.433(7)	C3	C4	1.367(8)
C21	C12	1.496(6)	C29	C28	1.390(7)
C21	C20	1.564(6)	C8	C9	1.361(9)
C21	C22	1.567(7)	C4	C5	1.402(9)
C12	O13	1.168(6)	C27	C26	1.362(9)
C23	C30	1.516(6)	C27	C28	1.383(8)
C23	C22	1.549(6)	C10	C9	1.402(8)
C23	C20	1.568(7)	C15	C16	1.387(11)
C20	C14	1.496(7)	C19	C18	1.381(8)
C22	C24	1.502(7)	C18	C17	1.379(11)
C6	C5	1.357(9)	C16	C17	1.339(13)
C6	C7	1.411(8)			

Table 5 Bond Angles for SB-FI-26A.

Atom	Atom	Atom	Angle/°	Atom	Atom	Atom	Angle/°
C12	O11	C1	115.6(4)	C8	C7	C6	122.5(5)
C10	C1	O11	119.9(5)	C8	C7	C2	119.2(5)
C10	C1	C2	122.3(5)	C6	C7	C2	118.3(6)
O11	C1	C2	117.7(5)	C19	C14	C15	117.7(6)
C3	C2	C1	123.9(4)	C19	C14	C20	123.9(5)
C3	C2	C7	119.0(5)	C15	C14	C20	118.4(6)
C1	C2	C7	117.1(5)	C26	C25	C24	121.5(6)
C12	C21	C20	112.2(4)	C29	C24	C25	117.6(5)
C12	C21	C22	117.1(4)	C29	C24	C22	123.3(5)
C20	C21	C22	89.6(3)	C25	C24	C22	119.1(5)
O13	C12	O11	121.6(4)	C4	C3	C2	120.7(5)
O13	C12	C21	126.9(4)	C24	C29	C28	121.1(6)
O11	C12	C21	111.5(4)	C9	C8	C7	121.2(5)
C30	C23	C22	114.5(4)	C3	C4	C5	120.5(6)
C30	C23	C20	115.6(4)	C26	C27	C28	119.8(5)
C22	C23	C20	90.1(3)	C1	C10	C9	120.2(6)
C14	C20	C21	117.8(4)	C8	C9	C10	120.0(6)
C14	C20	C23	118.4(4)	C6	C5	C4	120.4(6)
C21	C20	C23	89.3(4)	C16	C15	C14	120.6(8)
C24	C22	C23	120.9(4)	C27	C26	C25	120.3(6)
C24	C22	C21	120.4(4)	C14	C19	C18	121.4(7)
C23	C22	C21	89.9(4)	C27	C28	C29	119.6(6)
O32	C30	O31	119.6(5)	C17	C18	C19	119.6(8)
O32	C30	C23	124.3(5)	C17	C16	C15	120.6(8)
O31	C30	C23	116.1(5)	C16	C17	C18	120.1(8)
C5	C6	C7	121.1(6)				

Table 6 Hydrogen Atom Coordinates ($\text{\AA}\times 10^4$) and Isotropic Displacement Parameters ($\text{\AA}^2\times 10^3$) for SB-FI-26A.

Atom	<i>x</i>	<i>y</i>	<i>z</i>	U(eq)
------	----------	----------	----------	-------

H31	10571	13307	12172	97
H21	9578	11223	11194	49
H23	11581	13949	11731	51
H20	12870	11494	11614	54
H22	7837	13368	11376	49
H6	18210	15093	10052	82
H25	7062	15119	11010	61
H3	11955	14922	10641	64
H29	12958	15624	11408	71
H8	19090	12258	10168	82
H4	12791	17185	10393	82
H27	10873	18935	10860	77
H10	15089	9878	10699	74
H9	18172	9949	10395	86
H5	15931	17265	10098	92
H15	12642	9678	11990	93
H26	7688	17457	10772	75
H19	7310	10013	11481	79
H28	13548	18013	11176	80
H18	5770	7773	11686	101
H16	11050	7454	12196	134
H17	7728	6459	12036	126
H33A	2903	14894	12590	142
H33B	4574	15632	12370	142
H33C	5386	14247	12567	142
H1	4600(70)	13230(50)	12182(7)	10(3)

2.5. References

- (1) Loeser, J. D. *Relieving Pain in America*; National Academies Press: Washington, D.C., 2011; Vol. 28.
- (2) Robinson, J. Opioid (Narcotic) Pain Medications <http://www.webmd.com/pain-management/guide/narcotic-pain-medications?page=1#1> (accessed Jun 22, 2016).
- (3) DrugFacts: Marijuana <https://www.drugabuse.gov/publications/drugfacts/marijuana> (accessed Jul 4, 2016).
- (4) Iversen, L. Cannabis and the Brain. *Brain* **2003**, *126* (6), 1252–1270.
- (5) Kaczocha, M.; Rebecchi, M. J.; Ralph, B. P.; Teng, Y. H. G.; Berger, W. T.; Galbavy, W.; Elmes, M. W.; Glaser, S. T.; Wang, L.; Rizzo, R. C.; et al. Inhibition of Fatty Acid Binding Proteins Elevates Brain Anandamide Levels and Produces Analgesia. *PLoS One* **2014**, *9* (4), 1–11.
- (6) Kaczocha, M.; Vivieca, S.; Sun, J.; Glaser, S. T.; Deutsch, D. G. Fatty Acid-Binding Proteins Transport N-Acylethanolamines to Nuclear Receptors and Are Targets of Endocannabinoid Transport Inhibitors. *J. Biol. Chem.* **2012**, *287* (5), 3415–3424.
- (7) Ueda, N.; Puffenbarger, R. A.; Yamamoto, S.; Deutsch, D. G. The Fatty Acid Amide Hydrolase (FAAH). *Chem. Phys. Lipids* **2000**, *108* (1-2), 107–121.
- (8) Berger, W. T.; Ralph, B. P.; Kaczocha, M.; Sun, J.; Balius, T. E.; Rizzo, R. C.; Haj-Dahmane, S.; Ojima, I.; Deutsch, D. G. Targeting Fatty Acid Binding Protein (FABP) Anandamide Transporters - A Novel Strategy for Development of Anti-Inflammatory and Anti-Nociceptive Drugs. *PLoS One* **2012**, *7* (12).
- (9) Balius, T. E.; Mukherjee, S.; Rizzo, R. C. Implementation and Evaluation of a Docking-Rescoring Method Using Molecular Footprint Comparisons. *J. Comput. Chem.* **2011**, *32* (10), 2273–2289.
- (10) Balius, T. E.; Mukherjee, S.; Rizzo, R. C. Implementation and Evaluation of a Docking-Rescoring Method Using Molecular Footprint Comparisons. *J. Comput. Chem.* **2011**, *32* (10), 2273–2289.
- (11) Kaczocha, M.; Rebecchi, M. J.; Ralph, B. P.; Teng, Y.-H. G.; Berger, W. T.; Galbavy, W.; Elmes, M. W.; Glaser, S. T.; Wang, L.; Rizzo, R. C.; et al. Inhibition of Fatty Acid Binding Proteins Elevates Brain Anandamide Levels and Produces Analgesia. *PLoS One* **2014**, *9* (4), e94200.
- (12) Ichikawa, M.; Takahashi, M.; Aoyagi, S.; Kibayashi, C. Total Synthesis of (–)-Incarvilline, (+)-Incarvine C, and (–)-Incarvillateine. *J. Am. Chem. Soc.* **2004**, *126* (50), 16553–16558.
- (13) Chi, Y.-M.; Nakamura, M.; Yoshizawa, T.; Zhao, X.-Y.; Yan, W.-M.; Hashimoto, F.; Kinjo, J.; Nohara, T.; Sakurada, S. Pharmacological Study on the Novel Antinociceptive Agent, a Novel Monoterpene Alkaloid from *Incarvillea Sinensis*. *Biol. Pharm. Bull.* **2005**, *28* (10), 1989–1991.
- (14) Binas, B.; Danneberg, H.; McWhir, J.; Mullins, L.; Clark, a J. Requirement for the Heart-Type Fatty Acid Binding Protein in Cardiac Fatty Acid Utilization. *Faseb J* **1999**, *13* (8), 805–812.

- (15) Jamieson, C.; Moir, E. M.; Rankovic, Z.; Wishart, G. Medicinal Chemistry of hERG Optimizations: Highlights and Hang-Ups. *J. Med. Chem.* **2006**, *49* (17), 5029–5046.
- (16) Wang, S.; Li, Y.; Xu, L.; Li, D.; Hou, T. Recent Developments in Computational Prediction of hERG Blockage. *Curr. Top. Med. Chem.* **2013**, *13* (11), 1317–1326.
- (17) Kole, G. K.; Tan, G. K.; Vittal, J. J. Anion-Controlled Stereoselective Synthesis of Cyclobutane Derivatives by Solid-State [2 + 2] Cycloaddition Reaction of the Salts of Trans-3-(4-Pyridyl) Acrylic Acid. *Org. Lett.* **2010**, *12* (1), 128–131.
- (18) Oxford Diffraction. CrysAlis Pro. Oxford Diffraction Ltd: Abingdon, England 2016.
- (19) Farrugia, L. J. WinGX and ORTEP for Windows: An Update. *J. Appl. Crystallogr.* **2012**, *45* (4), 849–854.
- (20) Dolomanov, O. V.; Bourhis, L. J.; Gildea, R. J.; Howard, J. A. K.; Puschmann, H. OLEX2 : A Complete Structure Solution, Refinement and Analysis Program. *J. Appl. Crystallogr.* **2009**, *42* (2), 339–341.
- (21) Gruene, T.; Hahn, H. W.; Luebben, A. V.; Meilleur, F.; Sheldrick, G. M. Refinement of Macromolecular Structures against Neutron Data with SHELXL2013. *J. Appl. Crystallogr.* **2014**, *47* (1), 462–466.
- (22) Chang, J. W.; Coggnetta, A. B.; Niphakis, M. J.; Cravatt, B. F. Proteome-Wide Reactivity Profiling Identifies Diverse Carbamate Chemotypes Tuned for Serine Hydrolase Inhibition. *ACS Chem. Biol.* **2013**, *8* (7), 1590–1599.
- (23) Hsu, K.-L.; Tsuboi, K.; Adibekian, A.; Pugh, H.; Masuda, K.; Cravatt, B. F. DAGL β Inhibition Perturbs a Lipid Network Involved in Macrophage Inflammatory Responses. *Nat. Chem. Biol.* **2012**, *8* (12), 999–1007.

References

Chapter 1

- (1) WHO. Tuberculosis (TB) <http://www.who.int/topics/tuberculosis/en/> (accessed Jul 11, 2016).
- (2) WHO. Tuberculosis <http://www.who.int/mediacentre/factsheets/fs104/en/> (accessed Jul 11, 2016).
- (3) WHO. *Global Tuberculosis Report 2015*, 20th ed.; WHO Press: Geneva, 2015.
- (4) CDC. Latent TB Infection and TB Disease <http://www.cdc.gov/tb/topic/basics/tbinfectiondisease.htm> (accessed Jul 11, 2016).
- (5) CDC. Signs & Symptoms <http://www.cdc.gov/tb/topic/basics/signsandSYMPTOMS.htm> (accessed Jul 11, 2016).
- (6) Dobos, K. M.; Spotts, E. a.; Quinn, F. D.; King, C. H. Necrosis of Lung Epithelial Cells during Infection with Mycobacterium Tuberculosis Is Preceded by Cell Permeation. *Infect. Immun.* **2000**, *68* (11), 6300–6310.
- (7) Golan, D. E.; Tashjian Jr., A. H.; Armstrong, E. J.; Armstrong, A. W. *Principles of Pharmacology: The Pathophysiologic Basis of Drug Therapy*, 2nd Editio.; Williams & Wilkins: Philadelphia, PA, 2008.
- (8) European Medicines Agency. Delytba http://www.ema.europa.eu/ema/index.jsp?curl=pages/medicines/human/medicines/002552/human_med_001699.jsp&mid=WC0b01ac058001d124 (accessed Jul 11, 2016).
- (9) FDA. News & Events <http://www.fda.gov/NewsEvents/Newsroom/PressAnnouncements/ucm333695.htm> (accessed Jul 11, 2016).
- (10) Gupta, R.; Gao, M.; Cirule, A.; Xiao, H.; Geiter, L. J.; Wells, C. D. Delamanid for Extensively Drug-Resistant Tuberculosis. *N. Engl. J. Med.* **2015**, *373* (3), 291–292.
- (11) Tadolini, M.; Lingsang, R. D.; Tiberi, S.; Enwerem, M.; D'Ambrosio, L.; Sadutshang, T. D.; Centis, R.; Migliori, G. B. First Case of Extensively Drug-Resistant Tuberculosis Treated with Both Delamanid and Bedaquiline. *Eur. Respir. J.* **2016**, ERJ – 00637–02016.
- (12) Awasthi, D.; Kumar, K.; Ojima, I. Therapeutic Potential of FtsZ Inhibition: A Patent Perspective. *Expert Opin. Ther. Pat.* **2011**, *21* (5), 657–679.
- (13) Li, X.; Ma, S. Advances in the Discovery of Novel Antimicrobials Targeting the Assembly of Bacterial Cell Division Protein FtsZ. *Eur. J. Med. Chem.* **2015**, *95*, 1–15.
- (14) Nogales, E.; Wolf, S. G.; Downing, K. H. Structure of the Alpha Beta Tubulin Dimer by Electron Crystallography. *Nature* **1998**, *391* (6663), 199–203.
- (15) Kumar, K.; Awasthi, D.; Berger, W. T.; Tonge, P. J.; Slayden, R. A.; Ojima, I. Discovery of Anti-TB Agents That Target the Cell-Division Protein FtsZ. *Future Med. Chem.* **2010**, *2* (8), 1305–1323.
- (16) Haranahalli, K.; Tong, S.; Ojima, I. Recent Advances in the Discovery and Development of

- Antibacterial Agents Targeting the Cell-Division Protein FtsZ. *Bioorg. Med. Chem.* **2016**.
- (17) Slayden, R. A. Identification of Cell Cycle Regulators in Mycobacterium Tuberculosis by Inhibition of Septum Formation and Global Transcriptional Analysis. *Microbiology* **2006**, *152* (6), 1789–1797.
- (18) Sarcina, M. Effects of Tubulin Assembly Inhibitors on Cell Division in Prokaryotes in Vivo. *FEMS Microbiol. Lett.* **2000**, *191* (1), 25–29.
- (19) Kumar, K.; Awasthi, D.; Lee, S.-Y.; Zanardi, I.; Ruzsicska, B.; Knudson, S.; Tonge, P. J.; Slayden, R. A.; Ojima, I. Novel Trisubstituted Benzimidazoles, Targeting Mtb FtsZ, as a New Class of Antitubercular Agents. *J. Med. Chem.* **2011**, *54* (1), 374–381.
- (20) White, E. L. 2-Alkoxy-carbonylaminopyridines: Inhibitors of Mycobacterium Tuberculosis FtsZ. *J. Antimicrob. Chemother.* **2002**, *50* (1), 111–114.
- (21) Reynolds, R. C.; Srivastava, S.; Ross, L. J.; Suling, W. J.; White, E. L. A New 2-Carbamoyl Pteridine That Inhibits Mycobacterial FtsZ. *Bioorg. Med. Chem. Lett.* **2004**, *14* (12), 3161–3164.
- (22) Awasthi, D.; Kumar, K.; Knudson, S. E.; Slayden, R. A.; Ojima, I. SAR Studies on Trisubstituted Benzimidazoles as Inhibitors of Mtb FtsZ for the Development of Novel Antitubercular Agents. *J. Med. Chem.* **2013**, *56* (23), 9756–9770.
- (23) Nasielski-Hinkens, R.; Levêque, P.; Castelet, D.; Nasielski, J. The Four 6-Halo-7-Nitroquinoxalines. *Heterocycles* **1987**, *26* (9), 2433.
- (24) Turesky, R. J.; Goodenough, A. K.; Ni, W.; McNaughton, L.; LeMaster, D. M.; Holland, R. D.; Wu, R. W.; Felton, J. S. Identification of 2-Amino-1,7-dimethylimidazo[4,5- G]Quinoxaline: An Abundant Mutagenic Heterocyclic Aromatic Amine Formed in Cooked Beef. *Chem. Res. Toxicol.* **2007**, *20* (3), 520–530.
- (25) Valdez, J.; Cedillo, R.; Hernández-Campos, A.; Yépez, L.; Hernández-Luis, F.; Navarrete-Vázquez, G.; Tapia, A.; Cortés, R.; Hernández, M.; Castillo, R. Synthesis and Antiparasitic Activity of 1H-Benzimidazole Derivatives. *Bioorg. Med. Chem. Lett.* **2002**, *12* (16), 2221–2224.
- (26) Iddon, B.; Kutschy, P.; Robinson, A. G.; Suschitzky, H.; Kramer, W.; Neugebauer, F. A. 2H-Benzimidazoles (Isobenzimidazoles). Part 7. A New Route to Triclabendazole [5-Chloro-6-(2,3-Dichlorophenoxy)-2-Methylthio-1H-Benzimidazole] and Congeneric Benzimidazoles. *J. Chem. Soc. Perkin Trans. 1* **1992**, No. 22, 3129.
- (27) VanAllan, J. A.; Deacon, B. D. 2-MERCAPTOBENZIMIDAZOLE. *Org. Synth.* **1950**, *30* (September), 56.
- (28) Sekar, R.; Srinivasan, M.; Marcelis, A. T. M.; Sambandam, A. S-Arylation of Mercaptobenzimidazoles Using Cu(I) Catalysts—experimental and Theoretical Observations. *Tetrahedron Lett.* **2011**, *52* (26), 3347–3352.
- (29) Takahashi, S.; Kano, H. Benzimidazole N-Oxides. II. The Reactivity of 1-Alkoxybenzimidazoles. *Chem. Pharm. Bull. (Tokyo)*. **1964**, *12* (3), 282–291.
- (30) Harvey, I. W.; McFarlane, M. D.; Moody, D. J.; Smith, D. M. O-Nitroaniline Derivatives. Part 9. Benzimidazole N-Oxides Unsubstituted at N-1 and C-2. *J. Chem. Soc. Perkin Trans.*

I **1988**, No. 3, 681.

- (31) Jamieson, C.; Moir, E. M.; Rankovic, Z.; Wishart, G. Medicinal Chemistry of hERG Optimizations: Highlights and Hang-Ups. *J. Med. Chem.* **2006**, *49* (17), 5029–5046.
- (32) Wang, S.; Li, Y.; Xu, L.; Li, D.; Hou, T. Recent Developments in Computational Prediction of hERG Blockage. *Curr. Top. Med. Chem.* **2013**, *13* (11), 1317–1326.
- (33) Recanatini, M.; Poluzzi, E.; Masetti, M.; Cavalli, A.; De Ponti, F. QT Prolongation through hERG K⁺ Channel Blockade: Current Knowledge and Strategies for the Early Prediction during Drug Development. *Med. Res. Rev.* **2005**, *25* (2), 133–166.
- (34) Park, B.; Awasthi, D.; Chowdhury, S. R.; Melief, E. H.; Kumar, K.; Knudson, S. E.; Slayden, R. A.; Ojima, I. Design, Synthesis and Evaluation of Novel 2,5,6-Trisubstituted Benzimidazoles Targeting FtsZ as Antitubercular Agents. *Bioorg. Med. Chem.* **2014**, *22* (9), 2602–2612.
- (35) Oxford Diffraction. CrysAlis Pro. Oxford Diffraction Ltd: Abingdon, England 2016.
- (36) Farrugia, L. J. WinGX and ORTEP for Windows: An Update. *J. Appl. Crystallogr.* **2012**, *45* (4), 849–854.
- (37) Dolomanov, O. V.; Bourhis, L. J.; Gildea, R. J.; Howard, J. A. K.; Puschmann, H. OLEX2 : A Complete Structure Solution, Refinement and Analysis Program. *J. Appl. Crystallogr.* **2009**, *42* (2), 339–341.
- (38) Gruene, T.; Hahn, H. W.; Luebben, A. V.; Meilleur, F.; Sheldrick, G. M. Refinement of Macromolecular Structures against Neutron Data with SHELXL2013. *J. Appl. Crystallogr.* **2014**, *47* (1), 462–466.

Chapter 2

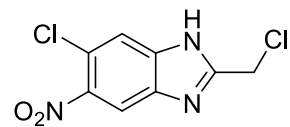
- (1) Loeser, J. D. *Relieving Pain in America*; National Academies Press: Washington, D.C., 2011; Vol. 28.
- (2) Robinson, J. Opioid (Narcotic) Pain Medications <http://www.webmd.com/pain-management/guide/narcotic-pain-medications?page=1#1> (accessed Jun 22, 2016).
- (3) DrugFacts: Marijuana <https://www.drugabuse.gov/publications/drugfacts/marijuana> (accessed Jul 4, 2016).
- (4) Iversen, L. Cannabis and the Brain. *Brain* **2003**, *126* (6), 1252–1270.
- (5) Kaczocha, M.; Rebecchi, M. J.; Ralph, B. P.; Teng, Y. H. G.; Berger, W. T.; Galbavy, W.; Elmes, M. W.; Glaser, S. T.; Wang, L.; Rizzo, R. C.; et al. Inhibition of Fatty Acid Binding Proteins Elevates Brain Anandamide Levels and Produces Analgesia. *PLoS One* **2014**, *9* (4), 1–11.
- (6) Kaczocha, M.; Vivieca, S.; Sun, J.; Glaser, S. T.; Deutsch, D. G. Fatty Acid-Binding Proteins Transport N-Acylethanolamines to Nuclear Receptors and Are Targets of Endocannabinoid Transport Inhibitors. *J. Biol. Chem.* **2012**, *287* (5), 3415–3424.
- (7) Ueda, N.; Puffenbarger, R. A.; Yamamoto, S.; Deutsch, D. G. The Fatty Acid Amide Hydrolase (FAAH). *Chem. Phys. Lipids* **2000**, *108* (1-2), 107–121.
- (8) Berger, W. T.; Ralph, B. P.; Kaczocha, M.; Sun, J.; Balius, T. E.; Rizzo, R. C.; Haj-

- Dahmane, S.; Ojima, I.; Deutsch, D. G. Targeting Fatty Acid Binding Protein (FABP) Anandamide Transporters - A Novel Strategy for Development of Anti-Inflammatory and Anti-Nociceptive Drugs. *PLoS One* **2012**, *7* (12).
- (9) Balias, T. E.; Mukherjee, S.; Rizzo, R. C. Implementation and Evaluation of a Docking-Rescoring Method Using Molecular Footprint Comparisons. *J. Comput. Chem.* **2011**, *32* (10), 2273–2289.
- (10) Balias, T. E.; Mukherjee, S.; Rizzo, R. C. Implementation and Evaluation of a Docking-Rescoring Method Using Molecular Footprint Comparisons. *J. Comput. Chem.* **2011**, *32* (10), 2273–2289.
- (11) Kaczocha, M.; Rebecchi, M. J.; Ralph, B. P.; Teng, Y.-H. G.; Berger, W. T.; Galbavy, W.; Elmes, M. W.; Glaser, S. T.; Wang, L.; Rizzo, R. C.; et al. Inhibition of Fatty Acid Binding Proteins Elevates Brain Anandamide Levels and Produces Analgesia. *PLoS One* **2014**, *9* (4), e94200.
- (12) Ichikawa, M.; Takahashi, M.; Aoyagi, S.; Kibayashi, C. Total Synthesis of (–)-Incarvilline, (+)-Incarvine C, and (–)-Incarvillateine. *J. Am. Chem. Soc.* **2004**, *126* (50), 16553–16558.
- (13) Chi, Y.-M.; Nakamura, M.; Yoshizawa, T.; Zhao, X.-Y.; Yan, W.-M.; Hashimoto, F.; Kinjo, J.; Nohara, T.; Sakurada, S. Pharmacological Study on the Novel Antinociceptive Agent, a Novel Monoterpene Alkaloid from *Incarvillea Sinensis*. *Biol. Pharm. Bull.* **2005**, *28* (10), 1989–1991.
- (14) Binas, B.; Danneberg, H.; McWhir, J.; Mullins, L.; Clark, a J. Requirement for the Heart-Type Fatty Acid Binding Protein in Cardiac Fatty Acid Utilization. *Faseb J* **1999**, *13* (8), 805–812.
- (15) Jamieson, C.; Moir, E. M.; Rankovic, Z.; Wishart, G. Medicinal Chemistry of hERG Optimizations: Highlights and Hang-Ups. *J. Med. Chem.* **2006**, *49* (17), 5029–5046.
- (16) Wang, S.; Li, Y.; Xu, L.; Li, D.; Hou, T. Recent Developments in Computational Prediction of hERG Blockage. *Curr. Top. Med. Chem.* **2013**, *13* (11), 1317–1326.
- (17) Kole, G. K.; Tan, G. K.; Vittal, J. J. Anion-Controlled Stereoselective Synthesis of Cyclobutane Derivatives by Solid-State [2 + 2] Cycloaddition Reaction of the Salts of Trans-3-(4-Pyridyl) Acrylic Acid. *Org. Lett.* **2010**, *12* (1), 128–131.
- (18) Oxford Diffraction. CrysAlis Pro. Oxford Diffraction Ltd: Abingdon, England 2016.
- (19) Farrugia, L. J. WinGX and ORTEP for Windows: An Update. *J. Appl. Crystallogr.* **2012**, *45* (4), 849–854.
- (20) Dolomanov, O. V.; Bourhis, L. J.; Gildea, R. J.; Howard, J. A. K.; Puschmann, H. OLEX2 : A Complete Structure Solution, Refinement and Analysis Program. *J. Appl. Crystallogr.* **2009**, *42* (2), 339–341.
- (21) Gruene, T.; Hahn, H. W.; Luebben, A. V.; Meilleur, F.; Sheldrick, G. M. Refinement of Macromolecular Structures against Neutron Data with SHELXL2013. *J. Appl. Crystallogr.* **2014**, *47* (1), 462–466.
- (22) Chang, J. W.; Cognetta, A. B.; Niphakis, M. J.; Cravatt, B. F. Proteome-Wide Reactivity Profiling Identifies Diverse Carbamate Chemotypes Tuned for Serine Hydrolase Inhibition. *ACS Chem. Biol.* **2013**, *8* (7), 1590–1599.

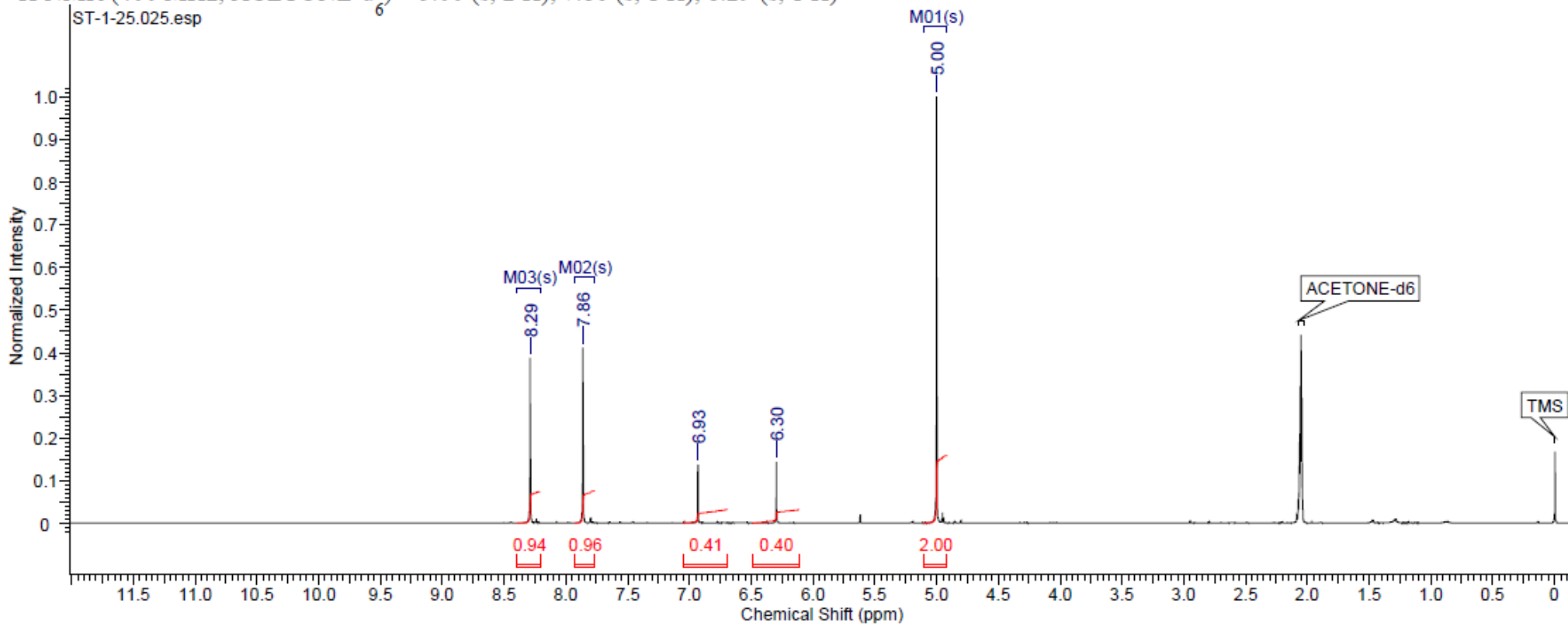
- (23) Hsu, K.-L.; Tsuboi, K.; Adibekian, A.; Pugh, H.; Masuda, K.; Cravatt, B. F. DAGL β Inhibition Perturbs a Lipid Network Involved in Macrophage Inflammatory Responses. *Nat. Chem. Biol.* **2012**, 8 (12), 999–1007.

Appendix

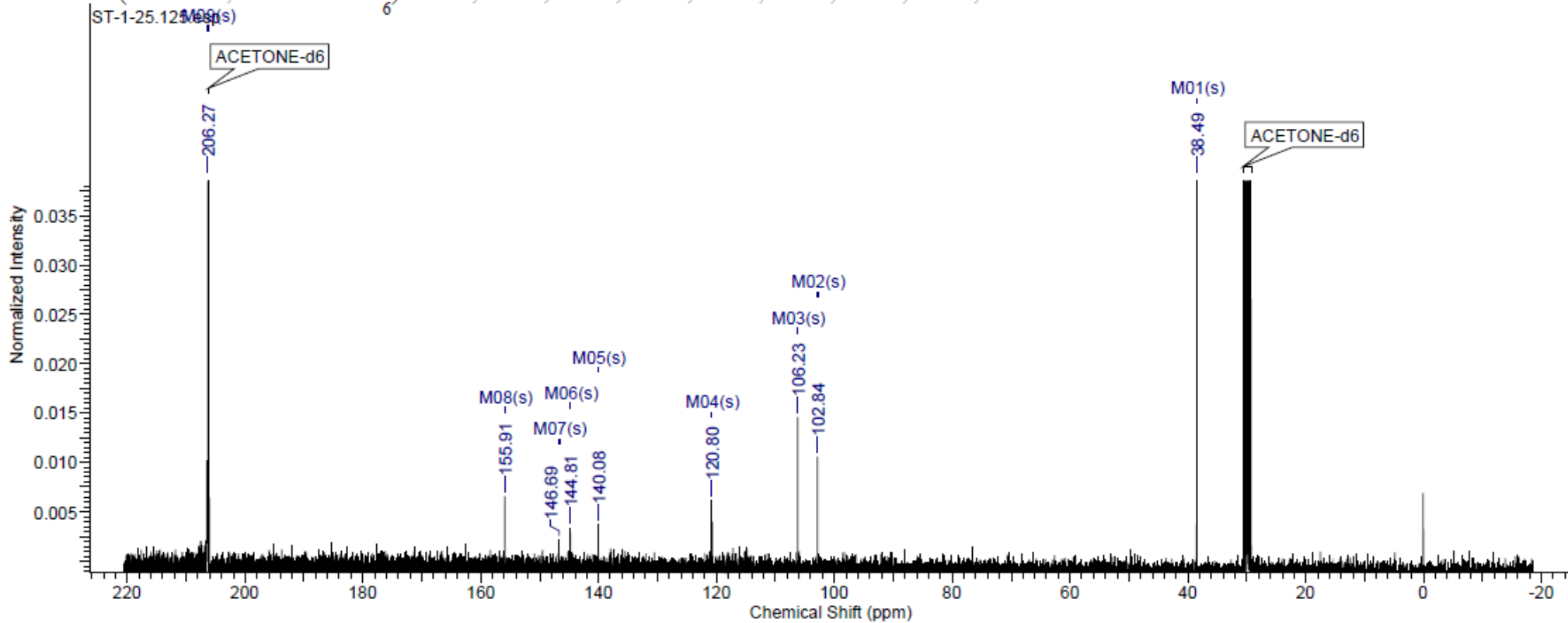
5-Chloro-2-chloromethyl-6-nitro-1H-benzo[d]imidazole



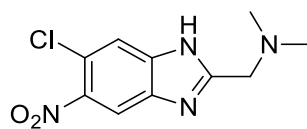
$^1\text{H NMR}$ (400 MHz, ACETONE- d_6) δ 5.00 (s, 2 H), 7.86 (s, 1 H), 8.29 (s, 1 H)



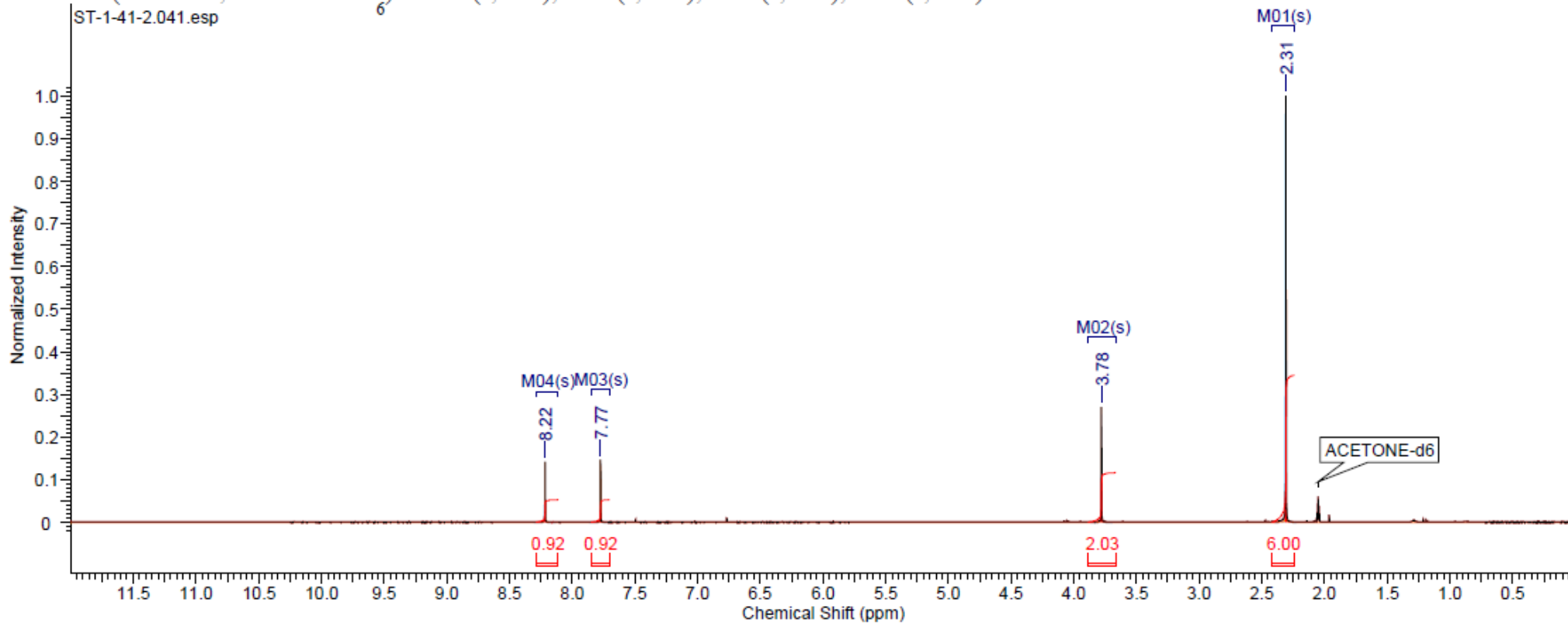
^{13}C NMR (101 MHz, ACETONE- d_6) δ 38.5, 102.8, 106.2, 120.8, 140.1, 144.8, 146.7, 155.9, 206.3



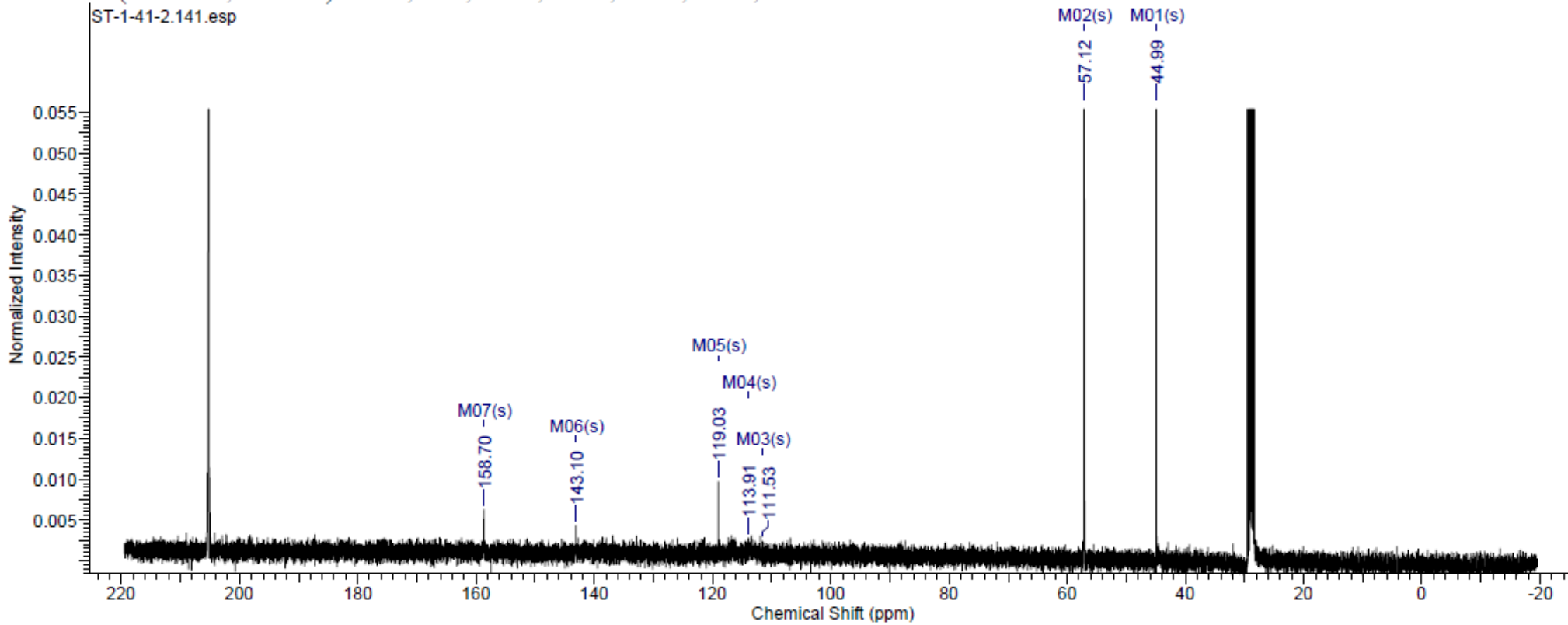
5-Chloro-2-dimethylaminomethyl-6-nitro-1H-benzo[d]imidazole



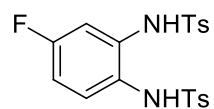
$^1\text{H NMR}$ (400 MHz, ACETONE- d_6) δ 2.31 (s, 6 H), 3.78 (s, 2 H), 7.77 (s, 1 H), 8.22 (s, 1 H)



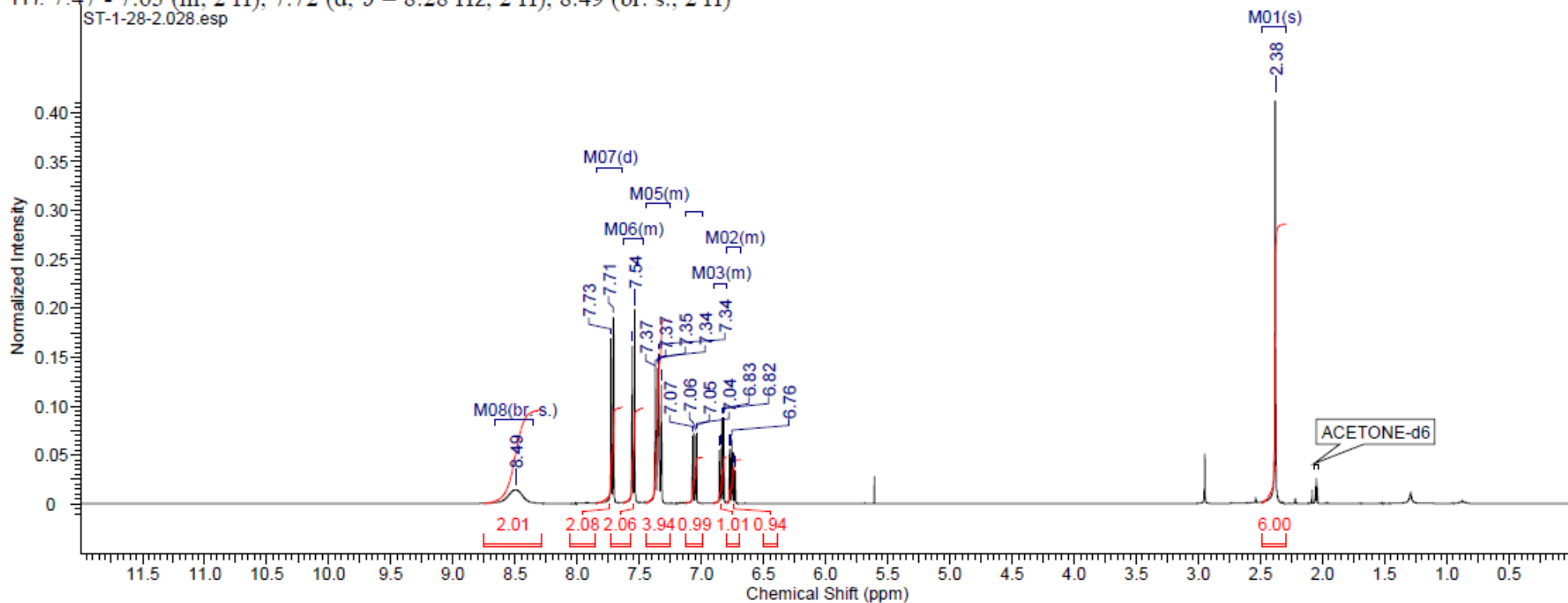
^{13}C NMR (101 MHz, Acetone) δ 45.0, 57.1, 111.5, 113.9, 119.0, 143.1, 158.7



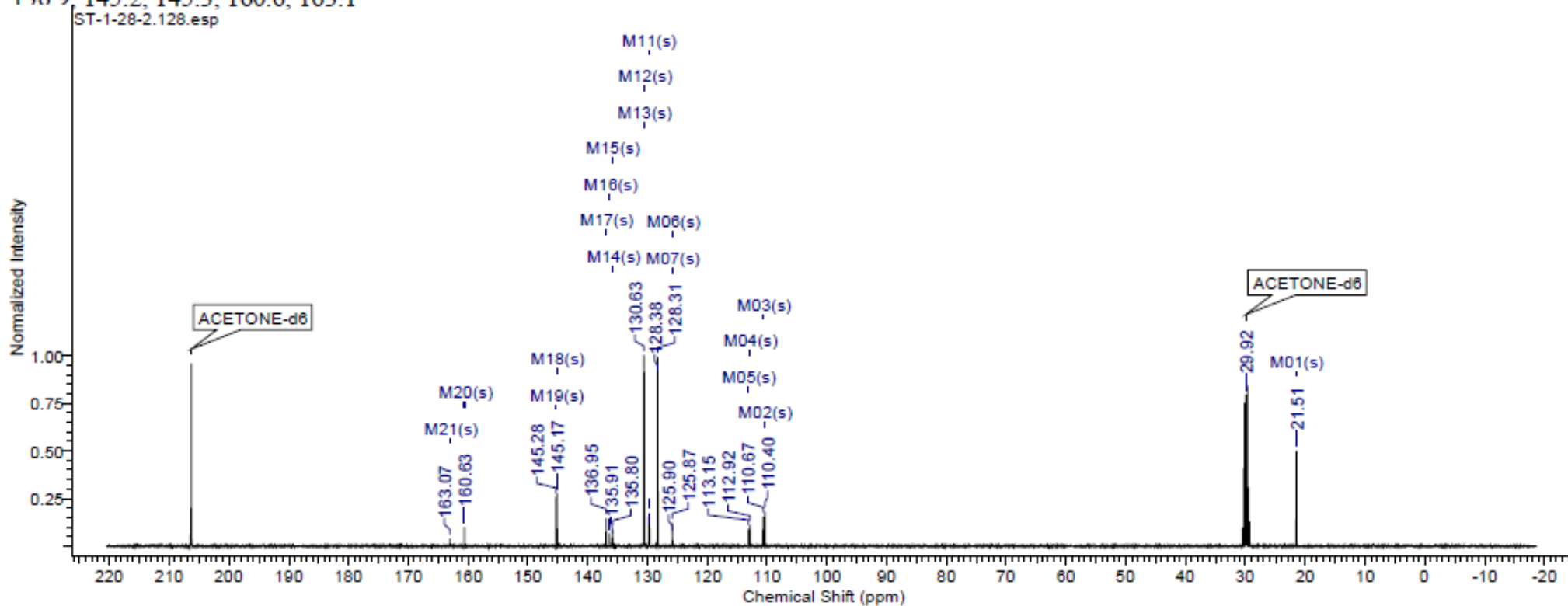
4-Fluoro-1,2-di (*p*-toluenesulfonylamino) benzene



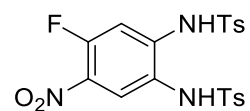
$^1\text{H NMR}$ (400 MHz, ACETONE- d_6) δ 2.38 (s, 6 H), 6.68 - 6.80 (m, 1 H), 6.80 - 6.90 (m, 1 H), 7.06 (dd, $J = 10.04, 2.76$ Hz, 1 H), 7.25 - 7.45 (m, 4 H), 7.47 - 7.63 (m, 2 H), 7.72 (d, $J = 8.28$ Hz, 2 H), 8.49 (br. s., 2 H)



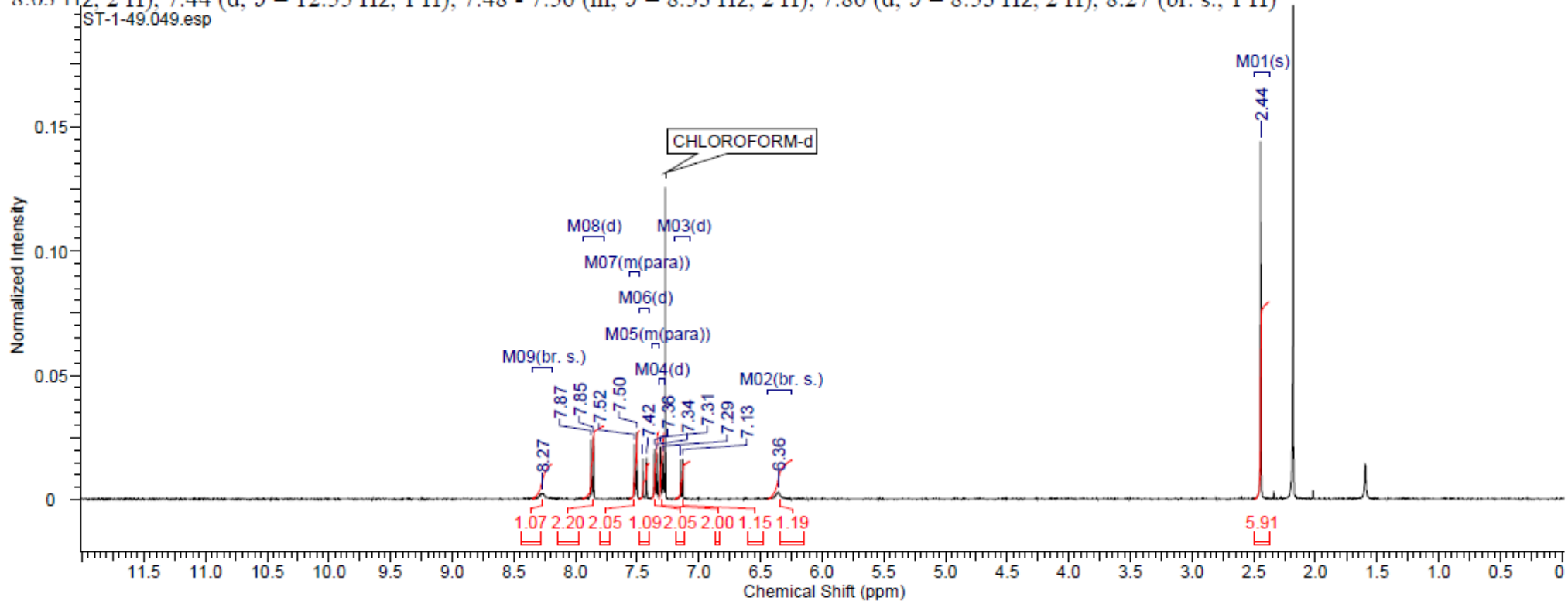
^{13}C NMR (101 MHz, ACETONE- d_6) δ 21.5, 110.4, 110.7, 112.9, 113.1, 125.9, 125.9, 128.3, 128.4, 129.7, 129.8, 130.6, 130.6, 135.8, 135.9, 136.4, 136.9, 145.2, 145.3, 160.6, 163.1



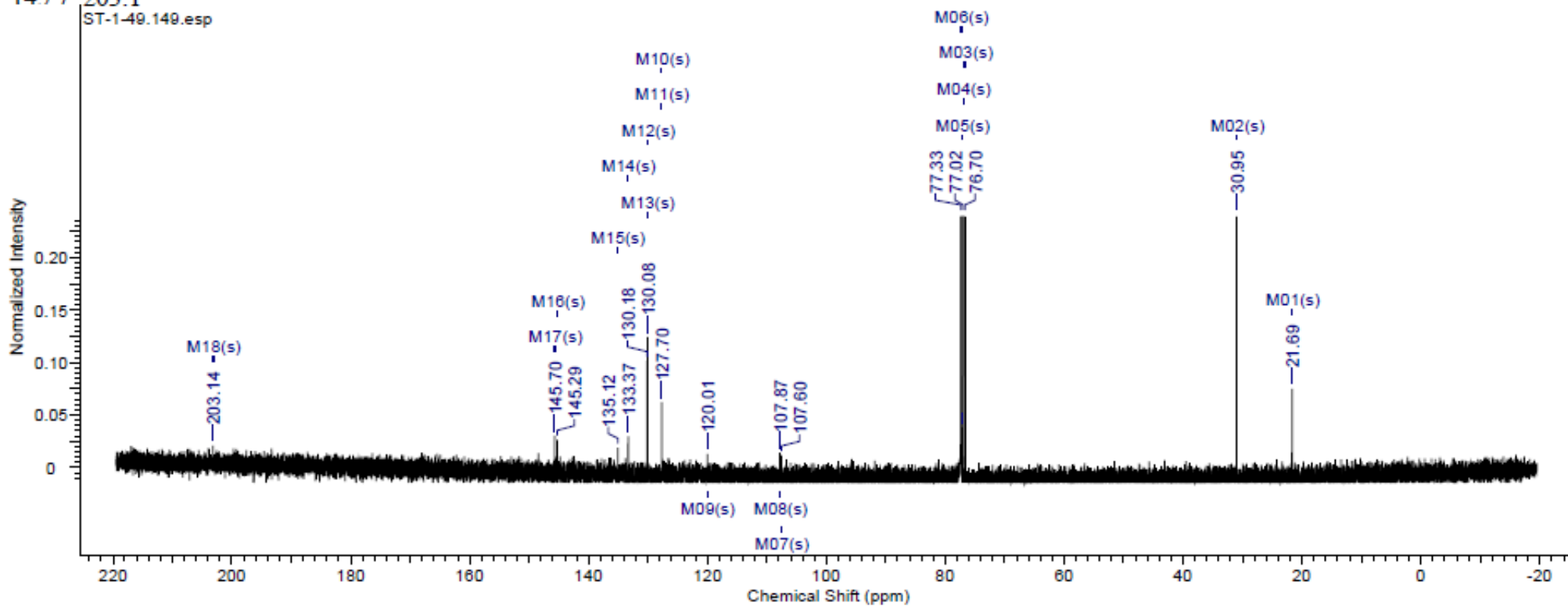
4-fluoro-5-nitro-1,2-di (*p*-toluenesulfonylamino) benzene



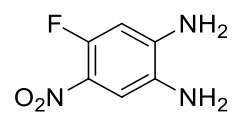
$^1\text{H NMR}$ (400 MHz, CHLOROFORM- d) δ 2.44 (s, 6 H), 6.36 (br. s., 1 H), 7.14 (d, $J = 7.53$ Hz, 1 H), 7.30 (d, $J = 8.03$ Hz, 2 H), 7.32 - 7.38 (m, $J = 8.03$ Hz, 2 H), 7.44 (d, $J = 12.55$ Hz, 1 H), 7.48 - 7.56 (m, $J = 8.53$ Hz, 2 H), 7.86 (d, $J = 8.53$ Hz, 2 H), 8.27 (br. s., 1 H)



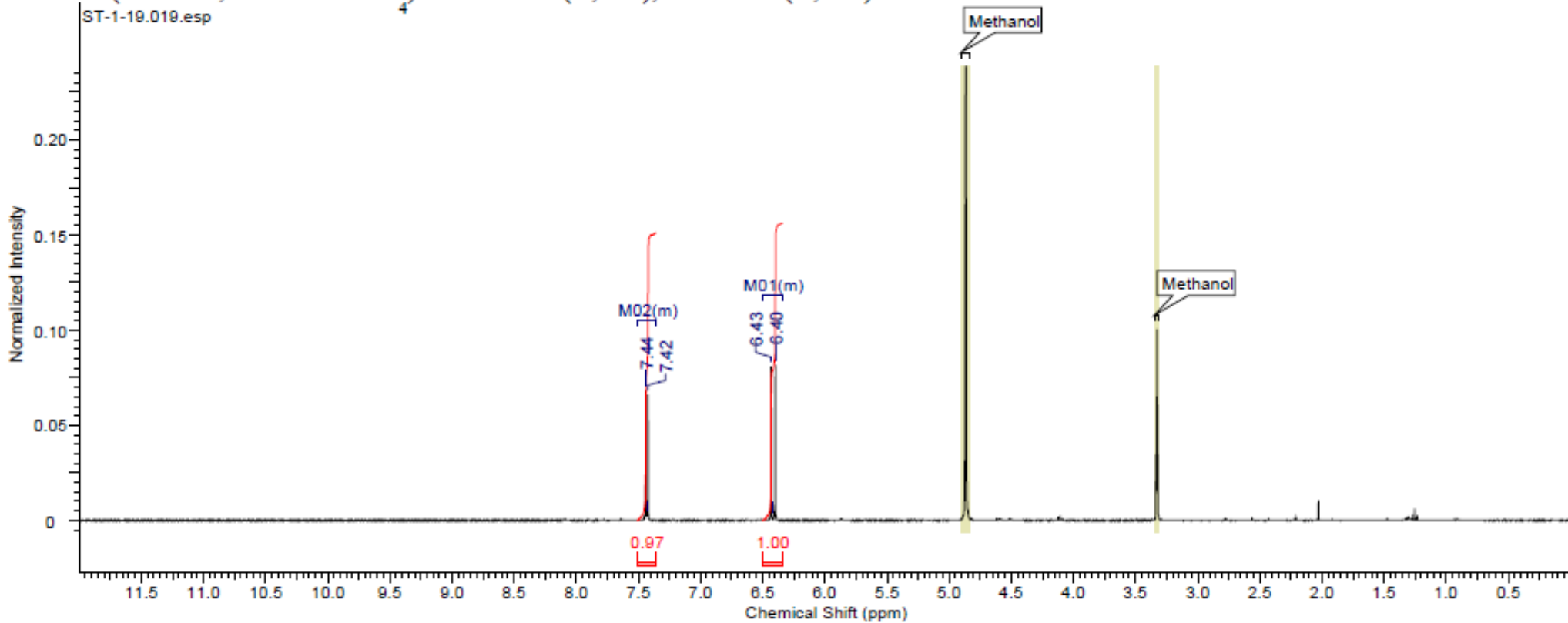
^{13}C NMR (101 MHz, CHLOROFORM- d) δ 21.7, 31.0, 76.7, 77.0, 77.2, 77.3, 107.6, 107.9, 120.0, 127.7, 127.7, 130.1, 130.2, 133.4, 135.1, 145.3, 145.7, 203.1



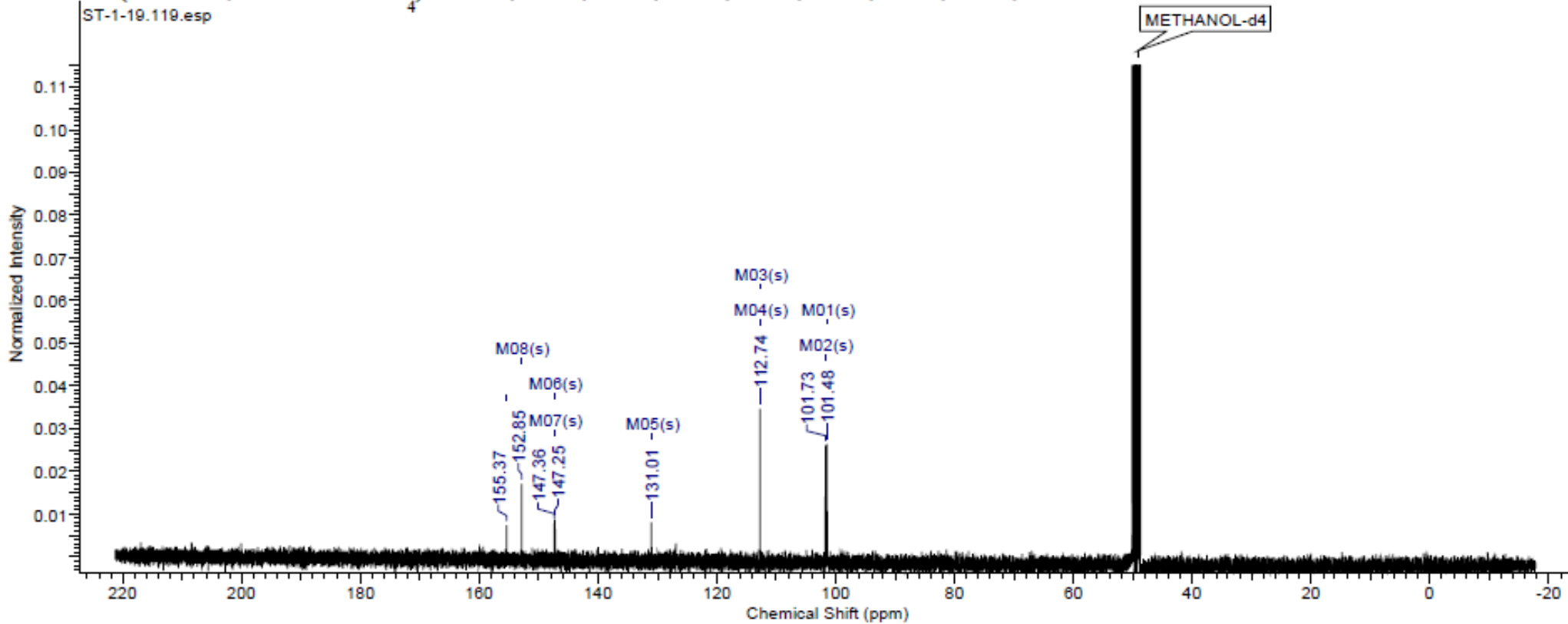
1,2-Diamino-4-fluoro-5-nitro benzene



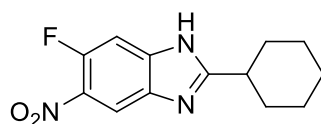
$^1\text{H NMR}$ (400 MHz, METHANOL- d_4) δ 6.34 - 6.50 (m, 1 H), 7.36 - 7.51 (m, 1 H)



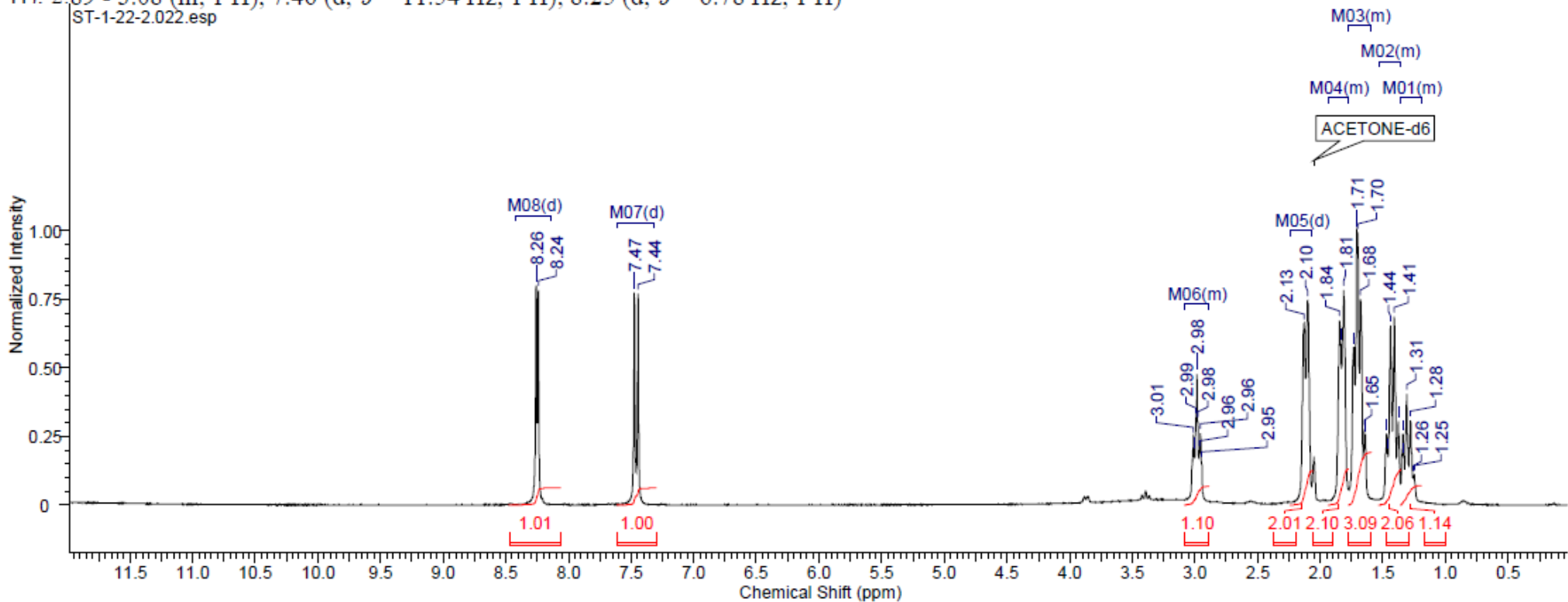
^{13}C NMR (101 MHz, METHANOL- d_4) δ 101.5, 101.7, 112.7, 112.8, 131.0, 147.3, 147.4, 152.8, 155.4



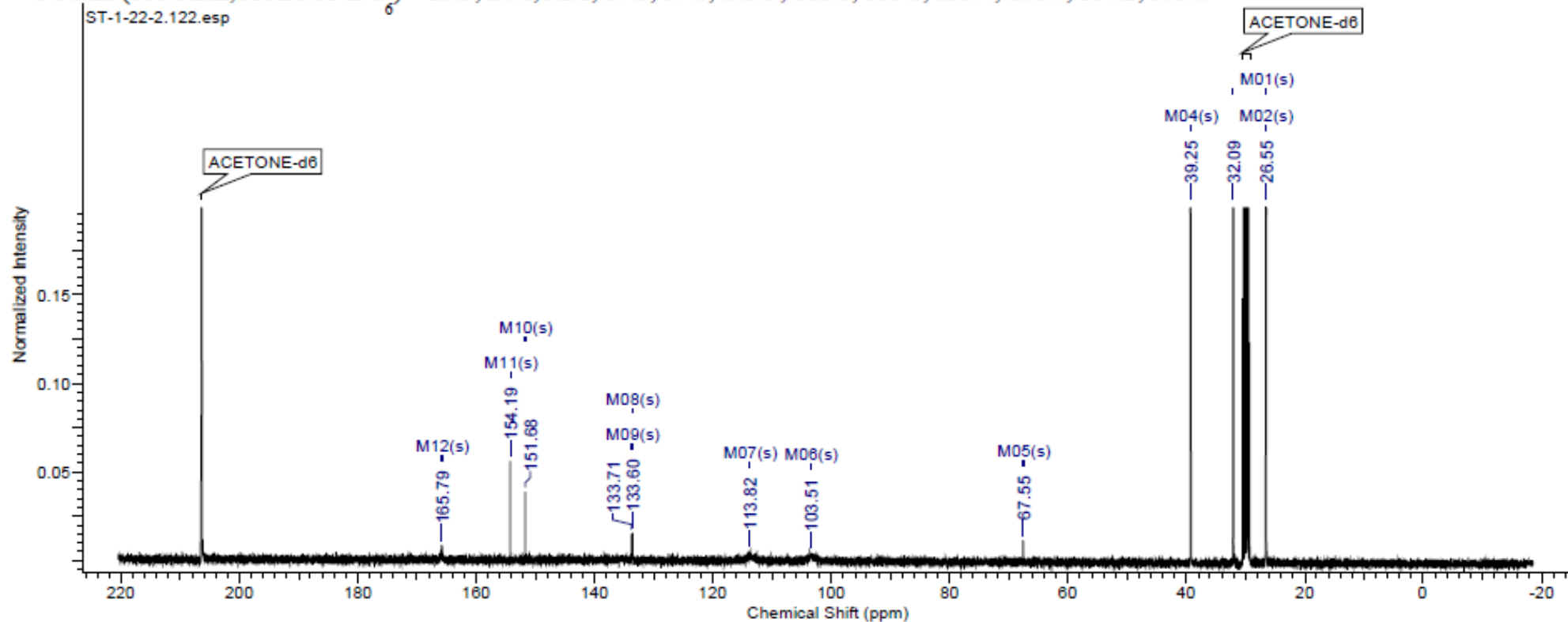
2-Cyclohexyl-5-fluoro-6-nitro-1H-benzo[d]imidazole



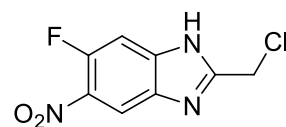
$^1\text{H NMR}$ (400 MHz, ACETONE- d_6) δ 1.19 - 1.36 (m, 1 H), 1.36 - 1.53 (m, 2 H), 1.59 - 1.77 (m, 3 H), 1.77 - 1.94 (m, 2 H), 2.11 (d, $J = 11.54$ Hz, 2 H). 2.89 - 3.08 (m, 1 H), 7.46 (d, $J = 11.54$ Hz, 1 H), 8.25 (d, $J = 6.78$ Hz, 1 H)



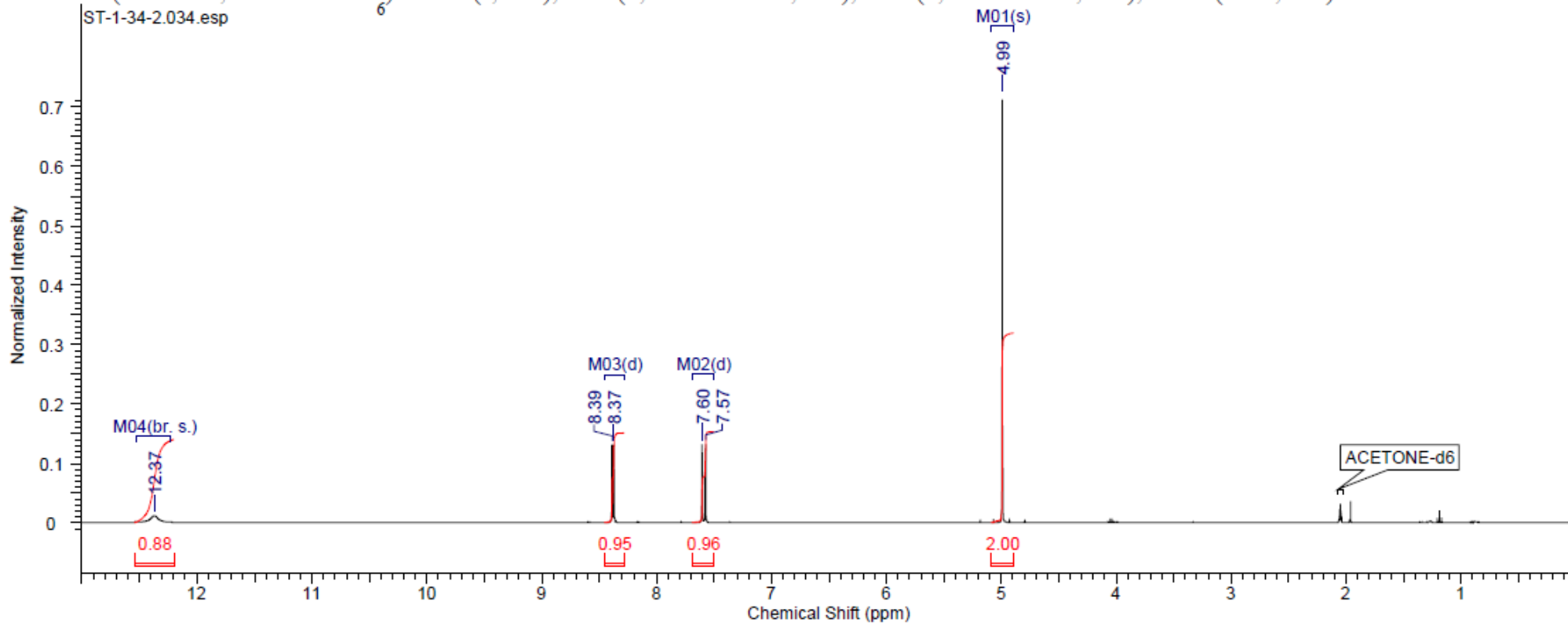
^{13}C NMR (101 MHz, ACETONE- d_6) δ 26.5, 26.6, 32.1, 39.3, 67.6, 103.5, 113.8, 133.6, 133.7, 151.7, 154.2, 165.8



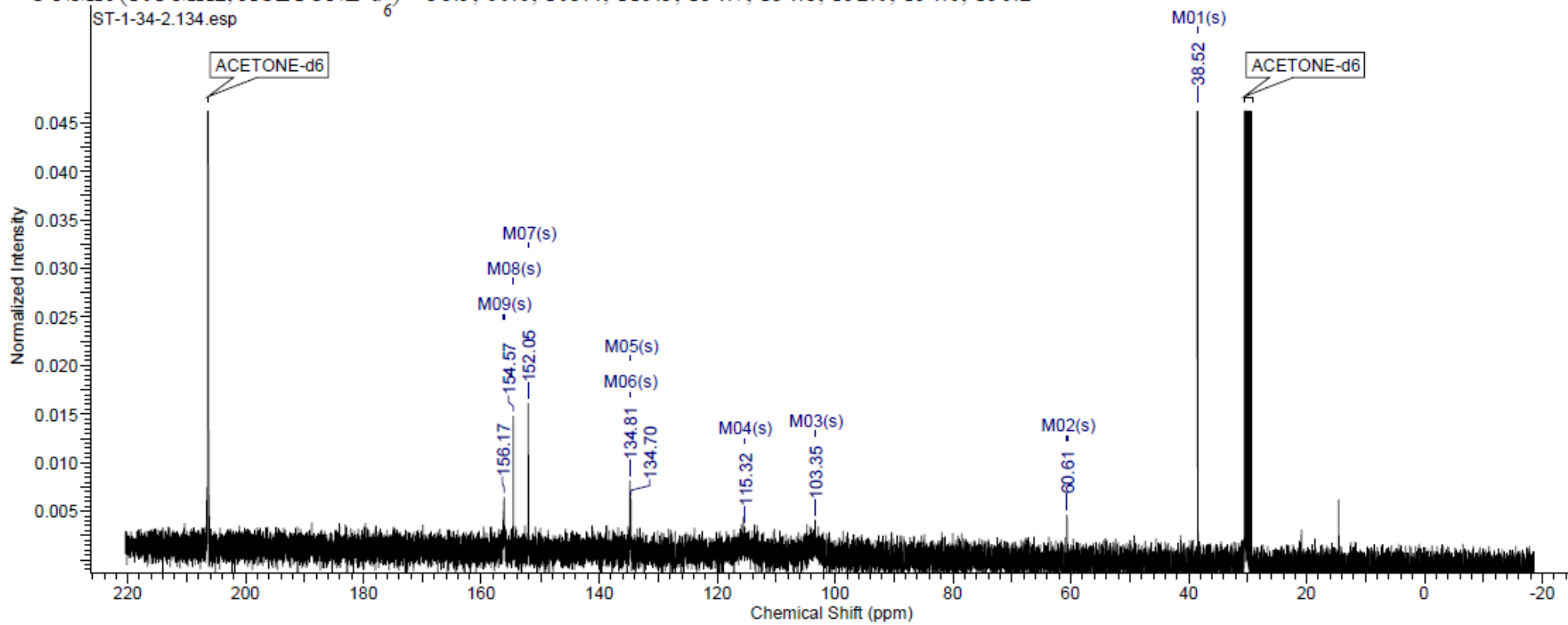
2-Chloromethyl-5-fluoro-6-nitro-1H-benzo[d]imidazole



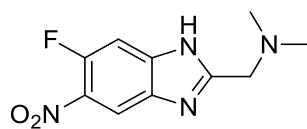
$^1\text{H NMR}$ (400 MHz, ACETONE- d_6) δ 4.99 (s, 2 H), 7.59 (d, $J = 11.54$ Hz, 1 H), 8.38 (d, $J = 6.78$ Hz, 1 H), 12.37 (br. s., 1 H)



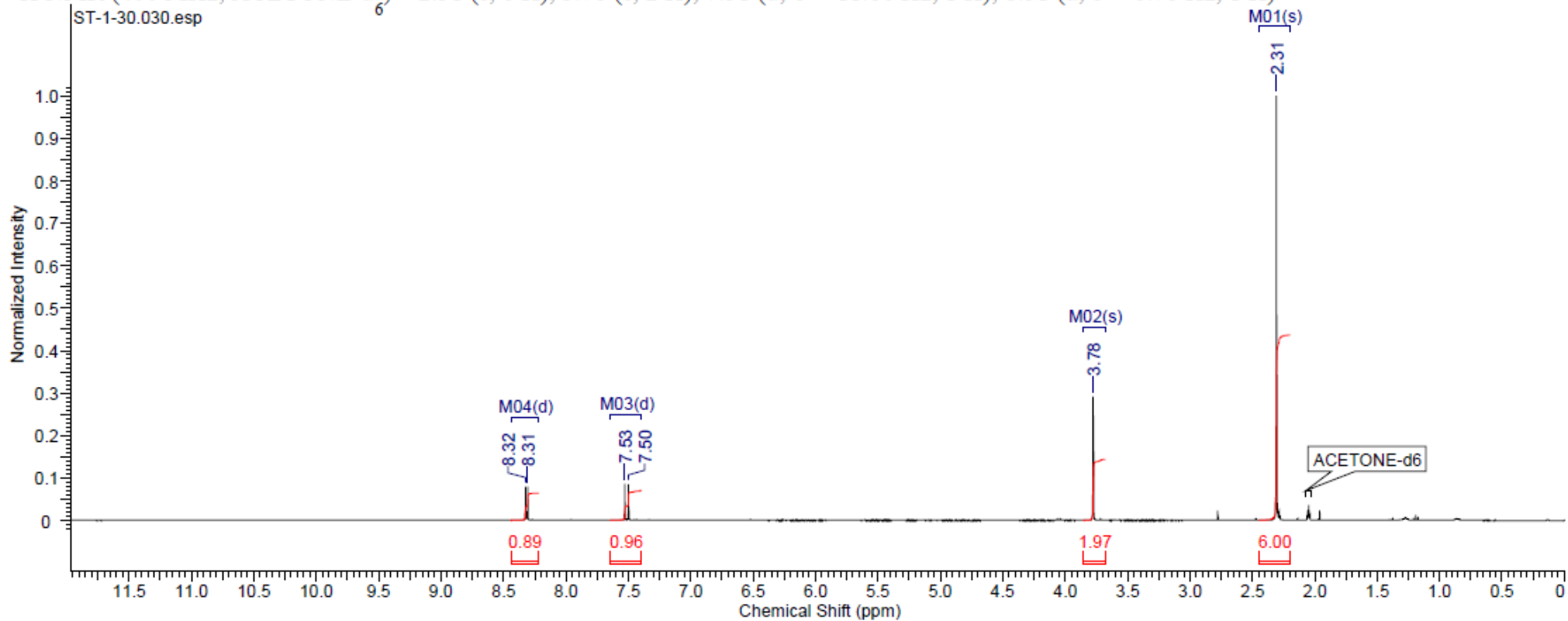
^{13}C NMR (101 MHz, ACETONE- d_6) δ 38.5, 60.6, 103.4, 115.3, 134.7, 134.8, 152.0, 154.6, 156.2



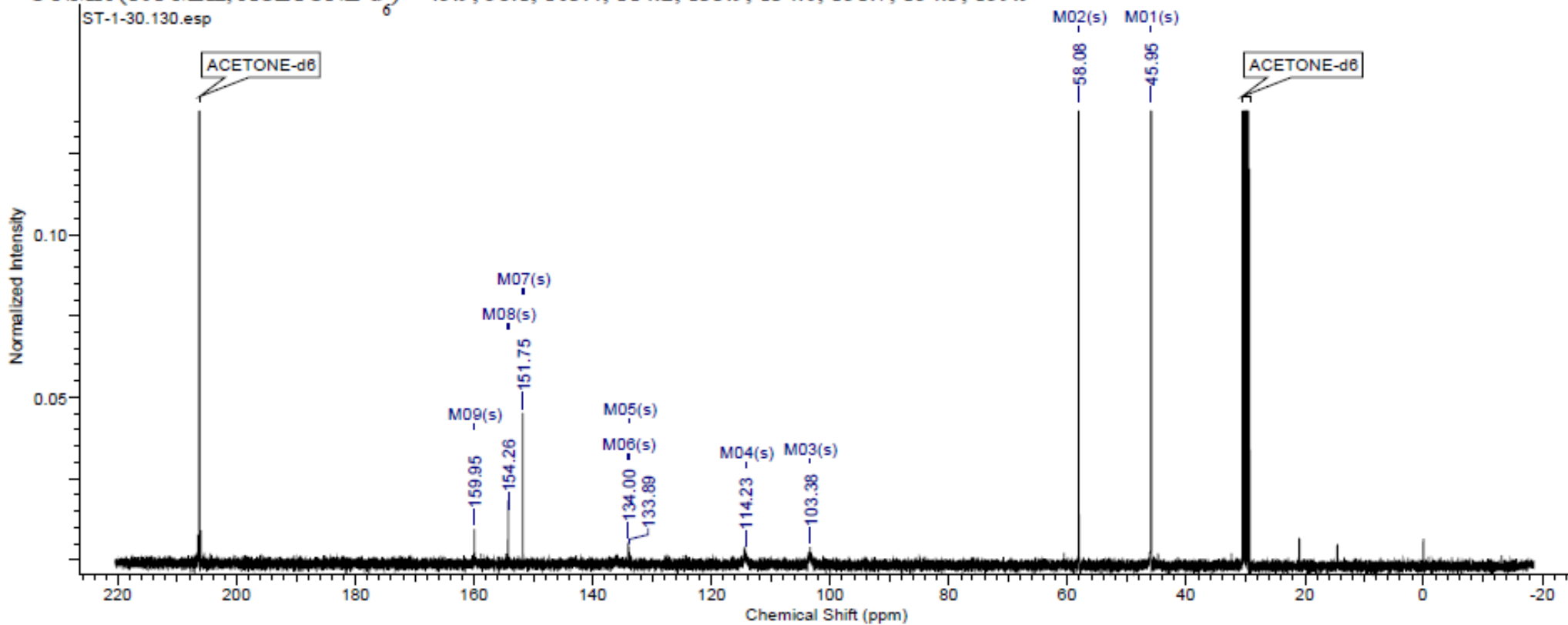
5-Fluoro-2-dimethylaminomethyl-6-nitro-1H-benzo[d]imidazole



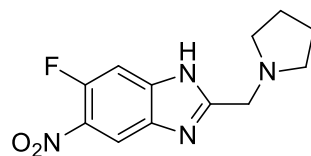
$^1\text{H NMR}$ (400 MHz, ACETONE- d_6) δ 2.31 (s, 6 H), 3.78 (s, 2 H), 7.51 (d, $J = 11.80$ Hz, 1 H), 8.31 (d, $J = 6.78$ Hz, 1 H)



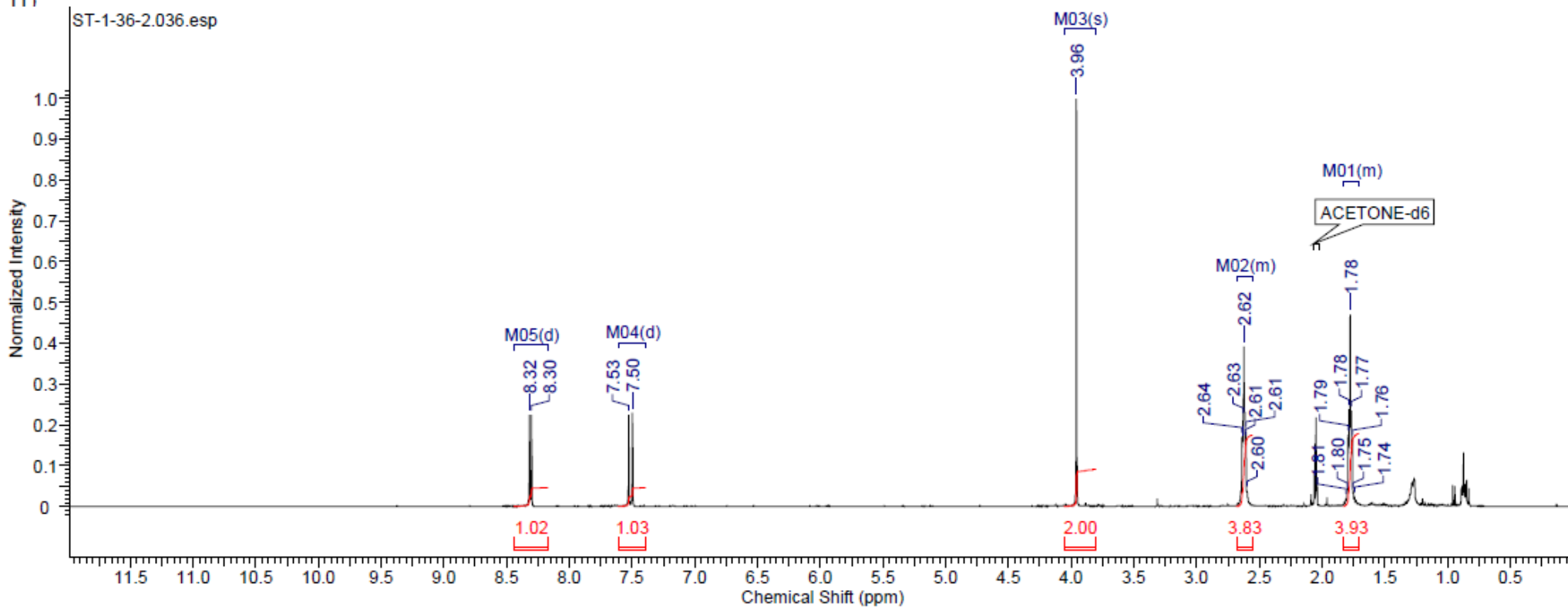
^{13}C NMR (101 MHz, ACETONE- d_6) δ 45.9, 58.1, 103.4, 114.2, 133.9, 134.0, 151.7, 154.3, 159.9



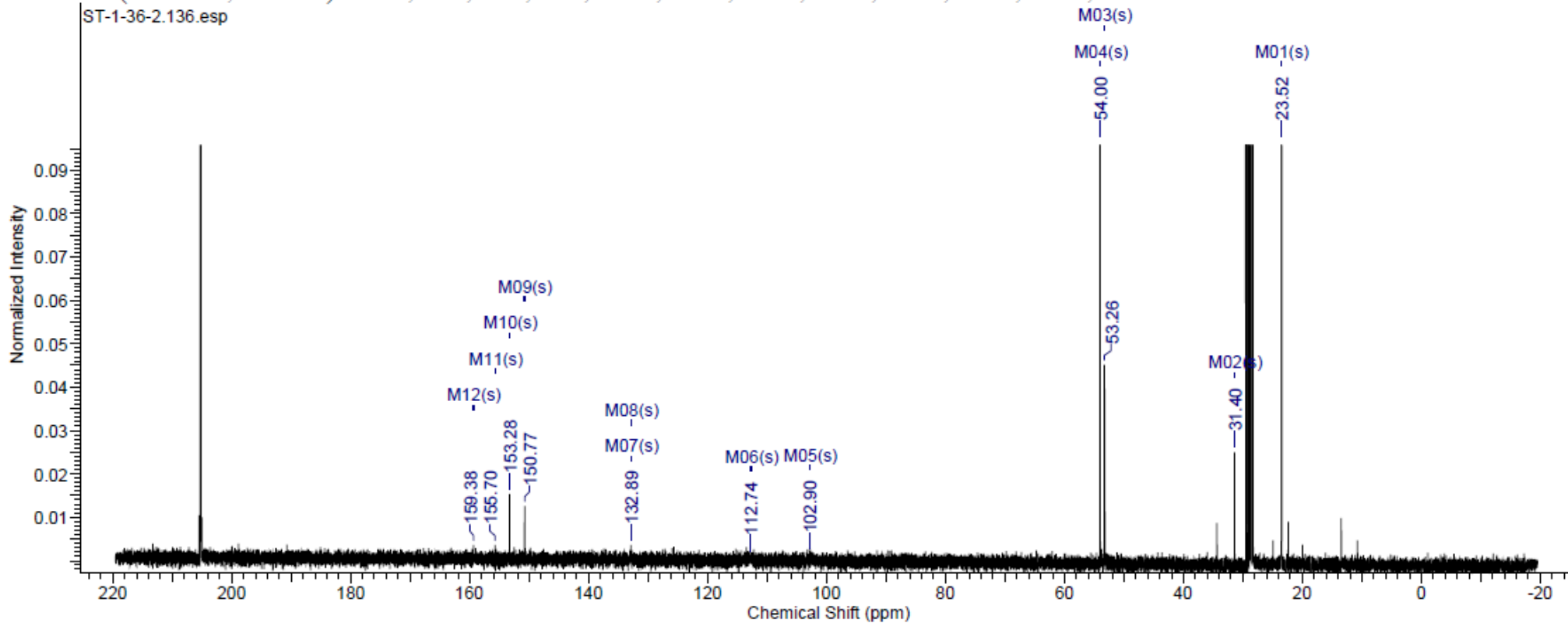
5-Fluoro-2-pyrrolidinylmethyl-6-nitro-1H-benzo[d]imidazole



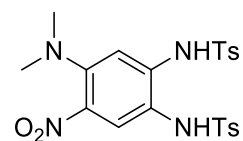
$^1\text{H NMR}$ (400 MHz, ACETONE- d_6) δ 1.71 - 1.83 (m, 4 H), 2.56 - 2.68 (m, 4 H), 3.96 (s, 2 H), 7.51 (d, $J = 11.54$ Hz, 1 H), 8.31 (d, $J = 6.78$ Hz, 1 H)



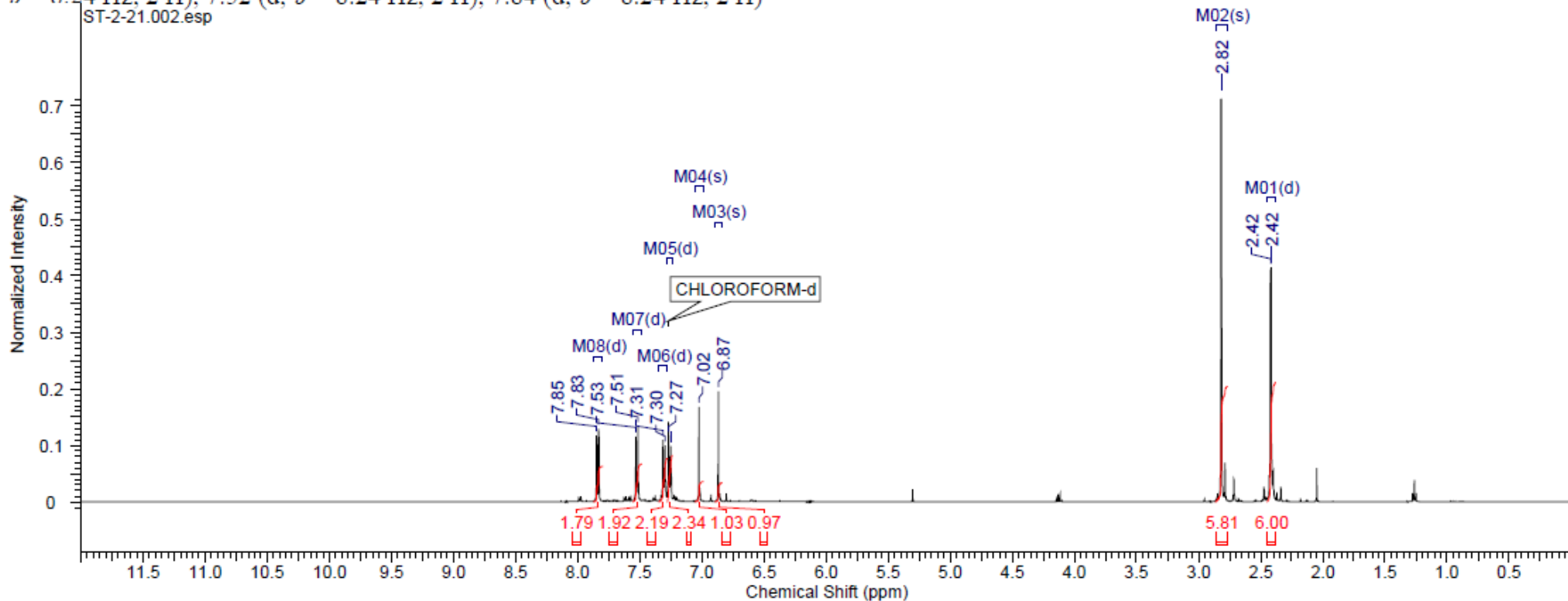
^{13}C NMR (101 MHz, Acetone) δ 23.5, 31.4, 53.3, 54.0, 102.9, 112.7, 132.9, 132.9, 150.8, 153.3, 155.7, 159.4



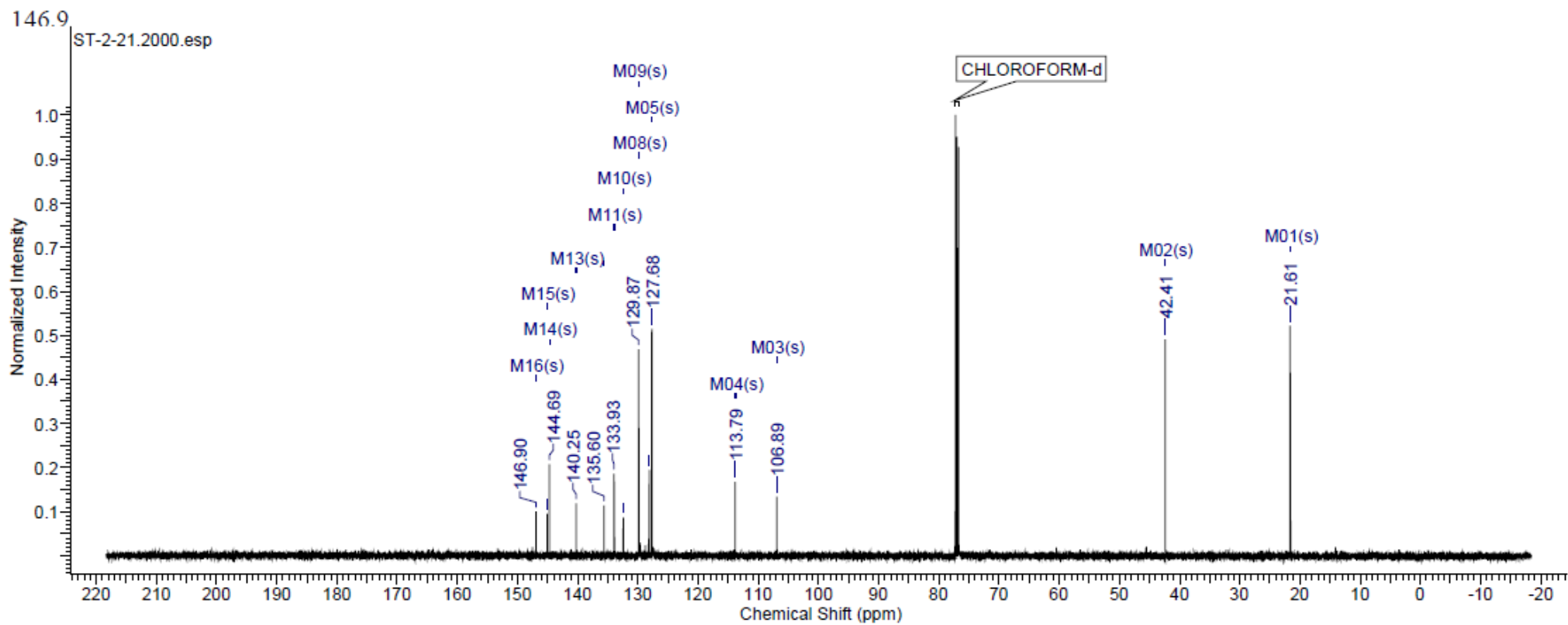
4-*N,N*-Dimethylamino-5-nitro-1,2-di (*p*-toluenesulfonylamino) benzene



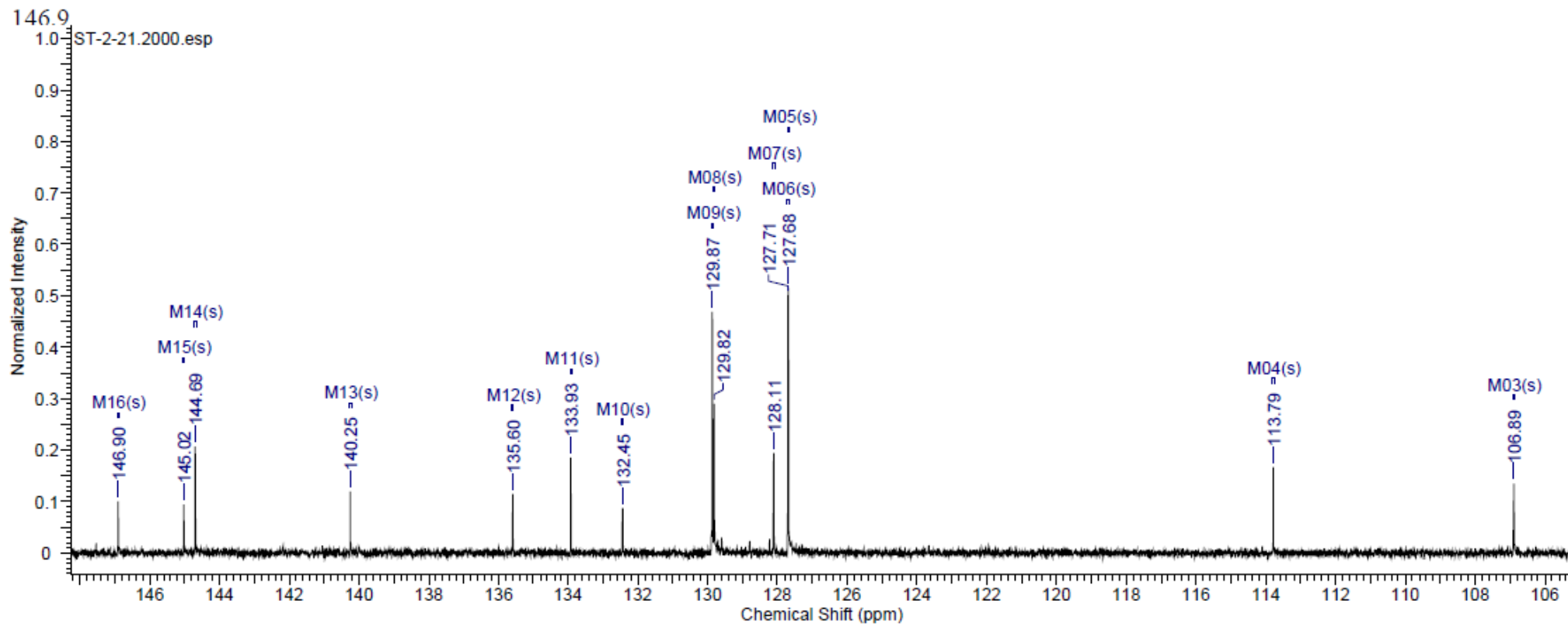
$^1\text{H NMR}$ (500 MHz, CHLOROFORM- d) δ 2.42 (d, $J = 2.14$ Hz, 6 H), 2.82 (s, 6 H), 6.87 (s, 1 H), 7.02 (s, 1 H), 7.26 (d, $J = 7.93$ Hz, 2 H), 7.31 (d, $J = 8.24$ Hz, 2 H), 7.52 (d, $J = 8.24$ Hz, 2 H), 7.84 (d, $J = 8.24$ Hz, 2 H)



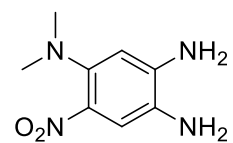
^{13}C NMR (126 MHz, CHLOROFORM- d) δ 21.6, 42.4, 106.9, 113.8, 127.7, 127.7, 128.1, 129.8, 129.9, 132.4, 133.9, 135.6, 140.2, 144.7, 145.0,



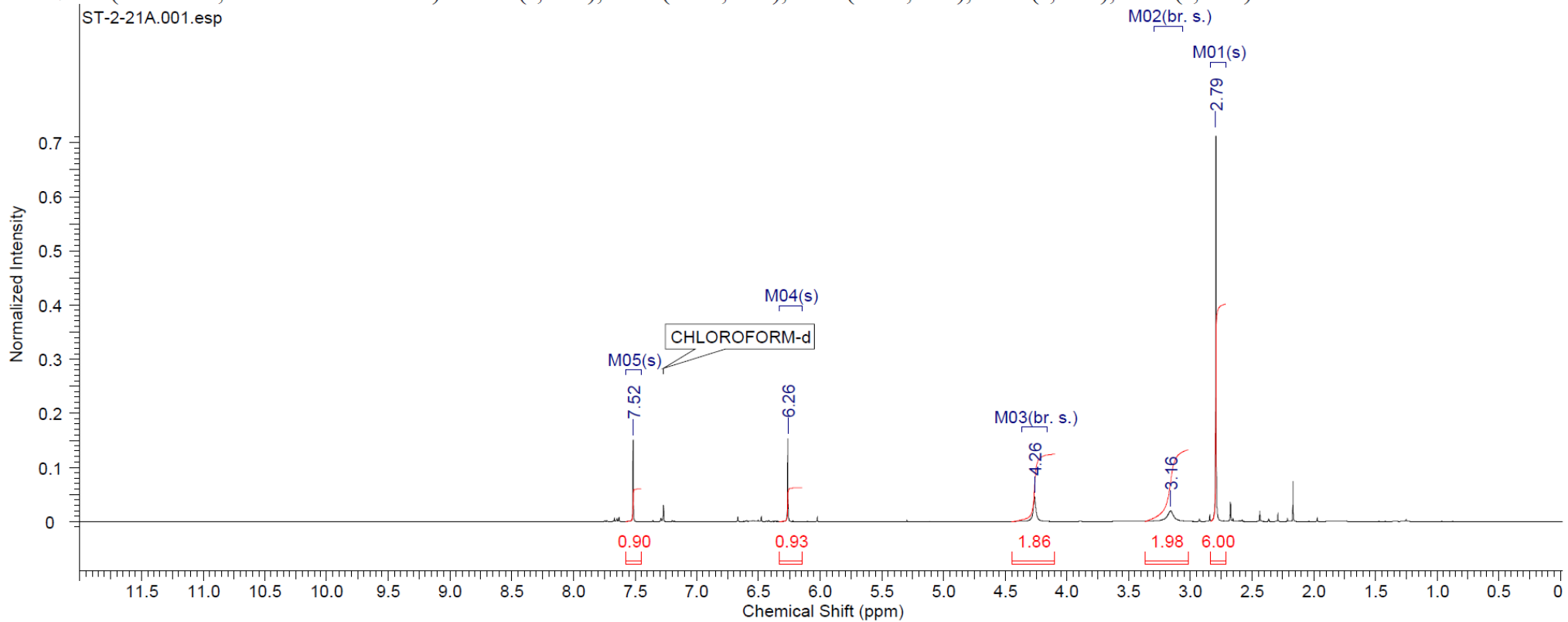
^{13}C NMR (126 MHz, CHLOROFORM- d) δ 21.6, 42.4, 106.9, 113.8, 127.7, 127.7, 128.1, 129.8, 129.9, 132.4, 133.9, 135.6, 140.2, 144.7, 145.0,



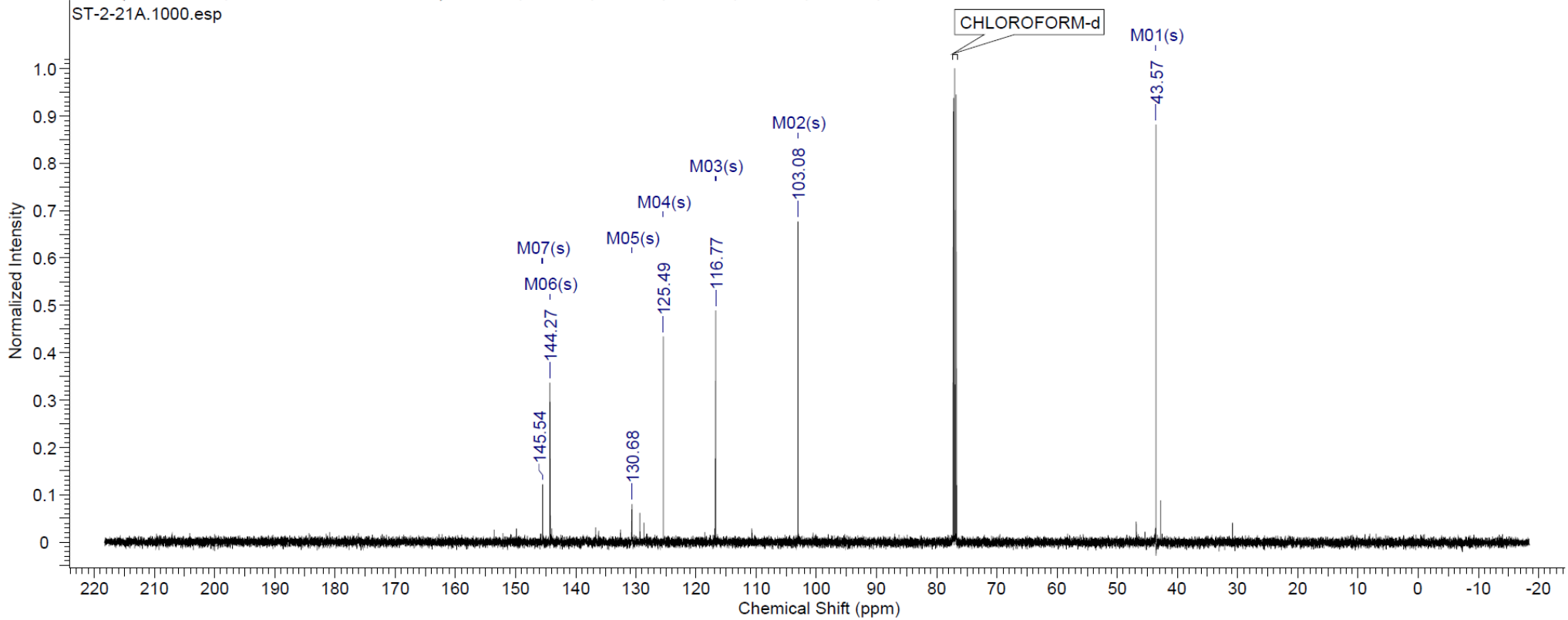
1,2-Diamino-4-*N,N*-dimethylamino-5-nitro benzene



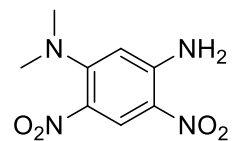
^1H NMR (500 MHz, CHLOROFORM- d) δ 2.79 (s, 6 H), 3.16 (br. s., 2 H), 4.26 (br. s., 2 H), 6.26 (s, 1 H), 7.52 (s, 1 H)



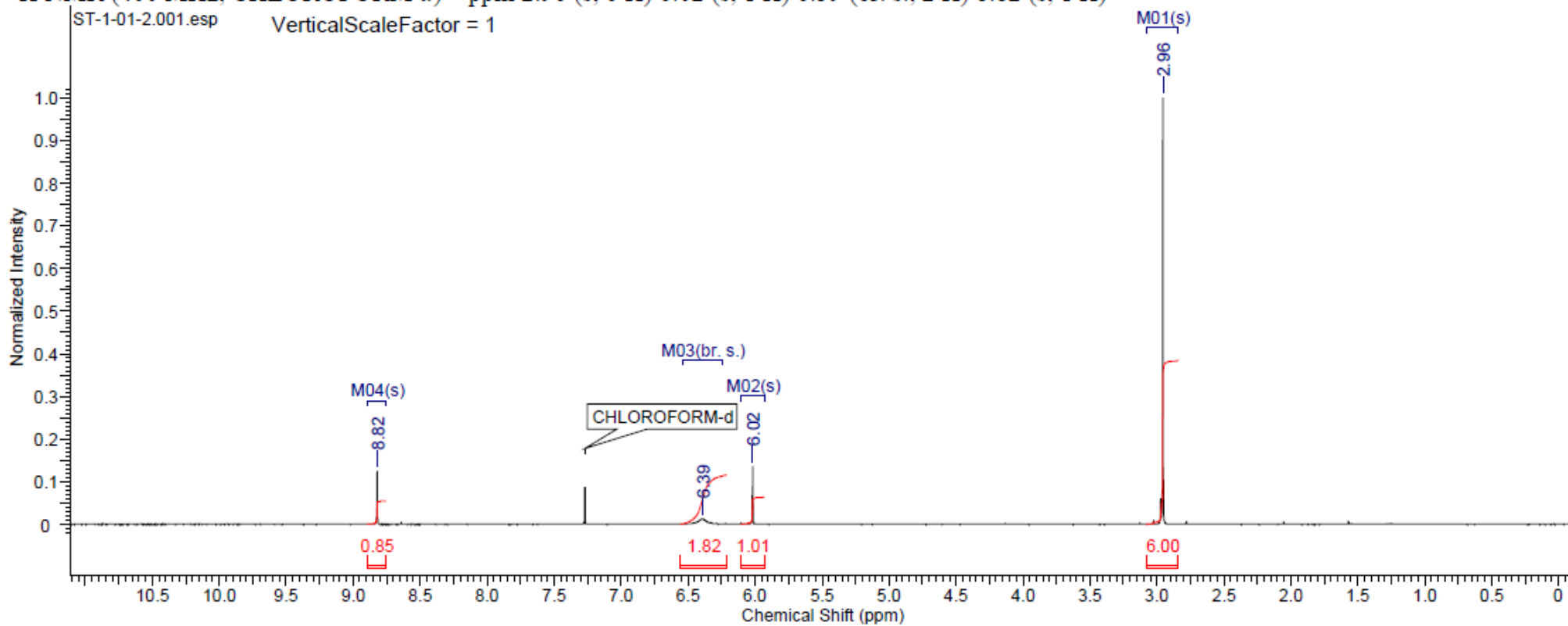
^{13}C NMR (126 MHz, CHLOROFORM-d) δ 43.6, 103.1, 116.8, 125.5, 130.7, 144.3, 145.5

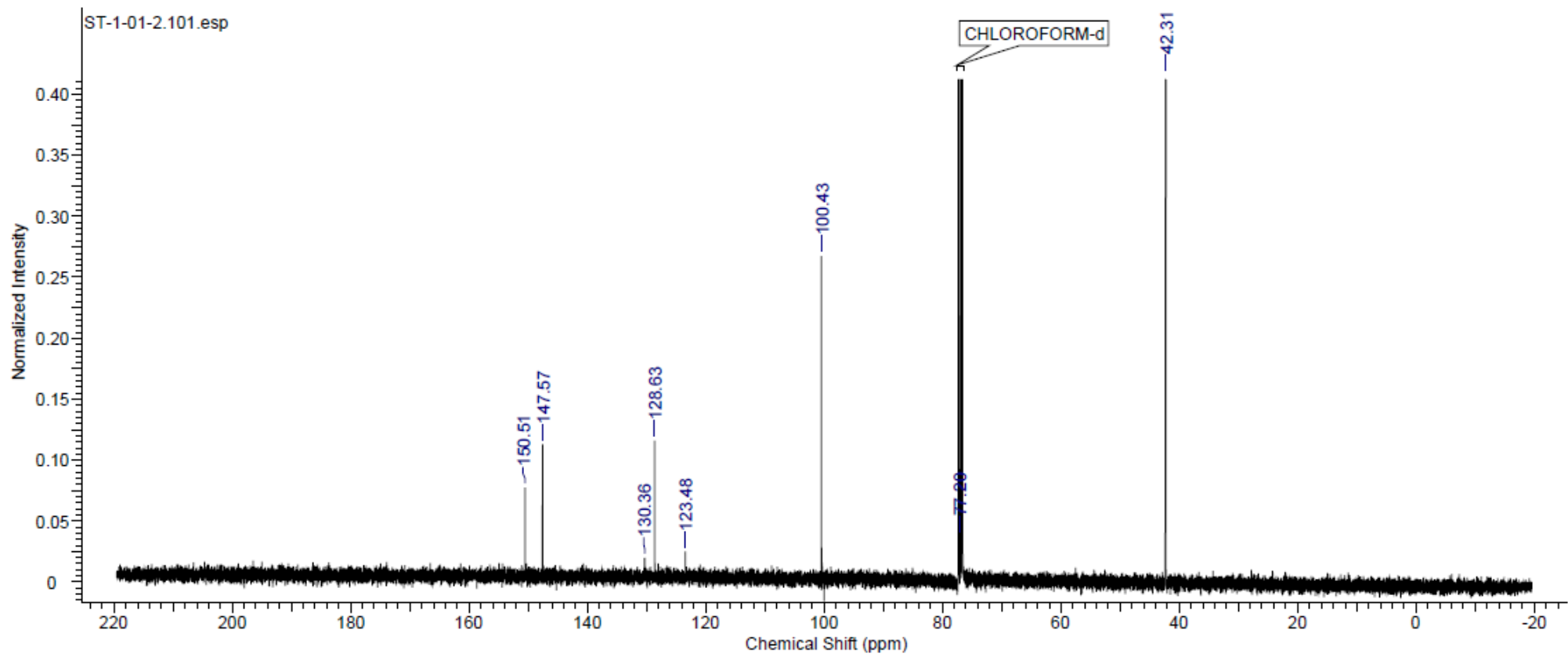


5-*N,N*-Dimethylamino-2,4-dinitro aniline

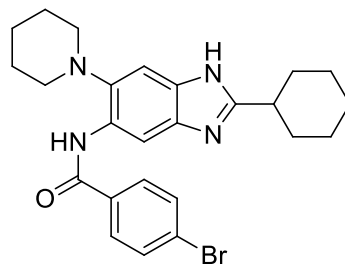


¹H NMR (400 MHz, CHLOROFORM-*d*) δ ppm 2.96 (s, 6 H) 6.02 (s, 1 H) 6.39 (br. s., 2 H) 8.82 (s, 1 H)

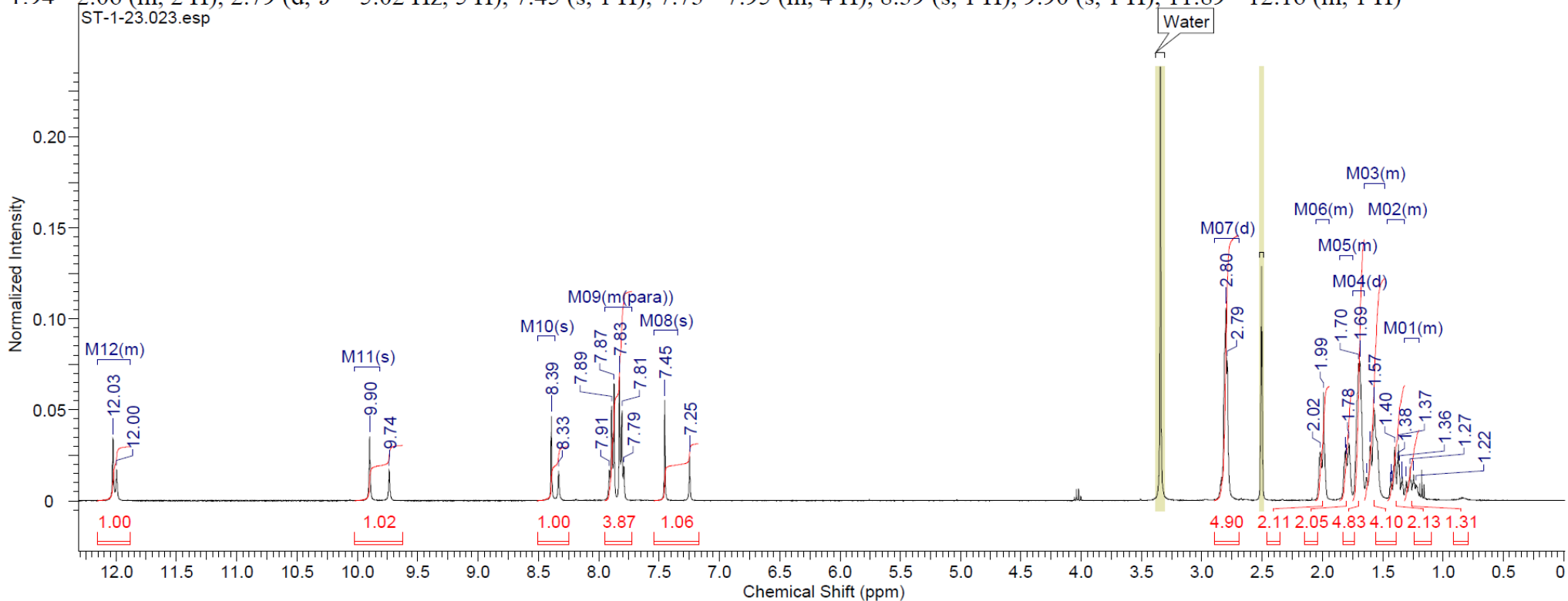




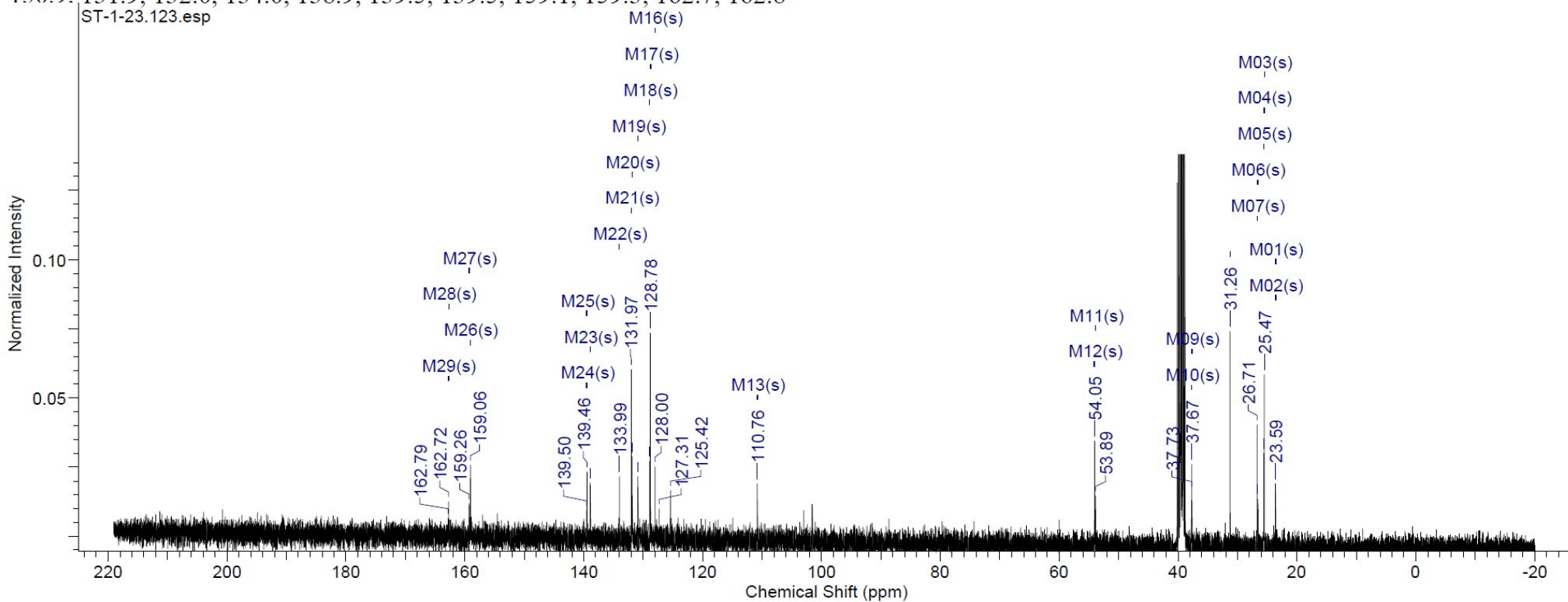
2-Cyclohexyl-5-(4-bromobenzamido)-6-piperidin-1-yl-1H-benzo[d]imidazole



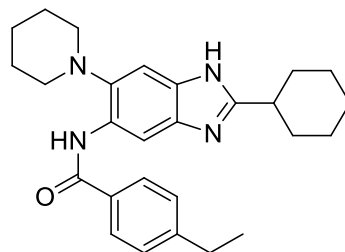
$^1\text{H NMR}$ (400 MHz, DMSO-d_6) δ 1.20 - 1.32 (m, 1 H), 1.32 - 1.46 (m, 2 H), 1.49 - 1.65 (m, 4 H), 1.70 (d, $J = 4.52$ Hz, 5 H), 1.75 - 1.86 (m, 2 H), 1.94 - 2.06 (m, 2 H), 2.79 (d, $J = 5.02$ Hz, 5 H), 7.45 (s, 1 H), 7.73 - 7.95 (m, 4 H), 8.39 (s, 1 H), 9.90 (s, 1 H), 11.89 - 12.16 (m, 1 H)



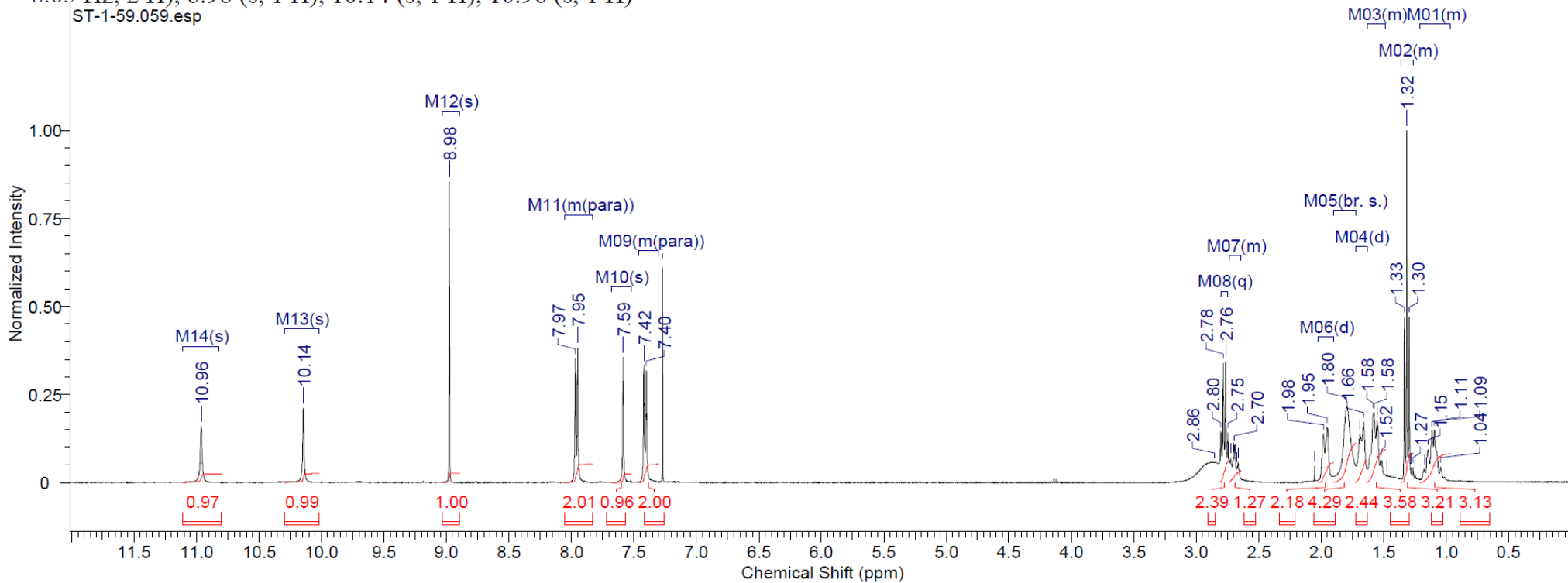
^{13}C NMR (101 MHz, DMSO- d_6) δ 23.6, 23.6, 25.5, 25.5, 25.6, 26.6, 26.7, 31.3, 37.7, 37.7, 53.9, 54.1, 110.8, 125.4, 127.3, 128.0, 128.8, 128.9, 130.9, 131.9, 132.0, 134.0, 138.9, 139.5, 139.5, 159.1, 159.3, 162.7, 162.8



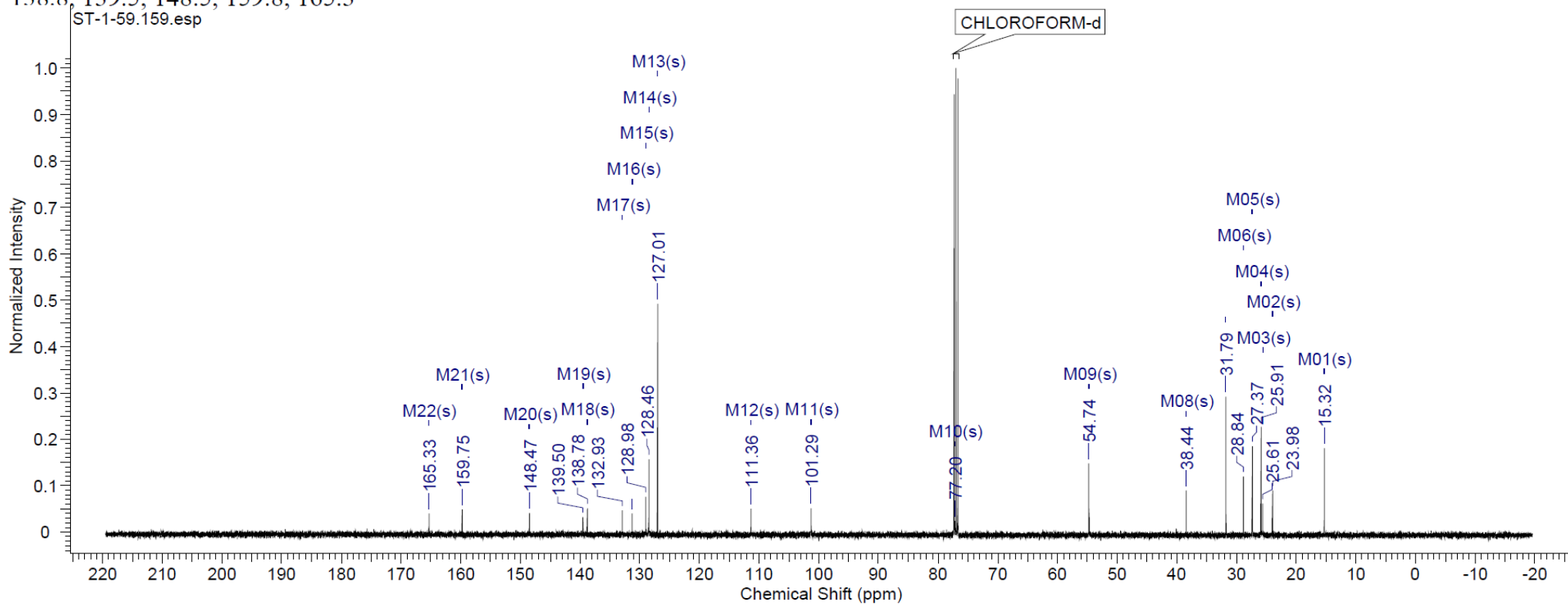
2-Cyclohexyl-5-(4-ethylbenzamido)-6-piperidin-1-yl-1H-benzo[d]imidazole



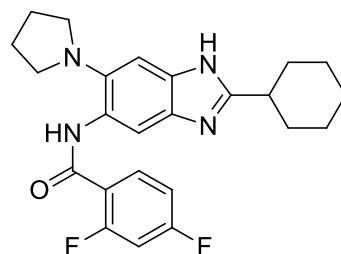
^1H NMR (400 MHz, CHLOROFORM- d) δ 0.97 - 1.21 (m, 3 H), 1.27 - 1.36 (m, 3 H), 1.48 - 1.63 (m, 4 H), 1.68 (d, J = 12.05 Hz, 2 H), 1.80 (br. s., 4 H), 1.97 (d, J = 12.55 Hz, 2 H), 2.64 - 2.73 (m, 1 H), 2.77 (q, J = 7.53 Hz, 2 H), 7.30 - 7.46 (m, J = 8.03 Hz, 2 H), 7.59 (s, 1 H), 7.83 - 8.05 (m, J = 8.03 Hz, 2 H), 8.98 (s, 1 H), 10.14 (s, 1 H), 10.96 (s, 1 H)



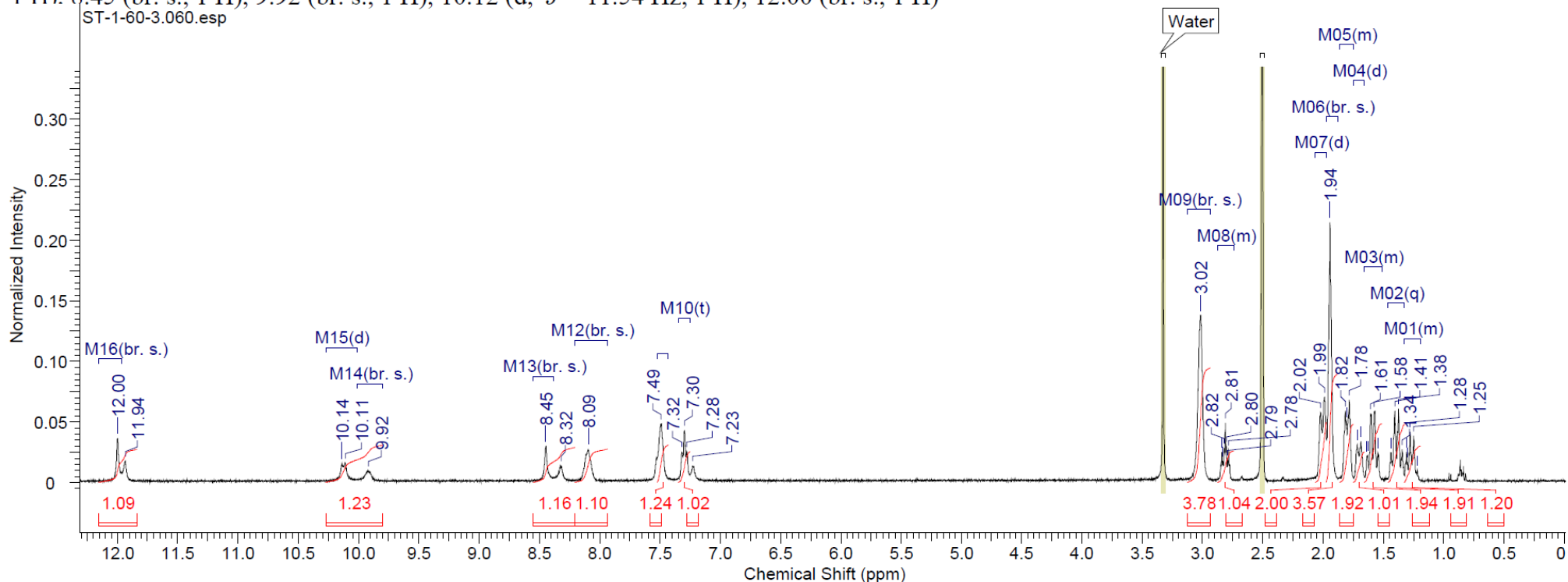
^{13}C NMR (101 MHz, CHLOROFORM- d) δ 15.3, 24.0, 25.6, 25.9, 27.4, 28.8, 31.8, 38.4, 54.7, 77.2, 101.3, 111.4, 127.0, 128.5, 129.0, 131.2, 132.9, 138.8, 139.5, 148.5, 159.8, 165.3



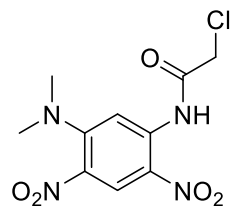
2-Cyclohexyl-5-(2,4-difluorobenzamido)-6-pyrrolidin-1-yl-1H-benzo[d]imidazole



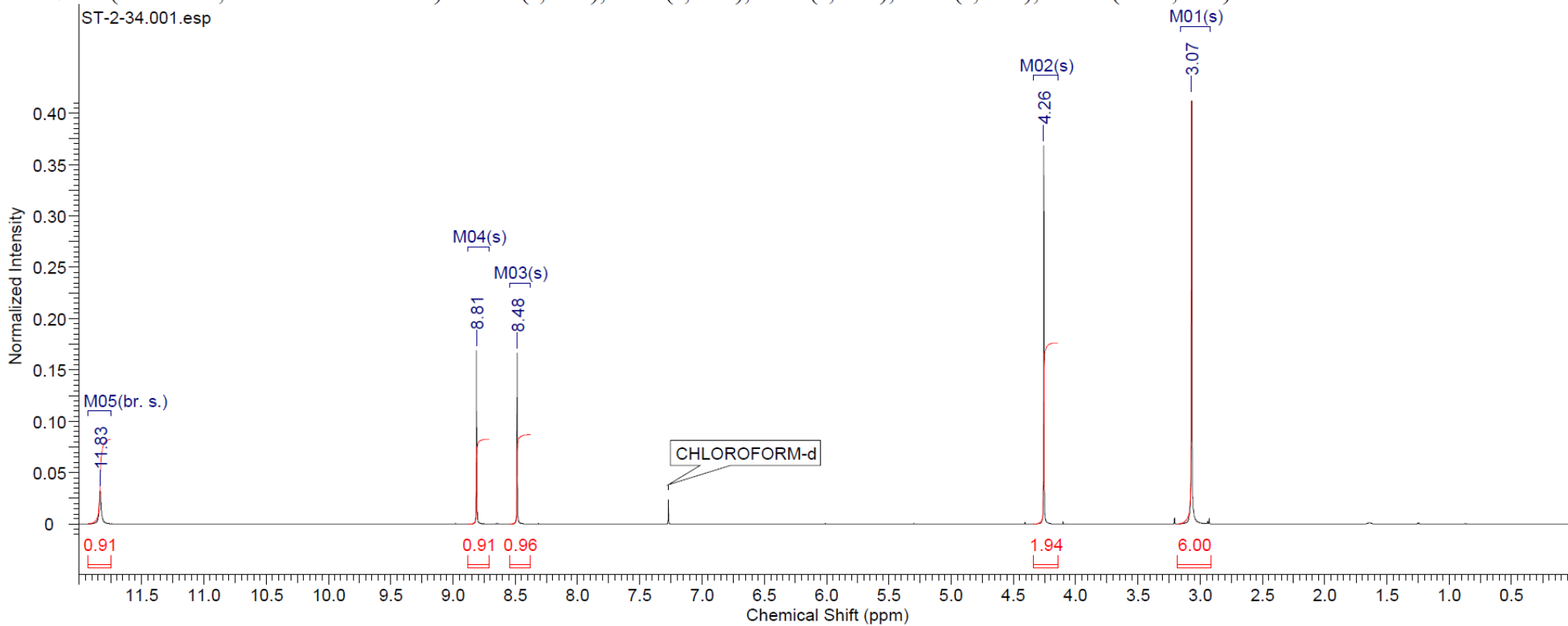
¹H NMR (400 MHz, DMSO-d₆) δ 1.19 - 1.33 (m, 1 H), 1.39 (q, *J* = 12.38 Hz, 2 H), 1.51 - 1.66 (m, 2 H), 1.70 (d, *J* = 12.55 Hz, 1 H), 1.75 - 1.86 (m, 2 H), 1.94 (br. s., 4 H), 2.00 (d, *J* = 12.30 Hz, 2 H), 2.74 - 2.88 (m, 1 H), 3.02 (br. s., 4 H), 7.30 (t, *J* = 8.03 Hz, 1 H), 7.49 (br. s., 1 H), 8.09 (br. s., 1 H), 8.45 (br. s., 1 H), 9.92 (br. s., 1 H), 10.12 (d, *J* = 11.54 Hz, 1 H), 12.00 (br. s., 1 H)



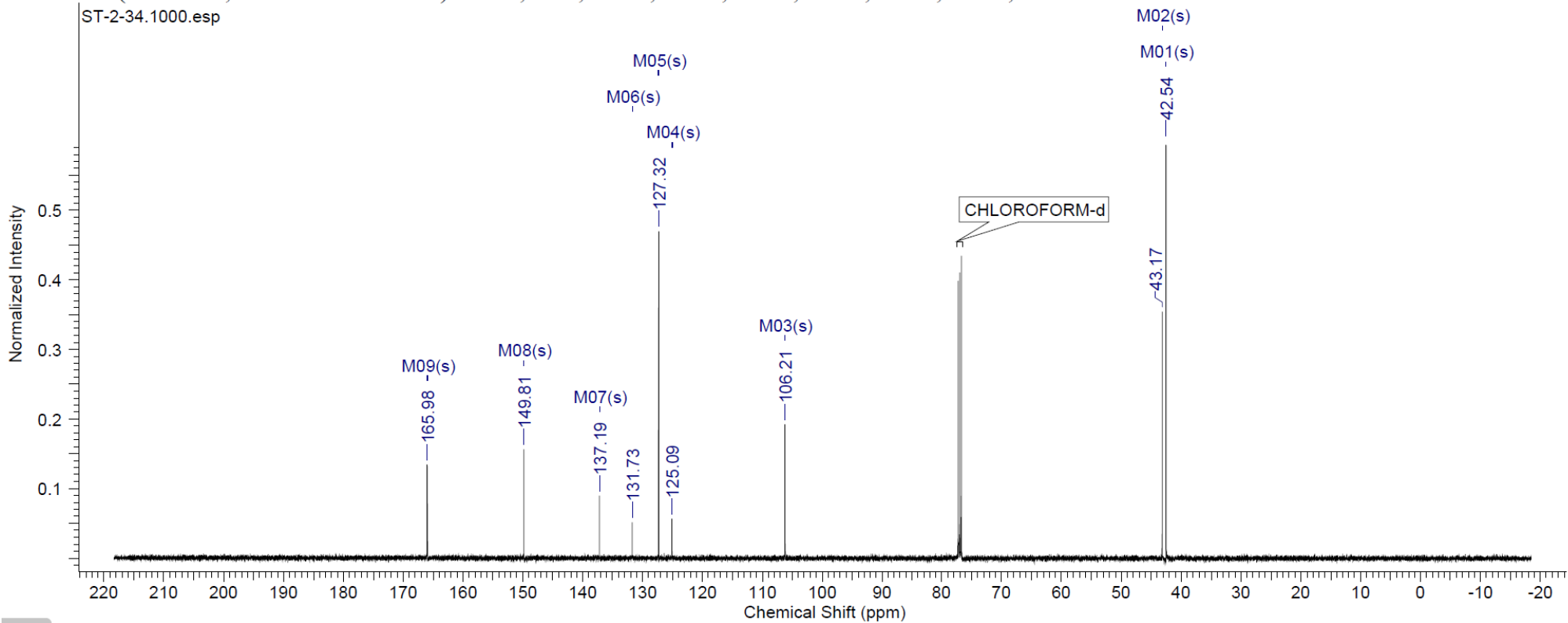
1-Chloroacetylcarboxamido-5-*N,N*-dimethylamino-2,4-dinitro benzene



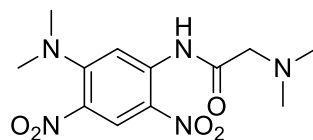
$^1\text{H NMR}$ (500 MHz, CHLOROFORM-*d*) δ 3.07 (s, 6 H), 4.26 (s, 2 H), 8.48 (s, 1 H), 8.81 (s, 1 H), 11.83 (br. s., 1 H)



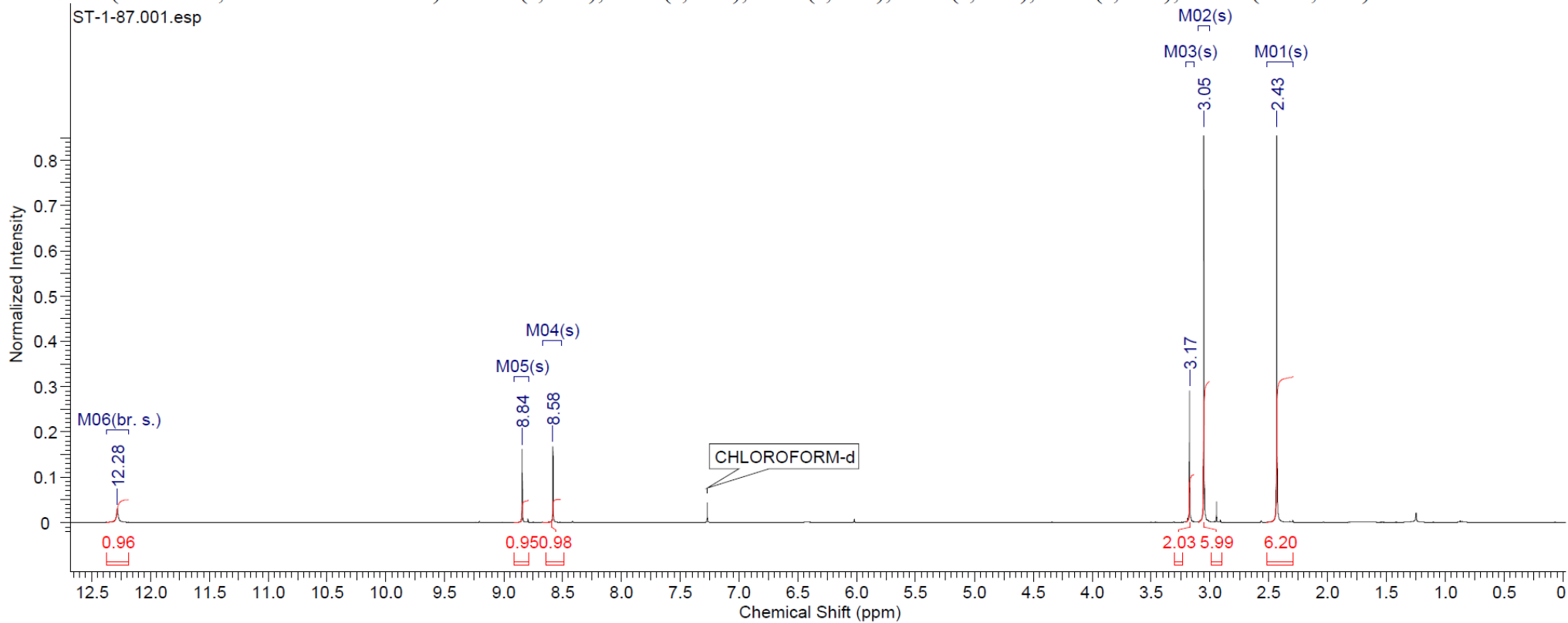
^{13}C NMR (126 MHz, CHLOROFORM-d) δ 42.5, 43.2, 106.2, 125.1, 127.3, 131.7, 137.2, 149.8, 166.0



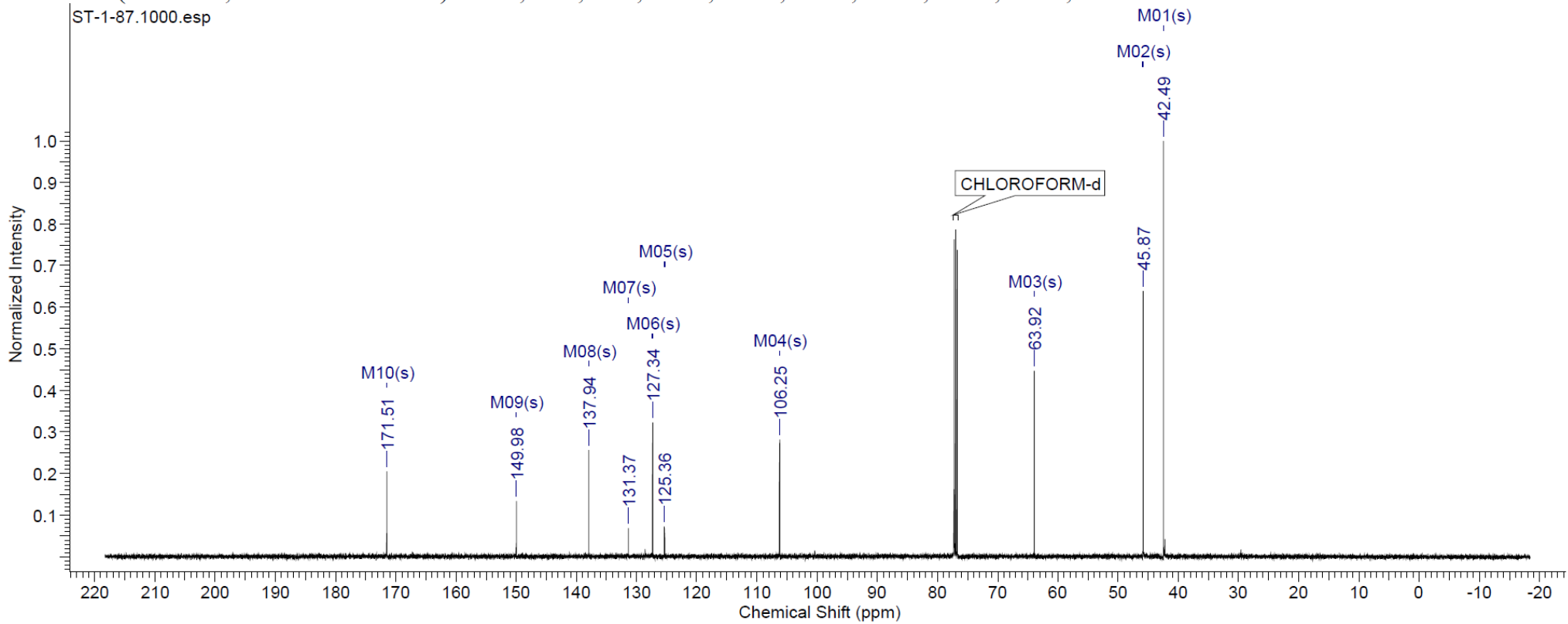
1-*N,N*-dimethylaminomethylcarboxamido-5-*N,N*-dimethylamino-2,4-dinitro benzene



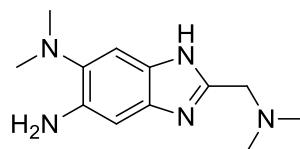
¹H NMR (500 MHz, CHLOROFORM-d) δ 2.43 (s, 7 H), 3.05 (s, 6 H), 3.17 (s, 2 H), 8.58 (s, 1 H), 8.84 (s, 1 H), 12.28 (br. s., 1 H)



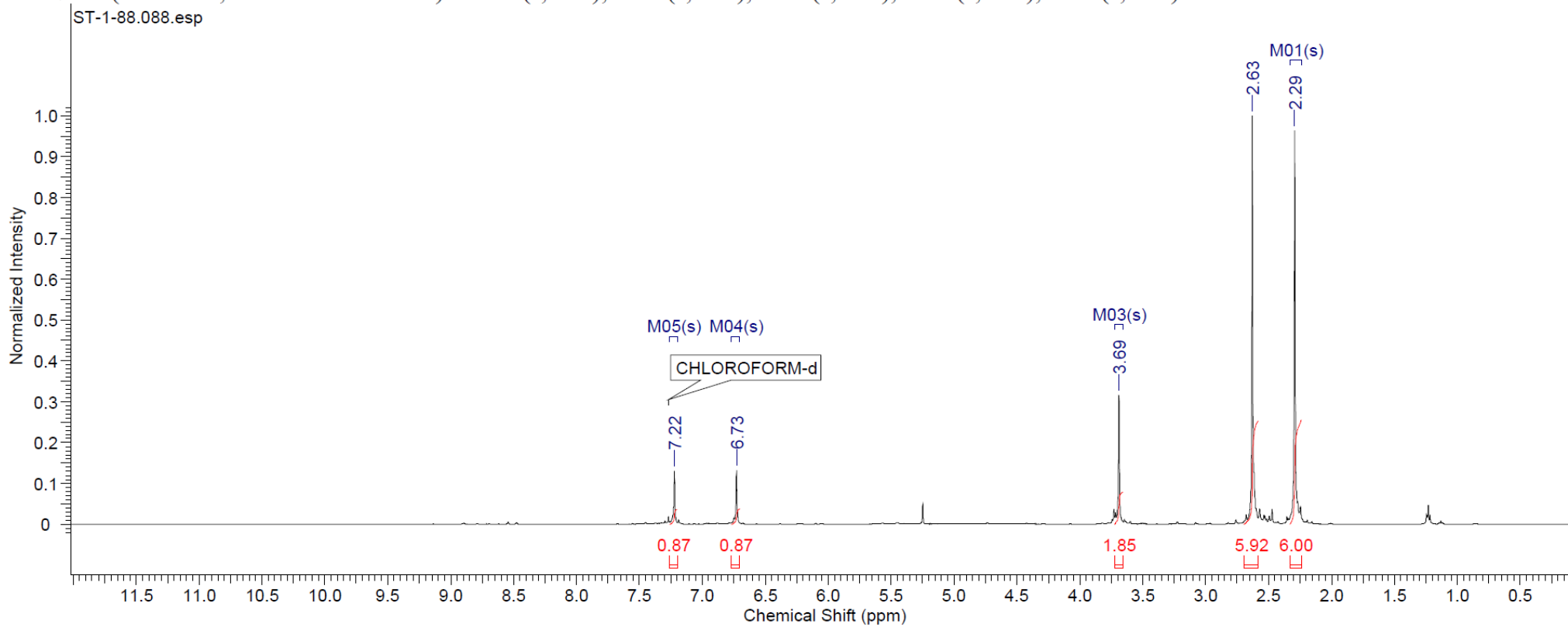
^{13}C NMR (126 MHz, CHLOROFORM-d) δ 42.5, 45.9, 63.9, 106.2, 125.4, 127.3, 131.4, 137.9, 150.0, 171.5



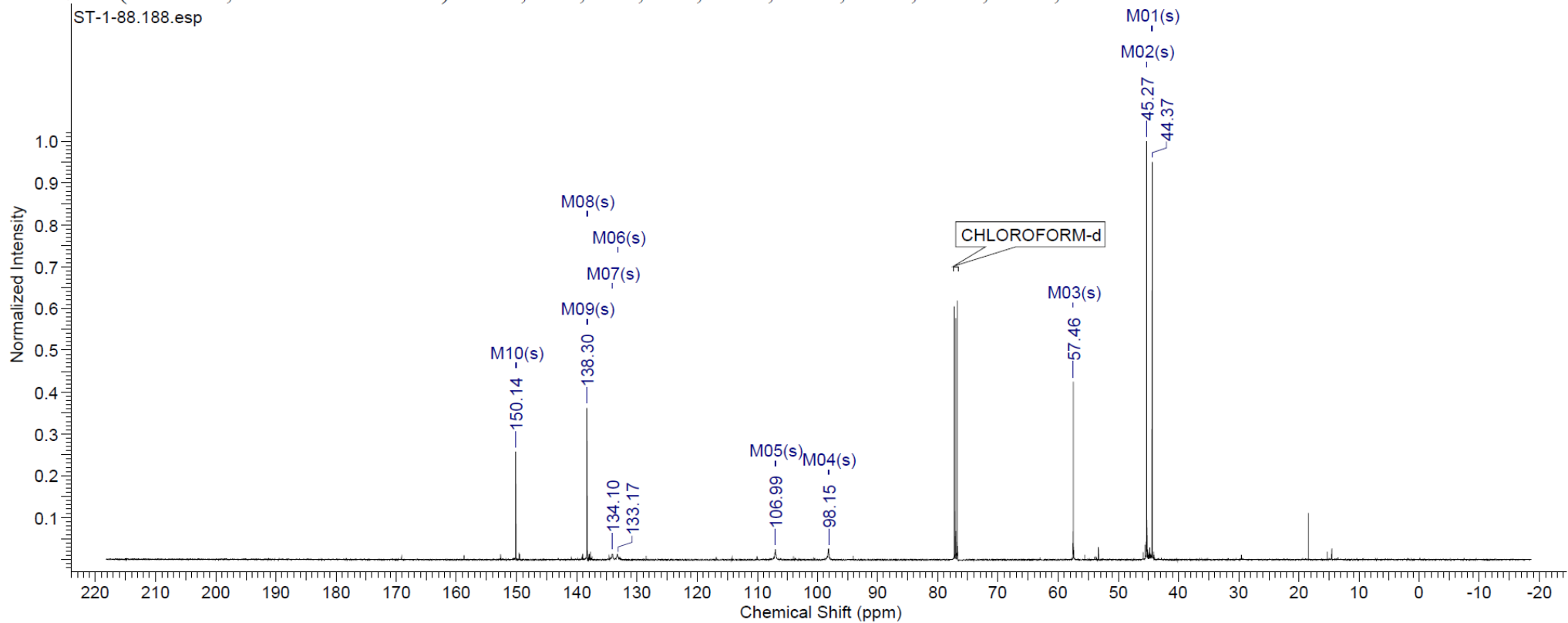
5-Amino-6-*N,N*-dimethylamino-2-*N,N*-dimethylaminomethyl-1*H*-benzo[d]imidazole



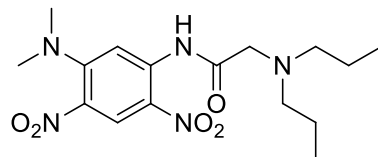
^1H NMR (500 MHz, CHLOROFORM-*d*) δ 2.29 (s, 6 H), 2.63 (s, 6 H), 3.69 (s, 2 H), 6.73 (s, 1 H), 7.22 (s, 1 H)



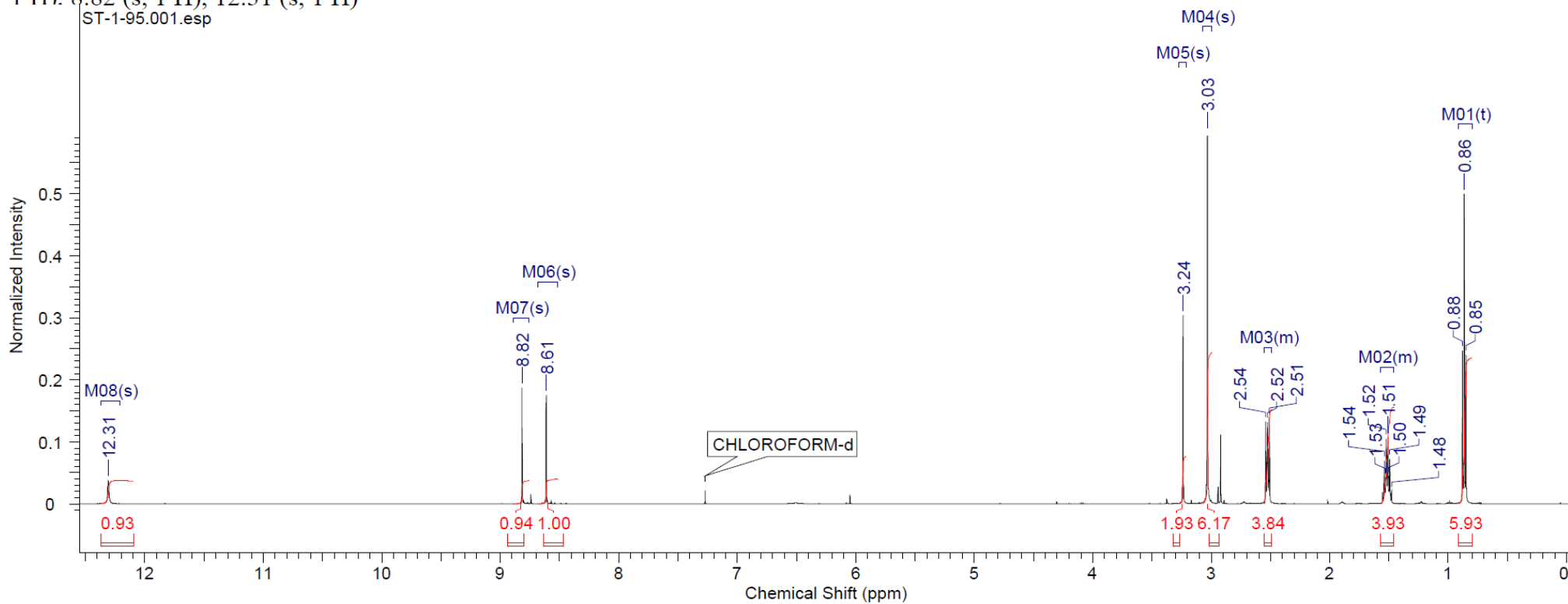
^{13}C NMR (126 MHz, CHLOROFORM-d) δ 44.4, 45.3, 57.5, 98.2, 107.0, 133.2, 134.1, 138.3, 138.3, 150.1



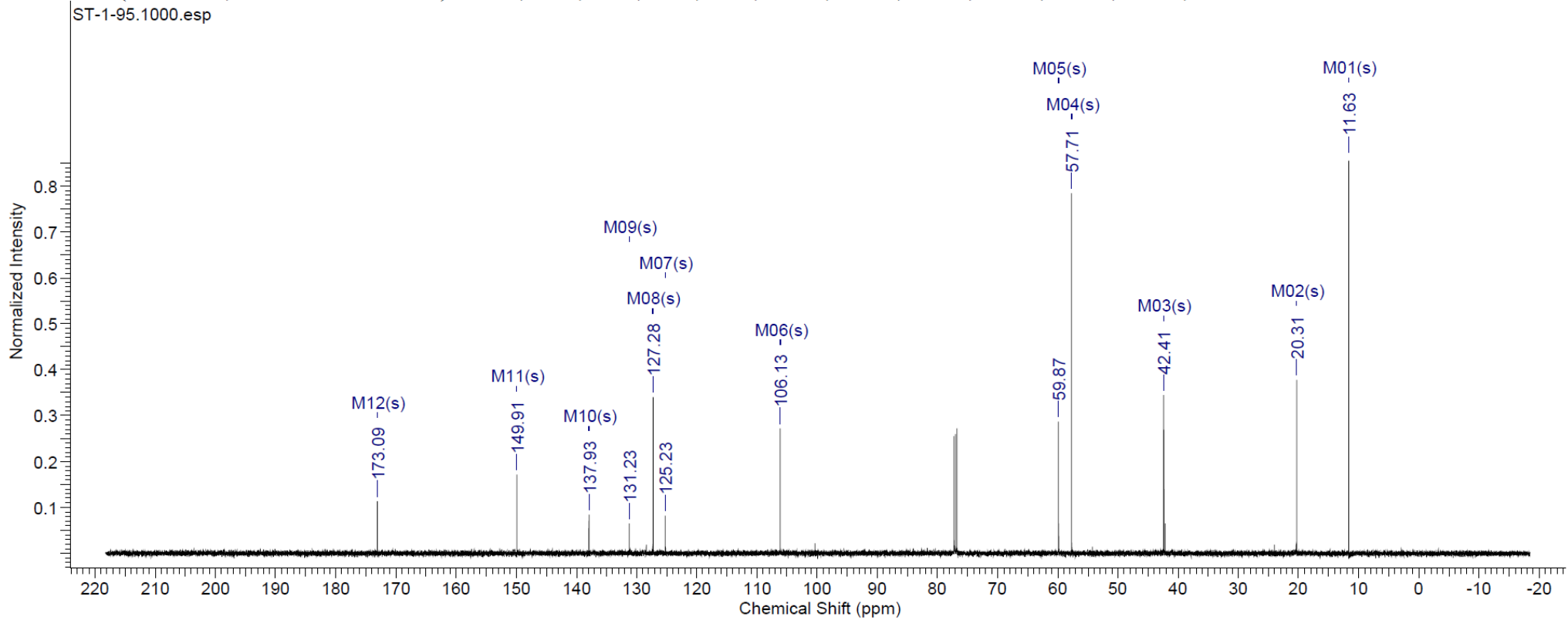
5-*N,N*-Dimethylamino-1-*N,N*-dipropylaminomethylcarboxamido-2,4-dinitro benzene



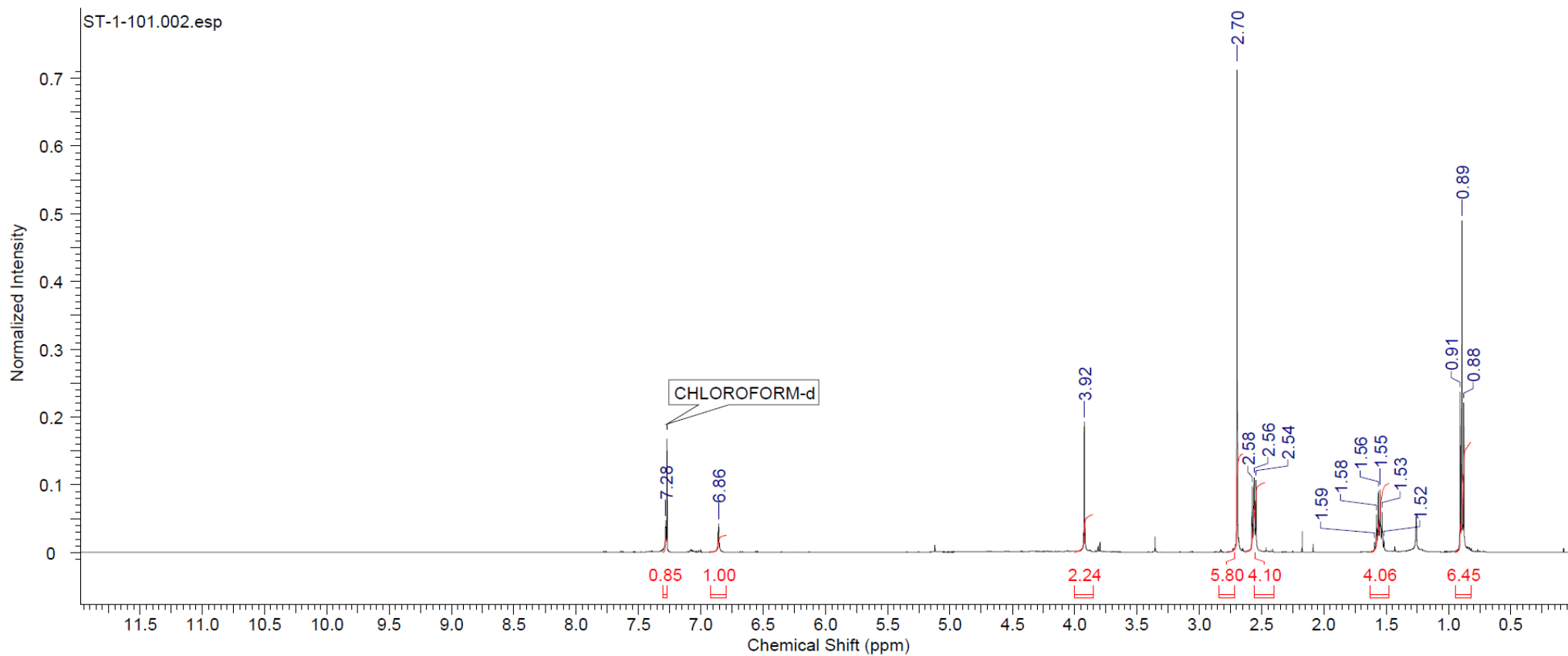
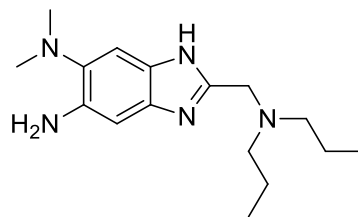
$^1\text{H NMR}$ (500 MHz, CHLOROFORM- d) δ 0.86 (t, $J = 7.32$ Hz, 6 H), 1.46 - 1.57 (m, 4 H), 2.49 - 2.55 (m, 4 H), 3.03 (s, 6 H), 3.24 (s, 2 H), 8.61 (s, 1 H), 8.82 (s, 1 H), 12.31 (s, 1 H)



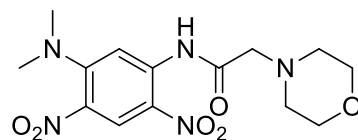
^{13}C NMR (126 MHz, CHLOROFORM- d) δ 11.6, 20.3, 42.4, 57.7, 59.9, 106.1, 125.2, 127.3, 131.2, 137.9, 149.9, 173.1



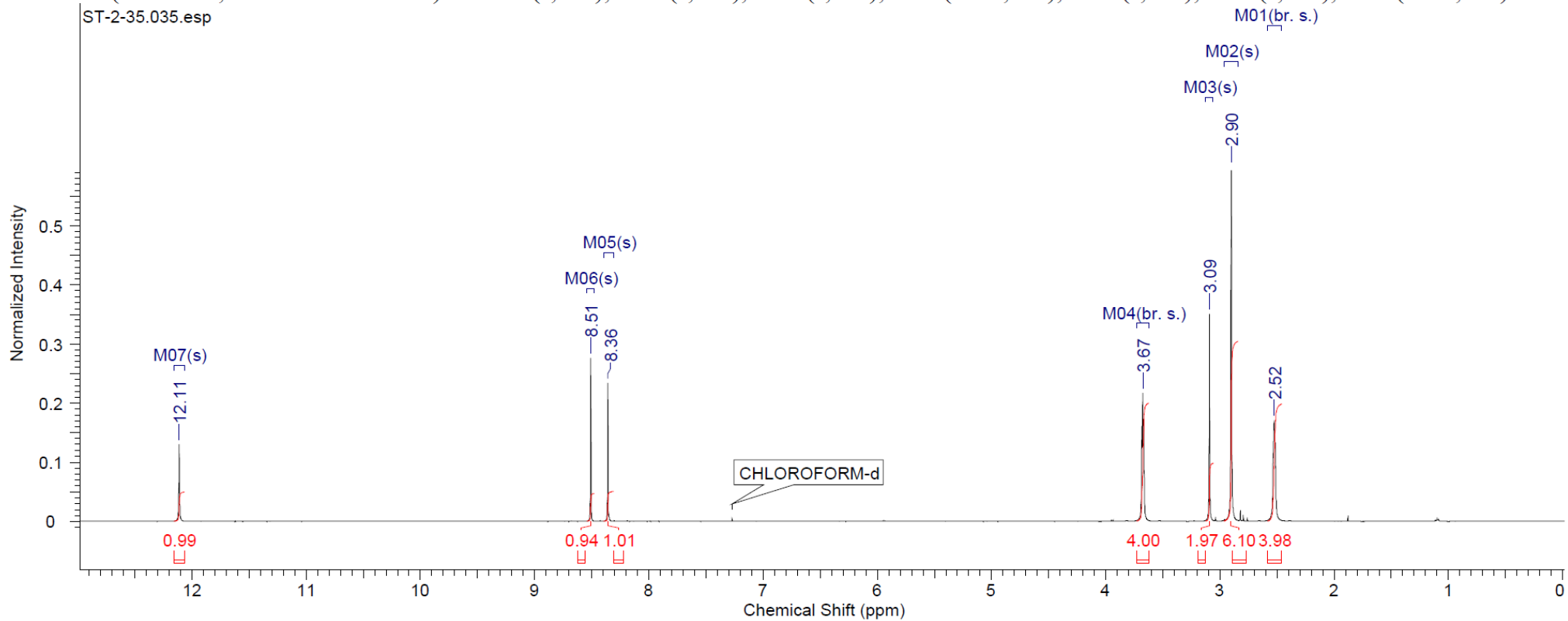
5-Amino-6-*N,N*-dimethylamino-2-*N,N*-dipropylaminomethyl-1*H*-benzo[d]imidazole



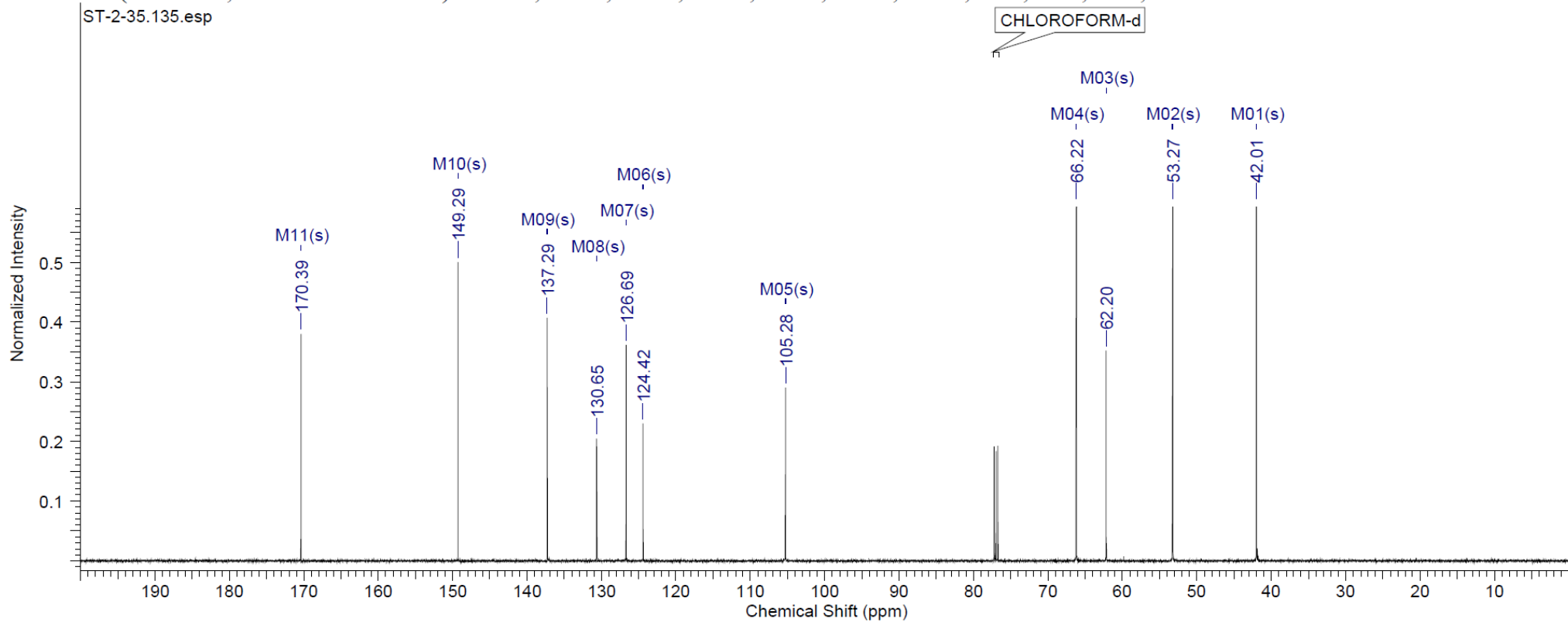
5-*N,N*-Dimethylamino-1-morpholin-1-ylmethylcarboxamido-2,4-dinitro benzene



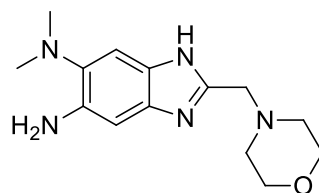
$^1\text{H NMR}$ (500 MHz, CHLOROFORM-*d*) δ 12.11 (s, 1H), 8.51 (s, 1H), 8.36 (s, 1H), 3.67 (br. s., 4H), 3.09 (s, 2H), 2.90 (s, 6H), 2.52 (br. s., 4H)



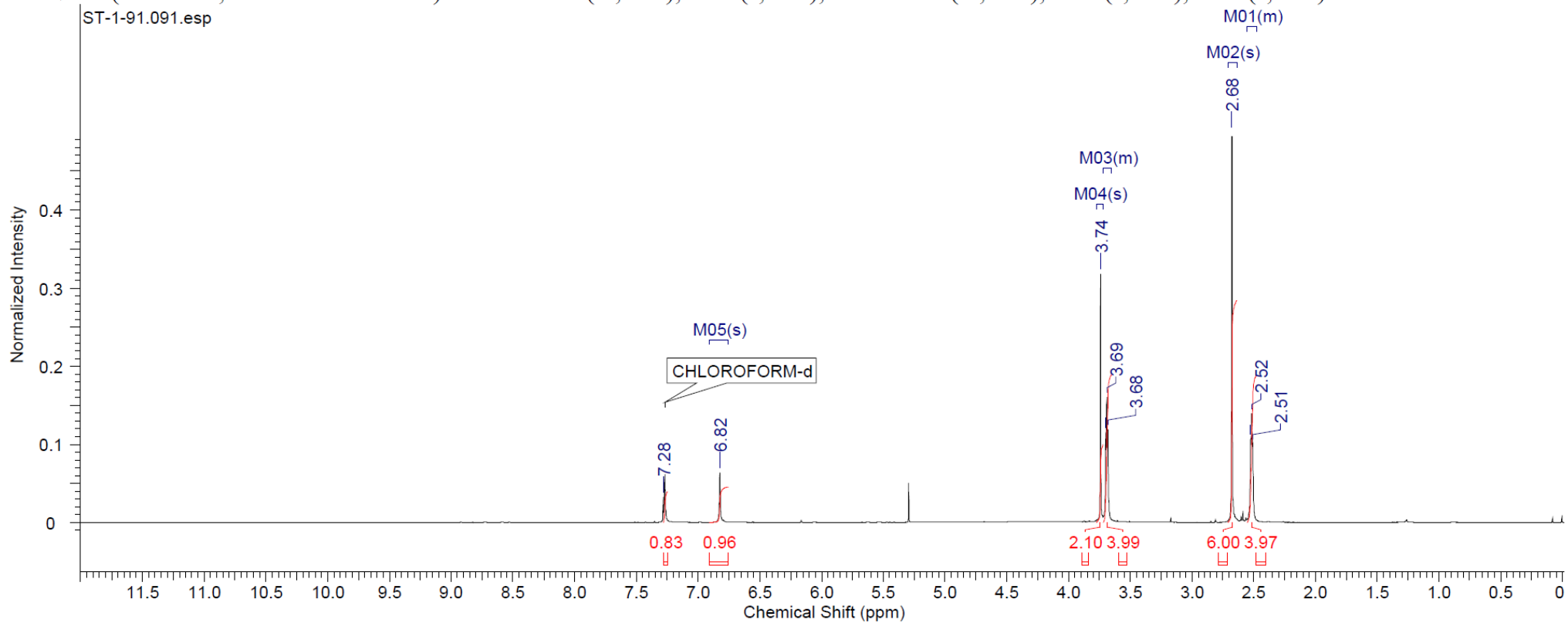
^{13}C NMR (126 MHz, CHLOROFORM-d) δ 170.4, 149.3, 137.3, 130.7, 126.7, 124.4, 105.3, 66.2, 62.2, 53.3, 42.0



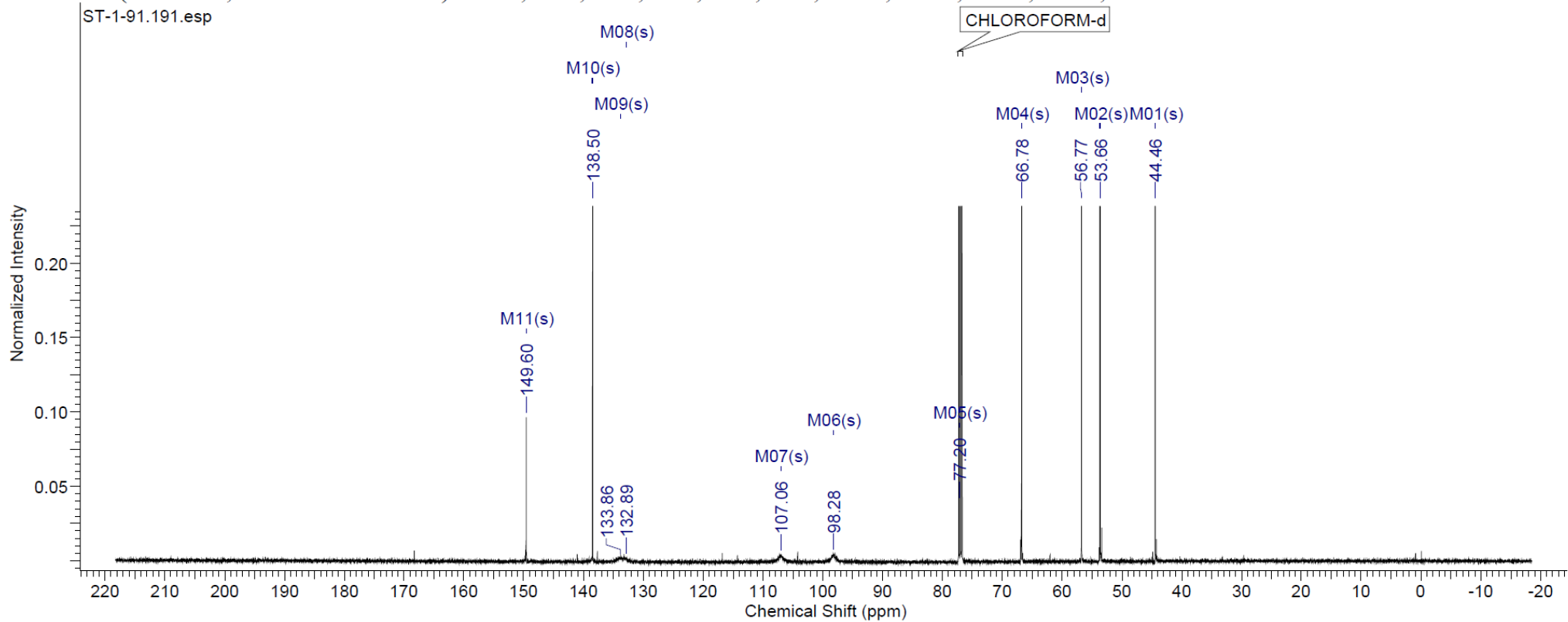
5-Amino-6-*N,N*-dimethylamino-2-morpholin-1-ylmethyl-1*H*-benzo[d]imidazole



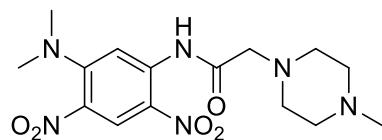
$^1\text{H NMR}$ (500 MHz, CHLOROFORM-*d*) δ 2.48 - 2.55 (m, 4 H), 2.68 (s, 6 H), 3.65 - 3.72 (m, 4 H), 3.74 (s, 2 H), 6.82 (s, 1 H)



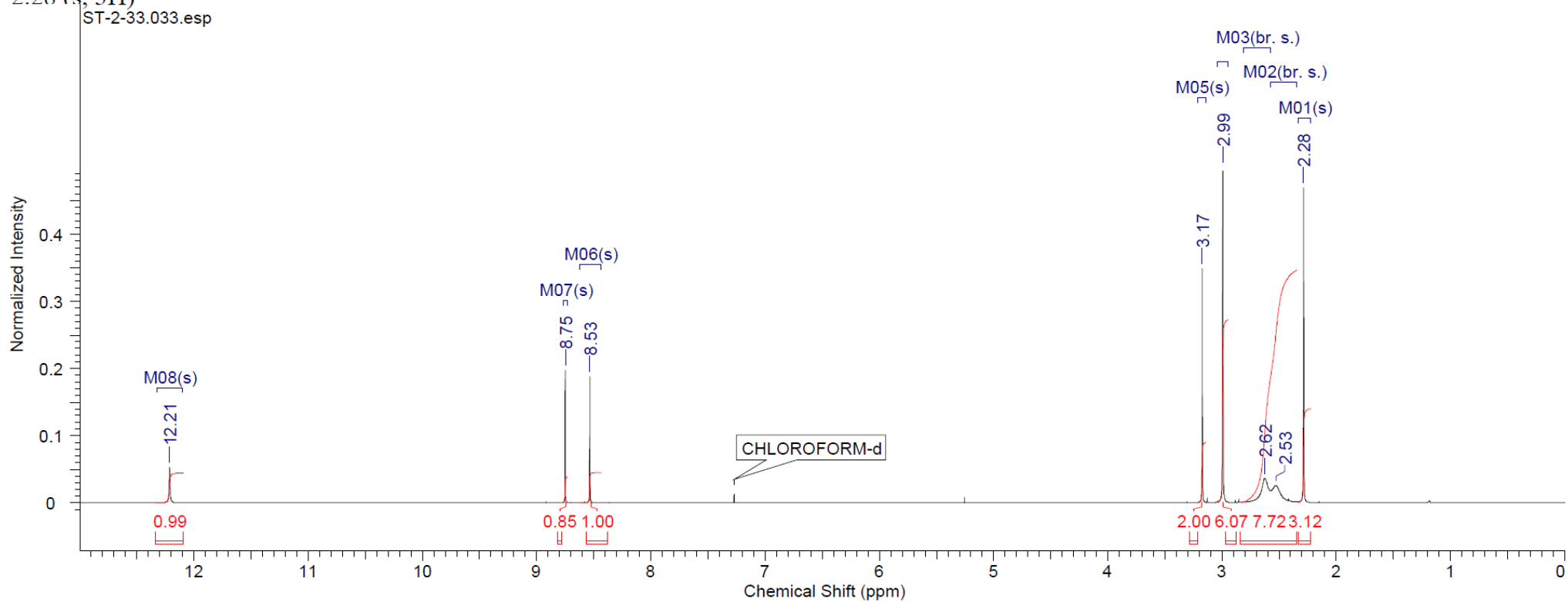
^{13}C NMR (126 MHz, CHLOROFORM-d) δ 44.5, 53.7, 56.8, 66.8, 77.2, 98.3, 107.1, 132.9, 133.9, 138.5, 149.6



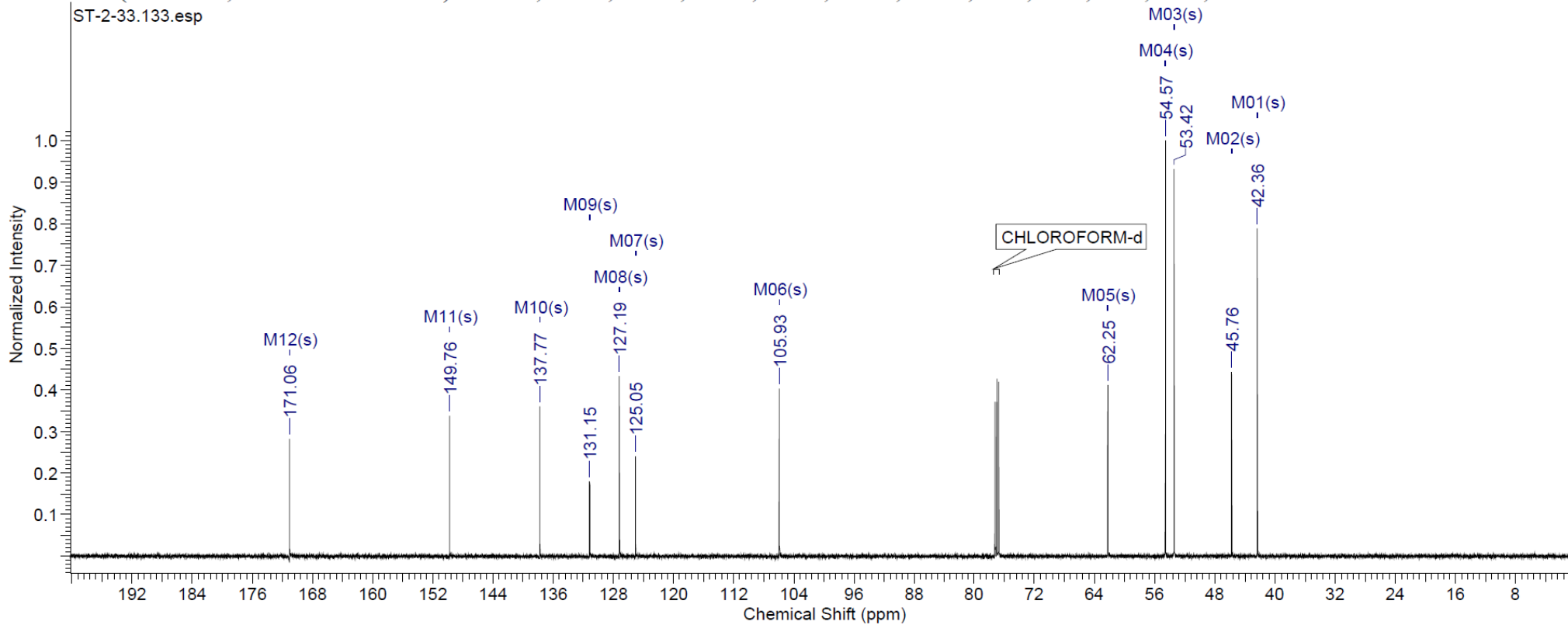
5-*N,N*-Dimethylamino-1-*N*-methylpiperazin-1-ylaminomethylcarboxamido-2,4-dinitro benzene



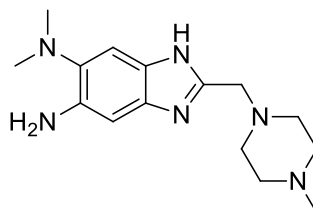
$^1\text{H NMR}$ (500 MHz, CHLOROFORM-*d*) δ 12.21 (s, 1H), 8.75 (s, 1H), 8.53 (s, 1H), 3.17 (s, 2H), 2.99 (s, 6H), 2.62 (br. s., 4H), 2.53 (br. s., 4H), 2.28 (s, 3H)



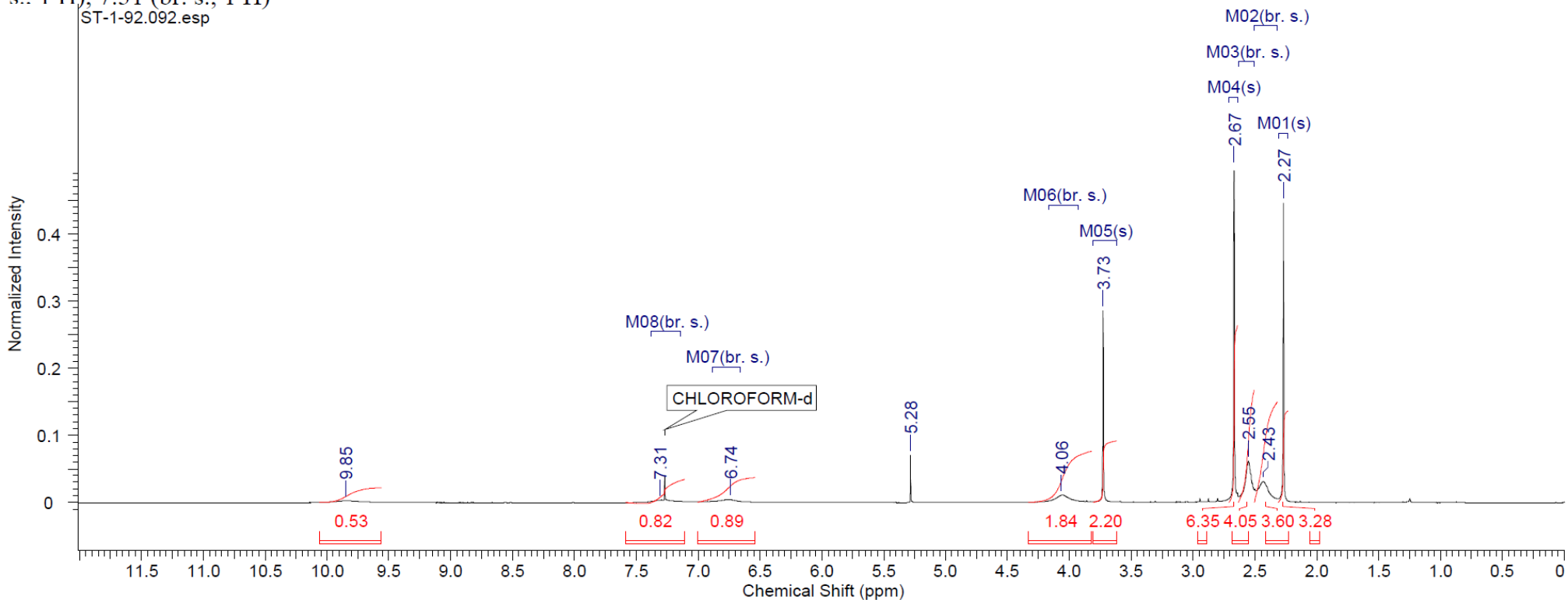
^{13}C NMR (126 MHz, CHLOROFORM- d) δ 171.1, 149.8, 137.8, 131.2, 127.2, 125.0, 105.9, 62.2, 54.6, 53.4, 45.8, 42.4



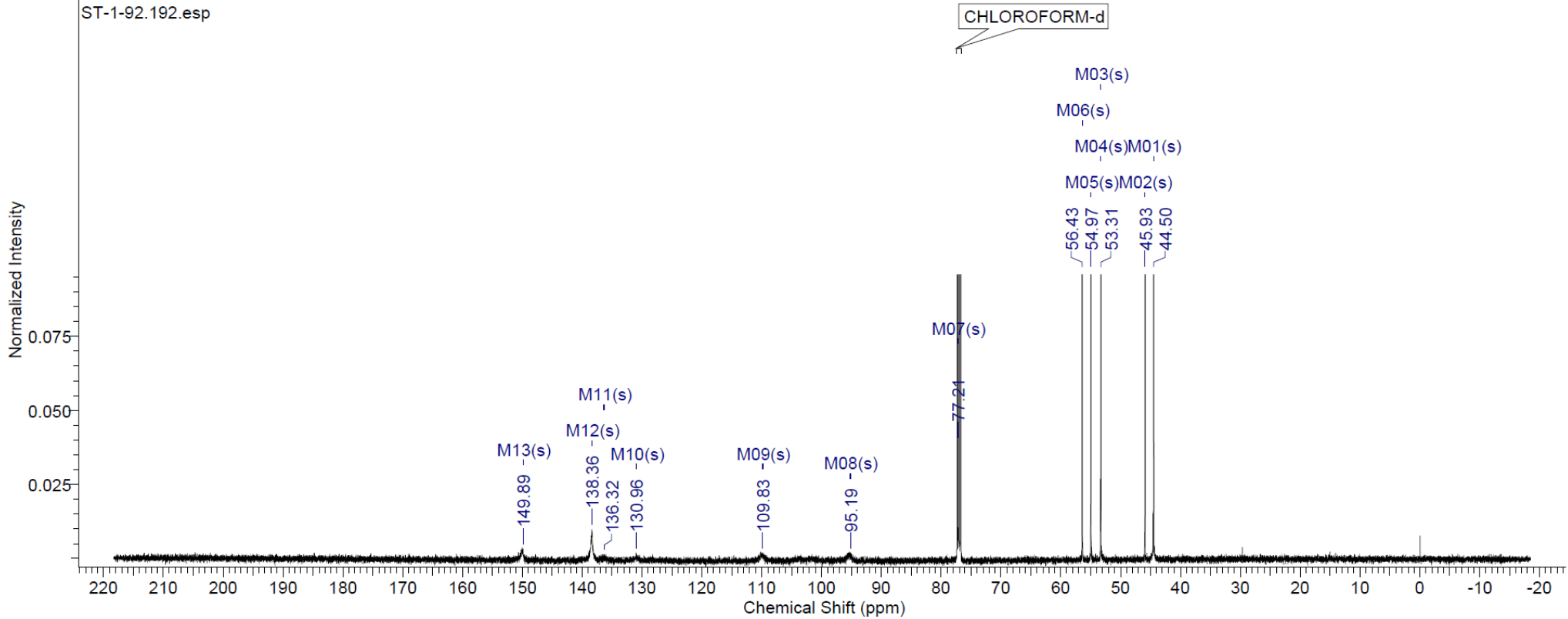
5-Amino-6-*N,N*-dimethylamino-2-*N*-methylpiperazin-1-ylmethyl-1*H*-benzo[d]imidazole



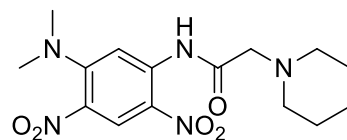
^1H NMR (500 MHz, CHLOROFORM-*d*) δ 2.27 (s, 3 H), 2.43 (br. s., 4 H), 2.55 (br. s., 4 H), 2.67 (s, 7 H), 3.73 (s, 2 H), 4.06 (br. s., 2 H), 6.74 (br. s., 1 H), 7.31 (br. s., 1 H)



^{13}C NMR (126 MHz, CHLOROFORM-d) δ 44.5, 45.9, 53.3, 53.4, 55.0, 56.4, 77.2, 95.2, 109.8, 131.0, 136.3, 138.4, 149.9

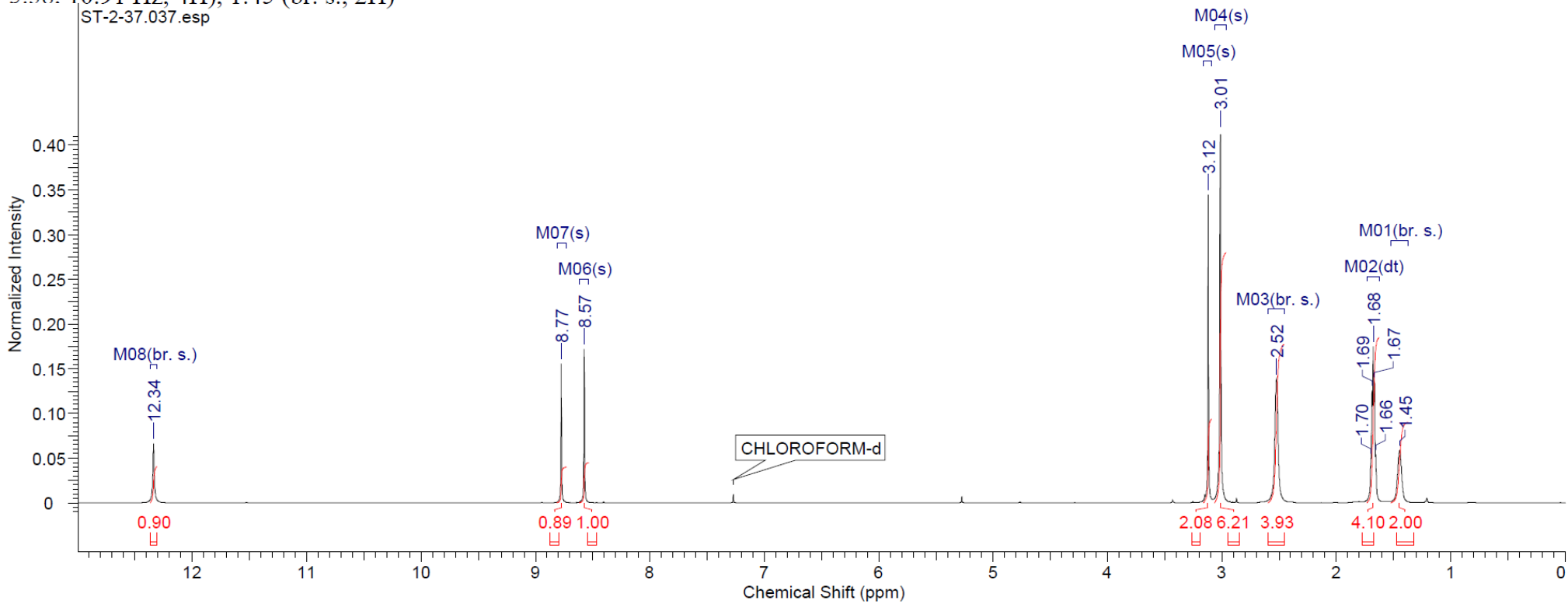


5-*N,N*-Dimethylamino-1-piperidin-1-ylmethylcarboxamido-2,4-dinitro benzene

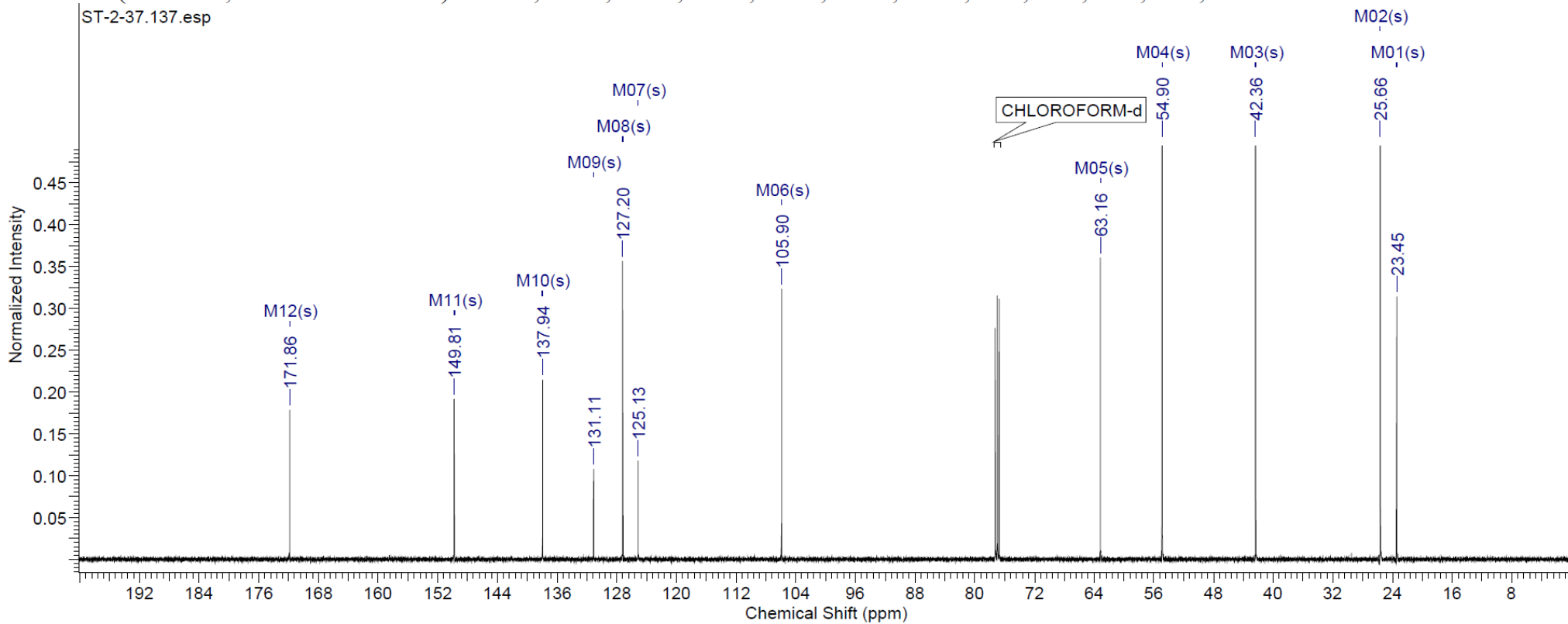


$^1\text{H NMR}$ (500 MHz, CHLOROFORM-*d*) δ 12.34 (br. s., 1H), 8.77 (s, 1H), 8.57 (s, 1H), 3.12 (s, 2H), 3.01 (s, 6H), 2.52 (br. s., 4H), 1.68 (td, $J =$

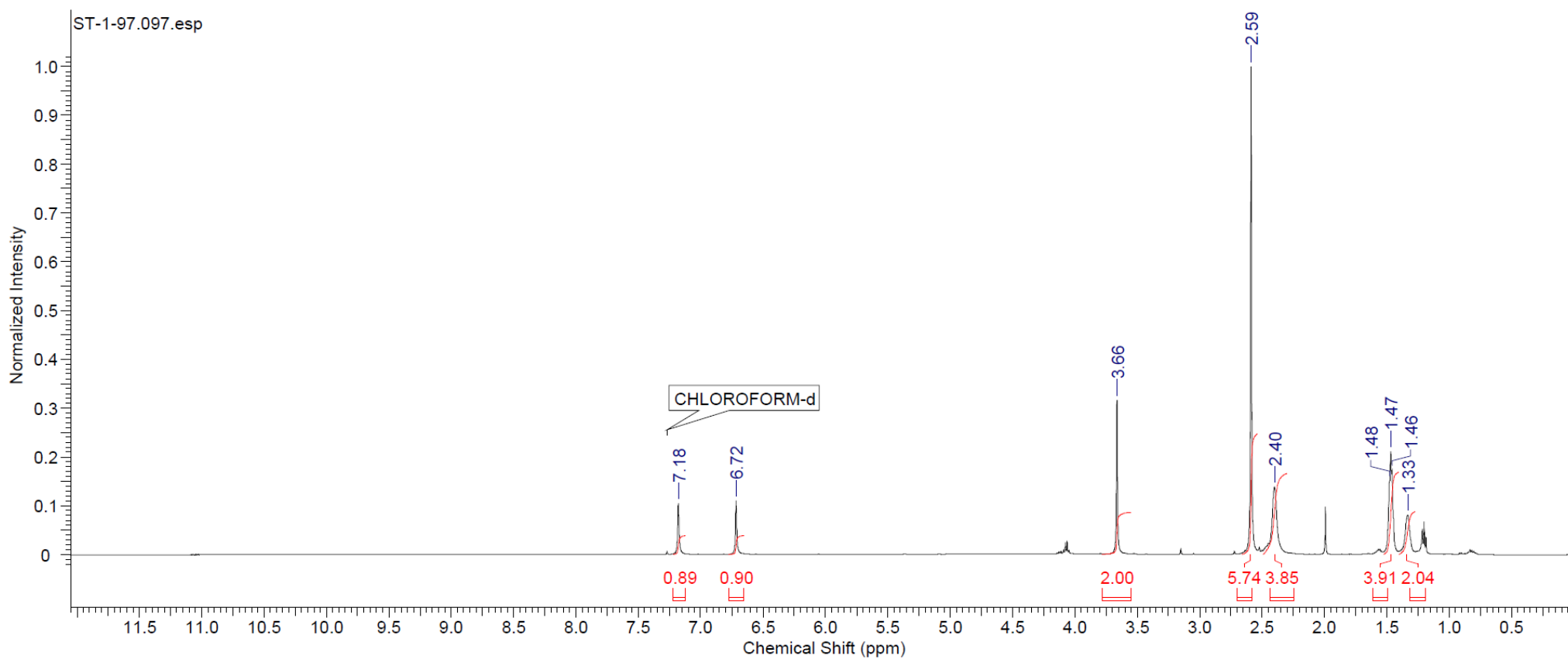
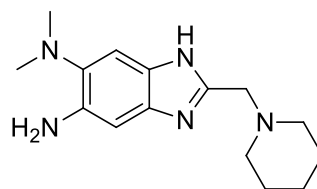
5.38, 10.91 Hz, 4H), 1.45 (br. s., 2H)



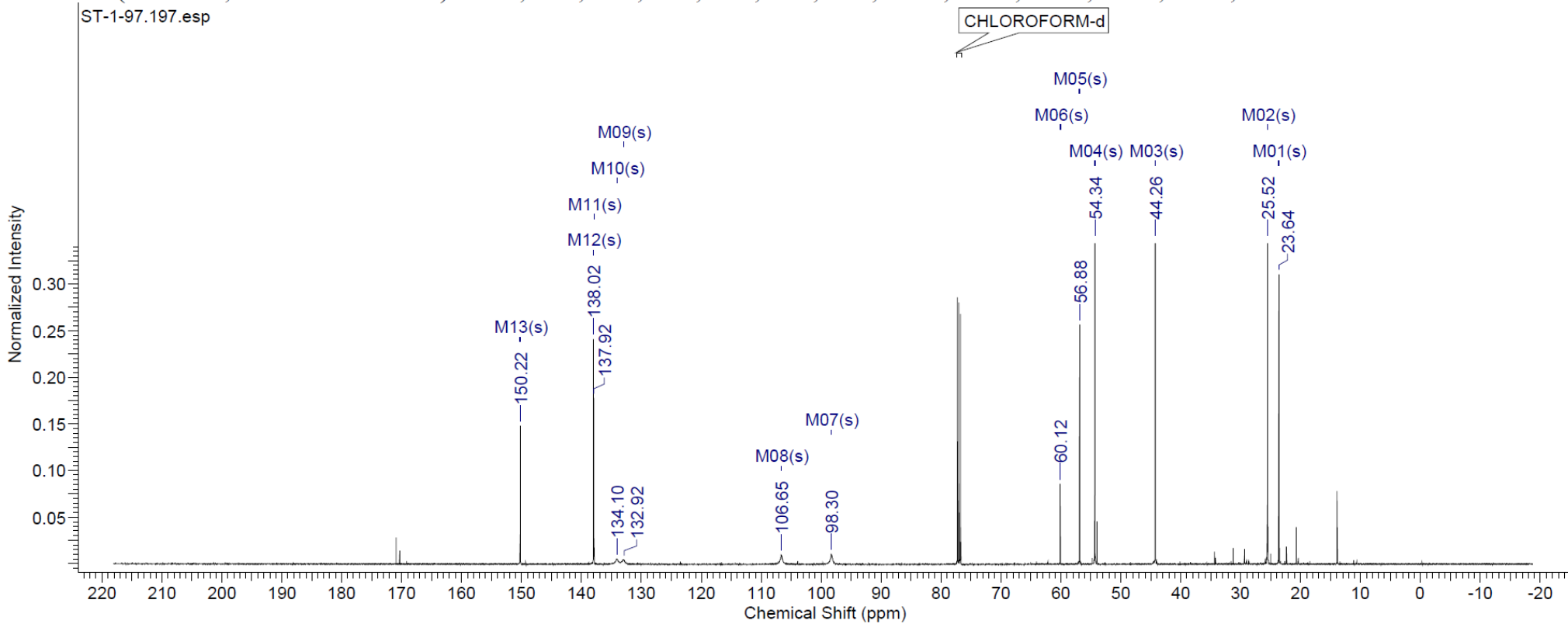
^{13}C NMR (126 MHz, CHLOROFORM-d) δ 171.9, 149.8, 137.9, 131.1, 127.2, 125.1, 105.9, 63.2, 54.9, 42.4, 25.7, 23.4



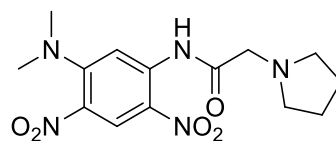
5-Amino-6-*N,N*-dimethylamino-2-piperidin-1-ylmethyl-1*H*-benzo[d]imidazole



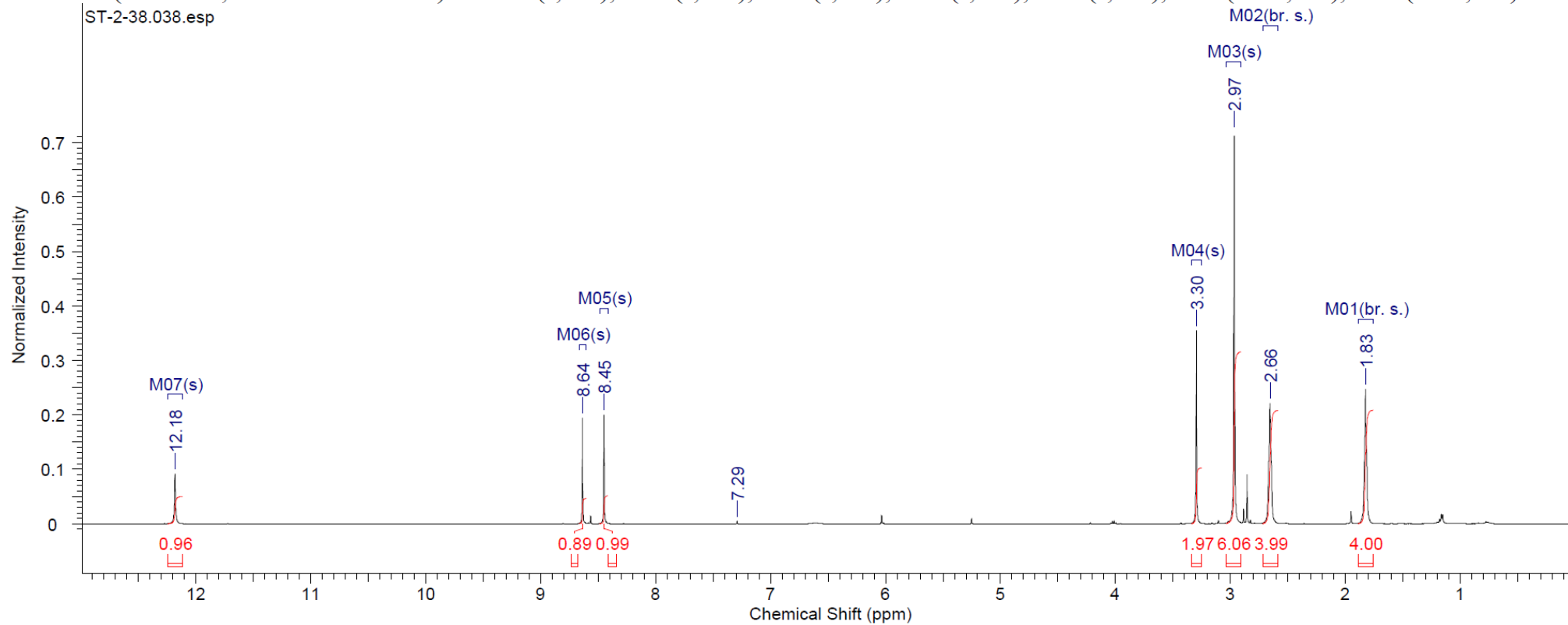
^{13}C NMR (126 MHz, CHLOROFORM- d) δ 23.6, 25.5, 44.3, 54.3, 56.9, 60.1, 98.3, 106.7, 132.9, 134.1, 137.9, 138.0, 150.2



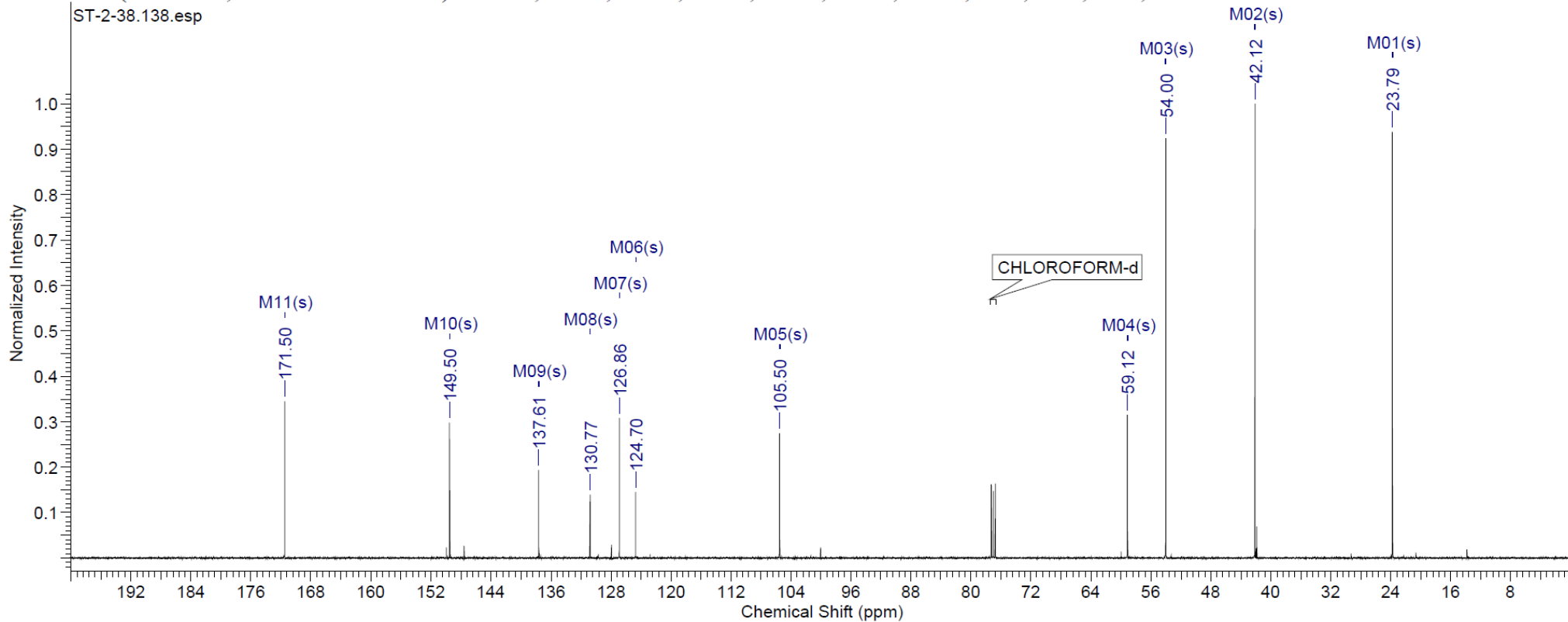
5-*N,N*-Dimethylamino-1-pyrrolidin-1-ylmethylcarboxamido-2,4-dinitro benzene



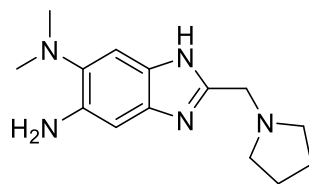
¹H NMR (500 MHz, CHLOROFORM-*d*) δ 12.18 (s, 1H), 8.64 (s, 1H), 8.45 (s, 1H), 3.30 (s, 2H), 2.97 (s, 6H), 2.66 (br. s., 4H), 1.83 (br. s., 4H)



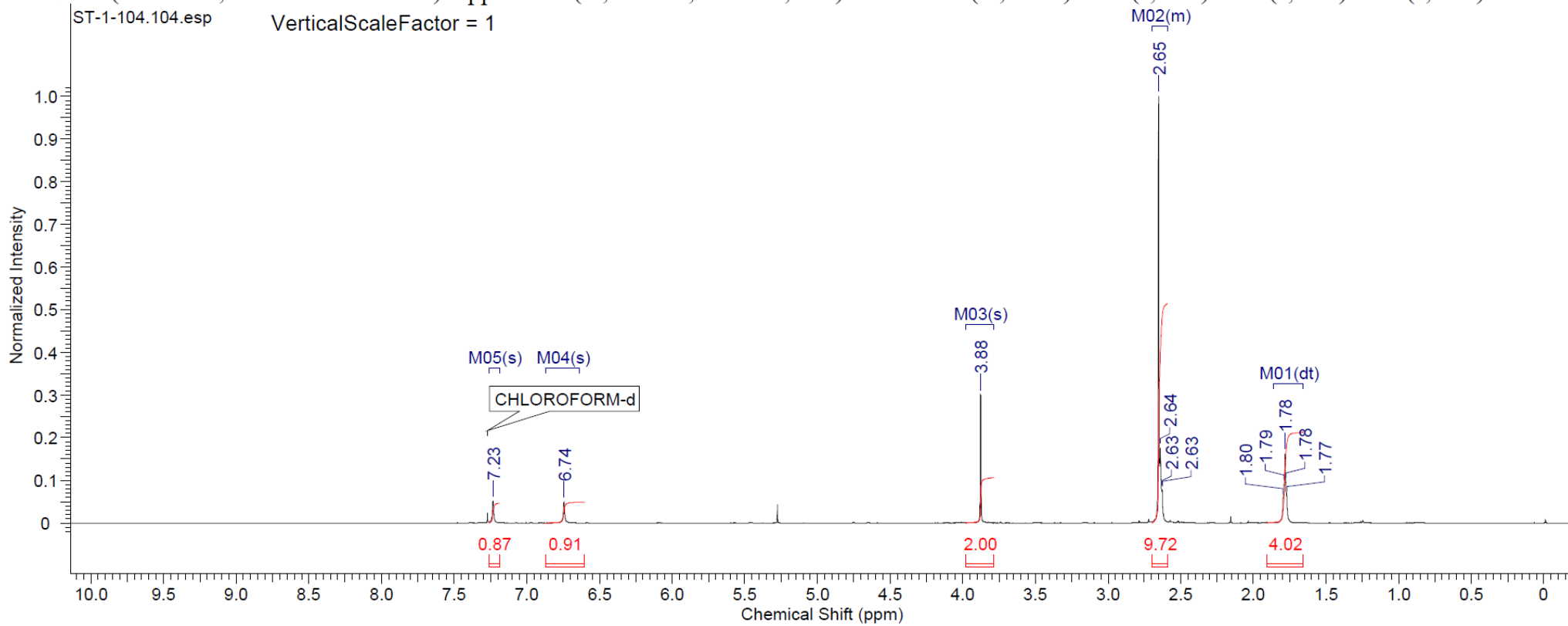
^{13}C NMR (126 MHz, CHLOROFORM- d) δ 171.5, 149.5, 137.6, 130.8, 126.9, 124.7, 105.5, 59.1, 54.0, 42.1, 23.8



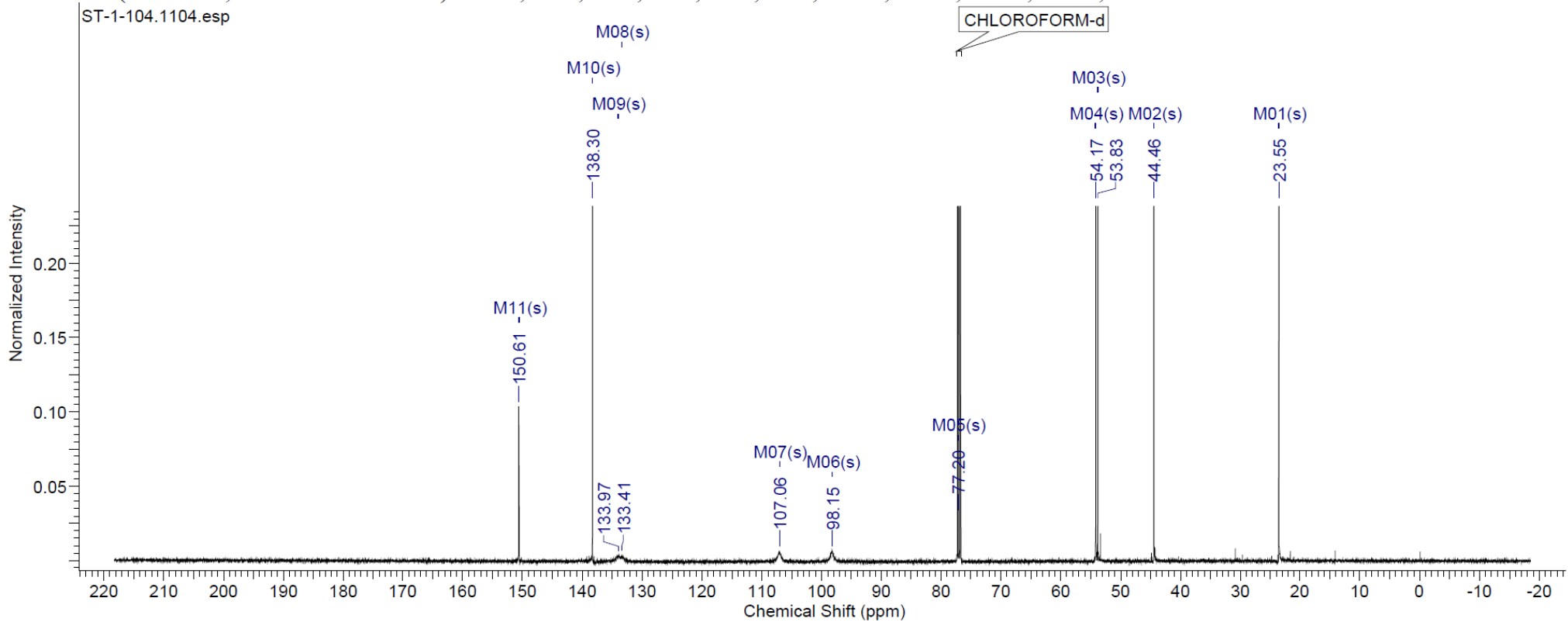
5-Amino-6-*N,N*-dimethylamino-2-piperidin-1-ylmethyl-1*H*-benzo[d]imidazole



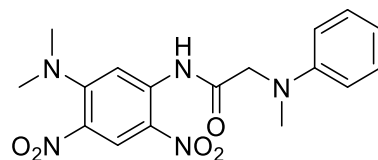
^1H NMR (500 MHz, CHLOROFORM-*d*) δ ppm 1.78 (dt, $J=6.48, 3.32$ Hz, 4 H) 2.59 - 2.70 (m, 10 H) 3.88 (s, 2 H) 6.74 (s, 1 H) 7.23 (s, 1 H)



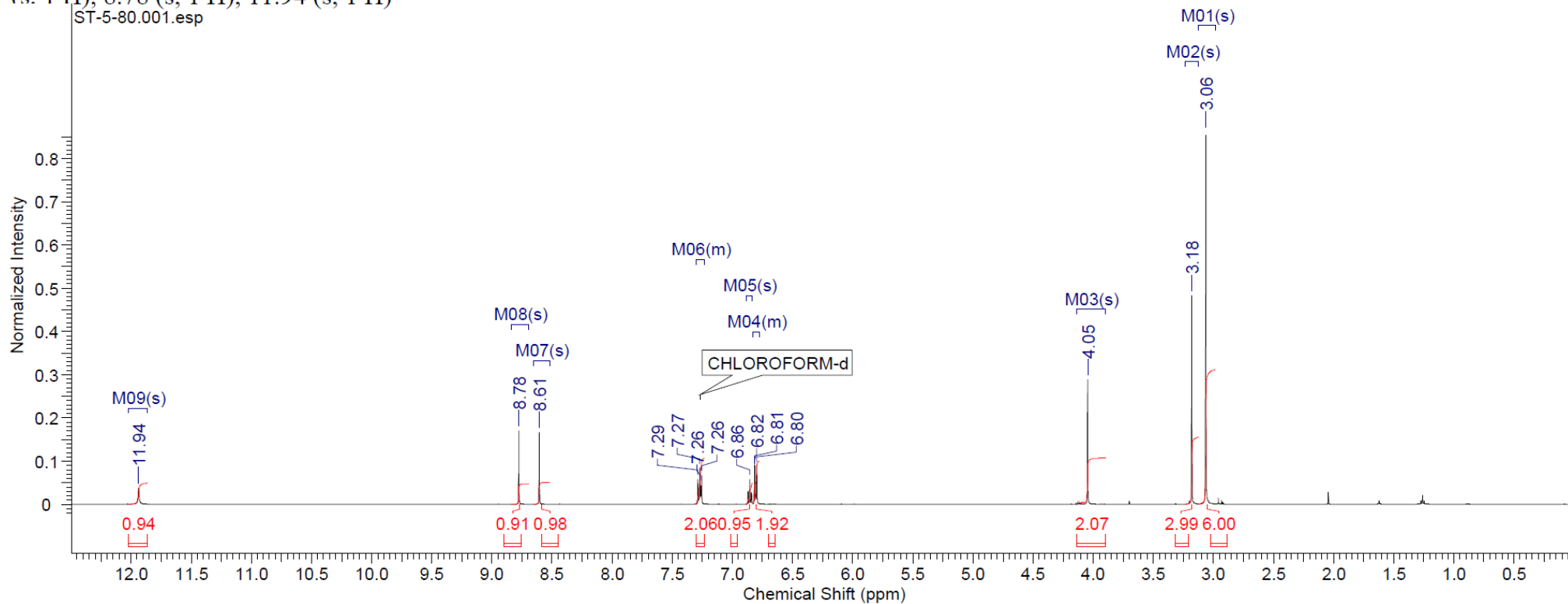
^{13}C NMR (126 MHz, CHLOROFORM-d) δ 23.5, 44.5, 53.8, 54.2, 77.2, 98.2, 107.1, 133.4, 134.0, 138.3, 150.6



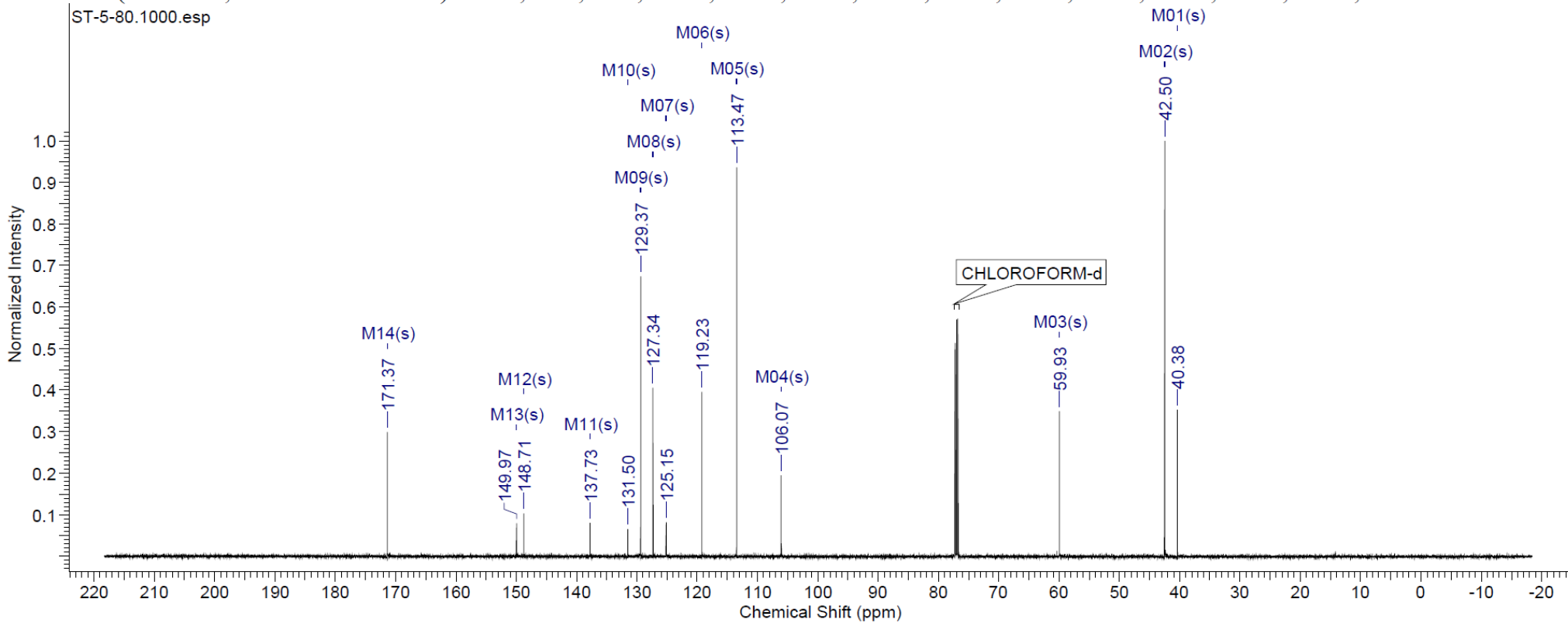
5-*N,N*-Dimethylamino-1-(*N*-methyl-*N*-phenylamino)methylcarboxamido-2,4-dinitro benzene



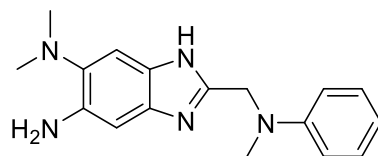
$^1\text{H NMR}$ (500 MHz, CHLOROFORM-*d*) δ 3.06 (s, 6 H), 3.18 (s, 3 H), 4.05 (s, 2 H), 6.78 - 6.83 (m, 2 H), 6.86 (s, 1 H), 7.23 - 7.30 (m, 2 H), 8.61 (s, 1 H), 8.78 (s, 1 H), 11.94 (s, 1 H)



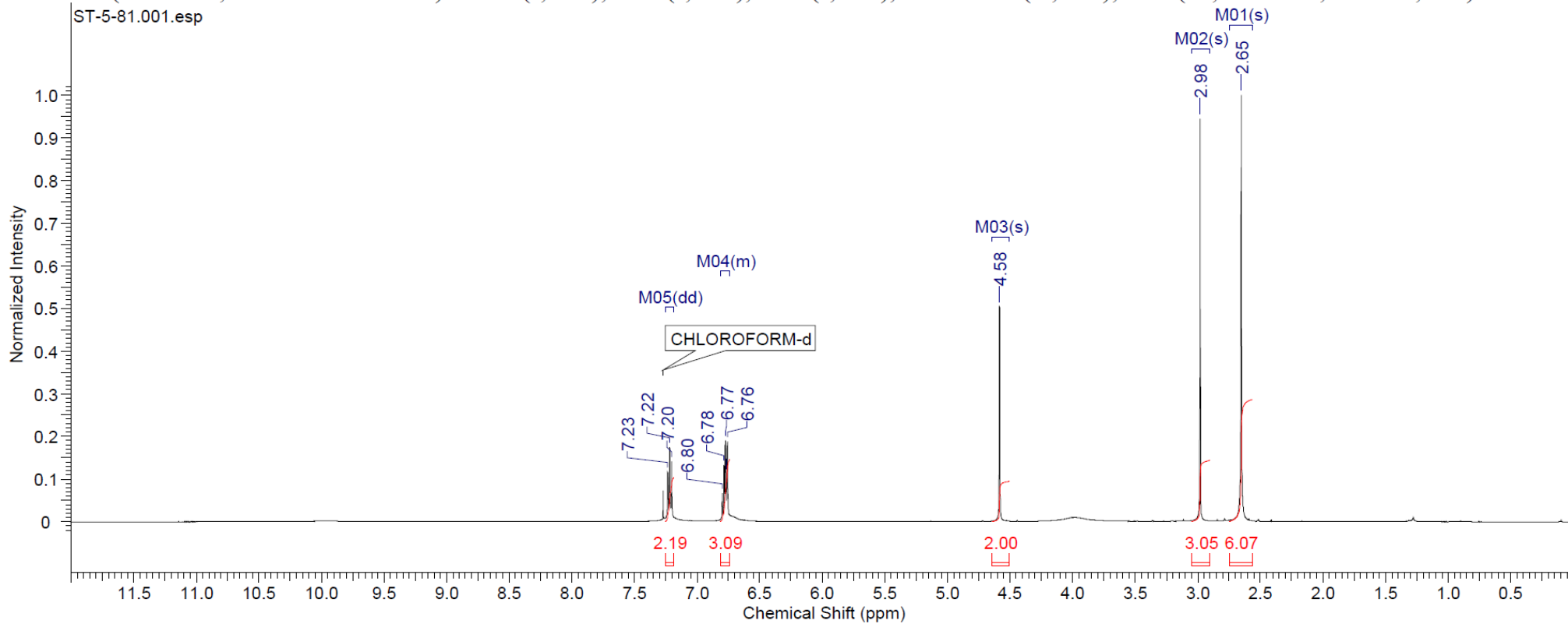
^{13}C NMR (126 MHz, CHLOROFORM- d) δ 40.4, 42.5, 59.9, 106.1, 113.5, 119.2, 125.1, 127.3, 129.4, 131.5, 137.7, 148.7, 150.0, 171.4



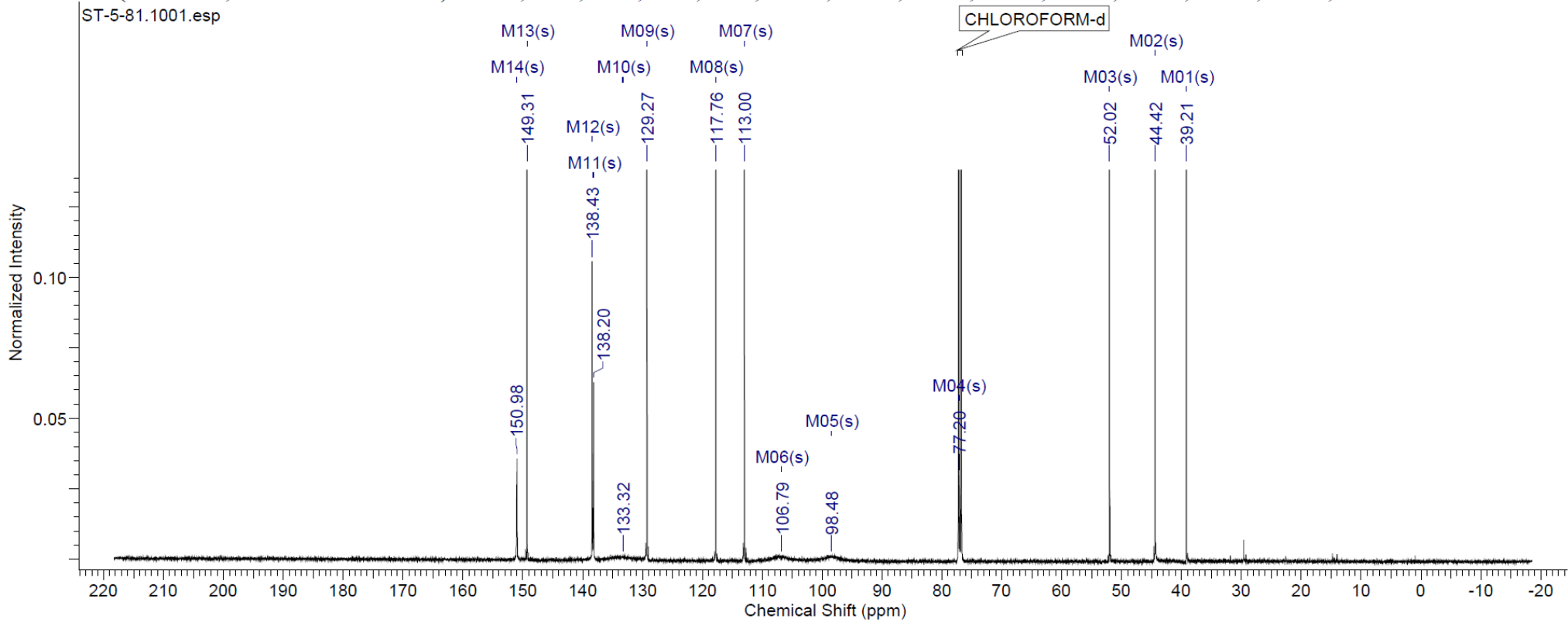
5-Amino-6-*N,N*-dimethylamino-2-(*N*-methyl-*N*-phenylamino)methyl-1*H*-benzo[d]imidazole



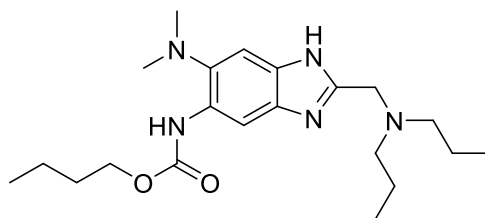
$^1\text{H NMR}$ (500 MHz, CHLOROFORM-*d*) δ 2.65 (s, 6 H), 2.98 (s, 3 H), 4.58 (s, 2 H), 6.74 - 6.81 (m, 3 H), 7.22 (dd, $J = 8.70, 7.48$ Hz, 2 H)



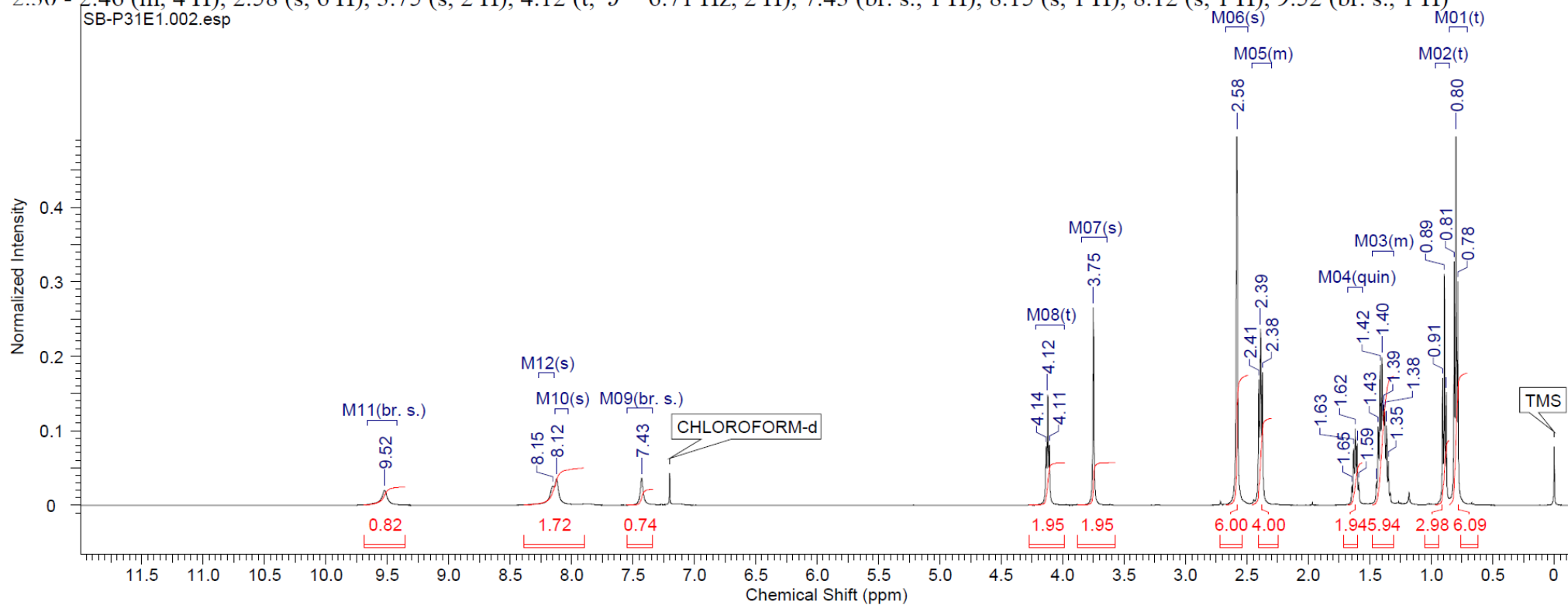
^{13}C NMR (126 MHz, CHLOROFORM-d) δ 39.2, 44.4, 52.0, 77.2, 98.5, 106.8, 113.0, 117.8, 129.3, 133.3, 138.2, 138.4, 149.3, 151.0



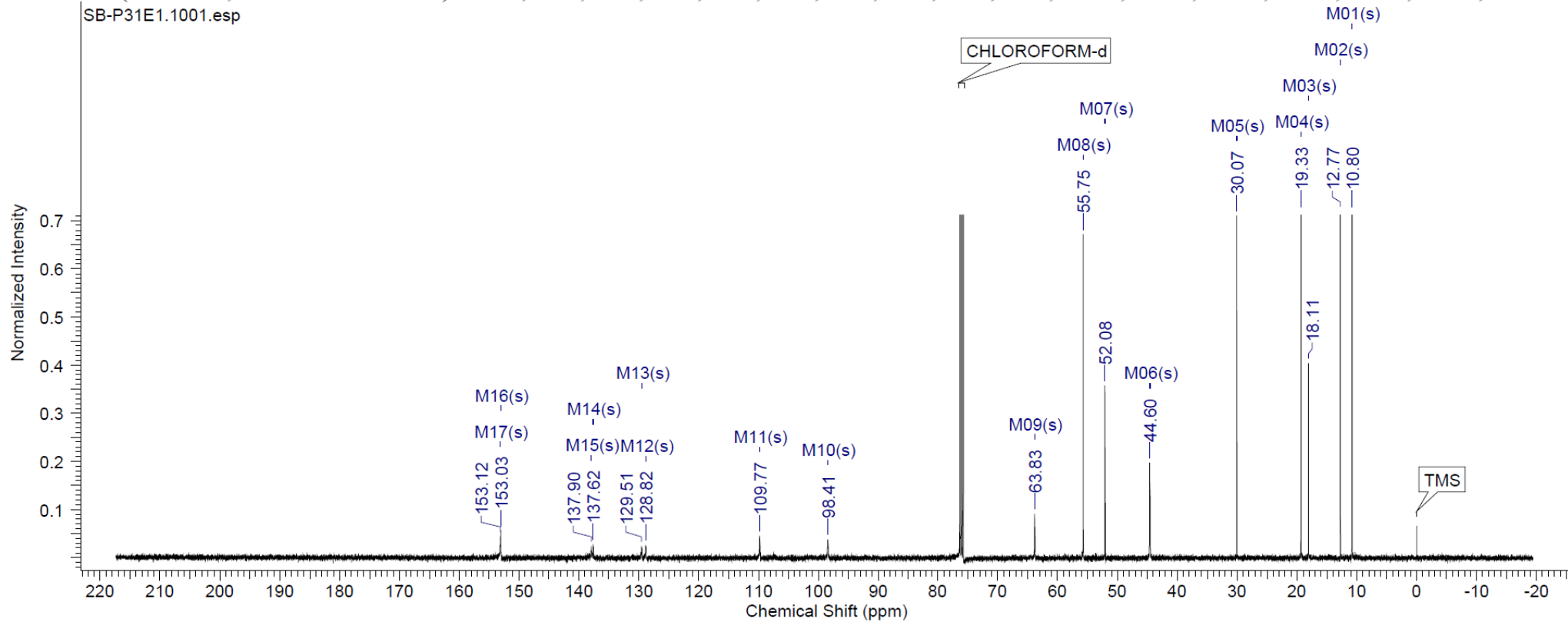
5-Butyloxycarbonylamino-6-*N,N*-dimethylamino-2-*N,N*-dipropylaminomethyl-1*H*-benzo[d]imidazole



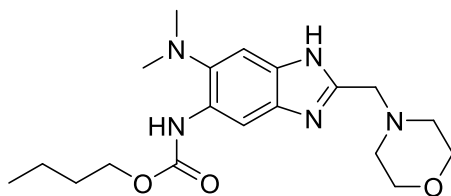
¹H NMR (500 MHz, CHLOROFORM-*d*) δ 0.80 (t, $J = 7.32$ Hz, 6 H), 0.89 (t, $J = 7.48$ Hz, 3 H), 1.31 - 1.48 (m, 6 H), 1.62 (quin, $J = 7.10$ Hz, 2 H), 2.30 - 2.46 (m, 4 H), 2.58 (s, 6 H), 3.75 (s, 2 H), 4.12 (t, $J = 6.71$ Hz, 2 H), 7.43 (br. s., 1 H), 8.15 (s, 1 H), 8.12 (s, 1 H), 9.52 (br. s., 1 H)



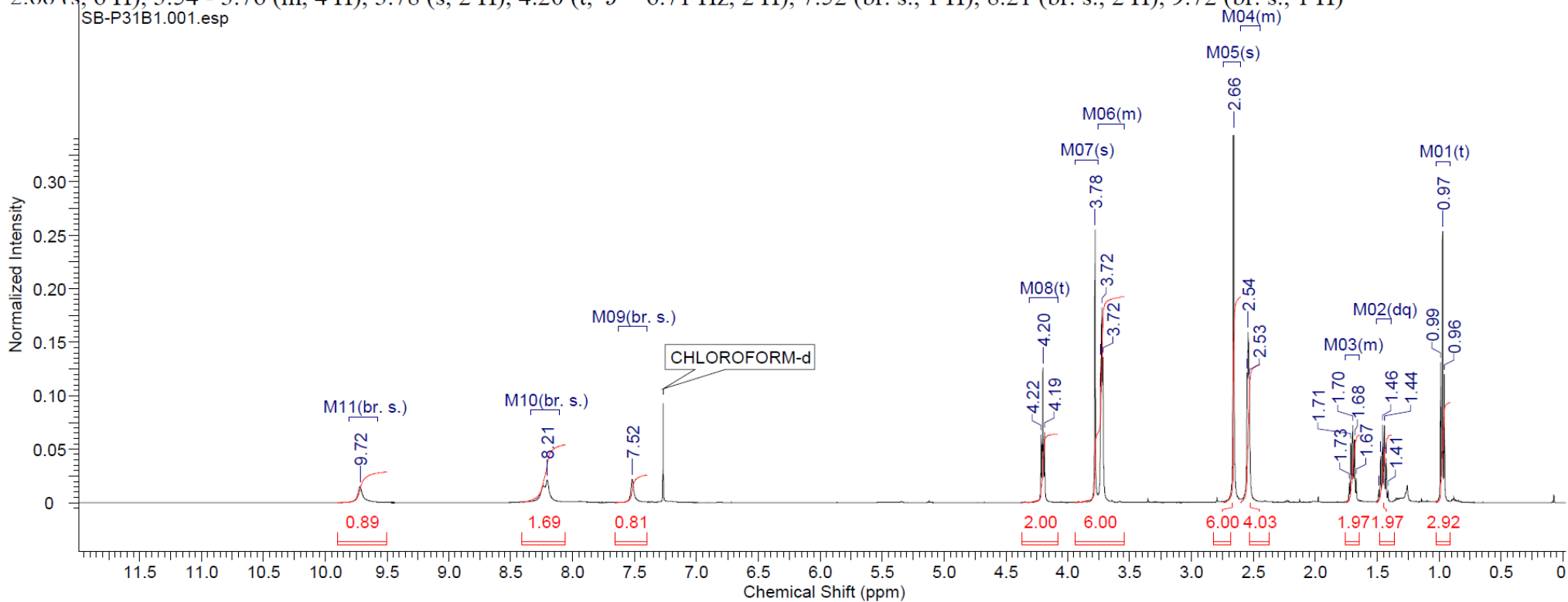
^{13}C NMR (126 MHz, CHLOROFORM-d) δ 10.8, 12.8, 18.1, 19.3, 30.1, 44.6, 52.1, 55.7, 63.8, 98.4, 109.8, 128.8, 129.5, 137.6, 137.9, 153.0, 153.1

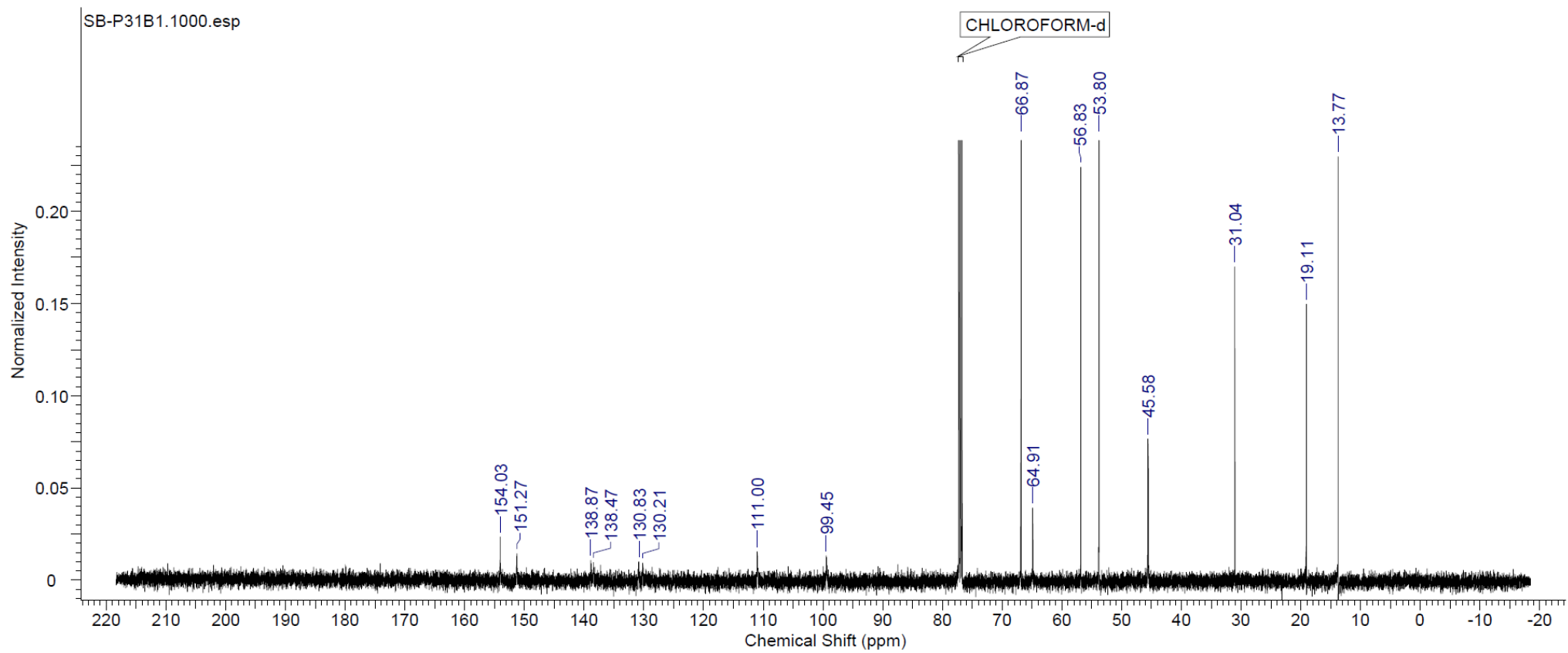


5-Butyloxycarbonylamino-6-*N,N*-dimethylamino-2-*N,N*-morpholinylmethyl-1*H*-benzo[*d*]imidazole

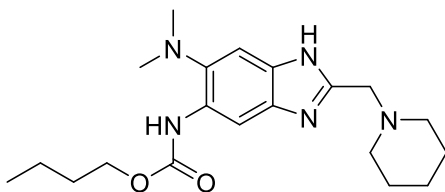


¹H NMR (500 MHz, CHLOROFORM-*d*) δ 0.97 (t, *J* = 7.32 Hz, 3 H), 1.45 (dq, *J* = 14.95, 7.53 Hz, 2 H), 1.64 - 1.76 (m, 2 H), 2.45 - 2.60 (m, 4 H), 2.66 (s, 6 H), 3.54 - 3.76 (m, 4 H), 3.78 (s, 2 H), 4.20 (t, *J* = 6.71 Hz, 2 H), 7.52 (br. s., 1 H), 8.21 (br. s., 2 H), 9.72 (br. s., 1 H)

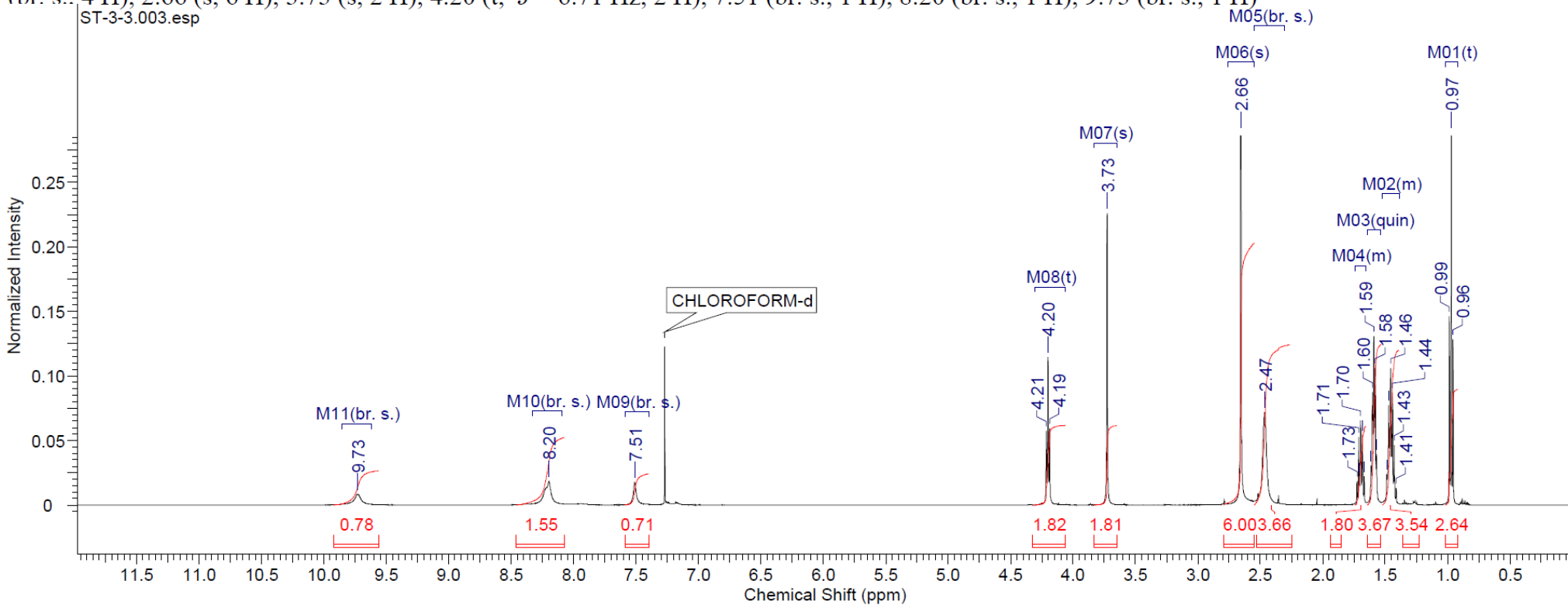




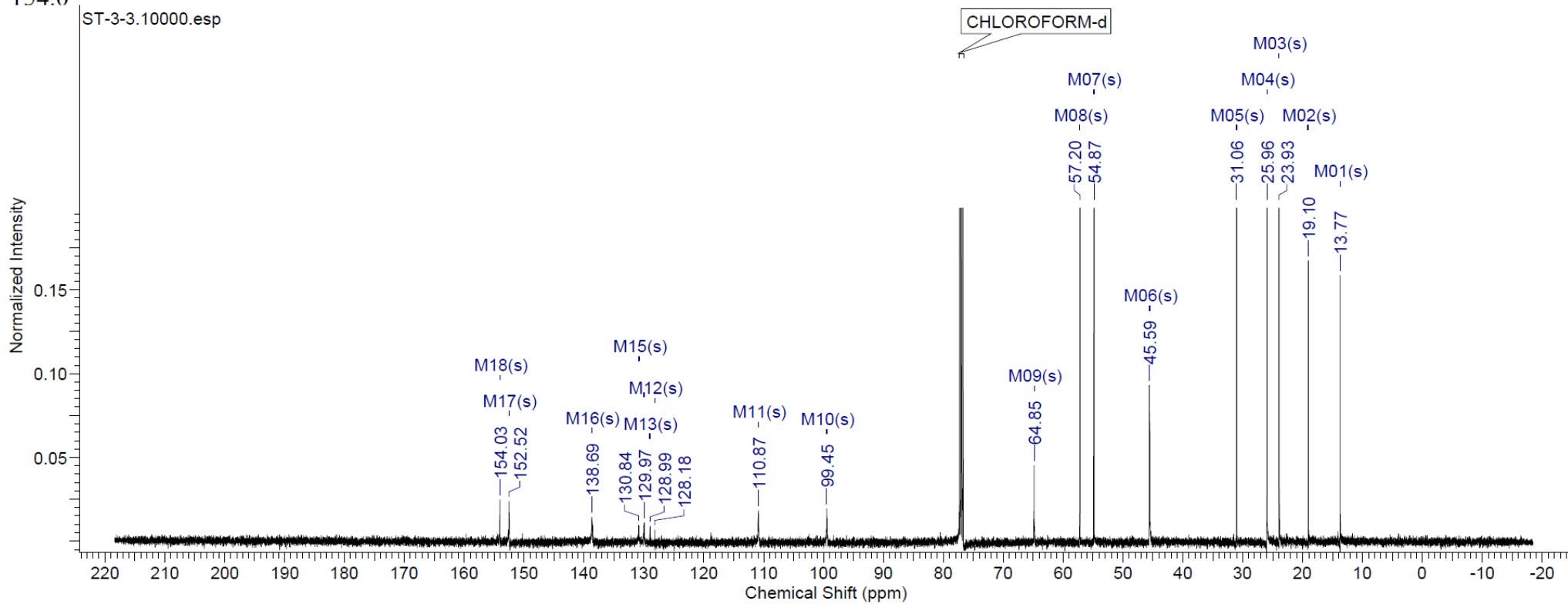
5-Butyloxycarbonylamino-6-*N,N*-dimethylamino-2-*N,N*-piperidinylmethyl-1*H*-benzo[d]imidazole



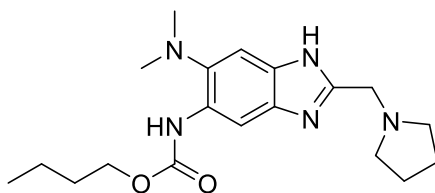
¹H NMR (500 MHz, CHLOROFORM-d) δ 0.97 (t, *J* = 7.32 Hz, 3 H), 1.39 - 1.52 (m, 4 H), 1.59 (quin, *J* = 5.57 Hz, 4 H), 1.66 - 1.74 (m, 2 H), 2.47 (br. s., 4 H), 2.66 (s, 6 H), 3.73 (s, 2 H), 4.20 (t, *J* = 6.71 Hz, 2 H), 7.51 (br. s., 1 H), 8.20 (br. s., 1 H), 9.73 (br. s., 1 H)



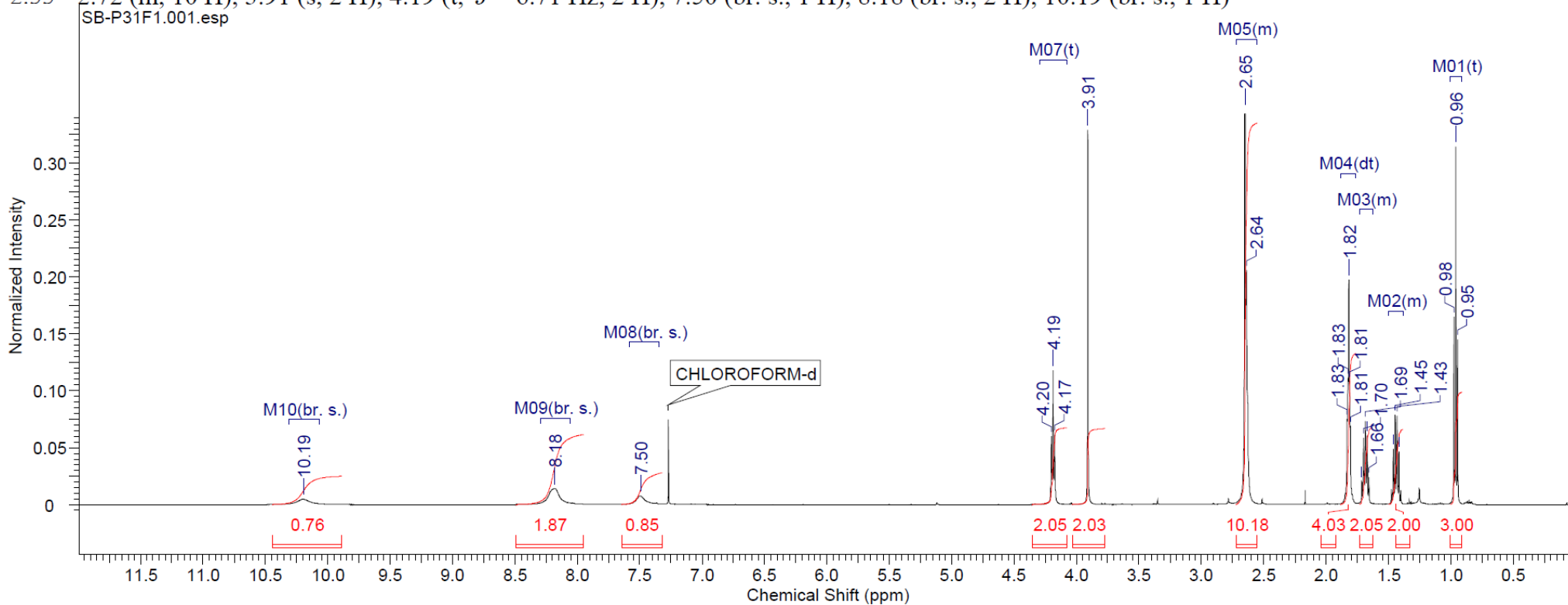
^{13}C NMR (126 MHz, CHLOROFORM-d) δ 13.8, 19.1, 23.9, 26.0, 31.1, 45.6, 54.9, 57.2, 64.9, 99.4, 110.9, 128.2, 129.0, 130.0, 130.8, 138.7, 152.5, 154.0



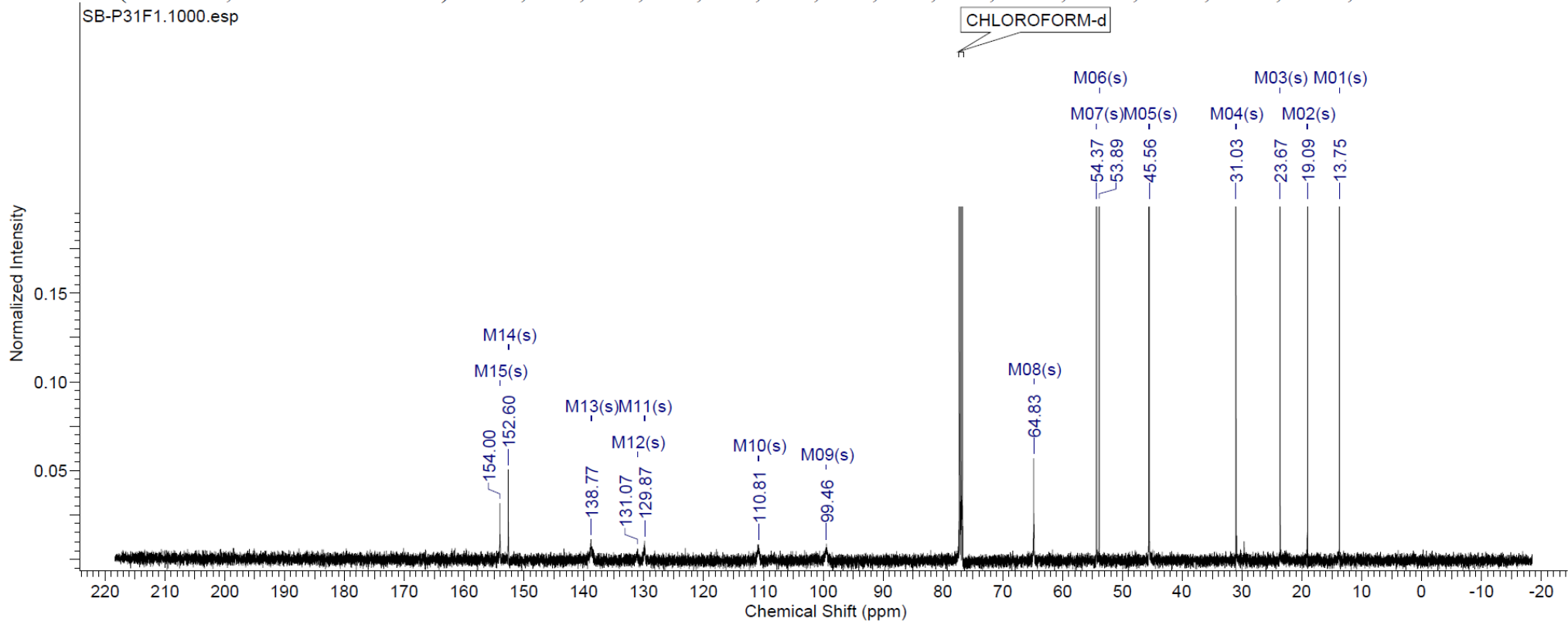
5-Butyloxycarbonylamino-6-*N,N*-dimethylamino-2-*N,N*-pyrrolidinylmethyl-1*H*-benzo[d]imidazole



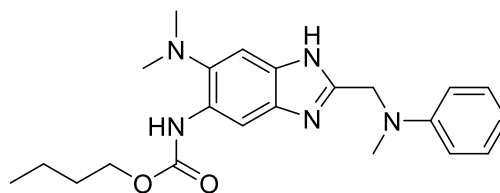
$^1\text{H NMR}$ (500 MHz, CHLOROFORM- d) δ 0.96 (t, $J = 7.48$ Hz, 3 H), 1.38 - 1.50 (m, 2 H), 1.63 - 1.73 (m, 2 H), 1.82 (dt, $J = 6.56, 3.13$ Hz, 4 H), 2.55 - 2.72 (m, 10 H), 3.91 (s, 2 H), 4.19 (t, $J = 6.71$ Hz, 2 H), 7.50 (br. s., 1 H), 8.18 (br. s., 2 H), 10.19 (br. s., 1 H)



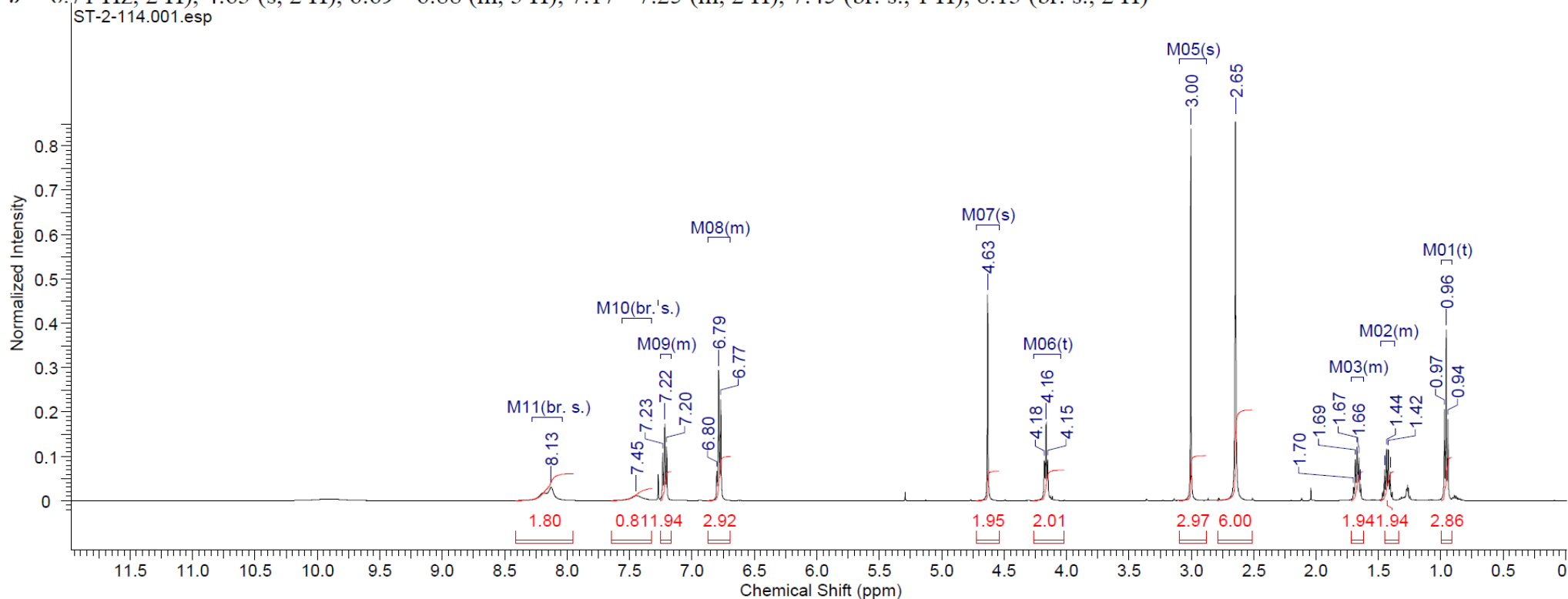
^{13}C NMR (126 MHz, CHLOROFORM-d) δ 13.8, 19.1, 23.7, 31.0, 45.6, 53.9, 54.4, 64.8, 99.5, 110.8, 129.9, 131.1, 138.8, 152.6, 154.0



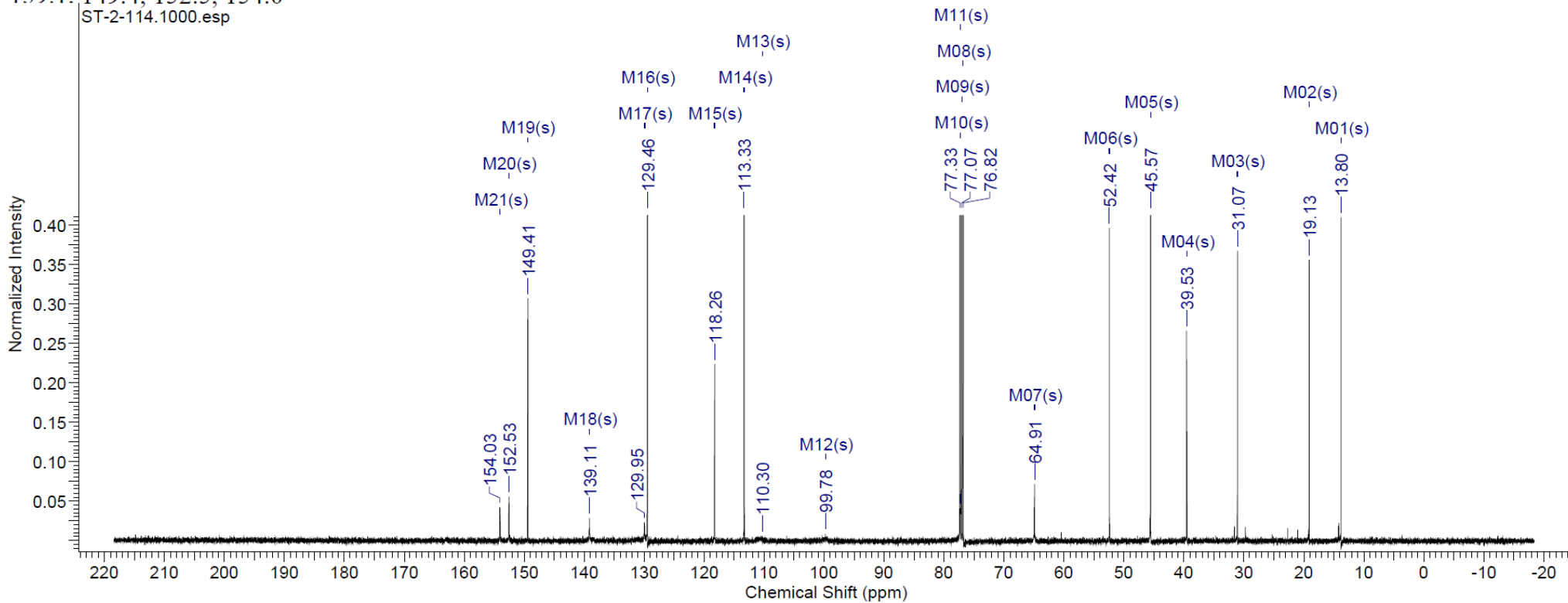
5-Butyloxycarbonylamino-6-*N,N*-dimethylamino-2-(*N*-methyl-*N*-phenylamino)methyl-1*H*-benzo[*d*]imidazole



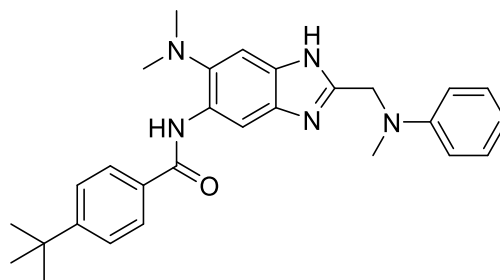
$^1\text{H NMR}$ (500 MHz, CHLOROFORM-*d*) δ 0.96 (t, $J = 7.48$ Hz, 3 H), 1.37 - 1.48 (m, 2 H), 1.62 - 1.72 (m, 2 H), 2.65 (s, 6 H), 3.00 (s, 3 H), 4.16 (t, $J = 6.71$ Hz, 2 H), 4.63 (s, 2 H), 6.69 - 6.88 (m, 3 H), 7.17 - 7.25 (m, 2 H), 7.45 (br. s., 1 H), 8.13 (br. s., 2 H)



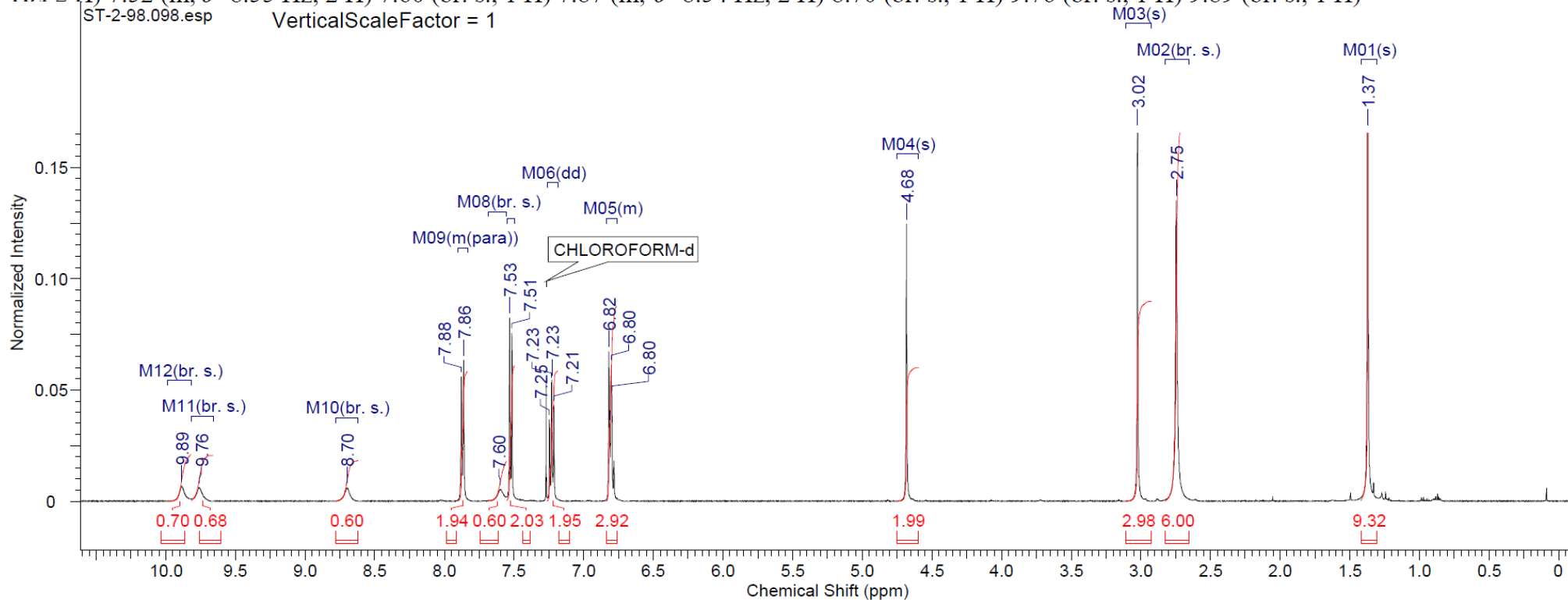
^{13}C NMR (126 MHz, CHLOROFORM- d) δ 13.8, 19.1, 31.1, 39.5, 45.6, 52.4, 64.9, 76.8, 77.1, 77.3, 77.3, 99.8, 110.3, 113.3, 118.3, 129.5, 129.9, 139.1, 149.4, 152.5, 154.0



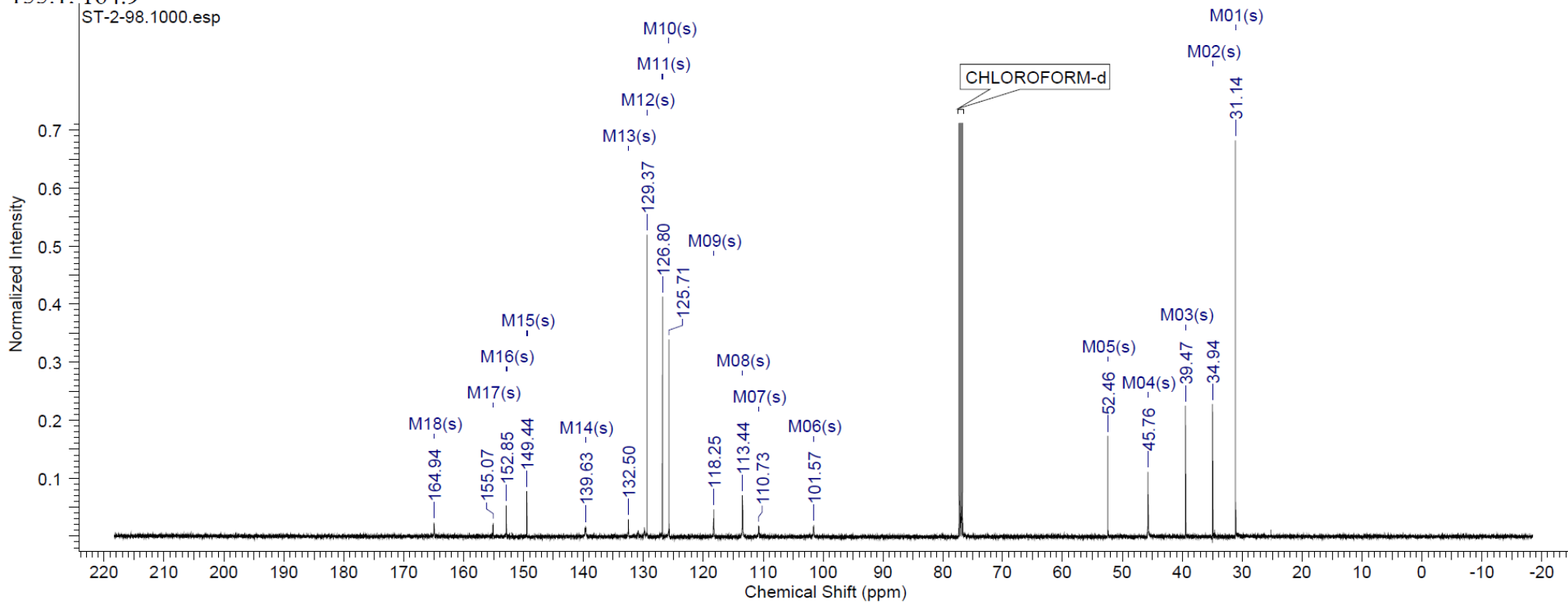
5-(4-Tert-butyl)benzamido-6-*N,N*-dimethylamino-2-(*N*-methyl-*N*-phenylamino)methyl-1*H*-benzo[d]imidazole



$^1\text{H NMR}$ (500 MHz, CHLOROFORM-*d*) δ ppm 1.37 (s, 9 H) 2.75 (br. s., 6 H) 3.02 (s, 3 H) 4.68 (s, 2 H) 6.76 - 6.84 (m, 3 H) 7.23 (dd, $J=8.85$, 7.32 Hz, 2 H) 7.52 (m, $J=8.55$ Hz, 2 H) 7.60 (br. s., 1 H) 7.87 (m, $J=8.54$ Hz, 2 H) 8.70 (br. s., 1 H) 9.76 (br. s., 1 H) 9.89 (br. s., 1 H)



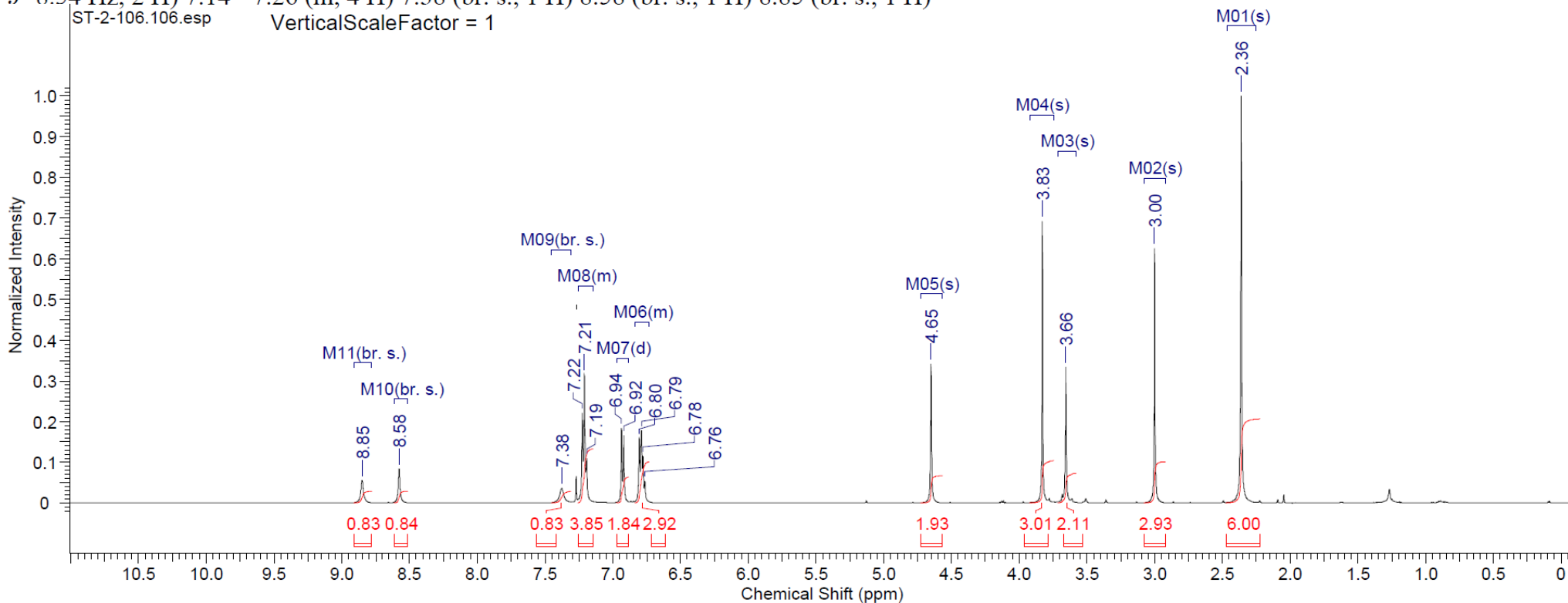
^{13}C NMR (126 MHz, CHLOROFORM-d) δ 31.1, 34.9, 39.5, 45.8, 52.5, 101.6, 110.7, 113.4, 118.2, 125.7, 126.8, 129.4, 132.5, 139.6, 149.4, 152.8, 155.1, 164.9



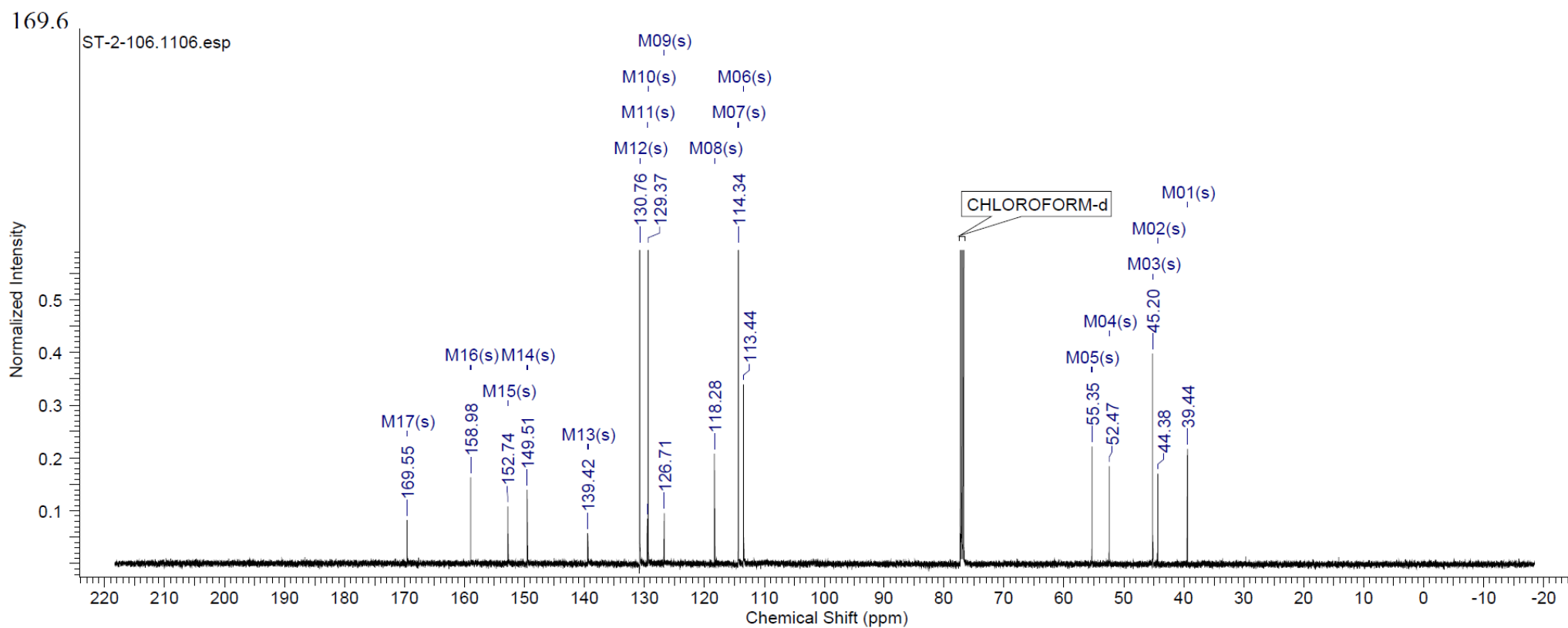
5-(4-Methoxyphenyl)ethanamido-6-*N,N*-dimethylamino-2-(*N*-methyl-*N*-phenylamino)methyl-1*H*-benzo[*d*]imidazole



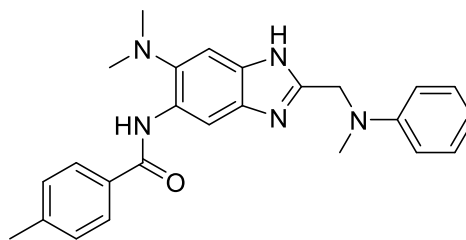
$^1\text{H NMR}$ (500 MHz, $\text{CHLOROFORM-}d$) δ ppm 2.36 (s, 6 H) 3.00 (s, 3 H) 3.66 (s, 2 H) 3.83 (s, 3 H) 4.65 (s, 2 H) 6.73 - 6.84 (m, 3 H) 6.93 (d, $J=8.54$ Hz, 2 H) 7.14 - 7.26 (m, 4 H) 7.38 (br. s., 1 H) 8.58 (br. s., 1 H) 8.85 (br. s., 1 H)



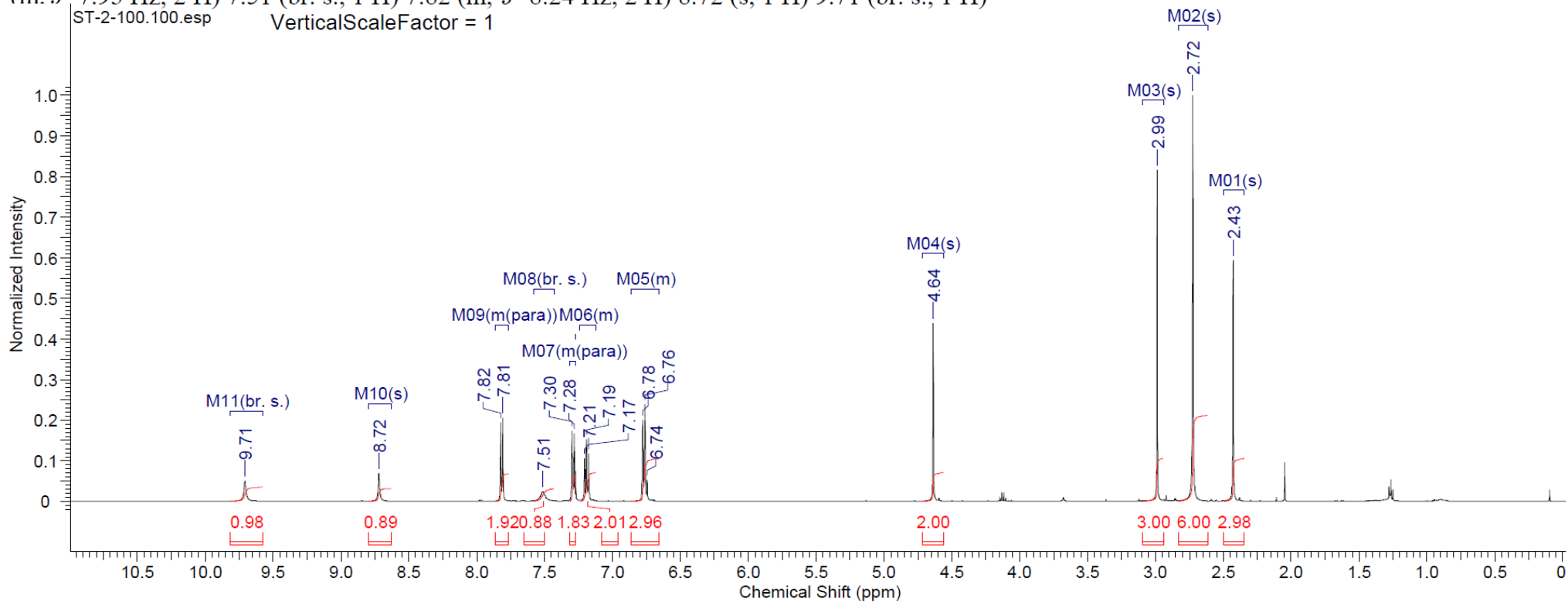
^{13}C NMR (126 MHz, CHLOROFORM-d) δ 39.4, 44.4, 45.2, 52.5, 55.3, 113.4, 114.3, 118.3, 126.7, 129.4, 129.5, 130.8, 139.4, 149.5, 152.7, 159.0, 169.6



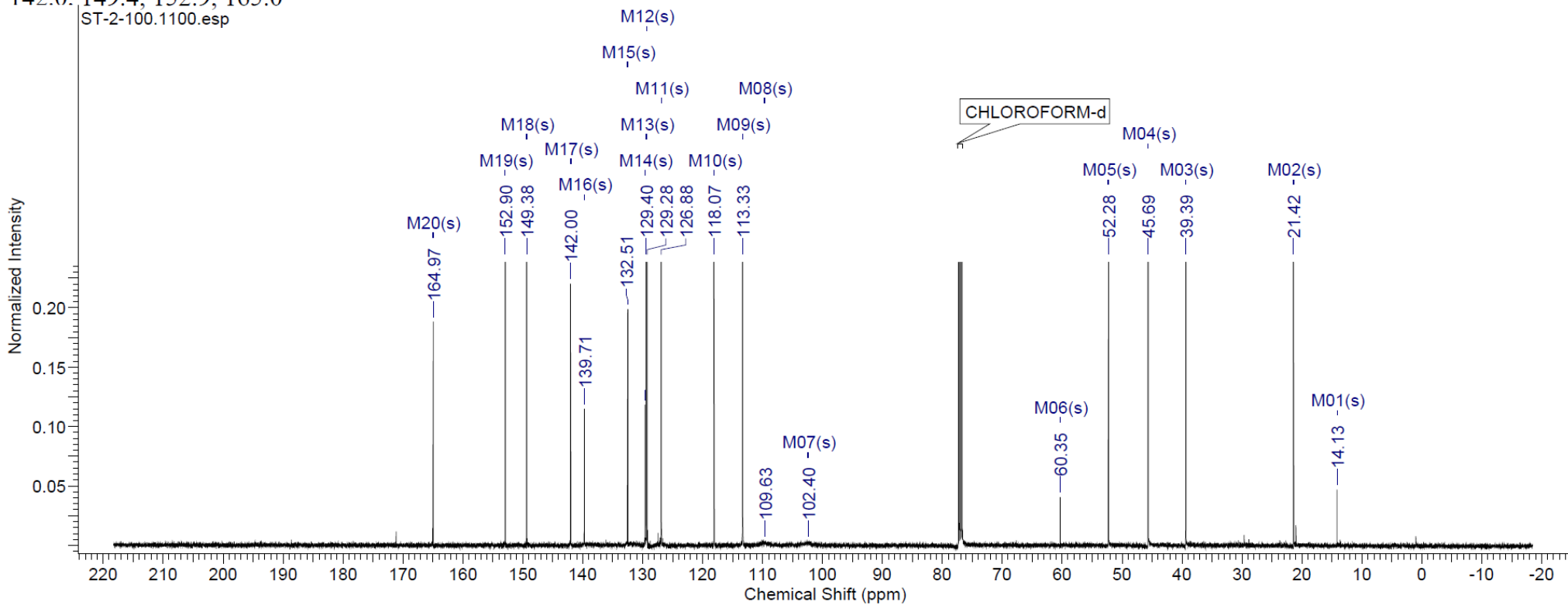
5-(4-Methyl)benzamido-6-*N,N*-dimethylamino-2-(*N*-methyl-*N*-phenylamino)methyl-1*H*-benzo[d]imidazole



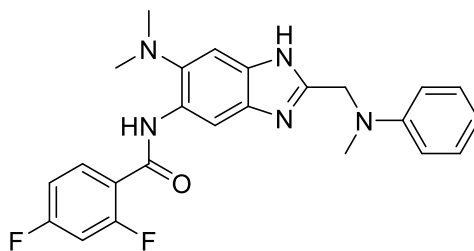
¹H NMR (500 MHz, CHLOROFORM-*d*) δ ppm 2.43 (s, 3 H) 2.72 (s, 6 H) 2.99 (s, 3 H) 4.64 (s, 2 H) 6.66 - 6.86 (m, 3 H) 7.12 - 7.24 (m, 2 H) 7.29 (m, *J*=7.93 Hz, 2 H) 7.51 (br. s., 1 H) 7.82 (m, *J*=8.24 Hz, 2 H) 8.72 (s, 1 H) 9.71 (br. s., 1 H)



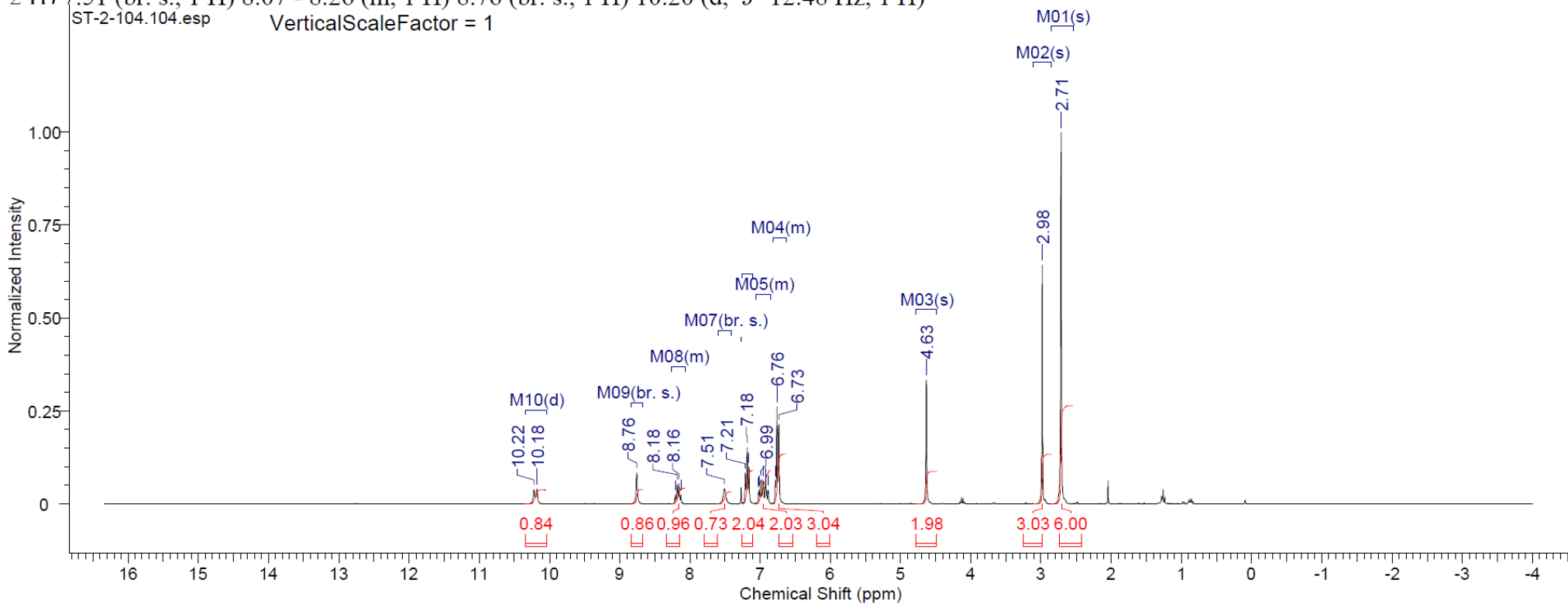
^{13}C NMR (126 MHz, CHLOROFORM-d) δ 14.1, 21.4, 39.4, 45.7, 52.3, 60.4, 102.4, 109.6, 113.3, 118.1, 126.9, 129.3, 129.4, 129.6, 132.5, 139.7, 142.0, 149.4, 152.9, 165.0



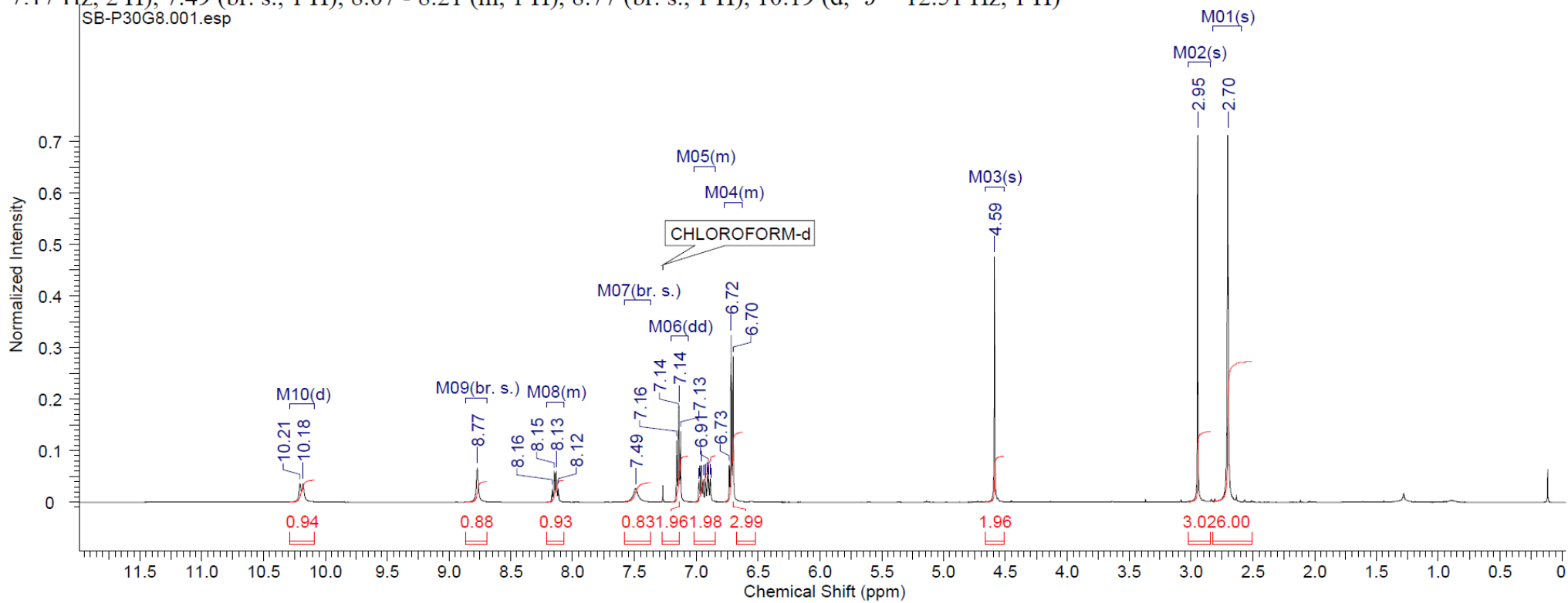
5-(2,4-Difluoro)benzamido-6-*N,N*-dimethylamino-2-(*N*-methyl-*N*-phenylamino)methyl-1*H*-benzo[d]imidazole



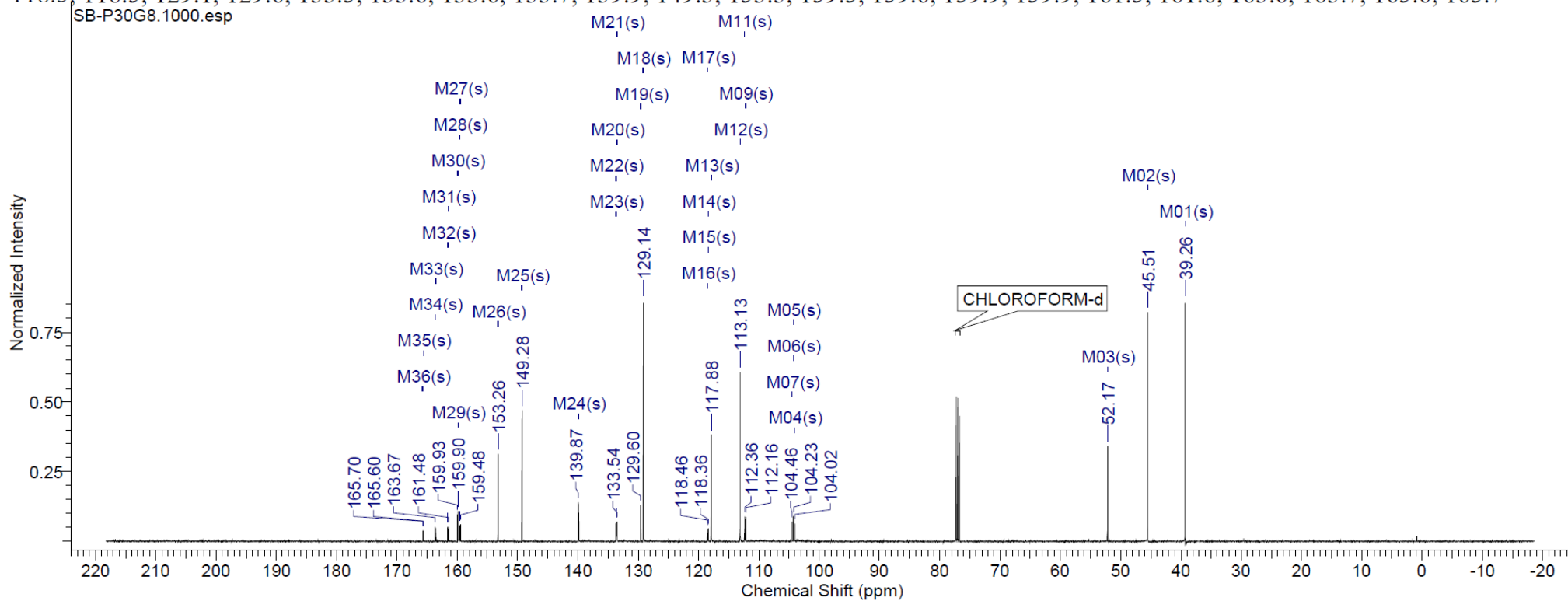
^1H NMR (300 MHz, CHLOROFORM-*d*) δ ppm 2.71 (s, 6 H) 2.98 (s, 3 H) 4.63 (s, 2 H) 6.63 - 6.82 (m, 3 H) 6.85 - 7.05 (m, 2 H) 7.18 (t, $J=7.82$ Hz, 2 H) 7.51 (br. s., 1 H) 8.07 - 8.26 (m, 1 H) 8.76 (br. s., 1 H) 10.20 (d, $J=12.48$ Hz, 1 H)



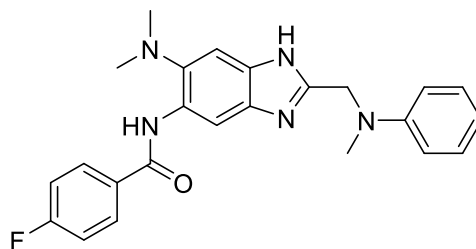
^1H NMR (500 MHz, CHLOROFORM- d) δ 2.70 (s, 6 H), 2.95 (s, 3 H), 4.59 (s, 2 H), 6.62 - 6.78 (m, 3 H), 6.85 - 7.02 (m, 2 H), 7.14 (dd, $J = 8.70$, 7.17 Hz, 2 H), 7.49 (br. s., 1 H), 8.07 - 8.21 (m, 1 H), 8.77 (br. s., 1 H), 10.19 (d, $J = 12.51$ Hz, 1 H)



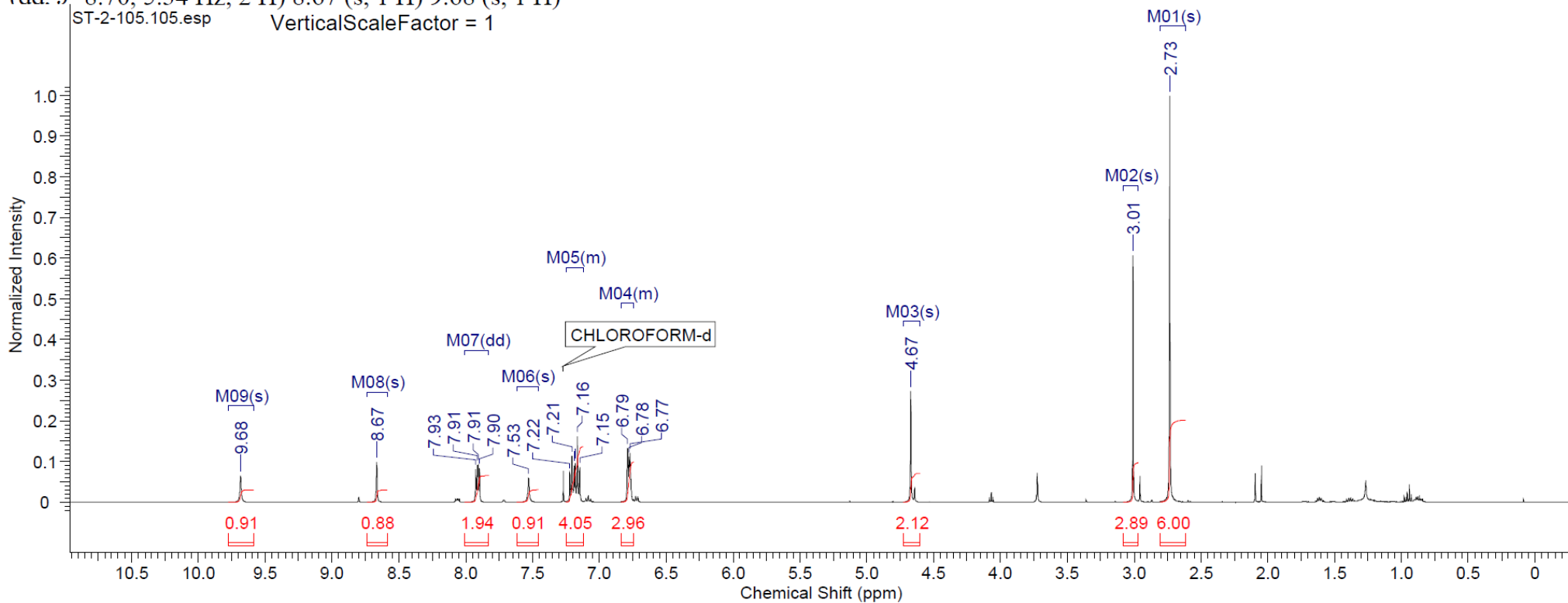
^{13}C NMR (126 MHz, CHLOROFORM-d) δ 39.3, 45.5, 52.2, 104.0, 104.2, 104.3, 104.5, 112.2, 112.2, 112.3, 112.4, 113.1, 117.9, 118.4, 118.4, 118.5, 118.5, 129.1, 129.6, 133.5, 133.6, 133.6, 133.7, 139.9, 149.3, 153.3, 159.5, 159.6, 159.9, 159.9, 161.5, 161.6, 163.6, 163.7, 165.6, 165.7



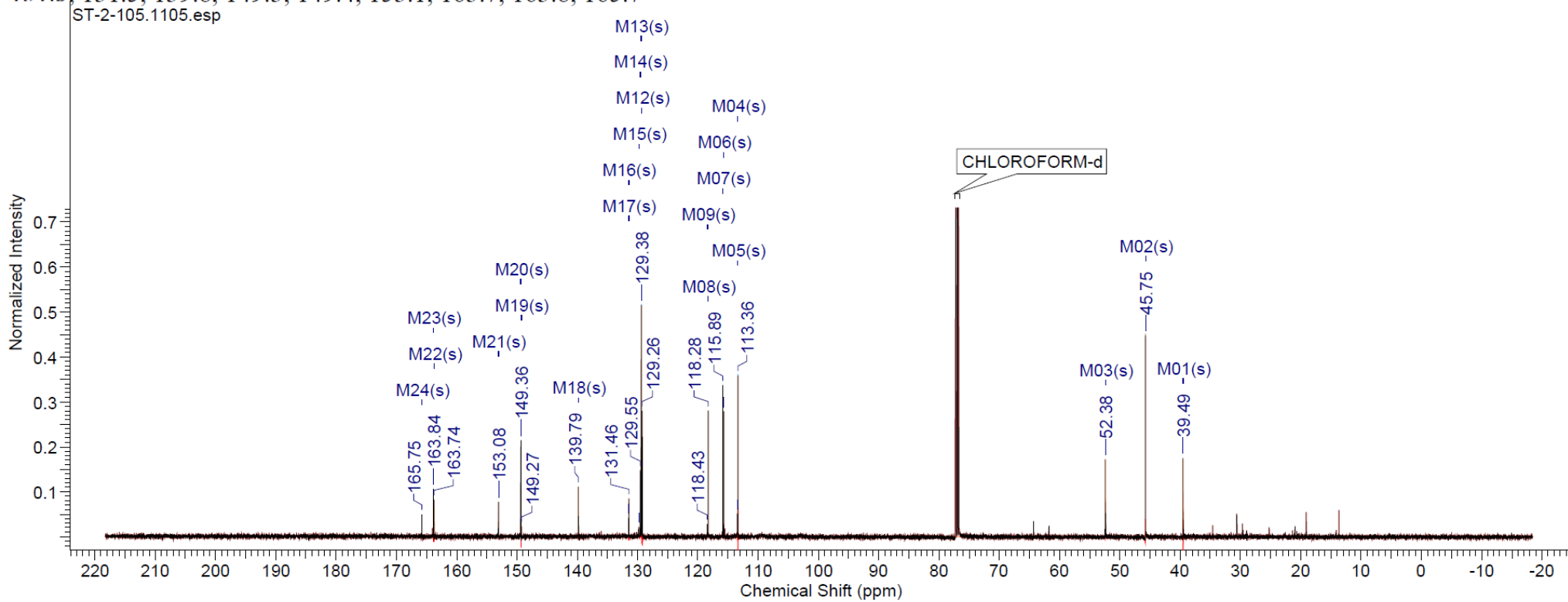
6-*N,N*-Dimethylamino-5-(4-fluoro)benzamido-2-(*N*-methyl-*N*-phenylamino)methyl-1*H*-benzo[d]imidazole



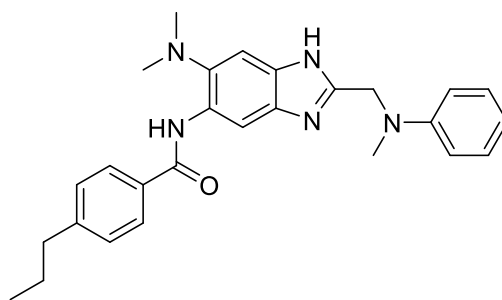
^1H NMR (500 MHz, CHLOROFORM-*d*) δ ppm 2.73 (s, 6 H) 3.01 (s, 3 H) 4.67 (s, 2 H) 6.74 - 6.84 (m, 3 H) 7.12 - 7.25 (m, 4 H) 7.53 (s, 1 H) 7.91 (dd, $J=8.70, 5.34$ Hz, 2 H) 8.67 (s, 1 H) 9.68 (s, 1 H)



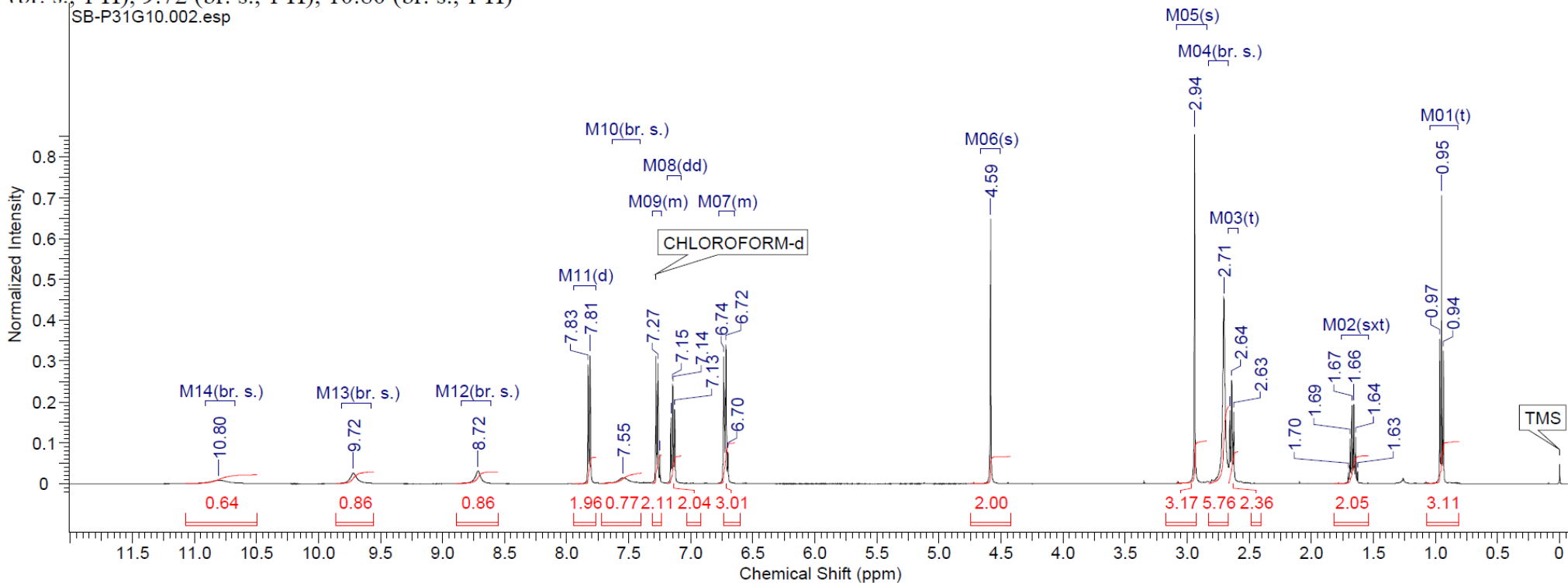
^{13}C NMR (126 MHz, CHLOROFORM-d) δ 39.5, 45.8, 52.4, 113.4, 113.4, 115.7, 115.9, 118.3, 118.4, 129.2, 129.3, 129.3, 129.4, 129.5, 129.8, 131.5, 131.5, 139.8, 149.3, 149.4, 153.1, 163.7, 163.8, 165.7



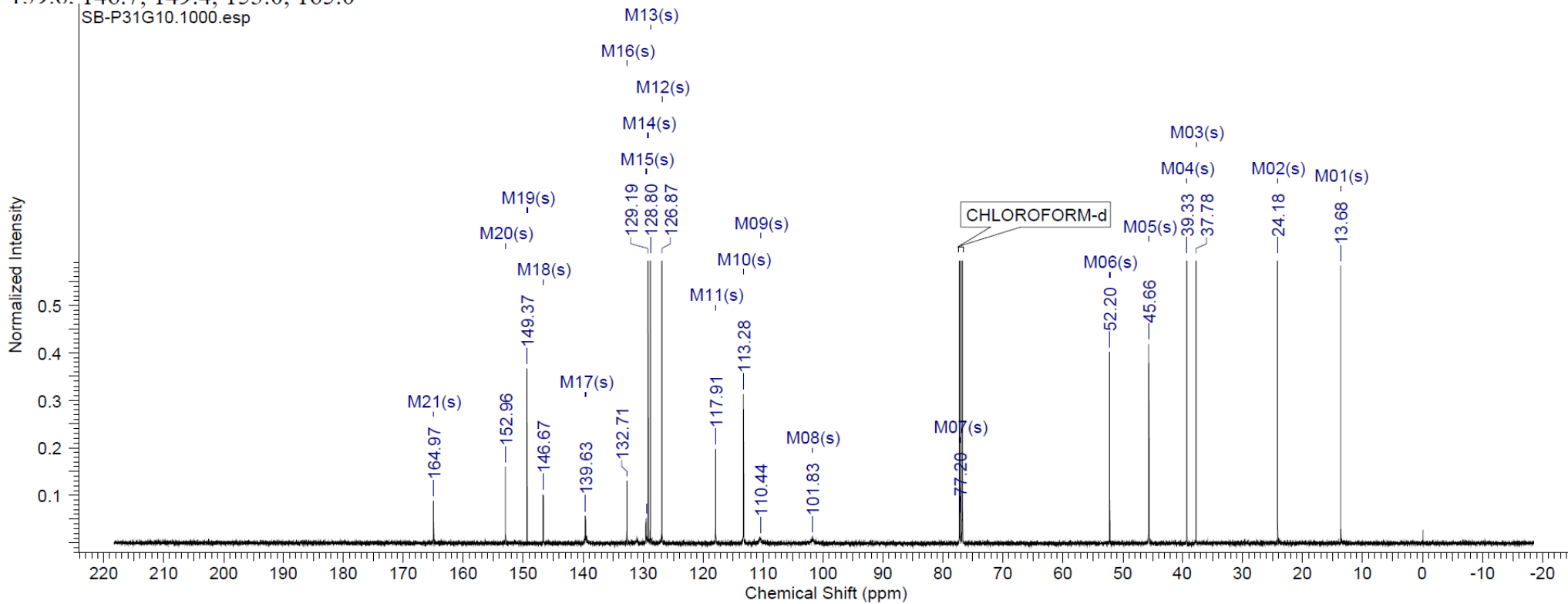
6-*N,N*-Dimethylamino-2-(*N*-methyl-*N*-phenylamino)methyl-5-(4-propyl)benzamido-1*H*-benzo[d]imidazole



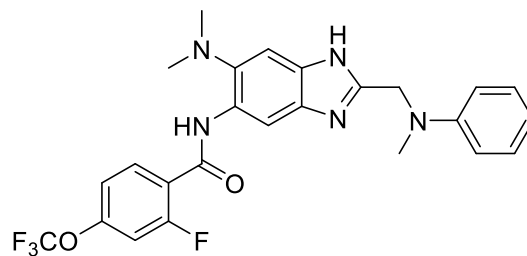
$^1\text{H NMR}$ (500 MHz, CHLOROFORM- d) δ 0.95 (t, $J = 7.32$ Hz, 3 H), 1.67 (sxt, $J = 7.45$ Hz, 2 H), 2.64 (t, $J = 7.63$ Hz, 2 H), 2.71 (br. s., 6 H), 2.94 (s, 3 H), 4.59 (s, 2 H), 6.65 - 6.78 (m, 3 H), 7.15 (dd, $J = 8.70, 7.17$ Hz, 2 H), 7.24 - 7.31 (m, 2 H), 7.55 (br. s., 1 H), 7.82 (d, $J = 8.24$ Hz, 2 H), 8.72 (br. s., 1 H), 9.72 (br. s., 1 H), 10.80 (br. s., 1 H)



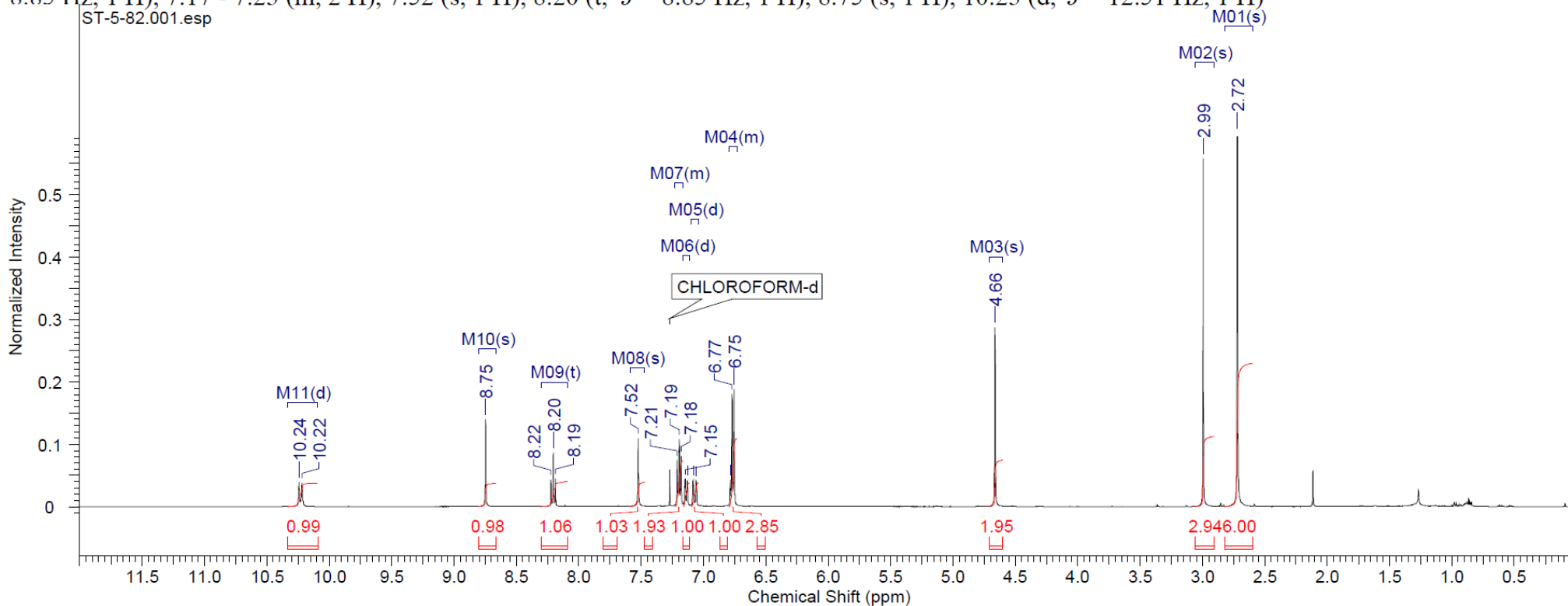
^{13}C NMR (126 MHz, CHLOROFORM- d) δ 13.7, 24.2, 37.8, 39.3, 45.7, 52.2, 77.2, 101.8, 110.4, 113.3, 117.9, 126.9, 128.8, 129.2, 129.5, 132.7, 139.6, 146.7, 149.4, 153.0, 165.0



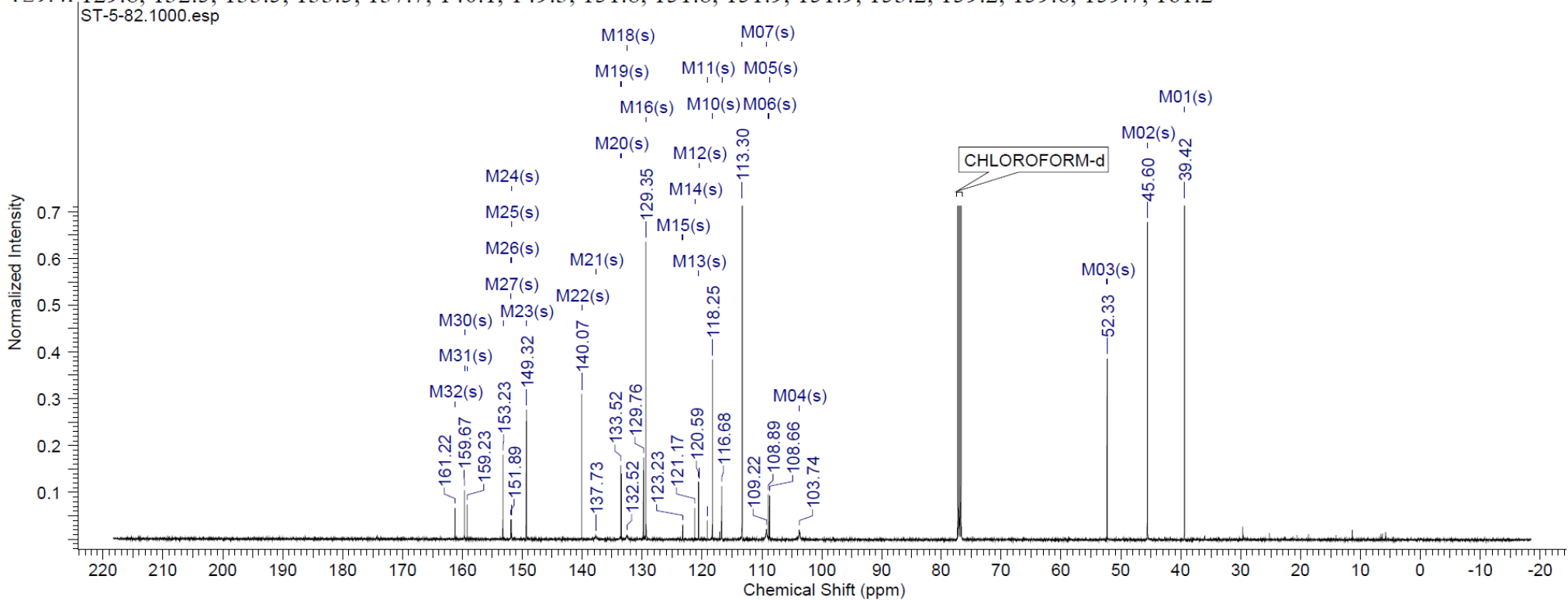
6-*N,N*-Dimethylamino-2-5-(2-fluoro-4-trifluoromethoxy)benzamido- (*N*-methyl-*N*-phenylamino)methyl-1*H*-benzo[d]imidazole



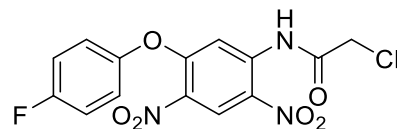
^1H NMR (500 MHz, CHLOROFORM-*d*) δ 2.72 (s, 6 H), 2.99 (s, 3 H), 4.66 (s, 2 H), 6.73 - 6.80 (m, 3 H), 7.07 (d, $J = 11.90$ Hz, 1 H), 7.14 (d, $J = 8.85$ Hz, 1 H), 7.17 - 7.23 (m, 2 H), 7.52 (s, 1 H), 8.20 (t, $J = 8.85$ Hz, 1 H), 8.75 (s, 1 H), 10.23 (d, $J = 12.51$ Hz, 1 H)



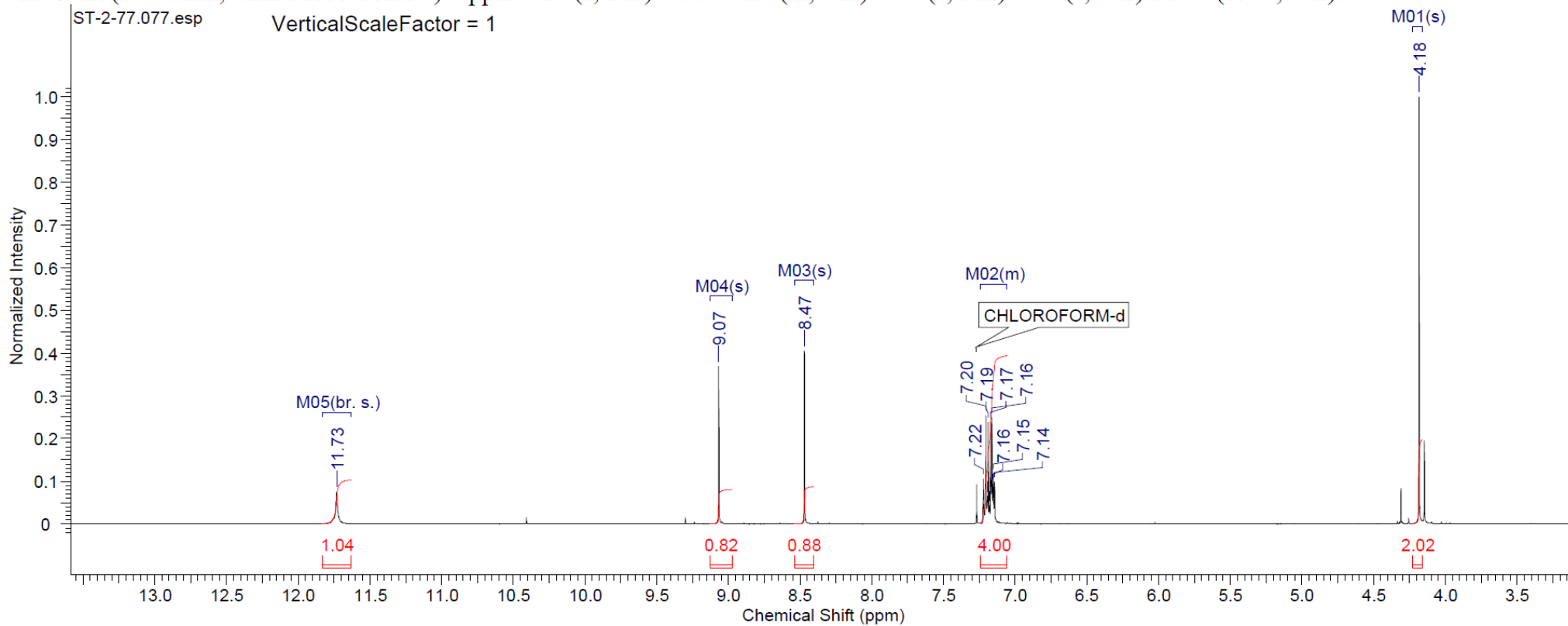
^{13}C NMR (126 MHz, CHLOROFORM- d) δ 39.4, 45.6, 52.3, 103.7, 108.7, 108.9, 109.2, 113.3, 116.7, 118.2, 119.1, 120.5, 120.6, 121.2, 123.2, 129.4, 129.8, 132.5, 133.5, 133.5, 137.7, 140.1, 149.3, 151.8, 151.8, 151.9, 151.9, 153.2, 159.2, 159.6, 159.7, 161.2



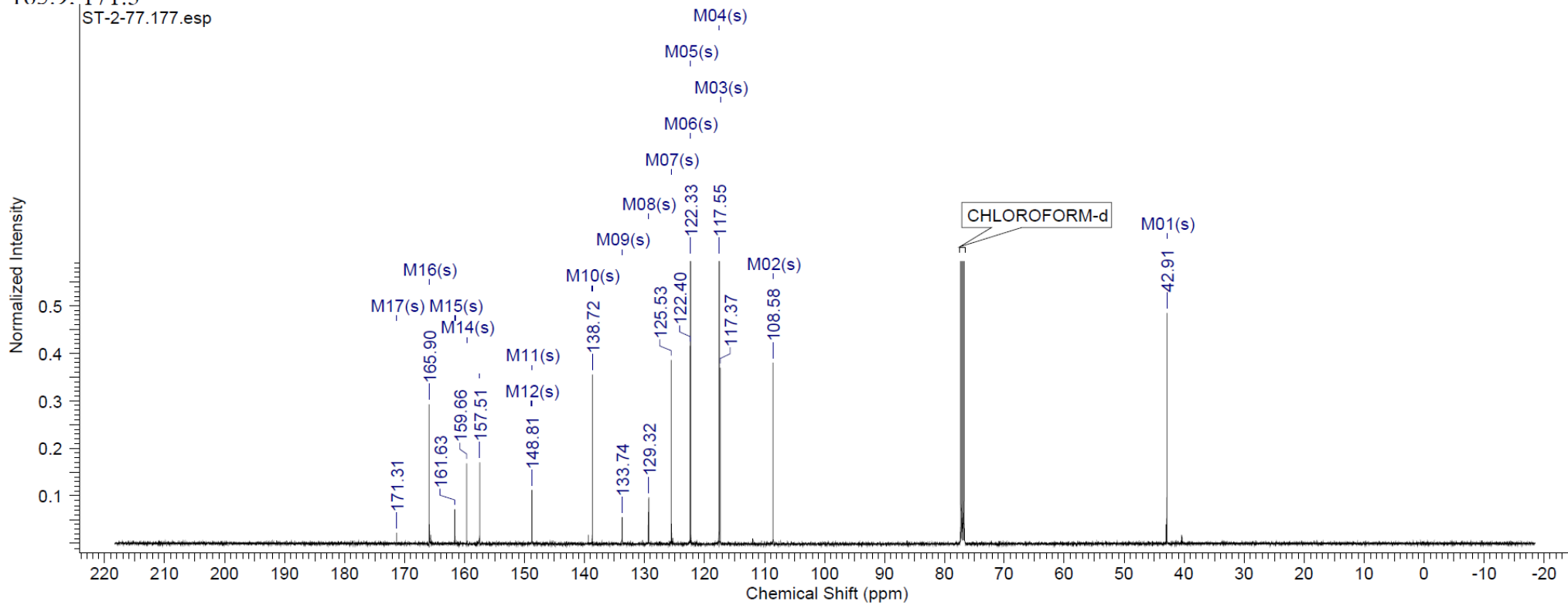
1-Chloromethylcarboxamido-5-(4-fluorophenoxy)-2,4-dinitro benzene



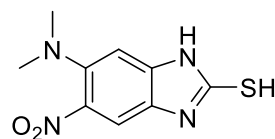
^1H NMR (500 MHz, CHLOROFORM-*d*) δ ppm 4.18 (s, 2 H) 7.06 - 7.24 (m, 4 H) 8.47 (s, 1 H) 9.07 (s, 1 H) 11.73 (br. s., 1 H)



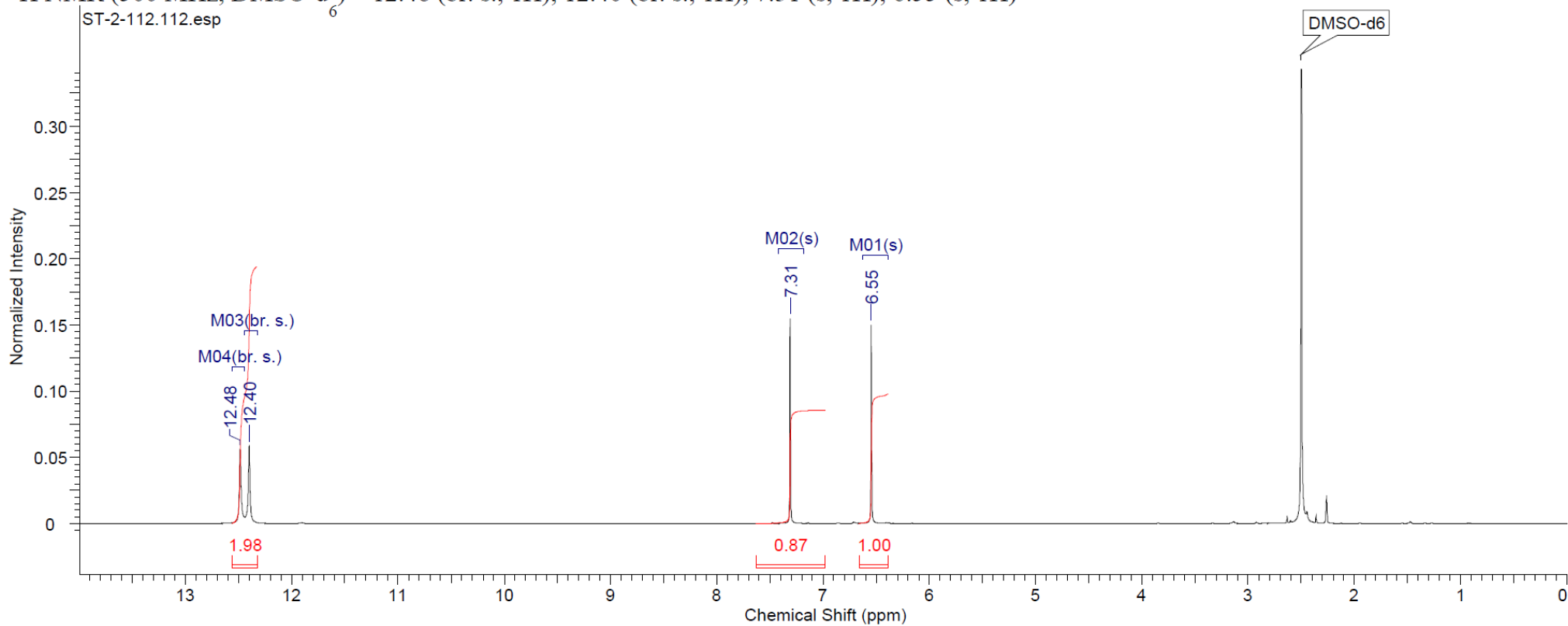
^{13}C NMR (126 MHz, CHLOROFORM- d) δ 42.9, 108.6, 117.4, 117.6, 122.3, 122.4, 125.5, 129.3, 133.7, 138.7, 148.8, 148.8, 157.5, 159.7, 161.6, 165.9, 171.3



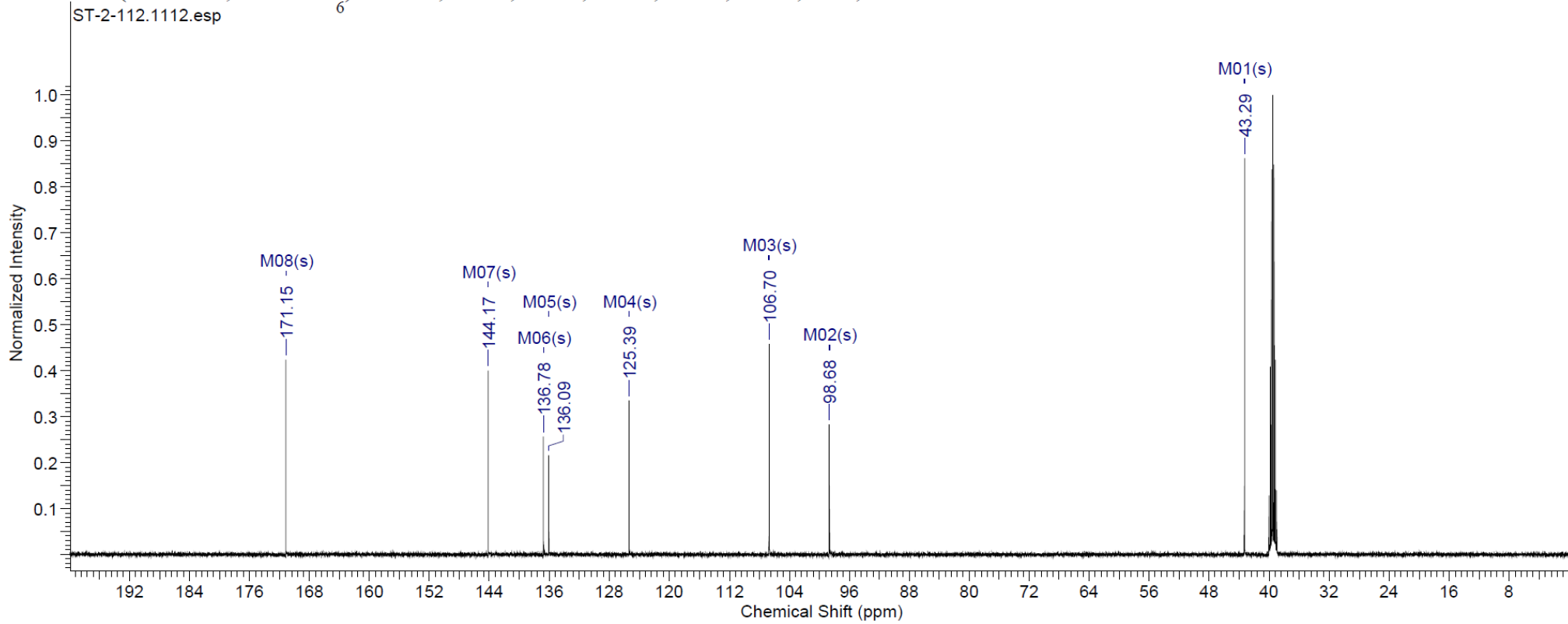
6-*N,N*-Dimethylamino-5-nitro -2-thio-1*H*-benzo[d]imidazole



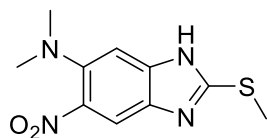
$^1\text{H NMR}$ (500 MHz, DMSO-d_6) δ 12.48 (br. s., 1H), 12.40 (br. s., 1H), 7.31 (s, 1H), 6.55 (s, 1H)



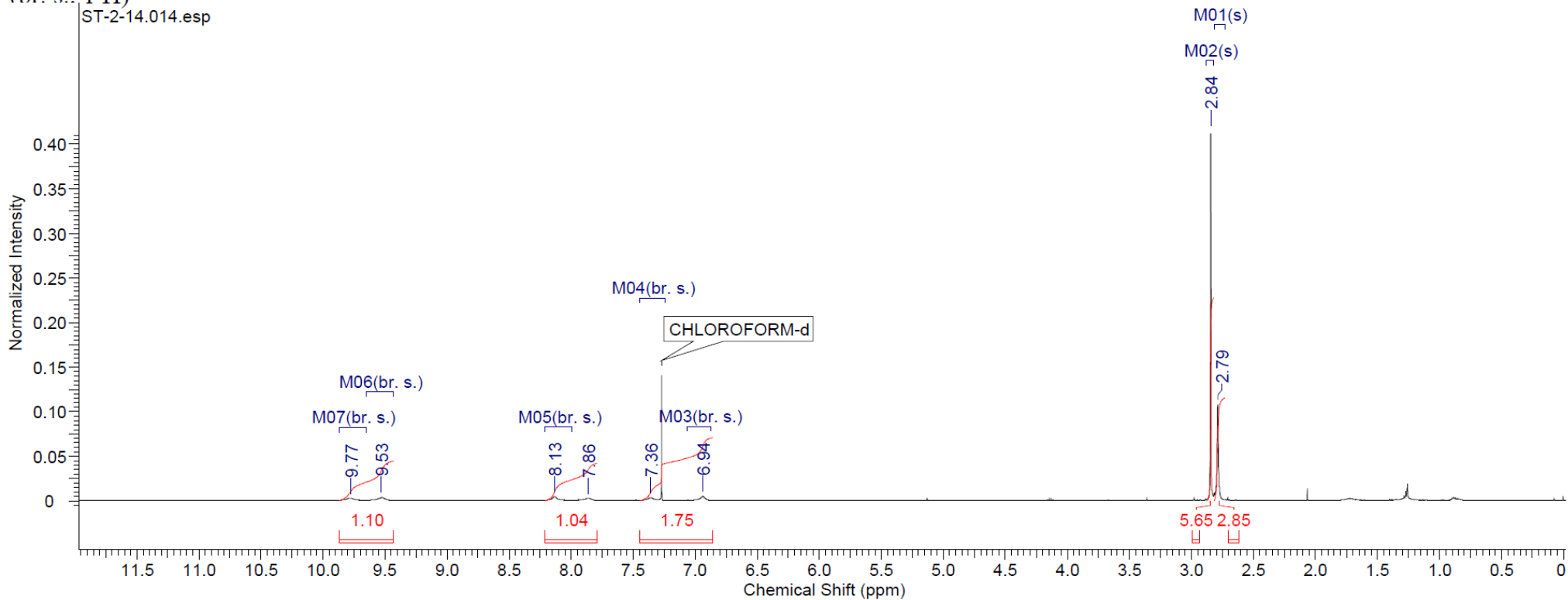
^{13}C NMR (126 MHz, DMSO- d_6) δ 171.2, 144.2, 136.8, 136.1, 125.4, 106.7, 98.7, 43.3



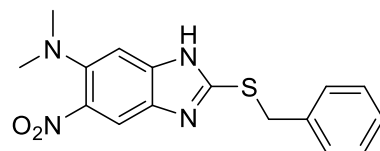
6-*N,N*-Dimethylamino-2-(methylthio)-5-nitro-1*H*-benzo[d]imidazole



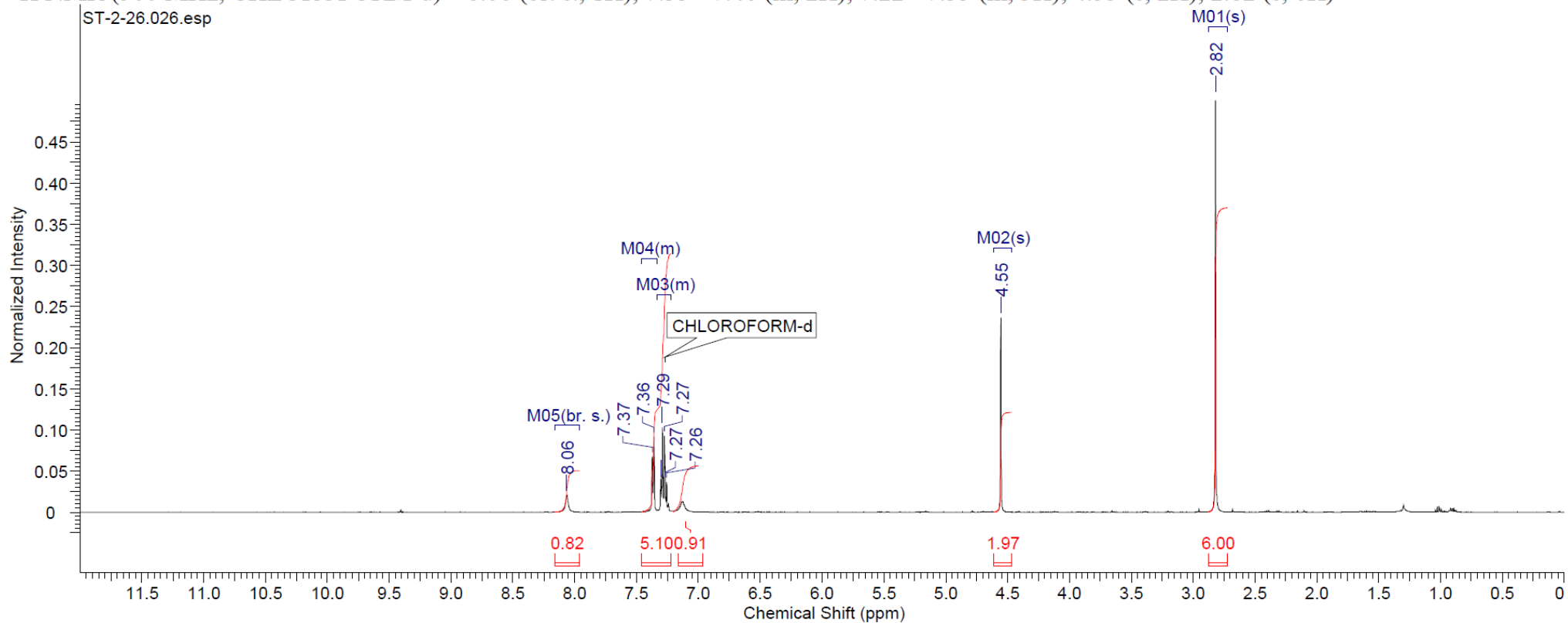
¹H NMR (500 MHz, CHLOROFORM-*d*) δ 2.79 (s, 3 H), 2.84 (s, 6 H), 6.94 (br. s., 1 H), 7.36 (br. s., 1 H), 8.13 (br. s., 1 H), 9.53 (br. s., 1 H), 9.77 (br. s., 1 H)



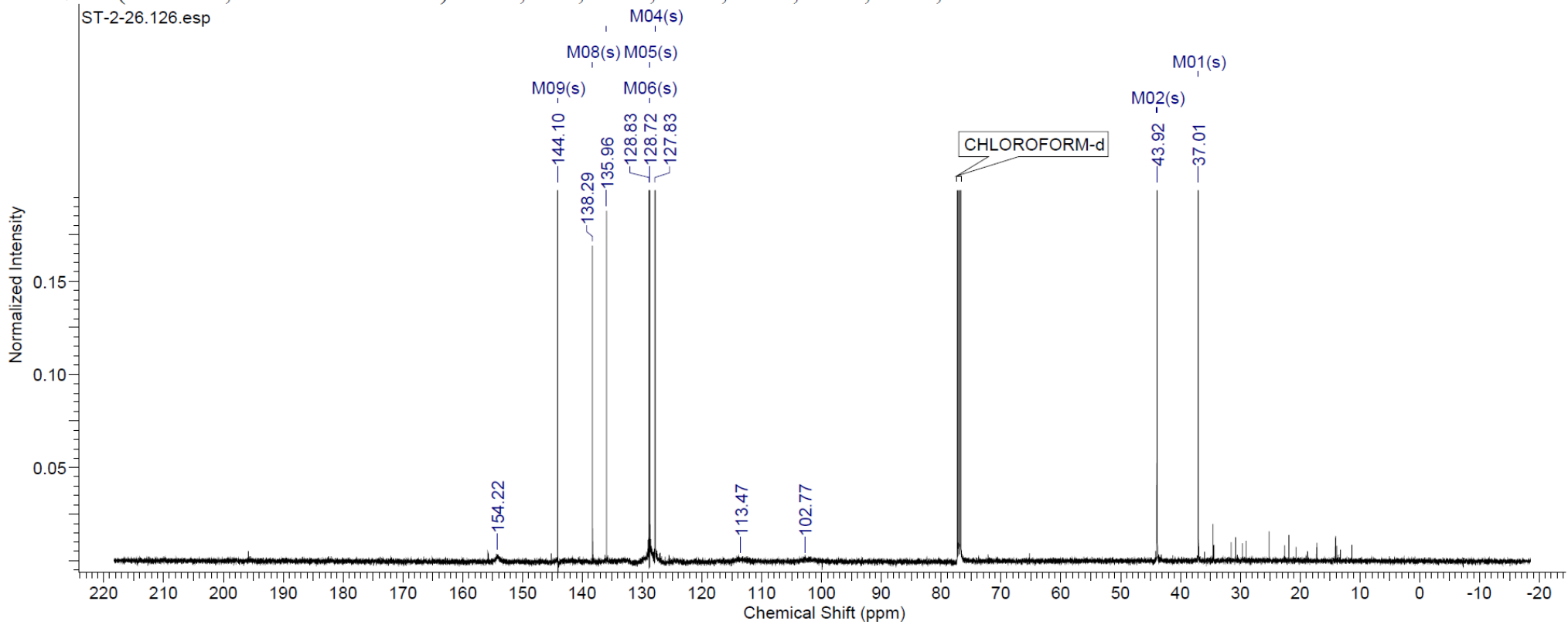
2-(Benzylthio)-6-*N,N*-dimethylamino-5-nitro-1*H*-benzo[d]imidazole



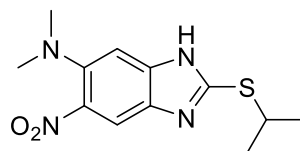
$^1\text{H NMR}$ (500 MHz, CHLOROFORM-*d*) δ 8.06 (br. s., 1H), 7.33 - 7.46 (m, 2H), 7.22 - 7.33 (m, 3H), 4.55 (s, 2H), 2.82 (s, 6H)



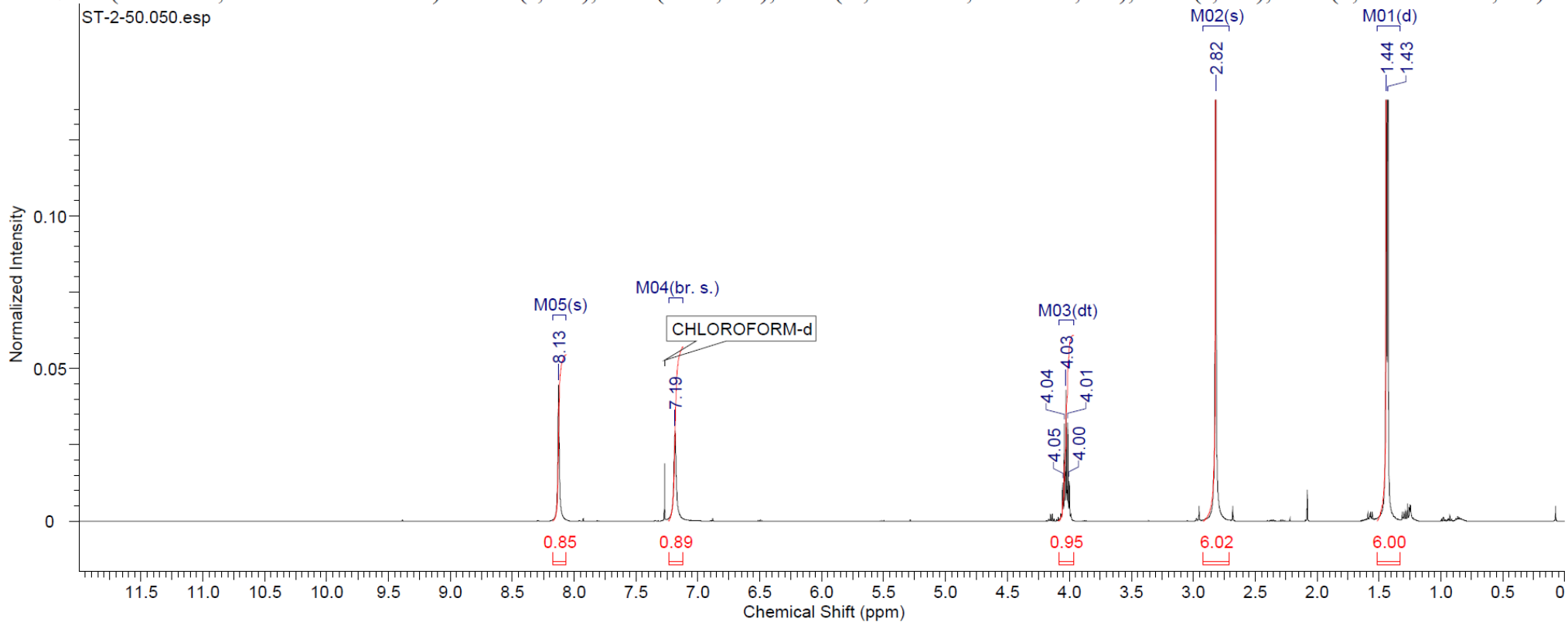
^{13}C NMR (126 MHz, CHLOROFORM-d) δ 37.0, 43.9, 127.8, 128.7, 128.8, 136.0, 138.3, 144.1



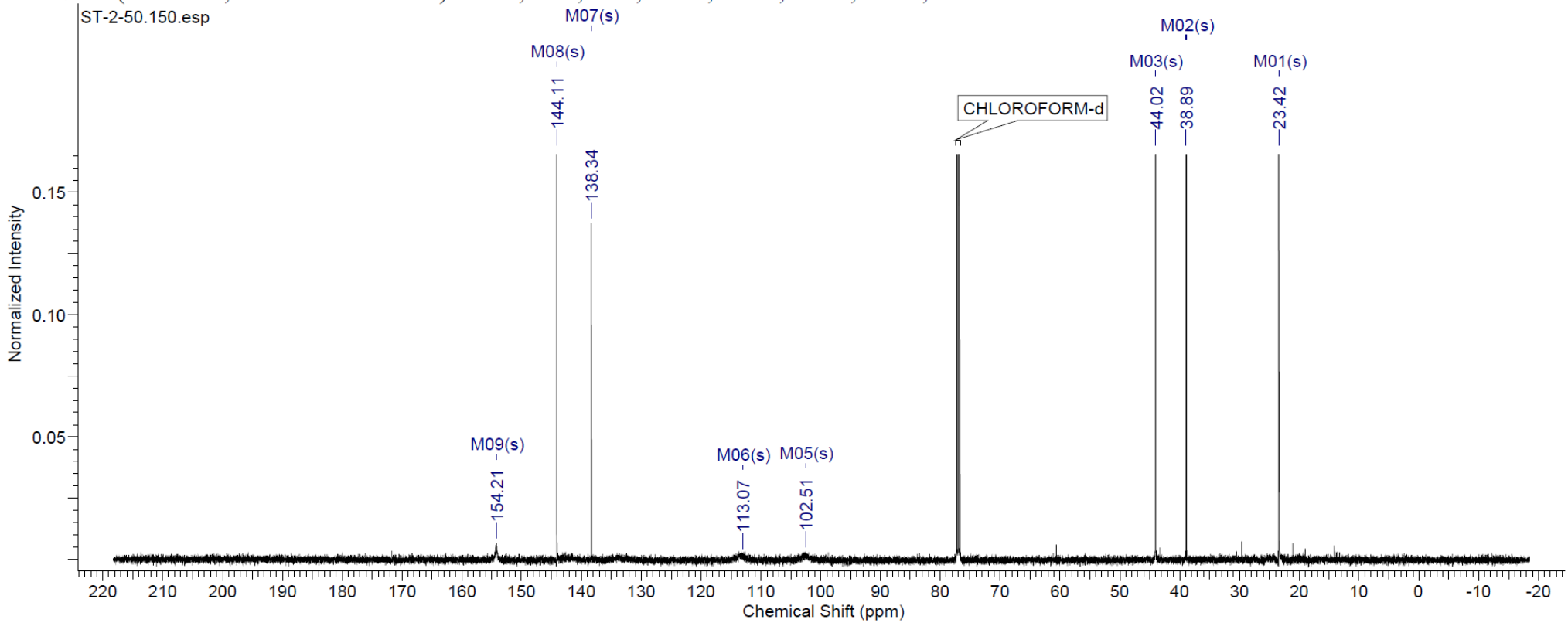
6-*N,N*-Dimethylamino-2-(isopropylthio)-5-nitro-1*H*-benzo[*d*]imidazole



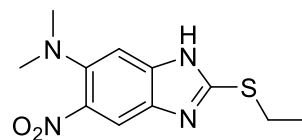
$^1\text{H NMR}$ (500 MHz, CHLOROFORM-*d*) δ 8.13 (s, 1H), 7.19 (br. s., 1H), 4.03 (td, $J = 6.71, 13.43$ Hz, 1H), 2.82 (s, 6H), 1.43 (d, $J = 7.02$ Hz, 6H)



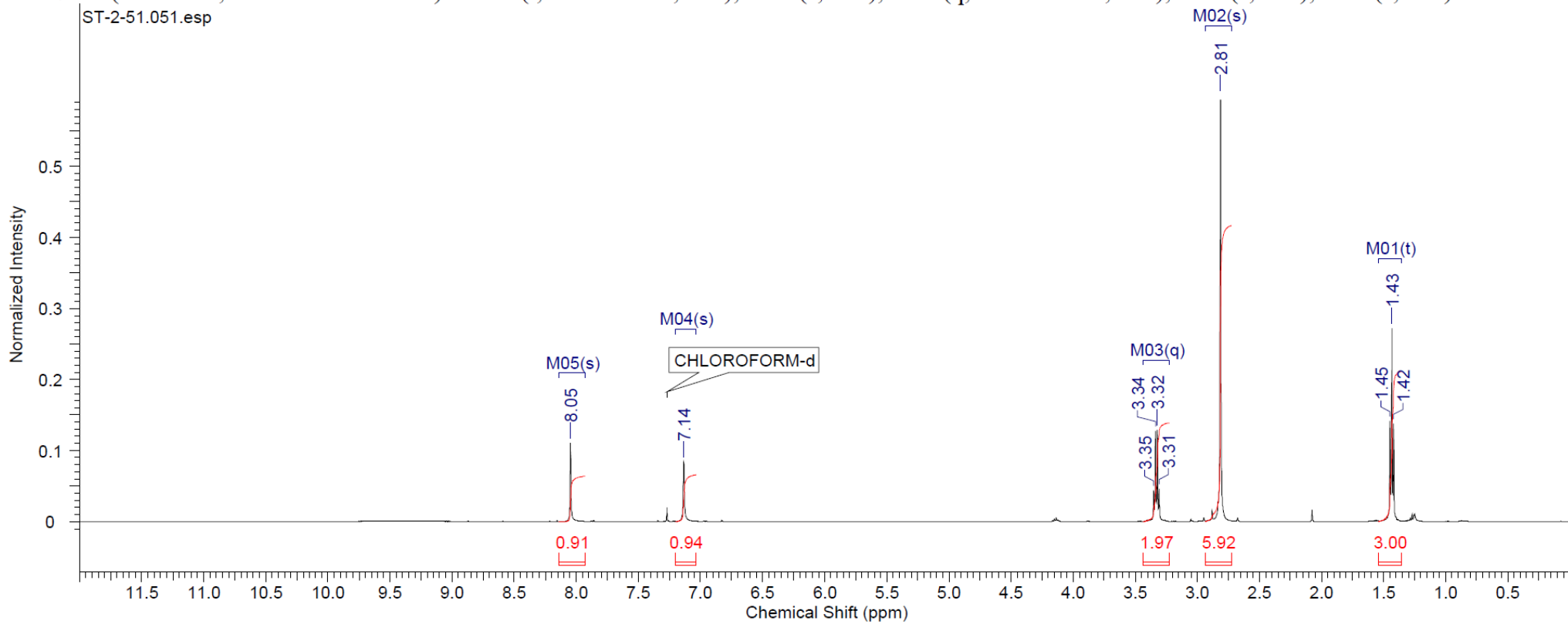
^{13}C NMR (126 MHz, CHLOROFORM-d) δ 23.4, 38.9, 44.0, 102.5, 113.1, 138.3, 144.1, 154.2



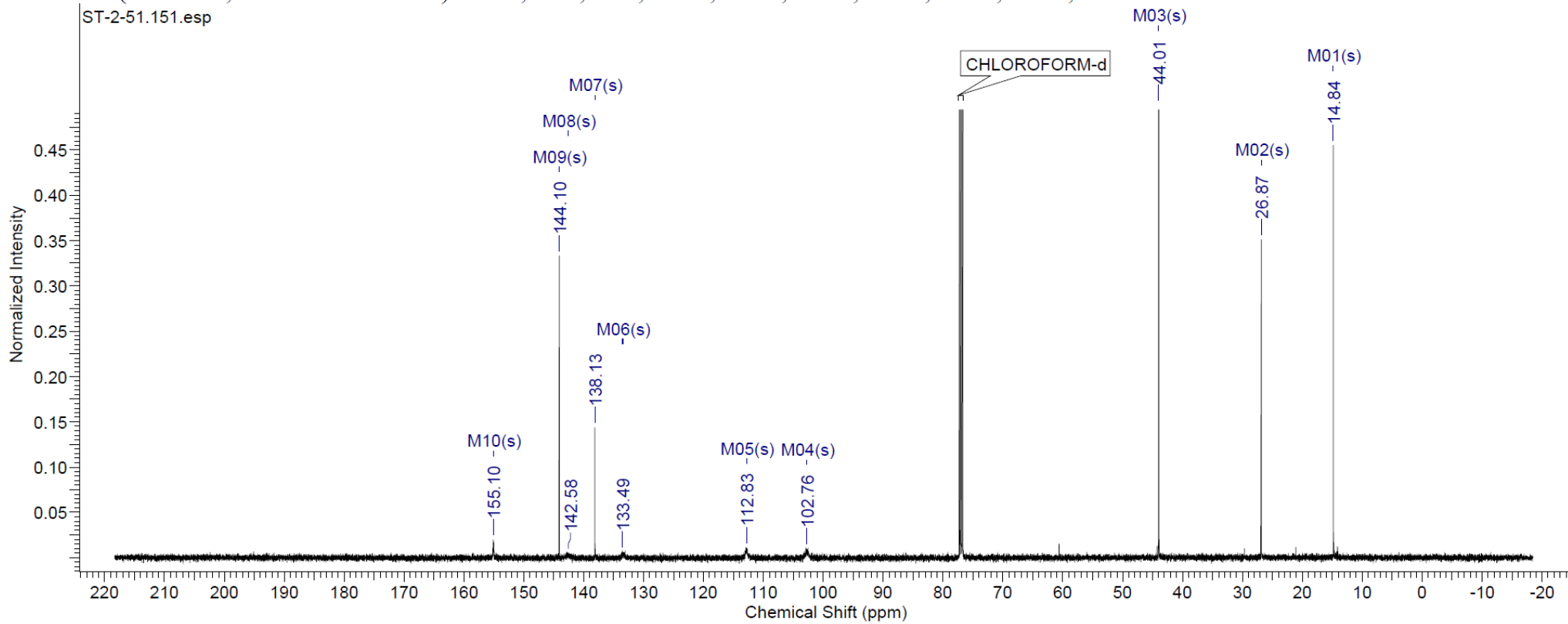
6-*N,N*-Dimethylamino-2-(ethylthio)-5-nitro-1*H*-benzo[d]imidazole



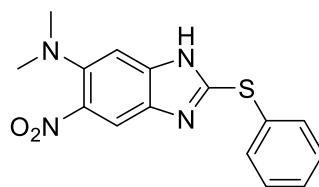
¹H NMR (500 MHz, CHLOROFORM-*d*) δ 1.43 (t, *J* = 7.32 Hz, 3 H), 2.81 (s, 6 H), 3.33 (q, *J* = 7.53 Hz, 2 H), 7.14 (s, 1 H), 8.05 (s, 1 H)



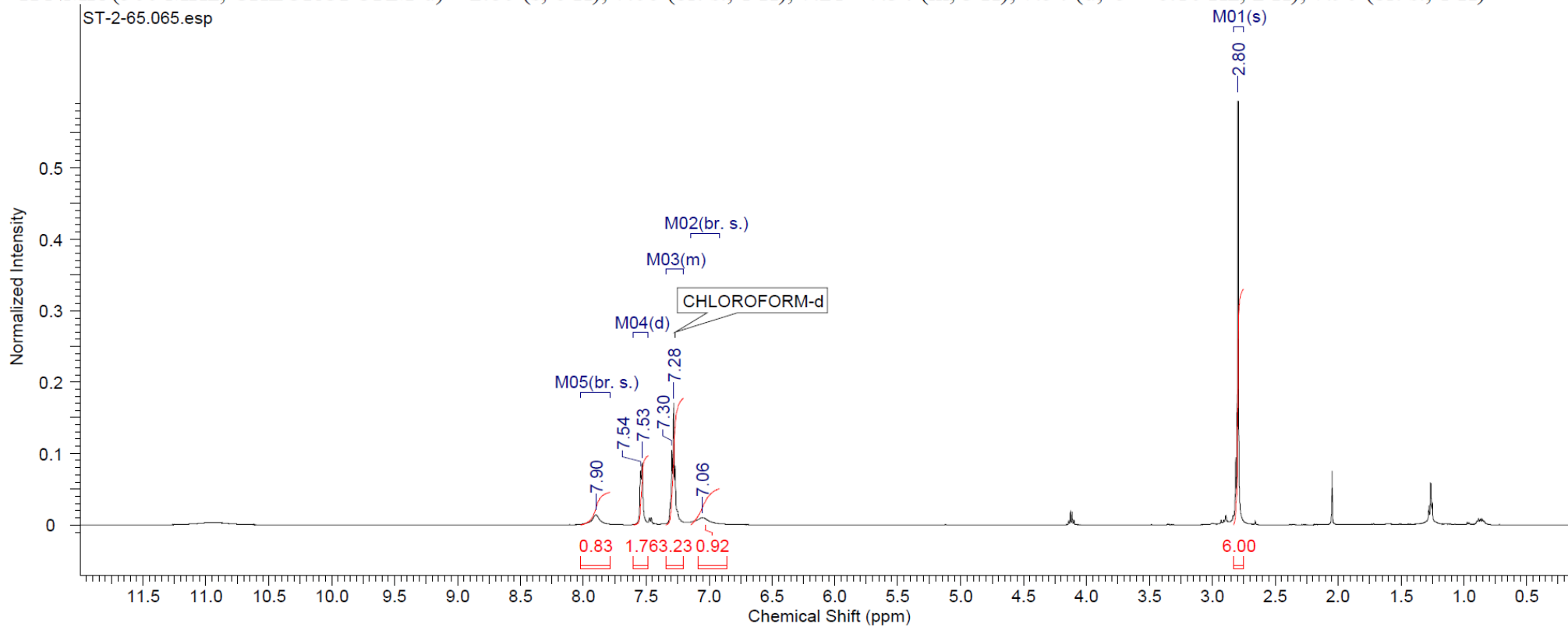
^{13}C NMR (126 MHz, CHLOROFORM-d) δ 14.8, 26.9, 44.0, 102.8, 112.8, 133.5, 138.1, 142.6, 144.1, 155.1



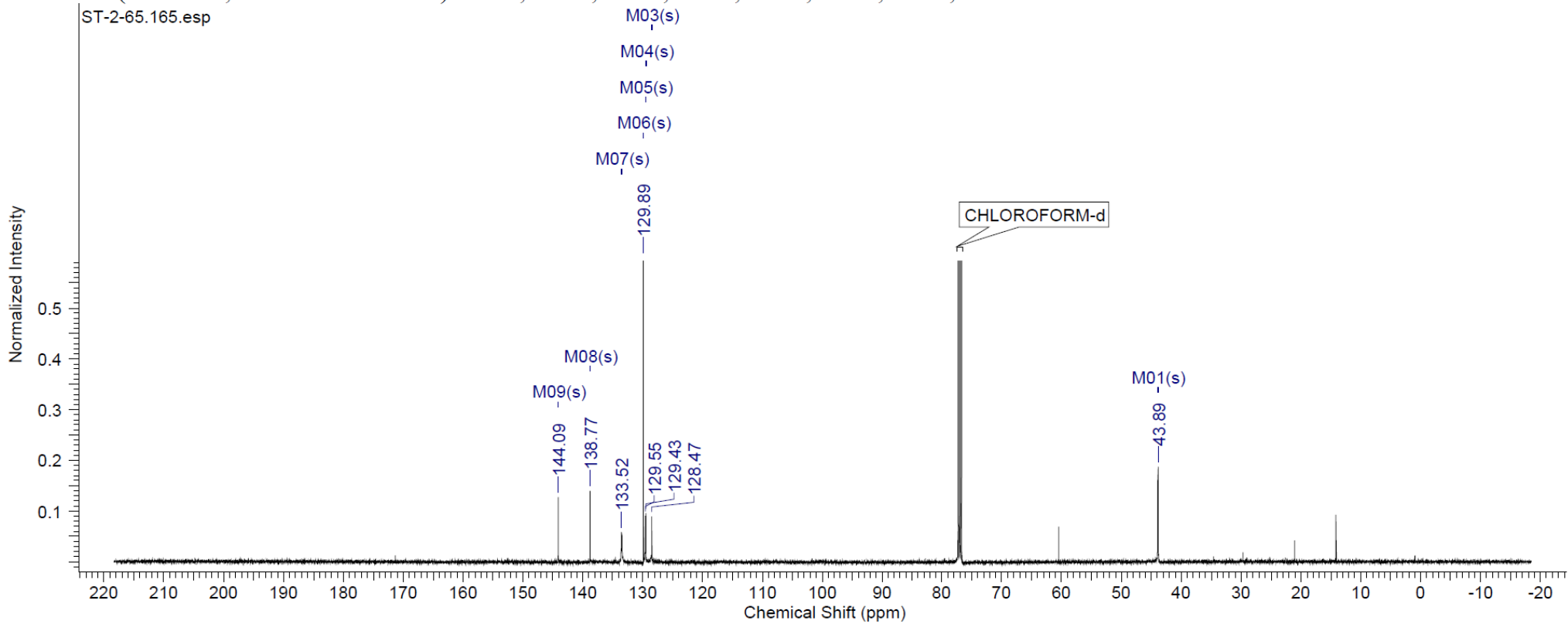
6-*N,N*-Dimethylamino-5-nitro-2-(phenylthio)-1*H*-benzo[d]imidazole



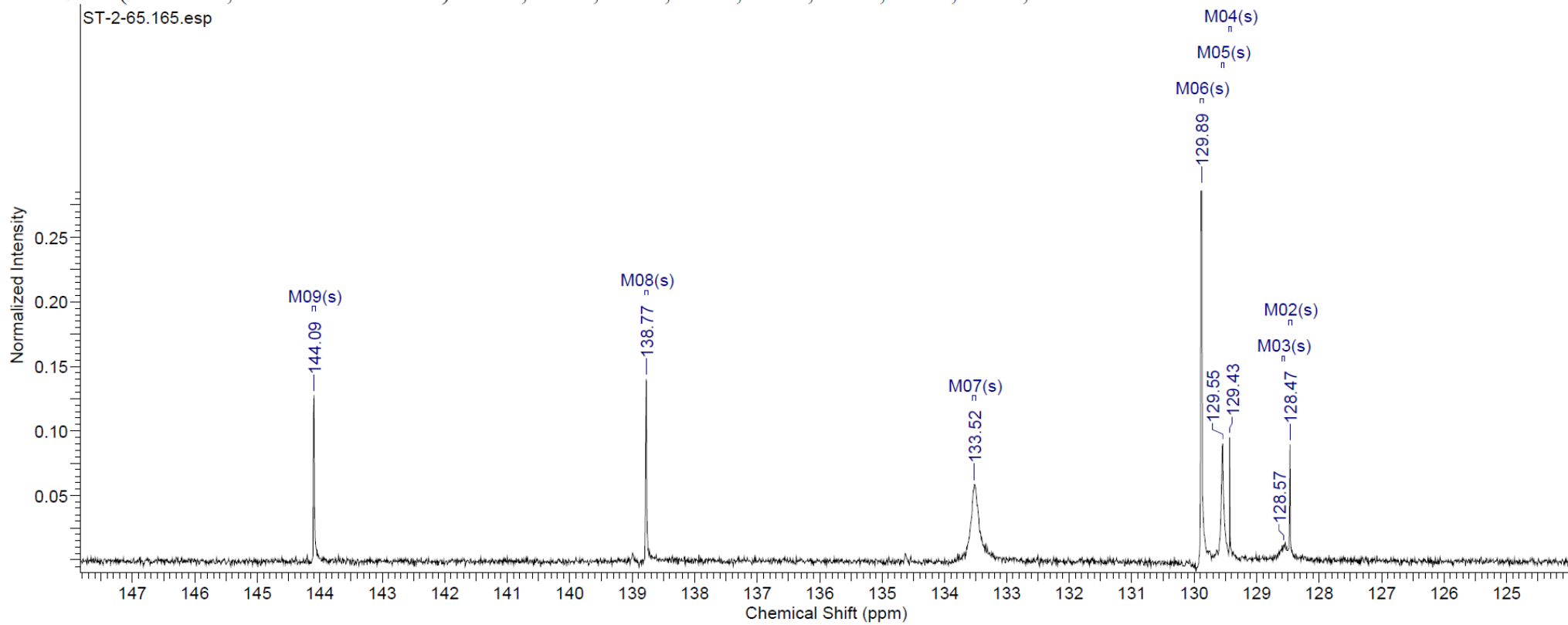
¹H NMR (500 MHz, CHLOROFORM-*d*) δ 2.80 (s, 6 H), 7.06 (br. s., 1 H), 7.21 - 7.34 (m, 3 H), 7.54 (d, $J = 6.10$ Hz, 2 H), 7.90 (br. s., 1 H)



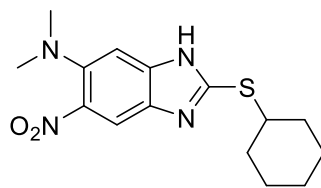
^{13}C NMR (126 MHz, CHLOROFORM-d) δ 43.9, 128.5, 129.4, 129.5, 129.9, 133.5, 138.8, 144.1



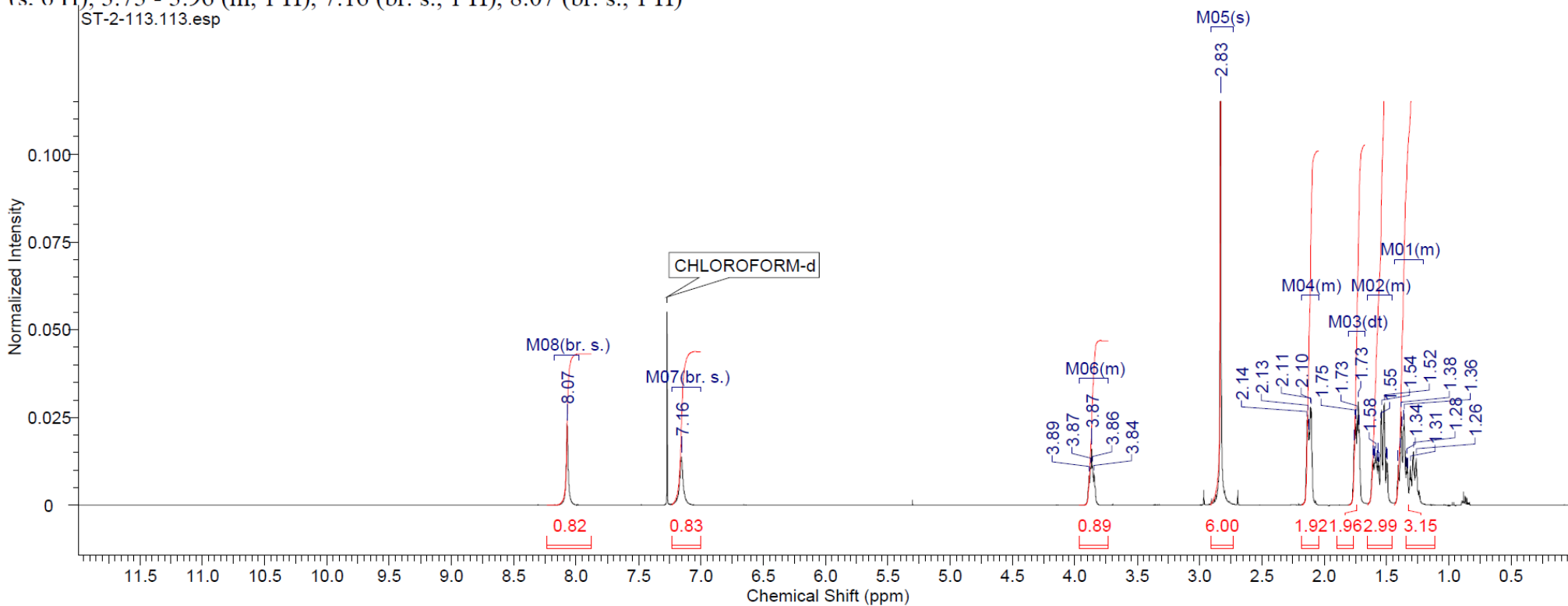
^{13}C NMR (126 MHz, CHLOROFORM- d) δ 43.9, 128.5, 128.6, 129.4, 129.5, 129.9, 133.5, 138.8, 144.1



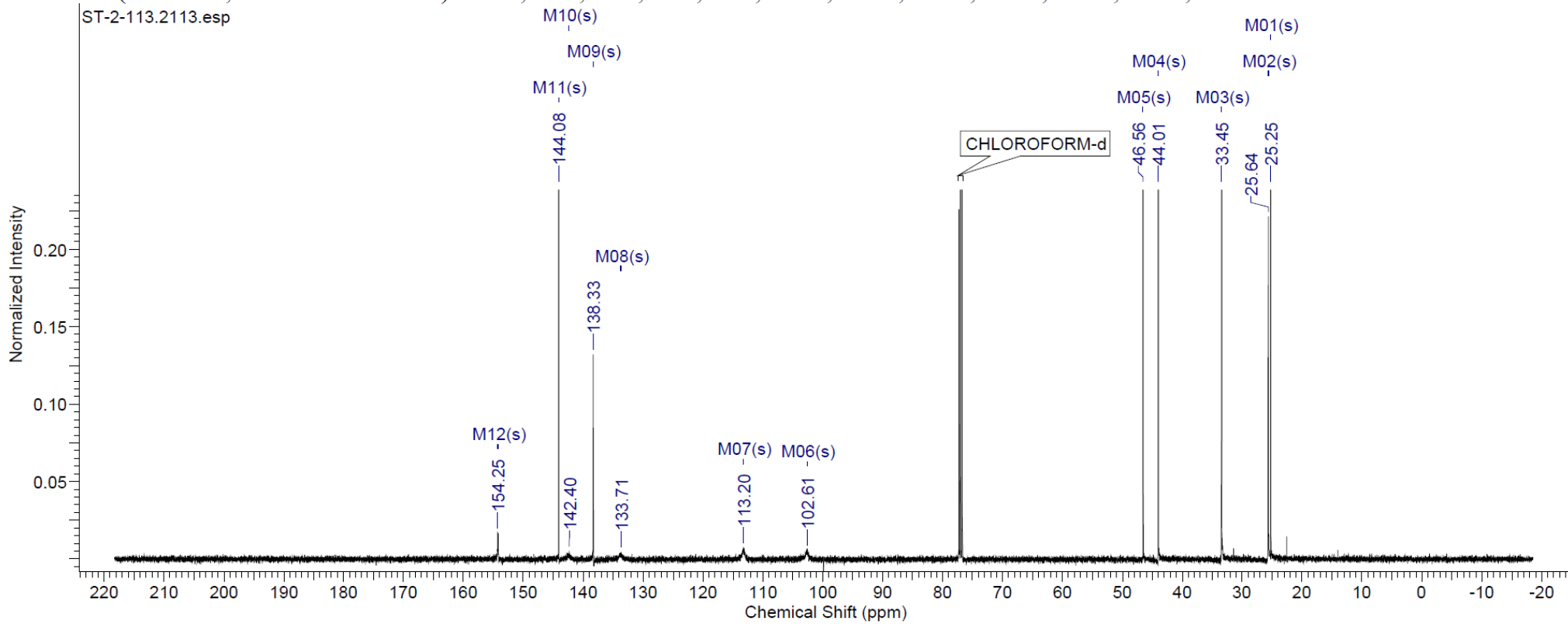
6-*N,N*-Dimethylamino-5-nitro-2-(cyclohexylthio)-1*H*-benzo[d]imidazole



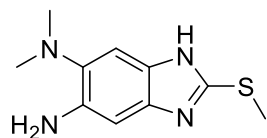
¹H NMR (500 MHz, CHLOROFORM-*d*) δ 1.21 - 1.44 (m, 3 H), 1.46 - 1.65 (m, 3 H), 1.74 (dt, $J = 13.28, 3.89$ Hz, 2 H), 2.04 - 2.18 (m, 2 H), 2.83 (s, 6 H), 3.73 - 3.96 (m, 1 H), 7.16 (br. s., 1 H), 8.07 (br. s., 1 H)



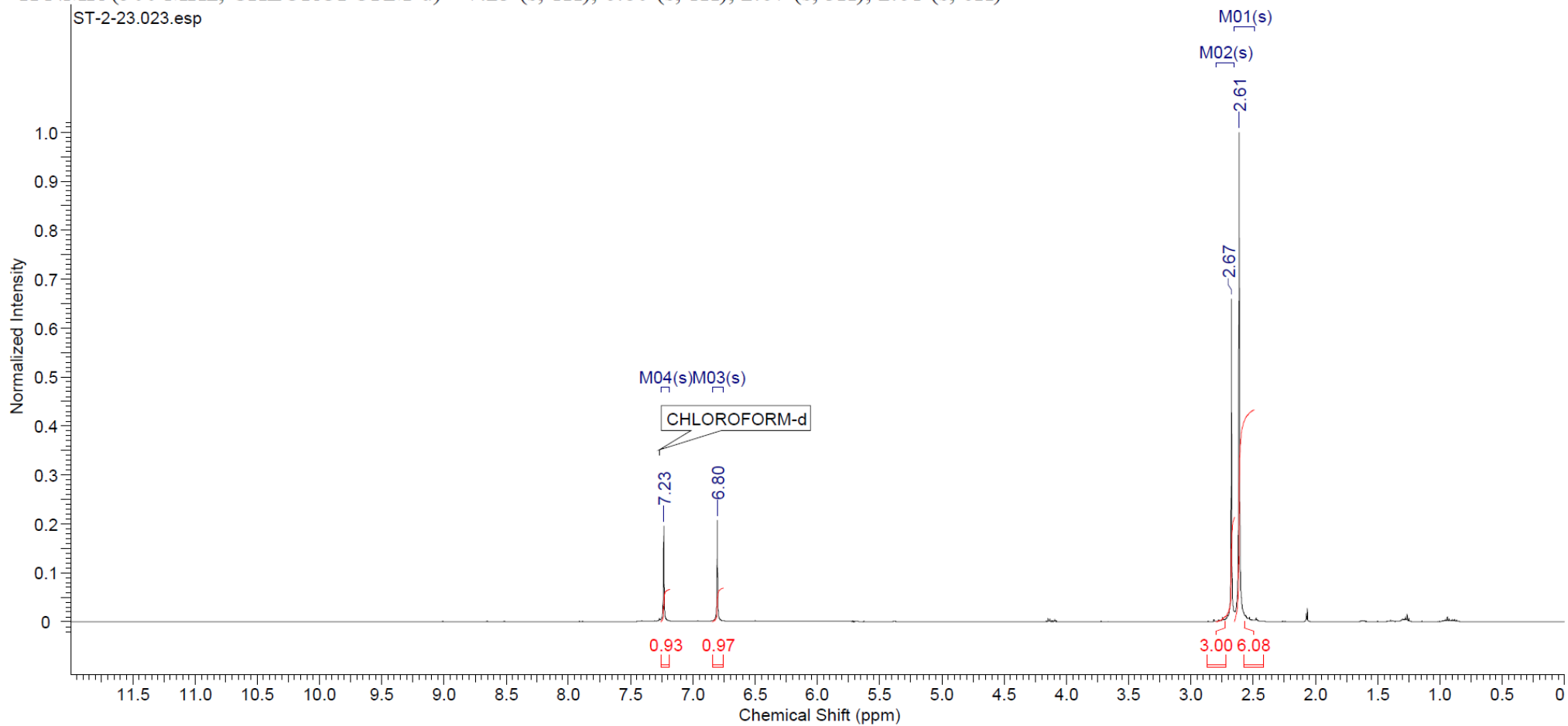
^{13}C NMR (126 MHz, CHLOROFORM-d) δ 25.3, 25.6, 33.4, 44.0, 46.6, 102.6, 113.2, 133.7, 138.3, 142.4, 144.1, 154.3



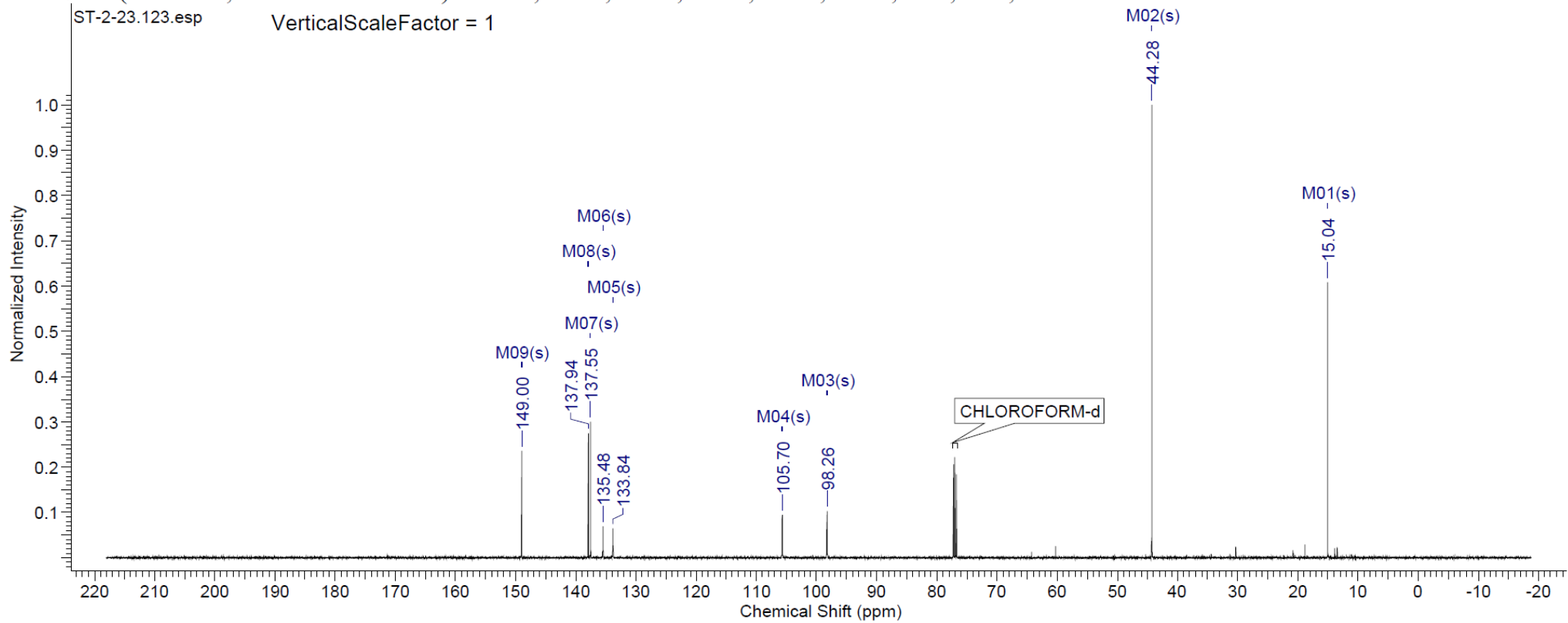
5-Amino-6-*N,N*-dimethylamino-2-(methylthio)-1*H*-benzo[d]imidazole



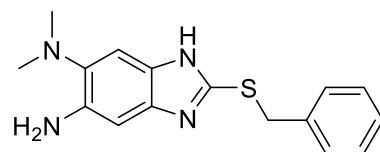
$^1\text{H NMR}$ (500 MHz, CHLOROFORM- d) δ 7.23 (s, 1H), 6.80 (s, 1H), 2.67 (s, 3H), 2.61 (s, 6H)



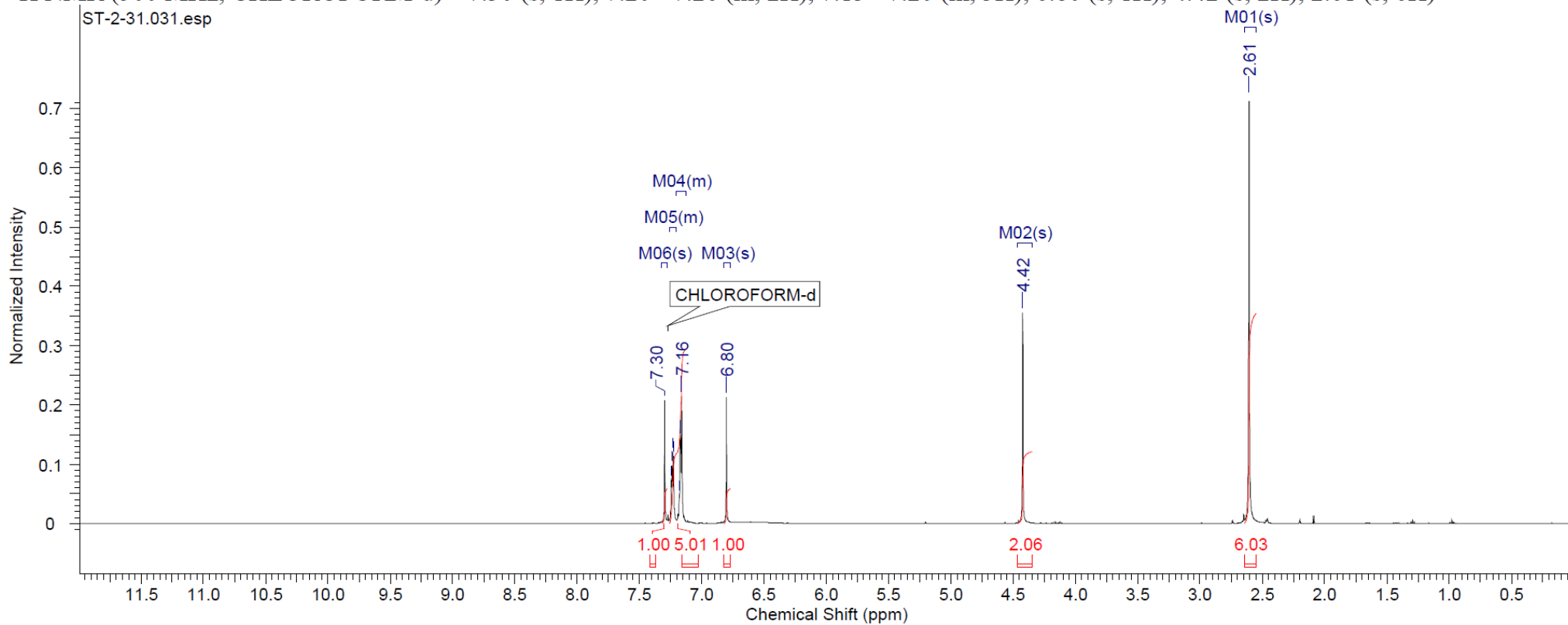
^{13}C NMR (126 MHz, CHLOROFORM- d) δ 149.0, 137.9, 137.5, 135.5, 133.8, 105.7, 98.3, 44.3, 15.0



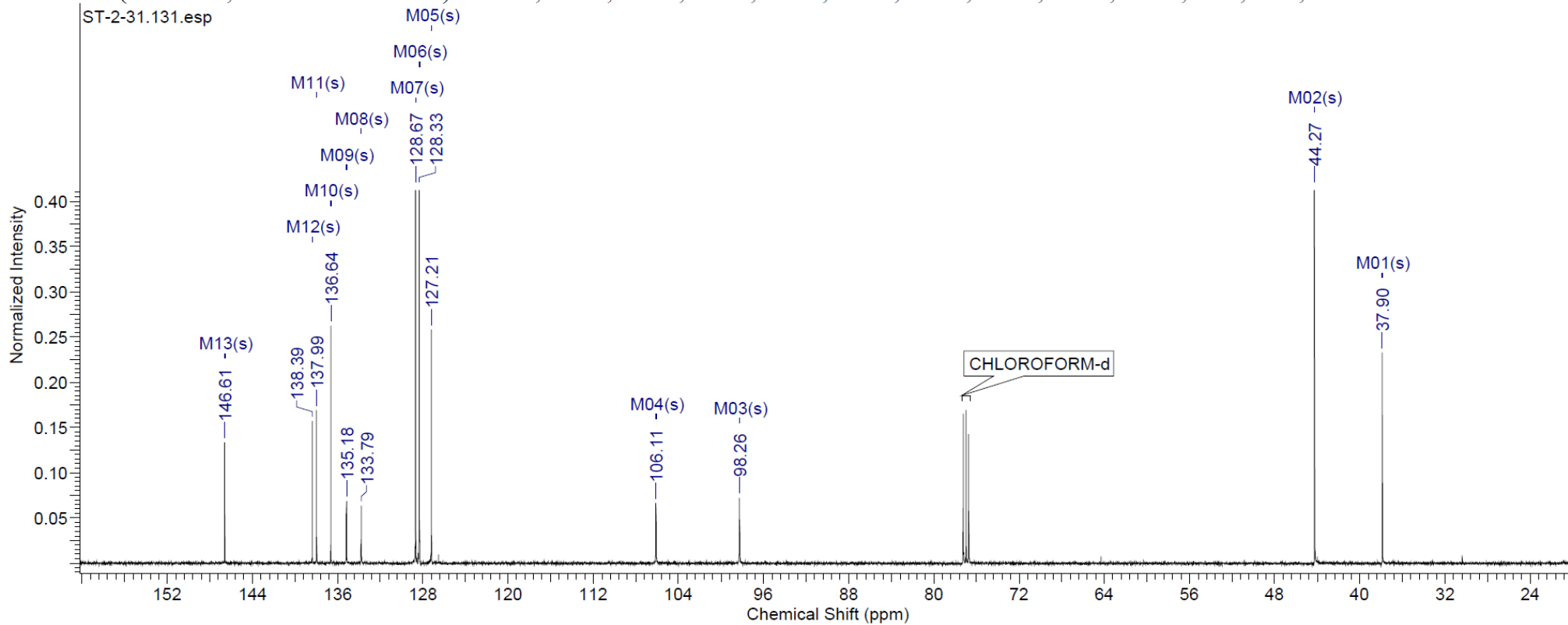
5-Amino-2-(benzylthio)-6-*N,N*-dimethylamino-1*H*-benzo[d]imidazole



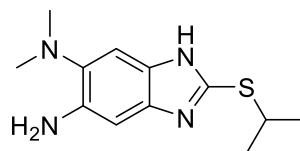
$^1\text{H NMR}$ (500 MHz, CHLOROFORM-*d*) δ 7.30 (s, 1H), 7.20 - 7.26 (m, 2H), 7.13 - 7.20 (m, 3H), 6.80 (s, 1H), 4.42 (s, 2H), 2.61 (s, 6H)



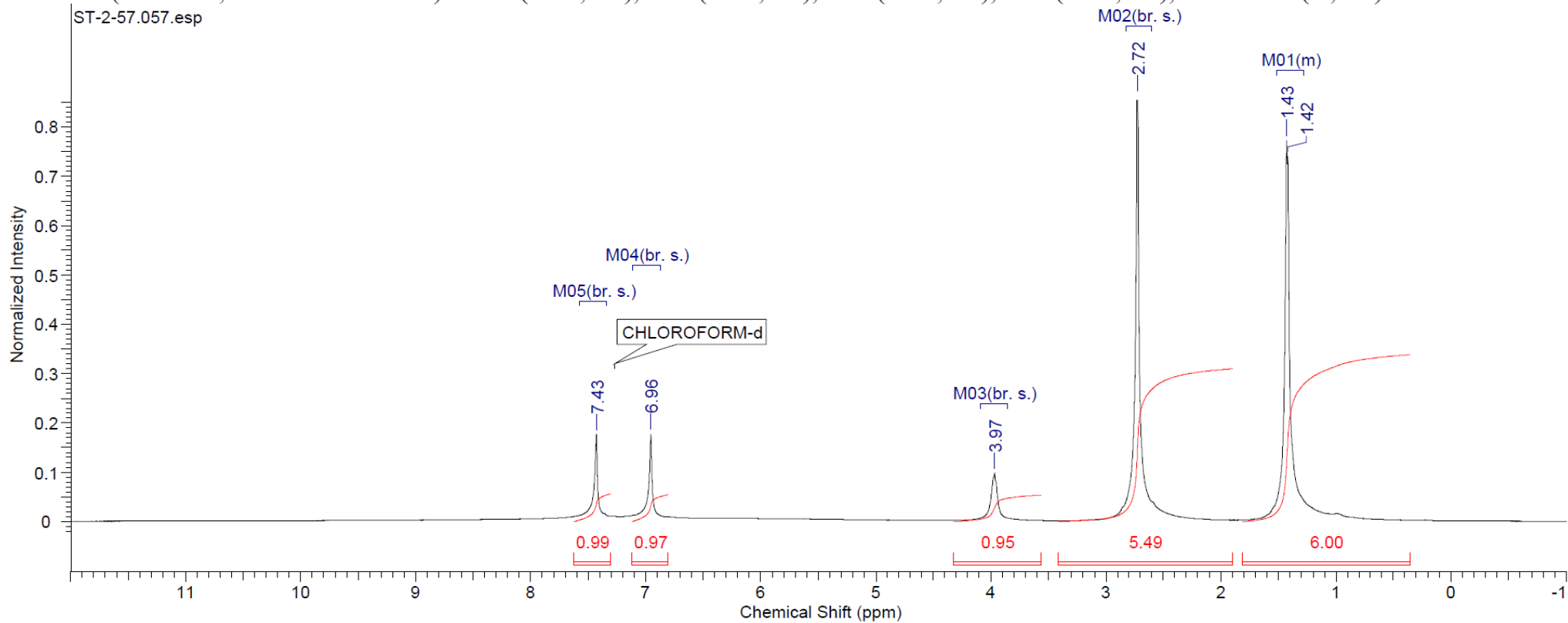
^{13}C NMR (126 MHz, CHLOROFORM- d) δ 146.6, 138.4, 138.0, 136.6, 135.2, 133.8, 128.7, 128.3, 127.2, 106.1, 98.3, 44.3, 37.9



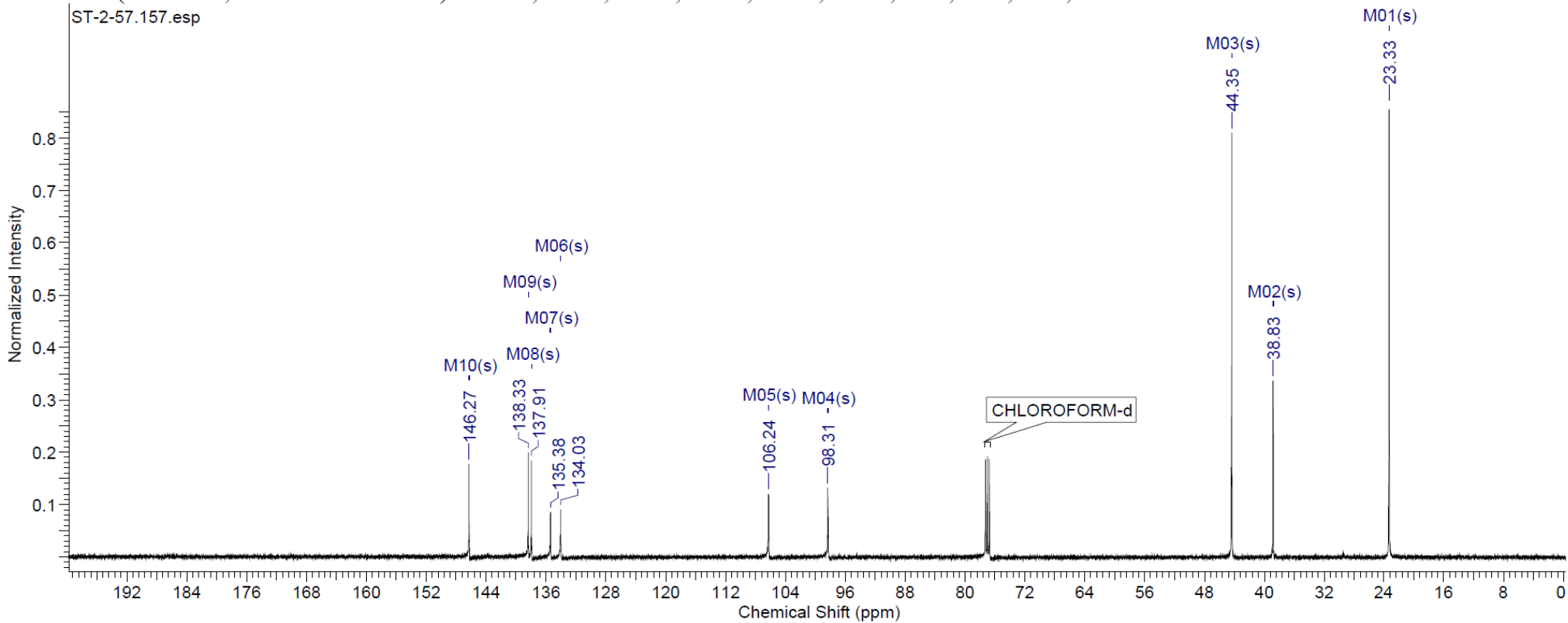
5-Amino-6-*N,N*-dimethylamino-2-(isopropylthio)-1*H*-benzo[d]imidazole



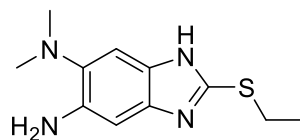
^1H NMR (500 MHz, CHLOROFORM-*d*) δ 7.43 (br. s., 1H), 6.96 (br. s., 1H), 3.97 (br. s., 1H), 2.72 (br. s., 6H), 1.28 - 1.51 (m, 6H)



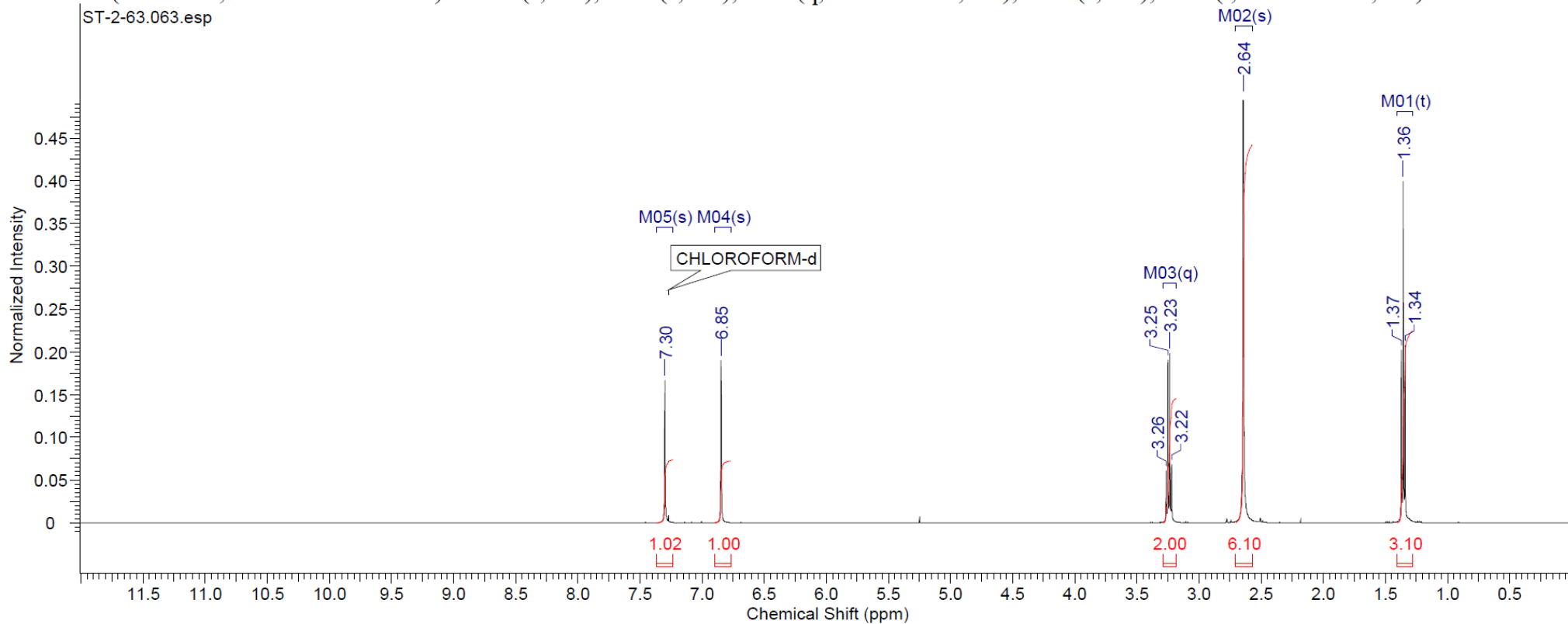
^{13}C NMR (126 MHz, CHLOROFORM-d) δ 146.3, 138.3, 137.9, 135.4, 134.0, 106.2, 98.3, 44.3, 38.8, 23.3



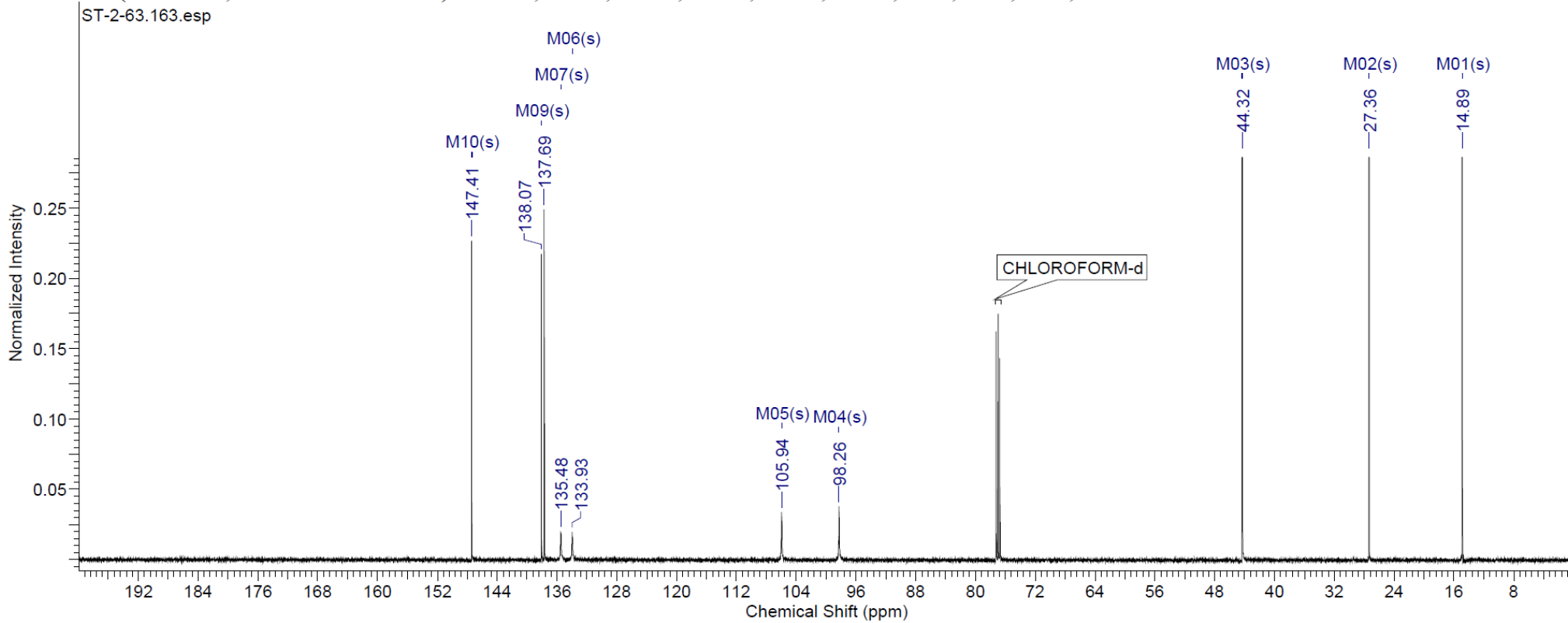
5-Amino-6-*N,N*-dimethylamino-2-(ethylthio)-1*H*-benzo[d]imidazole



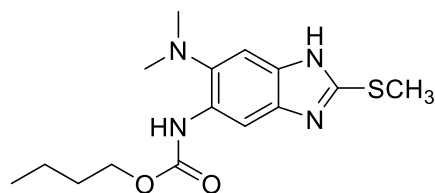
^1H NMR (500 MHz, CHLOROFORM-*d*) δ 7.30 (s, 1H), 6.85 (s, 1H), 3.24 (q, $J = 7.43$ Hz, 2H), 2.64 (s, 6H), 1.36 (t, $J = 7.48$ Hz, 3H)



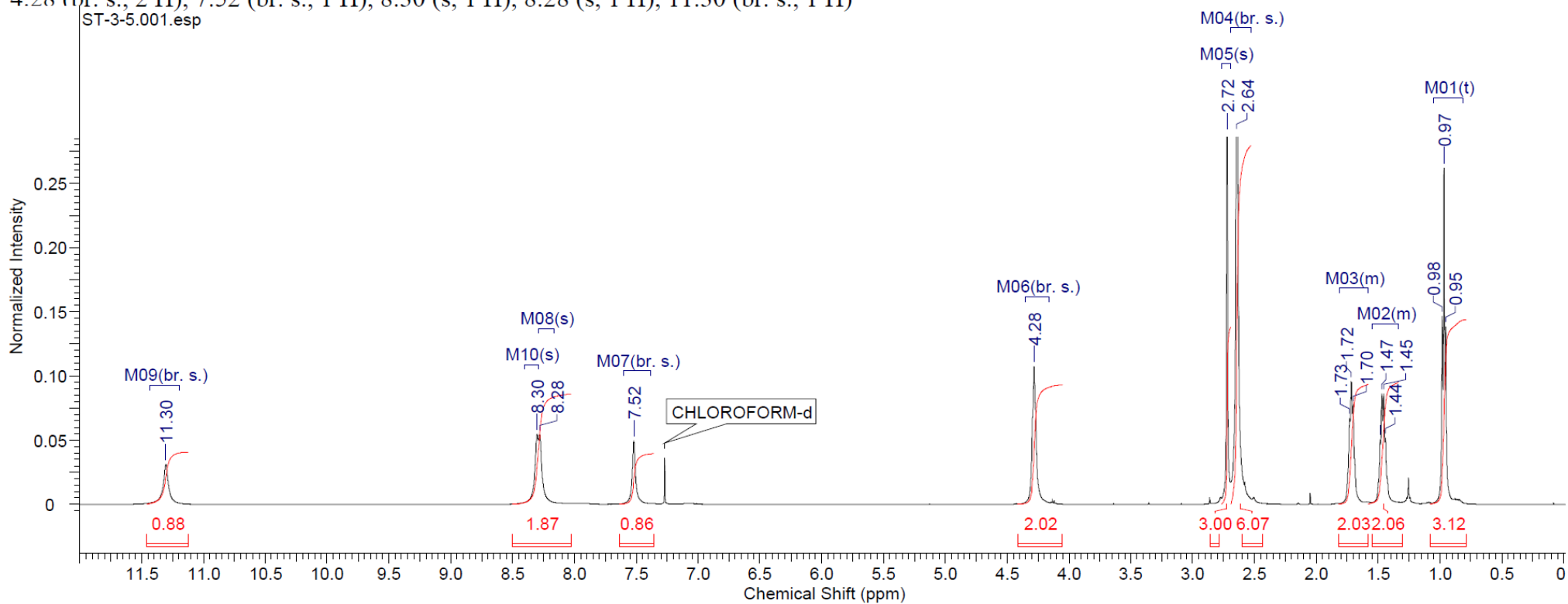
^{13}C NMR (126 MHz, CHLOROFORM-d) δ 147.4, 138.1, 137.7, 135.5, 133.9, 105.9, 98.3, 44.3, 27.4, 14.9



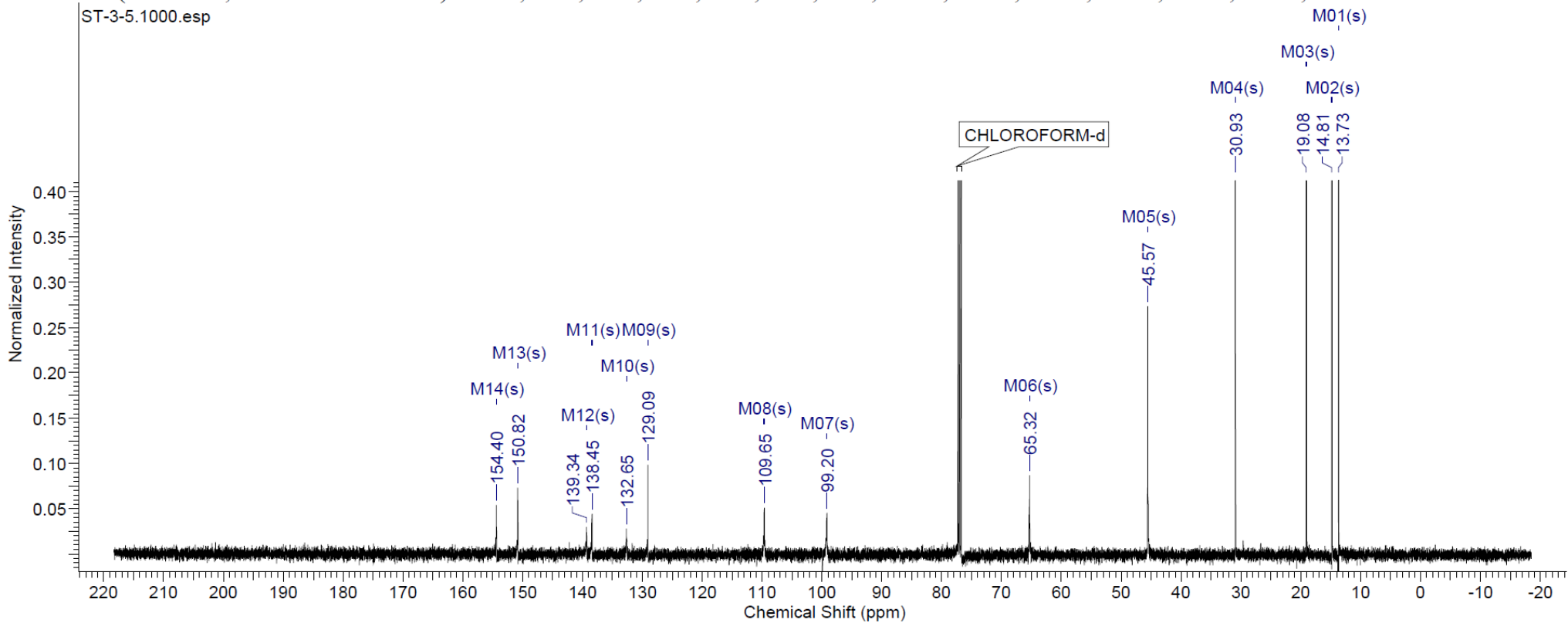
5-Butyloxycarbonylamino-6-*N,N*-dimethylamino-2-(methylthio)-1*H*-benzo[d]imidazole



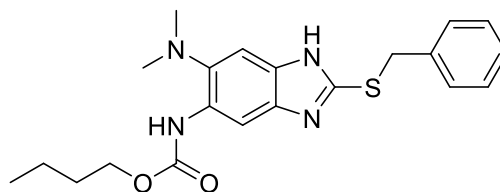
^1H NMR (500 MHz, CHLOROFORM-*d*) δ 0.97 (t, $J = 7.32$ Hz, 3 H), 1.34 - 1.55 (m, 2 H), 1.58 - 1.82 (m, 2 H), 2.64 (br. s., 6 H), 2.72 (s, 3 H), 4.28 (br. s., 2 H), 7.52 (br. s., 1 H), 8.30 (s, 1 H), 8.28 (s, 1 H), 11.30 (br. s., 1 H)



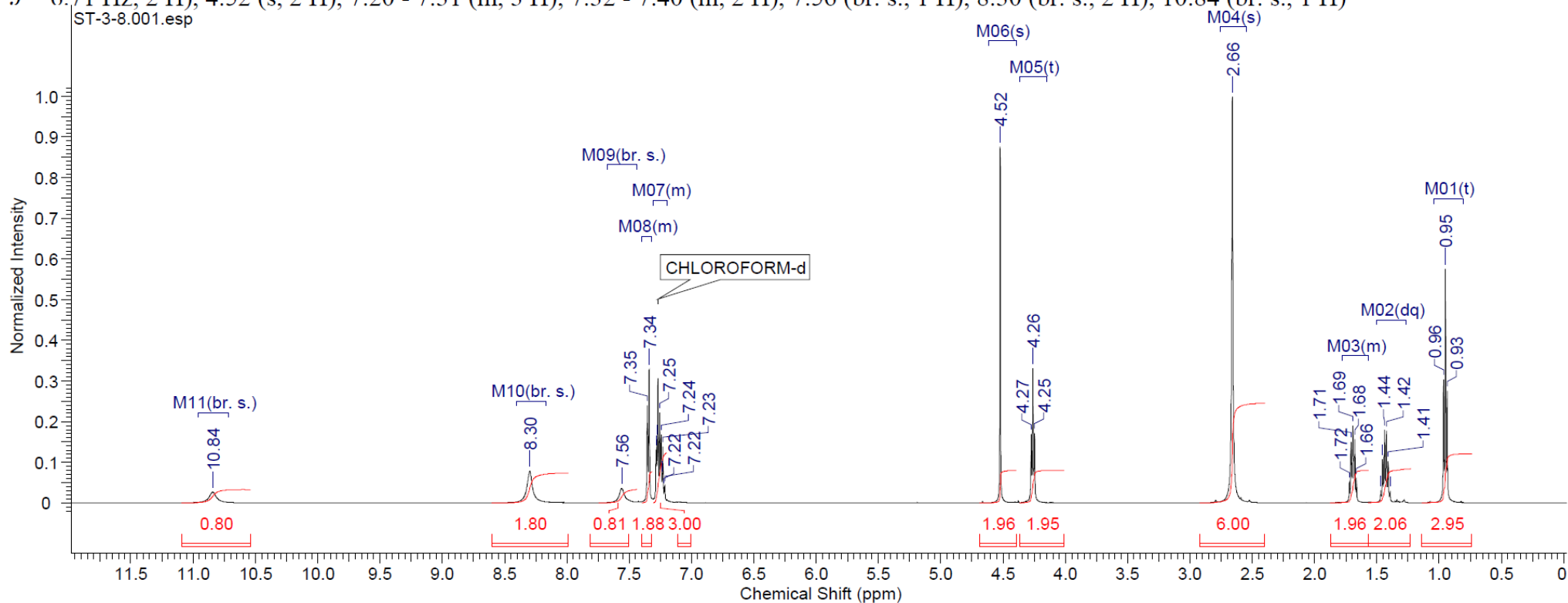
^{13}C NMR (126 MHz, CHLOROFORM-d) δ 13.7, 14.8, 19.1, 30.9, 45.6, 65.3, 99.2, 109.7, 129.1, 132.7, 138.4, 139.3, 150.8, 154.4



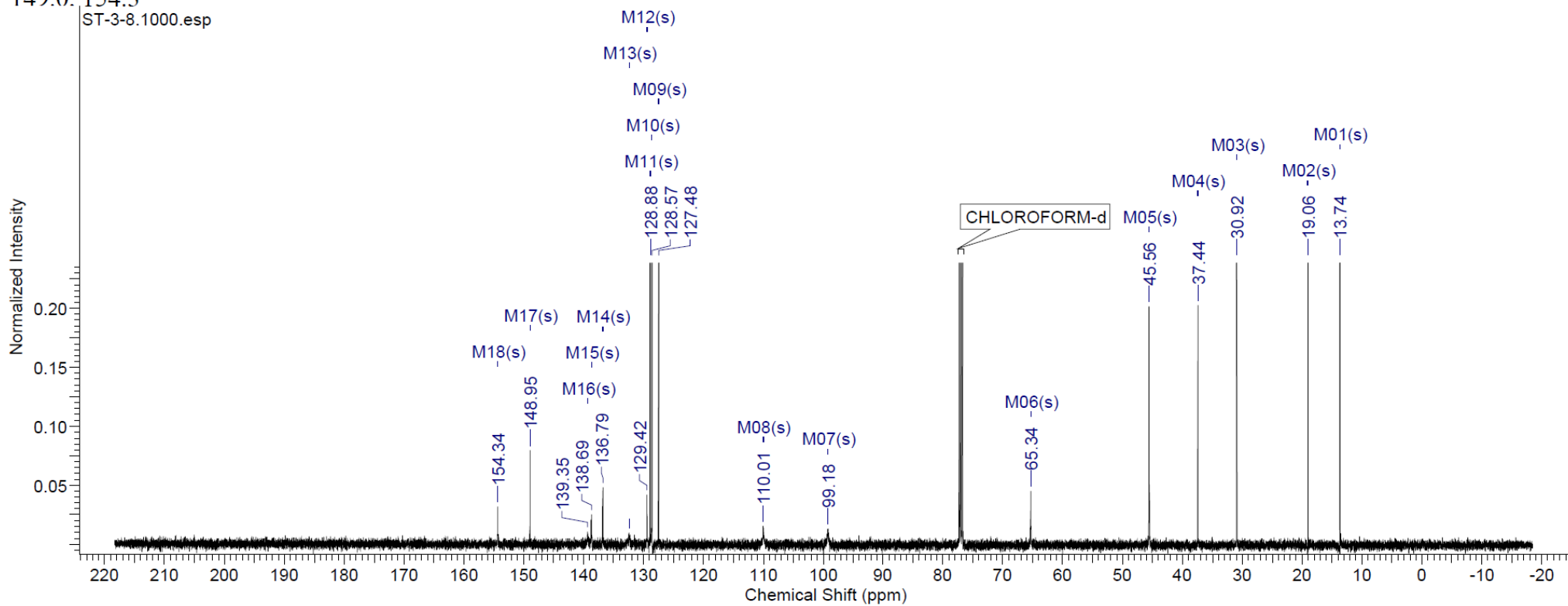
5-Butyloxycarbonylamino-6-*N,N*-dimethylamino-2-(benzylthio)-1*H*-benzo[d]imidazole



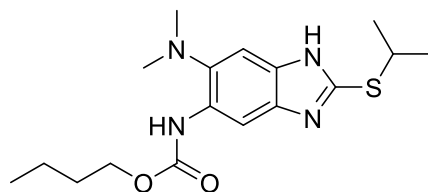
^1H NMR (500 MHz, CHLOROFORM-*d*) δ 0.95 (t, $J = 7.32$ Hz, 3 H), 1.43 (dq, $J = 15.03, 7.40$ Hz, 2 H), 1.57 - 1.78 (m, 2 H), 2.66 (s, 6 H), 4.26 (t, $J = 6.71$ Hz, 2 H), 4.52 (s, 2 H), 7.20 - 7.31 (m, 3 H), 7.32 - 7.40 (m, 2 H), 7.56 (br. s., 1 H), 8.30 (br. s., 2 H), 10.84 (br. s., 1 H)



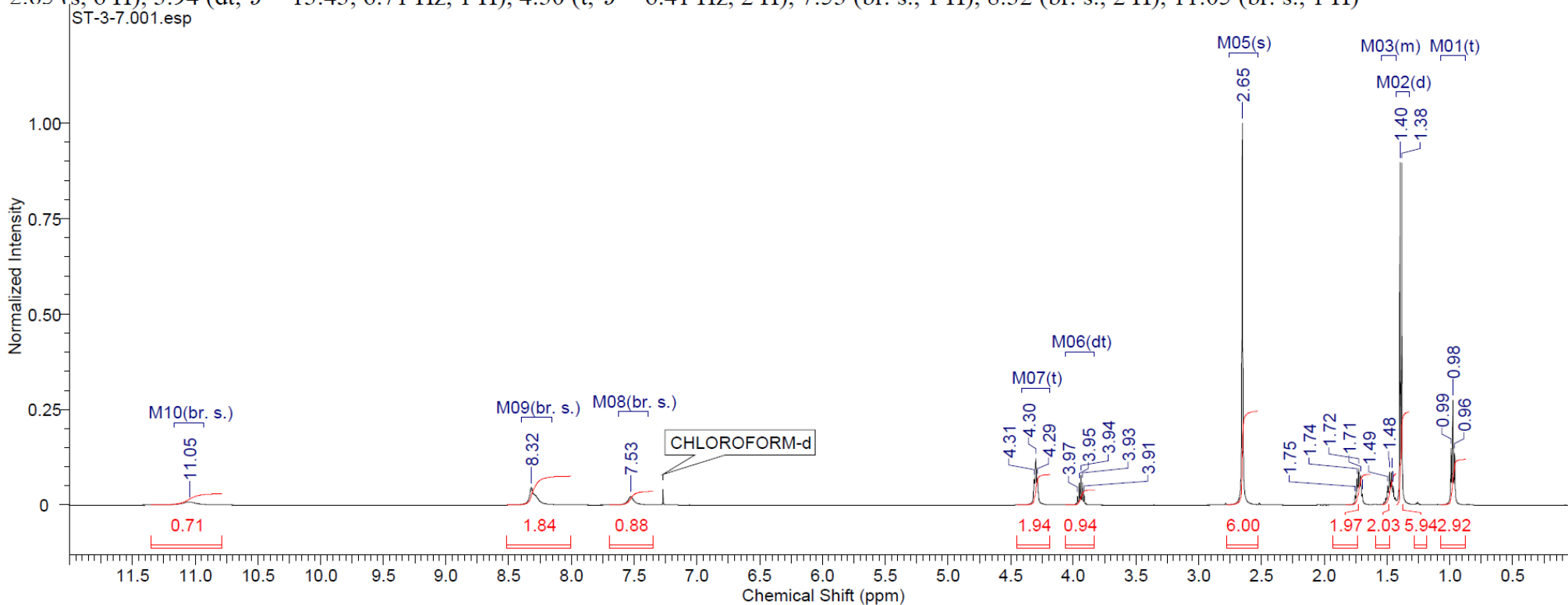
^{13}C NMR (126 MHz, CHLOROFORM- d) δ 13.7, 19.1, 30.9, 37.4, 45.6, 65.3, 99.2, 110.0, 127.5, 128.6, 128.9, 129.4, 132.4, 136.8, 138.7, 139.4, 149.0, 154.3



5-Butyloxycarbonylamino-6-*N,N*-dimethylamino-2-(isopropylthio)-1*H*-benzo[d]imidazole

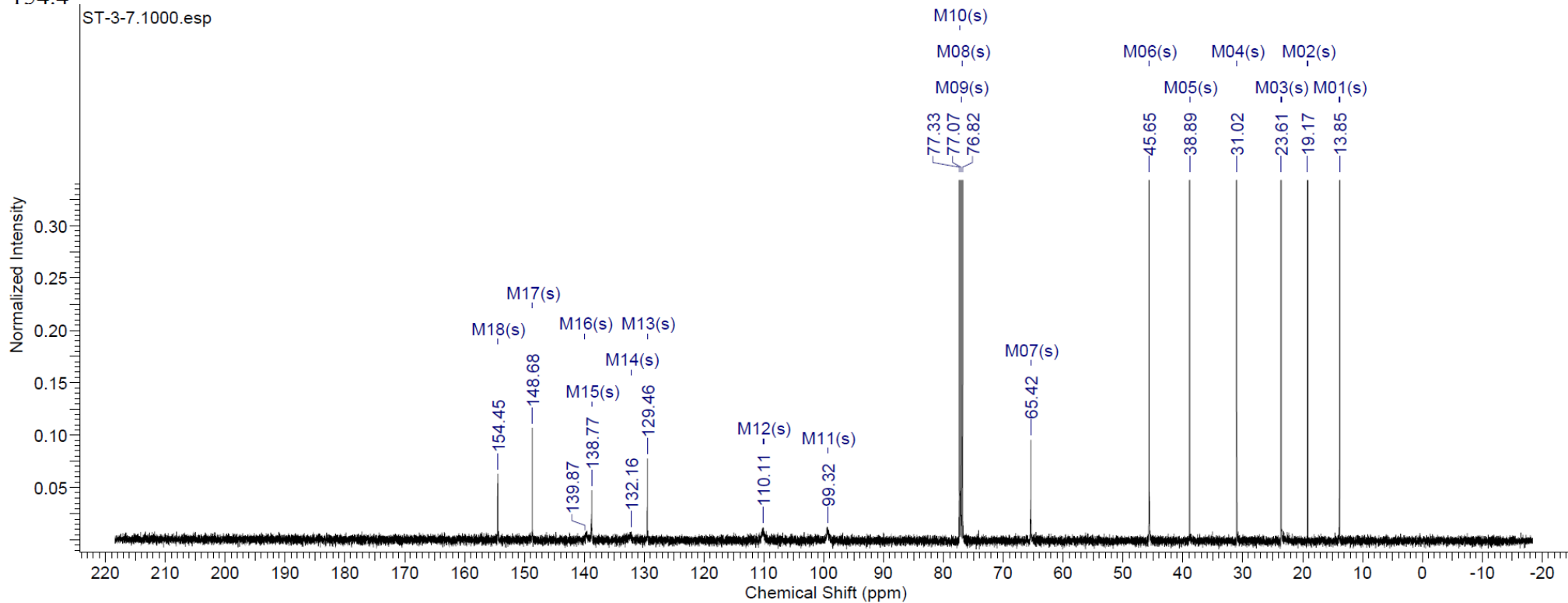


^1H NMR (500 MHz, CHLOROFORM-*d*) δ 0.98 (t, $J = 7.32$ Hz, 3 H), 1.39 (d, $J = 7.02$ Hz, 6 H), 1.43 - 1.54 (m, 2 H), 1.72 (quin, $J = 7.10$ Hz, 2 H), 2.65 (s, 6 H), 3.94 (dt, $J = 13.43, 6.71$ Hz, 1 H), 4.30 (t, $J = 6.41$ Hz, 2 H), 7.53 (br. s., 1 H), 8.32 (br. s., 2 H), 11.05 (br. s., 1 H)

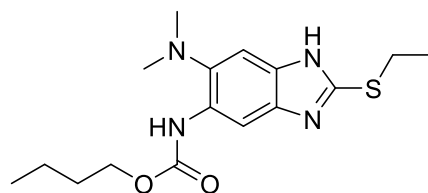


^{13}C NMR (126 MHz, CHLOROFORM- d) δ 13.8, 19.2, 23.6, 31.0, 38.9, 45.7, 65.4, 76.8, 77.1, 77.3, 99.3, 110.1, 129.5, 132.2, 138.8, 139.9, 148.7,

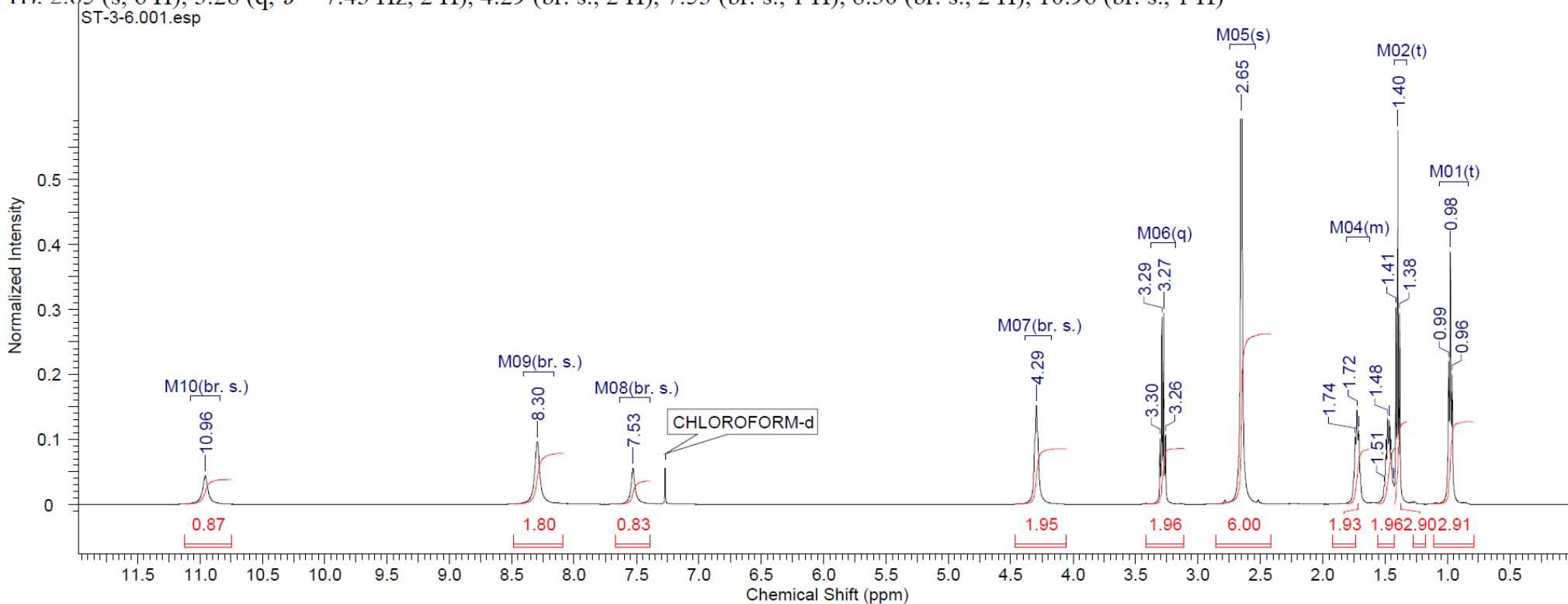
154.4



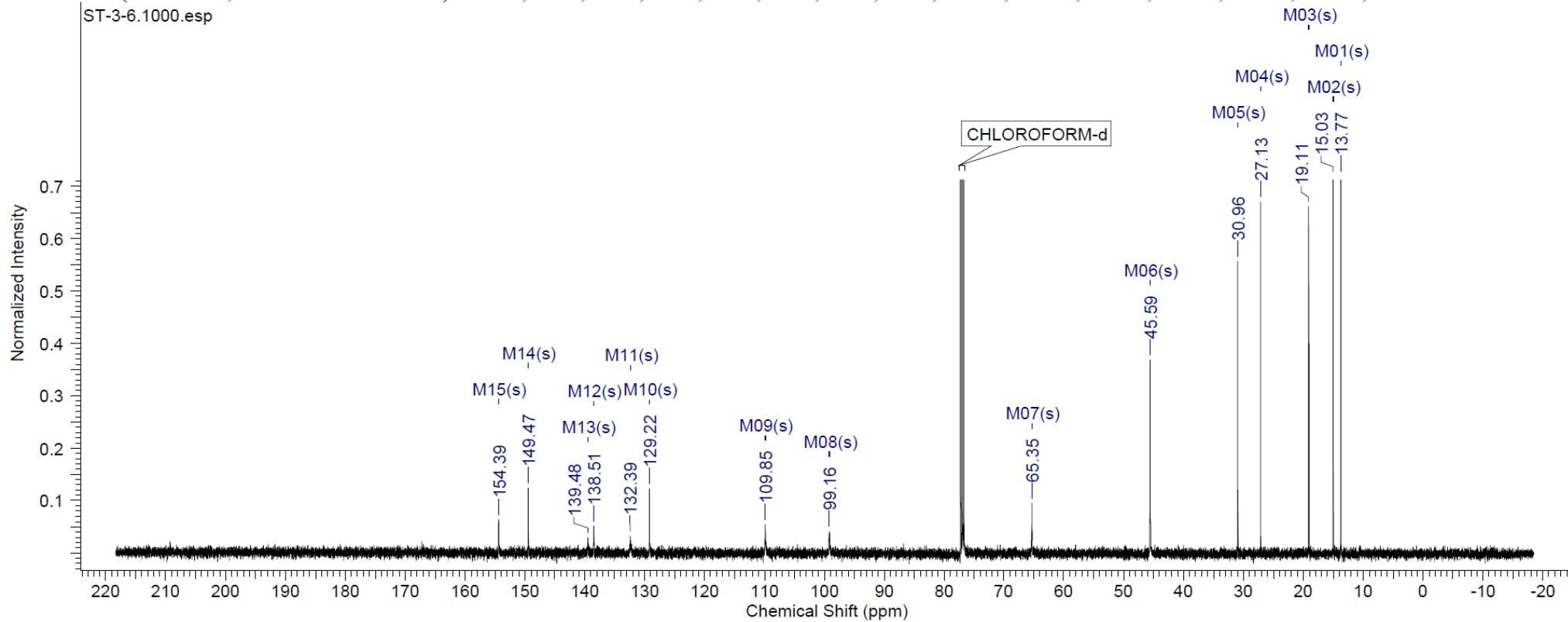
5-Butyloxycarbonylamino-6-*N,N*-dimethylamino-2-(ethylthio)-1*H*-benzo[d]imidazole



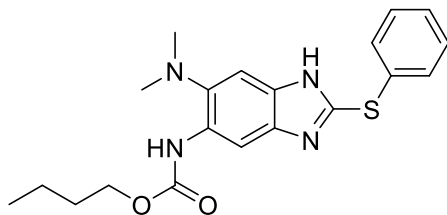
^1H NMR (500 MHz, CHLOROFORM-*d*) δ 0.98 (t, $J = 7.17$ Hz, 3 H), 1.40 (t, $J = 7.48$ Hz, 3 H), 1.47 (dq, $J = 14.61, 7.24$ Hz, 2 H), 1.62 - 1.81 (m, 2 H). 2.65 (s, 6 H), 3.28 (q, $J = 7.43$ Hz, 2 H), 4.29 (br. s., 2 H), 7.53 (br. s., 1 H), 8.30 (br. s., 2 H), 10.96 (br. s., 1 H)



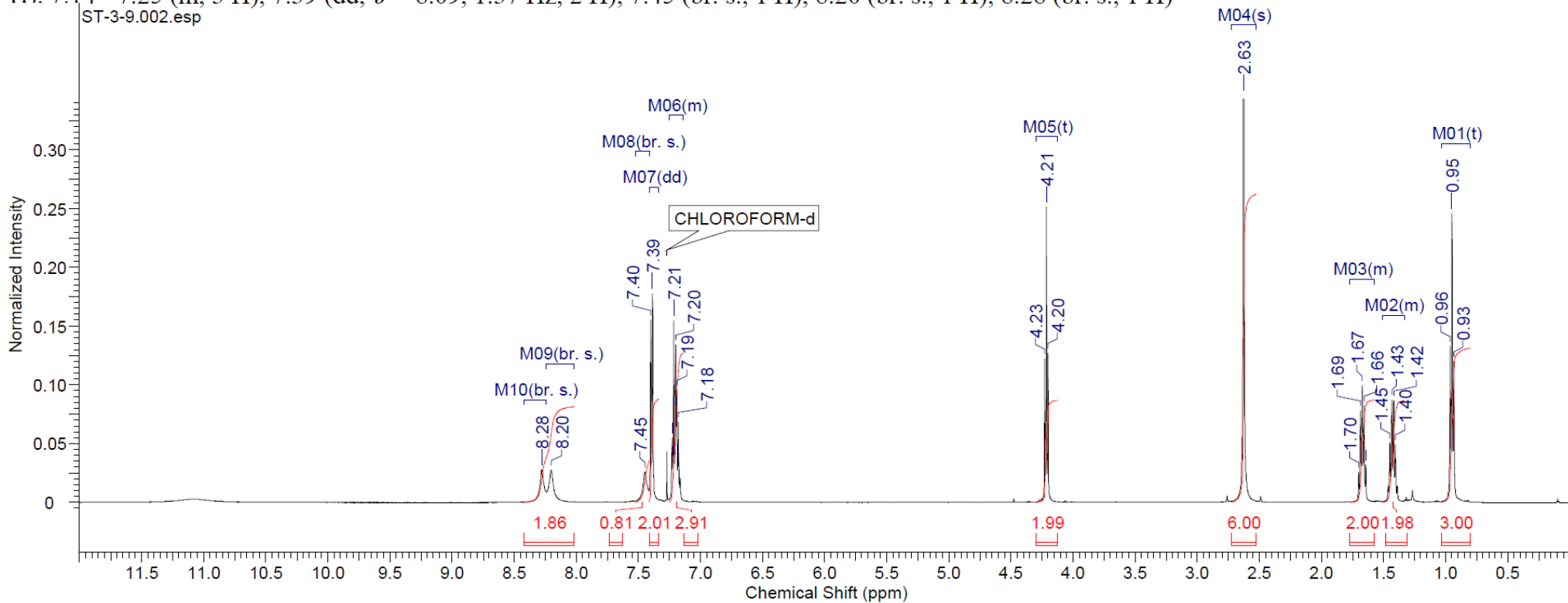
^{13}C NMR (126 MHz, CHLOROFORM-d) δ 13.8, 15.0, 19.1, 27.1, 31.0, 45.6, 65.4, 99.2, 109.9, 129.2, 132.4, 138.5, 139.5, 149.5, 154.4



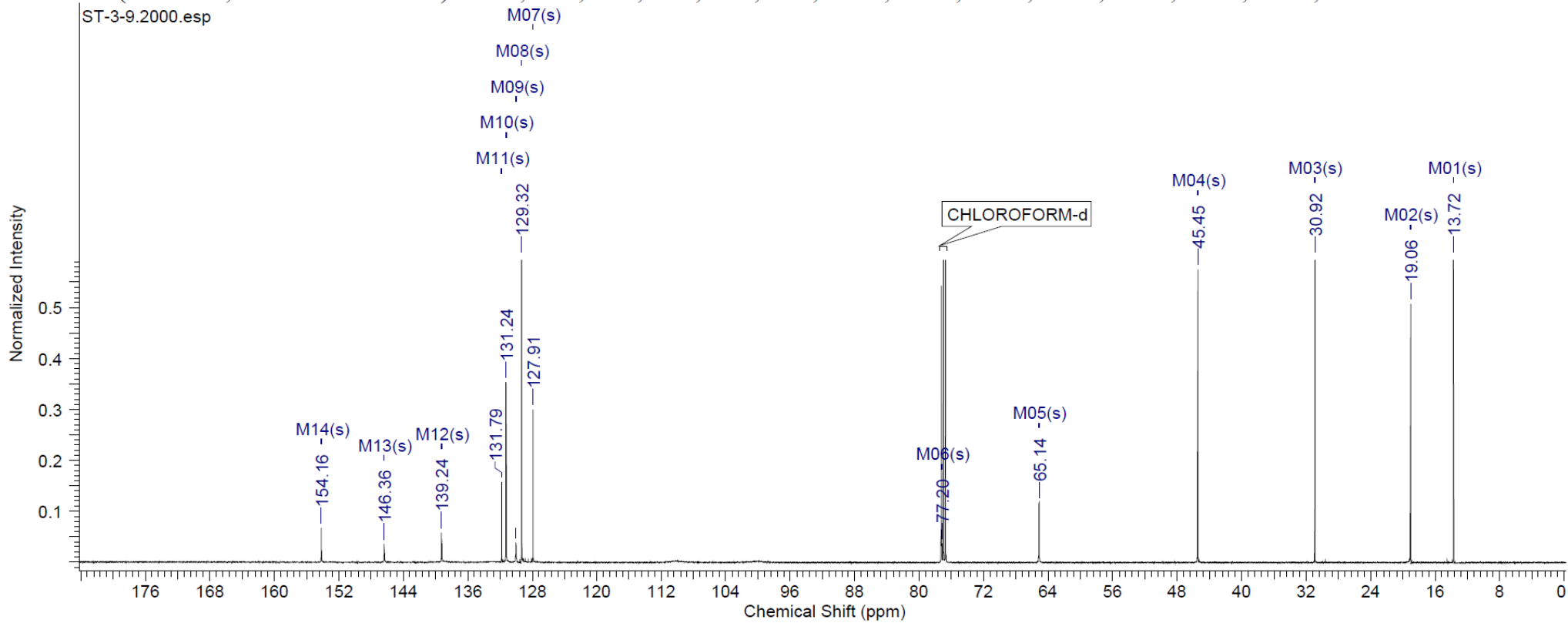
5-Butyloxycarbonylamino-6-*N,N*-dimethylamino-2-(phenylthio)-1*H*-benzo[d]imidazole



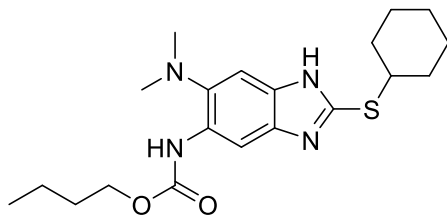
^1H NMR (500 MHz, CHLOROFORM- d) δ 0.95 (t, $J = 7.32$ Hz, 3 H), 1.33 - 1.51 (m, 2 H), 1.57 - 1.77 (m, 2 H), 2.63 (s, 6 H), 4.21 (t, $J = 6.71$ Hz, 2 H). 7.14 - 7.25 (m, 3 H), 7.39 (dd, $J = 8.09, 1.37$ Hz, 2 H), 7.45 (br. s., 1 H), 8.20 (br. s., 1 H), 8.28 (br. s., 1 H)



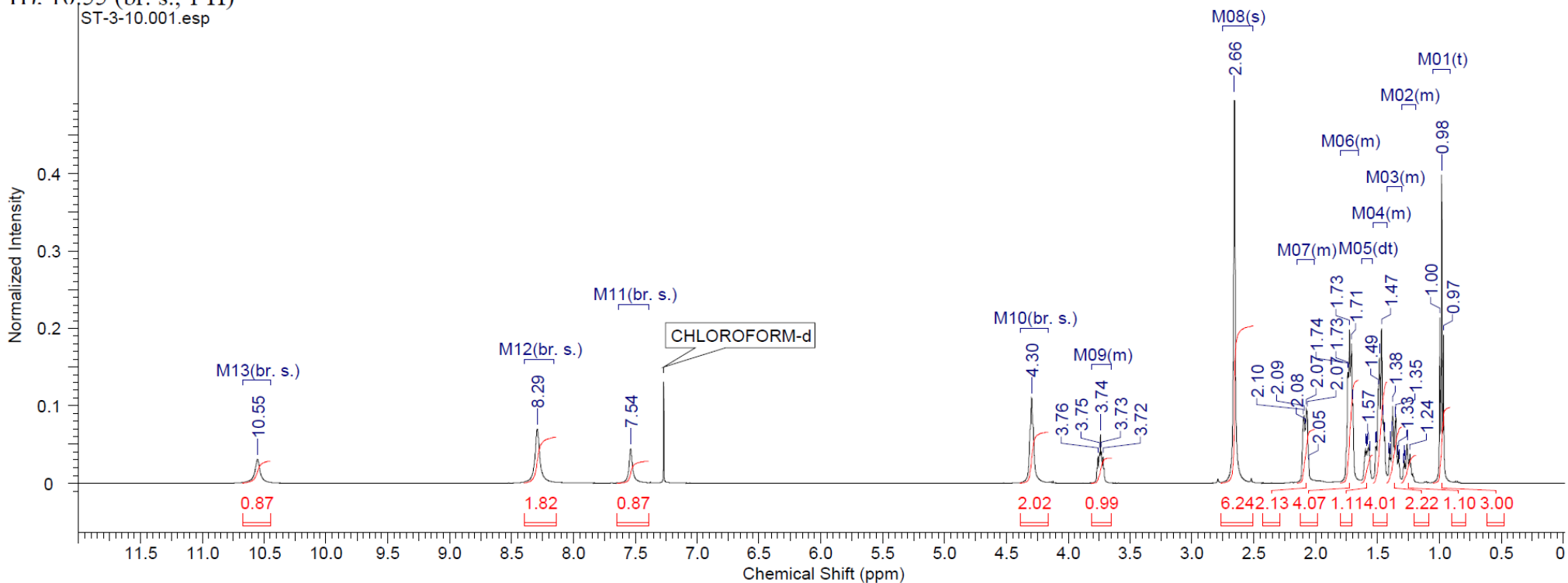
^{13}C NMR (126 MHz, CHLOROFORM-d) δ 13.7, 19.1, 30.9, 45.4, 65.1, 77.2, 127.9, 129.3, 130.0, 131.2, 131.8, 139.2, 146.4, 154.2



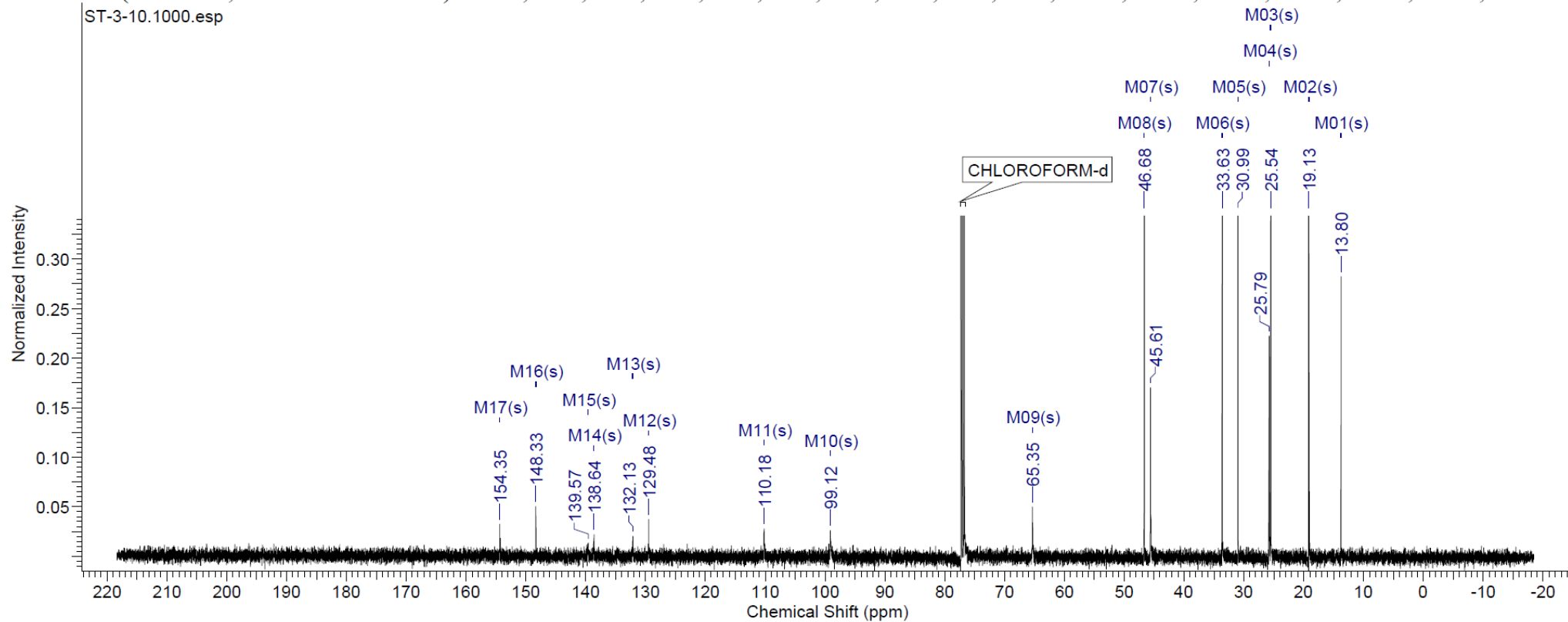
5-Butyloxycarbonylamino-2-(cyclohexylthio)-6-*N,N*-dimethylamino-1*H*-benzo[d]imidazole



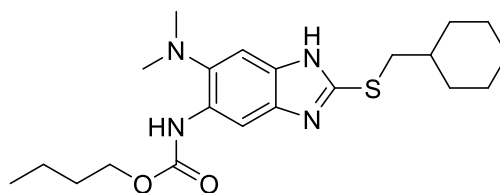
¹H NMR (500 MHz, CHLOROFORM-d) δ 0.98 (t, J = 7.32 Hz, 3 H), 1.19 - 1.31 (m, 1 H), 1.31 - 1.42 (m, 2 H), 1.42 - 1.53 (m, 4 H), 1.58 (dt, J = 8.39, 4.04 Hz, 1 H), 1.66 - 1.80 (m, 4 H), 2.01 - 2.15 (m, 2 H), 2.66 (s, 6 H), 3.65 - 3.81 (m, 1 H), 4.30 (br. s., 2 H), 7.54 (br. s., 1 H), 8.29 (br. s., 2 H), 10.55 (br. s., 1 H)



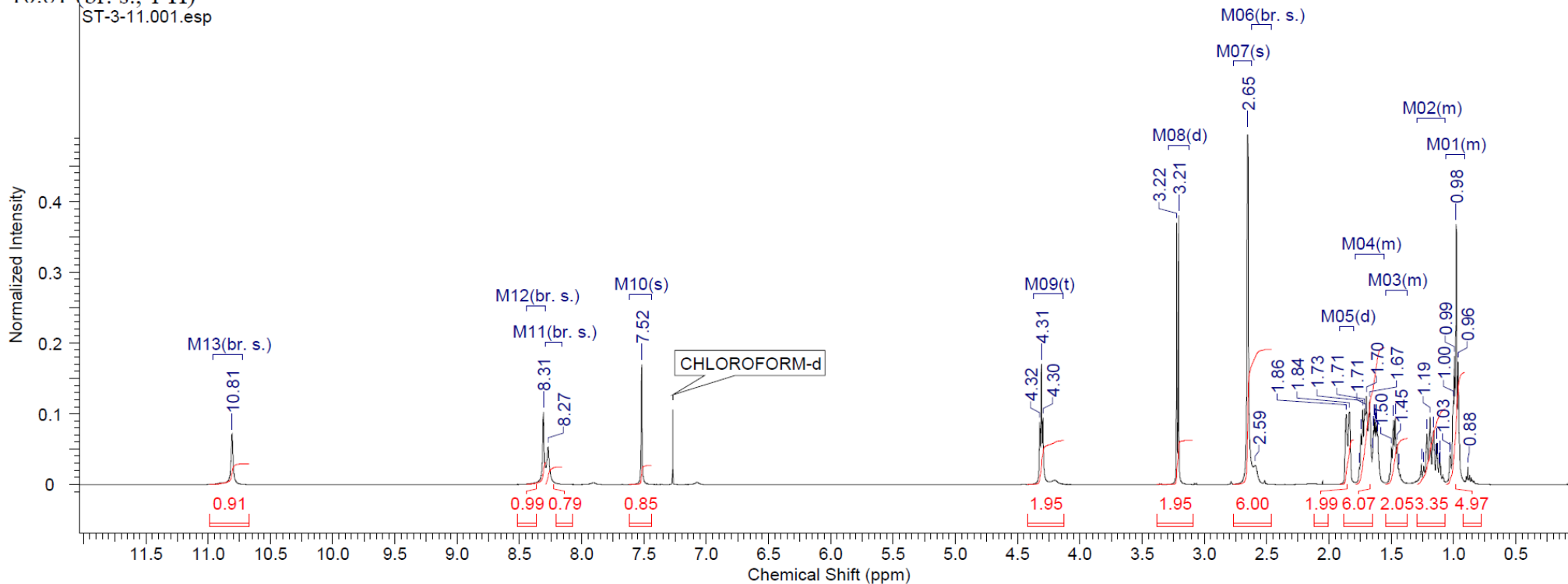
^{13}C NMR (126 MHz, CHLOROFORM-d) δ 13.8, 19.1, 25.5, 25.8, 31.0, 33.6, 45.6, 46.7, 65.3, 99.1, 110.2, 129.5, 132.1, 138.6, 139.6, 148.3, 154.4



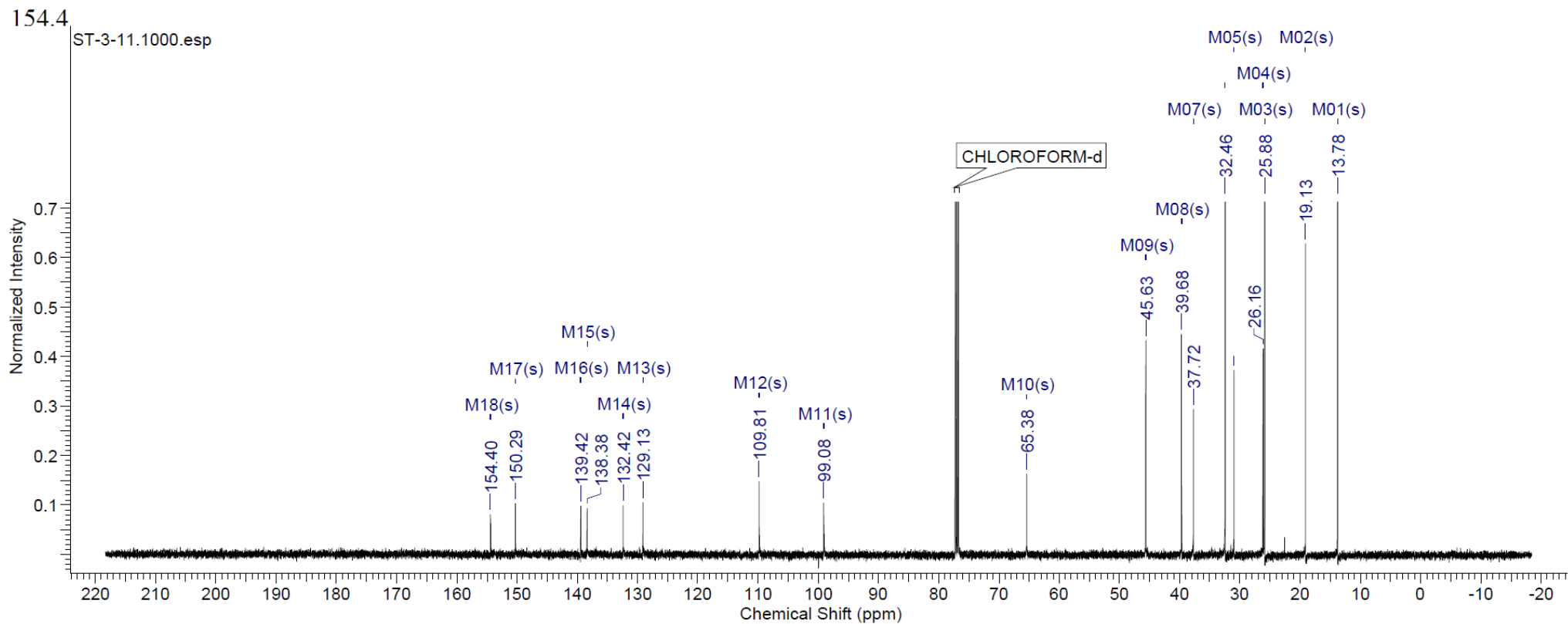
5-Butyloxycarbonylamino-2-(cyclohexylmethylthio)-6-*N,N*-dimethylamino-1*H*-benzo[d]imidazole



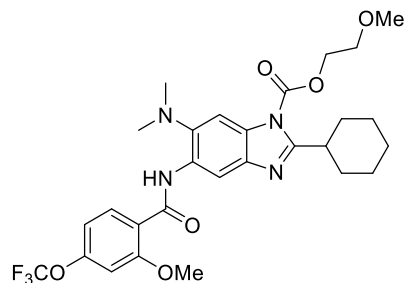
^1H NMR (500 MHz, CHLOROFORM-*d*) δ 0.91 - 1.06 (m, 5 H), 1.07 - 1.29 (m, 3 H), 1.37 - 1.55 (m, 2 H), 1.56 - 1.79 (m, 6 H), 1.85 (d, $J = 13.12$ Hz, 2 H), 2.59 (br. s., 1 H), 2.65 (s, 5 H), 3.22 (d, $J = 7.02$ Hz, 2 H), 4.31 (t, $J = 6.56$ Hz, 2 H), 7.52 (s, 1 H), 8.27 (br. s., 1 H), 8.31 (br. s., 1 H), 10.81 (br. s., 1 H)



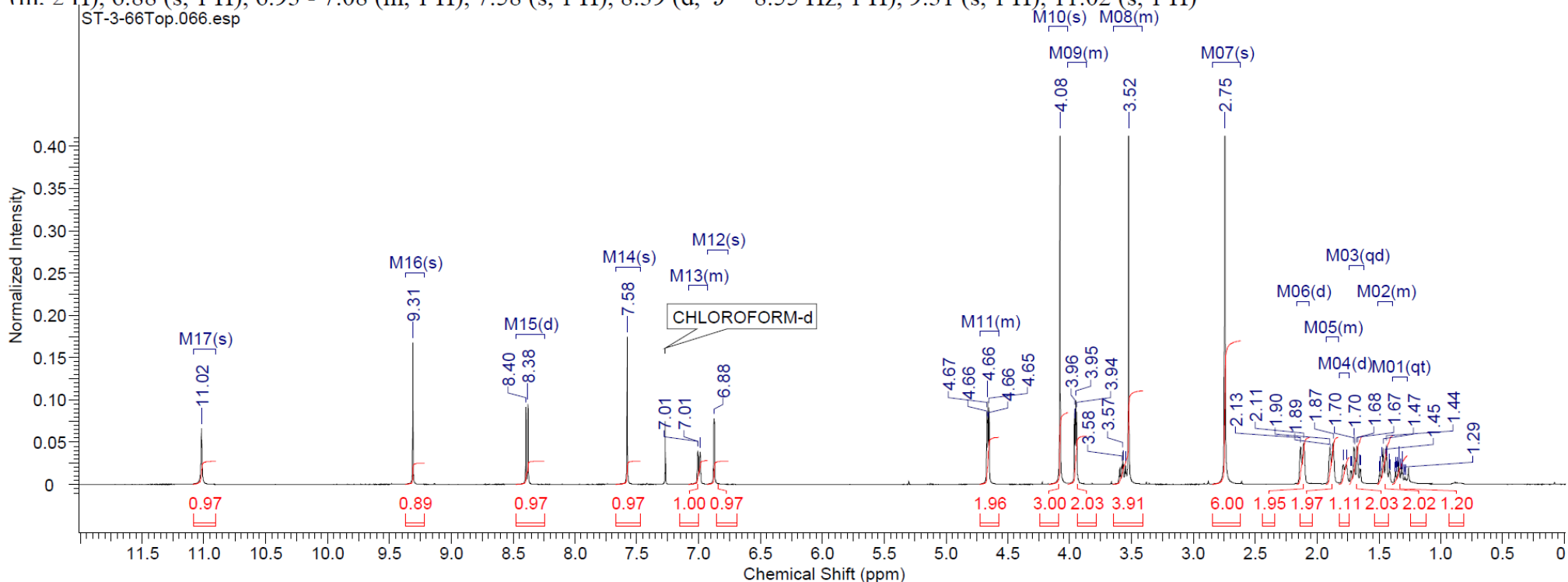
^{13}C NMR (126 MHz, CHLOROFORM- d) δ 13.8, 19.1, 25.9, 26.2, 31.0, 32.5, 37.7, 39.7, 45.6, 65.4, 99.1, 109.8, 129.1, 132.4, 138.4, 139.4, 150.3,



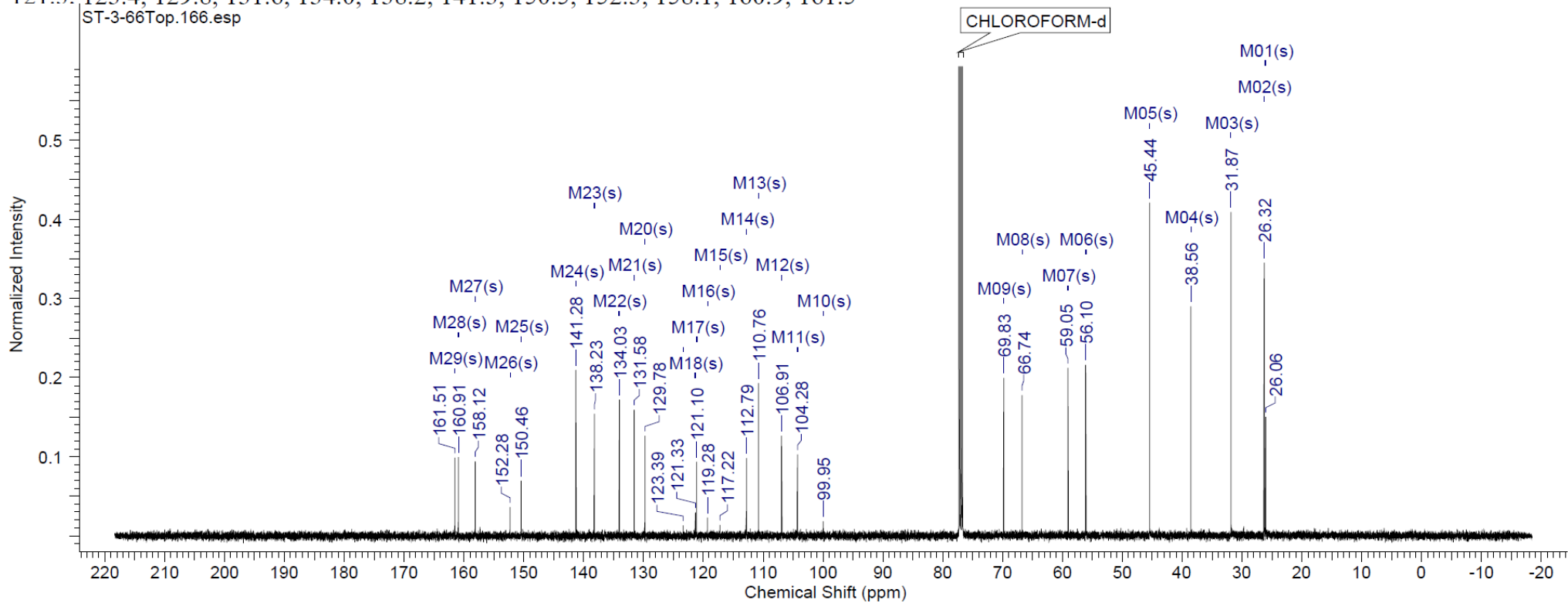
2-Cyclohexyl-6-*N,N*-dimethylamino-5-(2-methoxy-4-trifluoromethoxy)benzamido-1-(2-methoxyethoxy)carbonyl-1*H*-benzo[d]imidazole



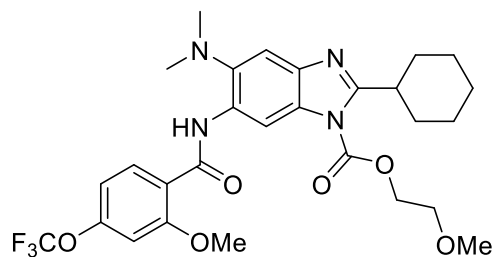
^1H NMR (500 MHz, CHLOROFORM-*d*) δ 1.33 (qt, $J = 12.72, 3.51$ Hz, 1 H), 1.39 - 1.51 (m, 2 H), 1.69 (qd, $J = 12.41, 3.05$ Hz, 2 H), 1.78 (d, $J = 12.51$ Hz, 1 H), 1.83 - 1.93 (m, 2 H), 2.12 (d, $J = 12.21$ Hz, 2 H), 2.75 (s, 6 H), 3.41 - 3.65 (m, 4 H), 3.86 - 4.01 (m, 2 H), 4.08 (s, 3 H), 4.58 - 4.73 (m, 2 H), 6.88 (s, 1 H), 6.93 - 7.08 (m, 1 H), 7.58 (s, 1 H), 8.39 (d, $J = 8.55$ Hz, 1 H), 9.31 (s, 1 H), 11.02 (s, 1 H)



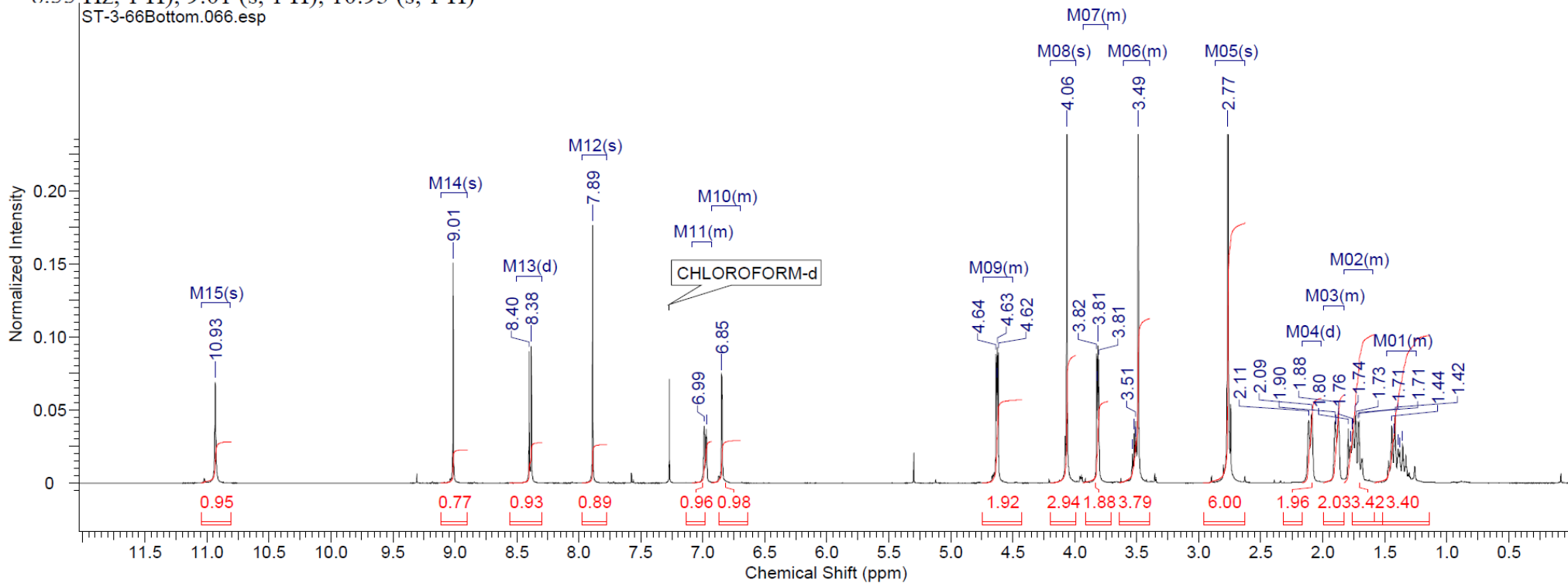
^{13}C NMR (126 MHz, CHLOROFORM- d) δ 26.1, 26.3, 31.9, 38.6, 45.4, 56.1, 59.1, 66.7, 69.8, 99.9, 104.3, 106.9, 110.8, 112.8, 117.2, 119.3, 121.1, 121.3, 123.4, 129.8, 131.6, 134.0, 138.2, 141.3, 150.5, 152.3, 158.1, 160.9, 161.5



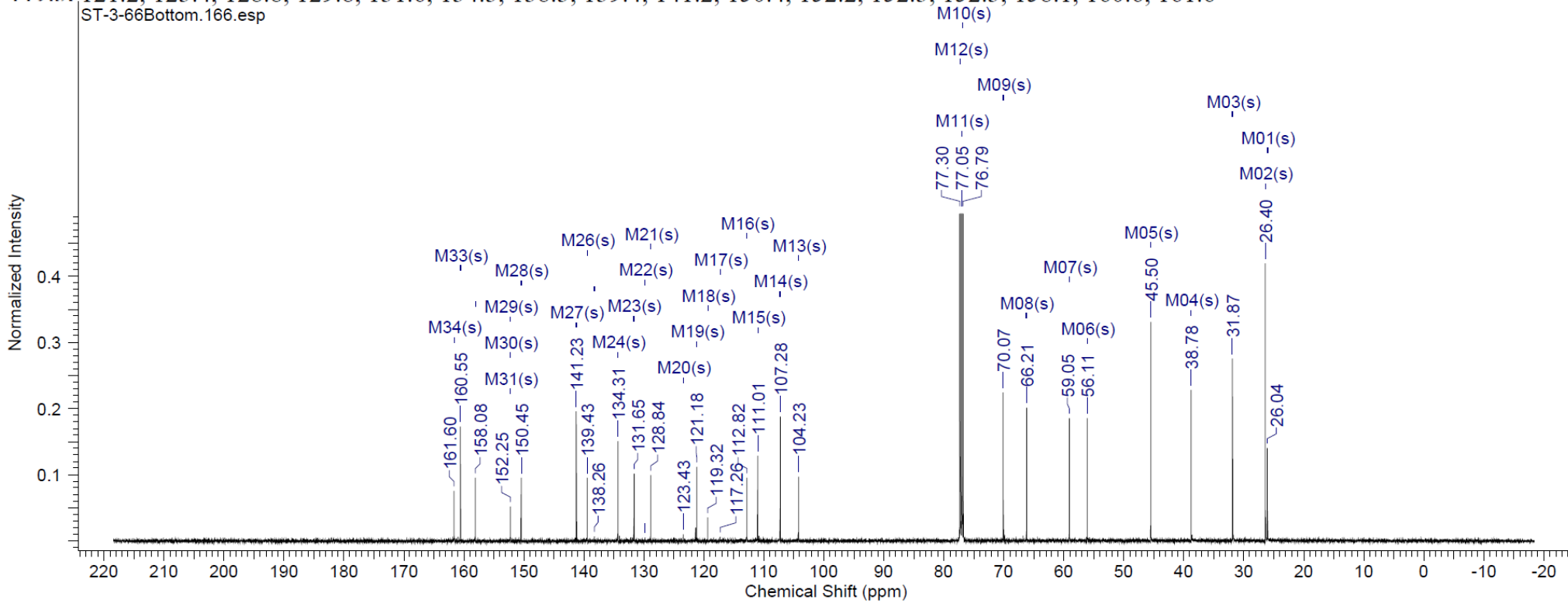
2-Cyclohexyl-6-*N,N*-dimethylamino-5-(2-methoxy-4-trifluoromethoxy)benzamido-3-(2-methoxyethoxycarbonyl)-1*H*-benzo[*d*]imidazole



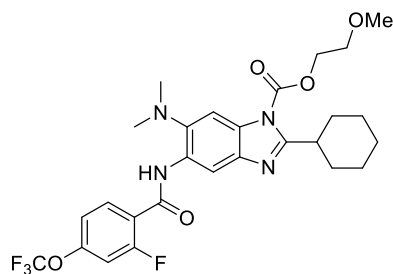
^1H NMR (500 MHz, CHLOROFORM-*d*) δ 1.25 - 1.49 (m, 3 H), 1.60 - 1.83 (m, 3 H), 1.83 - 2.00 (m, 2 H), 2.10 (d, $J = 11.90$ Hz, 2 H), 2.77 (s, 6 H), 3.40 - 3.61 (m, 4 H), 3.73 - 3.93 (m, 2 H), 4.06 (s, 3 H), 4.50 - 4.74 (m, 2 H), 6.70 - 6.93 (m, 1 H), 6.93 - 7.08 (m, 1 H), 7.89 (s, 1 H), 8.39 (d, $J = 8.55$ Hz, 1 H), 9.01 (s, 1 H), 10.93 (s, 1 H)



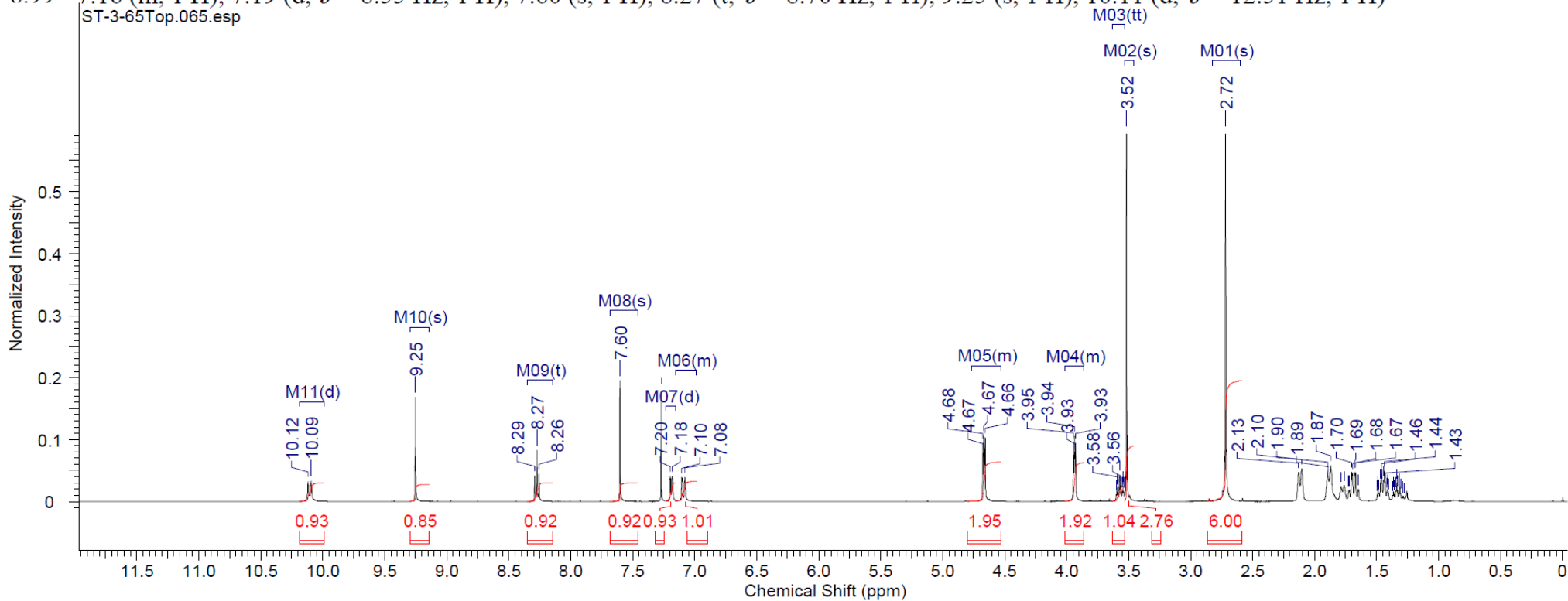
^{13}C NMR (126 MHz, CHLOROFORM- d) δ 26.0, 26.4, 31.9, 38.8, 45.5, 56.1, 59.0, 66.2, 70.1, 76.8, 77.0, 77.3, 104.2, 107.3, 111.0, 112.8, 117.3, 119.3, 121.2, 123.4, 128.8, 129.8, 131.6, 134.3, 138.3, 139.4, 141.2, 150.4, 152.2, 152.3, 152.3, 158.1, 160.6, 161.6



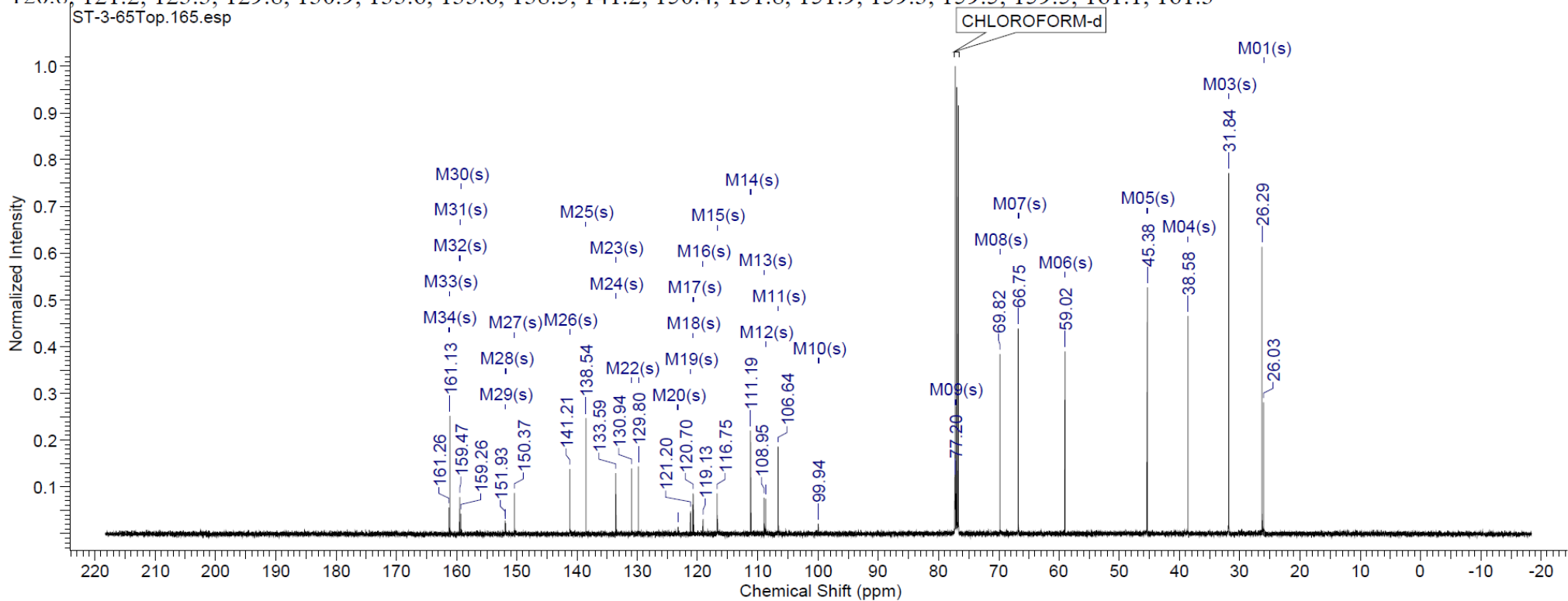
2-Cyclohexyl-6-*N,N*-dimethylamino-5-(2-fluoro-4-trifluoromethoxy)benzamido-1-(2-methoxyethoxy)carbonyl-1*H*-benzo[d]imidazole



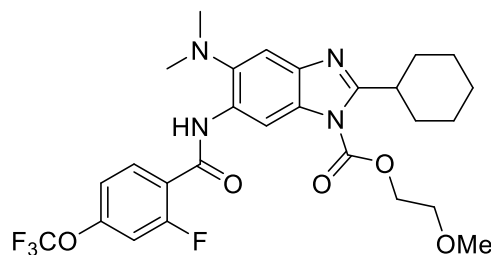
^1H NMR (500 MHz, CHLOROFORM-*d*) δ 2.72 (s, 6 H), 3.52 (s, 3 H), 3.57 (tt, $J = 11.60, 3.20$ Hz, 1 H), 3.86 - 4.01 (m, 2 H), 4.53 - 4.76 (m, 2 H), 6.99 - 7.16 (m, 1 H), 7.19 (d, $J = 8.55$ Hz, 1 H), 7.60 (s, 1 H), 8.27 (t, $J = 8.70$ Hz, 1 H), 9.25 (s, 1 H), 10.11 (d, $J = 12.51$ Hz, 1 H)



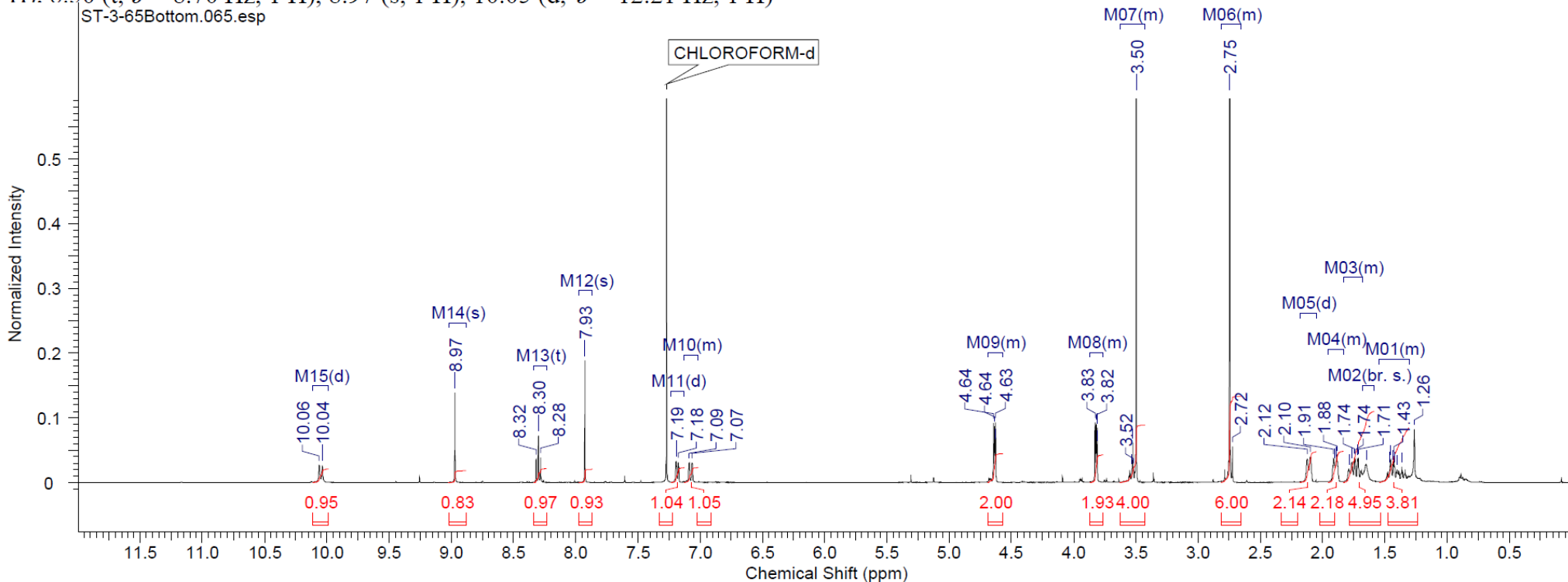
^{13}C NMR (126 MHz, CHLOROFORM- d) δ 26.0, 26.3, 31.8, 38.6, 45.4, 59.0, 66.8, 69.8, 77.2, 99.9, 106.6, 108.7, 108.9, 111.2, 116.8, 119.1, 120.7, 120.8, 121.2, 123.3, 129.8, 130.9, 133.6, 133.6, 138.5, 141.2, 150.4, 151.8, 151.9, 159.3, 159.5, 159.5, 161.1, 161.3



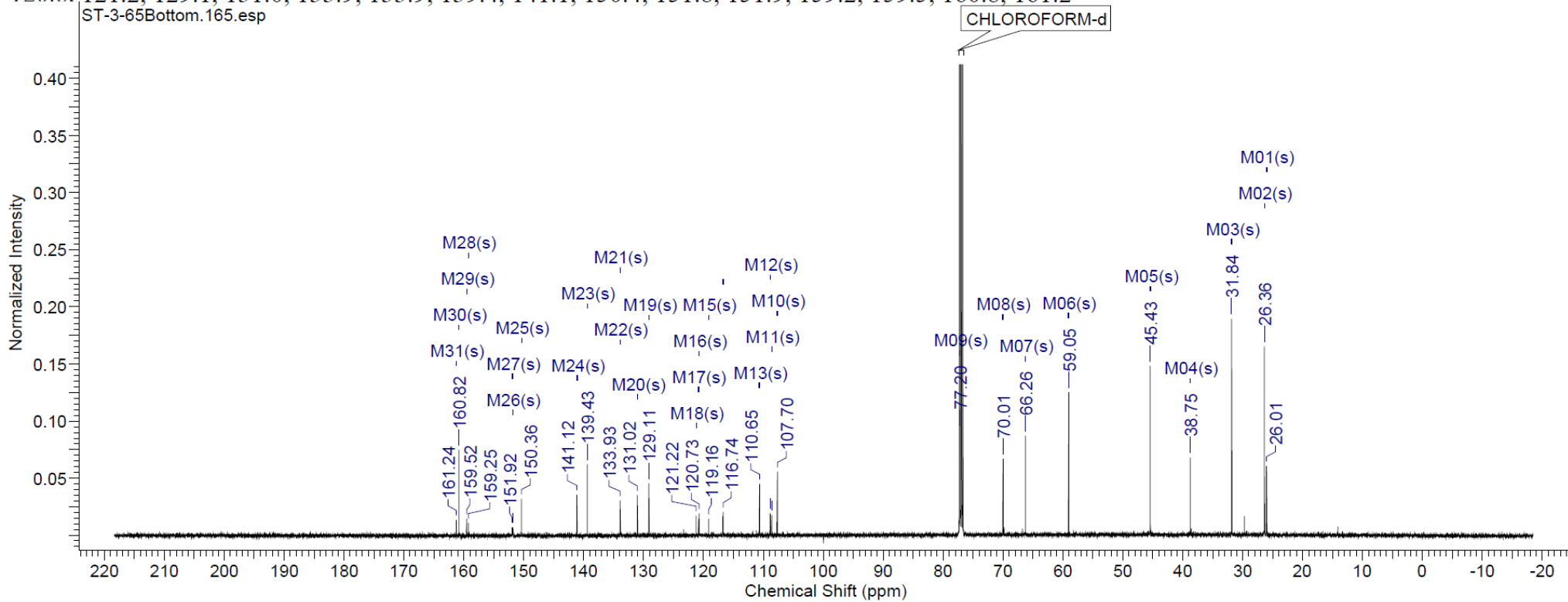
2-Cyclohexyl-6-*N,N*-dimethylamino-5-(2-fluoro-4-trifluoromethoxy)benzamido-3-(2-methoxyethoxy)carbonyl-1*H*-benzo[d]imidazole



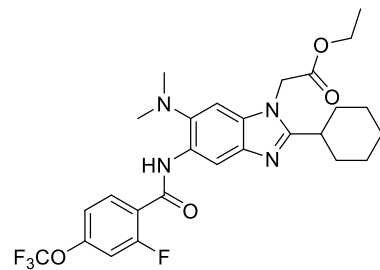
^1H NMR (500 MHz, CHLOROFORM-*d*) δ 1.31 - 1.54 (m, 4 H), 1.65 (br. s., 2 H), 1.68 - 1.83 (m, 3 H), 1.83 - 1.95 (m, 2 H), 2.11 (d, $J = 11.90$ Hz, 2 H), 2.66 - 2.81 (m, 6 H), 3.43 - 3.63 (m, 4 H), 3.76 - 3.87 (m, 2 H), 4.57 - 4.69 (m, 2 H), 7.01 - 7.13 (m, 1 H), 7.18 (d, $J = 8.55$ Hz, 1 H), 7.93 (s, 1 H), 8.30 (t, $J = 8.70$ Hz, 1 H), 8.97 (s, 1 H), 10.05 (d, $J = 12.21$ Hz, 1 H)



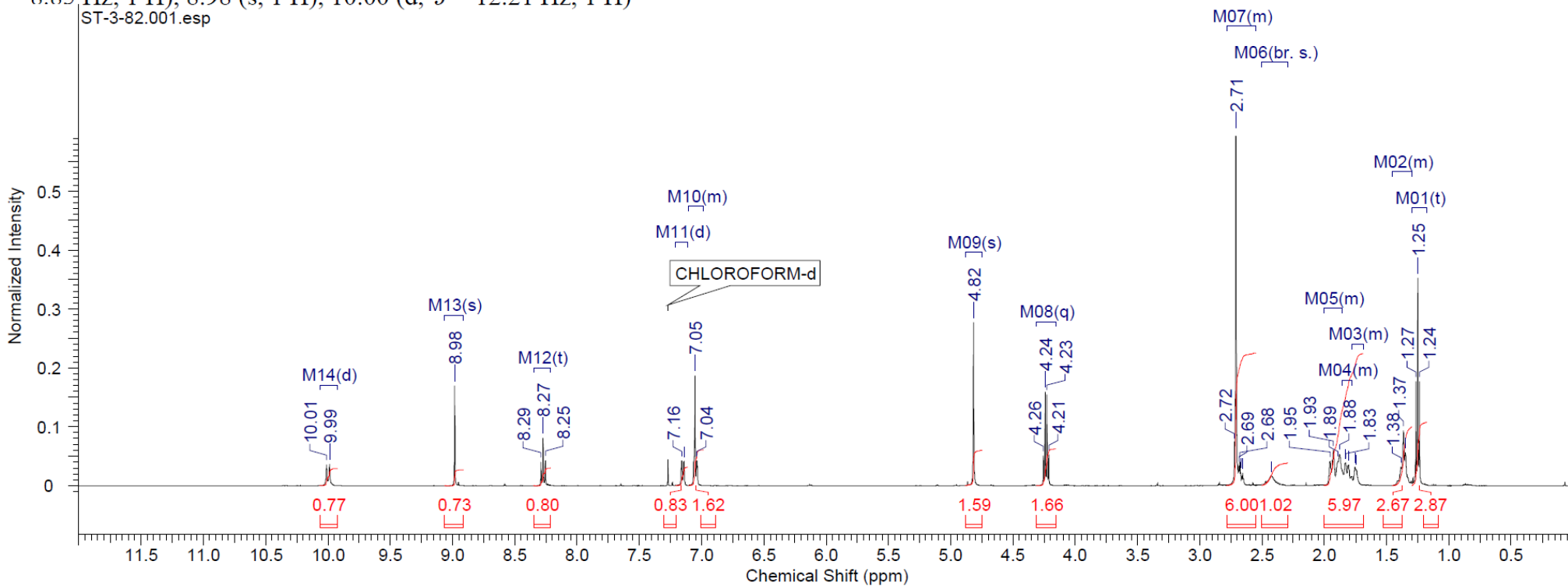
^{13}C NMR (126 MHz, CHLOROFORM- d) δ 26.0, 26.4, 31.8, 38.8, 45.4, 59.0, 66.3, 70.0, 77.2, 107.7, 108.6, 108.8, 110.7, 116.7, 119.2, 120.7, 120.8, 121.2, 129.1, 131.0, 133.9, 133.9, 139.4, 141.1, 150.4, 151.8, 151.9, 159.2, 159.5, 160.8, 161.2



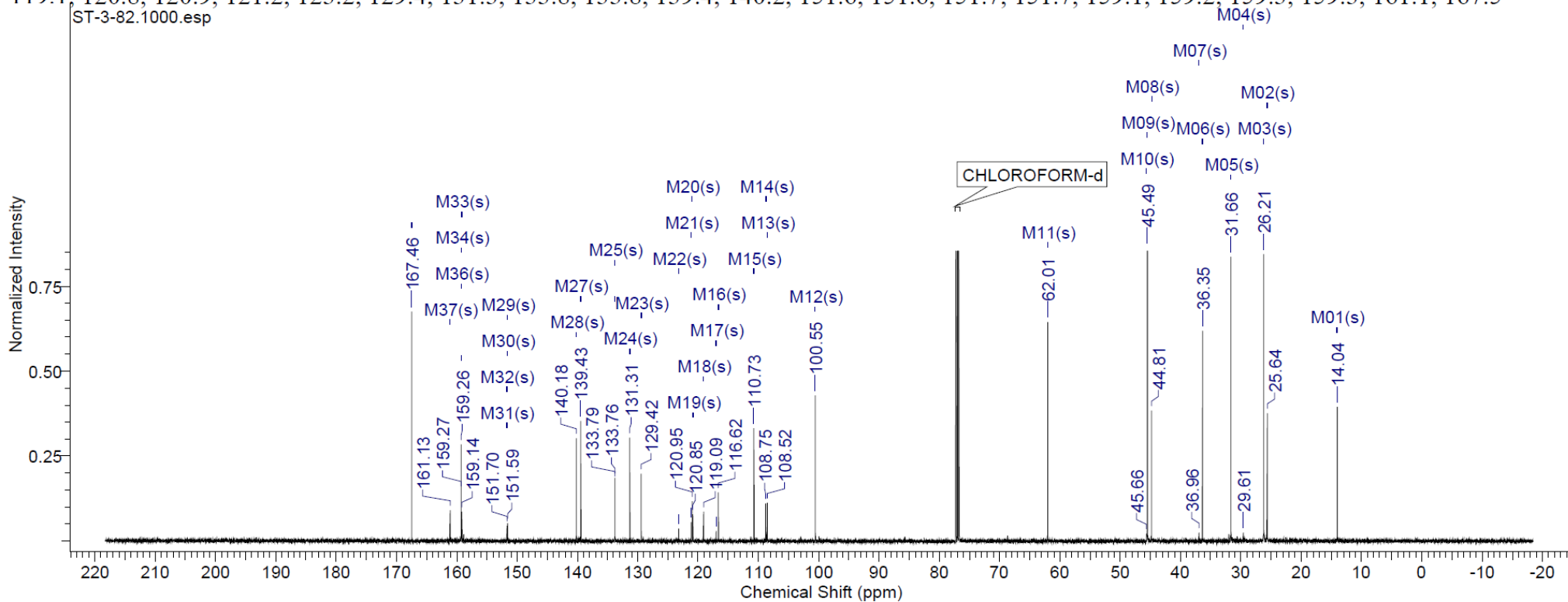
2-Cyclohexyl-6-*N,N*-dimethylamino-5-(2-fluoro-4-trifluoromethyl)benzamido-1-ethoxycarbonylmethyl-1*H*-benzo[d]imidazole



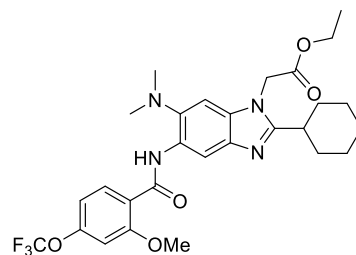
^1H NMR (500 MHz, CHLOROFORM- d) δ 1.25 (t, $J = 7.17$ Hz, 3 H), 1.30 - 1.46 (m, 3 H), 1.69 - 1.78 (m, 1 H), 1.78 - 1.86 (m, 2 H), 1.86 - 2.00 (m, 3 H), 2.43 (br. s., 1 H), 2.55 - 2.78 (m, 6 H), 4.23 (q, $J = 7.22$ Hz, 2 H), 4.82 (s, 2 H), 6.98 - 7.10 (m, 2 H), 7.15 (d, $J = 8.54$ Hz, 1 H), 8.27 (t, $J = 8.85$ Hz, 1 H), 8.98 (s, 1 H), 10.00 (d, $J = 12.21$ Hz, 1 H)



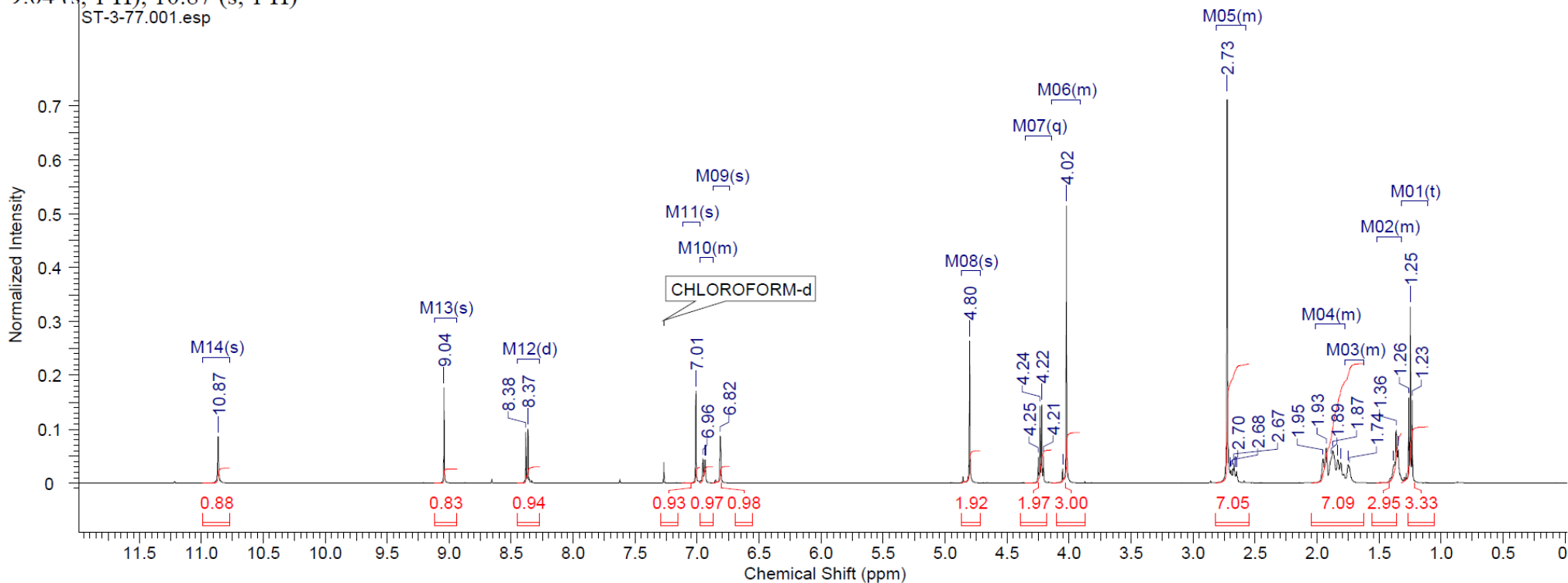
^{13}C NMR (126 MHz, CHLOROFORM-d) δ 14.0, 25.6, 26.2, 29.6, 31.7, 36.4, 37.0, 44.8, 45.5, 45.7, 62.0, 100.6, 108.5, 108.8, 110.7, 116.6, 117.0, 119.1, 120.8, 120.9, 121.2, 123.2, 129.4, 131.3, 133.8, 133.8, 139.4, 140.2, 151.6, 151.6, 151.7, 151.7, 159.1, 159.2, 159.3, 159.3, 161.1, 167.5



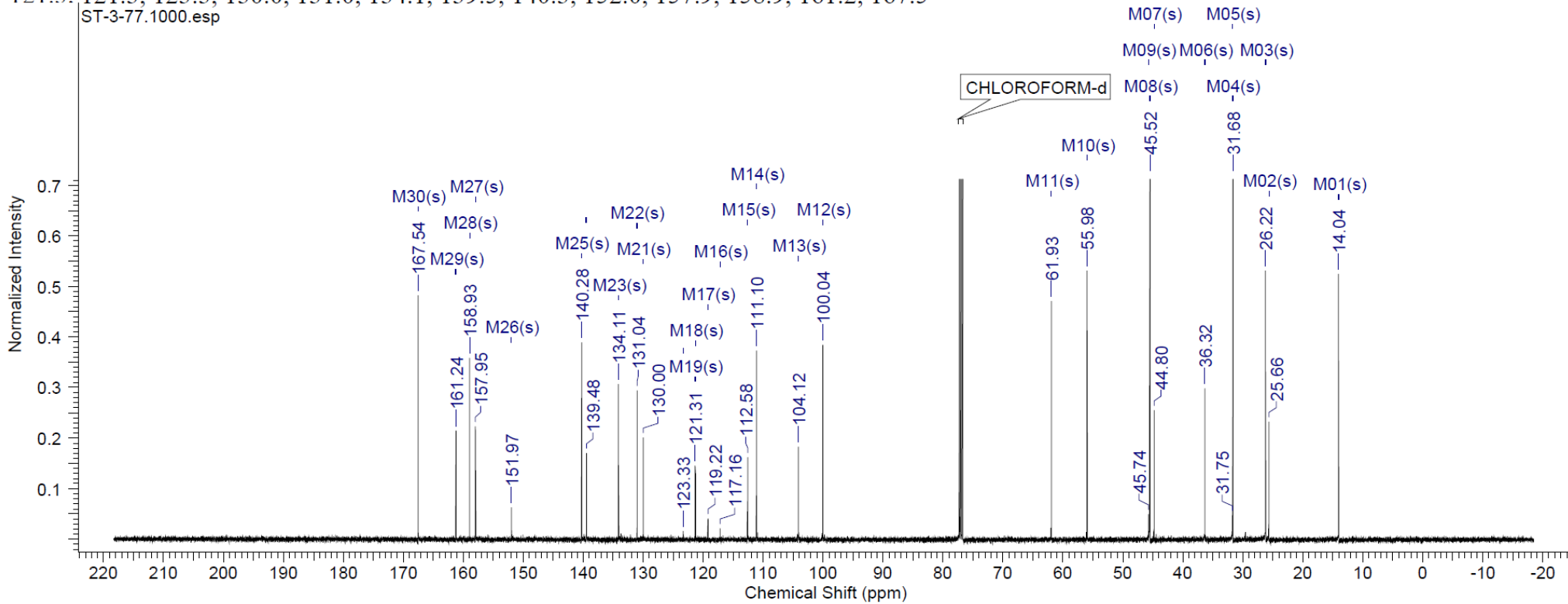
2-Cyclohexyl-6-*N,N*-dimethylamino-5-(2-methoxy-4-trifluoromethyl)benzamido-1-ethoxycarbonylmethyl-1*H*-benzo[d]imidazole



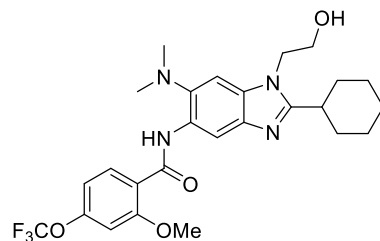
¹H NMR (500 MHz, CHLOROFORM-*d*) δ 1.25 (t, $J = 7.02$ Hz, 3 H), 1.32 - 1.52 (m, 3 H), 1.62 - 1.78 (m, 1 H), 1.78 - 2.02 (m, 6 H), 2.58 - 2.81 (m, 7 H), 3.92 - 4.14 (m, 3 H), 4.23 (q, $J = 7.02$ Hz, 2 H), 4.80 (s, 2 H), 6.82 (s, 1 H), 6.87 - 6.98 (m, 1 H), 7.01 (s, 1 H), 8.37 (d, $J = 8.85$ Hz, 1 H), 9.04 (s, 1 H), 10.87 (s, 1 H)



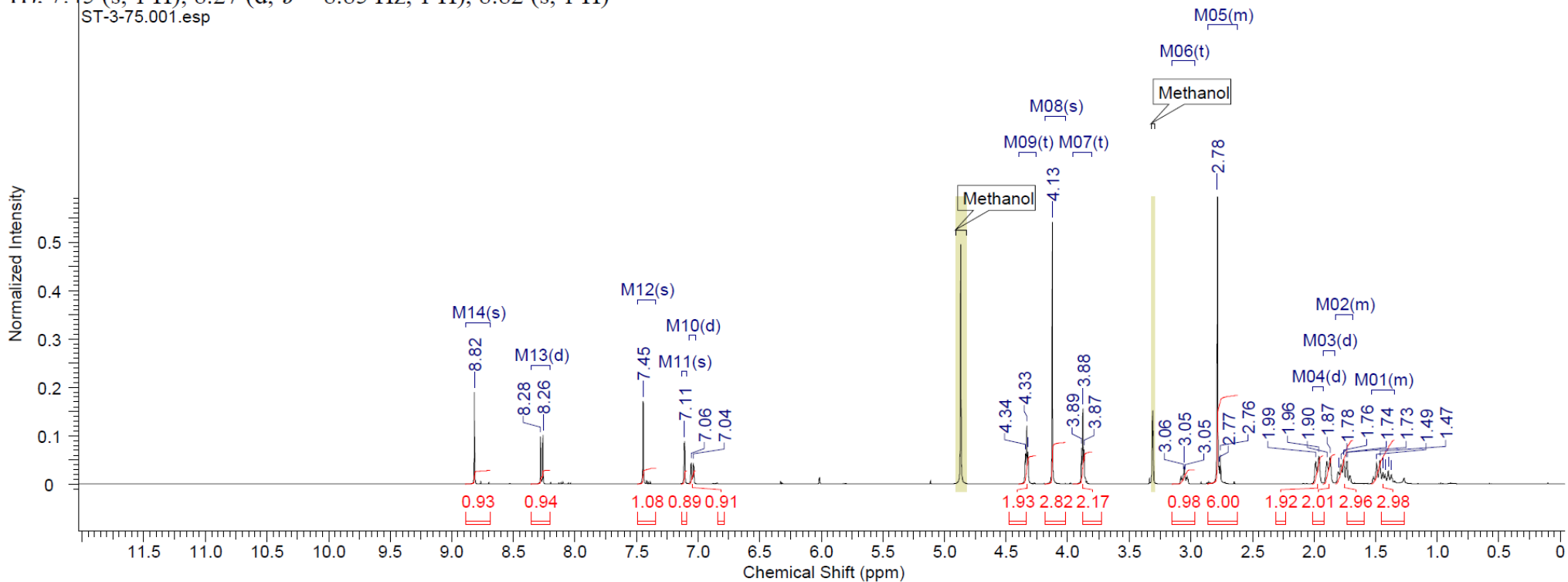
^{13}C NMR (126 MHz, CHLOROFORM- d) δ 14.0, 25.7, 26.2, 31.7, 31.7, 36.3, 44.8, 45.5, 45.7, 56.0, 61.9, 100.0, 104.1, 111.1, 112.6, 117.2, 119.2, 121.3, 121.3, 123.3, 130.0, 131.0, 134.1, 139.5, 140.3, 152.0, 157.9, 158.9, 161.2, 167.5



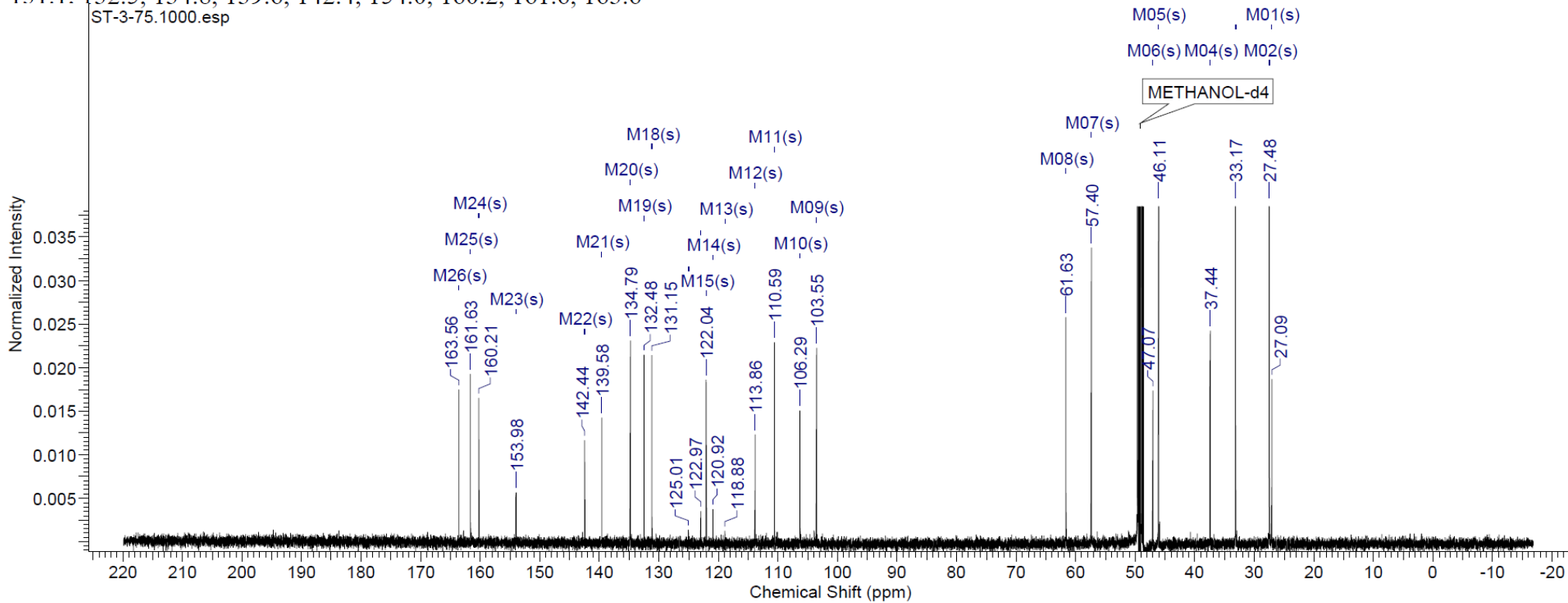
2-Cyclohexyl-6-*N,N*-dimethylamino-5-(2-methoxy-4-trifluoromethyl)benzamido-1-hydroxyethyl-1*H*-benzo[d]imidazole



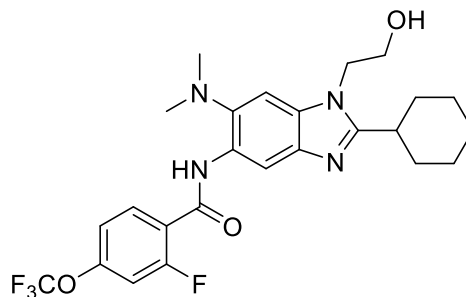
$^1\text{H NMR}$ (500 MHz, METHANOL- d_4) δ 1.35 - 1.53 (m, 3 H), 1.69 - 1.83 (m, 3 H), 1.88 (d, $J = 12.82$ Hz, 2 H), 1.97 (d, $J = 12.21$ Hz, 2 H), 2.62 - 2.86 (m, 6 H), 3.05 (t, $J = 3.20$ Hz, 1 H), 3.88 (t, $J = 5.34$ Hz, 2 H), 4.13 (s, 3 H), 4.33 (t, $J = 5.34$ Hz, 2 H), 7.05 (d, $J = 8.85$ Hz, 1 H), 7.11 (s, 1 H), 7.45 (s, 1 H), 8.27 (d, $J = 8.85$ Hz, 1 H), 8.82 (s, 1 H)



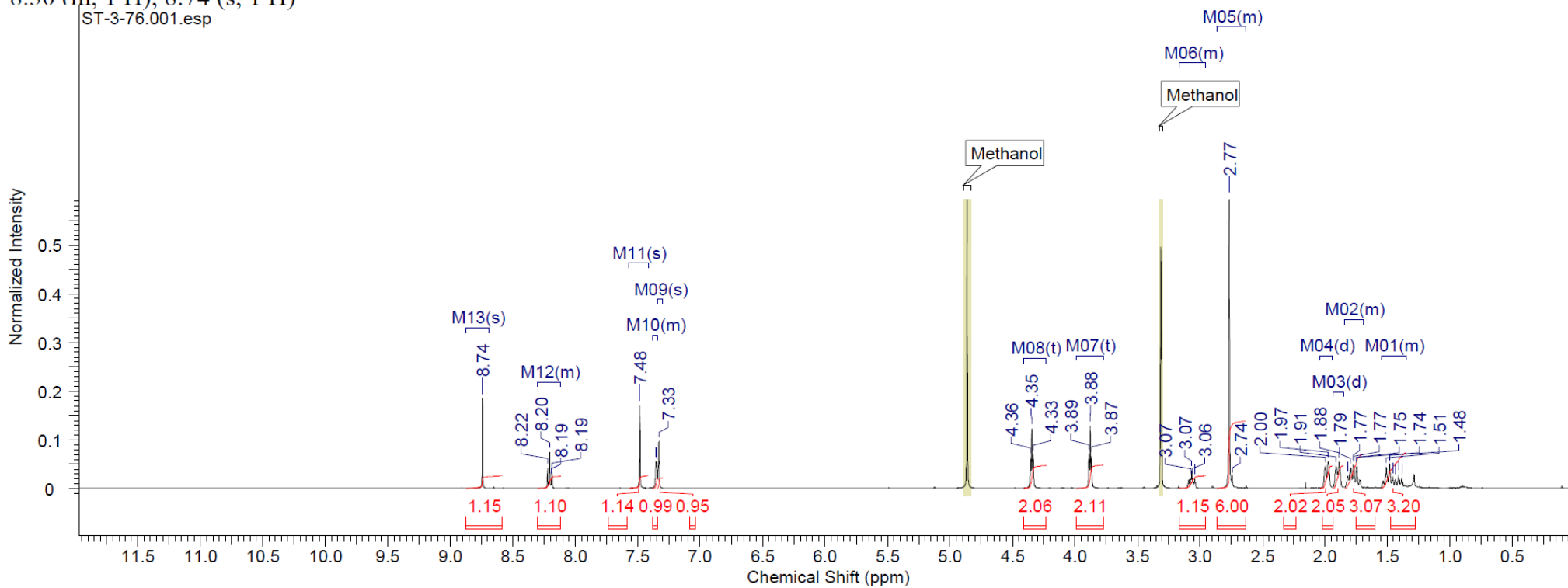
^{13}C NMR (126 MHz, METHANOL- d_4) δ 27.1, 27.5, 33.2, 37.4, 46.1, 47.1, 57.4, 61.6, 103.5, 106.3, 110.6, 113.9, 118.9, 120.9, 122.0, 123.0, 125.0, 131.1, 132.5, 134.8, 139.6, 142.4, 154.0, 160.2, 161.6, 163.6



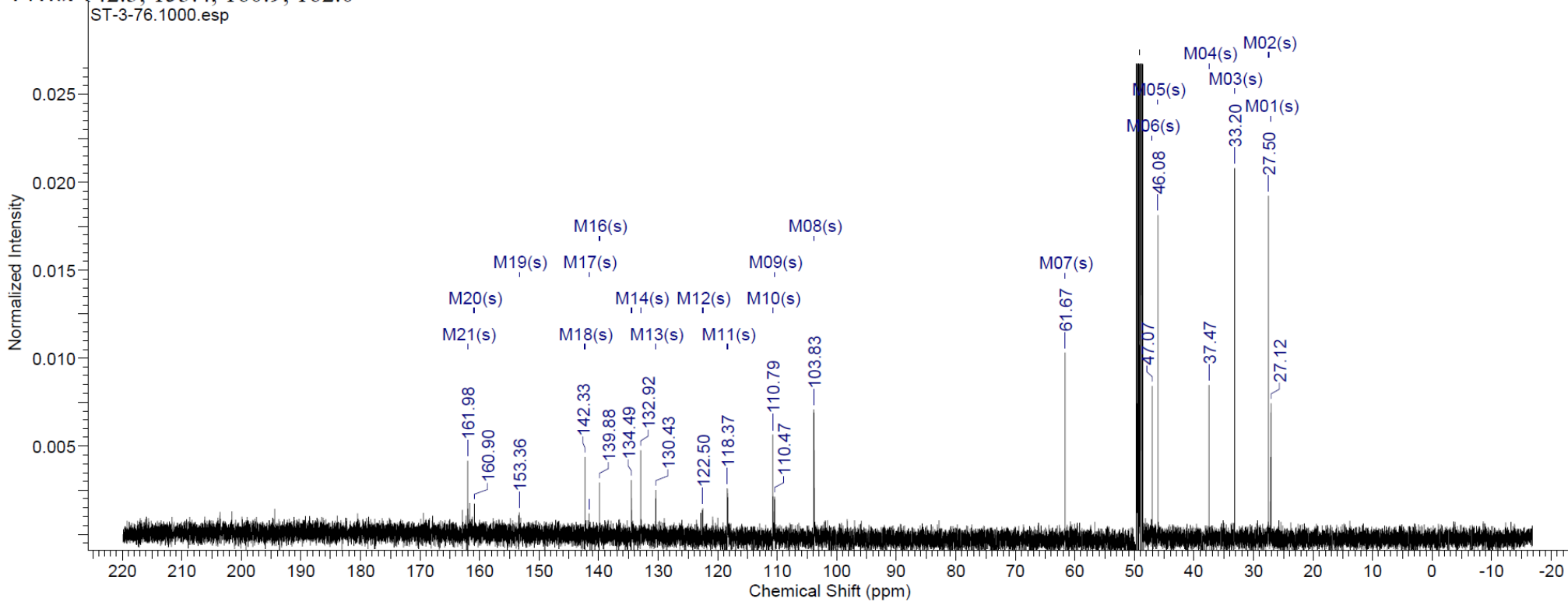
2-Cyclohexyl-6-*N,N*-dimethylamino-5-(2-fluoro-4-trifluoromethyl)benzamido-1-hydroxyethyl-1*H*-benzo[d]imidazole



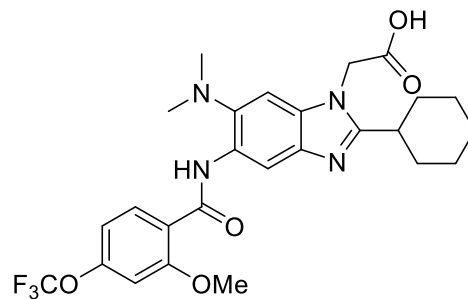
$^1\text{H NMR}$ (500 MHz, METHANOL- d_4) δ 1.35 - 1.55 (m, 3 H), 1.69 - 1.84 (m, 3 H), 1.90 (d, $J = 13.12$ Hz, 2 H), 1.99 (d, $J = 12.21$ Hz, 2 H), 2.64 - 2.86 (m, 6 H), 2.96 - 3.17 (m, 1 H), 3.88 (t, $J = 5.34$ Hz, 2 H), 4.35 (t, $J = 5.34$ Hz, 2 H), 7.33 (s, 1 H), 7.34 - 7.38 (m, 1 H), 7.48 (s, 1 H), 8.12 - 8.30 (m, 1 H), 8.74 (s, 1 H)



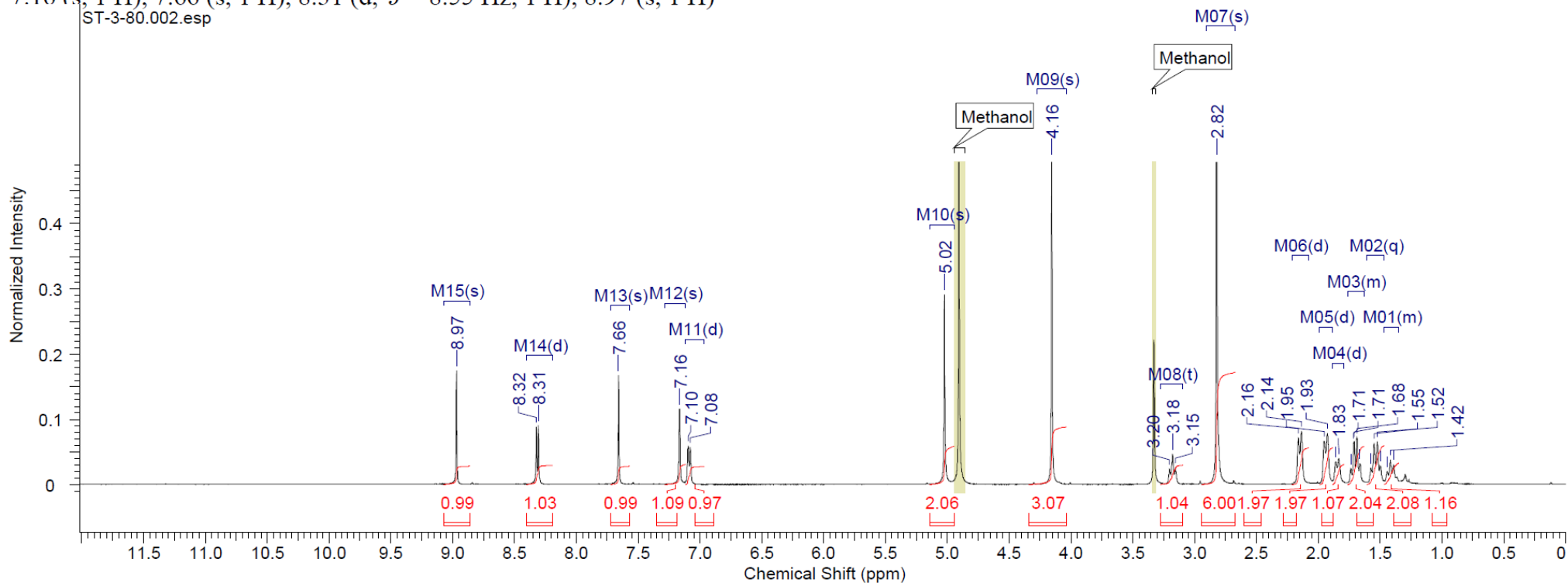
^{13}C NMR (126 MHz, METHANOL- d_4) δ 27.1, 27.5, 33.2, 37.5, 46.1, 47.1, 61.7, 103.8, 110.5, 110.8, 118.4, 122.5, 130.4, 132.9, 134.5, 139.9, 141.6, 142.3, 153.4, 160.9, 162.0



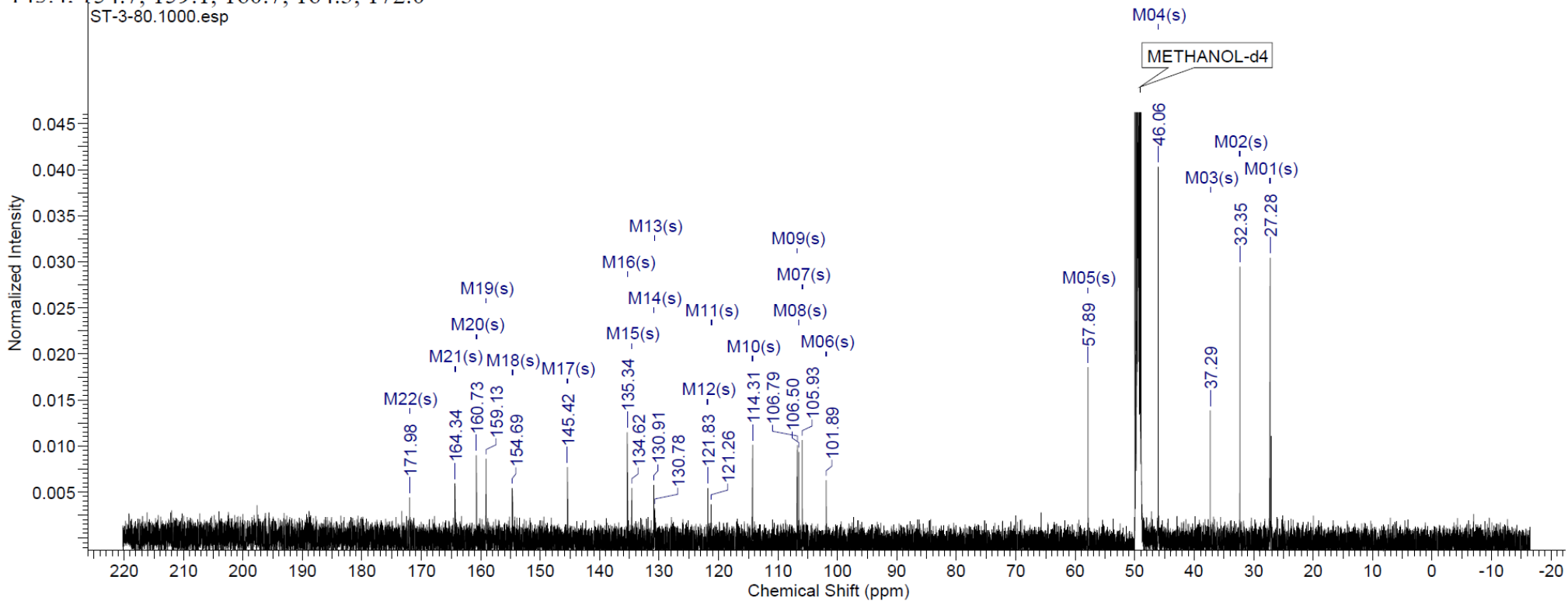
2-Cyclohexyl-6-*N,N*-dimethylamino-5-(2-methoxy-4-trifluoromethyl)benzamido-1-carboxymethyl-1*H*-benzo[d]imidazole



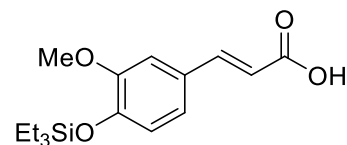
¹H NMR (500 MHz, METHANOL-*d*₄) δ 1.35 - 1.47 (m, 1 H), 1.53 (q, *J* = 12.92 Hz, 2 H), 1.63 - 1.76 (m, 2 H), 1.85 (d, *J* = 12.51 Hz, 1 H), 1.94 (d, *J* = 13.12 Hz, 2 H), 2.15 (d, *J* = 11.90 Hz, 2 H), 2.82 (s, 6 H), 3.18 (t, *J* = 12.05 Hz, 1 H), 4.16 (s, 3 H), 5.02 (s, 2 H), 7.09 (d, *J* = 8.55 Hz, 1 H), 7.16 (s, 1 H), 7.66 (s, 1 H), 8.31 (d, *J* = 8.55 Hz, 1 H), 8.97 (s, 1 H)



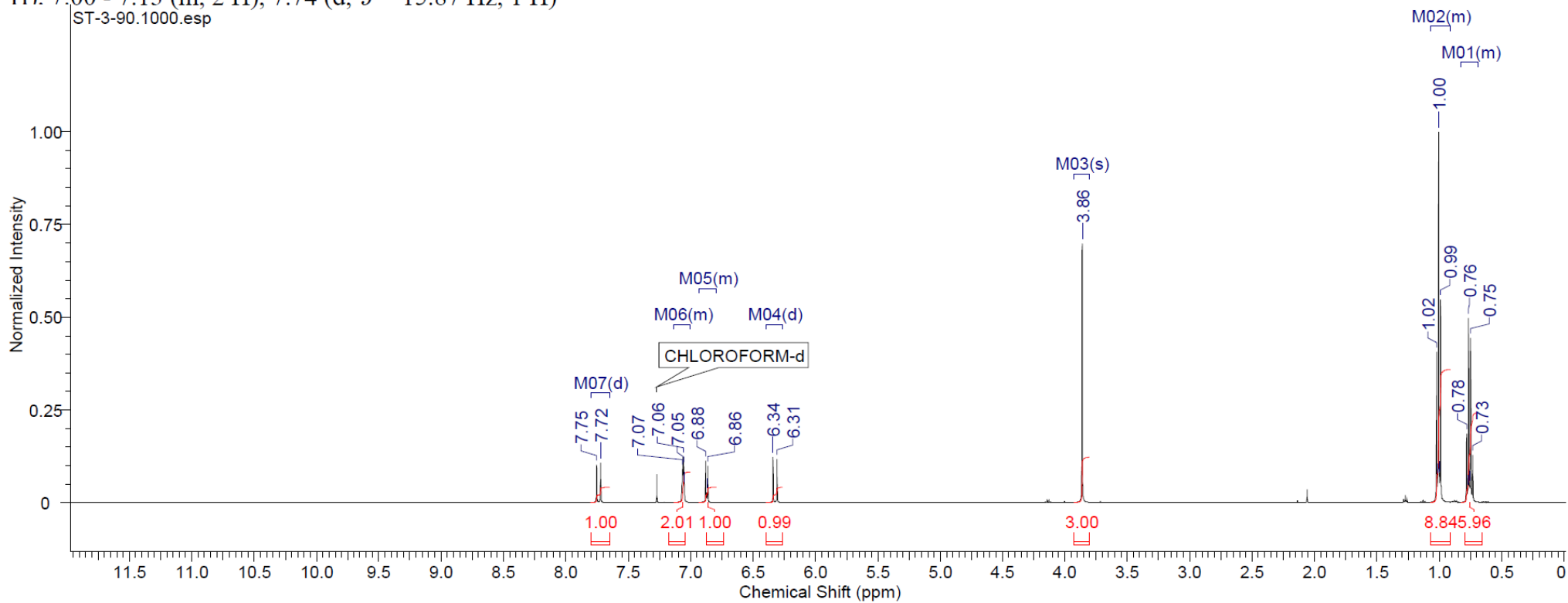
^{13}C NMR (126 MHz, METHANOL- d_4) δ 27.3, 32.4, 37.3, 46.1, 57.9, 101.9, 105.9, 106.5, 106.8, 114.3, 121.3, 121.8, 130.8, 130.9, 134.6, 135.3, 145.4, 154.7, 159.1, 160.7, 164.3, 172.0



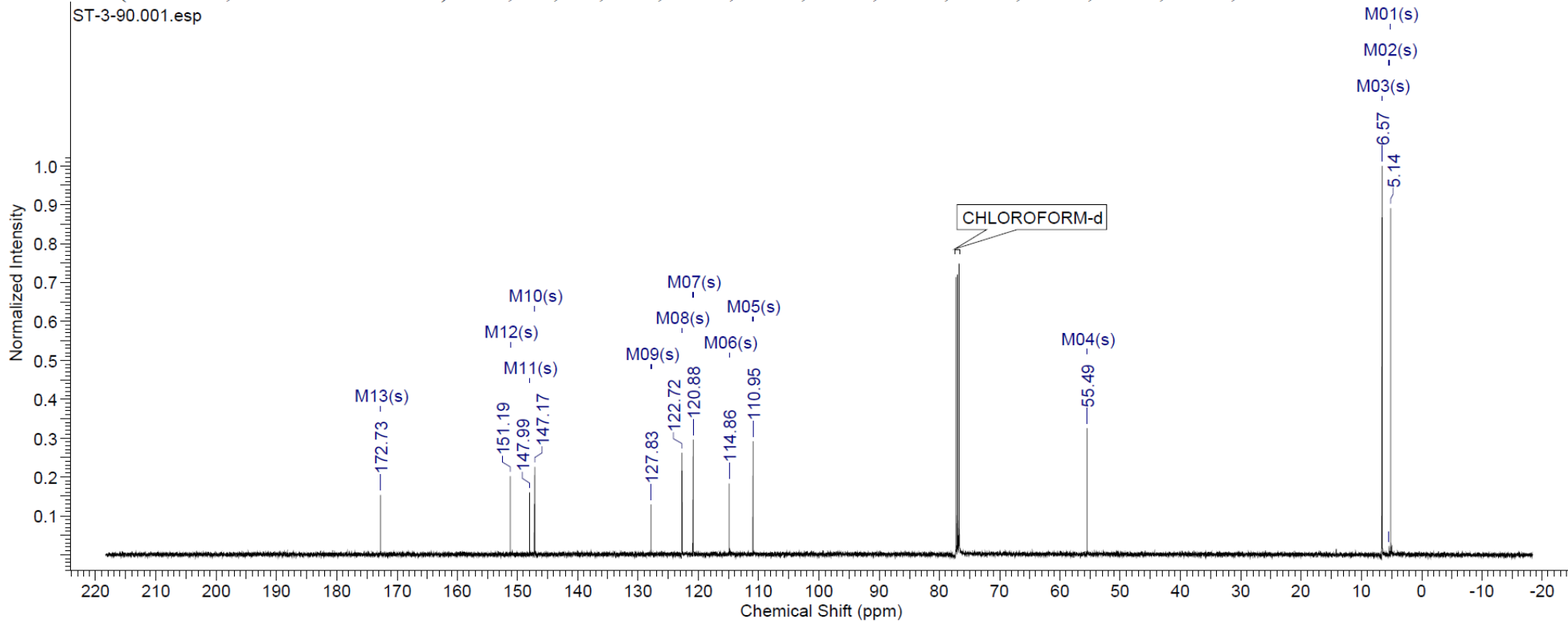
(2E)-3-(3-Methoxy-4-triethylsiloxyphenyl)-2-Propenoic acid



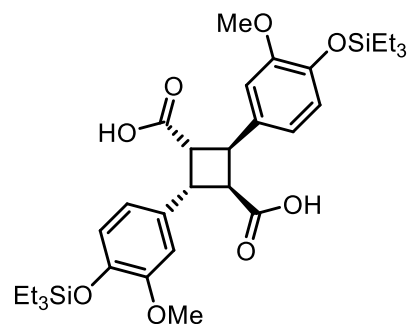
$^1\text{H NMR}$ (500 MHz, CHLOROFORM- d) δ 0.69 - 0.83 (m, 6 H), 0.91 - 1.07 (m, 9 H), 3.86 (s, 3 H), 6.32 (d, $J = 15.87$ Hz, 1 H), 6.79 - 6.93 (m, 1 H), 7.00 - 7.13 (m, 2 H), 7.74 (d, $J = 15.87$ Hz, 1 H)



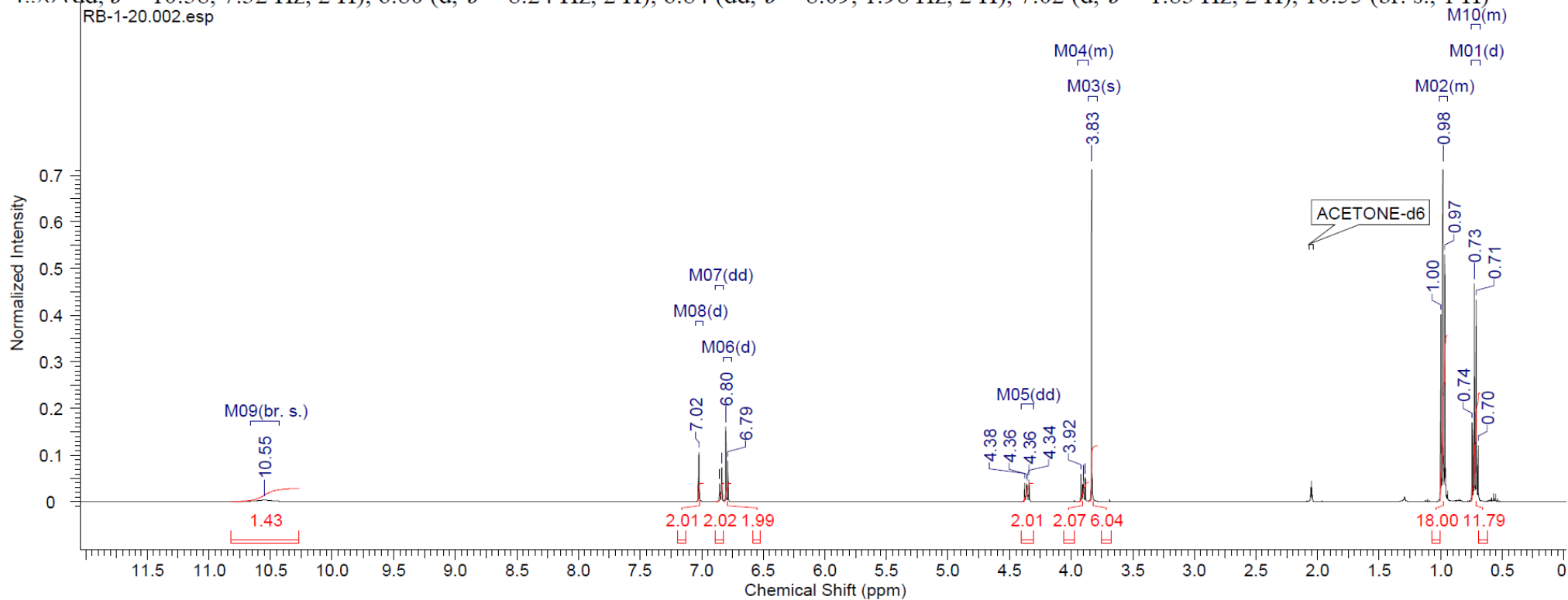
^{13}C NMR (126 MHz, CHLOROFORM-d) δ 5.1, 5.4, 6.6, 55.5, 110.9, 114.9, 120.9, 122.7, 127.8, 127.8, 147.2, 148.0, 151.2, 172.7



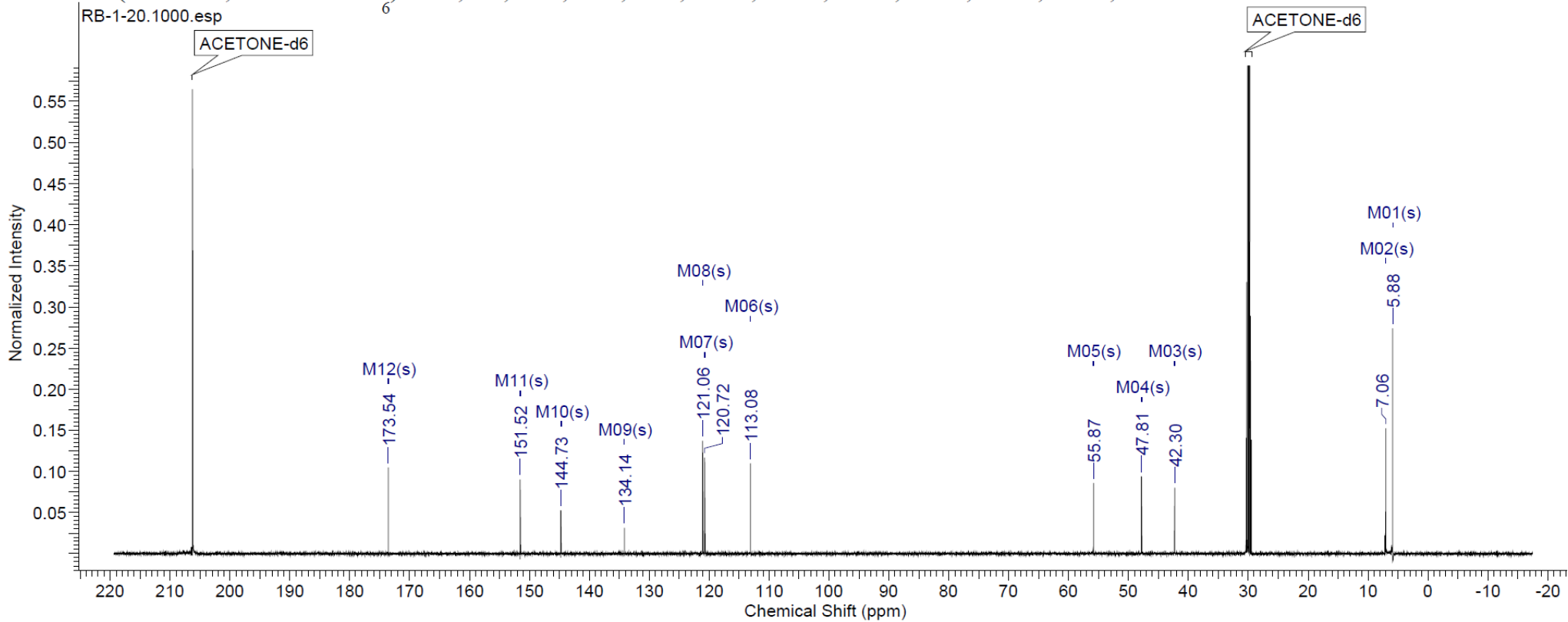
2,4-Bis(3-methoxy-4-triethylsiloxy)phenylcyclobutane-1,3-dicarboxylic acid



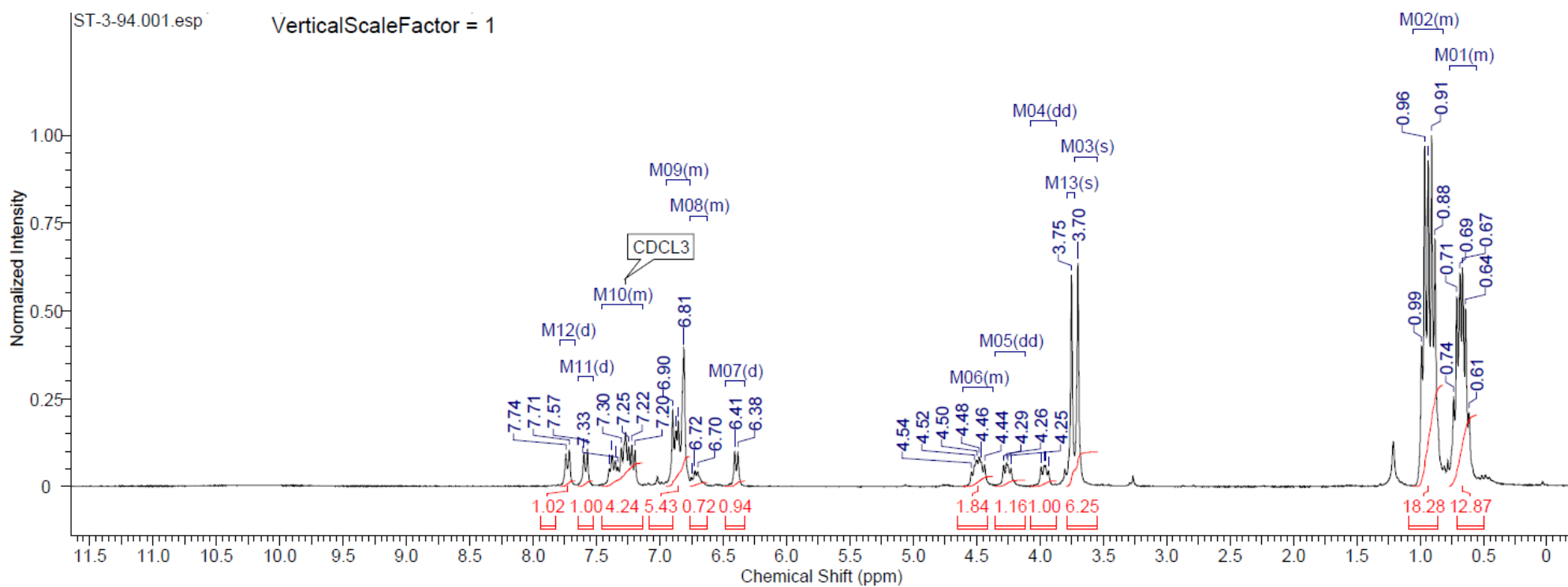
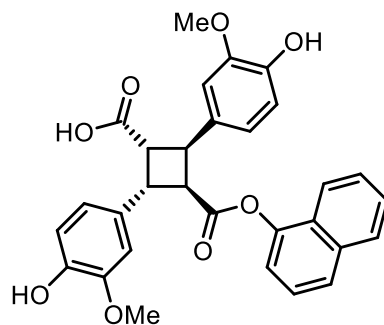
¹H NMR (500 MHz, ACETONE-d₆) δ 0.68 - 0.75 (m, 3 H), 0.72 (d, *J* = 7.93 Hz, 9 H), 0.95 - 1.01 (m, 18 H), 3.83 (s, 6 H), 3.86 - 3.95 (m, 2 H), 4.36 (dd, *J* = 10.38, 7.32 Hz, 2 H), 6.80 (d, *J* = 8.24 Hz, 2 H), 6.84 (dd, *J* = 8.09, 1.98 Hz, 2 H), 7.02 (d, *J* = 1.83 Hz, 2 H), 10.55 (br. s., 1 H)



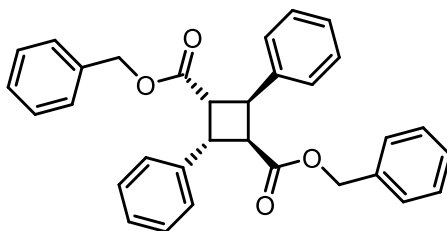
^{13}C NMR (126 MHz, ACETONE- d_6) δ 5.9, 7.1, 42.3, 47.8, 55.9, 113.1, 120.7, 121.1, 134.1, 144.7, 151.5, 173.5



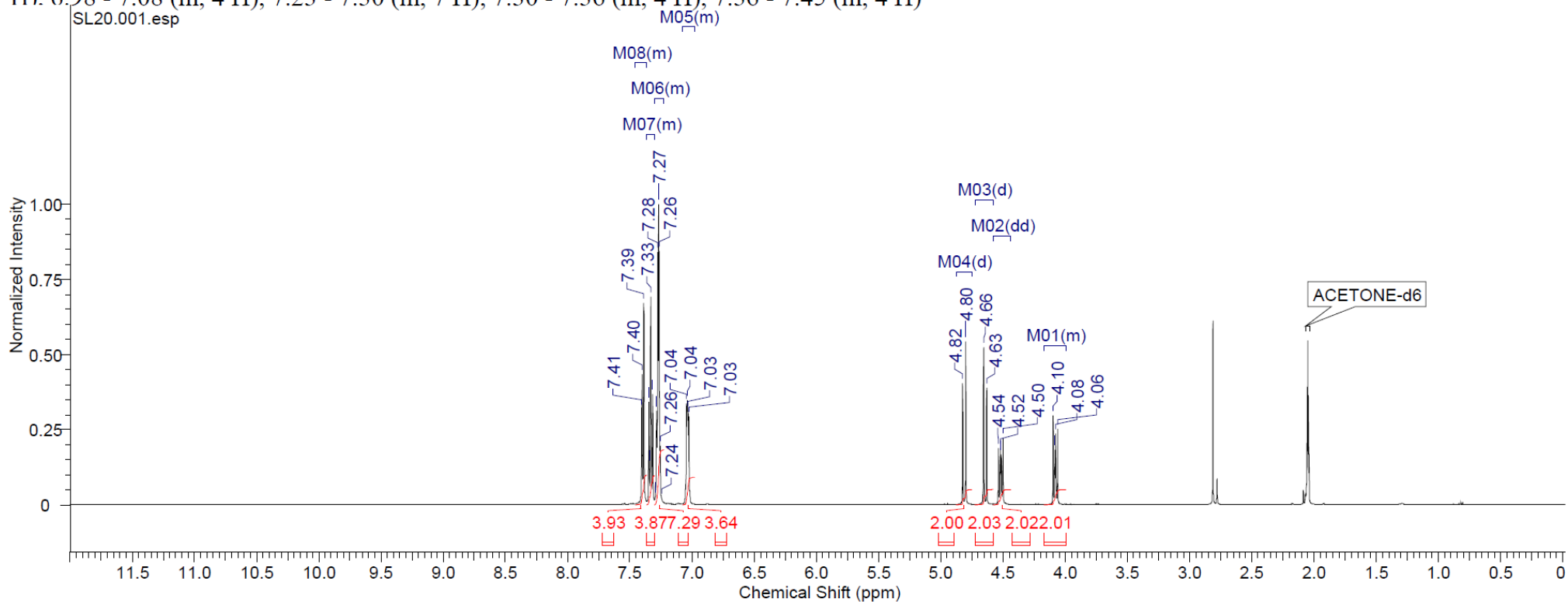
2,4-Bis(3-methoxy-4-hydroxy)phenylcyclobutane-1,3-dicarboxylic acid mono-1-naphthyl ester



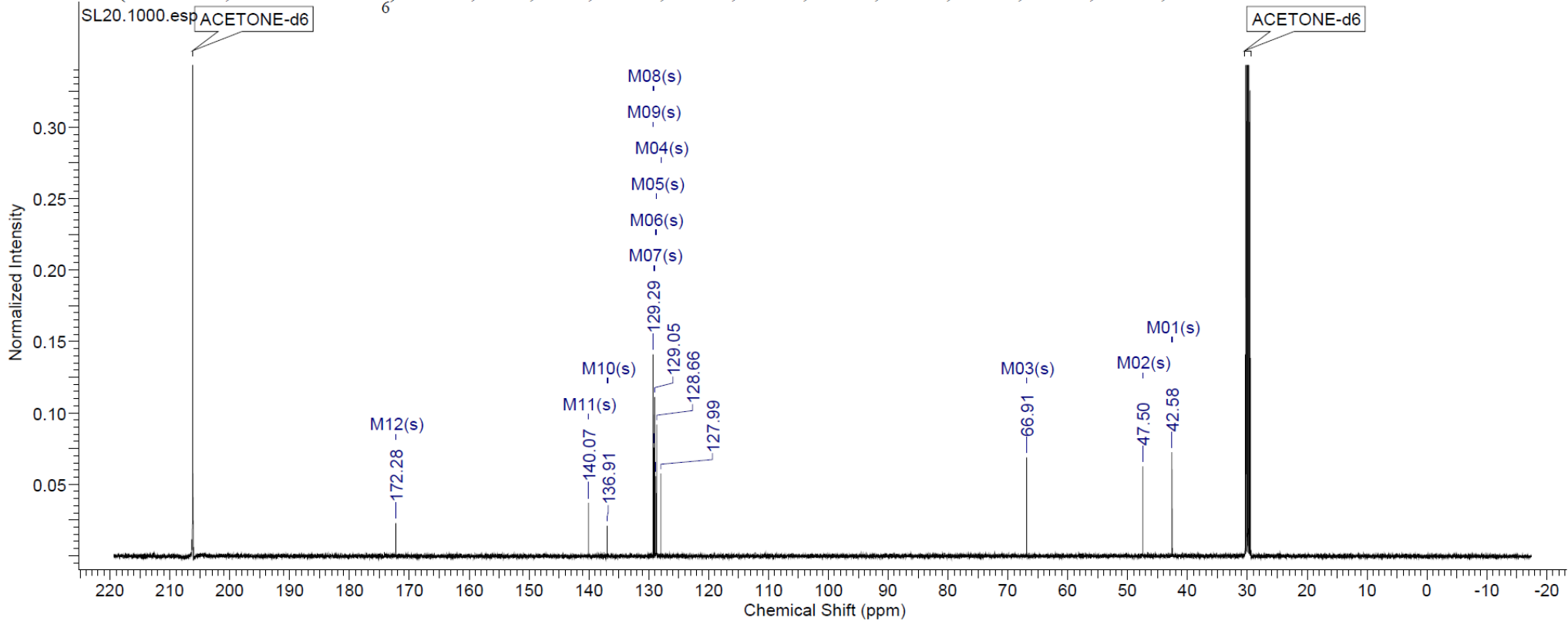
α -2,4-Diphenylcyclobutane-1,3-dicarboxylic acid di-benzyl ester (SB-FI-74)



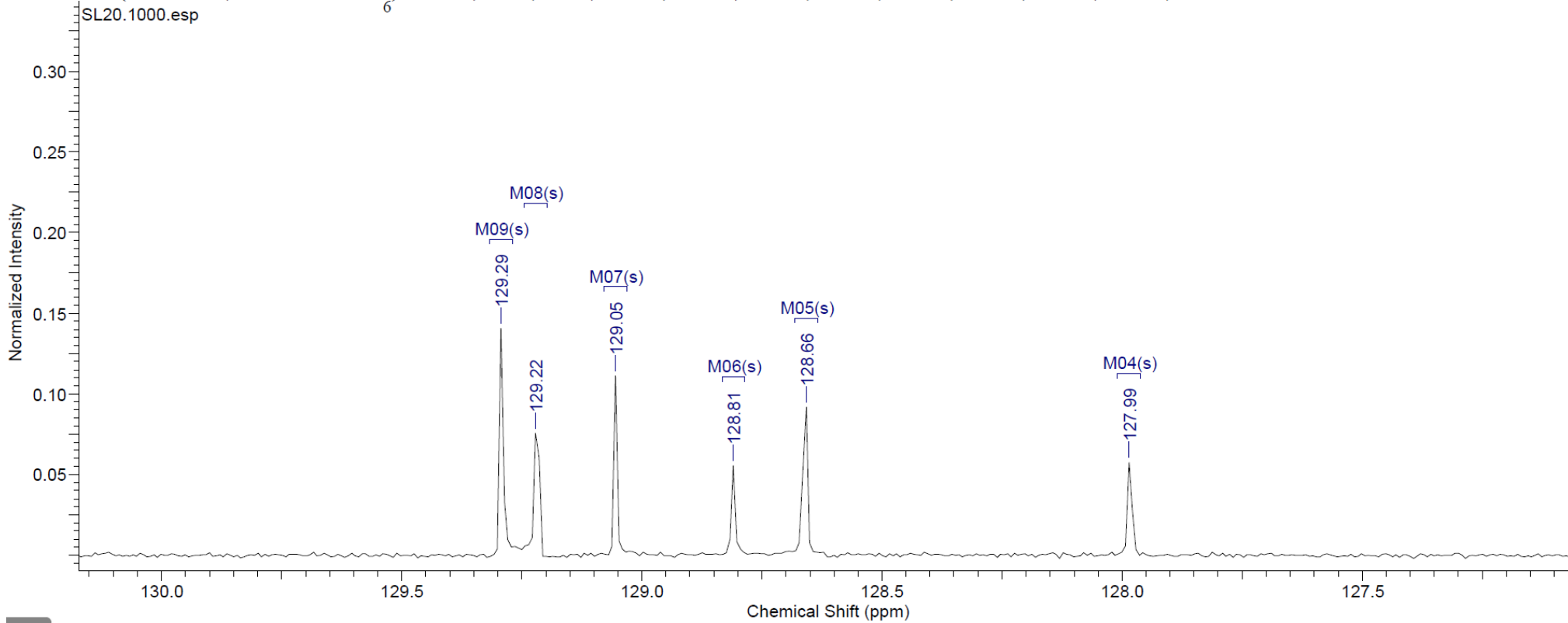
$^1\text{H NMR}$ (500 MHz, ACETONE- d_6) δ 3.99 - 4.17 (m, 2 H), 4.52 (dd, $J = 10.38, 7.32$ Hz, 2 H), 4.64 (d, $J = 12.21$ Hz, 2 H), 4.81 (d, $J = 12.51$ Hz, 2 H). 6.98 - 7.08 (m, 4 H), 7.23 - 7.30 (m, 7 H), 7.30 - 7.36 (m, 4 H), 7.36 - 7.45 (m, 4 H)



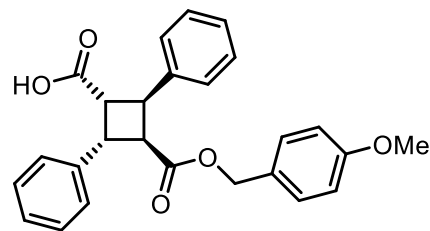
^{13}C NMR (126 MHz, ACETONE- d_6) δ 42.6, 47.5, 66.9, 128.0, 128.7, 128.8, 129.1, 129.2, 129.3, 136.9, 140.1, 172.3



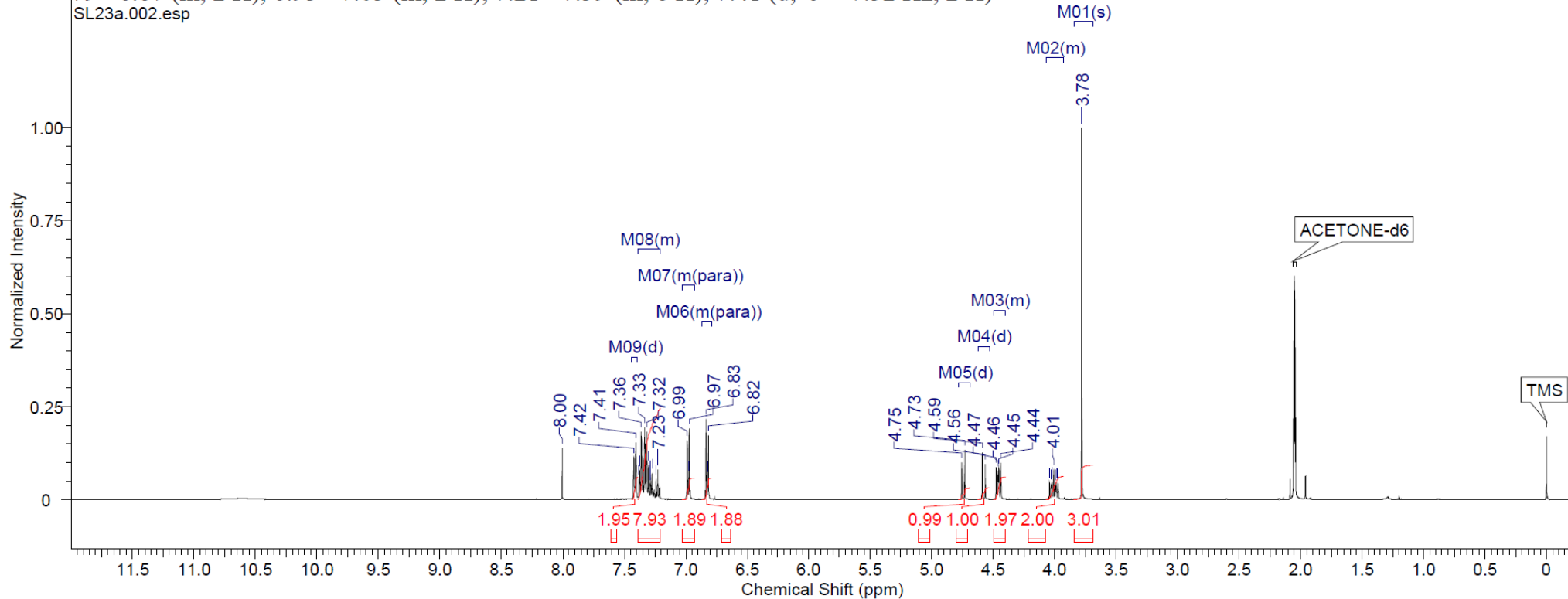
^{13}C NMR (126 MHz, ACETONE- d_6) δ 42.6, 47.5, 66.9, 128.0, 128.7, 128.8, 129.1, 129.2, 129.3, 136.9, 140.1, 172.3



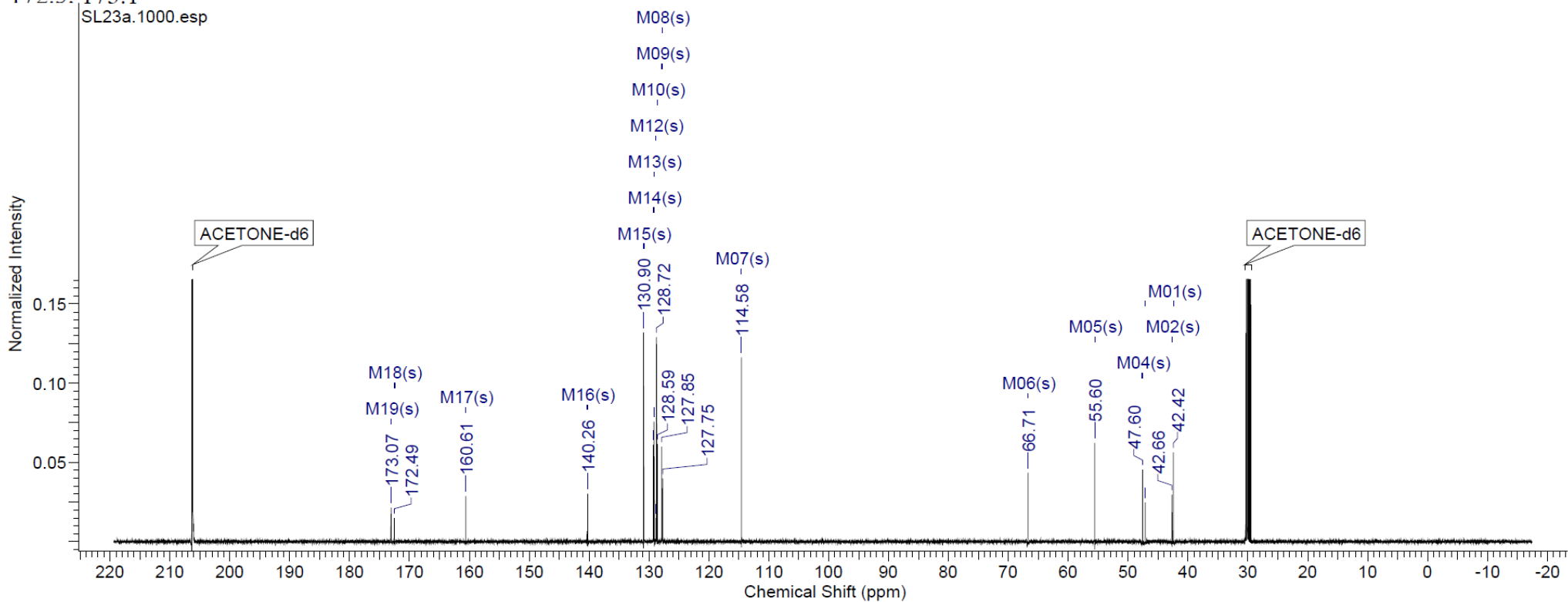
α -2,4-Diphenylcyclobutane-1,3-dicarboxylic acid mono-(4-methoxy)benzyl ester (SB-FI-75)



$^1\text{H NMR}$ (500 MHz, ACETONE- d_6) δ 3.78 (s, 3 H), 3.93 - 4.07 (m, 2 H), 4.40 - 4.50 (m, 2 H), 4.58 (d, J = 11.90 Hz, 1 H), 4.74 (d, J = 11.90 Hz, 1 H), 6.79 - 6.87 (m, 2 H), 6.93 - 7.03 (m, 2 H), 7.21 - 7.39 (m, 8 H), 7.41 (d, J = 7.32 Hz, 2 H)

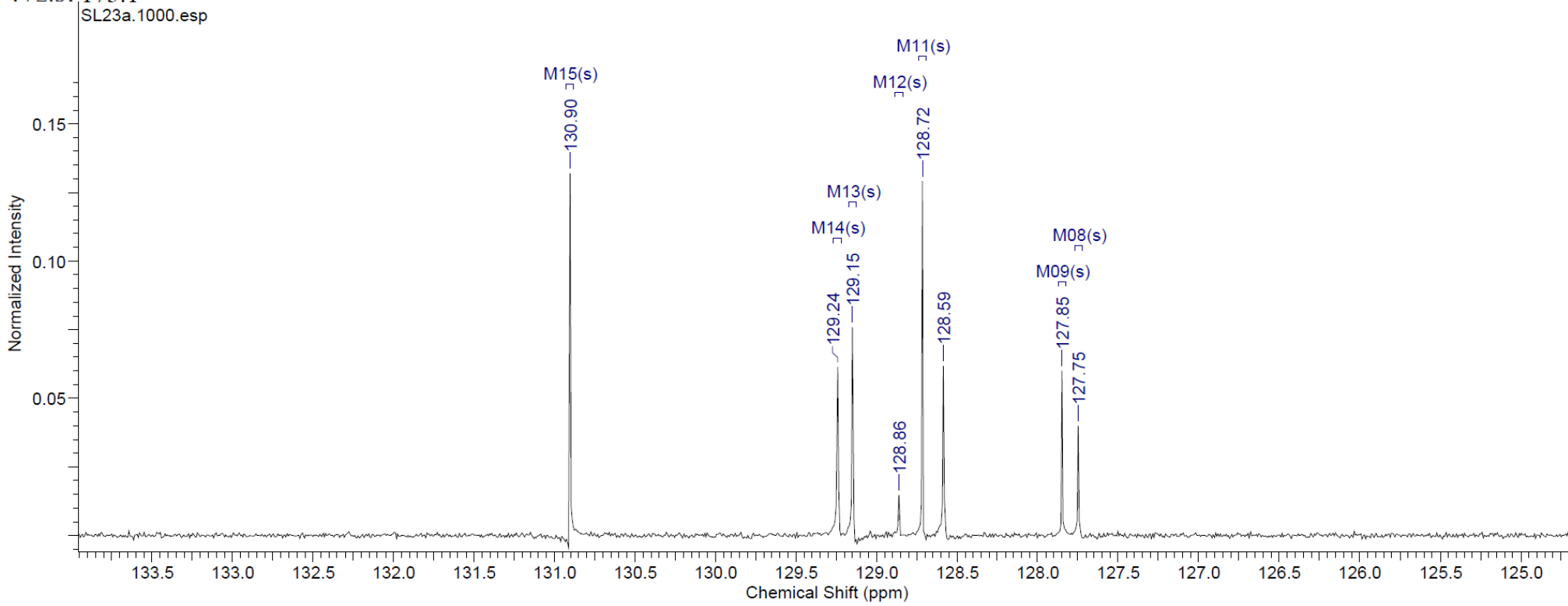


^{13}C NMR (126 MHz, ACETONE- d_6) δ 42.4, 42.7, 47.1, 47.6, 55.6, 66.7, 114.6, 127.7, 127.8, 128.6, 128.7, 128.9, 129.1, 129.2, 130.9, 140.3, 160.6, 172.5, 173.1

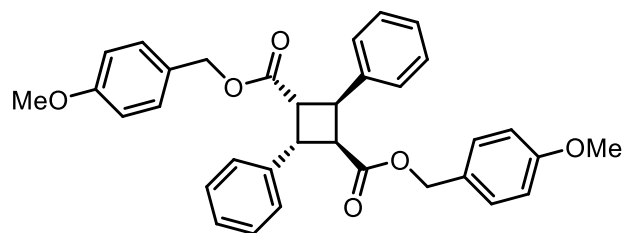


¹³C NMR (120 MHz, ACETONE-*d*₆) δ 42.4, 42.7, 47.1, 47.0, 55.0, 60.7, 114.0, 127.7, 127.8, 128.0, 128.7, 128.9, 129.1, 129.2, 130.9, 140.3, 100.0,

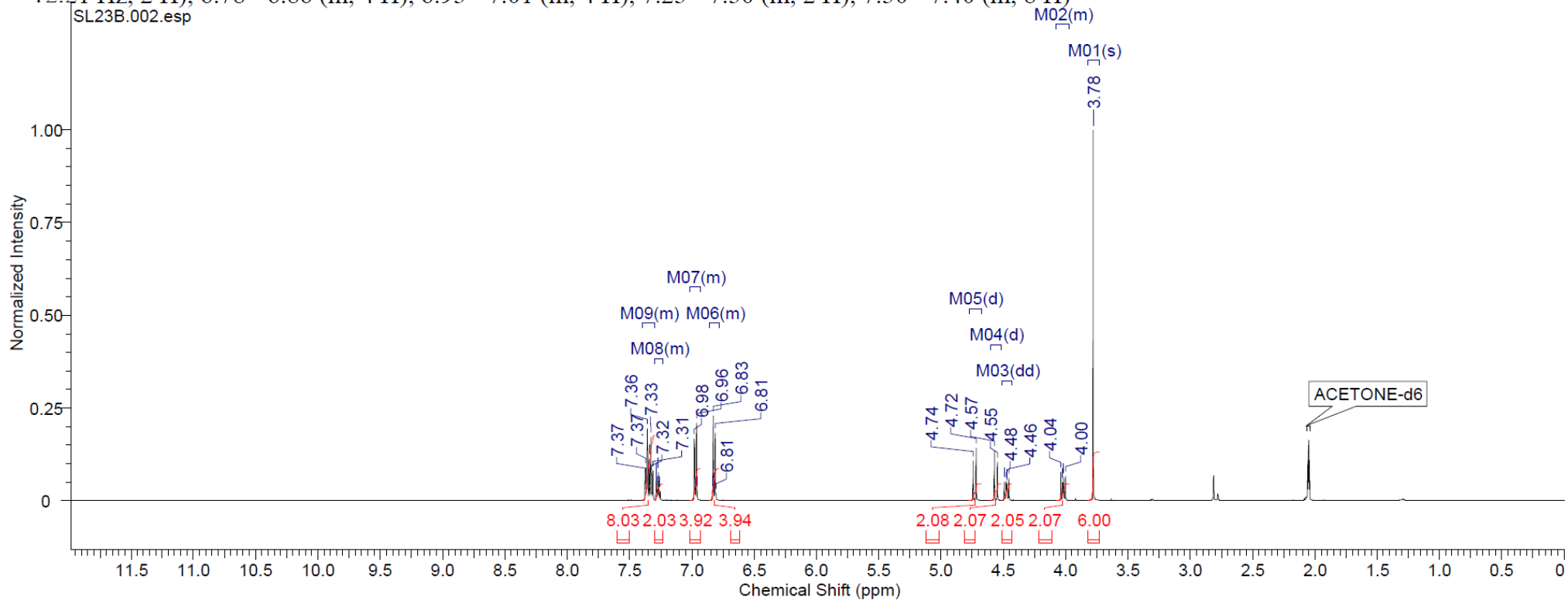
172.5, 173.1



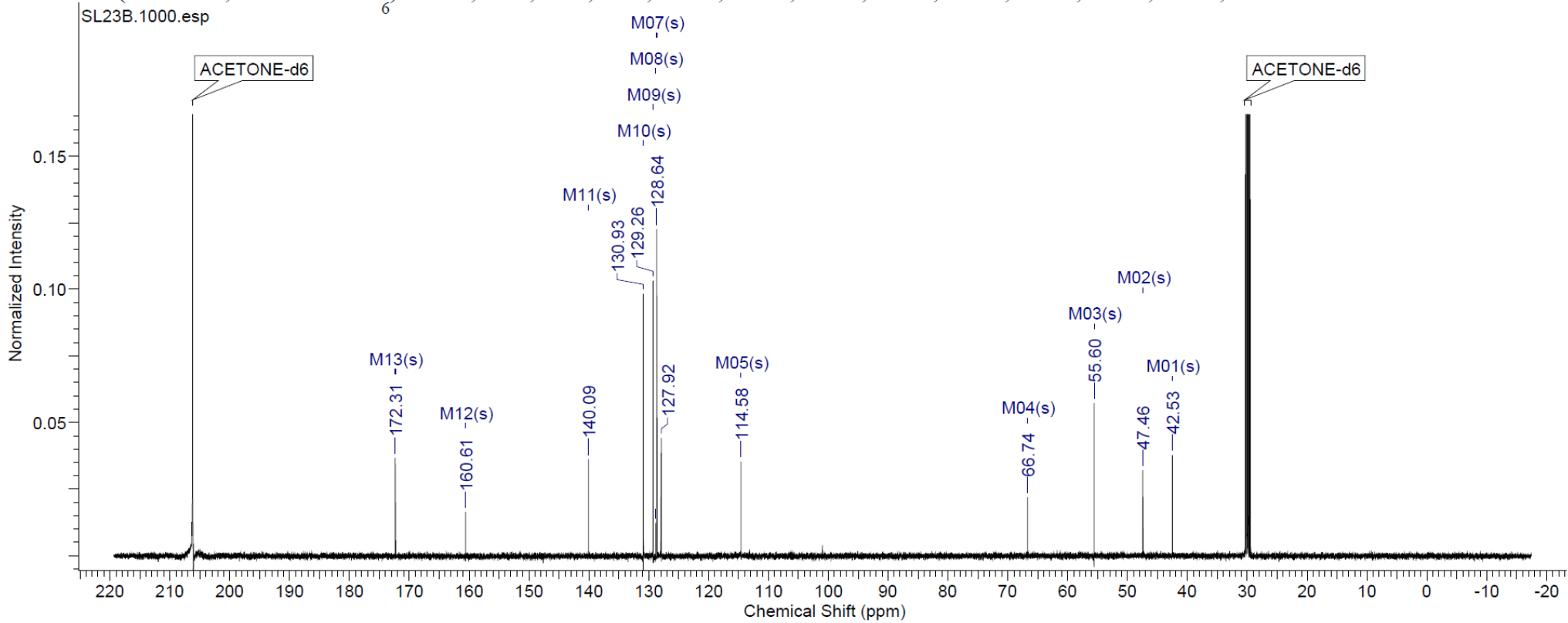
α -2,4-diphenylcyclobutane-1,3-dicarboxylic acid di-(4-methoxy)benzyl ester (SB-FI-76)



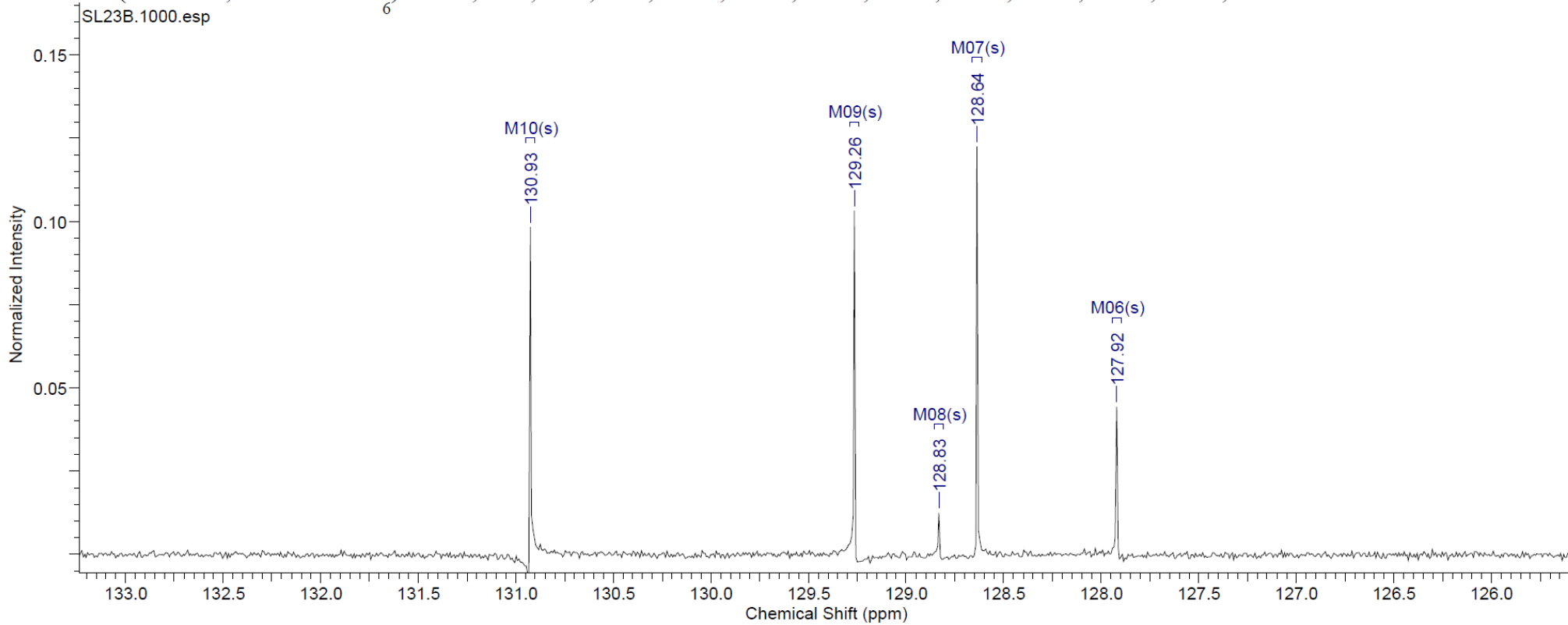
$^1\text{H NMR}$ (500 MHz, ACETONE- d_6) δ 3.78 (s, 6 H), 3.97 - 4.08 (m, 2 H), 4.47 (dd, $J = 10.38, 7.32$ Hz, 2 H), 4.56 (d, $J = 12.21$ Hz, 2 H), 4.73 (d, $J = 12.21$ Hz, 2 H), 6.78 - 6.86 (m, 4 H), 6.93 - 7.01 (m, 4 H), 7.23 - 7.30 (m, 2 H), 7.30 - 7.40 (m, 8 H)



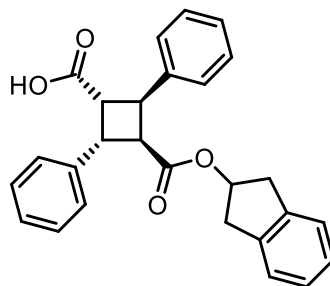
^{13}C NMR (126 MHz, ACETONE- d_6) δ 42.5, 47.5, 55.6, 66.7, 114.6, 127.9, 128.6, 128.8, 129.3, 130.9, 140.1, 160.6, 172.3



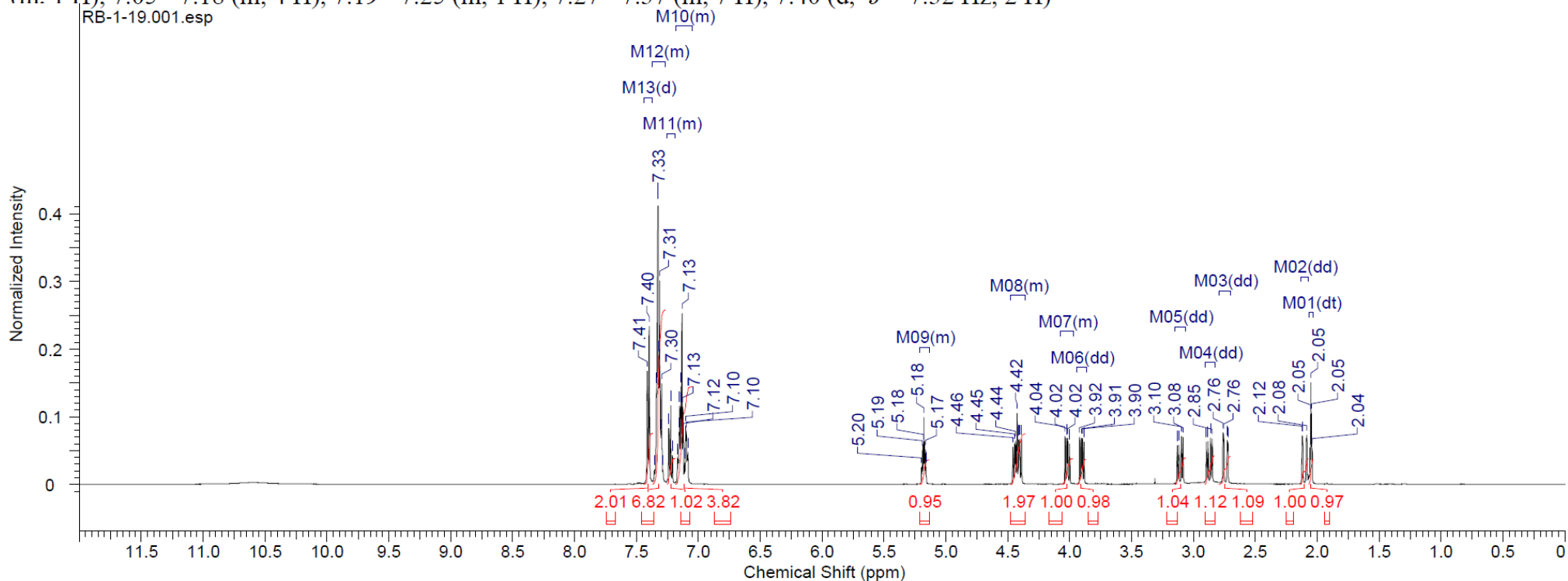
^{13}C NMR (126 MHz, ACETONE- d_6) δ 42.5, 47.5, 55.6, 66.7, 114.6, 127.9, 128.6, 128.8, 129.3, 130.9, 140.1, 160.6, 172.3



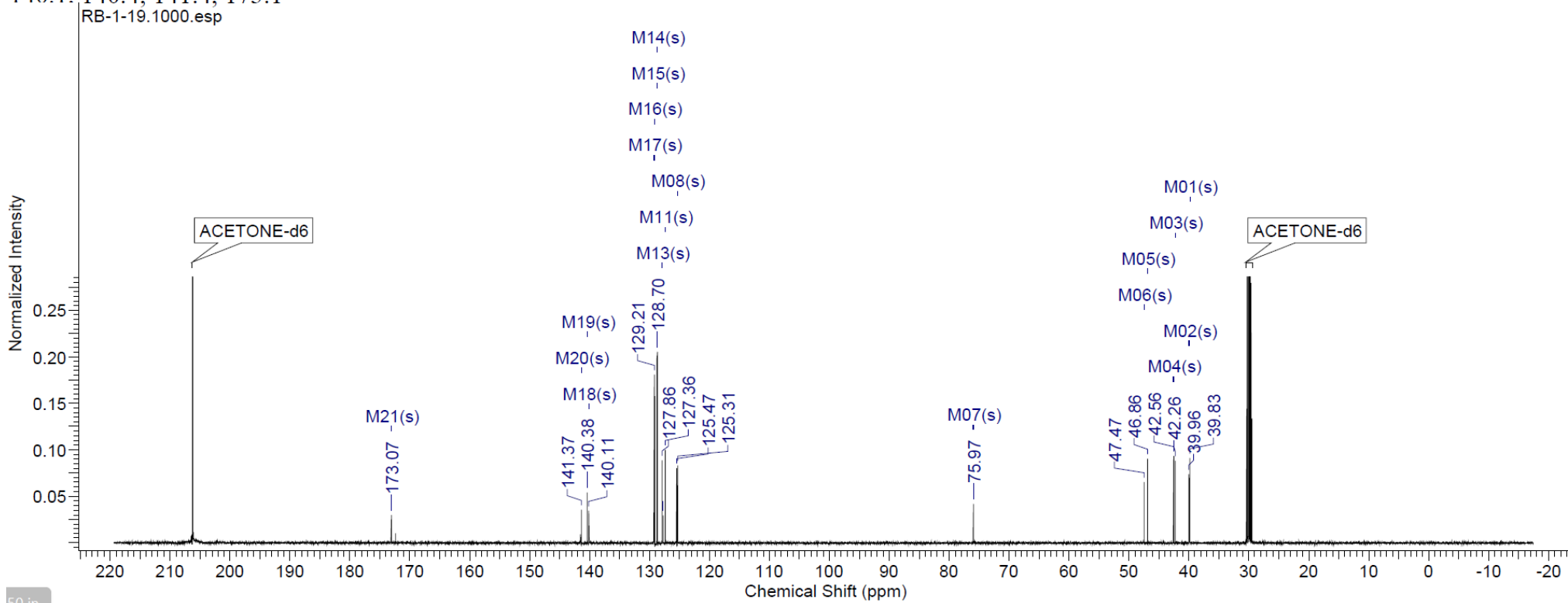
α -2,4-Diphenylcyclobutane-1,3-dicarboxylic acid mono-2-indanyl ester (SB-FI-77)



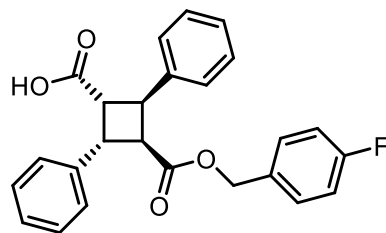
$^1\text{H NMR}$ (500 MHz, Acetone) δ 2.05 (dt, $J = 4.35, 2.25$ Hz, 1 H), 2.10 (dd, $J = 17.09, 2.44$ Hz, 1 H), 2.74 (dd, $J = 16.94, 2.59$ Hz, 1 H), 2.87 (dd, $J = 16.94, 6.26$ Hz, 1 H), 3.11 (dd, $J = 17.09, 6.41$ Hz, 1 H), 3.90 (dd, $J = 10.68, 6.71$ Hz, 1 H), 3.97 - 4.07 (m, 1 H), 4.36 - 4.48 (m, 2 H), 5.14 - 5.21 (m, 1 H), 7.05 - 7.18 (m, 4 H), 7.19 - 7.25 (m, 1 H), 7.27 - 7.37 (m, 7 H), 7.40 (d, $J = 7.32$ Hz, 2 H)



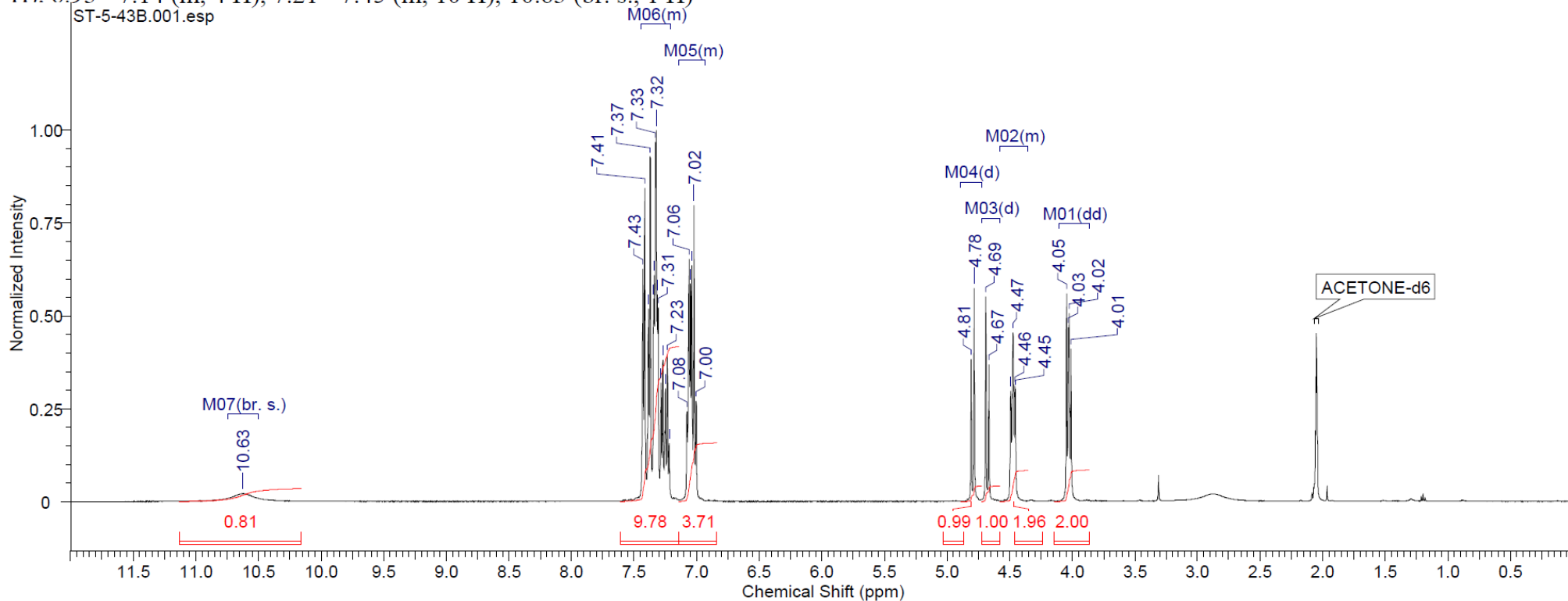
^{13}C NMR (126 MHz, ACETONE- d_6) δ 39.8, 40.0, 42.3, 42.6, 46.9, 47.5, 76.0, 125.3, 125.5, 127.3, 127.4, 127.7, 127.9, 128.7, 128.7, 129.1, 129.2, 140.1, 140.4, 141.4, 173.1



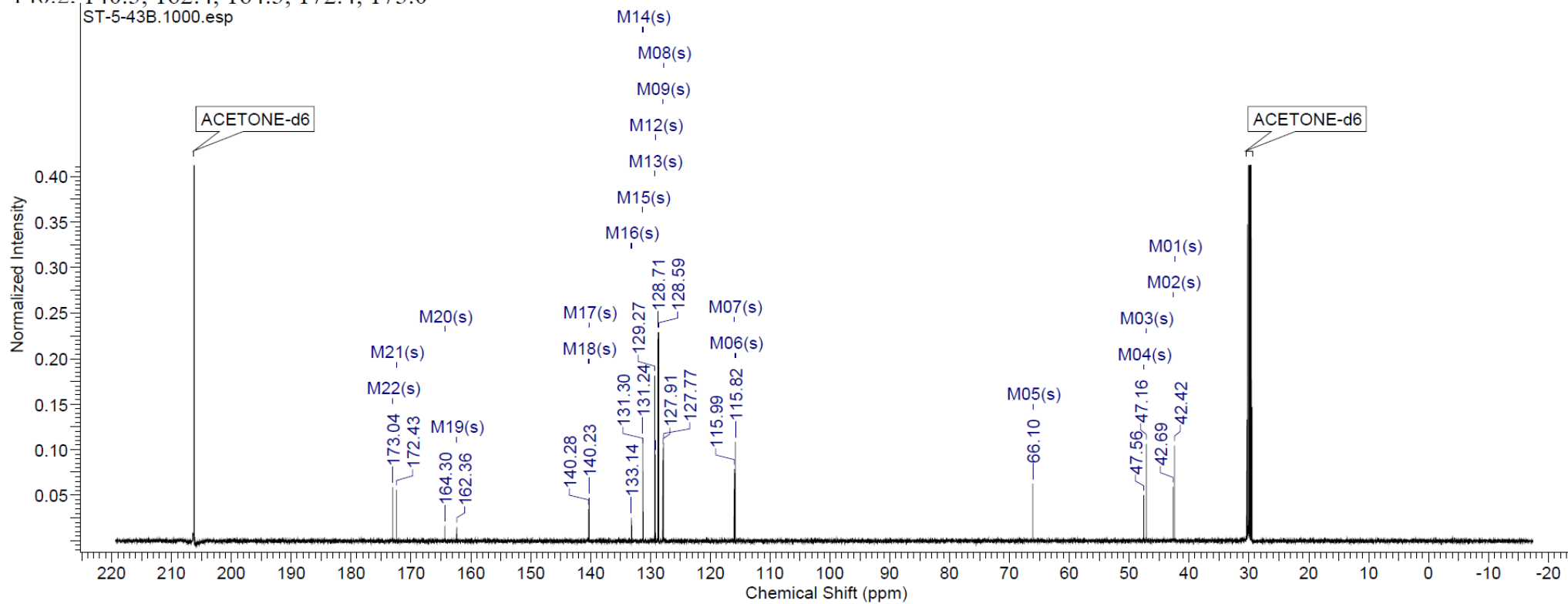
α -2,4-Diphenylcyclobutane-1,3-dicarboxylic acid mono-(4-fluoro)benzyl ester (SB-FI-78)



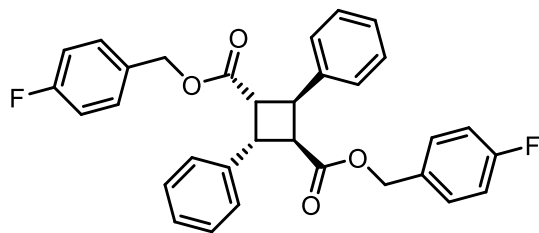
$^1\text{H NMR}$ (500 MHz, ACETONE- d_6) δ 4.03 (dd, J = 10.38, 7.32 Hz, 2 H), 4.35 - 4.58 (m, 2 H), 4.68 (d, J = 12.21 Hz, 1 H), 4.80 (d, J = 12.21 Hz, 1 H), 6.93 - 7.14 (m, 4 H), 7.21 - 7.45 (m, 10 H), 10.63 (br. s., 1 H)



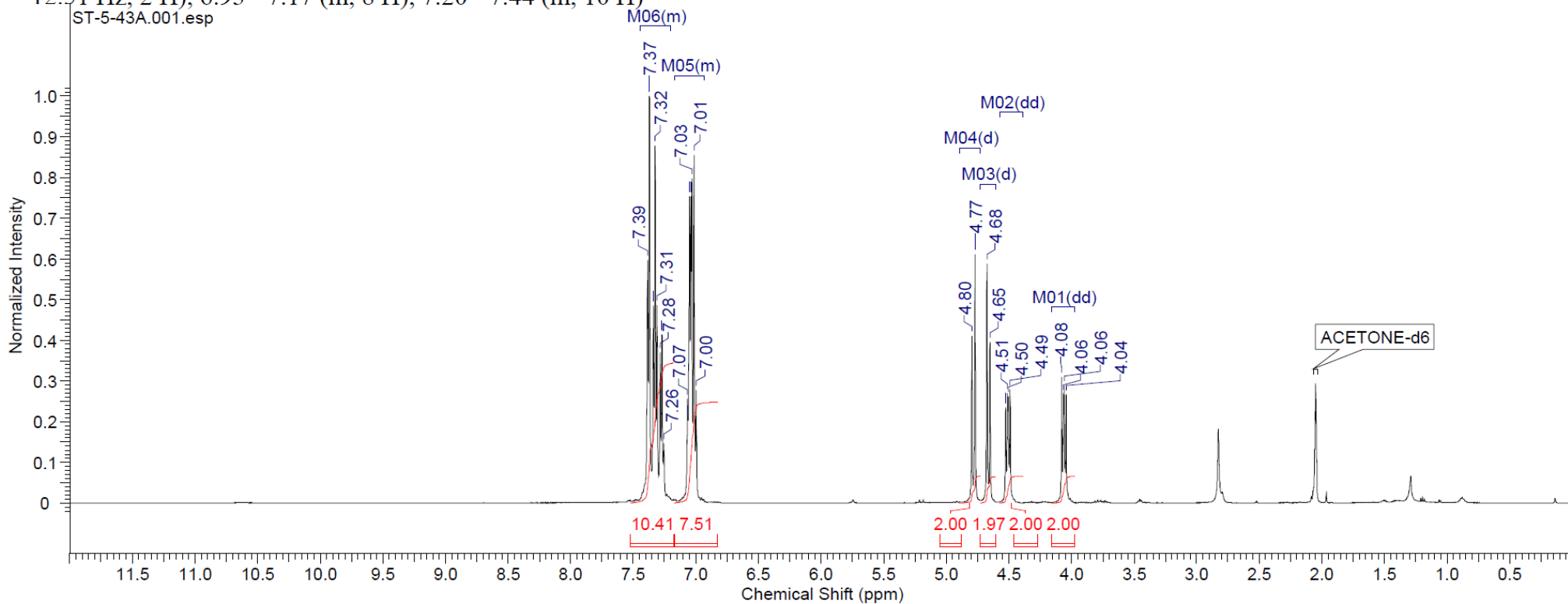
^{13}C NMR (126 MHz, ACETONE- d_6) δ 42.4, 42.7, 47.2, 47.6, 66.1, 115.8, 116.0, 127.8, 127.9, 128.6, 128.7, 129.2, 129.3, 131.2, 131.3, 133.1, 140.2, 140.3, 162.4, 164.3, 172.4, 173.0



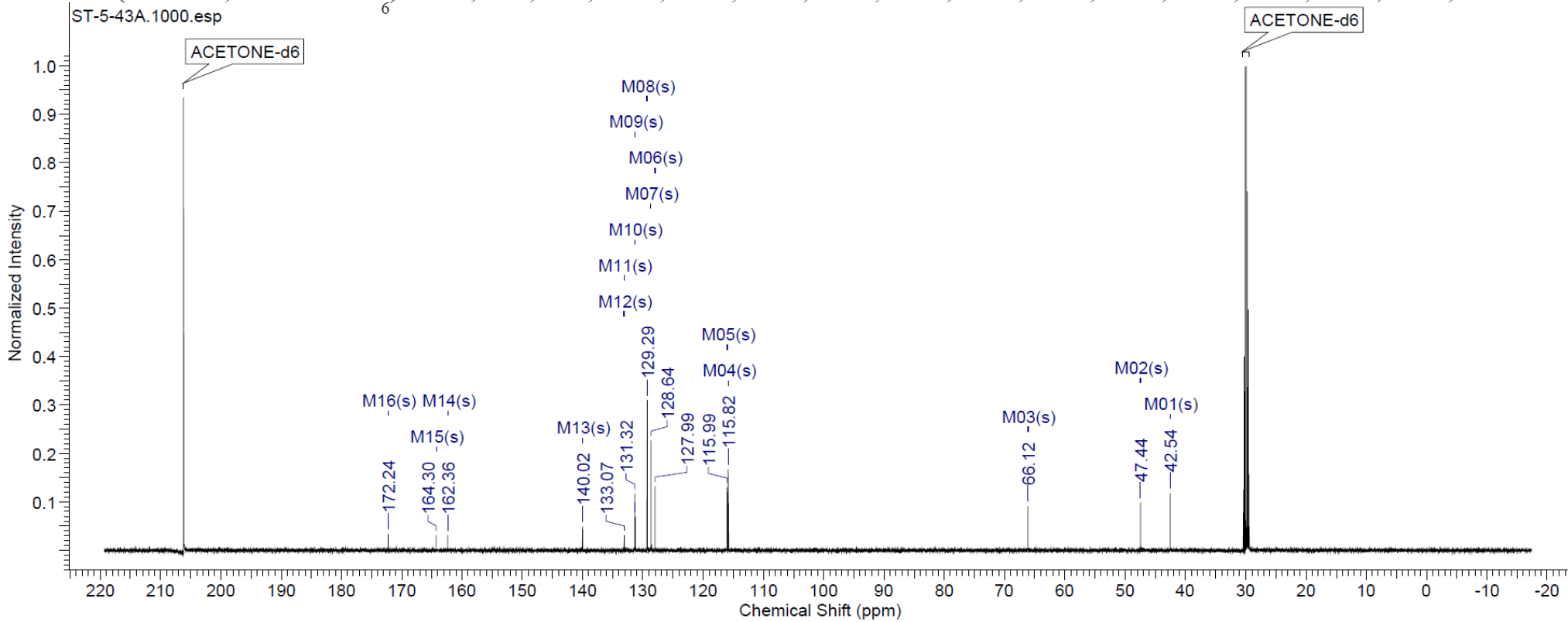
α -2,4-diphenylcyclobutane-1,3-dicarboxylic acid di-(4-fluoro)benzyl ester (SB-FI-79)



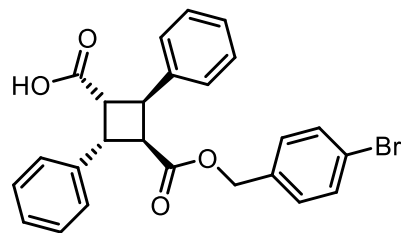
$^1\text{H NMR}$ (500 MHz, ACETONE- d_6) δ 4.06 (dd, J = 10.53, 7.48 Hz, 2 H), 4.51 (dd, J = 10.38, 7.32 Hz, 2 H), 4.66 (d, J = 12.21 Hz, 2 H), 4.78 (d, J = 12.51 Hz, 2 H), 6.93 - 7.17 (m, 8 H), 7.20 - 7.44 (m, 10 H)



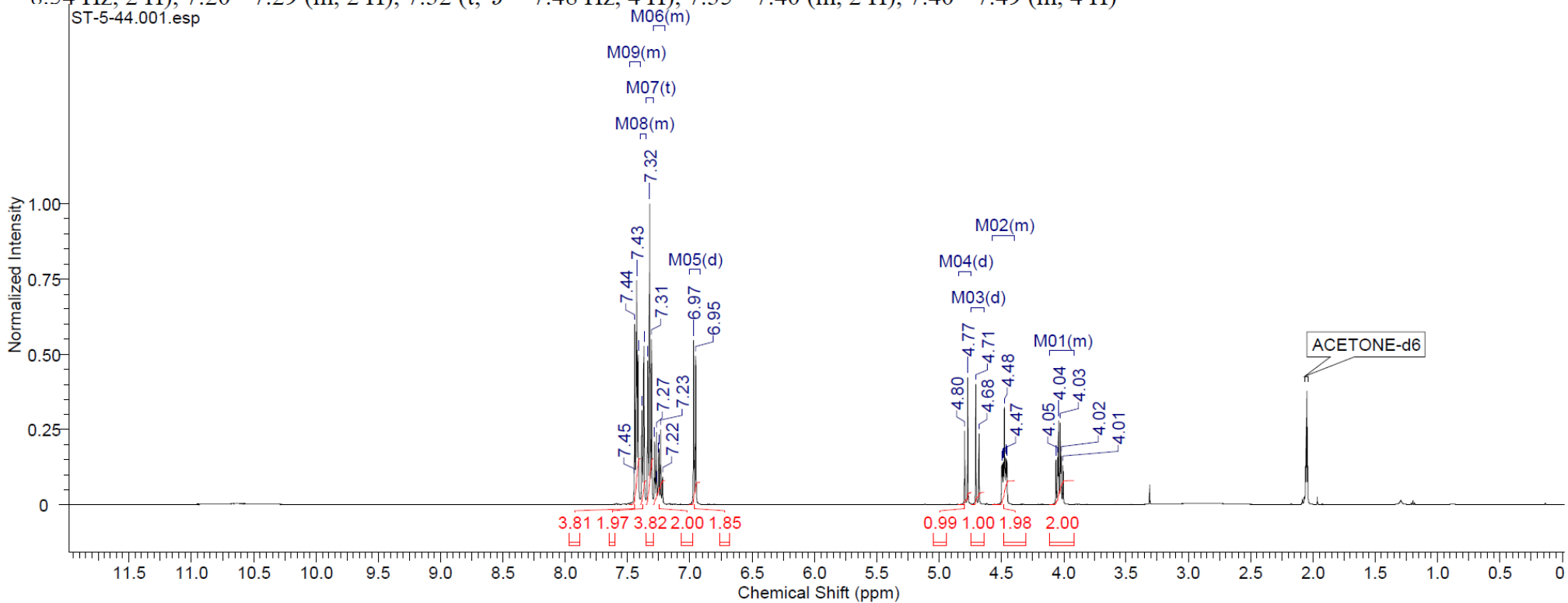
^{13}C NMR (126 MHz, ACETONE- d_6) δ 42.5, 47.4, 66.1, 115.8, 116.0, 128.0, 128.6, 129.3, 131.3, 131.3, 133.1, 133.1, 140.0, 162.4, 164.3, 172.2



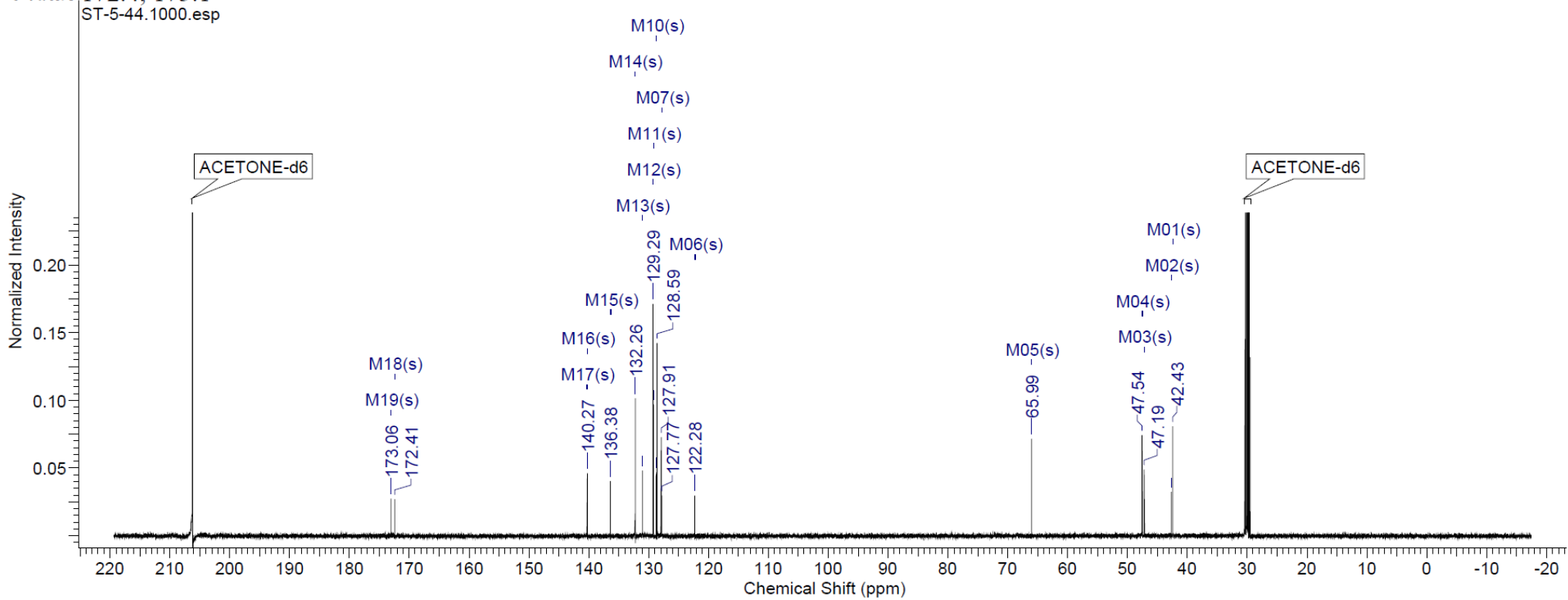
α -2,4-Diphenylcyclobutane-1,3-dicarboxylic acid mono-(4-bromo)benzyl ester (SB-FI-80)



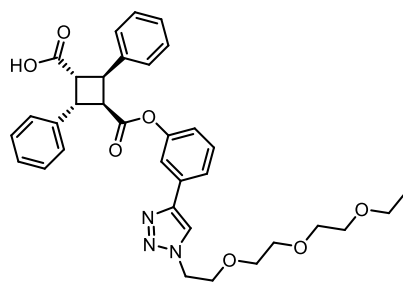
$^1\text{H NMR}$ (500 MHz, ACETONE- d_6) δ 3.92 - 4.11 (m, 2 H), 4.40 - 4.57 (m, 2 H), 4.69 (d, $J = 12.82$ Hz, 1 H), 4.78 (d, $J = 12.51$ Hz, 1 H), 6.96 (d, $J = 8.54$ Hz, 2 H), 7.20 - 7.29 (m, 2 H), 7.32 (t, $J = 7.48$ Hz, 4 H), 7.35 - 7.40 (m, 2 H), 7.40 - 7.49 (m, 4 H)



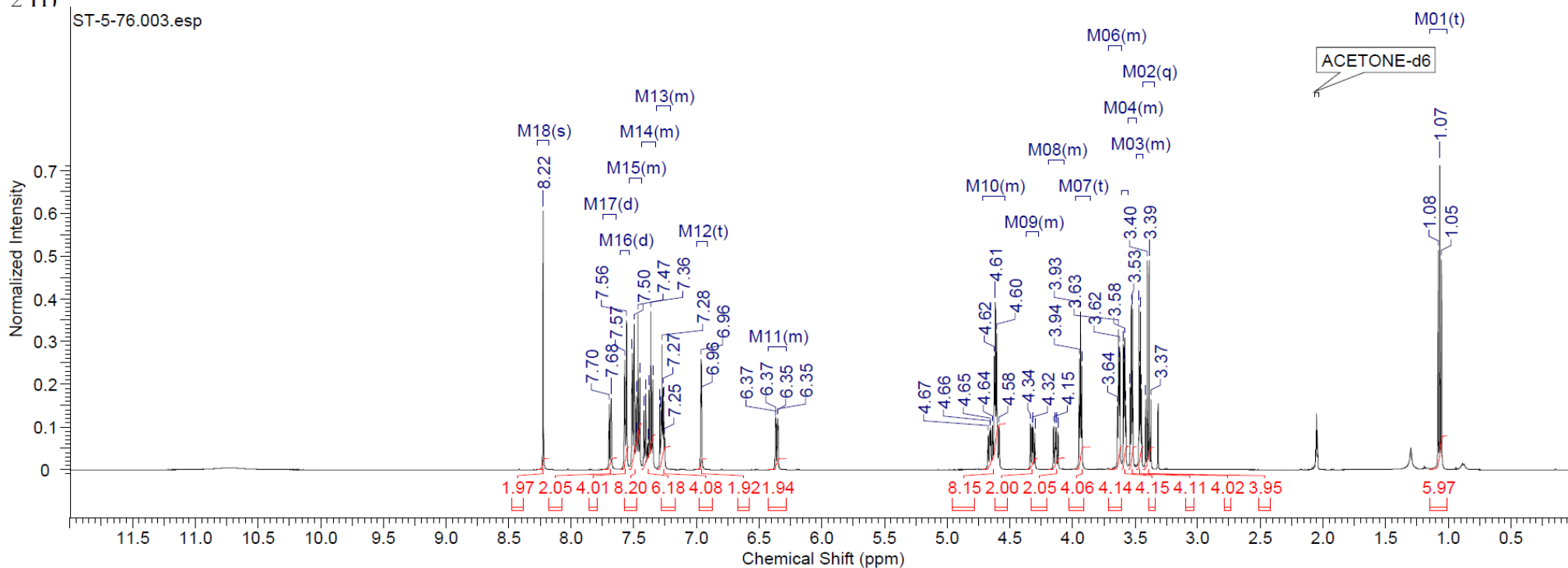
^{13}C NMR (126 MHz, ACETONE- d_6) δ 42.4, 42.7, 47.2, 47.5, 66.0, 122.3, 127.8, 127.9, 128.6, 128.7, 129.2, 129.3, 131.0, 132.3, 136.4, 140.2, 140.3, 172.4, 173.1



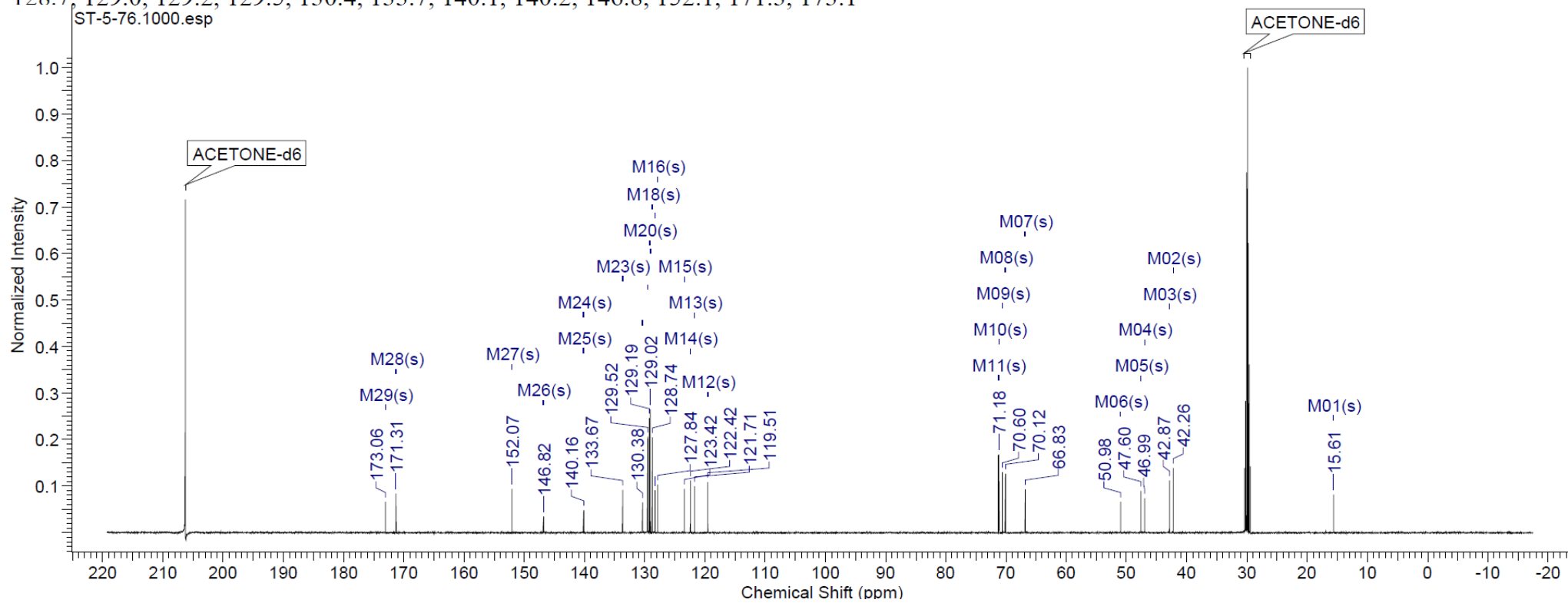
α -2,4-Diphenylcyclobutane-1,3-dicarboxylic acid mono-(3-(1-(2-(2-(2-ethoxyethoxy)ethoxy)ethyl)-1H-1,2,3-triazol-4-yl)phenyl ester (SB-FI-85)



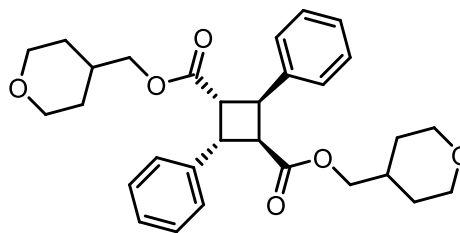
$^1\text{H NMR}$ (500 MHz, ACETONE- d_6) δ 1.07 (t, $J = 7.02$ Hz, 6 H), 3.39 (q, $J = 7.02$ Hz, 4 H), 3.43 - 3.49 (m, 4 H), 3.49 - 3.55 (m, 4 H), 3.55 - 3.61 (m, 4 H), 3.61 - 3.71 (m, 4 H), 3.93 (t, $J = 5.19$ Hz, 4 H), 4.06 - 4.19 (m, 2 H), 4.27 - 4.36 (m, 2 H), 4.54 - 4.72 (m, 8 H), 6.28 - 6.43 (m, 2 H), 6.96 (t, $J = 1.83$ Hz, 2 H), 7.21 - 7.32 (m, 4 H), 7.33 - 7.44 (m, 6 H), 7.44 - 7.54 (m, 8 H), 7.57 (d, $J = 7.32$ Hz, 4 H), 7.69 (d, $J = 7.93$ Hz, 2 H), 8.22 (s, 2 H)



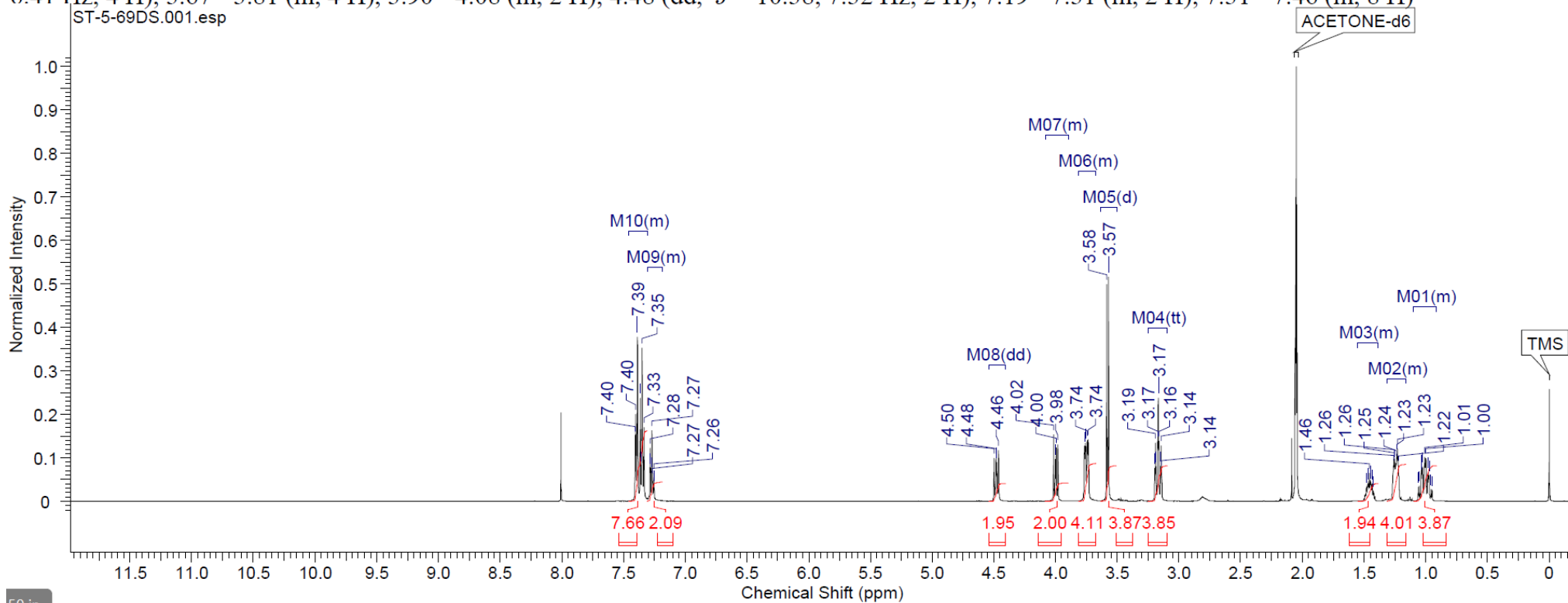
^{13}C NMR (126 MHz, ACETONE- d_6) δ 15.6, 42.3, 42.9, 47.0, 47.6, 51.0, 66.8, 70.1, 70.6, 71.2, 71.3, 119.5, 121.7, 122.4, 123.4, 127.8, 128.3, 128.7, 129.0, 129.2, 129.5, 130.4, 133.7, 140.1, 140.2, 146.8, 152.1, 171.3, 173.1



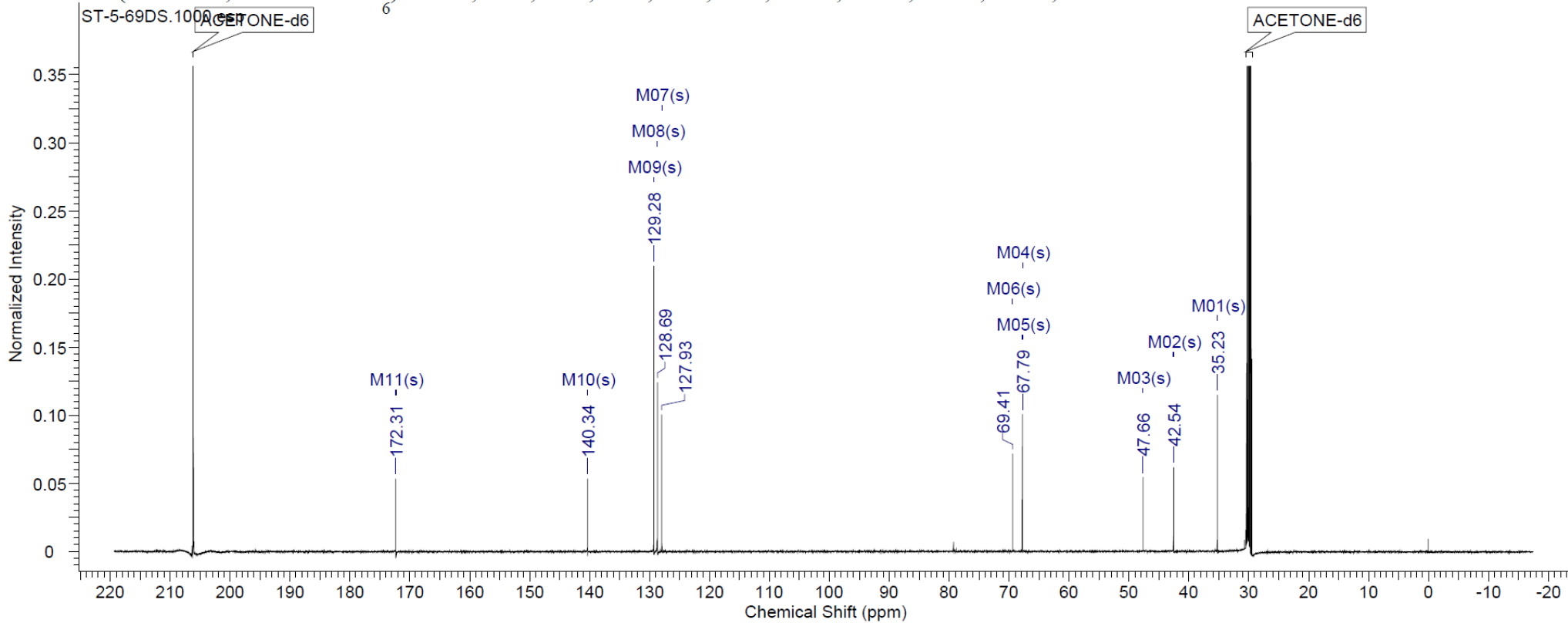
α -2,4-Diphenylcyclobutane-1,3-dicarboxylic acid di-tetrahydropyran-4-methyl ester (SB-FI-86)



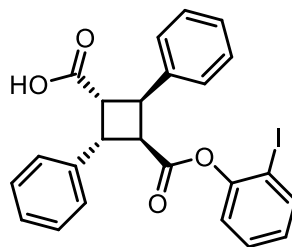
$^1\text{H NMR}$ (500 MHz, ACETONE- d_6) δ 0.91 - 1.10 (m, 4 H), 1.16 - 1.31 (m, 4 H), 1.38 - 1.55 (m, 2 H), 3.17 (tt, $J = 11.71, 2.33$ Hz, 4 H), 3.58 (d, $J = 6.41$ Hz, 4 H), 3.67 - 3.81 (m, 4 H), 3.90 - 4.08 (m, 2 H), 4.48 (dd, $J = 10.38, 7.32$ Hz, 2 H), 7.19 - 7.31 (m, 2 H), 7.31 - 7.46 (m, 8 H)



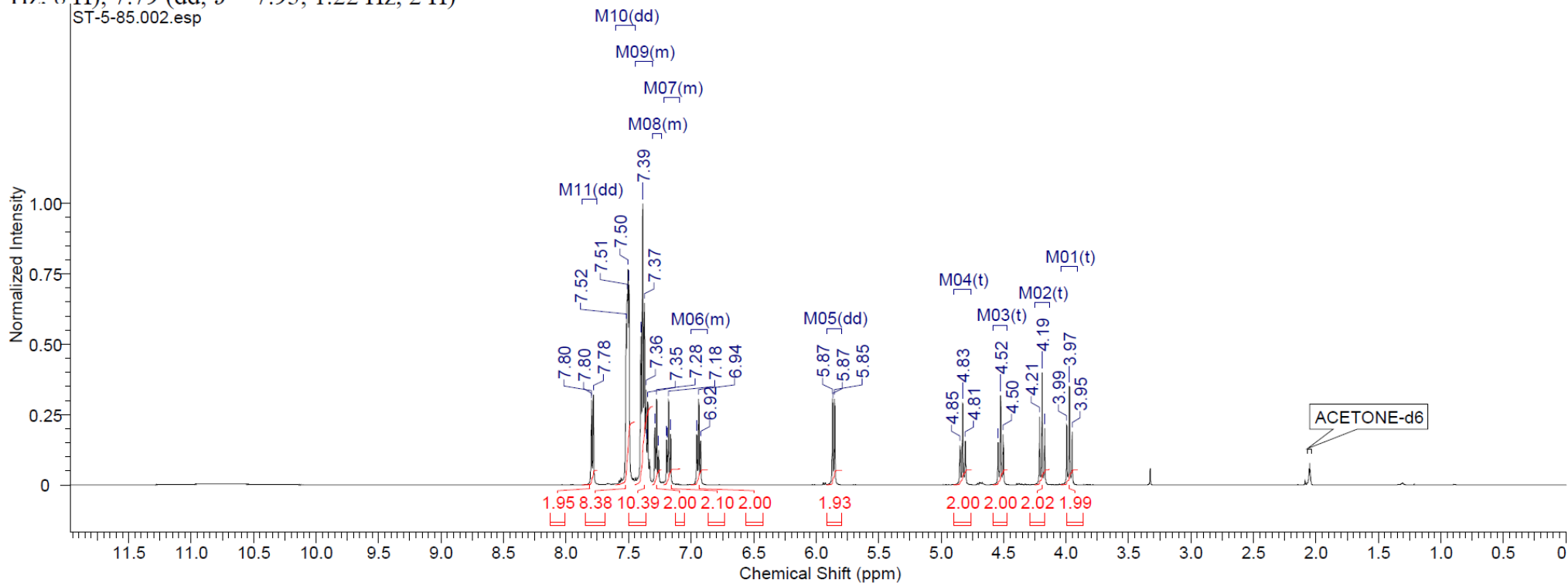
^{13}C NMR (126 MHz, ACETONE- d_6) δ 35.2, 42.5, 47.7, 67.8, 67.8, 69.4, 127.9, 128.7, 129.3, 140.3, 172.3



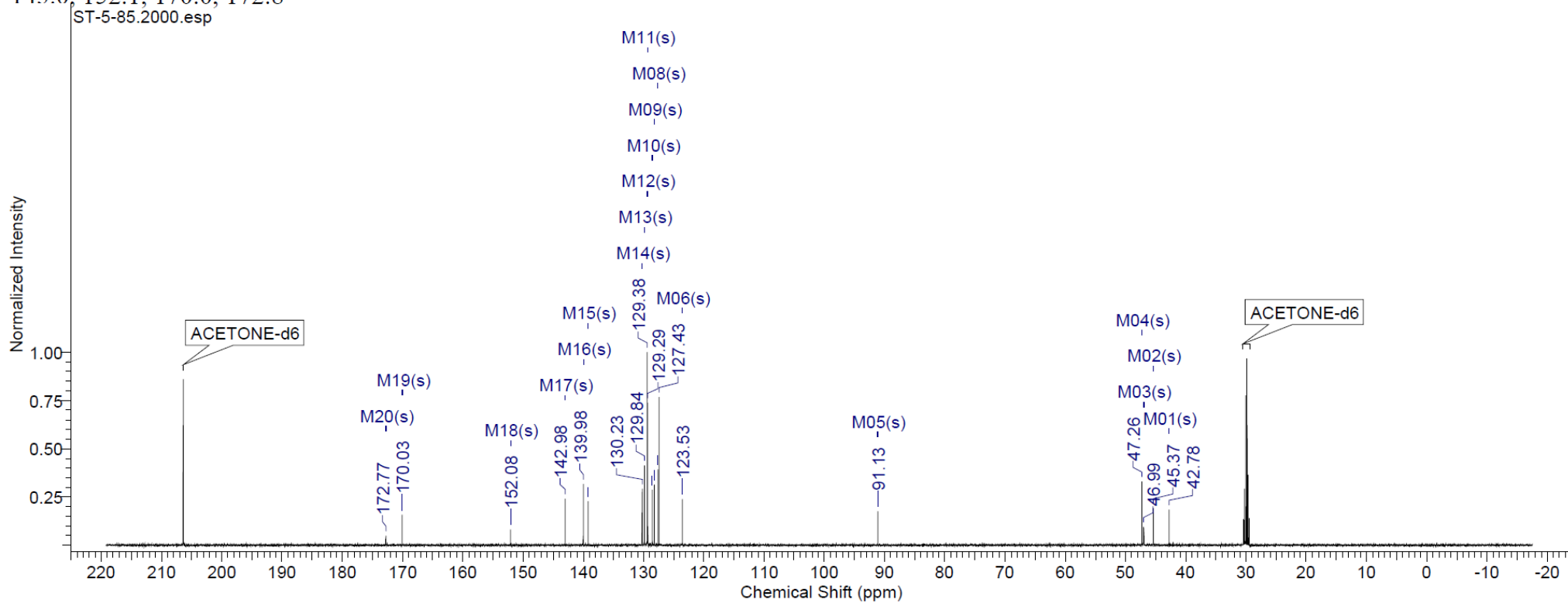
α -2,4-Diphenylcyclobutane-1,3-dicarboxylic acid mono-1-(2-iodo)phenyl ester (SB-FI-90)



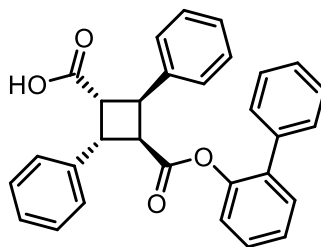
$^1\text{H NMR}$ (500 MHz, ACETONE- d_6) δ 3.97 (t, $J = 10.53$ Hz, 2 H), 4.19 (t, $J = 10.38$ Hz, 2 H), 4.52 (t, $J = 10.22$ Hz, 2 H), 4.83 (t, $J = 10.68$ Hz, 2 H), 5.86 (dd, $J = 7.93, 1.22$ Hz, 2 H), 6.87 - 7.00 (m, 2 H), 7.09 - 7.22 (m, 2 H), 7.24 - 7.31 (m, 2 H), 7.31 - 7.45 (m, 10 H), 7.51 (dd, $J = 7.02, 3.97$ Hz, 8 H), 7.79 (dd, $J = 7.93, 1.22$ Hz, 2 H)



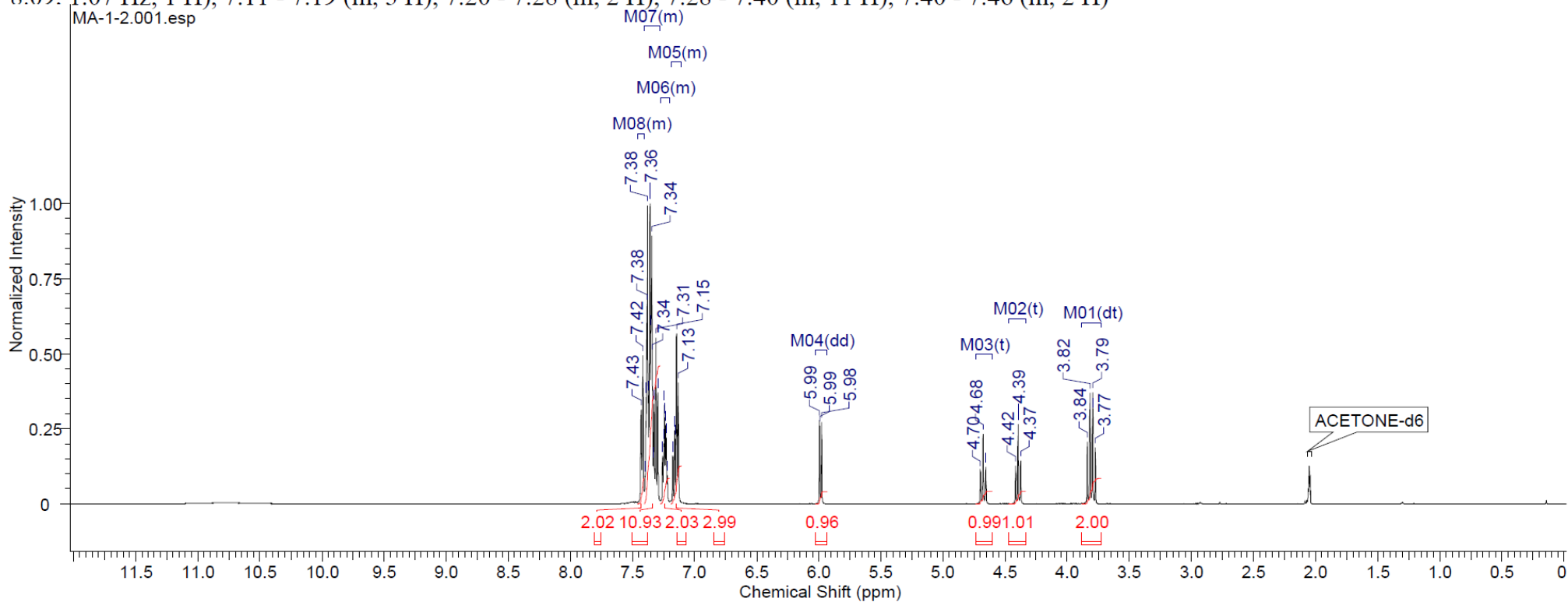
^{13}C NMR (126 MHz, ACETONE- d_6) δ 42.8, 45.4, 47.0, 47.3, 91.1, 123.5, 127.4, 127.6, 128.2, 128.5, 129.3, 129.4, 129.8, 130.2, 139.2, 140.0, 143.0, 152.1, 170.0, 172.8



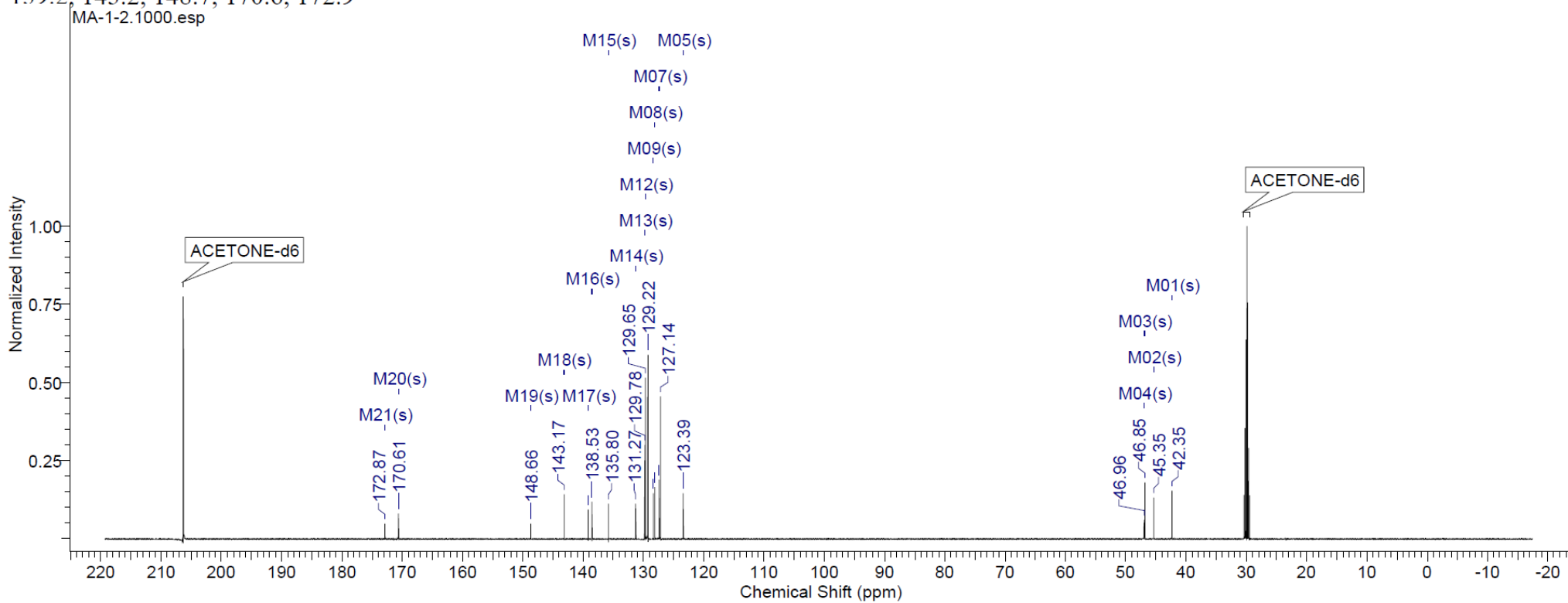
α -2,4-Diphenylcyclobutane-1,3-dicarboxylic acid mono-1-(2-phenyl)phenyl ester (SB-FI-91)

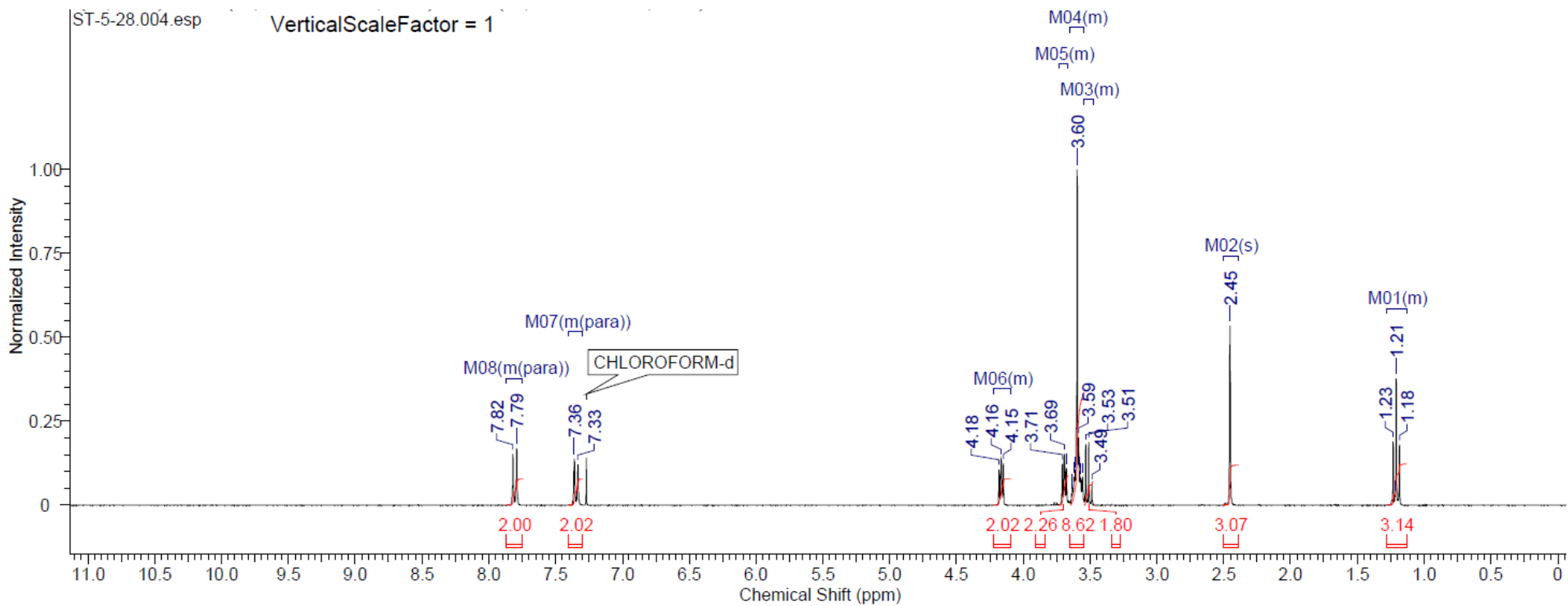
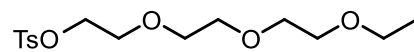


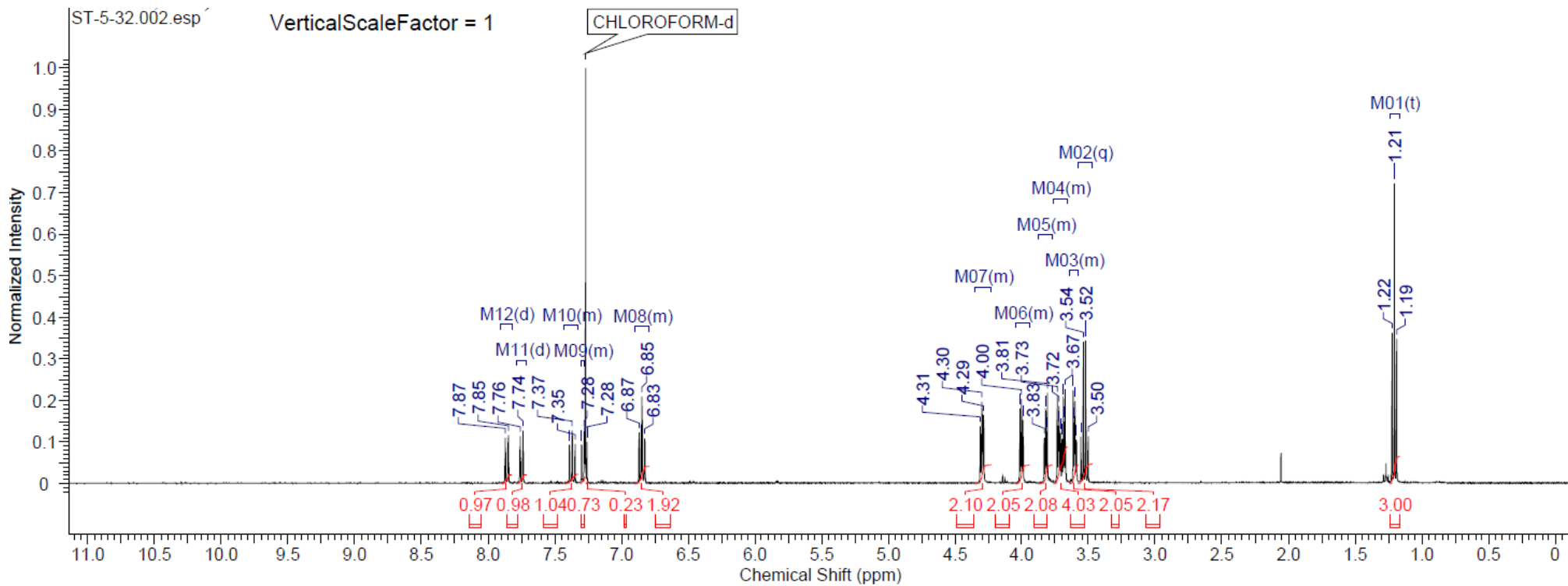
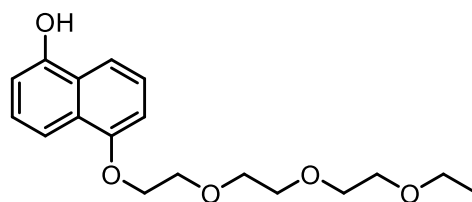
$^1\text{H NMR}$ (500 MHz, ACETONE- d_6) δ 3.81 (dt, $J = 11.67, 10.49$ Hz, 2 H), 4.39 (t, $J = 10.07$ Hz, 1 H), 4.68 (t, $J = 10.68$ Hz, 1 H), 5.99 (dd, $J = 8.09, 1.07$ Hz, 1 H), 7.11 - 7.19 (m, 3 H), 7.20 - 7.28 (m, 2 H), 7.28 - 7.40 (m, 11 H), 7.40 - 7.46 (m, 2 H)



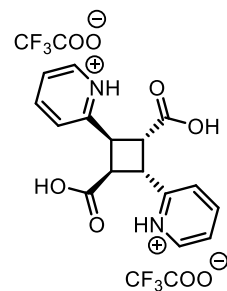
^{13}C NMR (126 MHz, ACETONE- d_6) δ 42.3, 45.4, 46.8, 47.0, 123.4, 127.1, 127.4, 128.1, 128.4, 129.2, 129.3, 129.6, 129.8, 131.3, 135.8, 138.5, 139.2, 143.2, 148.7, 170.6, 172.9



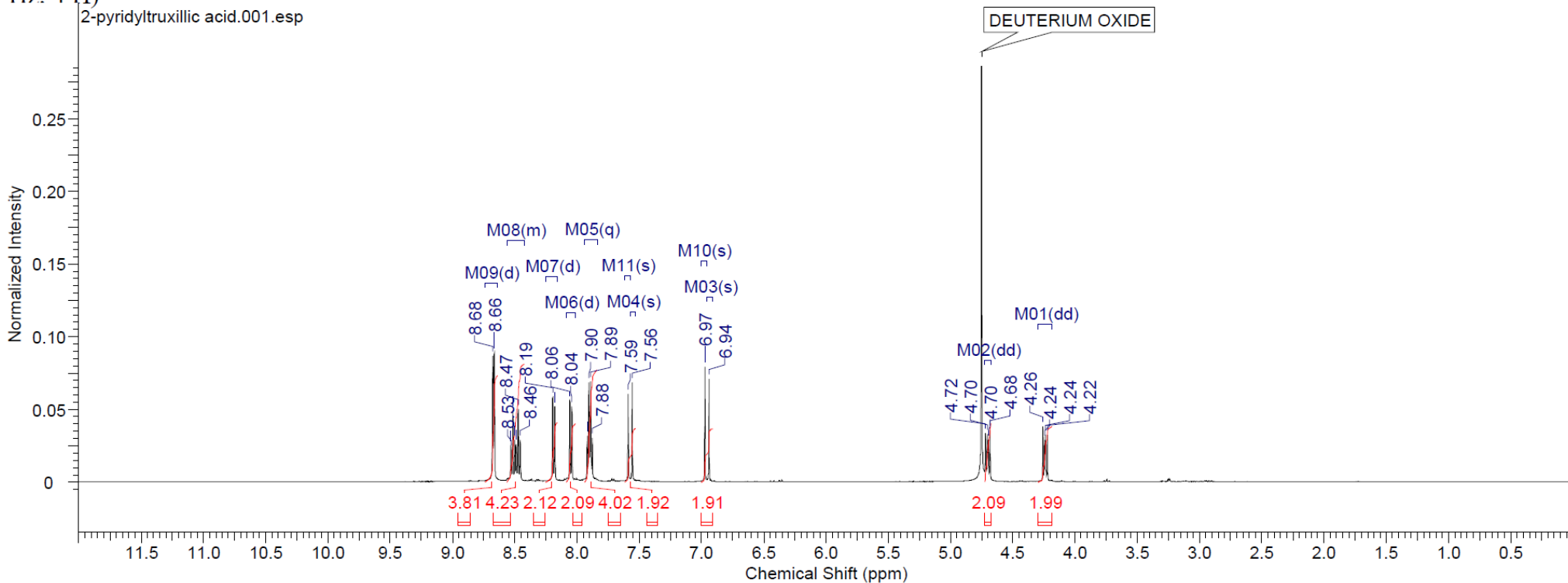




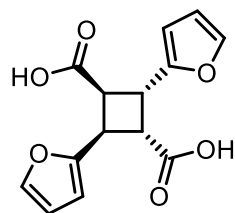
α -2,4-Di(pyridin-2-ium)cyclobutane-1,3-dicarboxylic acid trifluoroacetate



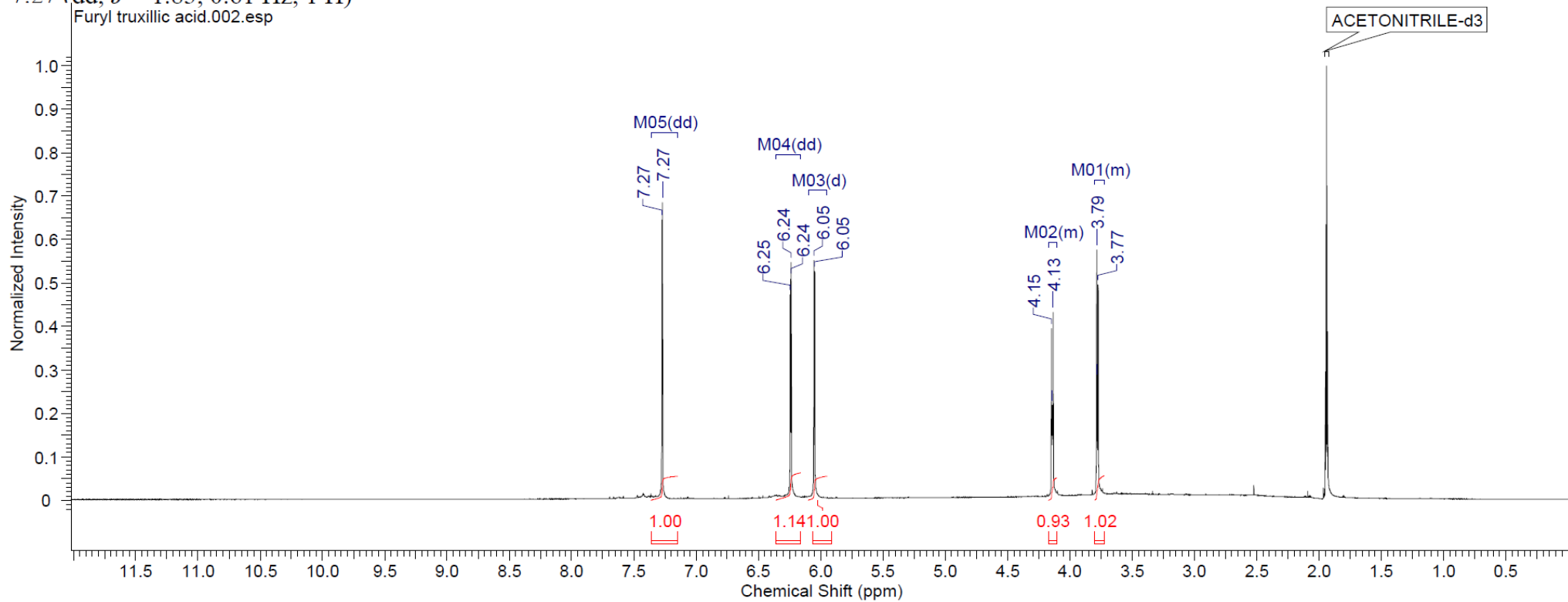
^1H NMR (500 MHz, DEUTERIUM OXIDE) δ 4.24 (dd, $J = 10.53, 7.17$ Hz, 2 H), 4.70 (dd, $J = 10.53, 7.48$ Hz, 2 H), 6.97 (s, 1 H), 6.94 (s, 1 H), 7.59 (s, 1 H), 7.56 (s, 1 H), 7.90 (q, $J = 6.41$ Hz, 4 H), 8.05 (d, $J = 8.24$ Hz, 2 H), 8.19 (d, $J = 8.24$ Hz, 2 H), 8.42 - 8.56 (m, 4 H), 8.67 (d, $J = 5.80$ Hz, 4 H)



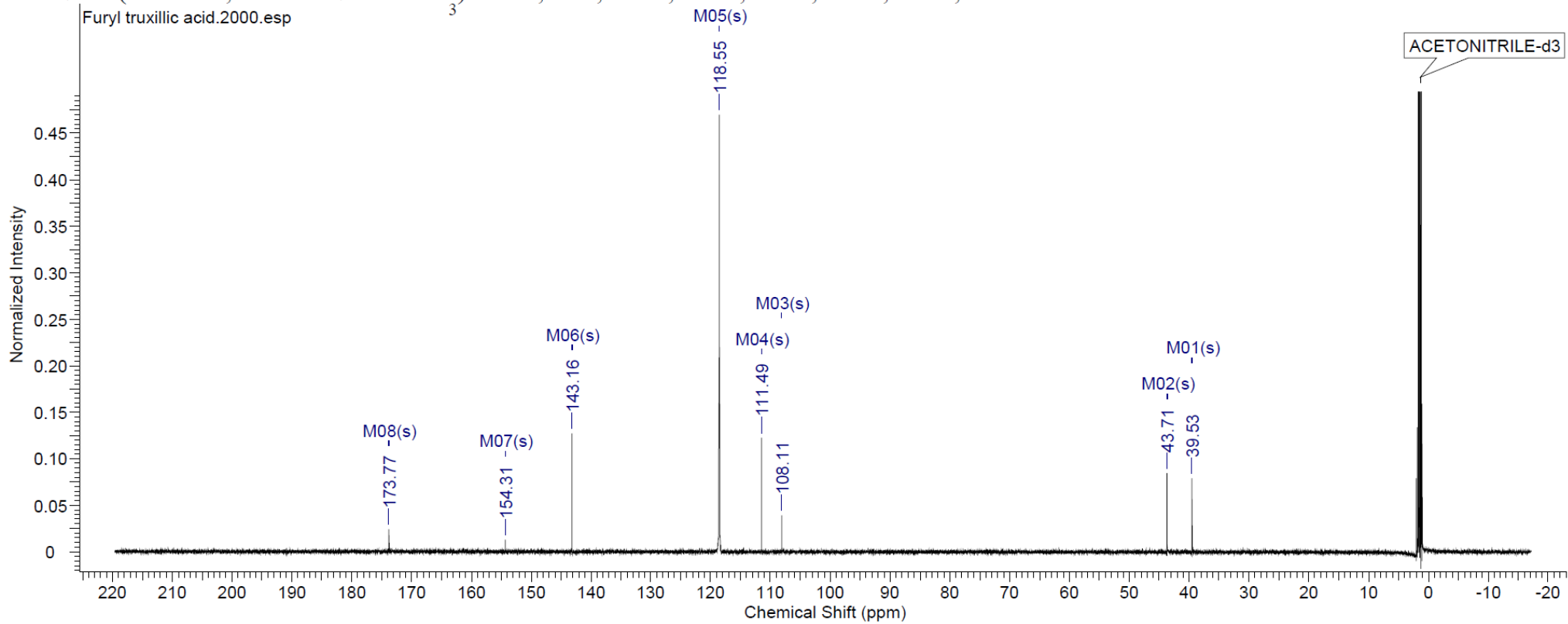
2,4-Di(furan-2-yl)cyclobutane-1,3-dicarboxylic acid



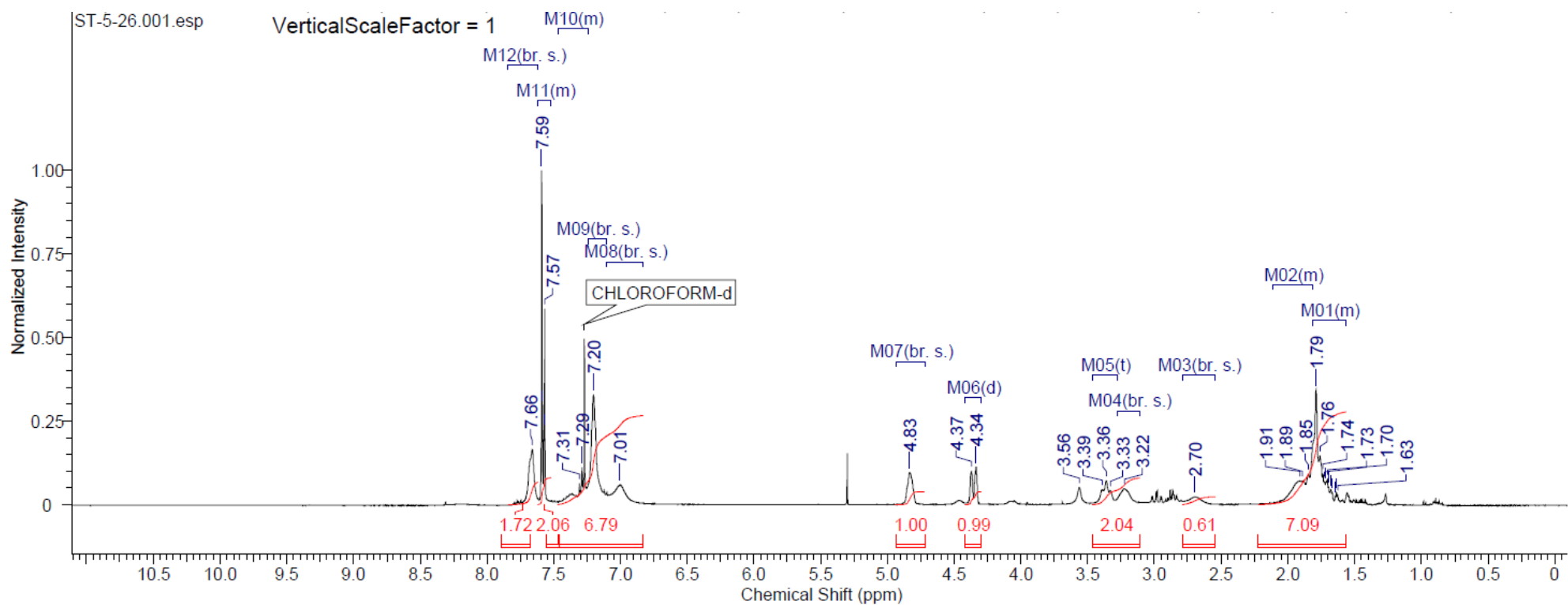
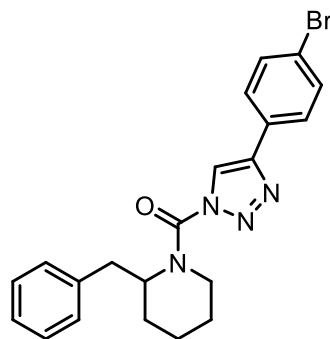
^1H NMR (500 MHz, ACETONITRILE- d_3) δ 3.73 - 3.80 (m, 1 H), 4.11 - 4.17 (m, 1 H), 6.05 (d, $J = 3.36$ Hz, 1 H), 6.24 (dd, $J = 3.05, 1.83$ Hz, 1 H), 7.27 (dd, $J = 1.83, 0.61$ Hz, 1 H)



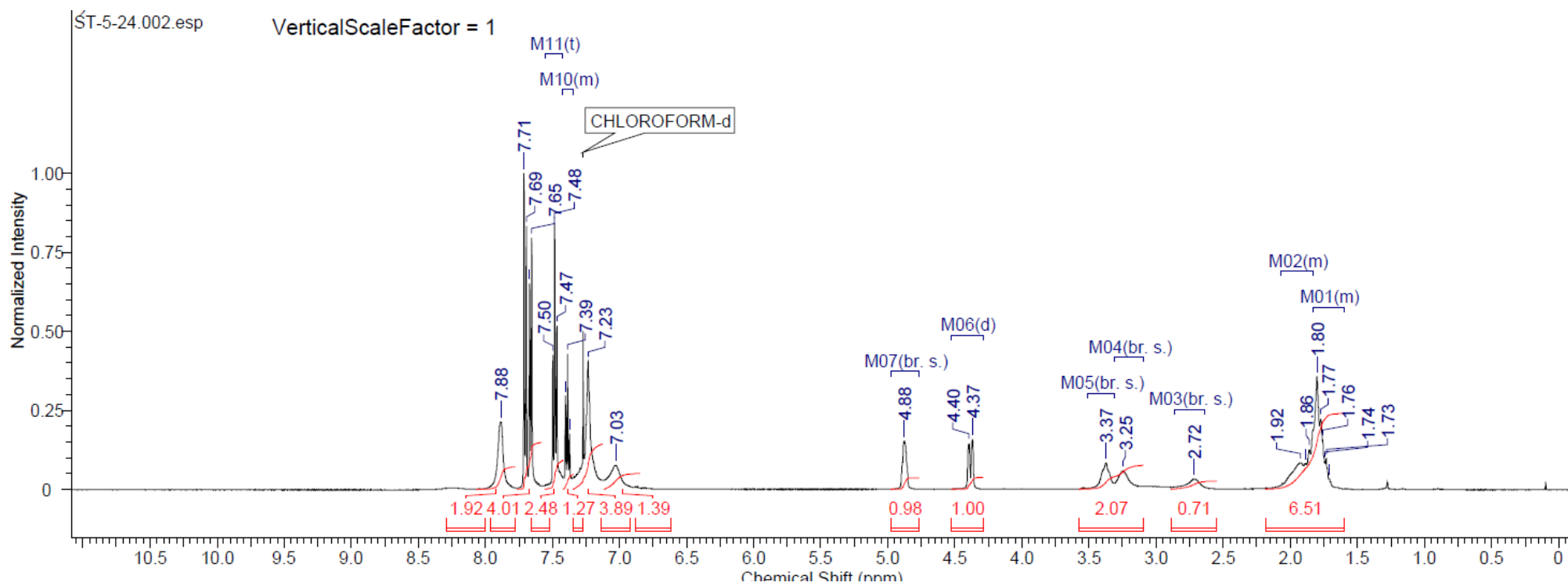
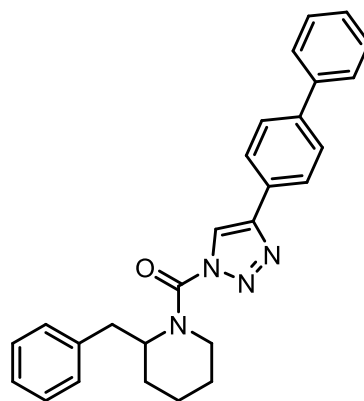
^{13}C NMR (126 MHz, ACETONITRILE- d_3) δ 39.5, 43.7, 108.1, 111.5, 118.6, 143.2, 154.3, 173.8



(2-Benzylpiperidin-1-yl)(4-(4-bromophenyl)-1H-1,2,3-triazol-1-yl)methanone²²



(4-([1,1'-Biphenyl]-4-yl)-1H-1,2,3-triazol-1-yl)(2-benzylpiperidin-1-yl)methanone²²



(2-Benzylpiperidin-1-yl)(4-(2'-methoxy-[1,1'-biphenyl]-4-yl)-1H-1,2,3-triazol-1-yl)methanone²²

